Proceedings

of

INTERNATIONAL CONFERENCE ON INNOVATIONS IN ENGINEERING AND MANAGEMENT

ICIEM '23

Organised by

DEPARTMENT OF MECHANICAL ENGINEERING

NSS COLLEGE OF ENGINEERING PALAKKAD

DATE : 21 & 22 JULY 2023

For any queries mail to :
iciem23@nssce.ac.in

PATRON

Sri. G. Sukumaran Nair
Chairman, Governing Body
NSSCE

CHAIRMAN

Dr. P. R. Suresh
Principal
NSSCE

ORGANISING CHAIRMAN

Dr. N. Rajeev
Head of the Department
Department of Mechanical Engineering
NSSCE

COORDINATORS

Dr. V. R. Pramod

Dr. B. Rajesh Menon

Dr. K. R. Kiron

LIST OF COMMITTEE MEMBERS

Technical Review Committee

Dr. Vinod V.

Dr. Aneesh Kumar P.

Dr. Sajeesh P

Sri Harish P

Programme Committee

Dr. Sudeep U

Prof. Sajesh M

Prof. Madhu Mohan

Sri. Manosh T.I

Publication Committee

Dr. Jyothi Sankar P.R.

Sri. Biju K.B.

Sri Ravisankar P

Sri Gopinath K

Sri. Arun V

Food Committee

Prof. Santhosh Kumar S

Sri Sreekumar C

Sri. Sunil P

Sri. Ajith Kumar C

Sri. Arjun Kumar M.K

Sri. Manikandan C

Transportation committee

Sri Sreekumar C

Sri. Suresh N.

Sri Vinayan V

Sri Renjithkumar CR

Sri Saneh KV

Sri Ramesh K

Stage & Decoration Committee

Sri Vimesh Nair K.

Sri Santhosh Kumar R

Sri. Suresh Kumar A

Sri. Kunjayyappan Pillai V

Sri. Jithu Chandrasekaran

Smt. Aiswarya S

LIST OF STUDENT COORDINATORS

M.Tech Students

Arun Krishnan C

Jithin Das M

Sreejith B

Sai Prasanth N

Akshay S Pillai

Harisankar T

Jayakrishnan K H

Sharan S Das

Viswas K

Yedhu Gopan

Phd Scholars

Kiran Vijayan

Ragesh P R

Jeevan Ealias

Manuraj K R

Sanoj T

ADVISORY COMMITTEE

- Dr. Mathew. T. Mathew, Director of faculty research, Professor (RT), University of Illinois College of Medicine Rockford.
- Dr. Nisha Nair, Clinical Assistant Professor of Business Administration, University of Pittsburgh.
- Dr. Mosa. S. Al. Haddad, Supply chain consultant, Senior Quality Consultant, Quality Esnad - Saudi Arabia, Dammam - Eastern Province - Kingdom of Saudi Arabia.
- Dr. D.K. Banwet, Former Professor, Dept. of Management Studies, IIT Delhi.
- Dr. S.R Devadasan, Professor, PSG College of Technology, Coimbatore.
- Dr. C. Sujatha, Former Professor, Dept. of Mechanical Engineering, IIT Madras.
- Dr. Jyothi S.N, Principal, Amrita Vishwa Vidyapeetham, Amritapuri Campus.
- Dr. Shalij P.R, Dean (Research), APJ Abdul Kalam Technological University, Kerala State.
- Dr. Jagathy Raj V. P, Director, School of Management Studies, Cochin University of Science and Technology, Kochi.
- Mr. K. Abdul Samad, Retired Unit Head, Malabar Cements, Cherthala.

INVITED TALKS

- Dr. Prahlad Vadakkepat, Associate Professor, Electrical & Computer Engineering, College of Design and Engineering, National University of Singapore & founder secretary of Federation of Int. Robot-soccer Association
- Dr. Sandeep Sangameswaran, PMP Director, Project & Program Management Philips, Innovation & Strategy, High Tech Campus 34,5656AE, Eindhoven the Netherlands.
- Mr. R. Radhakrishnan, AGM, Instrumentation Limited, Palakkad.
- Rekha Sharma, Operations Director, GRIP Global.
- Dr. V.R. Pramod, Professor, Dept. of Mechanical Engineering, NSS College of Engineering, Palakkad.
- Dr. Majeed Mohamed, Senior Principal Scientist, National Aerospace Laboratories, Ministry of Science and Technology, Govt. of India.

ABOUT THE DEPARTMENT

The department of mechanical engineering was started in 1960 and is the largest department of the institution. The department has highly committed faculty comprising of 18 Ph.D. holders from IIT/IISC/NIT/Reputed universities. The department is offering UG, PG and Doctoral programmes in mechanical engineering. Well-equipped laboratories and other infrastructure make the department to be the most sought after one in the state of Kerala.

MESSAGE FROM PRINCIPAL

I am delighted to learn that the Department of Mechanical Engineering is publishing conference proceedings associated with the International Conference on Innovations in Engineering and Management (ICIEM'23), which took place on July 21st and 22nd at our prestigious institution. This conference represented a collective effort to explore cutting-edge ideas and address challenges in the ever-evolving fields of engineering and management.

The theme, "Innovations in Engineering and Management," reflects our commitment to advancing knowledge and fostering innovation. The presentations and discussions held during the conference have undoubtedly contributed to the intellectual vibrancy of our academic community.

I congratulate the organizing committee, presenters, and participants for their dedication in making ICIEM'23 a successful event. Your collective efforts have enriched our academic landscape and laid the foundation for continued growth and collaboration.

As we peruse the pages of these proceedings, I am confident that the knowledge shared and collaborations formed during ICIEM'23 will contribute significantly to the ongoing advancements in the fields of engineering and management.

Congratulations to the Department of Mechanical Engineering for hosting such a noteworthy conference. I encourage all contributors to continue their pursuit of excellence in research and scholarship.

May these proceedings serve as a lasting testament to the intellectual achievements and collaborative spirit embodied by the participants of ICIEM 2023. Wishing you all continued success in your academic and professional endeavours.

Dr. P. R. Suresh
Principal
NSS College of Engineering
Palakkad

MESSAGE FROM HEAD OF DEPARTMENT

It is with great satisfaction that I reflect on the success of the International Conference on Innovations in Engineering and Management (ICIEM'23) held on July 21st and 22nd. Hosted by the Department of Mechanical Engineering, this event marked a significant milestone in our continuous effort to advance knowledge and foster innovation in the dynamic fields of engineering and management.

The selected theme, "Innovations in Engineering and Management," underscored our commitment to exploring cutting-edge ideas and addressing contemporary challenges in these interrelated domains. The conference provided a vibrant platform for researchers, academicians, and industry professionals to engage in insightful discussions and share their expertise in their respective areas.

I extend my sincere appreciation to the organizing committee for their diligent efforts in ensuring the success of the conference. Their dedication and meticulous planning played a pivotal role in creating a valuable and enriching experience for all participants.

As we look back on the presentations and discussions that unfolded during the two-day conference, I express my warmest gratitude to all participants. Your contributions were instrumental in making ICIEM'23 a great success, and I am confident that this gathering has laid the foundation for future collaborations and advancements in the fields of engineering and management.

I hope that everyone who participated actively engaged in the exchange of ideas, forged new connections, and explored the possibilities that arose from this collaborative endeavour. On behalf of the Department of Mechanical Engineering, I extend my sincere thanks for your contributions to the success of the International Conference on Innovations in Engineering and Management (ICIEM) July 2023.

Dr. Rajeev N
Professor & Head
Department of Mechanical Engineering
NSS College of Engineering
Palakkad

CONTENTS

SL.NO	TITLE	PAGE NO
1.	STIR CASTING, MICROSTRUCTURE AND MECHANICAL PROPERTIES OF AZ91D-TIB2-HAP HYBRID NANOCOMPOSITES	1 - 4
2.	AUTOMATED SOLAR POWERED GRASS TRIMMING ROBOT WITH INTERCHANGEABLE TOOL PROVISION	5 - 9
3.	AUTOMATED SYSTEM FOR CLEANING OF SOLAR CONCENTRATOR DISH	10 - 13
4.	MODEL FOR AGRI-FOOD DARK STORE ALLOCATION IN METRO CITIES	14 - 20
5.	EXPERIMENTAL STUDY OF EVACUATED TUBE HEAT PIPE SOLAR WATER HEATER	21 - 26
6.	RAILWAY BRAKE TECHNOLOGY FOR HIGH-SPEED TRAINS	27 - 35
7.	A REVIEW ON HOW STIRRING PROCESS PARAMETERS AFFECT THE STIR CASTING ROUTE WITH ALUMINIUM METAL MATRIX COMPOSITES	36 - 43
8.	RETROFITTING OF INTERNAL COMBUSTION VEHICLE TO ELECTRIC VEHICLE AND MATLAB-SIMULINK ANALYSIS	44 - 49
9.	DESIGN AND FABRICATION OF ELECTRIC VEHICLE SPECIFIC TEST RIG AND TESTING	50 - 54
10.	METHODS FOR MECHANICAL, THERMAL AND MORPHOLOGICAL INVESTIGATIONS ON NATURAL FIBRE REINFORCED COMPOSITES	55 - 60
11.	PERFORMANCE PREDICTION OF A TWO BED SOLAR ADSORPTION REFRIGERATION SYSTEM BASED ON ANN MODELING	61 - 65

12.	SPEED BUMP: A RENEWABLE ENERGY SOURCE	66 - 70
13.	FLUID FLOW AND HEAT TRANSFER CHARACTERISTICS OF SILVER GRANULE COATED MINICHANNEL WITH GRAPHENE OXIDE NANOFLUID AS COOLANT	71 - 76
14.	DESIGN AND FABRICATION OF AN ALL-TERRAIN VEHICLE INTEGRATED WITH SENSORS FOR THE IDENTIFICATION OF MATERIALS IN LANDSLIDE AFFECTED REGION	77 - 84
15.	DRIVER DROWSINESS DETECTION AND RIDER MONITORING FOR TWO WHEELERS	85 - 92
16.	MULTI LUG NUT REMOVER WITH DIFFERENTIAL DIAMETERS	93 - 101
17.	FIRE EXTINGUISHER AUTOMATIC ROBOT	102 - 106
18.	FABRICATION AND CHARACTERIZATION OF AZ91D MG MATRIX COMPOSITE WITH HYBRID REINFORCEMENT USING FRICTION STIR PROCESSING	107 - 111
19.	DESIGN AND FABRICATION OF FOLDING STAIRS FOR TRAIN	112 - 115
20.	DYNAMIC RESPONSE TESTING ON CONTROL VALVE WITH EVSP PACKING	116 - 120
21.	STUDY ON NOVEL MULTISEGMENT REPLACEABLE PROFILED STEEL SHEAR LINKS UNDER CYCLIC LOADING	121 - 127
22.	EFFECT OF DYNAMIC COUPLING OF LIQUID PROPELLANT SLOSHING ON THE RESPONSE AT SATELLITE OF A TYPICAL LIQUID PROPELLANT ROCKET	128 - 137
23.	EXPERIMENTAL INVESTIGATION ON SUGARCANE BAGASSE ASH BASED GEOPOLYMER BRICKS	138 - 143

24.	VALIDATION OF MODULAR GRIDDED BASE PLATFORM FOR THE STATIC STRUCTURAL TESTING OF AEROSPACE STRUCTURES USING M S ADAPTOR	144 - 148
25.	SUSTAINABILITY STUDIES AND LIFE CYCLE ASSESSMENT OF CONSTRUCTION MATERIALS – AN OVERVIEW	149 - 154
26.	AN ISOLATED SOFT SWITCHED HIGH POWER FACTOR RECTIFIER WITH MULTIPLE OUTPUT	155 - 160
27.	SOLAR-POWERED BICYCLE TEASHOP	161 - 165
28.	DESIGN OF A SMART CAR	166 - 169
29.	ADVANCED HELMET FOR TWO WHEELERS	170 - 174
30.	IMPLEMENTATION OF LEAN MANUFACTURING IN A SMALL AND MEDIUM ENTERPRISE USING VALUE STREAM MAPPING	175 - 180
31.	ANALYSIS OF DEFECTS FOR REDUCING THE REJECTION LOSSES IN A FORGING INDUSTRY	181 - 188
32.	CHARACTERIZATION AND ESTIMATION OF AREA BIASED SHUKLA DISTRIBUTION WITH APPLICATIONS OF MEDICAL SCIENCES	189 - 196
33.	SUJIT DISTRIBUTION AND ITS APPLICATIONS	197 - 200
34.	IMPACT OF COVID-19 ON LEARNERS LEARNING BEHAVIOR WITH SPECIALLY FOR THE ADOLESCENT GROUP	201 - 206
35.	ENTREPRENEURSHIP OPPORTUNITIES IN THE MECHANICAL ENGINEERING SECTOR: CHALLENGES AND SUCCESS FACTORS IN THE INDIAN CONTEXT	207 - 210
36.	STATISTICAL ANALYSIS AND CHARACTERISATION OF DIABETES MELLITUS DATA	211 - 219

37.	CUSTOMER RECEPTIVITY OF A TELECOM SERVICE SUPPLY CHAIN	220
38.	PERCEPTIONS OF INTERNAL CUSTOMERS ON A TELECOM SERVICE SUPPLY CHAIN	221
39.	EXPERT SYSTEM FOR COST-INTEGRATED VSM IMPLEMENTATION IN MSMES- A CASE STUDY	222 - 238
40.	NAVIGATING SERVICE QUALITY: A COMPREHENSIVE REVIEW OF SERVQUAL APPLICATIONS ACROSS DIVERSE INDUSTRIES	239 - 242
41.	QUALITY COST ANALYSIS: A LITERATURE REVIEW	243 - 246
42.	5S PRINCIPLES: A REVIEW OF THE LITERATURE	247 - 250
43.	LITERATURE REVIEW ON ISSUES FACED IN SMALL AND MEDIUM SCALE INDUSTRIES IN IMPLEMENTATION OF LEAN MANUFACTURING	251 - 254
44.	A REVIEW ON FACTORS INFLUENCING THE ECONOMIC PERFORMANCE OF SMALL AND MEDIUM ENTERPRISES	255 - 257
45.	FACTORS AFFECTING THE QUALITY OF INDIAN PLYWOOD: A LITERATUREREVIEW	258 - 261

Stir casting, Microstructure and Mechanical properties of AZ91D-TiB2-HAp hybrid nanocomposites

Shamla P C, Ramachandran K K and Bindu M D

Department of Mechanical Engineering, Government Engineering College Thrissur,

Thrissur-680009, Kerala, India

Abstract -

Magnesium metal matrix composites reinforced with hydroxyapatite (HAp) and titanium diboride (TiB2) were fabricated through the stir casting route. Mg alloy, AZ91D was used as the matrix material. The TiB2 composition was varied as 2%, 4% and 6% while keeping the HAp percentage constant at 5%. The microstructure of the developed composites were analyzed using SEM. The porosity, microhardness and tensile properties were assessed. An increase in tensile strength and hardness was observed with the increase of TiB2 reinforcement up to 4%. Beyond 4%, addition of TiB2 causes deterioration in mechanical properties due to increased porosity. Better microstructure and mechanical properties were observed for the composite fabricated with 4% TiB2.

Keywords -

Speed Bump, Planetary Gear Motor, Slider Crank Mechanism, Electromagnetic Induction

1 Introduction

Magnesium-based alloys have exceptional mechanical, biocompatible, and biodegradable characteristics, making them the best possible candidates for use in biomedical applications. Their biodegradable nature and excellent biocompatibility aid patients to avoid a second/revision surgery for the removal of the implant after bone healing or implant related issues. However, magnesium's extremely negative reduction potential and weak corrosion resistance in chloride-containing environments make them degrade faster much before the healing of the damaged bone tissue takes place. Hence, the corrosion rate of magnesium alloys has to be controlled while inside the body. Besides, the common magnesium alloys used as biomedical implants lose their mechanical properties as they corrode in the body environment. Hence the current researches are focussed on developing new Mg based composites that have controlled corrosion rate and ability to retain strength while inside the body.

Hydroxyapatite (HAp) is a naturally occurring mineral that has similar properties as that of natural bone and they are stable in the body fluids. HAp is a common material used on magnesium alloys as coatings to prevent corrosion or control the rate of corrosion [1]. TiB2 has been found to be effective in increasing the corrosion resistance of aluminum alloys [2]. TiB2 has been used as a biocompatible reinforcement in titanium based composites [3]. From the individual effects of HAp and TiB2, it can be presumed that their combined use as reinforcements can tailor the corrosion rate and strength of Mg alloy composites. To the best of knowledge, no studies on the fabrication/characterisation of HAp and TiB2 hybrid Mg alloy composite are reported in the literature. Therefore, in this paper, the fabrication of magnesium matrix composite reinforced with HAp and TiB2 nanoparticles and the effect of % of TiB2 reinforcement on the microstructure and mechanical properties of the composite are investigated.

2 Materials and Methods

The matrix material selected for this study was Mg alloy, AZ91D. The chemical composition of the alloy is given in Table 1. HAp nanoparticles of 10 nm size (99.5% pure) and TiB2 particles of 30 - 50 nm size (99.5% pure) were selected as the reinforcements. The hybrid nanocomposite was synthesized using the computerized bottom pouring stir casting machine with argon protection (Figure 1) available at Government Engineering College Thrissur.

Table 1. Composition of Mg alloy, AZ91D

Element	Fe	Ni	Zn	Al	Mn	Si	Mg
Wt (%)	0.005	0.002	0.38	8.2	0.15	0.01	bal

Pure magnesium has a melting point of 650°C, whereas AZ91D has a solidus temperature of 470°C and liquidus temperature of 595°C. Both the HAp and TiB2 nanoparticles were preheated to a temperature of 250°C and added into the molten magnesium in the furnace. The mixture was agitated using the stirrer at 450 rpm for about 20 minutes. Afterwards, the molten mixture was poured into the rectangular mold by actuating the bottom pouring valve. During the entire melting, stirring and pouring phases, argon gas protective environment was provided automatically by the Ar gas protection facility available in the machine.

Figure 1. Stir casting furnace with argon gas protection system

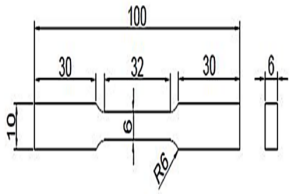

Figure 2. Tensile Test Specimen

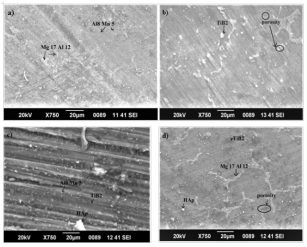

Figure 3. SEM images of a) as-cast AZ91D Mg alloy b) AZ91D with 5 % HAp 2% TiB2 c) AZ91D with 5 % HAp 4% TiB2 d) AZ91D with 5 % HAp 6 % TiB2

2.1 Mechanical Properties and Microstructure

Specimens of size 10 mm x 10 mm x 6 mm for microstructural observation and tensile specimens as shown in Figure 2 (according to the ASTM E8-M08 standard) were extracted from the raw cast ingots by EDM wire cutting. For the SEM analysis, the specimens were progressively rough polished using emery papers of grit 200 - 1500. The SEM images were captured using the Jeol 6390LA/ OXFORD XMX N SE microscope with accelerating voltage in the range 0.5 to 30 kV, available at STIC, CUSAT. To examine the tensile properties, two specimens each were prepared from each of the cast ingots. The tensile properties were evaluated using a computer controlled electromechanical universal testing machine (HEICO make) of capacity 25 kN at a crosshead speed of 5 mm/minute available at Government Engineering College Thrissur. The microhardness of the rough polished samples was measured using the Mitutoyo Vickers Hardness Tester according to the ASTM E 92 standard with an applied load of 50 gf and dwell time of 10 seconds. The porosity of the cast Mg composite samples is determined using the actual and theoretical densities of the composite. The theoretical density of the composite is calculated using the rule of mixtures relationship given in equation (1). The actual density was determined using the electronic balance-specific gravity apparatus available at Government Engineering College Thrissur.

$$(100/t) + (M/pm) = (R/pr) \quad (1)$$

Where, M is the matrix material weight percentage, R is the reinforcement weight percentage, pm, r and t are the densities of the matrix alloy, reinforcements and composite, respectively. From the measurements of weight of the samples in air and water, the theoretical density of the composite is calculated using equation (2).

$$e = (MassEair/MassEair - MassEwater) * pw \quad (2)$$

Where, w is the density of distilled water (1g/cc). The porosity of the Mg matrix composite is determined using equation (3)

$$Porosity = (pt - pe/pt) * 100 \quad (3)$$

2.2 Results and Discussions

SEM image of the as cast AZ91D base Mg alloy is shown in Figure 3(a). The microstructure of cast AZ91D alloy predominantly contains B-Mg17Al12 as strengthening precipitates. In addition to this, traces of Mg17Al12 (Zn) and Al18Mn5 intermetallics will also be present in the Mg matrix [4]. Accordingly, referring to Figure 3(a), the discontinuous, relatively large white patches are seemingly Mg17Al12 precipitates and the relatively less dominant very small dark gray and light gray ones are Mg17Al12 (Zn) and Al18Mn5 precipitates, respectively. The SEM images of AZ91D stir cast composite with 5 wt% HAp and different TiB2 wt% are shown in Figures 3(b)-(d). As shown in Figures 3(b)-(c), besides the strengthening precipitates, randomly distributed white lumps can be observed in the Mg matrix. These lumps are, probably, agglomerated HAp and TiB2 nanoparticles. At 6% TiB2 (Figure 3(d)), dark patches can be observed throughout the matrix. Though, in Figures 3(b) and (c) also such dark patches are present, they are very less in number. These

Table 2. Result of determination of porosity of the AZ91D alloy and composites

Material	Mass in air (g)	Mass in water (g)	Density (gm/cc)		Porosity (%)
			Theoretical	Measured	
AZ91D	5.6	2.328	1.73	1.71	1.633
AZ91D with 5 % HAp 2% TiB_2	2.7845	0.8702	1.8075	1.4545	19
AZ91D with 5 % HAp 4% TiB_2	2.3085	0.8256	1.864	1.6051	14
AZ91D with 5 % HAp 6% TiB_2	2.7067	0.8923	1.934	1.4233	26

dark patches may be due to the presence of porosity and as such, the AZ91D composite with 2% HAp and 6 % TiB2 possesses the highest level of porosity.

2.3 Porosity

The values of porosity of the as cast AZ91D alloy and AZ91D-HAp-TiB2 composites are given in Table 2. For the matrix alloy, porosity value is more or less consistent with the gravity-stir casting route of its manufacture. For composites with different TiB2 wt%, the porosity has not shown any consistency in its variation and the values are high for all the compositions and significantly high for the composite with 6 % TiB2. This observation is well in agreement with the increased amount of dark patches that are observed in the SEM image of the sample with 6 % TiB2. The addition of reinforcements can cause formation of porosity in metal matrix composites primarily due to the release of oxygen or other gasses and change in thermal-conductivity and thermal expansion coefficient. This further depends on the nature of the reinforcements and their size (particle size). Near the vicinity of the reinforcement particles, cooling occurs at a slower rate than the zones far from the particles. This fact together with the differential contraction due to the difference in the thermal expansion coefficient results in the formation of porosity.

2.4 Hardness measurements

Table 3. Microhardness

Material	Microhardness(HV)
AZ91D	59.2
AZ 91D with 5 % HAp 2% TiB_2	69.5
AZ 91D with 5 % HAp 4% TiB_2	72.3
AZ 91D with 5 % HAp 6% TiB_2	62.1

The average value of the microhardness of the as-cast AZ91D Mg alloy and the composites with different reinforcement proportions are given in Table 3. The AZ91D cast alloy is relatively soft when compared to the composites fabricated. For the composites with 2% and 4 % TiB2, the increase in microhardness is consistent with the presence of 5 wt% HAp and increase in the TiB2 concentration. But for the composite with 6 % TiB2, the microhardness is relatively low. This is certainly due to the presence of increased porosity, as evidenced from Figure 3(d) and the porosity values given in Table 2. For the composite with 4% TiB2, as seen in Figure 1(c), the near uniform distribution of the reinforcement particles and the relatively low porosity are the reasons for the highest observed microhardness.

Table 4. Tensile Test Results

Material	Elongation (%)	Ultimate tensile strength (MPa)
AZ91D	8.5	89.96
AZ 91D with 5 % HAp 2% TiB_2	8.4	138.50
AZ 91D with 5 % HAp 4% TiB_2	12.1	166.67
AZ 91D with 5 % HAp 6% TiB_2	9.3	144.47

2.5 Tensile Properties

The tensile properties of the cast AZ91D alloy and the hybrid composites are shown in Table 4. The ultimate tensile strength (UTS) of the base metal is low due to the relatively low proportion of discontinuous course precipitates and the bulk matrix of soft Mg metal as portrayed in Figure 3(a). The addition of HAp and TiB2 nanoparticles have caused an increase in strength of the AZ91D alloy. The highest UTS of 166.67 MPa is obtained for the composite with 4 wt% TiB2. The UTS of composite with 6% TiB2 is less than that at 4% TiB2, which may be attributed to the increased porosity of the composite. The exhibited UTS values are well in conformity with the microhardness and microstructure observations. Literature reports showed that for moderate TiB2 renforcement concentration, addition of (up to 12-15%) TiB2 reinforcements has shown increasing yield strength and UTS of the Mg-TiB2

composites. Therefore, the decreasing trend of UTS for the composites with TiB2 concentration in excess of 4% is not scientifically rational. Also, as stated above, the abnormally high sponginess that leads to the reduction in strength is not a scientific characteristic of the composite for the given TiB2 concentration. Thus, follow up studies are required to assess the real cause of the increased porosity, probably that exists in the synthesis route of the composites.

3 Conclusion

In this study, AZ91D-HAp-TiB2 Mg alloy hybrid composites were successfully fabricated through the stir casting route. The composites were fabricated with 5 wt% (constant) hydroxyapatite (HAp) and 2 wt%, 4 wt% and 6 wt% TiB2 nanoparticles as reinforcements. The microstructure, microhardness and tensile properties of the synthesized composites were evaluated and the following conclusions are derived from the study.

- The as cast AZ91D matrix alloy mostly composed of Mg17Al12 precipitates in soft Mg matrix with traces of Mg17Al12 (Zn) and Al18Mn5 precipitates
- All the fabricated AZ91D-HAp-TiB2 composites have shown near homogeneous distribution of the reinforcements without abnormal agglomeration.
- All the fabricated composites are observed with excessive porosity and the porosity at 6 wt% TiB2 is abnormally high.
- The highest ultimate tensile strength (UTS) is observed for the composite with5 wt% HAp and 4 wt% TiB2. When the concentration of TiB2 is increased, up to 4 wt%, the UTS is also increased. But for 6 wt% TiB2, the UTS has shown a decreasing trend.
- The UTS of the hybrid composites is well in agreement with the microhardness and microstructure of the composites.

References

[1] L.Chen, X.Zhang, W. Zheng, M. Wang, B Liu,W.Sun., Investigation on corrosion behaviors and mechanical properties of TiB2/7075Al composites with various particle contents (2023) Journal of Materials Research and Technology, pp. 2911-2923

[2] Sachiko Hiromoto and Masanari Tomozawa (2010) Corrosion Behavior of Magnesium with Hydroxyapatite Coatings Formed by Hydrothermal Treatment Materials Transactions, pp. 2080-2087

[3] F. M. Makau, K. Morsi, N. Gude, R. Alvarez, M. Sussman, and K. May-Newman (2013)Viability of Titanium-Titanium Boride Composite as a Biomaterial, International Scholarly Research Notices

[4] R. Floriano , D.R. Leiva , G.C. Melo , T.T. Ishikawa , J. Huot , M. Kaufman , S.J.A. Figueroa, L.A. Mendoza-Zelis , L.C. Damonte, W.J. Botta (2017) Low temperature rolling of AZ91 alloy for hydrogen storage , International journal of hydrogen energy., pp 1-12.

Automated Solar Powered Grass Trimming Robot With Interchangeable Tool Provision

Amal P C[1], Arun P[1], Aswin S[1], Jenson D cruz[1] and Arjun K S[2]

[1] B.Tech Students, NSS College of Engineering, Palakkad, Kerala, India
[2]Asst. Professor, Department of Mechanical Engineering, NSS College of Engineering, Palakkad, Kerala, India

Abstract -

This initiative focuses on creating an innovative and eco-friendly solution for grass cutting and floor mopping. By replacing traditional diesel-operated grass cutters with automated robots, we can eliminate pollution and reduce the need for manual labor. The prototype robot utilizes a combination of battery and solar power, with a solar panel attached to the top to charge the battery. Ultrasonic sensors are employed for obstacle detection, ensuring safe and efficient operation. The device is designed to be portable and versatile, capable of switching between grass cutting and floor mopping tasks by interchanging the trimming and mopping tools. By incorporating these features, this project aims to contribute to the development of a sustainable and environmentally friendly system.

Keywords -

Solar powered, automated, obstacle detection, remote monitoring

1 Introduction

In today's era of automation and sustainable technology, the demand for innovative solutions in various fields is on the rise. One such area is lawn maintenance, where traditional methods of grass trimming and maintenance can be time-consuming, labour intensive, and dependent on fossil fuels. To address these challenges, an automated solar powered grass trimming robot with interchangeable tool provision has emerged as a cutting-edge solution. This advanced robotic device harnesses the power of solar energy to operate autonomously, making it an environmentally friendly and cost-effective alternative to conventional grass trimming methods. By incorporating the capability to swap out different trimming tools based on specific requirements, this robot offers enhanced versatility and adaptability to suit various lawn maintenance needs. Through the utilization of solar panels and advanced technology, this automated grass trimming robot not only provides an efficient and sustainable solution but also reduces the manual effort and time required for maintaining outdoor spaces. With its interchangeable tool provision, it caters to different operating methods, allowing users to achieve precise results while customizing the robot's functionality to meet their specific preferences. With a simple swap of attachments, users can easily transform the robot's functionality to perform tasks. the robot can be seamlessly integrated with smart technology, allowing users to control and monitor its operation remotely. This article will delve into the key features and components of an automated solar powered grass trimming robot with interchangeable tool provision. From the solar power system and robotic operations to the grass trimming mechanism and autonomous operation, we will explore how this innovative robot revolutionizes lawn maintenance practices. Furthermore, we will discuss the benefits of such a solution, including its environmental impact, efficiency, and convenience for users seeking automated and sustainable alternatives for grass trimming. With its ability to operate independently, adapt to different cutting techniques, and utilize renewable energy, the automated solar powered grass trimming robot with interchangeable tool provision is poised to transform the way we approach lawn maintenance.

2 The object of the study (Model, Process, Device, Sample preparation etc.)

To develop a robot capable of automatically trimming grass in a designated area. The robot should be able to trim the grass to a required height as desired by the user.

2.1 Project planning

a. Develop a CAD model using solid edge ST7 with obtained data.
b. Research and select a suitable motor that aligns with the power requirements for the cutting.
c. Determine the appropriate battery capacity and type required to power the selected motor efficiently.
d. Fabrication of the working model by applying data.
e. Estimate the required calculations with obtained data.

3 Methods

The methodology of the project is found by analyzing various literatures. For the proper working of the machine the best design model is created using solid edge ST7 software. The size and dimensions are calculated from the

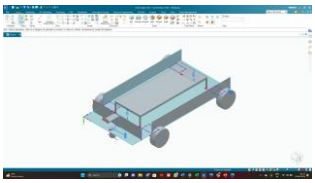

Figure 1. CAD Model

Figure 2. PV Panel

Figure 3. Ultrasonic Sensor

Figure 4. ACP Sheet

model. Firstly, a compactable solar panel of the required model is opted then its specifications are identified and the other components of the project are also selected. The components are placed in body provided by the ACP Sheet proper weight distribution. The fabrication of the model completed and various results and discussions estimated.

3.1 CAD Model

A 3D is developed using Solid edge software.

3.2 Components

The components used in project are described below;

3.2.1 PV Panel

A Solar panel is a collection of photovoltaic cells which can be used to generate electricity through photovoltaic effect. It helps in combating the harmful emissions of greenhouse gases and thus helps in reducing global warming. Solar panels do not lead to any form of pollution and are clean. They also decrease our reliance on fossil fuels (which are limited) and traditional power sources. The use of solar panel helps the machine to work continuously when working as it charges throughout the operation The maximum power obtained is 10W and maximum voltage is 12V.

3.2.2 Ultrasonic sensors

The ultrasonic sensor HC-SR04 is a device used for obstacle detection in the machine. The HC-SR04 has four pins something one ought to know about: VCC (power), Trig (trigger), Echo (getting), and GND (ground). One will uncover that setting up and involving this sensor for your first assortment observing mission is a pleasure. The sensor incorporates progressed control hardware that could likewise assist with keeping away from ”bouncy” information from the program.The operating voltage is 5V DC and current 15mA.

3.2.3 Sheet

Aluminium Composite Panel (ACP) or Aluminium Composite Material (ACM) is a widely-used term describing flat panels that consist of a non-aluminium core bonded between two aluminium sheets. ACP is very rigid and strong despite its light weight. The core is commonly low-density Polyethylene. The aluminium composite panel is a composite of a Polyethylene corebetween two Aluminium sheet and coated with extra durable PVDF (Fluoro Carbon Polymer) which features characteristics such as fire resistance and weather resistance. It also dampers vibration so no additional sound is necessary.

3.2.4 Battery

A lithium-ion or Li-ion battery is a type of rechargeable battery that uses the reversible reduction of lithium ions to store energy. The cutting motor and gear motor works by the energy produced by the battery. The chosen battery was 2.2V, 1200mAh lithium ion batteries connected in series to obtain a output voltage of 12V

3.2.5 Motor driver

This Arduino-compatible motor driving force protector is a packed solution that can handle four DC motors, two 4-cord steppers, and five-volt servos. It employs one L293D to command the DC motor and stepper, and Arduino pins 9 and 10 to run the servo. L293D is a four-channel main

Figure 5. Lithium – ion battery

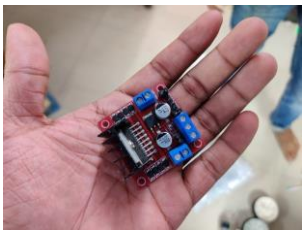

Figure 6. Motor driver

thrust with a solid coordinated high voltage, high current. The input voltage is between 3.2 V to 40V DC, the operating voltage is between 5V to 35V, the peak current is 2a and maximum power consumption is 20W.

3.2.6 Arduino uno

Arduino Uno is an open-source microcontroller board based on the processor ATmega328P. There are 14 digital I/O pins, 6 analog inputs, a USB connection, a power jack, an ICSP header, and a reset button. It contains all the necessary modules needed to support the microcontroller. Arduino is programmed to perform different functions of the components.The input voltage is 5V and DC current is 20mA.

3.2.7 Relay module

A power relay module is an electrical switch that is operated by an electromagnet. The electromagnet is activated by a separate low-power signal from a microcontroller. When activated, the electromagnet pulls to either open or close an electrical circuit. The input voltage is 5V and the switching current and voltage is 10A and 30V.

Figure 7. Arduino Uno

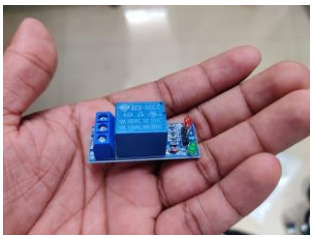

Figure 8. Relay Module

Figure 9. Bluetooth Module

3.2.8 Bluetooth module

It has a range of up to ¡100m which depends upon transmitter and receiver, atmosphere, geographic & urban conditions. It is IEEE 802.15.1 standardized protocol, through which one can build a wireless Personal Area Network (PAN). It uses frequency-hopping spread spectrum (FHSS) radio technology to send data over the air. It uses serial communication to communicate with devices. It communicates with a microcontroller using a serial port (USART).

3.2.9 Trimming and mopping tool

The trimmer tool located at the head of the cutting motor consists of nylon wire connected to the support . Mopping tool consists of sponge connected to the support. Sponge absorbs the water content in the floor thus making the floor dry. By using sponge the absorbing capability will be high and weight will be low thus increasing the rpm. There are several advantages offered by the nylon wire safety, versality, easy replacement and reduced noise. nylon cutting wire provides efficient and safe grass trimming.

Figure 10. Trimming Tool

Figure 11. Mopping Tool

Figure 12. Cutting motor

3.2.10 Cutting motor

A cutting motor is attached to the trimming or mopping tool to trim the grass at suitable height or to mop the floor.The rated speed of cutting motor is 1200 rpm and operating voltage is 12V.

3.2.11 Gear motor

A gear motor is usually a simple DC electric motor with a gear mechanism attached to it. The 4 electric motors include a three milli meter thread drill hole in the middle of a rod, making it simple to link them to tires.The rated speed of gear motor is 45rpm and the operating voltage is 12V.

Figure 13. Gear motor

3.3 Circuit diagram

3.4 Application control

The robot can be controlled through an application called ‘Arduino BlueControl’. It’s working is based on Bluetooth control. It has Automatic and Manuel control mode. It controls the wheel movement and action of the cutting motor.

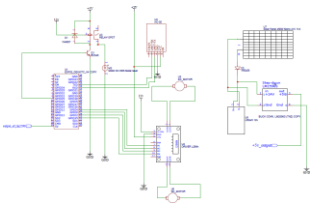

Figure 14. Circuit diagram

Figure 15. Application Interface

4 Results and Discussion

4.1 Model Fabricated

The proposed model is fabricated successfully. The project team analysed the data from machine operation. Through evaluation criteria and feedback, a suitable design concept was selected for further development.

4.2 Calculations

Efficiency of the solar panel = 20%
Energy (in watt-hours) = (1 mAh / 1000) * Voltage (in volts) * Time (in hours)
Sunlight intensity (in watts per square meter) = Energy (in watt-hours) / Time (in hours)
Sunlight Energy Required to change 1 mAh
Energy (in watt hour) = (1 mAh/1000)*V* t
The duration is 1hr 1mAh and voltage 12V
ie, Energy = (1 mAh*12*1)/1000
=0.012Whr
Sunlight Intensity =2 Energy (in watt-hr) / Time in hr
= 0.012/1
= 0.012W/m2̂

Figure 16. Automated solar powered grass trimming robot

Total Sunlight intensity for charge 1200 mAh battery
Sunlight Intensity = 1200*0.12 = 14.4 W/m$\hat{2}$
Assume that the charging efficiency = 50Charging rate = 12V * 0.50 = 6 W
Time Required to charge the battery to be full
Time (in hour) = Energy / Charge rate
= 14.4Whr/ 6 W
=2.4 hr

5 Conclusion

The automated solar grass trimming robot with tool exchange opens up new possibilities for automated lawn maintenance. Its autonomous capabilities reduce the need for manual labor, saving time and effort for homeowners and groundskeepers. The technology has the capacity to transform the way we maintain our outdoor spaces, providing efficient, eco-friendly, and versatile solutions for a greener future. The project demonstrates the potential of automated robotic systems powered by solar energy to revolutionize the lawn maintenance industry.

6 Acknowledgements

Any attempt at any level cannot be satisfactorily completed without the support and guidance of learned people. We owe to great many people whose constant support and motivation that has encouraged us to come up with this Project. We are greatly obliged to Dr. Rajeev N, Head of the Department, Department of Mechanical Engineering, for the encouragement and support that he has provided. We are immensely indebted to our very understanding Project guide, Arjun K S, Professor, Department of mechanical Engineering, for his constructive suggestions, guidance, and advice. Our Project in charge Dr. Aneesh Kumar P, Assistant Professor and Madhu Mohan, Professor, Department of Mechanical Engineering for his valuable guidance, support,and whole-hearted cooperation knowledgements and Reference heading should be left justified, bold, with the first letter capitalized but have no numbers. Text below continues as normal.

References

[1] Firas B. Ismail, Nizar F.O. Al-Muhsen, Fazreen A. Fuzi, A. Zukipli Design and Development of Smart Solar Grass Cutter Volume 09, Issue 2, December, 2019.

[2] Shaikh Mohd Sameer M.S.1, Venkatesh S. Thevar2, Suraj K. Patil3, Nitish S. Mangalpawar4, Pramod G. Design of Solar Grass Cutter Rahate Volume 08, Issue: 07, July 2021.

[3] Hemadri Chadalavada a, N. Bharath kumar b, P. Shaila srujan b, O. Lakshmi narayana b, C. Naveen kumar Solar Powered Semi-Automated Mutlipurpose Agriculture Machine,November 2020.

[4] Mr. Sudhir P1, Mr. Shibil PM2, Mr. Abdul Sufiyan Manaf3, Mr. Ebin Joseph4, Mr. Akmal Ahmed Solar Powered Automatic Grass Cutter Volume 05,Issue 07, July 2020.

[5] Aditya S. Rajmani, Appaji N. Gaonkar, Ajay Darak, Akshay Joshi Design and Fabrication of Hybrid Operating Grass Cutter Vol 8,Issue 05, May 2019.

Automated System for Cleaning of Solar Concentrator Dish

Abhinand P K[1], Akhil Dev[1], Alok J S[1], Aswanth P [1] and Sreeram P T[2]

[1] B.Tech Students, NSS College of Engineering, Palakkad, Kerala, India
[2]Asst. Professor, Department of Mechanical Engineering, NSS College of Engineering, Palakkad, Kerala, India

Abstract -

Renewable Energy is becoming increasingly important due to the resource shortage situation on the global level. Solar energy is one of the best and most efficient energy sources, and a solar concentrator dish focuses the solar energy arriving directly from the sun. However, shadow, snow, extremely high temperature, dust, dirt, bird dropping, sea salts, etc. can decelerate the efficiency. To increase power output, the panels must be cleaned. The project is divided into two parts: Cleaning System and Monitoring System. The cleaning task is completed according to the data received from the monitoring system, and a 3D printer mechanism is adopted for the X-Y axes movements of the cleaning system. The coded Arduino supports the movement of the nozzle throughout the dish and restricts the water to reach beyond the boundary of the concentrator dish.

Keywords -

Parabolic Solar Concentrator dish, Arduino, 3D Printer Mechanism, Renewable Energy

1 Introduction

Bright light and heat from the sun are regulated by a variety of technologies, including solar photovoltaic, solar thermal, and solar architectures. The use of solar photovoltaics is growing in popularity. It is sometimes asserted that after a few decades, it will unquestionably replace fossil fuels as the primary source of electricity. In the purpose of improving solar power plant efficiency, impressive research is being conducted in this area. Even though this approach focuses mostly on solar cell efficiency, there are several fundamental factors that influence the solar power output. Numerous studies have shown that maintaining and cleaning the panels still helps the plant's power output rise. The overall capacity of solar thermal energy increased by around 33.3 GW in 2018, bringing it up to about 480 GW, and this trend is expected to continue. The best locations for Concentrating Solar Power (CSP) facilities are often dusty and arid, which results in high rates of collector mirror soiling. For cleaning the mirrors, a typical 50 MW CSP power plant consumes 25,000,000 liters of water annually. The mirrors are washed on average once every two weeks, however sandstorms and other bad weather conditions may require more regular washing. Daily soiling causes a 0.5% reduction of reflectance in typical circumstances. A brand-new, flawless CSP mirror has a 97% reflection rating. Consequently, the mirror reflectivity will be less than 90%, and in some cases much lower, after two weeks without cleaning. The mechanism provided here works like a 3d printer for cleaning the dish. The stepper motors control the movement of the nozzle as a whole which is linked to the track joined in the frame that covers the concentrator dish. Arduino UNO is programmed for the proper movement of the water spraying throughout the dish.

2 The object of study (Model, Process, Device, Sample preparation etc.)

Fabricating two dishes, one with the cleaning system and the other without the cleaning system., the difference in the effectiveness of the heat collected is studied by comparing both values obtained from the two dishes after cleaning one of the dish. The feasibility of the machine is taken into account after the variation of heat at both dishes are studied.

2.1 Project Planning

- The materials in order to make the frame and the whole cleaning and sensing system are chosen and sorted to purchase
- Research regarding various existing technologies to clean the dishes and its feasibility was done.
- The innovative ideas from the surrounding world are analysed for a suitable option or solution for the cleaning of the dish economically.
- 3D printer movement is adopted for the nozzle and pressure variation in the flow.

2.2 Frame and track setting

- The GI pipe of 0.8 mm thickness is selected for the construction of frame after approximation of the load to the supported.
- The frame is welded and the sockets made of forex are used for the setting of track for easy periodic or unexpected maintenance.

- Threaded rod and steel rod as guideway are fixed by the nut connecting with the bearing attached plate for smooth movement of the system.
- The stepper motors are placed in appropriate positions for the X and Y axes movements.

2.3 Setting Arduino and coding

- The jumper wires are connected according to the code plan. The circuit is planned as to direct the movement of the nozzle throughout the dish to clean the whole dish. Two circuits are there , one which controls the X and Y axes movements of the nozzle and the other that connects all the sensors to the system. The 2 stepper switches are connected to draw back the nozzle carrier to the home position after the cleaning process.
- The code which is the brain of the whole system is to be uploaded to the Arduino uno board in order to perform action by the components in the system. Two circuits are to be coded to perform the total action.

3 Methods

The system is designed to clean parabolic solar concentrator dishes with water as the cleaningagent. It is a semi-automated mechanism that uses two-axis movement with the help of microcontrollers, Arduino and raspberry pi, and various data from sensors such as optical dustsensor, light dependent resistor, temperature sensor, etc. It is also equipped with a unit for filtering the used water for reusing purposes. By this method, we can reduce wastage of water and optimize the operational costs. Also, the system is scalable from small dishes with a diameter of 50 cm to big dishes.

The system is composed of six parts:

- Processing unit
- Supporting structure with Solar concentrator dish
- Sensing Unit
- Axis based movement unit
- Cleaning unit

3.1 Mechanism:

Processing unit is the brain of the system. It consists of microcontrollers and processors such as Arduino, Raspberry pi etc. The unit will analyze data from the sensing unit and send signalsto other units for enabling cleaning. It

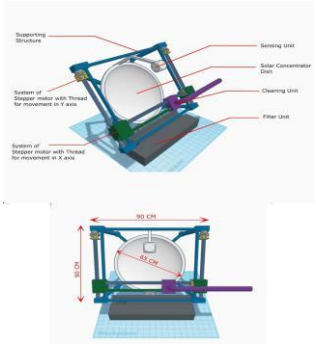

Figure 1. mechanism

also processes timings and frequencies of cleaning. Supporting structure for the system is mounted with the solar concentrator dish without affecting the sun tracker mobility. This structure provides the support for other units in the system including axis-based movement unit, cleaning unit and sensing unit. Sensing unit consists of various sensors such as optical dust sensor, light dependent resistor, temperature sensor, etc. It senses dust density in the air, temperature at the focal point, light level, and other factors. It helps the processing unit to determine the cleaning frequency and other variables. Axis based movement unit consists of stepper motors, threaded axes and its parallel axes. Thisunit will enable movement in both x and y axes, covering the plane in front of the solar concentrator dish with the help of microcontrollers. Cleaning unit consists of a pump, pipes, nozzle, and motors. It enables the cleaning of the dishwith water as cleaning agent. It can also provide various mechanisms such as sprinkling, unidirectional pumping, etc. for better efficiency.

3.2 Specification of the cleaning unit

There are a few equipment that will be very beneficial in properly gentle washing solar panels.On the one hand, a range of specialised rotating brushes are used to remove the soil from the panel. Any simple cleaning tool, like the one used on car windscreens, is also an option. However, employing water pressure tools like the Kercher High-Pressure Washer would let us to finish the job considerably more quickly while conserving a significant amount of water.

- The water from the nozzle blasts out their liquid at 1,000 to 1,200 PSI.
- For a pre-wash rinse, a 25 degree, or green, nozzle works well. This device shoots out a stronger spray
- The white or 40-degree nozzle works well for the typical wash. It is less intense andcovers a big region at once.

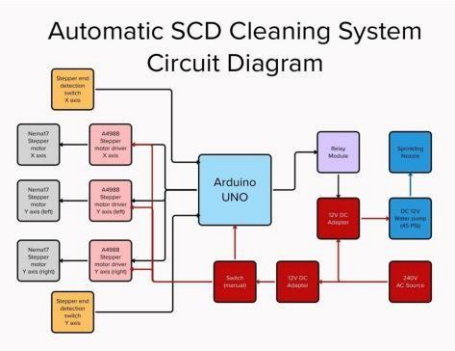

Figure 2. Circuit 1 : Here the code controls the working of stepper motors. The 3 stepper motors are controlled by the first circuit as the current from the adapter reaches the Arduino which is uploaded with the respective code, then through the A4988 motor driver to the stepper motors

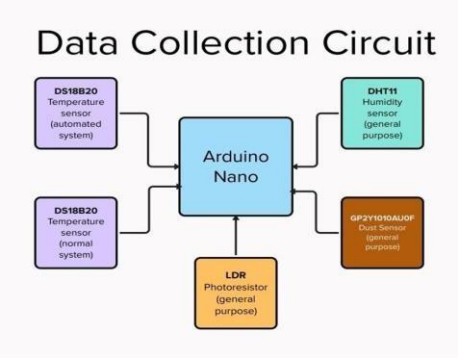

Figure 3. Circuit 2 : Here the sensors are being controlled by the code. The DS18B20 Waterproof Temperature sensor, DHT11 Humidity sensor, Optical dust sensor and LDR are being controlled by the second code developed

3.3 Testing

- Field testing : We can place the solar concentrator dish according to the seasonal changes. The direction of the dish to be placed is identified as south, since the location is in the Northern Hemisphere. The study says that change in seasons affect the lift in the placement of the dish.
- Dust selection : We had chosen wheat flour mixed with some of the curry powders that is available in the market and distributed evenly in the solar concentrator dish.The cleaning process was done very smoothly.
- Time slots for the test : Time slot selected according to the temperature,as the temperature sensor cannot withstand high temperature.So afternoon 3 30 PM TO 4 30 PM is selected
- Working of cleaning unit : Cleaning unit consists of 3 Nema 17 stepper motor, Arduino UNO, manual switch for power supply, stepper motor driver,3 lead screw,3 driving shafts,8mm journal bearings with couplings(4 nos),sprinkler for water spraying, circuit board,12 v AC to DC adapter. Firstly, the circuit board consists of an Arduino UNO module, stepper motor driver, manual switch and the connection to the aquarium pump and connection to the power source as well.12 v AC to DC adapter connected to the 220 v power source.
- Working of sensing unit : Sensing unit consists of temperature sensor, optical dust sensor, light intensity sensor, breadboard, Arduino UNO module, Arduino UNO cable and OTG to type c connector.

Firstly, the temperature sensor is fixed on the part where the focal point of the dish is located. The temperature sensor is connected to both the dish one with an automated system and other without it. The optical dust sensor, light intensity sensor and humidity sensor are fixed in a separate module along with the Arduino UNO to calculate the environmental conditions

We have taken afternoon 3 00 pm to 4 30 pm to take the readings, it is the suitable time as the temperature sensor does not get overheated. We had downloaded a software named Arduino UNO to take the readings from both the dishes. The OTG cable is connected to the computer to take the results. There is a slight change in settings to be updated in the software that need to do before connecting.

- Criteria for testing
  - with moisture

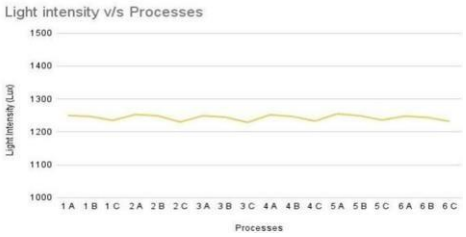

Figure 4. light intensity v/s processess

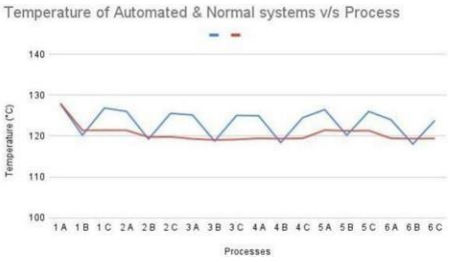

Figure 5. temperature v/s process

– without moisture

For each set of reading of reading the process is done by
A - Before dust
B - After dust
C - After cleaning

Results are taken in five consecutive days at regular intervals. Results and graphs are plotted accordingly.

4 Results and Discussion

Now we have taken the readings for evaluation, it is done by comparing the efficiency of both dishes. The dish without the Automated cleaning system has shown good result in the beginning but after four weeks its efficiency and amount of temperature absorption has decreased, as dust accumulated on it.The dish with the Automated cleaning system has shown good results in the beginning and slight variation at the end. Because cleaning has been done on a daily basis, there is only a slight change in the efficiency, and we have got good results.

5 Conclusion

This project emphasizes how much heat generation of the solar dish concentrator is affected by the external dusts, dirt, bird droppings and all. The regular cleaning of the mirrors could hold decelerating heat generation from the initial stage. It could maintain the fresh performance of the dish. A simple 3D printer movement replicating mechanism is used here. The human involvement in the process of cleaning gets just technical controlling work besides the manual cleaning. So that the system holds the global value due to this case. The more implanting of the solar dish concentrators could result in higher renewable energy production and the effective cleaning mechanism applied to each one could produce and retain the energy production capacity as that of the initial stage of the solar concentrator dish.

6 Acknowledgements

Any attempt at any level cannot be satisfactorily completed without the support and guidance of learned people. We owe to great many people whose constant support and motivation that has encouraged us to come up with this Project. We are greatly obliged to Dr. Rajeev N, Head of the Department, Department of Mechanical Engineering, for the encouragement and support that he has provided. We are immensely indebted to my very understanding Project guide, Sreeram P T, Assistant Professor, Department of Mechanical Engineering, for his constructive suggestions, guidance, and advice. Our project in charge Dr. Aneesh Kumar P, Assistant Professor and Madhu Mohan, Assistant Professor, Department of Mechanical Engineering for their valuable guidance, support, and wholehearted co-operation. We are thankful to our friends for their wholehearted co-operation during the preparation of the project. Last but not the least we wish our gratitude to our parents for their abundant blessing without which this project would not be successful.

References

[1] H., Andrea, Y., Pogrebnaya, T., Kichonge, B. (2019, December 20). Effect of Industrial Dust Deposition on Photovoltaic Module Performance: Experimental Measurements in the Tropical Region. Effect of Industrial Dust Deposition on Photovoltaic Module Performance: Experimental Measurements in the Tropical Region. https://doi.org/10.1155/2019/1892148

[2] Dacheng Li *, Marcus King, Mark Dooner, Songshan Guo, Jihong Wang"Study on the cleaning and cooling of solar photovoltaic panels using compressed airflow".

[3] PG Student, Dept. of Electronics Telecommunication, G.H.Raisoni Instituteof Engineering Technology, Pune, India . "Artificial Intelligence Based Solar Panel Cleaning Robot

Model for Agri-Food Dark Store Allocation in Metro Cities

Althaf Rasheed M [1], Kiran Kumar S [1], Nivedhidha Harikumar [1], Noufiya Siyad [1] and Dr. Regi Kumar V [2]

[1] BTech Student, College of Engineering Trivandrum, Kerala
[2] Professor, College of Engineering Trivandrum, Kerala

Abstract -

Dark stores are stores that have been repurposed to fulfil online orders in either the shortterm or long term, a new retail business model that began gaining attraction at the start of the pandemic. In agri-food supply chain, effective network distribution systems are essential and dark stores serve to reduce delivery and transit expensesas well as store acquisition prices. The deterministic multiinteger linear programming (MILP) model for facility allocation in the agricultural supply chain proposed in this article aims to promote 'express delivery' by converting current retail locations into 'dark stores' for online agri-food product sales in metro cities. The MILP model developed here is to achieve optimized distribution centre allocation, taking into account the elements like capacity of stores, delivery time, and distance from store to demand points. Two case studies were done in two cluster areas in the urban areas of Thiruvananthapuram, the capital metro city of Kerala and also verified the validity and practical applicability of the developed mathematical model. The result obtained from the developed model was analyzed using CPLEX software and validated with AnyLogistix. The scalable version of the developed mathematical model is recommended for real-world scenarios by taking into account the constraints. The generalized MILP model will enable effective allocation of dark stores by meeting all specified objectives of the scenario.

Keywords -

Dark Stores, Express delivery, On-demand Supply, Agri-food Supply Chain

1 Introduction

The agri-food supply chain faces a number of difficulties dueto the rising demand for fresh, high-quality food, including sea- sonality, perishability, and supply chain inefficiencies. Utiliz- ing dark stores, which are fulfilment facilities created solely to fulfil online orders, is one approach to overcome these diffi- culties. A dark storage allocation model for the agri-food sup- ply chain is what this article wants to create. According to demand, closeness to customers, and delivery time, the model will aid in maximizing the allocation of the demand points to the right dark store. The model's goal is to minimize supply chain costs and delivery time while ensuring that the appropri-ate products are available at the appropriate time and location to satisfy client demand. The goal of this article is to supply high-quality goods in an express delivery mode at reasonable delivery costs. The increasing customer preference for fresh and high-quality produce is one of the main reasons why this article is important. Customers now have higher expectations for the quality and freshness of vegetables and fruits as they aremore aware of the value of eating healthily and locally. The necessity of effective supply chain management is another fac- tor that contributes to relevance. This research also explores how the agri-food supply chain affects the environment. The article helps to reduce food miles and carbon emissions by re- ducing transportation distances and adopting a localized strat- egy through dark store allocation. our initiative attempts to cre-ate a dark store allocation model that converts retail stores into strategically placed fulfillment hubs, revolutionizing the agrifood supply chain. To satisfy customer expectations and help the agri-food sector expand, we work to reduce delivery times and increase supply chain effectiveness.

2 Literature Review

After exploring research articles , reports, and other sources, we were able to examine various aspects of agri-food supply chain. By analysing the available literature, his review aims to identify key trends , challenges, and opportunities in the agrifood industry which is experiencing a significant shift in consumer behavior, with a growing demand for e-commerce and express delivery of fresh products . This section examines the role of dark stores in agri-food supply chains. It explores the unique characteristics and challenges associated with the delivery of fresh agri-food products, highlighting the need for dedicated fulfillment centers. The review discusses the advantages and potential drawbacks of dark stores, emphasizing their potential to improve delivery speed, reduce transportation costs, and enhance customer satisfaction. The efficient delivery of fresh agri-food products is a growing concern in the age of e-commerce. Dark stores, dedicated fulfill-

ment centers for online orders, offer a potential solution for expedited delivery. This consolidated literature review examines various papers, reports, and research studies related to optimizing the allocation of dark stores to enable quick delivery of fresh agri-food products. Researchers have emphasized the importance of strategic dark store location selection. Smith et al. propose a mathematical model that considers factors such as demand density, transportation costs, and proximity to suppliers. Their study demonstrates that the strategic placement of dark stores can significantly reduce delivery time and enhance overall operational efficiency. Johnson and Davis(20XX) delve into the challenges specific to fresh food delivery through dark stores. They introduce a multi-objective optimization approach that accounts for product freshness, delivery time, and storagecapacity. Their findings suggest that an optimal dark store network design can improve the quality and speed of fresh food delivery. In conclusion, this consolidated literature review highlights the importance of strategic dark store location selection, accurate demand forecasting, last-mile delivery optimization, and technological innovations for achieving quick delivery of fresh agri-food products. By considering these factors and incorporating them into dark store network design, companies can meet the evolving demands of the market while ensuring the timely delivery of high-quality fresh agri-food products. Further research and empirical studies are needed to validate and expand upon these findings in real-world scenarios.

2.1 Research Gap

Despite the existing body of literature addressing the optimization of dark store allocation for quick delivery of fresh agri-food products, a notable research gap exists in the domain. One significant area for further investigation is the integration of sustainable practices into dark store operations. While studies have focused on operational efficiency and delivery speed, there is limited research on how to minimize the environmental impact associated with dark store networks. Sustainable considerations such as energy consumption, waste management, and carbon emissions are increasingly important in the agrifood sector. Exploring strategies to optimize dark store allocation while reducing the ecological footprint could contribute to a more environmentally responsible and sustainable supply chain. Future research endeavors should therefore aim to bridge this research gap by exploring and proposing innovative approaches that balance operational efficiency with sustainabilitygoals in dark store allocation for fresh agri-food product delivery

3 Methodology

As discussed in the previoussections, for the allocation of location, we use the concept of dark stores. We adopt the method of developing a mathematical model for the optimized allocation of dark stores for fulfilling our goal.

3.1 Descriptive Management Framework

This section presents a framework for efficient order management, divided into four phases: order response period, order picking time, order packing time, and order hand-over time. The system assigns orders to corresponding dark stores based on location, product availability, and proximity to the delivery point. Retailers are chosen based on store capacity, market proximity, traffic intensity, transportation facilities, and regional demand. Store staff pick and pack items according to orders, and orders are delivered within 30 minutes of order response time.

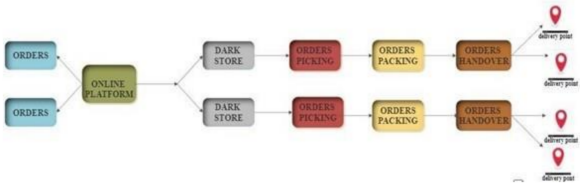

Figure 1. Descriptive Framework for Order Delivery System

3.2 Data Collection

A survey questionnaire was circulated on various online platforms, obtaining 390 responses. The survey covered aspects of online grocery shopping, including product quality, delivery time, cost, ease of use, time spent, local retailer preferences, and sustainable packaging. The results were analyzed using statistical software to identify trends and patterns. The survey provided valuable insightsinto consumer preferences and thoughts on online grocery shopping, aiding in decision-making and developing strategies for improving the experience. Secondary data included demand points, dark stores, warehouses, and travel distance. The survey aimed to gather detailed data and opinions from various stakeholders, including young people, to understand the article's impact, goals, objectives, target audience, and stakeholders. The survey was designed to cover multiple-choice and scale-based questions, allowing respondents to express their thoughts, preferences, and perceptions. The survey helped evaluate the article's goals and objectives, understand stakeholder impact, and identify areas for development. The results helped close the communication gap between the article team and stakeholders, fostering a collaborative approach

and ensuring stakeholder opinions were heard throughout the article's life cycle. The survey findings acted as an invaluable feed- back mechanism, enabling proactive planning to increase the article's effectiveness. The findings enabled the development of specialized interventions, resource allocation, and improved methods to maximize impact. The survey also enabled iteration and modification of the article, driving continual progress. The response analysis helps to enable the relationship between var-ious factors and their correlation. The survey reveals that customers prioritize quality, sustainability, reliable partners, and on-time delivery when shopping for groceries online. However, balancing these aspects with price can be challenging. Consumers are price-sensitive, and the online grocery platform must prioritize these factors to improve customer experience and foster adoption. To meet customer requests and expectations, the platform should offer highquality products, reliable delivery options, and a reputation for honesty and trust. It should also emphasize sustainability by providing environmentally friendly packaging, regional and organic goods, and sustainable farming methods. By adhering to sustainability values, the platform can attract environmentally conscious customers. A small portion of consumers currently shop online, but if the platform offers high-quality products at reasonable prices, adoption may expand.

4 Model Developed

Here deterministic Multi integer linear programming is used for modelling. In this model, we assume that the demand of each customer segment is a known parameter, lead time is considered to be zero, a single type of vehicle is used (Twowheelers), and only perishable goods are considered. Our proposed mathematical model is as follows:

Indices:

i = Indicates the dark store.

j = indices the demand point.

w = indicates the warehouse.

Parameters:

D_{ij} = distance between the data store and demand point.

T_{ij} = delivery time from the data store to demand point.

d_{ij} = The demand from location j to the data store.

C_j = The capacity of each data store.

wd_{wi} = distance between ware house and data store.

M_j = Maximum dark store required data store

R = Required delivery time from location dark store to demand point.

Decision variables:

$Assign_{ij}$ = 1 , If data store is assigned to location i, otherwise0.

$Open_i$ = 1 , If a data store is open, otherwise0.

Objective function:

Minimize: $\Sigma_i\Sigma_j D_{ij} * di_j * Assign_{ij} + \Sigma_w\Sigma_i Wd_{wi} * Open_i$

Subject to:

1. $\Sigma_i Assign_{ij} = 1, \forall i \in I$
2. $\Sigma_i Open_i \leq M$
3. $Assign_{ij} \leq Open_i \forall i \in I, j \in J$
4. $Assign_{ij} * T_{ij} \leq R \forall i \in I, jJ$
5. $\Sigma_i\Sigma_j \forall i \in I, jJ$
6. $Assign_{ij} \in 0, 1 \forall i \in I, j \in J$
7. $Open_i \in 0, 1 \forall i \in I$
8. $D_{ij} \geq 0 \forall i \in I, j \in J$
9. $T_{ij} \geq 0 \forall i \in I, j \in J$
10. $d_j \geq 0 \forall j \in J$
11. $Wd_{wi} \geq 0 \forall w \in W, i \in I$

Here our objective is to assign demand points to darkstore by minimizing total distance and time. It is subjected to certain constraints: 1) each demand point should be assigned exactly to one dark store 2) The number of dark store that should be opened should be less than the maximum darkstore that required. 3) Only the darkstore that opened should be assigned to the demand points. 4) shipment time should be less than the required delivery time. 5) demand should be less than the capacity of the darkstore.

5 Case Study

Inoder to ensure real life validity and scalability of model, two case studies were conducted by considering two clusters in Trivandrum region.

5.1 Cluster 1 (Sreekaryam Cluster)

The clusters optimize store allocation based on population density and proximity to demand points. The area is highly populated, with 18,000 people per square kilometer and nearly 100,000 residences. The region is home to academic institutions like the Government Medical College, the College of Engineering, and the University of Kerala. The busiest travel times are 7am to 9am and 5pm to 7pm. Factors affecting traffic include numerous marketplaces, educational institutions, and hospitals.

5.1.1 Data Collection

The data collected includes store locations, demand locations, distance, time, store capacity, and vegetable demand. Out of 23 stores, 10 are available, with varying capacities. Most stores closed due to low sales. The goal is to identify the proper allocation of stores using a developed model, considering the total capacity of all stores in a cluster to meet overall demand.

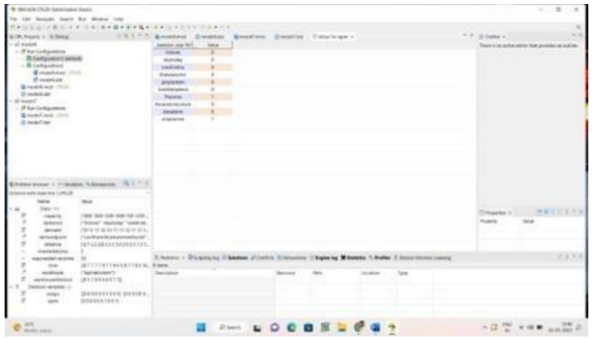

Figure 2. Allocated Stores using Cplex in Cluster 1

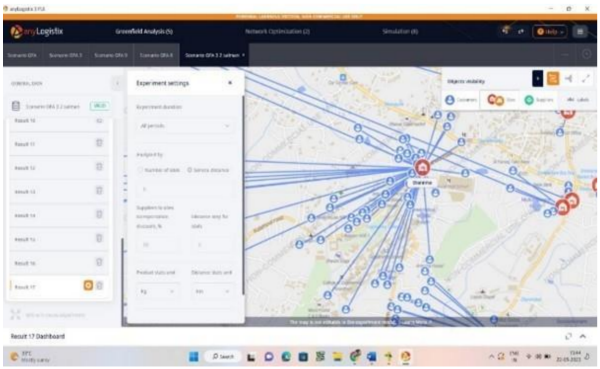

Figure 3. Allocation in AnyLogistix for Cluster 1

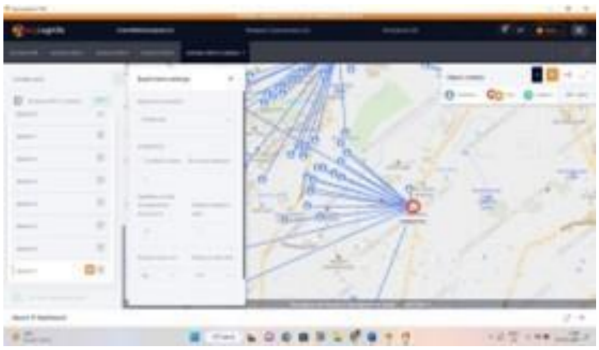

Figure 4. Allocation in AnyLogistix for Cluster 1

5.1.2 Validation

By using the data that we collected, the model has been validated by using two software; CPLEX and ANYLOGISTIX. The result obtained from those are compared and the efficient stores are identified along with their proper assignation of demand points. The stores that can deliver maximum orders within minimum time are taken. Any Logistix software utilizes GIS to visualize and analyze spatial data, allowing users to map demand points and store potential locations. It also enables resource constraints, such as facility capacity limitations, and provides scenario analysis, including Green Field Analysis (GFA) for distribution circles.CPLEX uses Optimisation Programming Language (OPL) to develop a model by incorporating data from various sources, such as potential locations, demand, capacity, demand, distance, and time, into the code. The result obtained from CPLEX is compared with the solution provided by ANYLOGISTIX.

5.2 Cluster 2 (Kazhakkottam Cluster)

Conducting case study 2 is crucial for acquiring residential points and confirming the utility and generalizability of a model across various clusters or circumstances. By analyzing the findings from multiple case studies, researchers can detect trends, similarities, and differences, allowing for a more thorough understanding of the model's effectiveness and adaptability to different situations. Kazhakkoottam, a rapidly expanding suburb in Thiruvananthapuram, is home to the Technopark, India's largest IT park, and has excellent road and rail connections. The area is home to around 100,000 people and has three markets: Santhi Nagar Market, Technopark Market, and Kazhakoottam Market. Kazhakkoottam's online grocery sector is rapidly expanding, with 1 million orders placed in 2022 and 2 million similarities, and differences, allowing for a more thorough understanding of the model's effectiveness and adaptability to different situations. Kazhakkoottam, a rapidly expanding suburb in Thiruvananthapuram, is home to the Technopark, India's largest IT park, and has excellent road and rail connections. The area is home to around 100,000 people and has three markets: Santhi Nagar Market, Technopark Market, and Kazhakoottam Market. Kazhakkoottam's online grocery sector is rapidly expanding, with 1 million orders placed in 2022 and 2 million by 2025. Popular online grocers include BigBasket, Grofers, and Amazon Fresh. Payment options include credit cards, debit cards, net banking, and cash on delivery. Home delivery and store pickup are the most common delivery choices.

5.2.1 Data Collection

The cluster covers 5.7 km from Vettuthura to Kaniyapuram and collects data on distance and time from stores to demand points using Google Maps. The capacity of stores is measured in kilograms, and the maximum daily capacity is 100 kg. The data is analyzed and sorted, and the developed model is validated using appropriate software. The figure below shows the collected data in cluster 2 using various sources.

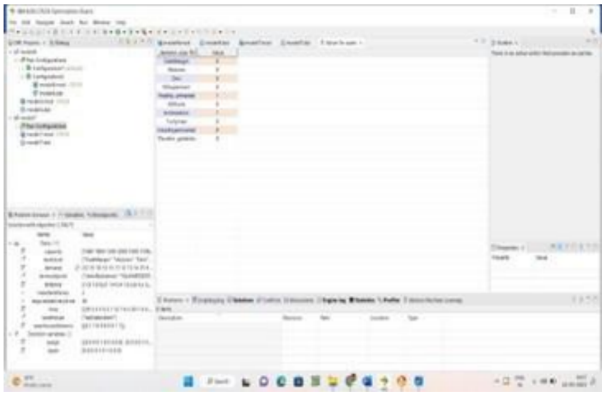

Figure 5. Allocated Stores using Cplex in Cluster 2

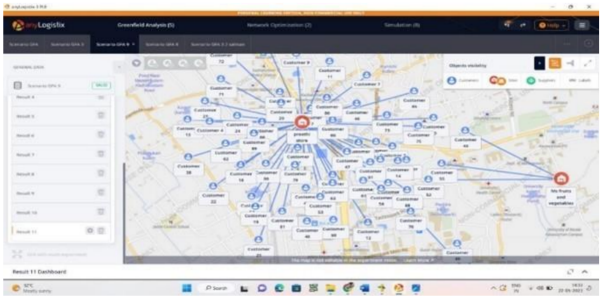

Figure 6. Allocation in AnyLogistix for Cluster 2

Figure 7.

5.2.2 Validation

Validation process is same as that of cluster 1 and is mentioned in section 5.1.2

5.3 Results and Discussions

This section analyzes case studies and inferences from comparing two softwares, determining the maximum store allocation for each cluster based on criteria.

5.4 Cluster 1 (Sreekaryam Cluster)

Using CPLEX, it obtain a result comprising of two stores allotted to Sreekaryam cluster. As earlier mentioned, the decision variable are binary, it shows 1 if it is allocated and 0 if it is rejected. In the given figure 2, the stores that show 1 to particular demand points shows that it is assigned to that corresponding demand points.AnylogistiX replicated a scenario, preserving 31 demand points for Annapurna store and allocating 39 to Thanima store as shown in figures 3 and 4. The inconsistent results were due to the use of displacement and distance parameters, and the manual mapping of store and demand points.

5.5 Cluster 2 (Kazhakkoottam Cluster)

CPLEX efficiently allocates stores in Kazhakkoottam cluster using mathematical models and optimization techniques. Two stores named Preethi and Krishna are chosen due to their capacity, proximity to demand points, and proximity to the ware- house. The figure 5 shows the allocated stores in Cplex. AnylogistiX simulated a scenario with 44 demand points allocated to Preethi store and 47 to Krishna store as shown in figures 6 and 7, resulting in disparities due to considering distance and displacement factors. The figure below shows the result from Any Logistx. The CPLEX program allocated 48 demand points to Preethi and 43 to Krishna stores, using an optimization algorithm to reduce time and distance between them. The difference in assigning demand points from the above software result are due to manual mapping in Any Logitix and data driven approach in CPLEX.

6 Conclusion

This paper presents an optimized mathematical model for online agri-food distribution and delivery, focusing on the alloca-tion of facilities for dark stores. The model is applied to hiring existing retail stores as dark stores and is verified using simula-tion with ANYLOGISTIX software. The article demonstrates how technology-driven methods can increase supply chain ef- fectiveness, save costs, and boost customer satisfaction. By us- ing a dark store for online delivery, businesses can streamline operations, reduce costs, and provide fast and reliable service to customers. One advantage of using a dark store is the abil- ity to better control the storage and handling of their products. By centralized fulfillment in a dedicated facility, businesses can ensure their products are stored and handled in a way that maxi- mizes freshness and quality. Additionally, customers can enjoythe convenience of having their products delivered directly to their door, especially for those living in rural or hard-to-reach areas or those with busy schedules. The article emphasizes the value of data integration and coordination among various players in the agri-food distribution system. By merging real- time data from multiple sources and integrating with

current systems, the model offers a promising solution for optimizing dark store allocation in express delivery and has significant im- plications for the future of logistics. The conclusions and sug- gestions from this article can be used as a starting point for future studies and applications in online agri-food delivery. 7.1. Future Scope of Work The future scope of this work involves instead of purchasing goods from warehouse, collecting and stocking products into stores, purchasing the goods directly from primary produc- ers can eliminate the intervention of supply vendors and multi- ple intermediaries in the network. This helps to deliver the freshproducts to customer within a minimal time. By integrating ad- vanced technologies and logistics techniques with the model can give insights regarding optimize crop planning, predicting demand patterns, and identify potential areas of store.

Acknowledgements

First and foremost, we thank the Almighty, without whose blessings we would have never completed our work. We ex- 7 press our deep gratitude to faculty guide and Head of Department, Department of Mechanical Engineering, College of Engineering, whose encouragement was a great source of inspiration. Our sincere gratitude is extended to all other teachers in the Department ofMechanical Engineering, and all our friends. We extend our heartfelt gratitude to our families, whose continued support andinspiration helped us accomplish this task.

References

[1] Bashir, R., Mehboob, I., Bhatti, W. K. (2015)," Effects of online shopping trends on consumer buying Behaviour: an empirical study of Pakistan", Journal of Management and Research, 2(2), 1-25.

[2] Meuter, M. L., Ostrom, A. L., Bitner, M. J., Roundtree, R. (2003)," The influence of technology anxiety on consumer use and experiences with self-service technologies", Journal of Business Research, 56(11), 899-906.

[3] Yeo, V. C. S., Goh, S. K., Rezaei, S. (2017), "Consumer experiences, attitude and behavioural intention toward online food delivery (OFD) services", Journal of Retailing and Consumer Services, 35, 150-162.

[4] Sultan, M. U., Uddin, M. (2011)," Consumers' Attitude towards Online Shopping: Factors influencing Gotland consumers to shop online", Unpublished Master's Thesis, Gotland University.

[5] Lin, Carrie. (2014)," Solving a Location, Allocation, and Capacity Planning Problem with Dynamic Demand and Response Time Service Level". Mathematical Problems in Engineering. 2014. 1-25. 10.1155/2014/492340.

[6] Pina-Pardo, Juan C. Moreno, Matheo Barros, Miguel Faria, Alexandre Winkenbach, Matthias Janjevic, Milena (2022)" Design of a two-echelon last-mile delivery model", EURO Journal on Transportation and Logistics. 11. 100079.10.1016/j.ejtl.2022.100079.

[7] H. Grillo, M.M.E. Alemany, A. Ortiz, V.S. FuertesMiquel, "Mathematical modelling of the order-promising process for fruit supply chains considering the perishability and subtypes of products", Applied Mathematical Modelling, 2017

[8] U. Okongwu, M. Lauras, L. Dupont, V. Humez," A decision support system for optimizing the order fulfilment process Prod. Plan. Control", 23 (8) (2011), pp. 581598, 10.1080/09537287.2011.566230

[9] P. Amorim, H.O. Gunther, B. Almada-Lobo," Multiobjective integrated production and distribution planning of perishable products", Int. J. Prod. Econ., 138 (1) (2012), pp. 89-101, 10.1016/j.ijpe.2012.03.005

[10] M. O nal, H.E. Romeijn, A. Sapra, W. Van den Heuvel," The economic lot-sizing problem with perishable items and consumption order preference", Eur. J. Oper. Res., 244 (3) (2015), pp. 881-891, 10.1016/j.ejor.2015.02.02S.S. Ali, J. Madaan, Chan F.T., S. Kannan, "Inventory management of perishable products: a time decay linked logistic approach", Int. J. Prod. Res., 51 (13) (2013), pp. 3864-3879, 10.1080/00207543.2012.752587

[11] A. Nagurney, A.H. Masoumi, M. Yu," Supply chain network operations management of a blood banking system with cost and risk minimization Comput", Manag. Sci., 9 (2) (2012), pp. 205-231, 10.1007/s10287-011-0133-z

[12] Melo M.T., Nickel S., Saldanha-da-Gama F," Facility location and supply chain management – a review", Eur. J. Oper. Res., 196 (2009), pp. 401-412

[13] Pasandideh, S. H. R., Niaki, S. T. A., Hajipour V, "A multi-objective facility location model with batch arrivals: Two parameter-tuned meta-heuristic algorithms", Journal of Intelligent Manufacturing, 24(2), 331–348.

[14] Bai, X., Wang, S., Sun, J., Yu, Y. (2018)." Research on express delivery mode selection and optimization". Applied Sciences, 8(9), 1545.

[15] Lu, C., Lu, C. (2020). "The impact of emerging technologies on express delivery service quality". Transportation Research Part E: Logistics and Transportation Review, 137, 101926.

[16] Lu, C., Lu, C. (2019). "Sustainable express delivery: A review of emerging technologies and practices". Sustainability, 11(7), 2009.

[17] Wang, H., Xu, K., Li, S., Cao, Q. (2020)." Collaborative transportation planning for express delivery considering customer demands and operational costs". Transportation Research Part E: Logistics and Transportation Review, 143, 102044

[18] Meng, Q., Wang, Q. (2015). "A study on the interplay between integrated express delivery and e-commerce in China". Transportation Research Part E: Logistics and Transportation Review, 77, 61-76.

[19] Beier, F., Vierhaus, I. (Eds.). (2019). "Agricultural supply chains, growth and poverty in sub-Saharan Africa: Market structure, farm constraints and grassroot institutions". Palgrave Macmillan.

[20] Hattum-Janssen, N. V., Semeijn, J. (2016). "Supply chain collaboration in the Dutch fruit and vegetable sector: An exploratory study". Journal of Transport Geography, 54, 132-141.

[21] Hwang, H., Kim, D., Na, S. (2021). Optimal location of perishable goods distribution center considering perishable inventory and quality decay. Applied Sciences, 11(6), 2734.

[22] Fei, R., Oguz, C. (2019). "Coordination mechanism for perishable agricultural products supply chain considering price-dependent demand". International Journal of Production Research, 57(4), 990-1007

Experimental Study of Evacuated Tube Heat Pipe Solar Water Heater

Abhinav N S[1], Akshay C Suresh[1], Arun Roy [1], Jayanath J B [1] Dr. Sajeesh P [2] and Dr. Suresh P R [3]

[1] Department of Mechanical Engineering, NSS College of Engineering, Palakkad, Kerala, India
[2] Asst. Professor, Department of Mechanical Engineering, NSS College of Engineering, Palakkad, Kerala, India
[3] Professor, Department of Mechanical Engineering, NSS College of Engineering, Palakkad, Kerala, India

Abstract -

Heat pipe solar water heaters which have proved to be much more efficient than conventional solar water heaters have paved the way for a more energy-efficient future for solar water heaters. The present project aims to perform an experimental investigation of introducing a heat- transferring oil inside the evacuated tube around the heat pipe to increase its contact and storage of heat thereby increasing its efficiency and nocturnal working hours. For conducting an experiment, the experimental setup is available. The experimental results of the project model are compared and checked with the base model. An increase in the efficiency of the system during nocturnal working hours is found and the effective system which gives that percentage increase is identified.

Keywords -

Evacuated Tube, Thermal Oil, Heat Pip, Solar Water Heater

1 Introduction

In the 21st century with population increase, the demand for resources is also increasing, and with the limited conventional resources, it is insufficient to meet the demands of everyone. Research and development in areas of science and technology have enabled mankind to explore new energy resources, which are available all around us in abundance in various energy forms. The major non-conventional energy resources are solar, wind, tidal, and geothermal energy whereas the conventional source of energy is oil, coal, etc. The increase in greenhouse gases makes it necessary to utilize renewable energy sources such as solar energy. Generally, the usage of solar heaters helps in reducing the annual energy costs when compared with electric water heaters or geysers. Since they do not need any additional energy source other than sunlight, they are ideal for heating water for various applications. The most important component of any solar system is the solar collector. Among various types of solar collectors, evacuated tube solar collector with heat pipe (ETCHP) has attracted much attention especially for the application in solar water heating systems (SWHs). And many experimental reviews have been carried out using heat pipe solar water heating systems and it is observed that it has major drawbacks such as poor heat transfer due to improper contact and its inability to maintain heat for a long time after sunset. To overcome this many other studies have been carried out such as by using different working fluid in evacuated tube heat pipe, using oil and foamed metal and by using phase change material (PCM).

2 The object of the study

The objective of the work is as follows:

•To develop an effective and efficient model of Evacuated tube heat pipe(ETHP) solar collector.
• Validate the model by conducting the experiment.
• The ETHP is then modified to overcome poor heat transfer due to improper contact and its inability to maintain heat for a long time after sunset.
• The above model is modified by adding thermal oil inside the evacuated tube.
• Temperature sensors were introduced inside the evacuated tube to identify the changes occurring inside the tube.
• Also, the experiment was conducted at different oil levels with varying water flow rates for a full day to find the changes occurring in the inner tubes of evacuated tube and to study the temperature change that occurs in the outlet water.
• Evaluate the effect of adding oil and inserting temperature sensor at different oil levels at varying water levels and compare the results with conventional ETHP collector.

3 Methods

Experimental study of evacuated tube heat pipe solar water heater is conducted on a custom-made experimental setup.

3.1 Experimental Setup

The experiment is carried out with a heat pipe evacuated tube solar water heater manufactured by V-Guard Industries Ltd. With a capacity of 100 liters/day. The schematic

layout of the experimental setup is shown in Fig.1. The setup consists of evacuated tube solar water heater, tanks, pipelines and measuring devices. The heater tank is supplied with water from the main tank with a capacity of 1000L. A secondary tank with 250L capacity is provided above the main tank which maintains a constant head of water in the main tank as it supplies water to the heater. The water from the heater tank is collected at the heater outlet and the flow is regulated with the help of a control valve.

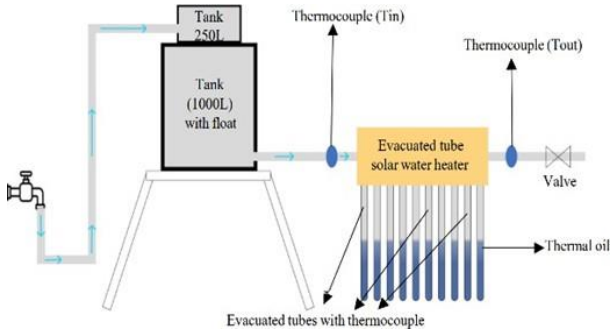

Figure 1. Schematic of Experimental Setup

The temperature inside the evacuated tube heat pipe, inlet and outlet water temperatures are measured using ds18b20 temperature sensor and the measured temperature is logged with the help of a data logger developed with Arduino UNO (The program code is provided in the appendix). The board is programmed to measure and log the temperature every 15 minutes. The temperature sensors are calibrated by standard calibration procedures by comparing the values with a standard Tank 250L Thermocouple (Tin) Thermocouple (Tout) Tank (1000L) with float Evacuated tube solar water heater Valve Thermal oil 21 thermometer.

3.2 Experimental Procedure

3.2.1 Trail 1

The experiment is carried out at three different flow rates of 110mL/min, 130mL/min and 150mL/min. Made holes in the alternate bushes of the solar water heater tube and inserted a thermocouple setup for taking the temperature readings. Developed a new Arduino setup for taking the temperature reading automatically. The parameters measured are inlet temperature, outlet temperature, temperature inside the evacuated tube heat pipes and solar irradiance. The readings were taken at 15 minutes intervals. For each flow rate the measurement and optimization of sensible heat storage in evacuated tube solar water heater is found out, thermal oil (Mobil-Therm 605) is introduced into the evacuated tube. The total amount of oil that can be filled in the evacuated glass tube is 2.0568 kg. The oil levels is varied, ie, from 0wt% of oil (no oil), 16.67wt% of oil (400mL), 50wt% of oil (1200Ml), and finally 100wt% of oil (2400mL), for the different levels of oil 3 sets of reading with flow rates 110mL/min, 130mL/min and 150mL/min respectively are taken to find the optimum levels at which the system gives the best performance. From the readings obtained, the graph is plotted. The experimental setup is shown in Fig 2&3.

The solar irradiance was measured using the LX-107 solar power meter manufactured by HTC as shown in Figure 3.4. The range of the device varies from 1-2000w/m .

3.2.2 Trail 2

From the trail 1 the characteristic of the system is known up to 7.00 PM. But the characteristic of the system after 7.00 PM is important to study the efficiency of the system during nighttime. Hence the data logger is made to record the cold-water temperature and hot water temperature for 24 hours. Solar flux is recorded for the frequency of 1 hour from 6.00 AM to 7.00 PM. But beyond 7.00 PM the solar flux is negligible, hence the flux is not recorded. From the data recorded in the logger, it is copied in the computer and graph is plotted.

Figure 2. Front view of Experimental Setup

Figure 3. Side view of Experimental Setup

3.3 Methodology

The equipment and components for the experimental setup are procured and the experimental setup is completed. The experiment is to be carried out with varying oil levels to find the best out characteristics The oil used is Mobiltherm-605. This oil was chosen since it is used in most of the industries for heat transfer. Mobiltherm heat transfer oils have good heat transfer efficiency, and their viscosities are such that they can be pumped readily at both start-up and operating temperatures. They demonstrate specific heat and thermal conductivities that provide more rapid heat dissipation. In table 1 containing all the properties of Mobiltherm-605 is shown below which helps in understanding why this thermal oil was chosen for increasing thermal efficiency of solar collector.

Table 1. Properties of Mobiltherm 605

Properties	Mobiltherm 605
Density @15ºC, Kg/l	0.857
Flash point, ºC	230
Kinematic viscosity @100ºC, mm²/s	5.4
Kinematic viscosity @40ºC, mm²/s	30.4
Pour point, ºC	-12

The efficiency of the system is calculated by,

$$\mu = \dot{m} * cp * [(Tout - Tin) / q * A] \quad (1)$$

$$\dot{m} = \dot{v}\rho \quad (2)$$

Where, $\dot{\mathbf{m}}$ = mass flow rate of water (kg/s), $\dot{\mathbf{v}}$ = volume flow rate (m3 /s), Cp is the specific heat of water = 4.182 J/g°C = 4182 J/kg °C, q solar heat flux (W/m2) and A= area (m2) Weight percentage of oil is calculated by,

$$wt\% = (\rho_0 * 9.81 * v_0) / (\rho_0 * 9.81 * v_0 t) \quad (3)$$

Where, wt% = weight % of oil, ρ_0 = density of oil (kg/m3), v_0 = volume of oil added (mL), $v_0 t$ = total volume of oil added (mL)

4 Results and Discussion

The experiment was conducted to analyze variations in the output temperatures and to find the increase in the percentage of outlet temperature as compared to outlet temperature of the solar water heater without thermal oil inside the evacuated tube. optimum oil level in evacuated tube solar water heaters using thermal oil. So, to find that, the inlet temperature, outlet temperature, and temperature inside the evacuated tube are noted.

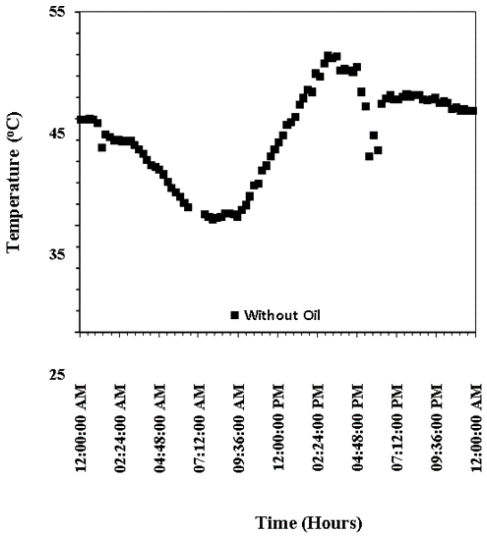

Figure 4. Outlet temperature vs Time graph for without oil

The first experiment was done with no thermal oil in the system and for the flow rate of 110mL/min, the variations in the outlet temperature due to available solar flux is recorded. All the readings are taken from morning 6 AM to the morning 6 AM the next day so completing 24 hours.

For the easiness of understanding the 12M to 6 AM part of the second day is plotted first. So, obtaining a graph of 12 AM to 11.59 PM. Here the reading was started on 30-04-2023 from 7.12 AM. From the graph, we can see that it has the least outlet temperature in the morning.

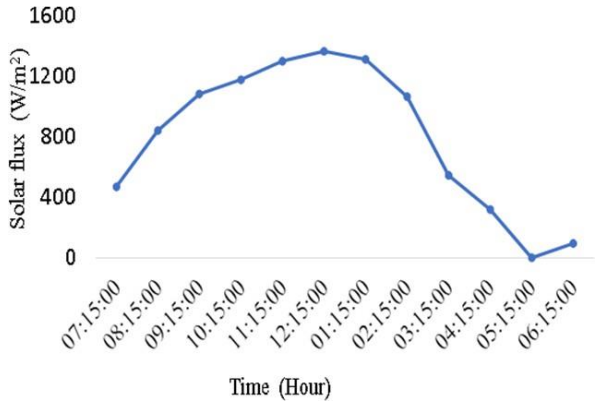

Figure 5. Solar flux vs time graph

Even though the temperature increases rapidly with the increase in flux, the temperature also drops very quickly if there is no solar flux. This can be seen from the slight rainy time 5 PM to 6 PM in the graph. Here the outlet temperature dropped quickly when there is no sun. So, it is also a reason to use thermal oil inside the solar water heater tubes that is to avoid these sudden drops in the outlet temperature. The temperature drops quickly in the absence of solar radiation in the nighttime as we can see in the graph. The graph between solar flux and time on the day 30-04- 2023 is shown in Fig 5. So, from the above graph Solar flux vs Time, we can see that the flux reading is very low in the morning time and it increases with the time reaching noon. Solar radiation reaches its peak value at noon in the range of 12 PM to 1 PM. Then The flux comes down as the solar radiation decreases. From the graph, we can see that the solar flux is about 0 W/M2 at 5 PM. It is due to the rainy atmosphere. So, during cloudy times, the flux comes down to zero and it suddenly affects the solar water heater also.

The working fluid gets heated from inside the vacuum tube, and it transfers heat towards the water. So, the outlet temperature depends on the temperature inside the tubes. The variation in the temperature inside the tube of the solar water heater without using thermal oil is plotted using the graph of Temperature versus Time shown in Fig 6. So, as we know that the temperature inside the tube influence the outlet temperature, because as the temperature inside the tube increases the working fluid get heated and it transfer the heat to water, thus resulting in the high-temperature water in the outlet. So, from the graph, when the solar

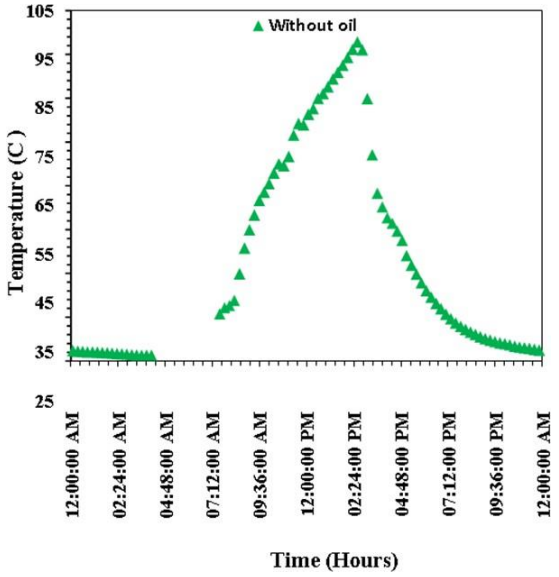

Figure 6. Temperature inside tube vs Time graph for without oil

radiation is very high; we can see the temperature inside the tube is also high and when the solar flux decreases the temperature inside the tube also decreases. From the morning to noon the solar flux increases and so the temperature inside the tube also increases. But as the time passes from noon to evening the solar flux decreases resulting in the decrease of the temperature inside the tube. These factors can be analyzed from the graphs. The advantage

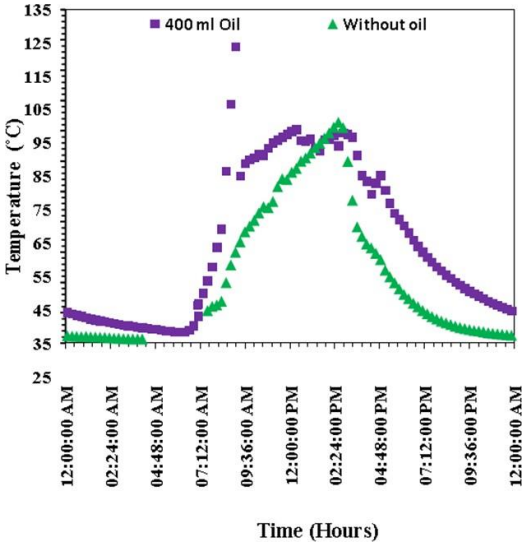

Figure 7. Temperature vs Time graph for with and without oil levels inside

of using thermal oil inside the evacuated tube helps to produce a more consistent outlet temperature during the day and nighttime. The variation in the temperature inside the tubes of the solar water heaters while using thermal oil and without using thermal oil are plotted using the graph of Temperature versus Time is shown in Fig.7 From the graph, the tube with oil has more temperature in the morning and other less solar flux timings because the oil can hold the heat for a longer time. The oil stores the heat and transfers the heat consistently to the water thereby heating it even the solar radiation is low. The temperature in the tube without oil is increasing rapidly during the daytime compared to the tubes with oil. This is because there is a time required to heat up the oil and then transfer that heat to the water through the working fluid. But when there is no oil, the working fluid is heated directly by solar radiation, and it heats the water quickly. From the graph, at nighttime the temperature starts dropping quickly in the tubes without oil as compared to the system with oil. Thus, by introducing oil to the tubes it traps heat and provides the required temperature at night times also in a very effective manner. These all are due to the heat-holding capacity of the oil since oil cools down slowly. It is found that outlet temperature of the system with oil has increased by an average of 40% during the nocturnal working hours.

5 Conclusion

In this paper, the thermal oil used is mobiltherm 605, which has a high specific heat capacity, due to which the nocturnal working of the solar water heater has improved. From the experiments conducted, it was found that the effect of varying solar flux causes considerable changes in the outlet temperature of the system during the night. The oil acts as a heat storage medium rather than a heat transfer medium. Due to this, as the amount of oil increases, the heat transfer rate of the system is reduced, and the peak temperature obtained at the outlet is decreased according to the increasing oil level inside the evacuated tube. This decrease in peak temperature is compensated by the high outlet temperature during the time of no input, i.e., during the night- time. It has been observed that outlet temperature of the system has been increased by 40% during the nocturnal workings hours when compared to the normal evacuated tube heat pipe solar water heater. From the results we have obtained, we can conclude that the introduction of this thermal oil increases the efficiency and performance of the solar water heater during nocturnal working conditions.

Acknowledgements

Any attempt at any level cannot be satisfactorily completed without the support and guidance of learned people. We owe to great many people whose constant support and motivation that has encouraged us to come up with this project. We are greatly obliged to Dr. Rajeev N, Head of the Department, Department of Mechanical Engineering, for the encouragement and support that he has provided. We are immensely indebted to my very understanding project guide, Dr. Suresh P R, Professor, Department of Mechanical Engineering, and Dr. Sajeesh P, Asst Professor, Department of Mechanical Engineering for their constructive suggestions, guidance, and advice. Our project in charge, Madhu Mohan, Asst.Professor, Department of Mechanical Engineering for his valuable guidance, support, and whole-hearted cooperation. We are thankful to our friends for their wholehearted co-operation during the preparation of our project. Last but not the least we wish our gratitude to our parents for their abundant blessing without which this project would not be successful.

References

[1] A. Shafieian et al. Thermal performance of an evacuated tube heat pipe solar water heating system in cold season, Applied Thermal Engineering 149 (2019) 644– 657

[2] S.M. Peyghambarzadeh et al. Thermal performance of different working fluids in a dual diameter circular heat pipe, Ain Shams Engineering Journal (2013) 4, 855- 861

[3] M.S. Abd-Elhady et al Improving the performance of evacuated tube heat pipe collectors using oil and foamed metals, Ain Shams Engineering Journal 9 (2018) 2683–2689

[4] Siva Kumar S et al. Experimental and Theoretical Investigation of Evacuated Tube Solar Collector with Heat Pipe, IJIRSET, Vol. 6, Issue 3, March 2017

[5] S.Sadhishkumar et al. Thermal performance of water in glass evacuated tube collector with and without phase change material, Indian J.Sci.Res. 20(2): 193-201, 2018.

[6] C. Wannagosit et al. Validated mathematical models of a solar water heater system with thermosyphon evacuated tube collectors, Case Studies in Thermal Engineering 12 (2018) 528– 536

[7] J. Yang et al. A Study on Thermal Performance of a Novel All-Glass Evacuated Tube Solar Collector Manifold Header with an Inserted Tube, International Journal of Photoenergy Volume 2015.

[8] S. Hlaing, M.M.Soe et al. Design Calculation and Heat Transfer Analysis of Heat Pipe Evacuated

Tube Solar Collector for Water Heating , IJSETR Vol.03,Issue.12 June-2014.

[9] Marco Ricci et al. Experimental Tests of Solar Collectors Prototypes Systems, / Energy Procedia 82 (2015) 744 – 751

Railway Brake Technology for High Speed Trains

Fayad Samad[1] **and Dr.Vinod V** [2]

[1] M. S. Student, RWTH Aachen University, Germany
[2] Professor, NSS College of Engineering, Palakkad, Kerala, India

Abstract -
The railway industry plays a crucial role in transportation, requiring efficient and reliable braking systems to ensure safe operations. This article provides an overview of recent advancements in railway brake equipment, focusing on technologies that enhance safety and efficiency. It explores various types of braking systems, including air brakes, disc brakes, electro-pneumatic brakes, and dynamic brakes. The article discusses the evolution of these systems, highlighting their benefits and drawbacks. Additionally, it delves into emerging technologies such as electrodynamic brakes and magnetic track brakes, which offer potential improvements in braking performance. The article also examines the concept of brake blending, a strategy that combines different brake types to optimize performance. Furthermore, it explores the importance of wheel slide protection systems in preventing wheel slip and enhancing safety. Overall, this article provides valuable insights into the advancements in railway brake equipment, offering a comprehensive understanding of the technologies driving safety and efficiency in the railway industry.

Keywords -
Brake technology; safety; elctrodynamic brakes; magnetic track brakes; brake blending.

1 Introduction

Railway brake equipment is a fundamental aspect of train operations, ensuring the safety, control, and efficient deceleration of trains in various operating conditions. Over the years, extensive research and development efforts have been dedicated to advancing railway brake technology, leading to significant improvements in braking systems. These advancements have been driven by the need for enhanced safety, improved performance, and increased operational efficiency in the railway industry. This article aims to provide an overview of the evolution and innovations in railway brake equipment, exploring the various types of braking systems and technologies that have transformed the field. By examining the historical development and recent advancements in railway brake equipment, this article seeks to shed light on the crucial role these technologies play in ensuring safe and reliable train operations.

2 Evolution of train brakes

The evolution of train braking systems has been a gradual process over the last two centuries. Railway brakes are a critical component of the train system, responsible for slowing and stopping the train as it travels along the track. Over the years, railway brakes have undergone significant changes and advancements, from the early days of hand-operated brakes to the sophisticated computer-controlled systems used today. In this report, we will explore the different types of railway brakes and how they have evolved over time. Here are some key milestones. In the early days of railways, trains were stopped by applying brakes to individual wheels. This was a time-consuming process, and it was not very effective. In the mid-1800s, the vacuum brake system was invented. This system used a vacuum to apply brakes to all the wheels simultaneously, making it much more efficient than the earlier systems. Air Brakes: In the late 1800s, the air brake system was developed by George Westinghouse. This system used compressed air to apply brakes to all the wheels simultaneously, and it quickly became the standard for train braking systems. Electro-Pneumatic Brakes: In the early 1900s, the electro-pneumatic brake system was developed. This system used electricity to control the compressed air, making it more precise and easier to control. Dynamic Brakes: In the 1930s, dynamic brakes were developed. These brakes used the energy of the moving train to slow it down, making them especially useful for descending steep grades. In recent years, computerized braking systems have been developed that use sensors and algorithms to optimize braking performance. These systems can take into account factors such as train weight, track conditions, and weather to provide the safest and most efficient braking. Overall, the evolution of train braking systems has been driven by a need for greater efficiency, safety, and control, and it is likely that further advances will continue to be made in the future.

2.1 Early brakes

In the early days of railways, trains were stopped using hand-operated brakes. These brakes were located on individual cars and required an individual to manually turn a wheel to apply the brakes. This process was time-consuming and often resulted in uneven stopping of the train. The invention of vacuum brakes in the mid-1800s improved the braking system significantly.

Figure 1. A brakeman at work : source: https://www.american-rails.com/brakeman.html

2.2 Vacuum brakes

In the early days of railways, trains were stopped using hand-operated brakes. These brakes were located on individual cars and required an individual to manually turn a wheel to apply the brakes. This process was time-consuming and often resulted in uneven stopping of the train. The invention of vacuum brakes in the mid-1800s improved the braking system s The vacuum brake system was invented by George Westinghouse in the 1860s. This system used a vacuum to apply the brakes to all the wheels of the train simultaneously. The system consisted of a vacuum cylinder mounted on the locomotive and a brake pipe that ran the length of the train. When the driver wanted to apply the brakes, he would create a vacuum in the brake pipe by opening a valve. This would cause the vacuum cylinder on the locomotive to open and apply the brakes. The vacuum brake system was an improvement over the earlier hand-operated brakes as it was faster, more efficient, and more reliable. The system was also safer as it allowed the brakes to be applied uniformly, preventing the train from jerking or swaying.

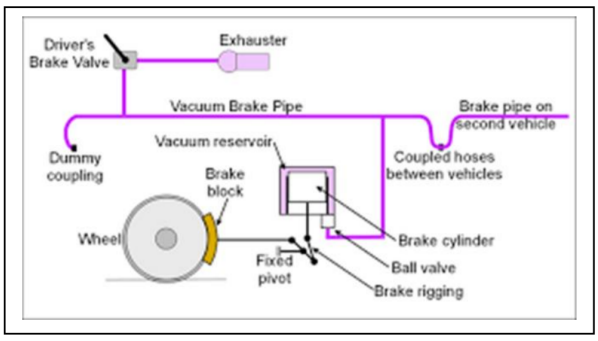

Figure 2. Schematic of Vacuum brake : source: The Railway technical Website

2.3 Air brakes

The vacuum brake system served as the primary braking system for many years, but it had limitations. The vacuum could only be maintained for a certain distance, which meant that the braking distance was limited. In the late 1800s, the air brake system was developed by George Westinghouse. This system used compressed air to apply the brakes to all the wheels of the train. The system was also safer as it allowed for faster and more efficient braking. The air brake system worked by using a compressor to pressurize the air tank on the locomotive. The compressed air was then sent to the brake cylinders on each car, which applied the brakes to the wheels. The driver controlled the system by manipulating the brake valve, which regulated the amount of air pressure in the system.. Over the years, the air brake system has undergone several improvements to improve its safety and performance.

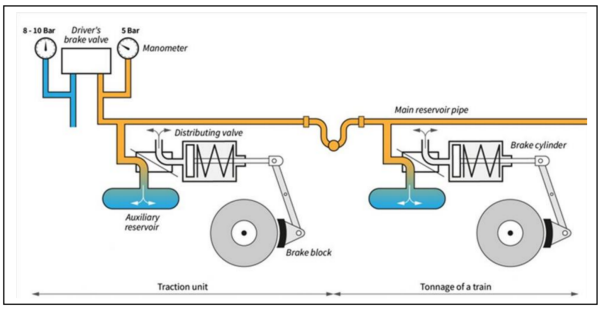

Figure 3. Schematic of direct air brakes : source: Société Nationale des Chemins de Fer Luxembourgeois

2.3.1 How the Air brake system works

The air brake system uses compressed air to apply the brakes to all the wheels of the train simultaneously. The system consists of a compressor, air storage tanks, brake valves, brake cylinders, and brake shoes as shows in fig.3. When the train is in operation, the compressor continually pumps air into the storage tanks or auxiliary reservoirs, which are located on each car of the train. The brake valves or distribution valves control the release of the compressed air from the storage tanks to the brake cylinders, which are located on each wheel of the train. When the train operator applies the brakes, the brake valves release the compressed air from the storage tanks to the brake cylinders, causing the brake shoes to press against the wheels and slow down the train.

2.3.2 Advantages of the Air brake system

The air brake system has several advantages over other types of braking systems. One of the main advantages

is its efficiency. The system allows for quick and precise braking, which is essential for safe and efficient train operations. The system is also responsive, meaning that the brakes can be applied and released quickly, which is important for maintaining the speed and stability of the train during operation. Another advantage of the air brake system is its reliability. The system is relatively simple and easy to maintain, making it less prone to failure than other types of braking systems. Additionally, the system is designed to be fail-safe, meaning that in the event of a failure, the brakes will automatically apply, bringing the train to a stop.

2.3.3 Challenges and Innovations in the Air brake system

Although the air brake system has been a reliable and efficient system for many years, there have been some challenges and innovations in the field of railway braking. One challenge has been the development of longer and heavier trains. As trains have become longer and heavier, the air brake system has had to be adapted to ensure that it can provide adequate braking power to slow down and stop the train. One innovation has been the introduction of distributed power systems, which use multiple air compress throughout the train to improve the distribution of braking power. Another challenge has been the development of faster and more advanced train operations. As trains have become faster and more advanced, the air brake system has had to be adapted to ensure that it can provide the precise and responsive braking necessary for safe and efficient train operations. One innovation has been the use of electronic brake systems, which use sensors and computer control to provide more precise and responsive braking.

2.4 Electro-Pneumatic brakes

Electro-pneumatic brakes are a type of braking system that combines the use of electricity and compressed air to stop a train. This type of braking system is widely used in modern trains and is known for its efficiency, reliability, and safety.

2.4.1 How the Electro-Pneumatic brake system works

Electro-pneumatic brakes work by using an electric control system as shown in fig.4 to control the release of compressed air to the brake cylinders. When the train operator applies the brake, an electrical signal is sent to a control valve, which releases compressed air from the brake reservoir to the brake cylinders. This causes the brake pads to clamp down on the wheels, creating friction that slows down and stops the train.

2.4.2 Advantages of the Air brake system

Electro-pneumatic brakes offer several advantages over other types of braking systems. One of the main advantages is their responsiveness. The electric control system allows for precise and immediate braking, which is important for ensuring the safety and efficiency of train operations. Another advantage of electro-pneumatic brakes is their flexibility. The system can be easily adjusted to accommodate different speeds, loads, and track conditions, which makes it a versatile and reliable option for train braking. Additionally, electro-pneumatic brakes are known for their durability and low maintenance requirements. The system is designed to be resistant to wear and tear and requires minimal maintenance, which can reduce the overall cost of train operations.

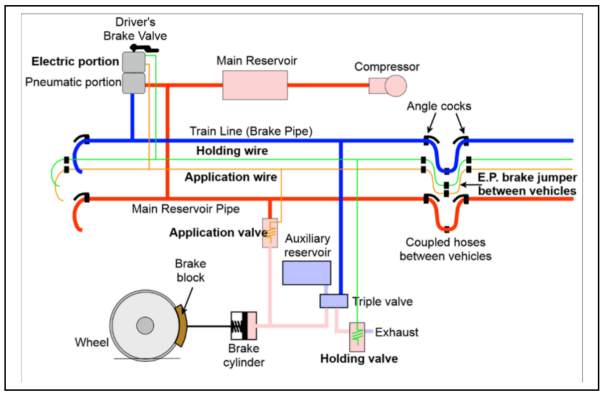

Figure 4. Schematic of Electro-Pneumatic brake : source: The Railway Technical Website

2.4.3 Challenges and Innovations in the Electro-Pneumatic brake system

One of the main challenges with electro-pneumatic brakes is their reliance on electricity and compressed air, which can be affected by adverse weather conditions and other external factors. Additionally, the system can be complex and requires specialized knowledge and training to maintain and repair. However, there have been several innovations in the field of electro-pneumatic brakes that have addressed some of these challenges. For example, some manufacturers have developed advanced control systems that are designed to be more efficient and reliable. Additionally, some systems incorporate sensors and monitoring devices that can provide real-time data on the condition of the braking system and alert operators to any potential issues.

2.5 Dynamic brakes

Electrodynamic brakes, also known as regenerative brakes, are a type of braking system used in modern trains that rely on the principle of electromagnetic induction to slow down and stop the train. Unlike traditional friction brakes, which convert the kinetic energy of the train into heat energy, electrodynamic brakes convert this energy into electrical energy, which can be used to power other systems on the train.

2.5.1 How Dynamic brakes work

Electrodynamic brakes use the principle of electromagnetic induction to generate a braking force. When the train's wheels turn, they rotate a set of magnets that are fixed to the axle. This creates a magnetic field that interacts with a set of stationary coils located near the wheels. As the magnetic field moves through the coils, it generates an electrical current, which creates a secondary magnetic field that opposes the rotation of the wheels. This creates a braking force that can slow down and stop the train.One of the key advantages of electrodynamic brakes is their ability to generate a significant amount of braking force, even at high speeds. They are also very efficient and can convert a large amount of the train's kinetic energy into electrical energy, which can be used to power other systems on the train, such as the lighting or air conditioning.

2.5.2 Types of Electrodynamic brakes

There are two main types of electrodynamic brakes used in trains: rheostatic brakes and regenerative brakes. Rheostatic brakes use electrical resistance to slow down and stop the train. When the brakes are applied, a set of resistors, mounted on the top of trains as shown in fig.5, is connected to the train's electrical system, which creates a load that slows down the rotation of the wheels. This load converts the kinetic energy of the train into heat energy, which is dissipated through the resistors. Regenerative brakes, on the other hand, use electromagnetic induction to generate an electrical current that can be fed back into the train's electrical system. When the brakes are applied, the energy generated by the rotation of the wheels is converted into electrical energy, which can be used to power other systems on the train, such as the traction motors or the lighting.

2.5.3 Advantages of Electrodynamic brake system

Dynamic brakes offer several advantages over other types of braking systems. One of the main advantages is their efficiency in recovering energy. When the dynamic brake is applied, the electrical energy generated by the traction motors can be used to power other systems on the train, such as lighting and heating, or it can be returned to the power grid. Another advantage of dynamic brakes is their ability to reduce wear and tear on other braking systems. Because dynamic brakes are able to slow down the train without relying solely on friction, they can help reduce the wear and tear on brake pads and other components. Additionally, dynamic brakes are known for their quiet operation, which can be important in urban areas where noise pollution is a concern.

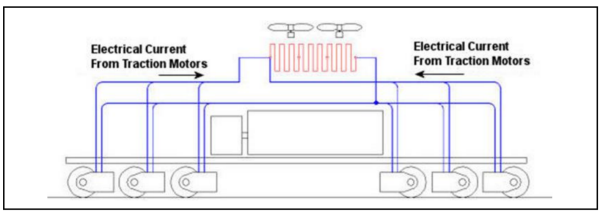

Figure 5. Electro Dynamic braking - Rheostatic: source: 2010 Philip J. O'Keefe, PE, MLE

2.5.4 Challenges and Innovations in the Electrodynamic brake system

One of the main challenges with electrodynamic brakes is that the force generation is related to speed. When in stand still there is not braking force possible and also due to construction limitations, when speed increases, the regenerative force decreases. This can be seen from the ED brake performance curve. Another challenge is their inability to provide a quick and immediate stopping force in emergency situations. Because the braking force is generated by the rotation of the wheels, it takes some time for the brakes to fully engage and slow down the train. This can be a concern in emergency situations, where quick and reliable stopping power is essential. To address this challenge, some trains are equipped with a combination of electrodynamic brakes and traditional friction brakes. This allows for a quicker and more reliable stopping force, while still providing the energy-saving benefits of electrodynamic braking.

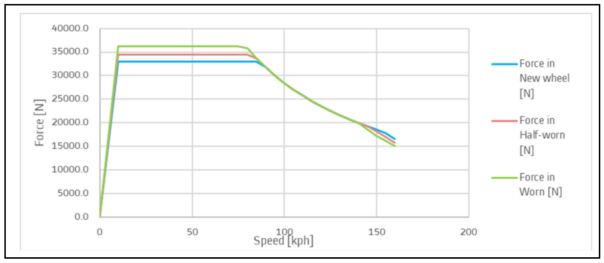

Figure 6. Electro Dynamic braking - Rheostatic: source: 2010 Philip J. O'Keefe, PE, MLE

3 Wheel Rail Adhesion

Wheel and rail adhesion is a term used to describe the amount of traction or grip that exists between the wheels of a locomotive or train and the rails upon which they run. This adhesion is critical for ensuring that the train is able to move smoothly and safely along the tracks, especially when accelerating or braking. The level of adhesion between the wheels and rails can be affected by various factors, such as the weight of the train, the condition of the track, the speed of the train, and the weather conditions. For example, in wet or icy conditions, the adhesion between the wheels and rails may be reduced, making it more difficult for the train to maintain traction and move along the tracks. To ensure that trains are able to operate safely and efficiently, it is important to monitor and maintain adequate levels of wheel and rail adhesion. This can involve using specialized equipment to measure the level of adhesion, as well as taking steps to improve track conditions or adjust train speeds as needed. In simple terms this is the ratio of the forces exerted between the wheel and rail. From a brake system perspective, this is the ratio of the braking force to the weight of train. And can be expressed as

$$T_s = \frac{F}{P} = \frac{(M+m)\gamma - R_a}{(M+m)g} \simeq \frac{\gamma}{g} \quad (1)$$

Ts – Adhesion ratio, F – Tangential force on wheel frail contact, P – Vertical wheel load, M – Static masses, m – equivalent rotating masses, – equivalent deceleration, g – gravitational acceleration, Ra – running resistances It is quite important to notice that this formula is only valid for braking as normally in a train all axles are braked. Now in the above equation, ignoring the resistances, this is the ratio of effective deceleration over gravitational constant. This is quite interesting if we round up g to 10 m/s2. Then the required adhesion becomes the 10th of a required deceleration. For a deceleration of around 1-1.5 m/s2 an adhesion is required between 10-15Wheel rail contact and adhesion cannot be sufficiently explained without contact theories. A few of which are explained below. Hertzian contact theory is a mathematical model that is used to analyze the stresses and deformations that occur when two curved surfaces, such as cylinders, come into contact with each other. The theory was developed by Heinrich Hertz in the late 19th century, and it has since been widely used in engineering and materials science to design and analyze various mechanical systems. When two cylinders come into contact with each other, the Hertzian contact theory predicts that the stresses and deformations that occur are concentrated in a small area, known as the contact patch. The contact patch is a small elliptical area where the maximum pressure occurs and is located at the center of the cylinders' point of contact. The Hertzian contact theory can be used to calculate the maximum pressure that occurs in the contact patch, as well as the size and shape of the contact patch. The theory is based on several assumptions, such as that the cylinders are perfectly elastic, the contact surfaces are smooth and have no defects or irregularities, and the deformation of the cylinders is small compared to their overall size. The theory is a powerful tool for predicting the behavior of mechanical systems, but it is important to keep in mind its limitations and assumptions. In practice, many mechanical systems may have non-ideal surfaces, may not be perfectly elastic, or may experience large deformations that cannot be accurately predicted using the Hertzian contact theory alone. Kalker's Theory is a mathematical model developed by Professor Michael Kalker in the 1970s to simulate the contact behavior between the wheel and rail in a train system. The theory takes into account the elastic and plastic deformation of the wheel and rail, as well as the friction and adhesion between the two surfaces. The model is based on the idea that the contact behavior between the wheel and rail can be described as a set of springs and dampers, which represent the elastic and damping properties of the materials. The model also includes a friction model to account for the effect of friction between the two surfaces. The Kalker's Theory is a numerical method that can be implemented on a computer to simulate the contact behavior between the wheel and rail. The model predicts the contact pressure, the size and shape of the contact patch, and the forces and moments that occur between the wheel and rail. The model can also predict the wear and damage that can occur over time due to repeated contact between the two surfaces. The theory is widely used in the field of rail vehicle engineering to optimize the design of train components, such as wheels and rails, and to evaluate the performance of train systems. The model has been validated through experimental tests and has been shown to provide accurate predictions of wheel-rail contact behavior. Now coming back to the wheel rail contact During sliding, the adhesion characteristics between the wheel and rail change significantly compared to when the two surfaces are in pure rolling contact. In pure rolling, the adhesion between the two surfaces is mainly due to the deformation of the surface asperities, which creates a mechanical interlocking effect. However, during sliding, the adhesion is dominated by the chemical interactions between the two surfaces, such as van der Waals forces and chemical bonding. The adhesion characteristics during sliding depend on several factors, including the materials of the wheel and rail, the temperature, the speed of the train, and the level of contamination on the surfaces. In general, the adhesion coefficient (the ratio of the tangential force to the normal force) is much lower during

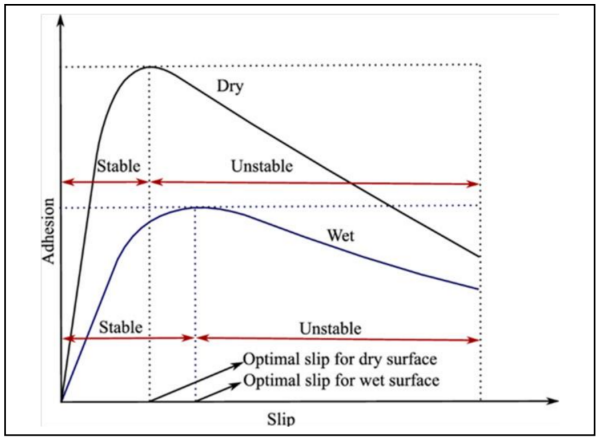

Figure 7. Adhesion charectiristic during sliding: source: 2020, Zirek, A., Onat, A

sliding than during pure rolling. This can cause problems such as wheel slipping, which can reduce the efficiency and safety of the train. To improve the adhesion characteristics during sliding, researchers and engineers have developed several strategies, including the use of friction modifiers and the optimization of the surface texture of the wheel and rail. Friction modifiers are chemicals that are added to the rail to improve the adhesion characteristics, while the optimization of the surface texture can enhance the mechanical interlocking effect between the two surfaces. Overall, understanding the adhesion characteristics during sliding is important for improving the performance and safety of train systems, especially in adverse weather conditions or when the surfaces are contaminated.

3.1 Regeneration of Wheel Rail adhesion

When the full contact zone is sliding, pure rolling conditions do not hold any more, and macroscopic sliding between the wheel and the rail occurs. In this phase, the adhesion coefficient depends on the absolute slip. The relationship between the adhesion coefficient μ and the absolute sliding w was investigated by many researchers because its behaviour is fundamental for the performance anti-skid and WSP devices. Sliding is impossible to prevent. Hence it is interesting to note a second peak, well into the sliding region as can be seen in the figure 8. There are two curves; the continuous one represents a loss of adhesion, or an increase in slip, while the dashed curve represents a recovery of adhesion, or a decrease in slip, and their usual shapes are obviously different. The second peak is a more stable region compared to very low sliding region. Even though the coefficient of adhesion is reduced, the second peak provides a favorable region of operation as sliding is inevitable. The secondary stable region is usually between 10-15% of slip.

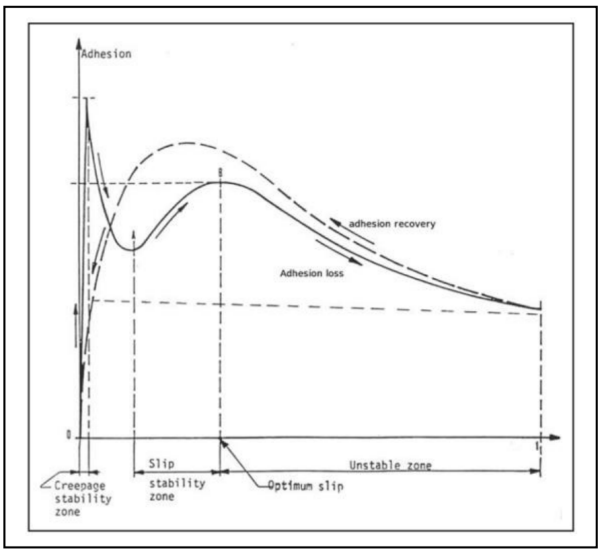

Figure 8. Typical qualitative behaviour of the slip/adhesion curve: source: Boiteux et al

4 Brake Blending

Brake blending is a technique used in modern train braking systems to optimize braking performance and efficiency by blending different types of brakes to achieve the desired braking force. This technique is important because different types of brakes have different characteristics, such as response time, stopping power, and wear and tear, which can affect the overall performance of the braking system.

4.1 How it works

In most modern trains, brake blending is achieved through a combination of electronic and mechanical systems. When the brakes are applied, the electronic system receives signals from various sensors throughout the train, such as speed sensors and brake pad wear sensors , to determine the optimal combination of brakes to achieve the desired braking force. For example, at low speeds, when there is more time available to slow down and stop the train, the electronic system may rely primarily on regenerative and friction brakes to slow down the train. Regenerative brakes are used to convert the kinetic energy of the train into electrical energy, which can be stored in batteries or used to power other systems on the train. Friction brakes, such as disc brakes or tread brakes, are used to provide additional stopping power when needed. At higher speeds, when there is less time available to slow down and stop the train, the electronic system may rely more heavily on

friction brakes to achieve the desired braking force. This is because regenerative brakes are less effective at high speeds, and may not be able to generate enough stopping power to slow down the train quickly enough.

4.2 Rules and parameters

Usual parameters taken into consideration during brake blending are:
• Braking Modes (service brake or emergency brake)
• Configuration of train (motor bogies and trailer bogies)
• Presence of dynamic brake
• Current status of equipment (if active or there are isolated points of failure)
• Type of brake control (to analyze where the blending can be achieved)

Basic rules considered for blending
• Prioritize dynamic brakes
• Distribute mechanical brake effort
• Use other brakes only in case of emergencies

4.3 Advantages of brake blending

One of the key benefits of brake blending is improved efficiency and reduced wear and tear on the braking system. By using a combination of different types of brakes, the system can optimize braking performance while minimizing the amount of wear and tear on any one component. This can help to reduce maintenance costs and improve the overall lifespan of the braking system. Another benefit of brake blending is improved safety. By using a combination of different types of brakes, the system can provide a more reliable and consistent braking force, which can help to prevent accidents and improve passenger safety.

4.4 Blending Strategies

4.4.1 Equi-adhesion

In an equi adhesion brake blending strategy, the braking force is distributed among the wheels of the train in a way that ensures that each wheel has the same level of adhesion with the track. This strategy is mainly used during emergency braking, which means electrodynamic braking is often not available for this strategy and the entire effort is achieved by mechanical brakes. As can be seen from the chart, the adhesion in all of the bogies is same. To achieve this a control algorithm monitors the brake force generated in each bogie and adjust it accordingly to have a constant level of adhesion throughout the train.

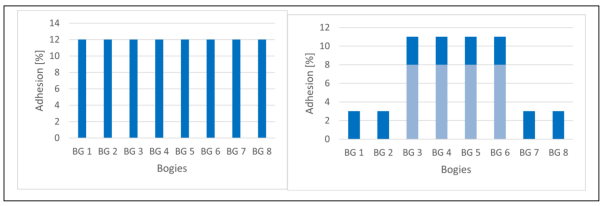

Figure 9. a. Equi adhesion, b. Equi distribution: source: Alstom Transport Deutschland

4.4.2 Equi-power

The Equi Power Brake Blending strategy is another approach optimizing the performance of train braking systems. It is based on the concept of distributing the braking force equally among all the axles of the train, rather than just among the individual wheels. This approach helps to prevent wheel slip and ensures that the braking force is applied evenly across the train, regardless of the weight distribution. The Equi Power Brake Blending strategy is particularly useful for long trains with a large number of axles, where weight distribution can be a significant challenge. By distributing the braking force equally across all the axles, this strategy helps to improve braking performance, reduce the risk of wheel slip, and improve overall safety. To achieve this the control algorithm prioritizes the ED brake, and deficiency in braking force is met by sharing the load equally among all the friction force elements.

5 Wheel Slide Protection - WSP

Brake blending is a technique used in modern train braking systems to optimize braking performance and efficiency by blending different types Wheel slide protection is an important feature in modern railway braking systems, and is designed to prevent wheel slip and improve the safety and efficiency of train operations. Wheel slip occurs when the wheels of a train lose traction with the track, typically due to excessive braking force or poor track conditions. This can cause the train to skid or derail, which can be dangerous and costly. The development of WSP devices started in the 1960s when the running speed started increasing to 160kph, 200kph. At these high speeds the operators started facing reduced levels of adhesion and force transmission in degraded conditions. The early WSP equipment were purely mechanical devices based on small weights and inertia attached to the end of axles. The main aim was only to prevent wheel locking and thereby wheel flats. So they were just operating in a binary manner. They are completely turned off the braking force, so that the wheel locking is prevented and once the wheel starts rolling the brake force was reapplied. In the 1980s by the working group B164 of UIC, with the discovery of the sec-

ond peak in adhesion around 15first wheel slide protection system of the second generation was developed. A continuous control and precise adjustment were possible at this point in time thanks to digital electronics. Present day wheel slide protection systems are complex systems designed to detect the onset of wheel slip monitoring speeds and automatically adjust the braking force to prevent it from occurring. There are several different types of wheel slide protection systems, including:

• Electro-pneumatic braking systems: These systems use sensors to detect the onset of wheel slip, and adjust the braking force by releasing the brakes on the affected wheels. This helps to prevent the wheels from locking up and allows them to regain traction with the track.

• Anti-lock braking systems (ABS): ABS systems work by monitoring the speed of each wheel and adjusting the braking force to prevent them from locking up. This helps to prevent wheel slip and allows the train to maintain traction with the track.

• Electronic brake control (EBC): EBC systems use a combination of sensors, computer algorithms, and hydraulic valves to adjust the braking force and prevent wheel slip. These systems are highly advanced and can adjust the braking force in real-time based on a wide range of factors, including speed, weight distribution, and track conditions.

• Wheel slide protection devices: These devices are installed on the train wheels and work by automatically adjusting the braking force to prevent wheel slip. They typically use a hydraulic or mechanical system to adjust the braking force, and are effective in preventing wheel slip in a wide range of conditions.

Overall, wheel slide protection is an important feature in modern railway braking systems, and is essential for preventing accidents and improving the safety and efficiency of train operations. By detecting the onset of wheel slip and adjusting the braking force in real-time, these systems help to prevent accidents and ensure that trains can operate safely and efficiently in a wide range of conditions.

6 Conclusion

In conclusion, my internship at Alstom Transport Deutschland has been an incredibly valuable experience that has provided me with the opportunity to gain practical skills and knowledge in the railway brakes and air supply domain. Over the course of my internship, I have had the chance to work on a variety of projects and tasks, and have learned a great deal about the inner workings of the railway manufacturing industry. Throughout my internship, I have had the chance to work with a team of experienced professionals who have been incredibly supportive and helpful in guiding me through my work. Their guidance and feedback have been invaluable in helping me to develop my skills and knowledge, and I am grateful for the opportunity to have worked with such a talented group of individuals. In addition to the technical skills I have acquired, my internship has also taught me the importance of effective communication, teamwork, and adaptability in the workplace. These soft skills are essential for success in any professional environment, and I feel that my experience at Alstom Transport Deutschland has prepared me well for a career in the railway brakes domain. Overall, I am incredibly grateful for the opportunity to have completed my internship at Alstom, and would like to thank all of the staff and management for their support and guidance throughout my time here. I believe that the skills and knowledge I have gained will serve me well in my future career, and I look forward to applying them in my future work.

References

[1] UIC CODE 540 - International Union of Railways - Brakes - Air Brakes for freight trains and passenger trains.

[2] UIC 541-1 : 8ED 2013 - SAI Global - Brakes - Regulations concerning the design of brake components.

[3] UIC CODE 541-4 - International Union of Railways - Brakes – Brakes with composite brakes blocks.

[4] EN 15329 - Railway applications — Braking — Brake block holder and brake shoe key for railway vehicles.

[5] EN16541- Railway applications - Braking – Brake pad holder.

[6] EN16207 Railway applications - Braking - Functional and performance criteria of Magnetic Track Brake systems for use in railway rolling stock.

[7] EN14535-1 Brake discs for railway rolling stock – Part 1: Brake discs pressed or shrunk onto the axle or drive shaft, dimensions and quality requirements.

[8] EN14535-2 Brake discs for railway rolling stock - Part 2: Brake discs mounted onto the wheel, dimensions and quality requirements.

[9] EN14535-3 Brake discs for railway rolling stock – Part 3: Brake discs, performance of the disc and the friction couple, classification.

[10] UIC 541-4 Brakes – Brakes with composite brakes blocks.

[11] EN 15328 Railway applications - Braking – Brake pads.

[12] EN 16451 Railway applications - Braking – Brake pad holder.

[13] UIC 541-3 : Disc brakes and their application – General conditions for the certification of brake pads.

[14] Alstom Brake conception guidelines.

A Review on how stirring process parameters affect the Stir Casting Route with Aluminium Metal Matrix Composites

Lakshmi Rajan P S[1], Dr. Sujatha I [2] and Dr. Arun M S [3]

[1] Research scholar, Department of Production Engineering, Govt Engineering college, Thrissur
[2] Associate Professor, Department of Production Engineering, Govt Engineering college, Thrissur
[3] Associate Professor, Department of Mechanical Engineering, RIT, Kottayam

Abstract -

Aluminium metal matrix composites are preferred candidates for industries nowadays due to their tremendous mechanical properties. A high strength to weight ratio at an economical rate with good wear and fatigue properties makes it stand out in the materials world. The simplicity and economical nature of stir casting process has attracted the attention of mass production scale industries nowadays. There are different process parameters that affect the quality of the final stir casted product. Some of the process parameters which have a great influence are studied here. This includes wettability, stirrer speed and time, stirrer design and dimensions, position of stirrer, reinforcement feeding rate and preheat temperature. The focus of this paper is to provide a good insight to the upcoming researchers regarding the selection of various processing features for different AMMC's and HAMC's.

Keywords -

Composite, Metal matrix composite (MMCs), Stir Casting, Process Parameters, Aluminium metal matrix composites (AMMC's), Hybrid Aluminium matrix composites (HAMC's)

1 Introduction

The reason for preferring Metal matrix composites by industries is due to its high strength to weight ratio, which makes it an ideal candidate for an economical material. A metal matrix composite comprising of two or more reinforcements is said as hybrid MMC's. With regard to hybrid aluminium matrix (HAMC), more than one reinforcement is mixed with aluminium matrix. The reinforcements may be either calculated in weight percentage or volume percentage and the form may vary from particles to fibres. Mostly Aluminium matrix composites which are particle reinforced are widely used for advanced components. It offers a wide range of properties like good wear resistance, better stability at high temperatures, better fatigue characteristics, high thermal and electrical conductivity and high strength to weight ratio [2, 3,4–7]. These properties make it an ideal candidate for various aerospace applications compared to other metal alloys. Various factors affect the fabrication of Aluminium matrix composites. A process widely accepted to use for the fabrication of Aluminium matrix composites are Friction stir casting (Figure 1). This can not only be applied to Aluminium MMC's but also to metals like magnesium. While doing this casting process, reinforcement particles are usually preheated. The purpose behind this is to avoid moisture, to reduce porosity and other defects. Higher preheating temperatures and lower mixing rate ensures a better quality of final Al MMC's. The friction stir process has its origin from Friction stir welding, a process found in 1991 by Cambridge university, UK. Aluminium alloys are widely stir casted nowadays due to various properties like better machining properties, better homogenous mixing of reinforcement with the matrix, and an added advantage of reduced porosity defect. The mechanical and physical properties of the final composite is also enhanced due to the stirring effect in stir casting machine [8-9]. Fabrication of MMC's can be carried out in different ways. It can be a solid state technique ie., powder metallurgy, a liquid state technique like casting or some other methods like infiltration [10-12]. While considering the product quality, solid state as well as infiltration methods give a better quality product with regard to its properties, reinforcement distribution etc. Industries still go behind stir casting technique because of its low manufacturing cost and simplicity. This allows industries to widely accept it and use in mass production scale [13].

2 STIR CASTING TECHNIQUE

A stir caster consists of a furnace, a mechanical Stirrer and a reinforcement feeder either attached with it or externally placed. The stir casting setup is shown in Figure 1. Melting of the matrix material is carried out in the furnace and the reinforcements are preheated in the preheater attached. In order to avoid the particle settling at the bottom, a bottom pouring setup was employed with a stir caster. Thus, melt can be suddenly poured from its melt state. The stirrer provided will create a vortex motion which will help in the proper mixing of the reinforcement particle with the

matrix. Stirrer has a stirrer rod with impeller blades attached to it. The rotation in the stirrer is brought by a variable speed motor which has a regulator attached with it. The number of blades as well the geometry of the blades may vary according to the vortex required. Usually as per many studies axial flow which is obtained by three blade system is preferred. This also helps in reducing power consumption. Reinforcements are fed through the feeder after preheating in the powdered form. After melting, the mixture is poured into the mould, either a sand mould or a permanent mould. The primary most concern associated with stir caster is with its nonuniform distribution of reinforcement particles with the matrix which leads to less efficiency of the process in obtaining required properties for the final product [14,15]. Various process parameters like the stirrer speed, angle of the stirrer etc affects the distribution of reinforcements with the matrix. A flow diagram of various steps involved in stir casting is depicted in Figure 2. In the first step, the matrix is melted in a bottom pouring furnace. Along with the melting done, the preheater with reinforcement is switched ON. Preheating will allow in eliminating excess moisture or any other impurity present in the reinforcement. After complete melting of the matrix material, the stirrer is switched ON. The stirring time and stirrer speed are set according to the needs and specifications of the material property. The impact of this will be discussed later in the coming sections. Now the preheated reinforcement is added to the melt and the stirring is continued. After a certain time, the melt is poured to the mould and is allowed for solidification and natural cooling. To improve the material characteristics, post casting process such as heat treatment may be done followed by machining, testing, inspection etc.

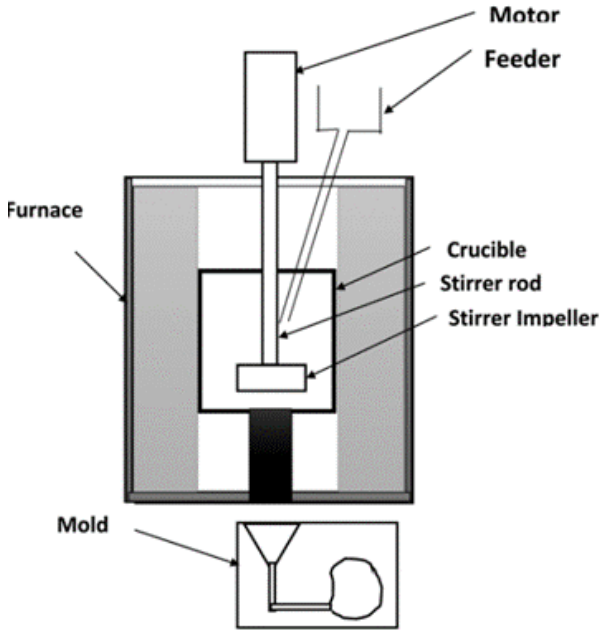

Figure 1. Schematic of stir casting machine [16]

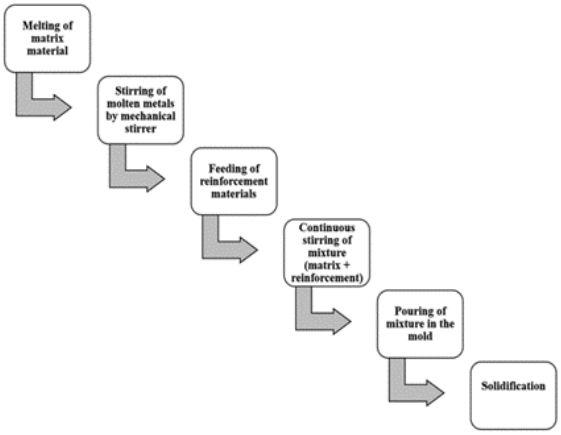

Figure 2. Process of stir casting [16]

3 IDENTIFICATION OF RESEARCH GAP

According to Turan et al [15] despite of various advantageous features offered by stir casting process like lower running cost, hassle free operation etc, there are still some loop holes which need to be studied further as depicted in Figure 3. The identified gaps are listed below:

1. Related with temperature.
2. Related with material
3. Related with the stirrer

These gaps will allow the researcher to study further regarding different process parameters and its effects with the stir casting process

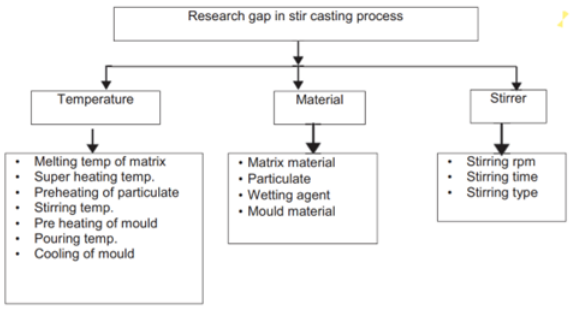

Figure 3. Research gaps in stir casting process [15]

4 STIR CASTING PROCESS

4.1 Melting of matrix material

• Melting of the matrix material is carried out in an Automatic bottom pouring furnace, which will allow the melt to be poured to the mould immediately after the melt is completed. This type of furnaces is mostly used in investment casting industry. In stir casting process, the matrix material is melted in the furnace and the reinforcement is preheated in a separate furnace or a preheater attached with the stir casting setup and then once the melt is completed, the reinforcement particles are added to the melt and held with stirring for some time.

4.2 Wettability factors

Wettability is the rate of measure of the interfacial attraction of liquid with another liquid or with solid. This is the property by virtue which the liquid material will maintain a balance of cohesive and adhesive forces with the solid material. The reinforcement particles are non-uniformly distributed in the matrix due to many problems. One of which is the formation of the oxide layer on the molten metal surface. This oxide layer has to be skimmed off before adding the reinforcement particles. Next is the wettability factors, which are quite difficult to overcome in case of ceramic particles. In order to improve wettability, one has to focus on surface tension of liquid melt with the reinforcement particles. Surface tension between these has to be reduced. This can be achieved in a variety of ways as per many studies.

One of them is the addition of Magnesium in a very low percentages (about 1 %) to the melt. This will act as a surfactant and will reduce the surface tension and will thereby promote the interfacial attraction between solid liquid interface. High oxygen affinity of magnesium with the surface of reinforcement particles is the reason behind this [17-19,24]. Another way of improving wettability is to carry out stirring process in a semi solid state. This will increase the melt viscosity and will reduce the surface tension and will also allow particles to be uniformly distributed into the melt. Jasmi Hashim et al. has stated in his studies that stirring process if carried out in fully molten condition will cause the reinforcement particles to stay at the top of melt without proper distribution [20]. Rao and Ramanaiah stated that wettability of Magnesium alloy (ZE-42) melted at 6500 oC in an electric furnace was improved by adding boron carbide and multiwalled carbon Nano Tubes in molten state [21]. Various factors, like chemical reactions, contaminants, surface roughness, gas layer, density, temperature and pressure, time of contact, particle size and materials and its crystallinity al etc affects the wetting properties of MMC's. Mechanical stirring has been stated as a very effective method in improving the wettability in ceramic-metal composites [22]. Different types of stirrers with different blade design and the number of blades has been used to improve agitation. When the size of particles is reduced, the porosities and voids within the composite will increase, thereby, decreasing particle size and increasing weight fraction will reduce wetting [23]. This is because if the particle size is smaller, then a high shearing force will need to be applied to separate clusters and to deagglomerate these particles. It has been reported that cleaning the outer surface of the reinforcement a particles either by ultrasonic treatment will cause changes in the surface properties and will give way in changing the contact angle thereby introducing wetting properties. Shao et al. [26] added rare element La in a 2% proportion to molten Aluminium to improve its wetting properties with Al2O3. This reduced the surface tension of and the contact angle was reduced from 90.5° in Al- Al2O3 to ¡ 80° in Al-La- Al2O3 system. Qin An et al. [25] studied the effect of alloying elements Si and Cu on the wettability of SiC-Al system and it was concluded that the addition of Si improved the wettability whereas Cu deteriorates the wettability. However, the formation of Al4C3 intermetallics was denied by both the alloying elements. It has been noted that zirconium improved the wettability in Al2O3/Al composite. The reason stated was that the exothermic reaction in the interface between Zr and Al. Heat release during this reaction will retard the formation of oxide layer and thereby promoting the formation of ZrAl3 leading to improvement in wettability of Zr-coated Al2O3 reinforced Al matrix composites [27]. Chromium has also been stated as an effective alloying element in improving the wettability properties. By the addition of 1 wt% Chromium in a Cu/graphite combination, the wetting angle was reduced from 140° to 43° at 1573 K [28]. Initially, 140° indicated very poor wetting of graphite particles in the graphite matrix. Molybdenum is also considered as a good wetting agent, as the wettability between TiC-Al matrix nano composites were improved by its addition. This was obtained by improving the chemical stability of TiC in Al melt, thereby interfacial reactions are controlled, and thus improving ductility and mechanical strength [29]. Different coating techniques like Physical/Chemical vapour depositions, cementations, thermal spraying etc are also used to improve the wettability [30]. Apart from this, some metals like Cu, Ni, Ag, Co, Sn, Sb or Cr, can also be considered as an alternative in improving wettability as liquid metals have a better tendency to wet metals [25].

4.3 Stirring Speed and time

Stirring speed has a great influence in the stir casting process, as this decides the mixing of the particulate reinforcement in the matrix phase. Microstructure of the

composite gets varied depending upon the stirring speed and time. An optimal stirring speed and time ensures proper mixing of the reinforcement in the matrix. The amount of the reinforcement added as well as the its size also affects the stirring parameters. A longer stirring time is expected to improve better incorporation of the reinforcement particles in the matrix, moreover it also leads to more power consumption and thereby a rise in the total fabrication cost of the composite. A stirring time less than 3 mins is generally not preferred as this will not give a chance for the particles to get well distributed in the melt. The working temperature of some combinations like that with Boron Carbide in Aluminium matrix which turns around 800-950 oC may also damage the impeller of the stirrer. A study conducted by Prabu et al. [22] on the effect of stirring time on the microstructure and hardness of Al/SiC composite, suggested a stirring time of 10 mins, as this ensured a uniform value of hardness as well as a better mixing of the reinforcements with the matrix throughout the composite. It was observed that an effective inclusion of SiC particles were not obtained when stirred for 5 mins and clustering in some localized regions were observed. While increasing the stirring time to about 10 to 15 mins, a better distribution of particles was obtained. Thereby increasing stirring speed and time was found to be optimal. The microstructures viewed were having better characteristics at this point. From a hardness point of view, as SiC particles being harder, when distributed in softer Aluminium matrix increases the hardness of the final composite, thereby restricting the plastic deformation of the matrix and also making the material stiffer and stronger. But this would depend upon the distribution of the reinforcement particle. If the distribution is uneven, it may lead to significant change in the hardness value at particular places. It was observed that hardness values at some places were minimum and at some places were maximum at lower stirring speeds. The presence of SiC particles ensured a higher hardness value and a lower value was observed at places where the SiC particle accumulation were lower. The study also pointed out that the optimal stirring speed was 600 rpm and stirring time was 10 mins. The hardness value obtained for a stirring speed lower than 600 rpm were uneven [22].

A study by Vishal et al [32] on the microstructure of the final composite pointed out that the clustering of particles were found at lower stirring speeds of 150-300 rpm. A better distribution was obtained when the stirring speeds were raised to 500 rpm. A hardness study was also conducted mentioning the influence of stirring speed on the hardness of the final composite. In as- cast condition, a higher stirring speed ensured better hardness.

4.4 Stirring Temperature

Holding time of stirring and working temperature also affects the viscosity of the matrix phase. It was observed that, an increase in the holding time of stirring resulted in a reduction in the viscosity of the matrix, thereby increasing the chemical reaction between reinforcement and matrix phase [31]. Viscosity would also affect the distribution of the reinforcement particles in the matrix phase. An optimal stirring temperature from various studies were found out to be 800 °C.

4.5 Reinforcement Pre-heat Temperature

For better surface activity of particles as well as to improve the wettability of the particles to the melt, it is preferred to preheat the reinforcement particles/powder. This will help in trapping the moisture or any other gases that may affect the processing or property of the composite [33]. Rajesh Kumar et al. [38] found an optimal reinforcement preheat temperature at 500 °C for a time of 30 mins. This resulted in better wettability between the particles. A study on different preheat temperature and stirring speed combinations were conducted by Vishal et al [32], and a table was created showing different properties and characteristics of different composites obtained. The matrix used here was Al6061 and the reinforcement selected was SiC. It was observed that almost all the researchers focused on a preheat temperature of 400-800 °C and this significantly increase the wettability of the reinforcement particles with the matrix.

4.6 Mould pre-heat temperature

Moulds are usually preheated to remove any entrapped gases present in the slurry and this may also remove the porosity from the final casted composite. Thus, preheating the mould will enhance the property of the cast composite as well help in reducing the bubble formation while pouring the molten composite. [32]

4.7 Stirrer design and dimensions

The process efficacy of stir casting can be enhanced by proper design of the stirrer. For solid suspension in liquids, it is best to use axial flow impellers [34]. A pitched blade stirrer is more preferred than propeller type as it causes a smooth vortex motion because of its unique flow design pattern causing mixed flow ie., both axial and in radial directions, thereby allowing better incorporation of the reinforcement particles in the matrix. A propeller type stirrer creates a vigorous turbulent flow which causes splashing of the melt outside the crucible. A better blade angle will ensure a homogenous distribution of the reinforcement with the matrix in minimum stirring time. A simulation

study conducted by S. Naher et al. [35] pointed out that the optimal blade angle with minimum stirring time for better incorporation as 60 °.[35]. Sahu and Sahu et al. [16] and Lu and Lu [37] concluded that in order to achieve proper axial flow and shearing action, the blade angle should be selected appropriately. The reinforcement particles from the liquid surface are transferred to the melt as a cause of the vortex motion. The shearing action would assist in breaking the accumulation of the reinforcement particles, thereby allowing a uniform distribution throughout the melt. A water model study conducted by Ravi et al. [3] to investigate on the effect of the impeller blade angle revealed that on a range of blade angles selected ie., 15, 30, 45, 60 and 90 o, a lower blade angle of 15o created a particle dispersion below the stirrer. Whereas a blade angle of 30 o created a uniform dispersion of the particles without concentration at a particular area. When the blade angle was increase to more than 30 o, it was found that the solid particles tend to concentrate near the tip of the impeller. Thereby the study concluded that an optimal blade angle for better distribution as 30 o with respect to the stirrer axis. This was in compromise with the FEM model created. The stagnant and the dead zones, which are considered as the inactive zones in the cylindrical and bottom portions of the crucible were attempted to reduce by changing the impeller blade angles through 30, 45, 60 and 90 o. An increase in the blade angle to more than 90 o, would lead to higher shear flow and thereby consuming high power as well. Shearing action is said to aid the solid particle suspension in the melt, but without and axial inward pressure it makes difficult for solid particles to evenly mix in the melt. The studies also showed that by decreasing the blade angle, it is quite possible to increase the axial flow and a flow near the liquid surface was obtained for a blade angle of 30 o [3, 37, 39]. The diameter of the impeller with respect to the diameter of the crucible is termed as the impeller blade size. It is essential to select properly sized impeller for better distribution of the reinforcement phase. If the impeller size is too large, then it may result in the reinforcement particles to get concentrated in the centre of the crucible, whereas if the impeller size is too small, this may result in the particles to get suspended at the edges of the crucible. Thereby the optimal diameter of the impeller was confirmed by a relation,

$$d = 0.5D \tag{1}$$

where d is the optimal diameter of the impeller and D is the diameter of the crucible in the case of single stage stirring for a flat base crucible at 550 rpm [16] (Figure 4). For a semi spherical base crucible for multistage stirring at 1000 rpm [37], the relation was termed as

$$d = 0.55D \tag{2}$$

And the blade width b is given as 0.1 to 0.2 times D [39].

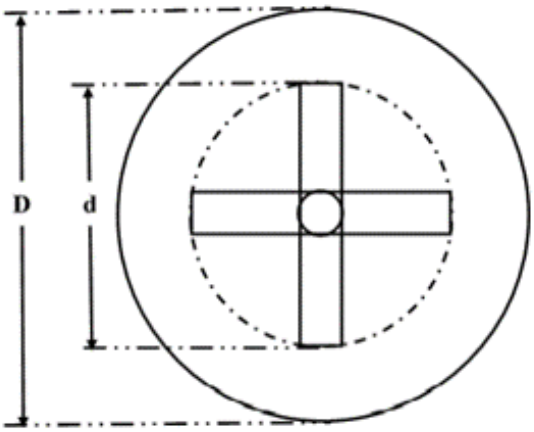

Figure 4. Impeller and crucible diameter.[16]

4.8 Pouring Rate

While pouring the molten slurry of the composite, the rate of pouring should be constant. Otherwise entrapping of gases may occurs which affect the mechanical property of the composite materials. [39]

4.9 Feeding rate

Particle feed rate has an important role to play in the quality of the final cast composite. For proper mixing and distribution of the reinforced particles in the matrix, feed rate is to be taken care of. Clustering of the particles may occur, if the feed rate is non uniform and this may lead to inclusion defect. Usually, the reinforcements are fed to the center of the vortex created by the mechanical stirrer. Feeder should be designed in such a way that the feed rate is neither too high nor too low to allow continuous flow of the particles. High feeding rate may lead to the accumulation of particles in the composite whereas a low feed rate may lead to lump formation of the reinforcement particles. An optimal feeding rate as per studies was found to be between 0.8-1.5 g/s. This resulted in preventing the accumulation of reinforcements in the composite and thereby achieving uniform distribution of particles in the final composite [39,40,41]. Different types of feeding techniques have been employed to feed the reinforcement particles to the matrix. In normal feeding techniques, the reinforcement particles are simply added to the matrix material in its molten state. Apart from the regular feeding, two feeding method is also in usage. Here the matrix material is preheated and the reinforcement particles are added to the matrix melt. In the second stage, a piece of Aluminium alloy and reinforcement particles are added to the molten metal. The matrix metal as well as the reinforcement particles like ceramics are added at the same

time in pre-melt feeding method. Whereas in capsulated feeding technique, an Aluminium sheet is used to cover the ceramic particles as a capsule and is preheated for about 350 oC. In the second stage, this capsule is added to the molten matrix material. A layer by layer feeding technique called double layer feeding technique is used, where the matrix material is placed as a layer at the bottom of the furnace and on top of it, a layer of reinforcement material is added and then a layer of matrix material is again placed on top of this filler material. From a study conducted by Prakash et al,[42] it was concluded that among different techniques adopted, the double layer feeding technique gave better feeding option and this ensured an improved bonding between the matrix material and the ceramics. This feeding method gave reduced porosity, lesser clustering and agglomeration of particles. An increase in the Ultimate tensile strength, yield strength and microhardness of the final casting was also obtained.

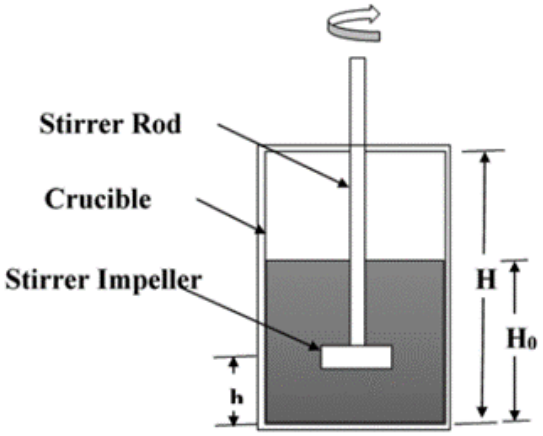

Figure 5. Position of stirrer impeller in crucible [16]

4.10 Position of stirrer

The position of the stirrer should be well taken care of to get better efficiency of the stir casting process. A study conducted by Nagata [43] revealed that, the stirrer impeller should be placed below 30% of the melt height from the bottom of the crucible, in order to avoid the clustering of the particles at the bottom of the furnace [43]. This result was agreed by the simulations done by J.Hashim et al,[39] that in order to obtain better turbulence in the melt, it is essential for the stirrer blade to be kept at 0.1 and 0.7 of the melt height. The required vortex motion will not be obtained if the blade is placed very close to the bottom of the crucible. In such a case, the effect of stirring can only be experienced at the bottom portion of the crucible [39]. A relation given in the equation (3) has been formed between the height of the impeller (h) from the bottom of the crucible [39] (Figure 5).

$$h \geq 0.3H_0 \tag{3}$$

here H_0 is the height of the fluid.

5 Conclusion

This review paper covers the importance of the stirring parameters, affecting the properties of the final cast composite as per the requirements of the industry. The following conclusions can be made from the above studies.

(1) The impeller should be placed at not more than 30% of the melt height to obtain better incorporation of the reinforcement particles to the melt.
(2) In order to achieve better shearing action and axial flow, it is necessary to maintain the blade angle at 30 o. This will ensure lower power consumption.
(3) The stirring speed ranges from 200 to 1000 rpm, and this may vary depending upon the type of reinforcement, matrix material and chemical properties. This varies for single stage impellers and multi stage impellers. The stirring time from different studies showed that , an optimal stirring time as 10 mins for a uniform distribution of the filler material in the matrix.
(4) Wettability of the reinforcement particles in the matrix should be well taken care of to avoid clustering or accumulation of the particles in the matrix.
(5) A pitched blade stirrer is more preferred than propeller type as it causes a smooth vortex motion because of its unique flow design pattern causing mixed flow ie., both axial and radial directions, thereby allowing better incorporation of the reinforcement particles in the matrix.
(6) An optimal reinforcement preheat temperature was obtained at 500 °C for a time of 30 mins. This resulted in better wettability between the particles.
(7)A Feed rate of 0.9–1.5 g/s is better suited to avoid the clustering of reinforcement particles.

References

[1] A. Kumar, S. Kumar, N.K. Mukhopadhyay, “Effect of SiC Reinforcement and Its Variation on the Mechanical Characteristics of AZ91 Composites”, Materials 13-21 (2020) 4913.

[2] Singh J, Chauhan A. “Characterization of hybrid Aluminium matrix composites for advanced applications – A review”. Journal of Materials Research and Technology. 2016; 5:159-169.

[3] Ravi KR, Sreekumar VM, Pillai RM. “Optimiza-

tion of mixing parameters through a water model for metal matrix composites synthesis". Materials and Design. 2007 :871- 881.

[4] Surappa MK. "Aluminium matrix composites: Challenges and opportunities".2003;319-334. DOI: 10.1007/BF02717141

[5] Suresha S, Sridhara BK. "Wear characteristics of hybrid aluminium matrix composites reinforced with graphite and silicon carbide particulates". Composites Science and Technology.2010;1652-1659. DOI: 10.1016/j.compscitech.2010.06.013

[6] Rajmohan T, Palanikumar K, Ranganathan S. "Evaluation of mechanical and wear properties of hybrid aluminium matrix composites". Transactions of the Nonferrous Metals Society of China. 2013;2509-2517.

[7] Sahu MK, Valarmathi A, Baskaran S, Anandakrishnan V, Pandey RK. "Multi-objective optimization of upsetting parameters of Al-TiC metal matrix composites: A grey Taguchi approach". Proceedings of the Institution of Mechanical Engineers, Part B: Journal of Engineering Manufacture. 2014; 228:1501-1507.

[8] S. Soltani, R. Azari Khosroshahi, R. Taherzadeh Mousavian, Z.-Y. Jiang, A. Fadavi Boostani, D. Brabazon, "Stir casting process for manufacture of Al–SiC composites", Rare Metals 36 ;7: (2017) 581–590.

[9] V.S. Srivastava, T.K. Gupta, A.K. Srivastava, S. Chauhan, P.K. Chauhan, "Effects of cutting parameters on aluminium alloys-A review" , Materials Today : Proceedings, 2021.

[10] D. K. Koli, G. Agnihotri, and R. Purohit, "Properties and Characterization of Al-Al2O3 Composites Processed by Casting and Powder Metallurgy Routes-Review" , International journal of Latest Trends in Engineering Technology,2013 , vol. 2, no. 4, 486–496.

[11] K. M. S. Manu, L. A. Raag, T. P. D. Rajan, M. Gupta, and B. C. Pai, "Liquid Metal Infiltration Processing of Metallic Composites: A Critical Review", Metallic Material Transition. B, no. Metal matrix composites, 2016.

[12] M. T. Sijo and K. R. Jayadevan, "Analysis of stir cast aluminium silicon carbide metal matrix composite: A comprehensive review", Procedia Technology, vol. 24, 2016, 379–385.

[13] W. C. Harrigan, "Commercial processing of metal matrix composites", Material Science and Engineering. A, vol. 244, 1998, 75–79.

[14] S. Kumar, A. Yadav, V. Patel, B. Nahak, A. Kumar, "Mechanical behaviour of SiC particulate reinforced Cu alloy-based metal matrix composite", Materials Today Proceedings 41 ,2021, 186–190.

[15] M.E. Turan, M. Rashad, H. Zengin, I. Topcu, Y. Sun, M. Asif, "Effect of Multiwalled Carbon Nanotubes on Elevated Temperature Tensile and Wear Behavior of Al-2024 Matrix Composites Fabricated by Stir Casting and Hot Extrusion", Journal of Materials Engineering and Performance, 2020 , 5227–5237.

[16] M. K. Sahu and R. K. Sahu, "Fabrication of Aluminum Matrix Composites by Stir Casting Technique and Stirring Process Parameters Optimization", Intechopen , London, UK, 2018.

[17] R. M. Pillai, "Review Role of magnesium in cast aluminium alloy matrix composites", Journal of material science, vol. 30, 2014. 1903–1911.

[18] O. F. Materials, "The wettability and the reaction for SiC particle/Al alloy system", Journal of material science, vol. 28, 1993, 684–690.

[19] L. Poovazhagan, K. Rajkumar, P. Saravanamuthukumar, S. Javed Syed Ibrahim, and S. Santhosh, "Effect of Magnesium Addition on Processing the Al-0.8 Mg-0.7 Si/SiC Metal Matrix Composites", Application of mechanical materials, vol. 787, 2015, 553–557.

[20] A. Baradeswaran and A. E. Perumal, "Influence of B 4 C on the tribological and mechanical properties of Al 7075–B4C composites", Composites. Part B, vol. 54, 2013, 146–152

[21] Rao,E.S. and Ramanaiah, N., "Intermetallic reinforced boron carbide composites produced through stir casting processing". Composite Materials: An International Journal, Vol. 1(2),2016, 58-66.

[22] Prabu, S.B, Karunamoorthy, L.; Kathiresan, S., Mohan, B. "Influence of stirring speed and stirring time on distribution of particles in cast metal matrix composite". Journal of material processing and technology, 2006, 268–273.

[23] Sajjadi, S.A, Ezatpour, H.R, Beygi, H. "Microstructure and mechanical properties of Al–Al_2O_3 micro and nano composites fabricated by stir casting". Material science Engineering. 2011, 528, 8765–8771.

[24] Pai, B, Ramani, G., Pillai, R., Satyanarayana, K. "Role of magnesium in cast aluminium alloy matrix composites". Journal of material science and Engineering,1995, 30, pp :1903–1911.

[25] Qin An, Xiao-shuang Cong, Shen Ping., Jiang Qui Chuan. "Roles of alloying elements in wetting of SiC by Al". Journal of Alloys and compounds. 2019, 784, 1212–1220

[26] Shao N, Dai J W, Li. G.Y, Nakae H, Hane T, "Effect of La on the wettability of Al_2O_3 by molten Aluminium". Materials letters; 2004, 58, 2041–2044

[27] Qian-Gang Xu, Li-Wei Guo, Li Zhang.; Hong Liu. "Wettability of zirconium-coated alumina by molten Aluminium". Surface and coatings technology, 2016, 302, 150–157

[28] Kennedy A, Wood J, Weager B, "The wetting and spontaneous infiltration of ceramics by molten copper". Journal of material science and engineering, 2000, 2909–2912.

[29] Shuaihang Pan, Zeyi Guan., Gongcheng Yao, Yuan Jie; Xiaochun Li. "Mo-enhanced chemical stability of TiC nanoparticles in molten Al". Journal of Alloys and Compounds. 2021, 856, 158-169.

[30] Malaki M.,Fadaei Tehrani, A., Niroumand B., Gupta Manoj, "Wettability in Metal Matrix Composites". Metals, 2021, 11(7), 1034.

[31] S. S. S. T. S. J. Dattatraya, N. Lawate, "study of process parameters in stir casting method for production of particulate composite plate", international journal of innovations in engineering research and technology [IJIERT], vol. 3, 1-5, 2016.

[32] S Vishal Shankar Srivastava, Tarun Kumar Gupta , Akash Nigam,. "Study of stirrer speed and preheat temperature on stir cast aluminium matrix composite materials – A review", Article in Materials Today, Proceedings, July 2021

[33] S. Suresha and B. K. Sridhara,. "Effect of silicon carbide particulates on wear resistance of graphitic Aluminium matrix composites", Materials and Design , vol. 31, 2010, 4470–4477.

[34] Edward L. Paul, Victor A. Atiemo-Obeng, and Suzanne M. Kresta, 2004. Handbook of industrial mixing. New Jersey, John Wiley & Sons,

[35] S. Naher, D. Brabazon, and L. Looney, " Simulation of the stir casting process", vol. 144, 2003, 567–571.

[36] Abdel rahman Elsayed , Adel Nofal , Galal Attia, "Optimization of Stir Casting Process Parameters for Producing MMC Aluminium Sacrificial Anode Incorporated with Manganese Dioxide Concentrate Powder" ,International Journal of Engineering Research and Technology,Volume 13, no.10, 2020, 2651-2659

[37] Lu J, Lu Z. "Optimization of stirring parameters through numerical simulation for the preparation of Aluminium matrix composite by stir casting process". Journal of Manufacturing Science and Engineering, 2010, 1-7

[38] Vijaya Ramnath B, Elanchezhian C, Jaivignesh M, Rajesh S, Parswajinan C, Siddique Ahmed Ghias A. "Evaluation of mechanical properties of aluminium alloy–alumina– boron carbide metal matrix composites". Materials and Design. 2014;332-338.

[39] Hashim J, Looney L, Hashmi MSJ. Particle distribution in cast metal matrix composites— Part II. Journal of Materials Processing Technology. 2002., 258-263.

[40] Baradeswaran A, Vettivel SC, Elaya Perumal A, Selvakumar N, Franklin Issac R. "Experimental investigation on mechanical behaviour, modelling and optimization of wear parameters of B_4C and graphite reinforced Aluminium hybrid composites". Materials and Design. 2014; 620-632.

[41] Auradi V, Rajesh GL, Kori SA. "Processing of B_4C particulate reinforced 6061Aluminum matrix composites by melt stirring involving two-step addition". Procedia Materials Science. 2014;1068-1076.

[42] S. Prakash, R. Sasikumar, Elango Natarajan, B. Suresha, "Influence of Feeding Techniques in Bottom Tapping Stir Casting Process for Fabrication of Alumina Nano-filler-reinforced Aluminium Composites", The Indian Institute of Metals - IIM 2020

[43] S. Nagata, Mixing-principles and applications. New York, Wiley,1976

Retrofitting Of Internal Combustion Vehicle to Electric Vehicle and MATLAB-Simulink Analysis

Dr.Vinod V, Amal Pious, Anirudh M, Arjun S, Dhanush Babu, Mohammed Razal Rafeeq, Muraleekrishnan S, Pranav A, P Yadukrishnan

NSS College of Engineering,Palakkad,678008,Kerala,India

Abstract -

This initiative focuses on converting a conventional Internal Combustion Engine (ICE) vehicle into an Electric Vehicle (EV). An EV is an automobile that is propelled by one or more electric motors, relying solely on energy stored in batteries. Compared to ICE vehicles, electric cars offer advantages such as quieter operation, improved performance, low maintenance costs, and zero exhaust emissions. Replacing ICE cars with EVs brings numerous benefits, including a significant reduction in local air pollution by eliminating the emission of pollutants like carbon monoxide, hydrocarbons, ozone, lead, and nitrogen oxides. To evaluate the performance characteristics of the converted EV, a simulation is conducted using MATLAB Simulink, and the results are compared with real-time data.

Keywords -

BLDC Motor, Lead Acid Battery, Retrofitting, MATLAB;

1 Introduction

In order to achieve India's goal of reaching net-zero carbon emissions by 2050, merely purchasing electric vehicles (EVs) will not be sufficient. Retrofitting offers a potential solution to address the urgent global climate emergency. Retrofitting involves utilizing a conventional vehicle as a foundation for constructing an electric vehicle. The process begins with a meticulous project that thoroughly analyzes the dimensions, weights, and potential obstacles associated with integrating specific components into a particular vehicle model. The Indian government has taken a step towards promoting this approach by legalizing electric conversion kits for gasoline vehicles through an amendment implemented by ARAI in September 2018. During the retrofitting process, the original engine and associated components of the vehicle are replaced, and a new alternative energy source is integrated into the existing vehicle frame. This allows individuals to continue using their valuable vehicles instead of having them discarded, which is both cost-effective and environmentally beneficial. However, it is essential to ensure that the retrofit kit has obtained approval from a designated testing agency as outlined in rule 126 of CMVR 1989.

2 Literature study

Electric vehicles (EVs) have gained significant attention due to their efficiency and cost-effectiveness in comparison to traditional petrol or diesel vehicles.[1] To retrofit existing vehicles, previous studies focused on connecting electric motors directly to the vehicle's differential.[2] While this approach facilitated weight reduction, it presented certain limitations, such as the need for a more powerful motor, a fixed gear ratio, and limited top speed.[3] This study aims to rectify these shortcomings by proposing a retrofitting process that integrates the electric motor with the existing gearbox, thus reducing fabrication requirements. By utilizing gearboxes, the advantages include the ability to employ lower-power motors and adjust gear ratios to suit different driving situations. In addition, the implementation of brushless DC (BLDC) motors offers affordability, enhanced power control, and reduced maintenance.[5] The sizing of the motor is accomplished through the use of MATLAB Simulink software, which determines the appropriate motor capacity based on the vehicle's specifications.[6]

3 Methods

Retrofitting a Ford Ikon 2006, weighing 1 ton car converted into a BLDC motor-powered car involves several steps and considerations. To determine the power and torque necessary to propel the motor, MATLAB-Simulink software was utilized. A simulation was conducted, neglecting air resistance and aerodynamic forces, to obtain accurate results. The simulation results indicated that a 4.5kW motor, powered by a 60V lead acid battery supply, was sufficient to meet the required torque for propelling the vehicle. These findings provide valuable insights into the powertrain requirements for retrofitting the Ford Ikon into an electric vehicle. Further research and experimentation could focus on incorporating additional factors, such as air resistance and aerodynamic considerations, to refine the retrofitting process and optimize the performance of the converted vehicle. Here are the details for the retrofitting process

3.1 Process Planning

This research aims to conduct a thorough assessment of the Ford Ikon 2006 car during the planning phase of an electric vehicle conversion project. The assessment includes analyzing the car's dimensions, weights, and structural integrity. Furthermore, a suitable 4.5kW BLDC motor is researched and selected, taking into account power requirements and dimensions. Finally, the appropriate battery capacity and type required to power the BLDC motor efficiently are determined.

3.1.1 Motor and Powertrain Integration

The first phase involves the removal of the internal combustion engine (ICE) and associated components, making way for the integration of a Brushless DC (BLDC) motor. Compatibility with the Ford Ikon's transmission system is ensured, and necessary modifications are made for seamless integration. The BLDC motor is then installed in the engine bay, aligning it with the vehicle's drivetrain.

3.1.2 Battery System Installation

Selected a suitable battery type, 70 AH 12V Lead acid connected in series to obtain a combined voltage of 60V.We determine the optimal placement of the battery pack in the vehicle, considering weight distribution and available space and we placed the battery packs in the boot of the vehicle

3.1.3 Control and Power Management

As the final step, we Incorporated an electronic motor controller to regulate the BLDC motor's speed, torque, and direction. Then connected the motor controller to the vehicle's control system, such as the throttle pedal and brake system, for smooth acceleration

3.2 Components

The components used in retrofitting are described below:

3.2.1 BLDC Motor

A BLDC (Brushless DC) motor is a type of motor that operates using direct current and utilizes electronic commutation to achieve continuous rotation.BLDC motors offer numerous advantages over traditional brushed motors, including higher efficiency, longer lifespan, and reduced maintenance requirements. They operate using electronic commutation rather than brushes, resulting in smoother operation and lower electrical noise. With their compact size and high power-to-weight ratio, BLDC motors are commonly used in various applications, including electric vehicles, robotics, industrial automation, and renewable energy systems. Their precise control, reliability, and power output make them a popular choice for demanding applications requiring efficient and dependable motor performance. Within the retrofitting process, a 4.5KW Brushless DC (BLDC) motor is employed, characterized by its exceptional performance specifications. This motor exhibits a maximum rotational speed of 4000 rpm, while under loaded conditions it operates at 3000 rpm. When connected to a 60V power supply, the BLDC motor generates a maximum torque of 16.8m, and this torque value is 12.8Nm when connected to a 48V supply.

Figure 1. BLDC Motor

3.2.2 Motor Power Controller

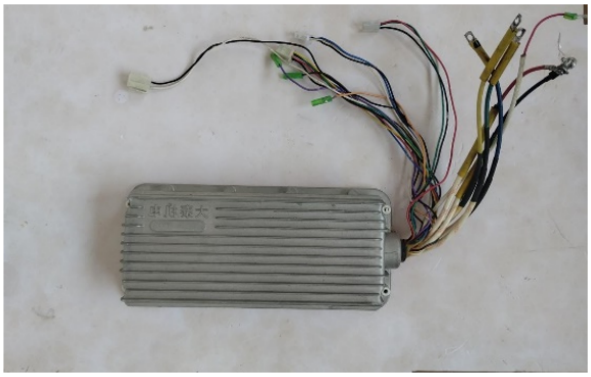

Figure 2. Motor power controller

To control the power and operation of a BLDC motor, a motor controller is specifically designed for BLDC motors is used. The motor controller is responsible for regulating the speed, direction, and other parameters of the motor based on the input signals it receives

Figure 3. Foot Operated Electric Throttle Accelerator

3.2.3 Foot Operated Electric Throttle Accelerator

A foot-operated electric throttle accelerator, also known as an electronic throttle controller or electronic accelerator pedal, is a device used in vehicles to control the throttle opening and acceleration. It replaces the traditional mechanical linkage between the accelerator pedal and the throttle body with an electronic system. Instead of a physical cable, the foot-operated electric throttle accelerator uses sensors and electronic signals to transmit the driver's input to the BLDC motor power controller.

3.2.4 Lead Acid Battery

Figure 4. Lead Acid Battery

A lead-acid battery is a type of rechargeable battery that uses a chemical reaction between lead, lead dioxide, and sulfuric acid to store and release electrical energy. Lead-acid batteries have been widely used for various applications due to their relatively low cost and robustness. The chosen battery was a 70 AH 12V Lead acid batteries connected in series to obtain a output voltage of 60V.

3.2.5 Love joy coupling

Figure 5. Love joy coupling

When connecting a BLDC motor to a gearbox, a coupling is used to transmit torque and rotational motion between the motor shaft and the gearbox input shaft. The coupling ensures proper alignment and minimizes misalignment-induced stresses on the motor and gearbox components. The selection of the coupling depends on factors such as the torque requirements, misalignment tolerance, speed, and specific application needs.

3.3 MATLAB Simulation

Simulation plays a significant role in the development, analysis, and optimization of electric vehicles. It enables performance evaluation, battery and energy management, powertrain design, range estimation. Simulation helps in modeling of EV before actually prototyping it and modifications can be easily made in simulation. We have modelled a simple EV power train and simulated it with actual forces and resistance the vehicle has to endure in real world scenarios. We have coupled it with blocks such as vehicle body, tires, etc., in order to include data such as wheel friction, input power, battery parameters etc. We are testing how we can utilize MATLAB Simulink to simulate different scenarios. The drive cycle which is available in the default setting is an FTP 75, which is a mandatory dynamometer test used as an industry standard. FTP 75 are series of tests defined by US Environmental Protection Agency to measure tailpipe emissions and fuel economy of passenger cars. The high and low velocity makes it a good drive cycle to check the parameters of the drivetrain. The FTP75 drive cycle is shown below:

3.3.1 Simulation Diagram

We modelled a electric vehicle of weight 1000kg because the car we have chosen Ford Ikon has a kerb weight

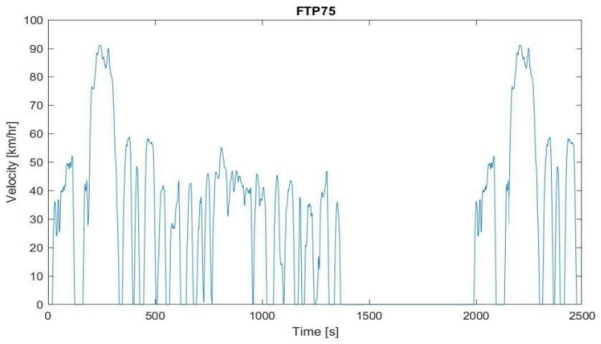

Figure 6. Input Drive Cycle.

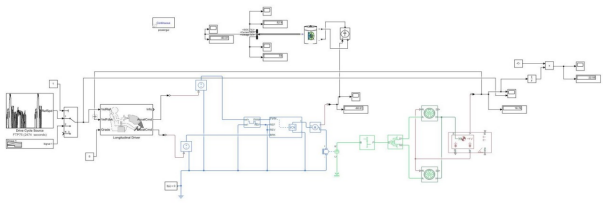

Figure 7. Simulation Diagram.

of 998kg, which runs on a 4.5 KW BLDC motor and energy for propulsion is provided by a 100AH 48V.The drive cycle used for testing is FTP75, is a mandatory dynamometer testing cycle. State of Charge, range, speed, current variation,voltage variation etc. are obtained as output for the given drive cycle. Aerodynamic forces and wind resistance are neglected during our testing. If these are taken into consideration these values can be entered to the vehicle body component in the MATLAB-Software.

3.4 Results of simulation

3.4.1 State of Charge (SoC)

The state of charge (SOC) is a measurement of the amount of energy available in a battery at a specific point in time expressed as a percentage. On inputting the FTP75 drive cycle for 2474 seconds, the charge dissipates to 48% of battery capacity.

3.4.2 Speed(km/hr)

As shown in the graph maximum speed obtained is 62km/hr. From 1500 seconds to 2000 seconds the vehicle is in stationary condition therefore the speed during that period is zero.

3.4.3 Range(km)

Range test is performed for 2474 seconds. EV has a range of 23km by using approximately half the power of battery. Therefore, approximate total range of EV is almost 46km.

3.4.4 Current

As shown in the graph the current fluctuates throughout the driving cycle due to changing input driving condition and when the car is in idle condition, the current supplied becomes steady and obtains a linear line. The peak points indicate the high requirement for electric current to start the vehicle from rest condition.

3.4.5 Voltage.

As shown in the graph, the voltage decreases throughout the driving cycle which signifies that the battery is being discharged to power the electric motor. The peak drop after 2000 seconds is due to the sudden acceleration of the motor from stationary condition.

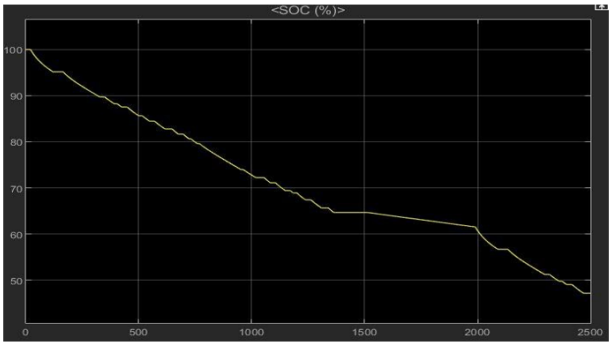

Figure 8. Soc (%) vs Time(s)

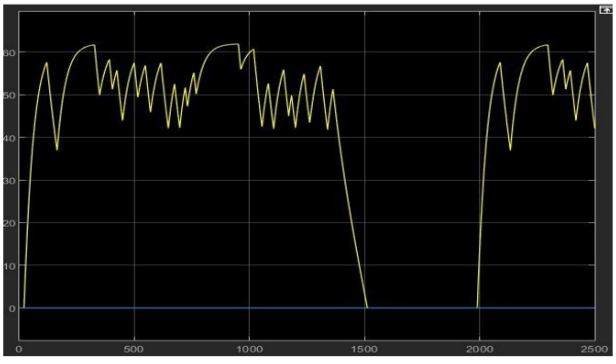

Figure 9. Speed(km/hr) vs Time(s)

4 Results and Discussion

The retrofitting of a 4.5 kW BLDC motor into the Ford Ikon 2006 model was carried out successfully, involving

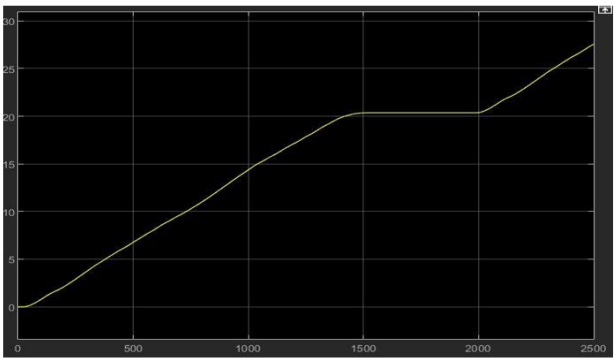

Figure 10. Range (km) vs Time (s)

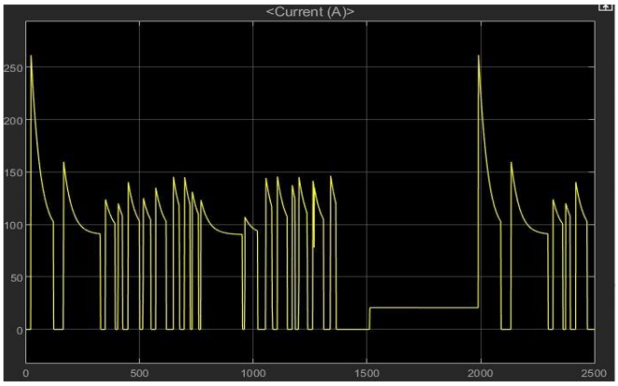

Figure 11. Current(A) vs Time(s)

the removal of the internal combustion engine and its substitution with the BLDC motor. The motor was seamlessly coupled with the existing gearbox. In the retrofitting pro-

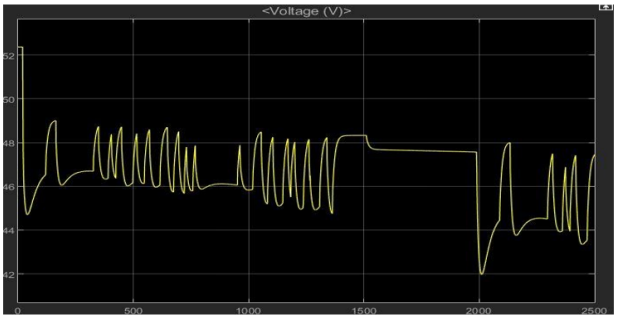

Figure 12. Voltage (V) vs Time(s)

cess, the BLDC motor is seamlessly connected to the gearbox using a Lovejoy coupling. The motor is subsequently linked to a power controller, which offers the capability to incorporate an ignition switch, electronic accelerator, and reverse switch. These connections exemplify the effective integration of components in the retrofitting procedure. The powertrain for propulsion in this retrofitting project

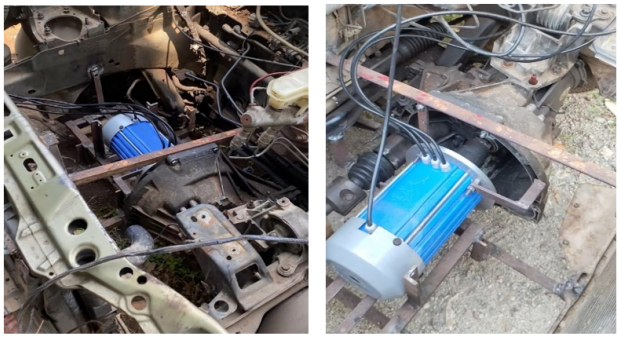

Figure 13. Motor Connection setup

utilizes a series connection of five 70AH 12V batteries, resulting in a 60V supply. This voltage selection is preferred over a 48V supply due to its ability to generate higher torque in the motor. The ignition switch serves as the initial step to activate the powertrain, allowing for gear shifting and subsequent motor acceleration. The foot accelerator serves as a responsive input, controlling the rotation speed of the motor based on acceleration demand.

5 Conclusion

TStep-by-step analytical calculation of Electric Vehicle (EV) was presented in this paper. Based on the analytical calculation, EV was modelled in MATLAB-Simulink environment. The simulation results are summarized. The drive cycle used for testing is FTP75, is a mandatory dynamometer testing cycle. State of Charge, range, speed, current variation, voltage variation etc. are obtained as output for the given drive cycle. Battery discharges from 100% to 23%, when vehicle runs for 3600 seconds. The maximum speed of the simulated model is 63kmph.On running the vehicle through the drive cycle for 2747 seconds, Vehicle consumed 52% of its total battery charge and obtained a maximum range of 23 kms. Therefore, approximate maximum range of our model is around 45 kms. In the simulation aerodynamic forces and wind resistances are neglected during test. Road inclination is assumed zero. Because we consider testing the model on a straight road. If we consider the road inclinations, range and top speed decreases and power consumption increases. The peak points in current vs time graph indicate the high current requirement of motor to start from rest. Retrofitting has been successfully completed and test runs were performed to check the stability of the motor and frame. Retrofitted vehicle easily achieved the top speed of 35- 40 kmph on the first gear. We made use of 1st,2nd and reverse gear according to our power and torque requirements

Acknowledgements

Any attempt at any level cannot be satisfactorily completed without the support and guidance of learned people. We owe to great many people whose constant support and motivation that has encouraged us to come up with this Project. We are greatly obliged to Dr. Vinod V, Dr. Rajeev N, Dr. Aneesh Kumar P , Madhu Mohan ,Department of Mechanical Engineering, for the encouragement and support that he has provided. We are deeply grateful to Mr. Muralidharan TV and Mrs. Rani for believing in our project and their willingness to support us by providing the car. We also extend our gratitude towards Mr. Sathish, Positive Business Solutions, Palakkad, Mr. Navin CC Megh Neel motors, Coimbatore for their support.

References

[1] Fabian Hoeft;Internal combustion engine to electric vehicle retrofitting: Potential customer's needs, public . . , perception, and business model implications; Transportation research interdisciplinary perspectives 9,2021,1-8

[2] Agus PurwadiJimmy DozenoNana Heryana ,Testing Performance of 10 kW BLDC Motor and LiFePO4 Battery on ITB-1 Electric Car Prototype,Procedia technocology.Volume 13-2013,1075-1081.

[3] Delfim Pedrosa, Vítor Monteiro, Henrique Gonçalves, Júlio S. Martins, João L. Afonso."A Case Study on the . Conversion of an Internal Combustion Engine Vehicle into an Electric Vehicle". IEEE Powered and propulsion .. . . . .conference.Portugal October 2014,1-10.

[4] Susumu SatoYu Jade JiangRobert L. RussellJ. Wayne MillerGeorgios KaravalakisThomas D. DurbinKent C. Johnson .Experimental driving performance evaluation of battery-powered mediumand heavy duty all-electric vehicles.International journal of electric power and energy systems .Volume 141- 2012,100-108

[5] Tahir Aja Zarma, Ahmadu Adamu Galadima, Maruf A Aminu, A Review of Motors for Electric Vehicle; Nile university of Nigeria, Abuja,2017,1-4

[6] Hitesh S1, C. Sunanda.Modeling and Performance Analysis of an Electric Vehicle with MATLAB/Simulink . . International Research Journal of Engineering and Technology (IRJET)-June2020,1098-1104

Design And Fabrication Of Electric Vehicle Specific Test Rig And Testing

Dr.Vinod V , Mohammed Razal Rafeeq , Muraleekrishnan S , Pranav A and P Yadukrishnan

NSS College of Engineering,Palakkad,678008,Kerala,India

Abstract -

This initiative focuses on designing an electric vehicle test rig to conduct various test on the electric vehicle to find the electrical energy consumption of the vehicle. For this we designed an electric vehicle specific chassis dynamometer to apply various loads to the drive wheels of the vehicle. In this chassis dynamometer hydraulic braking system of the vehicle undergoing testing is implemented as the loading system in the dynamometer. Various loads are applied on the brake pedal of dynamometer that may be acted on the vehicle during different driving conditions and measure the energy consumption of the electric vehicle by measuring the voltage current and state of charge of the electric vehicle battery. After these tests we can arrive at the amount of energy consumed by the electric vehicle for different drive conditions. By this we can generate the real time range and this can resolve range anxiety issues of the electric vehicle owners which is one of the problems facing by the popularity of electric vehicles in the market.

Keywords -

Chassis Dynamometer, EV Testing, EV Test Rig, Energy Consumption.

1 Introduction

An electric vehicle (EV) chassis dynamometer is a testing device that allows engineers to evaluate the performance and efficiency of an EV by simulating real-world driving conditions in a controlled laboratory setting. The EV is mounted onto the dynamometer, consisting of a platform that rotates to simulate the vehicle's motion. The load on the EV is applied through hydraulic brakes, which provide precise and consistent resistance to the vehicle's wheels. During testing, the EV is driven at a variety of speeds and loads to simulate different driving conditions, such as uphill and downhill grades, acceleration and deceleration, and highway and city driving. The dynamometer measures a variety of parameters, including the EV's voltage, current, power output, energy consumption, and efficiency. This information is used to optimize the EV's performance and identify any issues that may need to be addressed. Chassis dynamometer testing is a key part of the EV development process, as it allows engineers to fine-tune the vehicle's design and ensure that it meets performance and efficiency targets.

2 Methods

2.1 LITERATURE STUDY

2.1.1 Suraj Kothale, V.P Jagtap, C.S. Choudhari: Design of Chassis Dynamometer for light motor vehicle of service stations (2016);

This journal paper is about design of chassis dynamometer for lightweight vehicles. Here the dynamometer works as an energy absorption device. It could only be used to conduct basic tests like acceleration between two-speed points, maximum speed test, different gears speed test, load test and fuel consumption test.

2.1.2 Fabrico Leonardo Silva, Fabio Mazzariol Santiciolli, Ludmila C.A. Silva.; Vehicle and twin-roller chassis dynamometer model considering slip tire interactions (2022)

This journal paper is about showcasing the design of disc brake system, force acting on the pad of the brake from the fluid from the wheel cylinder, how much the force is getting multiplied from brake pedal to wheel cylinder and the force analysis.

2.1.3 Agus Purwadi, Jimmy Dozeno, Nana Heryana; Testing performance of a 10KW BLDC motor and LiFePO4 Battery on ITB-1 electric prototype (2013)

This journal paper is about the fabrication of a electric car prototype with a 10Kw BLDC motor are explained, in this paper a 10KW BLDC motor and its energy storage that is LiFePO4 will be evaluated based on the performance results based on the tests.

2.2 DESIGN OF ELECTRIC VECHICLE TEST RIG

A specialized test rig for electric vehicles, specifically designed for testing a retrofitted Ford Ikon. To ensure accuracy and relevance, the dimensions of the test rig should match those of the vehicle. In this case, the Ford Ikon has a width of 1560mm, and a clearance of 10mm is provided to accommodate any protrusions. The wheelbase, which is the distance between the front and rear axles, is 2486mm. The tire width is 190mm. Considering safety concerns

and the maximum load of the converted electric vehicle, which is approximately 1000kg, the test rig is designed to bear a load of 1500kg. This ensures a sufficient safety margin. To facilitate testing, a ramp is incorporated into the design. The ramp is elevated 366mm above the ground level, providing the necessary clearance for the vehicle to climb onto it. For easy vehicle maneuverability, the ramp is inclined at an angle of 25 degrees with respect to the ground level.

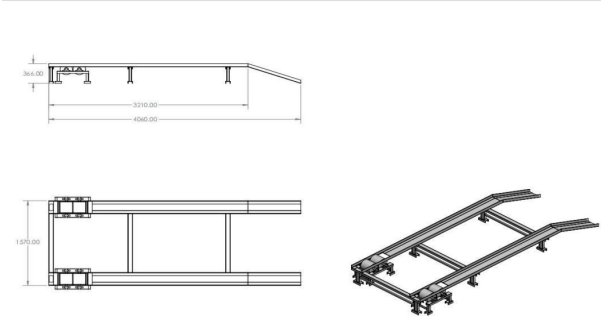

Figure 1. Design of electric vehicle test rig.

2.3 FORCE ANALYSIS OF TEST RIG

As the vehicle undergoing testing which is a retrofitted ford ikon which weigh around 1000kg. By considering the safety concerns a 1500 kg load is applied and distributed equally through the four wheels of the vehicle. As the front wheel ie, the drive wheels are placed on the roller and the back wheels are 2486mm behind front wheels the load is acted uniformly as point loads in these four points.

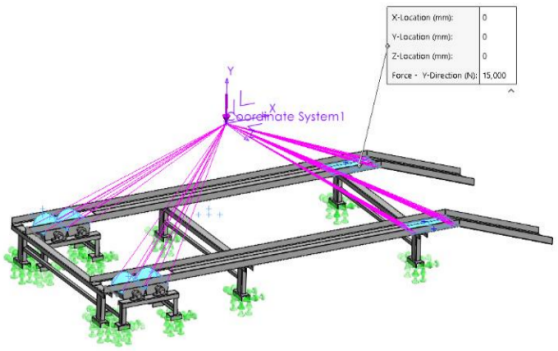

Figure 2. Load distribution on the test rig.

The entire 3D model is modeled in solid works software 2022. mild steel is the material used for the entire

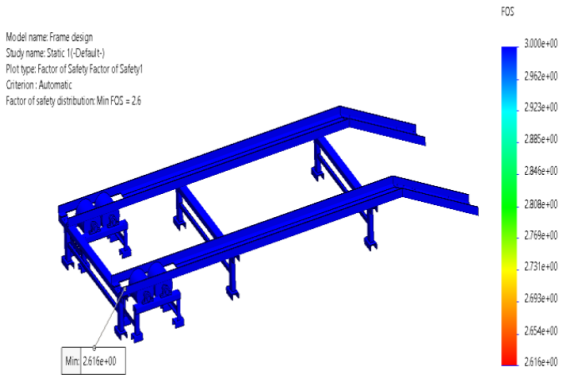

Figure 3. Factor of safety analysis

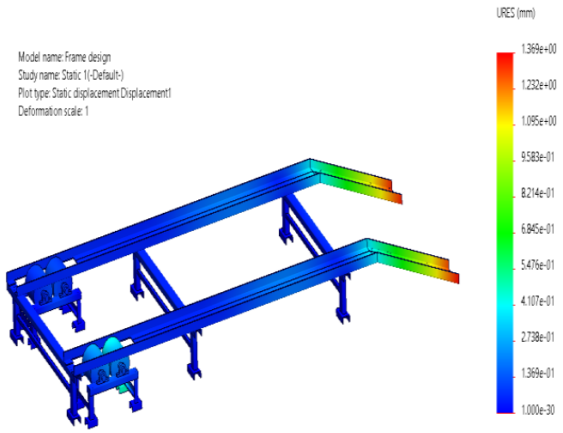

Figure 4. Deformation analysis.

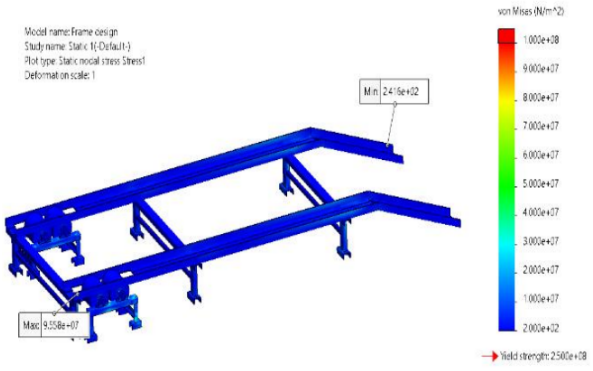

Figure 5. Stress analysis

model. Static stimulation study is assumed for this analysis.Assume boundary conditions, the boundary conditions are set on the basis that the front two wheels or the drive

wheels are placed on the center of two rollers and the rear wheel is 2450mm behind the front wheels. Therefore the force is applied on four points uniformly, where the wheel come in contact with the ramp. all the base frames are fixed and remote load of 15000 N is applied As the total force applied by the testing vehicle and the solution is solved using solid works simulation. As per the simulation three results are obtained one is total deformation another one is von mises stresses and last one is safety factor. From the deformation analysis it is evident that model undergoes very less deformation, the maximum deformation occurred is 1.369mm the result of deformation analysis is shown in fig 4.7.from the von mises stresses it is noted that the maximum stress value is below the yield stress value of the entire model, the maximum stress value obtained for the model is 9.558e+07 N/m2 and minimum value is 2.416e+02 N/m2 and the yield strength value is 2.500e+08 N/m2 the result of stress analysis is shown in fig 4.6. from the factor safety analysis it is evident that the factor of safety for the entire model is above 3 and the minimum value of factor of safety obtained is 2.668.

2.4 TESTING

The retrofitted ford ikon is to be tested in the electric vehicle specific test rig. For this the vehicle is placed on the test rig with proper alignment of the rollers of the test rig. After placing the vehicle on the test rig proper electric connections where made according to the circuit diagram. Mainly concentrated on two types of tests that is constant rpm test at various loads and constant load test at various rpm. Here we are conducting all the tests in the first gear as it produces more torques and all the other gears doesn't consume that much energy as in the first gear. Here we are taking readings corresponding to 100-400 rpm at 4 diffferent loads including no load condition. At a constant rpm 0,200,600 and 800 Newtons of load is applied by the brake to resist the motion of the vehicle. And these tests are repeated among several rpms.

Figure 6. Testing setup

3 Results and Discussion

3.1 Constant RPM test

3.1.1 No Load to 800 N at 100 RPM

Variation and relationship of the load applied to the voltage, current, power and energy consumption corresponding to the 100 rpm were found and tabulated and according to their relationship graphs were plotted as shown below.

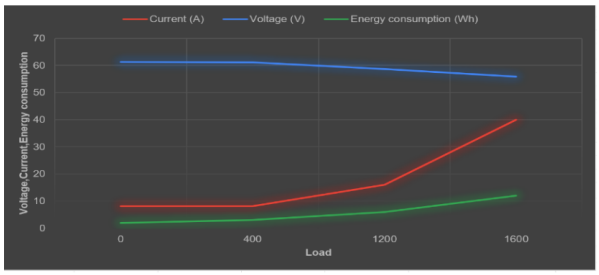

Figure 7. Relation between Voltage, Current and Energy consumption with Load.

3.1.2 No load to 800 N at 200 RPM

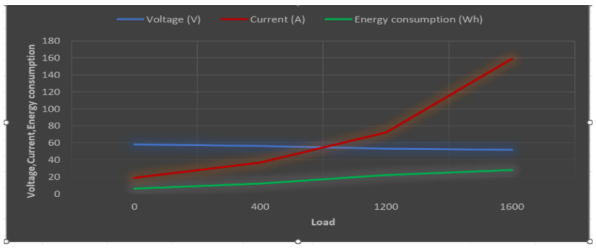

Figure 8. Relation between Voltage, Current and Energy consumption with Load.

3.1.3 No load to 800N at 300 RPM

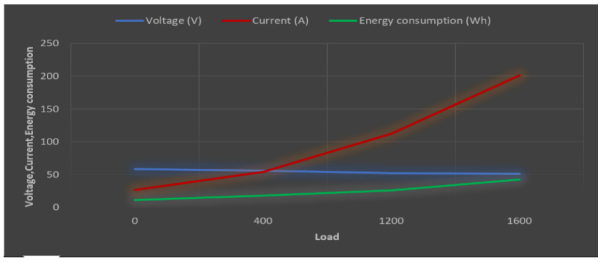

Figure 9. Relation between Voltage, Current and Energy consumption with Load.

3.1.4 No load to 800 N at 400 RPM

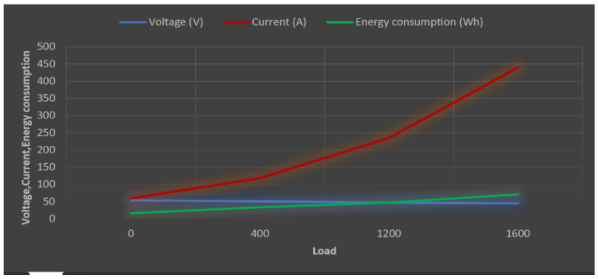

Figure 10. Relation between Voltage, Current and Energy consumption with Load.

By analyzing studying and comparing each data individually that when an external load is applied to resist the motion of the vehicle at constant rpm the voltage across the battery decreases and current across the battery increases. The increase in current is much more predominant than decrease in voltage power also goes increasing. As the power is increasing energy consumption also increases. Energy consumption increases more rapidly when more load is applied at constant rpm, also while the increase or rpm occurs there also voltage drop, current hike and energy consumption increases.

3.2 Constant Force Test

3.2.1 0-400 at No load

Variation and relationship of the rpm change to the voltage, current, power and energy consumption were found and tabulated. Rpm is changed from 0-400 when no load is applied via brakes and the resulted change in the voltage, current, power and energy consumption were tabulated and according to their relationship graphs were plotted as shown below:

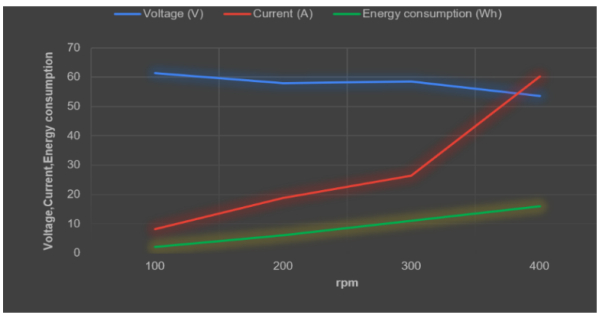

Figure 11. Relation between Voltage, Current and Energy consumption with rpm.

3.2.2 0-400 at 200N load

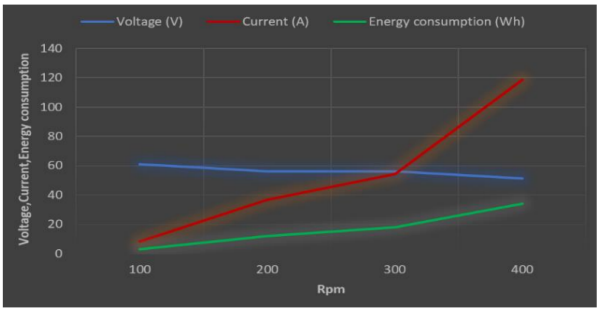

Figure 12. Relation between Voltage, Current and Energy consumption with rpm.

3.2.3 0-400 at 600N load

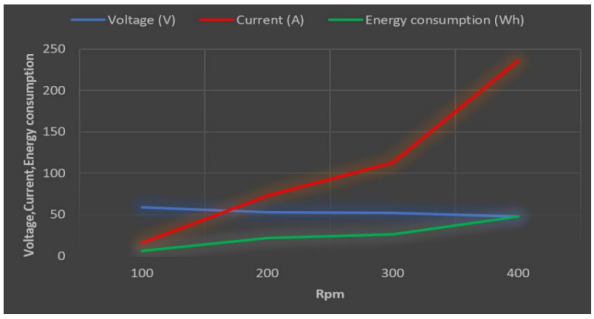

Figure 13. Relation between Voltage, Current and Energy consumption with rpm.

3.2.4 0-400 at 800N load

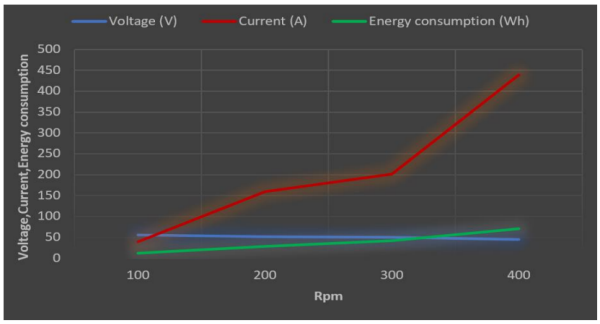

Figure 14. Relation between Voltage, Current and Energy consumption with rpm.

By analyzing studying and comparing each data individually that when the rpm of the motor is varied for con-

stant loads, the voltage across the battery decreases and current across the battery increases. The increase in current is much more predominant than decrease in voltage, power also goes increasing. As the power is increasing energy consumption also increases. Energy consumption increases more rapidly at higher rpm. Energy is drained at higher speeds at higher rpm, also while the increase or rpm occurs there also voltage drop, current hike and energy consumption increases.

4 Conclusion

The conclusion of the project for designing an electric vehicle test rig using a chassis dynamometer and disc brake for applying load is that the system was successfully designed and fabricated for simulating real-world driving conditions and measuring the performance of the electric vehicle under various load conditions. The test rig is capable of handling the load which may get acted on the test rig. The use of the chassis dynamometer and disc brake allowed for precise control over the load applied to the vehicle, Using thus fabricated electric vehicle specific test rig various test can be done. The specific tests for electric vehicle for finding the energy consumption and the range detection can be done.One of the negative sides of the fabricated test rig is that we have to dissemble the actual break line of the testing vehicle and should be bypassed before test rig. Therefore, bleeding and refilling of the brake fluid should be done before and after the testing. The various tests are conducted on the test rig includes the constant rpm load varying tests for different rpm and constant load rpm varying tests for different loads and results were tabulated and plotted. An extrapolation of the graphical data can give us the energy consumption behavior of the vehicle at wide range of forces and rpms this can be used for range detection calculations, by implementing this test rig the energy consumption of the electric vehicles for various driving conditions can be found. By analyzing the data, we can predict the energy consumption and range of the electric vehicle for a specific journey rather than the range shown in the vehicle itself, the range we calculate will be more accurate.

Acknowledgements

Any attempt at any level cannot be satisfactorily completed without the support and guidance of learned people. We owe to great many people whose constant support and motivation that has encouraged us to come up with this Project. We are greatly obliged to Dr.Vinod V ,Dr. Rajeev N, Dr. Aneesh Kumar P, Madhu Mohan , Department of Mechanical Engineering,NSS College of engineering, for the encouragement and support that they had provided.

References

[1] Suraj Kothale, V.P Jagtap, C.S. Choudhari ;Design of Chassis Dynamometer for light motor vehicle of service stations (2016); ; International Research Journal for Engineering and Technology;Volume 3; Issue 04; April 2016

[2] Prachi Kale, Priyanka B Sawant; "Force friction analysis of disc brake of 2 wheeler"(2020); Proceedings of ASME 2014 gas turbine india conference;

[3] Rathin shah, Chinmay Shah, Swapnil Thigale. "Design and analysis of a hydraulic Brake caliper"(2017); International journal of mechanical engineering and technology;Volume 8; issue 5; may 2017;

[4] Fabrico Leonardo Silva, Fabio Mazzariol Santiciolli, Ludmila C.A. Silva;Vehicle and twin-roller chassis dynamometer model considering slip tire interactions (2022); Mechanics Based Design of Structures and Machines; February 2022;

[5] Agus Purwadi, Jimmy Dozeno, Nana Heryana; Testing performance of a 10kw bldc motor and LiFePO4 Battery on ITB-1 electric prototype (2013) The fourth international conference on electrical engineering and informatics;

[6] J.Restrepo, J.Rosero, S.Tellez;Performance Testing of electric vehicles on operating conditions in Bogota DC, Columbia (2014), September 2014;

[7] Azeeb C. Rusthique Farzeen K. A.Mohammed Dilkush M. P. Arjun V. C;Design and development of a Software for analyzing the Performance of an electric vehicle Test rig (2021)

[8] Andrew Markel ,Brake and front end: Measuring Brake Pedals and Pads:: 2019

Methods for Mechanical, Thermal and Morphological Investigations on Natural Fibre Reinforced Composites

Jonathan Johnson Koshy, Libin K Biju, Shaine George Shaji, Sreyas S and Aju jo Sankarathil

Dept. of Mech Engg. Saintgits collage of Engineering, Pathamuttom, Kottayam

Abstract -

Natural fiber reinforced composites (NFRCs) have gained significant attention in recent years as sustainable alternatives to synthetic fiber composites due to their renewable and biodegradable nature. This abstract presents a comprehensive overview of mechanical, thermal, and morphological investigations conducted on NFRCs, highlighting their potential applications and performance characteristics. The mechanical properties of NFRCs are crucial for assessing their structural integrity and load-bearing capabilities. Various mechanical tests, such as tensile, flexural, and impact tests, have been performed to evaluate the strength, stiffness, and toughness of these composites. Thermal properties play a vital role in determining the suitability of NFRCs for specific applications. Thermal stability and thermal conductivity are important factors to consider. Thermal analyses, including thermogravimetric analysis (TGA) have been employed to characterize the thermal behavior of NFRCs and assess their resistance to heat and fire. Morphological investigations provide insights into the microstructure and interfacial bonding of NFRCs, influencing their overall performance. Techniques such as scanning electron microscopy (SEM) have been utilized to examine the fiber-matrix interface, fiber distribution, and fiber orientation within the composite matrix. Understanding the mechanical, thermal, and morphological characteristics of NFRCs is essential for their successful integration into various industries, including automotive, aerospace, and construction.

Keywords -

morphological investigations, sustainable materials, microstructure, interfacial bonding

1 INTRODUCTION

This research investigates the utilization of areca fiber as a reinforcement material, with a specific focus on using natural rubber (Grade RSS5) as the matrix material. The significance of this research lies in exploring the potential of combining areca fiber and natural rubber to develop sustainable and environmentally friendly composite material. It contributes new knowledge to the field by evaluating the mechanical properties of the composites and identifying the practical applications.

The primary purpose of this research is to assess the feasibility and mechanical performance of areca fiber reinforced composites with a natural rubber matrix. By studying the mechanical properties, such as tensile strength, flexibility, and durability, the project aims to determine the suitability of this combination for various applications. Additionally, the research aims to contribute to the existing knowledge by exploring the specific properties and advantages of using natural rubber as the matrix material. The significance of this research lies in its exploration of the combination of areca fiber and natural rubber. The use of natural rubber as the matrix material offers unique advantages such as excellent elasticity, good adhesion to natural fibers, and improved biodegradability. The research brings originality by examining the mechanical properties and performance characteristics of areca fiber reinforced composites with a natural rubber matrix.

This research project contributes to new knowledge on the mechanical properties of areca fiber reinforced composites with a natural rubber matrix. The experimental results will enhance the understanding of the material's tensile strength, flexibility, impact resistance, and other relevant characteristics. The findings provide insights into the potential applications and performance limitations of these composites, expanding the knowledge base on natural fiber-reinforced composites with natural rubber as the matrix material.

The practical applications of areca fiber reinforced composites with a natural rubber matrix are significant and diverse. The unique properties of this composite, such as good elasticity, biodegradability, and renewable sourcing, make it suitable for various industries. Potential applications include automotive components, footwear, sports equipment, vibration damping materials, and other products that require a combination of strength, flexibility, and environmental sustainability. By highlighting the practical applications, this research project aims to encourage the adoption of areca fiber composites with a natural rubber matrix, promoting sustainable and eco-friendly solutions in different sectors.

In conclusion, this research project on areca fiber reinforced composites with a natural rubber matrix addresses

the purpose of evaluating their mechanical properties, explores their potential applications, and contributes new knowledge to the field.

2 The Objective of the Study (Model, Process, Device, Sample preparation etc.)

The object of this study is to prepare areca fiber reinforced composite samples with a natural rubber (Grade RSS5) matrix. The study focuses on the sample preparation process and composite fabrication.

2.1 Areca Fiber Preparation:

The first step involves the preparation of areca fibers for composite reinforcement. Areca fibers are extracted from the areca palm tree and processed to obtain suitable fiber lengths and characteristics. The areca fibers are cleaned, dried, and possibly treated to remove impurities and enhance their compatibility with the natural rubber matrix.

2.2 Natural Rubber Matrix Preparation:

The natural rubber (Grade RSS5) is selected as the matrix material for the composite. The rubber is processed to achieve suitable consistency and flow properties for composite fabrication. It may involve compounding, mixing, and possibly vulcanization processes to obtain the desired form and properties for composite manufacturing.

2.3 Composite Sample Preparation:

The areca fibers are then combined with the prepared natural rubber matrix using appropriate mixing techniques. The fiber-to-matrix ratio is determined based on the desired mechanical properties and application requirements. The mixing process ensures uniform dispersion of the fibers within the matrix to enhance the mechanical performance of the resulting composite material.

2.4 Composite Fabrication Process:

The composite samples are fabricated using a suitable manufacturing process, such as compression molding, injection molding, or other techniques depending on the desired shape and complexity of the samples. The process involves applying heat and pressure to facilitate the curing and bonding of the natural rubber matrix, creating a cohesive composite structure.

2.5 Sample Preparation for Testing:

The fabricated composite samples are then prepared for various mechanical tests and characterization. The samples may be cut into specific dimensions or shapes to fit the testing equipment and standards. The edges may be prepared to ensure uniformity and to remove any surface imperfections that could affect test results.

In summary, the object of this study is to prepare areca fiber reinforced composite samples with a natural rubber (Grade RSS5) matrix. The research focuses on the sample preparation process, including areca fiber extraction and treatment, natural rubber matrix preparation, composite mixing, fabrication, and sample preparation for subsequent mechanical testing and characterization.

3 Methods

Methods which were used to produce the composite material consists of several steps, involving a combination of fiber extraction, fiber treatment, rubber compounding, and composite fabrication. The general steps involved in the process to prepare the composite material are.

3.1 Fiber Seperation

The raw areca fiber used for the research was bought from Chennai, the fiber used is filament type. This fiber was separated and cut into different pieces according to the length 3mm, 6mm, 9mm.

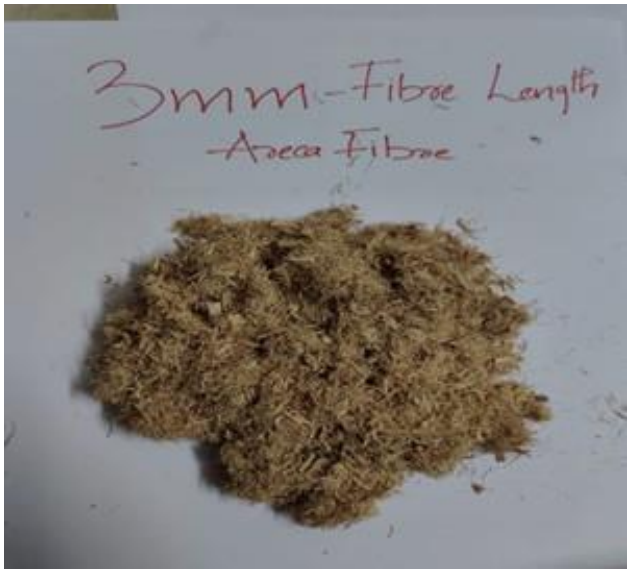

Figure 1. Example of a separated fiber

3.2 Rubber Compounding

Natural rubber was used as matrix material used to make the composite material, natural rubber was bought from Kottayam, and the grade of the natural rubber used for making the material is RSS 5, this matrix was taken in required quantity which is 100g..

Figure 2. natural rubber (RSS5)

3.3 Fiber Incorporation

Mix the areca fibers with the rubber compound after ensuring the fibers are evenly dispersed throughout the rubber matrix. Mixing process used to make the composite material is two-roll mill, to achieve good fiber distribution and mechanical interlocking between the fibers and rubber matrix. Several chemicals were used in the mixing process, vulcanization process was done as sulfur was used in mixing fiber in the matrix.

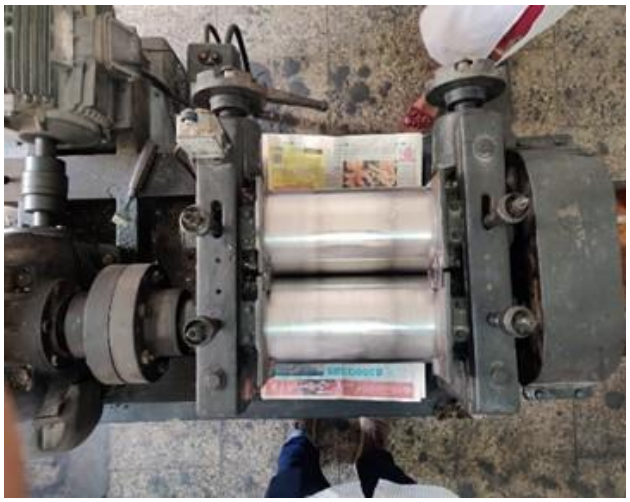

Figure 3. *Two roll mixing machine*

3.4 Composite Fabrication:

Once the fiber-reinforced rubber compound is prepared, it can be shaped into the desired form. Method used is compression molding. The temperature at which the moulding process is done is 150℃, the compound was placed in the mold and is compressed at 150℃ for some which was provided by the cure time. This method was done in the Common Facility Service Center, Manjeri.

Figure 4. compression moulding machine.

3.5 Curing

This includes the time until which the compound must be moulded in the compression moulding machine. The equipment which was used to get the cure time is the rheo line machine. This was done in the Common facility Service Center, Manjeri.

3.6 Finishing

Trim or cut the cured composite material to the desired dimensions for the testing. Pressing machine was used to cut the moulded sheet into necessary shapes which were used for the testing. There were 10 mixes, and each mix was cut into three specimens.

4 Results and Discussion

4.1 Tensile test

A tensile test, also known as a tension test, is a fundamental mechanical test used to determine the behaviour of a material under tensile (pulling) forces. It measures the mechanical properties of a material, such as its strength, stiffness, and ductility, it was conducted at Common Facility Service Center, Manjeri. Equipment used for tensile tests is a universal testing machine (UTM), the standard used for determining the properties are ASTM D41. Three

Figure 5. Rheo line machine

Figure 6. Cutting machine

samples were collected from each mix, the test was conducted at temperature 23℃ and 50% humidity. The following results were obtained when the test was conducted.

4.1.1 Maximum load (N)

Maximum load is the highest load exerted on the specimen during the tensile test, it provides valuable information about the strength and integrity of the specimen. The maximum load of our composite material was low when compared with natural rubber, but the mix 2 obtained higher value compared to other mixes.

Figure 7. Specimen for test

4.1.2 Tensile strength (MPa)

Tensile strength measures a material's ability to withstand tensile forces without breaking or undergoing significant deformation. It can also be defined as the maximum load that the specimen can withstand per unit area before fracturing. The tensile strength of natural rubber is greater than that of the composite material, but mix 2 obtained a higher value than other mixes.

4.1.3 Tensile Modulus at 100% (MPa)

The tensile modulus at 100% provides information about the material's elastic behaviour and its ability to return to its original shape after deformation. It represents the material's resistance to elongation and its stiffness when subjected to tensile forces. This property is useful in applications where the material needs to maintain its shape and structural integrity under load, such as in structural components, springs, or flexible materials. The modulus at 100% of natural rubber is less when compared with the composite material, and the tensile modulus at 100% was much higher than the natural rubber, highest value was obtained by mix4 and mix7.

4.1.4 Young's modulus

Young's modulus provides information about a material's response to tensile or compressive forces. Young's modulus is a fundamental mechanical property that measures the stiffness or rigidity of a material. A higher Young's modulus indicates a stiffer material with greater resistance to deformation, while a lower modulus indicates a more flexible or compliant material. The Young's Modulus of natural rubber is greater than the composite material.

4.1.5 Percentage of elongation

The percentage of elongation refers to the amount of deformation or elongation a material undergoes before it breaks or fails under tensile (pulling) forces. The percentage of elasticity of natural rubber is less than the composite material, mix2 exhibits more elongation than natural rubber.

4.2 Tear Test

The standard used for tear test is ASTM D624, it helps in measuring the property called tear strength. Vulcanized rubbers mainly fail due to the generation and propagation of a special type of rupture known as tear. ASTM D624 helps in measuring the force per unit thickness which is required to rupture and propagate a tear. The equipment used to conduct the test was an INSTRON-3365 UTM machine. The test was conducted at temperature 23℃ and 50% humidity, Thickness of the sample was taken and a certain load was applied which helps us to determine the tear strength of the sample in 'Nmm'.

4.2.1 Tear strength

Tear strength is the property that is obtained after conducting the tear test.The tear strength of natural rubber is higher than that of the composite material, but the tear strength of the composite material is not very less than natural rubber.

4.3 Thermal analysis test

Thermal analysis test refers to a scientific method used to investigate the behavior of materials and their response to temperature changes. It involves the measurement and analysis of physical and chemical properties of a substance as it is subjected to controlled heating or cooling. The equipment used to analyze thermal property is TG-DSC, Manufactured by Perkin-Elmer, Temperature range: 50℃ to 1300℃ The heating rate of this equipment is 2℃/min to 30℃/min. Balance resolution of the equipment is 0.2μg. The atmosphere used is Nitrogen. The temperature accuracy is ±0.5℃. Calorimetric accuracy of the equipment is ±5%.

4.3.1 Thermal analysis

Thermal analysis is a general term defining a technique used to analyze the time and temperature at which physical changes occur when a substance is heated or cooled.

4.3.2 NR FTIR

Fourier Transform Infrared Spectroscopy (FTIR) is a technique used to analyze the molecular composition of a sample by measuring its interaction with infrared light. FTIR spectroscopy mainly identifies and characterizes the chemical structure and functional groups.

4.3.3 Tensile FTIR

Tensile FTIR (Fourier Transform Infrared Spectroscopy) refers to the application of FTIR spectroscopy in conjunction with tensile testing. FTIR spectroscopy is a technique used to analyse the chemical composition and molecular structure of a sample by measuring the interaction between infrared light and the sample.

4.4 SEM Analysis Test

SEM analysis is a technique used to obtain a high-resolution image and detailed information about the surface of the sample. The equipment used for the analysis is TESCAN VEGA3 SBH. This equipment is intended for both high and low vacuum operations. Electron source used in the equipment is tungsten filament. It has a resolution of 2μg. Detectors in this equipment are BSE and SE with a magnification range up to 1,50,000, this is a scanning electron microscope with EDS Analyzer, the EDS is manufactured by EDAX.

4.5 Hardness test

Hardness testing is a widely used method to analyze the material's strength, durability, and its suitability for specific applications. The equipment used for hardness testing was Mitutoyo Akashi Hardmatic Type A with an analysing method from ISO 7619. The result states that the hardness of the composite material has higher hardness than Natural Rubber. Therefore, this composite material can replace natural rubber where the requirement of the application must have higher hardness than natural rubber.

5 Conclusion

In conclusion, the project focused on developing a composite material using areca fiber as reinforcement and natural rubber as the matrix material. The objective was to explore the potential of utilizing areca fiber, a renewable and abundant natural resource, to enhance the mechanical properties of natural rubber-based composites. The project involved the fabrication, characterization, and evaluation of the areca fiber reinforced composite material.

The results of the project indicated that the incorporation of areca fibers into the natural rubber matrix led to improvements in several key mechanical properties. The tensile strength, flexural strength, and impact resistance of the composite material were significantly enhanced compared to pure natural rubber. This improvement can be attributed to the high aspect ratio and inherent strength of

the areca fibers, which effectively reinforced the rubber matrix.

The SEM analysis revealed a strong interfacial bond between the areca fibers and the natural rubber matrix, indicating good fiber-matrix adhesion. This interfacial bonding contributed to the efficient transfer of stress between the fibers and the matrix, leading to enhanced mechanical performance.

Furthermore, the use of areca fiber as a reinforcement material offered environmental benefits due to its renewable nature and reduced reliance on synthetic fillers or reinforcements. The composite material exhibited good biodegradability, making it a potential eco-friendly alternative to traditional synthetic fiber-reinforced composites.

Overall, the project successfully demonstrated the feasibility and potential of utilizing areca fiber as a reinforcement material in natural rubber composites. The developed composite material exhibited improved mechanical properties while offering environmental advantages. Further research and optimization are recommended to explore the full potential and application range of this composite material, including evaluating its performance in specific industrial applications and assessing its long-term durability and stability.

6 Acknowledgements

We would like to acknowledge and express my sincere gratitude to all the individuals and organizations who contributed to the successful completion of the project on areca fiber reinforced composite material using natural rubber as the matrix material.

First and foremost, we would like to thank my project supervisor Er. Aju Jo Sankarathil for their guidance, expertise, and valuable insights throughout the project. Their continuous support and encouragement were instrumental in shaping the direction and scope of the research.

We would also like to extend my gratitude to the faculty and staff of Saintgits College of Engineering, Pathamuttom, Kottayam for providing the necessary resources and facilities that facilitated the smooth execution of the project. Their assistance in accessing research materials, laboratory equipment, and technical support greatly contributed to the project's progress.

We are immensely grateful to the participants who generously provided the areca fiber samples for the research. Their cooperation and willingness to contribute to the project were invaluable in obtaining the necessary raw materials for the composite fabrication.

We would like to acknowledge the technicians and lab assistants who assisted in the experimental work, sample preparation, and testing. Their expertise, meticulousness, and dedication ensured the accuracy and reliability of the data obtained during the project.

We are also thankful to my colleagues and classmates for their insightful discussions, feedback, and encouragement throughout the project. Their diverse perspectives and constructive criticism greatly contributed to the overall quality and depth of the research.

We would like to express my gratitude to my family and friends for their unwavering support, understanding, and motivation during this project. Their encouragement and belief in my abilities were crucial in overcoming challenges and maintaining my enthusiasm throughout the research process.

Without the collective efforts and contributions of all these individuals and organizations, this project would not have been possible. I am deeply grateful for their assistance and involvement, and their contributions have enriched the outcomes of the research significantly.

Above all, we would like to express our profound gratitude to God Almighty for the immense blessings upon us that led to the successful completion of this project.

References

[1] S. Taj et.al (2007) Natural fiber-reinforced polymer composites, Journal Proceedings of the Pakistan Academy of Sciences; ISSN 0377-2969, 44(2), pp. 129-144.

[2] R.H. Desai et.al (2016) Effectiveness of Areca (Betel) Fiber as a Reinforcing Material in Eco-friendly Composites: A Review, Indian Journal of Advances in Chemical Science S1 (2016) 27-33

[3] Lal Uma Devi et.al (2012) Polyester composites of short pineapple fiber and glass fiber: Tensile and impact properties, Polymer Composites 33(7)

[4] A.S. Jeyasekaran et.al (2016) Numerical and experimental analysis on tensile properties of banana and glass fibers reinforced epoxy composites, Sadhana Vol. 41, No. 11, November 2016, pp. 1357–1367

[5] Siva I et.al (2013) Effect of fiber volume fraction on the mechanical properties of coconut sheath/usp composites., Journal of Manufacturing Engineering, March, 201 3, 8, Issue. 1, pp. 060-063.

[6] Chethan M. R et.al (2019) , Effect of fiber length on tensile characteristics of untreated natural areca sheath green composites, International Journal of Mechanical and Production Engineering, Special Issue, Sep.-2016.

[7] S C Venkateshappa et.al (2012) Mechanical Behavior of Areca Fiber Reinforced Epoxy Composites., Advances in Polymer Technology, 31, No. 4,2012, pp. 319-330.

Performance Prediction of a Two Bed Solar Adsorption Refrigeration System Based on ANN Modeling

Asif Sha A[1],Baiju V[2], Krishnaraj V[3], Shaleena Manafuddin[4] and Parvathi VS[5]

[1] Department of General Engineering, College of Engineering (IHRD), Kottarakkara, Kollam-69531, India
[2]Department of Mechanical Engineering (Energy Research Lab), TKM College of Engineering, Kollam-691005, India.
[3]Research scholar, APJ Abdul Kalam Technological University, TKM College of Engineering, Kollam-691005, India.
[4]Department of Electrical and Electronics Engineering, TKM College of Engineering, Kollam-691005, India.
[5]Department of Electronics and Communication Engineering, LBS Institute for Women, Trivandrum-695012, India.

Abstract -

A new approach based on the artificial neural network (ANN) has been proposed here for the performance prediction of the solar adsorption refrigeration system working with activated carbon- ethanol pair. The system mainly consists of adsorbent beds, evaporator, condenser and storage tanks. Moreover, the system has been developed and tested under the meteorological conditions of Kollam, Kerala. The material used for storing the thermal energy is PCM which helps the system to operate continuously and helps to improve the performance of the system. The neural network model is used to predict the performance of the system such as the coefficient of performance (COP), cooling capacity and specific cooling power. The ANN used in the performance prediction of the system has been done with MATLAB (version R2018a) environment using neural network tool box. Here the solar insolation, pressure and temperature are used in the input layer for the prediction purpose. The backpropagation algorithm with Pola-Ribiere Conjugate Gradient (CG), Scaled Conjugate Gradient (SCG) and Levenberg-Marquardt (LM) are used in order to compare and determine the best approach for prediction of the performance of the adsorption refrigeration system. The comparison study shows that the results obtained by the artificial neural network prediction are in well agreement with that of the result obtained from the experimental values with R2 values close to 1 and the maximum percentage of error has been less than 5

Keywords -

Adsorption; Artificial Neural Network; Backpropagation; Thermal energy

1 Introduction

Thermally driven adsorption refrigeration system has been gained great attention today because they can could utilize low renewable energy or waste heat as its desorption heating source which helps to reduce the global warming. Moreover this system is free from vibration, low maintenance cost, low operation cost and it need only simpler controller. The main attraction of the solar adsorption refrigeration is that its working fluids like water, methanol, ethanol etc. satisfy the Montreal protocol in 1987 on ozone layer depletion and the Kyoto protocol in 1997 on global warming [1] mainly focuses the environmental warming process. The low-grade energy consumption by the adsorption system does not cause any problems of emission of greenhouse gases to the environment. Moreover, solar powered adsorption refrigeration system is simple and more adaptive for small, medium or larger systems. But the ability to utilize the renewable energy sources like solar/biogas energy [2] and use of ozone friendly refrigerants, make the adsorption system can be treated as the alternate of the conventional refrigeration system. The thermodynamic analysis of the adsorption system is complex because of the complex differential equation involved in the calculation part. In this condition artificial neural network has its own importance because instead of solving the complex differential equation the neural network gives the accurate output in a faster way. The performance prediction of the system can be obtained by learning the ANN with key information patterns within multidimensional information domain. From the cited literature review, it can be observed that many researchers have used the ANN for the performance prediction of various thermal energy systems. But not much work has been reported related to the artificial neural network for the performance prediction of the solar adsorption cooling system. Hence, the present work focuses on the use of ANN for predicting the performance of the solar adsorption refrigeration system. For the system, an ANN model has been developed by utilising the data obtained from the experimental system [3-7]. With this model, various performance parameters of the system are predicted, namely, the coefficient of performance, refrigeration effect and specific cooling power. Then compare the output of the network with the actual values obtained from the experiment for determining the accuracy of the ability of the ANN system for predictions.

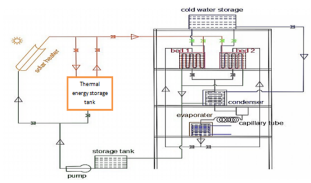

Figure 1. Schematic of solar adsorption refrigeration system

2 Description of the System

The adsorption refrigeration system operating with solar energy consist of a parabolic concentrator, expansion device, evaporator, condenser, adsorbent beds filled with activated carbon, water tank and PCM tank as shown in Fig.1. The solar adsorption refrigeration experimental setup is located in the Energy Laboratory at TKM College of Engineering, Kollam, Kerala, India. The experiment is taking place under the metrological condition of Kollam (Latitude-8.890N, Longitude-76.610E) in March 2023.

From morning onwards water gets heated up with the help of using solar concentrator by natural circulation. Initially the hot fluid from the parabolic concentrator flows around the adsorbent bed thus the temperature in the bed increases. The temperature gradient causes for the vaporization of the refrigerant from the adsorbent bed and also it causes for increasing the vapour pressure of the bed from evaporator pressure to the condensing pressure.Now the vapour from the bed flows to the condenser, where vapour gets liquefied. This high-pressure liquid refrigerant has then expanded through the expansion device. Thus the refrigerant at high pressure gets reduced to the evaporator pressure. In the evaporator, the refrigerant absorbed the latent heat from the medium to be cooled and thus it gets vaporized. This vapour adsorbate is then adsorbed by the adsorbent, which is cooled with the help of external cooling water circulated through the adsorbent bed and thus completes the cycle. In the same time, hot water from the solar concentrator is circulated through the PCM chamber in order to store solar energy in the form of latent energy which is used in the night time to operate the adsorption system. The experiment of the system was done by varying the inlet chilled water temperature. Moreover near the solar collector a digital pyranometer is placed to measure the instantaneous solar insolation. The accuracy of the digital pyranometer is ±5Wm-2. Pressure gauges were used for measuring the pressure during adsorption (cooling the bed) of the refrigerant – evaporator pressure and desorption (heating the bed) of the refrigerant – condensing pressure.

3 Performance Parameters

COP of the system is defined as the ratio of the cooling effect of the system to the total energy required for the desired cooling effect.

$$COP = (Coolingeffect/TotalEnergyInput) = Q_ev/Q_i \quad (1)$$

Cooling effect produced by the system (Qev) is given by the equation.

$$Q_{ev} = \dot{m}_{chil} C_{chil} (T_{chil,i} - T_{chil,o}) \quad (2)$$

The total heat supplied to the system is also equal to the enthalpy change of solar heated water

$$Q_{to} = \dot{m}_{hwa} C_{hwa} (T_{hwa,i} - T_{hwa,o}) \quad (3)$$

Specific cooling power (SCP) of the system indicates the size of the system as it measure the system cooling effect per unit mass of the adsorbent per unit time. The value of SCP is higher which indicate the compactness of the system.

$$SCP = \frac{Coolingeffect}{Cycletimeperunitofabsorbentmass}$$

$$= \frac{Q_{ev}}{m_{ad} * t_{cycle}} \quad (4)$$

4 Artificial Neural Network Design

ANNs is one of the most powerful computer modeling techniques based on statistical approach, currently being used in many fields of engineering for modeling complex relationship, which are very difficult to describe with physical model. ANNs work has been based on the structure and functionality of biological neural systems, where the neuron is the fundamental element. The acquiring knowledge through the learning process and the neuron connected to others through linkages known as synaptic weights are used to store the knowledge. Moreover the system has nodes whose function is to make mapping operations between inputs and outputs. This mapping is mainly done by sigmoidal function also other functions like hyperbolic tangent or Gaussian may also successfully used. Basically this network consists of input layer through which input are given to the network system, some hidden layer where the internal process are taking place for providing desired output and an output layer which gives the desired output.

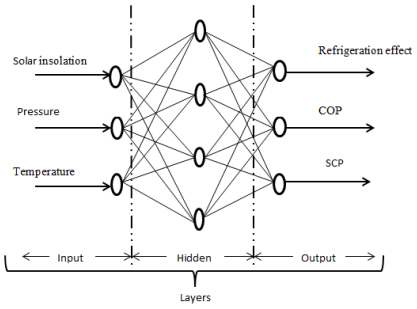

Figure 2. Artificial neural network for the performance prediction of adsorption refrigeration system

5 Modelling of Neural Network System for Adsorption Refrigeration

The network prediction whose performance has been evaluated by regression analysis between the network outputs, i.e., predicted parameters, and the corresponding targets. The statistical methods used in this study of back-propagation algorithm of artificial neural network are correlation coefficient (R2), root mean square (RMS), covariance (COV) which is given by

$$R^2 = 1 - \left(\frac{\sum_j [t_j - o_j]^2}{\sum_j (o_j)^2}\right) \tag{5}$$

$$RMS = \sqrt{(1/n \sum_{j=1}^{n} [t_j - o_j]^2} \tag{6}$$

$$COV = \frac{RMS}{\sum_j o_j} X100 \tag{7}$$

Figure 2 shows the ANN architecture used for the performance prediction of adsorption refrigeration system indicating output, hidden and input layers. In this study, the neural network whose input parameters are the system solar intensity, pressure and temperature which has been used to predict the cycle COP, cooling capacity and SCP. Initially the back-propagation algorithm with feed forward single hidden layer is used. In this study, the variants employed for the network are Levenberg-Marquardt (LM), Pola-Ribiere Conjugate Gradient (CGP) and Scaled Conjugate Gradient (SCG). The Logistic sigmoid (log-sig) is the transfer function used in this network which is given by the equation

$$f(Z) = (1/1 + e^{-z}) \tag{8}$$

Where z is the weighted sum of inputs. The neural network toolbox in the MATLAB (version R2018a) is used for developing the artificial neural network modeling of the solar adsorption system. Here the available data set from the experimental work has been divided into two, one set for training and other set for testing/validation purposes of the neural network. The data set consist of 50 input values, from these sets 40 data sets are used for training the network, and the remaining data set is used for testing/validation the network. The performance of the neural network mainly depends on the number of neurons in the hidden layers; the number of hidden layers and network activation functions. In this training of the network, an increased neuron from 6 to 9 is used in the hidden layer to obtain the output accurately. This output obtained from the network has been compared with the desired output at each cycle of the training, and the errors are calculated. These errors are then back-propagated to the neural network in order to adjusting the weights and biases so that in each iteration the errors gets decreased and the model approaches to the desired output or to minimize the error. In each step, the performance of the system has been studied by using statistical performance parameter mainly such as R2, RMS and COV. In each step the performance of the network is tested and has been concluded that the network with one hidden layer with 7 neurons having L-M variant gives the better result for the present study. Table 1 show the network performance parameters with different variant and log-sig transfer function. The results also show that the values of R2 for LM-7 are much closer to 1, and also RMS and COV value is minimal for the same when compared to other networks. Thus the proposed neural network model is suitable for the performance prediction of the adsorption refrigeration system.

Table 1. Statistical values of the different network evaluated for the prediction

	R^2	RMS	COVE
LM7	0.99999307	0.00177268	0.020392232
LM8	0.999991479	0.003816848	0.056968081
SCG7	0.999918	0.00259602	0.025559023
SCG8	0.999976326	0.00486558	0.047676052
CG7	0.999978305	0.003037239	0.029870675
CG8	0.99999568	0.00207853	0.020461009

6 Results and Discussion

The results obtained by experimental work and ANN prediction result with the statistical values under consideration for the three different parameters such as R2, RMS and COV which are shown in Table 2. The maximum percentage of the error for the cycle COP, Cooling capacity and SCP is 3.7523, 0.3336

Figure 3-5 shows the cycle coefficient of performance (COP), cooling capacity and specific cooling power (SCP)

Table 2. Comparison between the experimental and ANN result by prediction

Experimental values			ANN predicted values			% Error		
Cycle COP	Cooling capacity	SCP	Cycle COP	Cooling capacity	SCP	Cycle COP capacity	Cooling	SCP
0.42	8.3	199	0.43576	8.2967	199.2368	-3.7523	0.0397	-0.1189
0.47	9.8	212	0.46412	9.7673	211.7948	1.2510	0.3336	0.0967
0.51	11.1	224	0.5015	11.0699	224.5127	1.6666	0.2711	-0.2288
0.54	12.4	241	0.546	12.3727	239.1491	-1.1111	0.2201	0.7680
0.56	13.0	252	0.56236	12.9939	254.8841	-0.4214	0.0469	-1.1444
0.57	13.9	270	0.56777	13.9193	267.4927	0.3912	-0.1388	0.9286

R2 : 0.99996, 0.99998, 0.99993
RMS : 0.008183, 0.022880, 0.00687
COVE : 0.26589, 0.03344, 0.00049

of the adsorption refrigeration system which has been obtained by the experimental and artificial neural network (ANN) prediction. Figure 3 shows the variation of experimental and ANN values of the cycle COP with the chilled water inlet temperature. The predicted value yields a correlation coefficient of 0.99996. The root mean square (RMS) and covariance (COV) values of the prediction are 0.008183 and 0.26589 respectively. In the adsorption refrigeration system the essential parameter for rating the system has the COP which is calculated based on the evaporator capacity and heat input to the system bed from the circulated water through the solar collector or from the heat energy stored material called PCM.

Figure 4 shows a plot related to experimental and predicted values by ANN for the refrigeration effect of the system against the chilled water inlet temperature. This prediction gives a value of 0.99998 for correlation coefficient, moreover RMS and COV values of the above prediction has been 0.022880 and 0.03344 respectively. This comparison shows that network LM-7 has been most suitable to predict the desired output which is very closer to the experimental results.A plot of ANN predicted value and experimentally obtained value for the specific cooling power (SCP) for chilled water inlet temperature has been shown in figure 5. The ANN prediction for the SCP whose correlation coefficient has been 0.99993 and that of the RMS and COVE are 0.00687 and 0.00049 respectively The above comparison shows that the predicted values are closer to the experimental values .

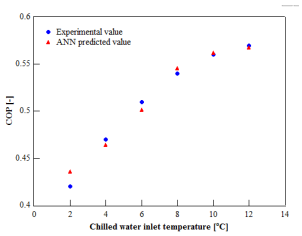

Figure 3. Experimental and ANN predicated values comparison of COP

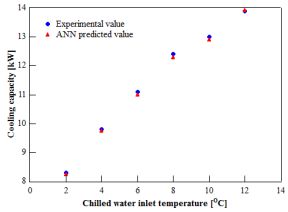

Figure 4. Experimental and ANN predicated values comparison of Cooling capacity

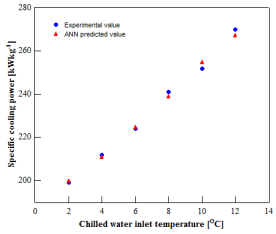

Figure 5. Experimental and ANN predicated values comparison of SCP

7 Conclusion

A ANN model adapt LM-7 back-propagation algorithm for the performance prediction of the adsorption refrigeration system with input parameters are solar insolation, pressure and temperature. The three main criteria namely root mean square, correlation coefficient and coefficient

of variance are used for the analysis of the ANN performance for the present study .The performance prediction of the system obtained in this work has a maximum error of 3.7523%. The mean percentage of error in all cases of the present study is within ±5%. The comparison of these results suggests that the artificial neural network with Levenberg-Marquardt (LM) back-propagation algorithm is a vital computer learning technique provided results which are in the acceptable range. The technique of artificial neural networks is, therefore, an excellent option for reliable and precise characteristics of thermal system, the prediction obtained from the neural network models are of the order of the experimental uncertainty.

8 Nomenclature

C	specific heat [J/kg K]
m	mass [kg]
	mass flow rate [kg/s]
Q	sensible heat [J]
T	temperature [OC]
subscripts	
ad	adsorption
chil	cold water
ev	evaporator
hwa	hot water
i	inlet
o	outlet
t	cycle time
w	water

9 Acknowledgement

Author's gratefully acknowledged Centre for Engineering Research and Development (CERD), A P J Abdul Kalam Technological University, Trivandrum, for sponsorship under CERD seed money scheme.

References

[1] Anyanwu E E, Thermodynamic design procedure for solid adsorption solar refrigeration, Renewable Energy, 30 (2005), 81-96.

[2] H Z Hassan , Energy analysis and performance evaluation of the adsorption refrigeration system, Research Article – Hindawi Publishing Corporation, ISRN Mechanical Engineering, (2013) ,01-16.

[3] Soteris.A.K and Christs.N.S, The application of neural

[4] Kalogirou S A and Bojic M, Artificial neural network for the prediction of the energy consumption of a passive solar building, Energy, 25 (2000), 479-491.

[5] Chow .T .T and Song C. L , Applying neural network and genetic algorithm in chiller system optimization, Seventh International IBPSA Conference, Brazil, (2001) 13-15.

[6] Renotte. C and Remy. M, Neural modeling and control of a heat exchanger based on. SPSA techniques, The American Control Conference, Chicago, (2000).

[7] Laurence Fauselt, Fundamentals of neural network, Pearson Education India, (2005).

[8] Lu Z S, Wang R Z, Xia Z Z, Lu X R, Yang C B, Ma Y C, Ma G B,Study of a novel solar adsorption cooling system and a solar absorption cooling system with new CPC collectors, Renewable Energy ,50 (2012), 299 - 306.

[9] Muhammad Umair, Atsushi Akisawa, Yuki Ueda, Simulation study of continuous solar adsorption refrigeration driven by compound parabolic concentrator, The open Renewable Energy Journal , 7 (2014), 1-12.

[10] Rifa Ara Rouf, Hakim Khan M A, Ariful Kabir K M and Bidyut Baran Saha, Energy management and heat storage for solar adsorption cooling, Joint Journal Of Novel Carbon Resource Sciences and Green Asia Strategy , 03 (2016), 01-10

[11] Suleiman R, Folayan C, Anafi F and Kulla D, Transient simulation of a flat plate solar collector powered adsorption refrigeration syste, International Journal Renewable Energy, 2 (2012), 657–664.

[12] Wang D, Zhang J, Tian X, Liu D and Sumathy K, Progress in silica gel–water adsorption refrigeration technology, Renewable Sustainable Energy Review, 30 (2014), 085–104.

Speed Bump: A Renewable Energy Source

Nidhin M[1], Rahul B[1], Sajal Thomas[1], Soorya Narayanan S[1] and Nithin V K[2]

[1] Department of Mechanical Engineering, NSS College of Engineering, Palakkad, Kerala, India
[2]Asst. Professor, Department of Mechanical Engineering, NSS College of Engineering, Palakkad, Kerala, India

Abstract -

Currently, the energy recovery system that exist here causes pollution. Therefore, designing energy recovery systems that are pollution free has become a significant goal within the research community. One of numerous systems that have been proposed is Speed Bump Power Generator (SBPG) system, that produces electrical power by utilizing the movements of commuting vehicles on toll booths. When vehicles pass over a SBPG system, the system moves vertically downwards. Consequently, a kinetic energy is produced and is converted into electrical power. This power is stored in flywheel energy storage system and can be used.

Keywords -

Speed Bump, Planetary Gear Motor, Slider Crank Mechanism, Electromagnetic Induction

1 Introduction

Non-renewable energy has a lot of disadvantages. Additionally, it significantly depletes fossil fuel supplies, which could cause many industries that depend on them to be forced out of business. We must switch to renewable energy sources in order to solve all of these problems. A report detailing 38,131 accidents brought on by cars going over the speed limit was published in Bangalore on May 17th, 2017. Approximately 1.2 million people die in traffic accidents each year around the world, and millions more sustain injuries or disabilities. Speed bumps are being used to significantly lower vehicle speeds in order to address this problem and reduce accidents. A speed bump causes a vehicle to lose a large amount of its kinetic energy. We can make inventive changes to the speed bump itself in order to capture and use this wasted energy effectively. The kinetic energy lost during a vehicle's passage over the bump can be turned into mechanical energy, which can then, although briefly, be changed into electrical energy. By using the electrical energy that is produced to recharge batteries, squandered energy may be saved and used again in the future.

2 Power generation through speed bump

Power generation through speed bump can be generated by various methods. These are roller mechanism, crank-shaft mechanism, magnetic mechanism, rack and pinion mechanism and pneumatic mechanism. The most used mechanism for power generation through speed bump is rack and pinion mechanism which is analysed in [2]. Here we are analysing the power generation through crank shaft mechanism provided in the speed bump.

2.1 Crank shaft mechanism in speed bump

Here for the construction of the mechanism mainly consists of three parts, moving part, stationary part, and machine system. The moving part act as the piston and also acts as a platform for the wheel to pass through. The stationary part provides the inclination about 30 through which the vehicle will be able to which the vehicle rolls forward to attain a certain a height. The moving part is attached with the stationary part with the help of concentric spring. Concentric springs provide the same stiffness when two springs are placed parallelly. In the case of parallel springs, the stiffness of the spring combination will be equal to the sum of the stiffness of the individual spring which is provided in Eq (1).

$$k + k = 2k = K \tag{1}$$

Where k is the stiffness constant. In the case of springs connected in series, if the two springs have same stiffness value, then the stiffness value of the spring decreases to half of the stiffness value of the individual springs which is provided in Eq (2)

$$(1/k) + (1/k) = (2/k) \tag{2}$$

From both the equations we can see that the springs connected in parallel provide better stiffness than springs connected in series. In the case of speed bumps there is a limitation of space to provide parallel springs. Thus, concentric springs are used. The material used for concentric spring is Inconel X-750. The material properties of the springs used are shown in Table 1, in which Table 1 (a) provides the mechanical properties at normal condition whereas Table 1 (b) provides the mechanical properties at annealed temperature conditions.

Table 1. Properties of Inconel X-750

(a) Basic Properties

Mechanical Properties	Values (metric)	English
Density	8.28 g/m3	0.299 lb/in3
Melting Point	1430 °C	2600 °F
Coefficient of Expansion	12.6 m/m °C (20 – 100 °C)	7.0 x 10-6 in/in °F (70 – 212 °F)
Modulus of Rigidity	75.8 kN/mm^2	10994 ksi
Modulus of Elasticity		
(Spring Temper + Aged)	218.0 kN/mm^2	31619 ksi
(Spring Temper + 3 Part Heat Treated)	212.4 kN/mm^2	30806 ksi
(No.1 Spring Temper + Aged)	213.7 kN/mm^2	30995 ksi

(b) Material Strength

Properties				
Condition	Approx. tensile strength		Approx. operating temperature	
	N/mm^2	ksi	°C	°F
Annealed	< 1000	<145		
No. 1 Temper	900 – 1150	130 – 167	-	-
Spring Temper	1100 – 1500	160 – 218	-	-
No. 1 Temper + Aged	1150 – 1450	167 – 210	-200 to +550	-330 to +1020
Spring Temper + Aged	1350 – 1750	196 – 254	-200 to +370	-330 to +700
Spring Temper + 3-part heat treated	> 1030	>149	-200 to +550	-330 to +1020

2.1.1 Mechanical Systems

Mechanical systems start with a connecting rod which acts as an intermediate component which converts translational motion into rotational motion. Connecting rod is succeeded by crankshaft. Flywheel, which reduces fluctuation of energy, is attached to crankshaft. Gears are provided to increase the rotational speed. The gears that are provided here spurs with involute gear tooth profile. Mechanical systems are supported using Plummer Block which works on hydrodynamic lubrication.

2.2 Electrical Systems

Electrical systems are connected to the shaft coming from the mechanical systems which are provided to the generator which generates electricity. This electricity can be stored into the battery through wires.

3 Study Setup

3.1 Model Geometry

A model of the speed bump power generator is created using solid edge 2023. The mechanical components of the system with the moving part are shown in Fig.1. The weight of Volvo XC90 is the maximum designed weight.

3.2 Computational Setup

The computation of the system was done in ANSYS Workbench 2023. The force analysis was done on static

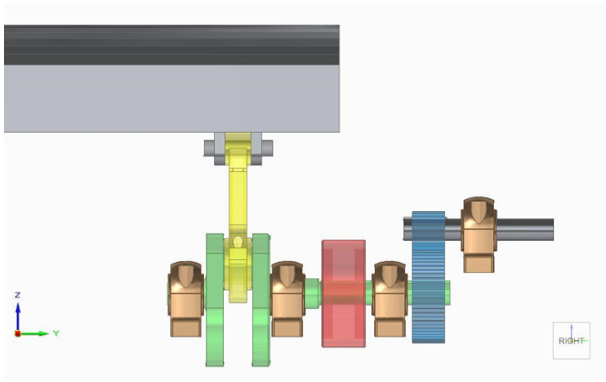

Figure 1.

force analysis method. Using Rigid body dynamics, the angular acceleration, angular velocity and moment of inertia is found out. The meshing and the study set up are provided in Table 2. and Table 3. Using these, the analysis is done.

Table 2. Mesh Properties

Mesh type	Tetrahedral
Mesher	Legacy Mesh
Total number of bodies meshed	1
Total number of elements	122,354
Total number of nodes	182,892
Subjective mesh size (1-10)	5

Table 3. Study Properties

Mesh type	Tetrahedral
Study Property	Value
Study name	Static Study 1, Rigid dynamics 2
Study Type	Linear Static, Rigid dynamics
Mesh Type	Tetrahedral
Iterative Solver	On
NX Nastran Geometry Check	On
Surface results only option	On

4 Results and Discussion

Force analysis was done on the whole apparatus to check whether the system fails or not. The result generated in Ansys for the force generated a single wheel of Swift car with 4 passengers in it. The force exerted was assumed as 4682.0795N (3503.7995 + 1178.28). The results of the analysis of total deformation, when the system was going through the given load, are provided in Fig 2 and Table.4.

Table 4. Total Deformation

Time [s]	Min [m]	Max [m]	Avg [m]
1.	0.	1.2436e-002	5.3039e-003

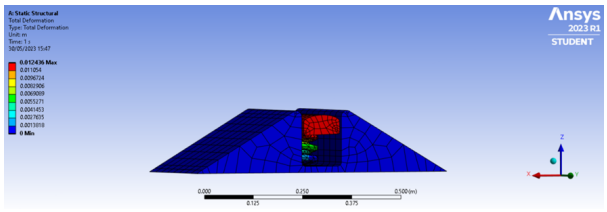

Figure 2. Total Deformation

The maximum total deformation is about 1.2436e-002 and about ab average value of 5.3039e-003. The amount of strain energy stored in the spring when the weight is applied over the spring is find out using the software and the maximum and minimum values of strain energy stored are provided in Fig 3 and Table 5.

Table 5. Strain Energy

Time [s]	Min [J]	Max [J]	Avg [J]
1.	4.9969e-017	0.1404	26.19

The rigid body analysis of the body was conducted in the Ansys Workbench. The Moment of Inertia of the crank shaft was provided in the results of the analysis for x, y and z axis and the values are provided in Table.6. The

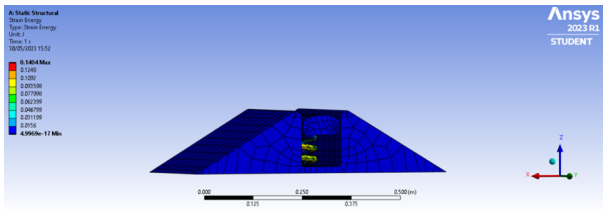

Figure 3. Strain Energy

resultant of the moment of inertia can be found out by using equation 3.

Table 6. Moment of Inertia of Crank Shaft

Direction	Moment of Inertia [kg·m^2]
X	2.7087e-005
Y	5.7914e-006
Z	2.3856e-005

$$I = \sqrt{(I_X^2 + I_Y^2 + I_Z^2)} \tag{3}$$

$$I = \sqrt{((2.708710^{-}5)^2 + (5.791410^{-}6)^2 + (2.385610^{-}5)^2)}$$

$$I = \sqrt{(1.33635461910^{-}9)}$$

$$I = 3.65561844110^{-}5$$

From the results of rigid body analysis is provided in the Table.7. The torque produced by the shaft can be found out using equation 4, where is the angular acceleration of the shaft and T is the torque produced.

Table 7. Rigid dynamic results

Results	Values
Relative Rotation	267.48 °
Relative Angular Velocity	-58.444 rad/s
Relative Angular Acceleration	-5482 rad/s^2

$$T = I \tag{4}$$

$$=3.655618441\times10^{-}55482$$

$$= 0.2004010029Nm$$

Let P be the power produced by the crankshaft and n be the angular velocity of the shaft n rps. Then power produced by the crankshaft can be calculated using equation 5. Then torque calculated using equation 7.4 can be equated with the equation 7.5 to get the power produced by the crankshaft.

$$P = T \tag{5}$$

= 0.2004010029 × 58.444

= 11.71143461 W

So, we can get 73.5W power from the one wheel of the front part of the vehicle. While considering the overall vehicle, we can get about 297W power. More power can be produced with the help of more vehicles.

5 Conclusion

In the current scenario there is a huge depletion in fossil fuels, by the introduction of renewable energy the depletion of the fossil fuels can be reduced and thus providing some for the future generations. By the implementation of this system, overall usage of electric energy can be decreased and thus saving for future generations. This project's main goal was to investigate whether it was possible and practical to harvest energy from speed bumps in order to aid in the transition to renewable energy on a worldwide scale. Speed bumps' energy has been wasted up until this point. Additionally, more speed bumps are being installed to reduce accidents. Utilizing the wasted energy from speed bumps is a novel concept worldwide. So extensive investigation was necessary. This report presents the findings of the research and design. A suitable work plan has been developed. The brainstorming process is complete. Numerous literary sources have been examined. The mechanism was in place. The component material selection has been completed. There have been some upgrades. Solid Edge is used to design components. ANSYS software is used to conduct a number of analyses. Materials for the components are selected by analyzing several factors. Some are mentioned below. The decision to employ ABS plastic as a building material was based on the two results of the stationary section where two distinct materials, stainless steel and ABS plastic, were used. This is so because the factors of safety (FOS) for both materials 927 for stainless steel and 174 for ABS and are incredibly high. FOS of 174 is sufficient, and ABS is inexpensive and lightweight. ABS weighs 15.642 kg, whereas stainless steel weighs about 118.378 kg. Choosing steel as the material of the moving portion was based on two outcomes that uses the above-mentioned results. This is due to the fact that the FOS of steel is higher than the FOS of ABS, at 253 vs. 23. Additionally, ABS deforms more than steel, which deforms less. The moving component must be somewhat heavy because it is the component that distributes the load to the connecting rod. ABS material weighs only 1.356 kg as compared to 10.259 kg for stainless steel. Numerous methods and technologies have been investigated and put into practice to transform the kinetic energy of moving objects into useful electrical energy. To maximize energy conversion efficiency, a slider crank mechanism and electromagnetic systems have been developed and evaluated. These results have opened the door for prospective improvements and enhancements in speed bump energy system deployments in the future. However, it's important to note that while the concept of speed bumps as a renewable energy source shows promise, there are practical challenges that need to be addressed. Factors such as durability, maintenance, cost-effectiveness, and integration with existing infrastructure require further research and development. These considerations will play a crucial role in determining the feasibility and scalability of speed bump energy systems in real-world applications.

5.1 Future Possibility and Uses

The newly rising world is looking for the maximum utilization of energy especially when a lot of energy is wasted in day-to-day life. As conversion of these waste energy into productive ones is the main objective of this mechanism, this can be very useful in the present and future generations. The apparatus can be completely set up as portable and can be easily transported from one place to another. The design of the apparatus is highly durable so that it can be used for years. As it is connected to a portable battery as the storage, this battery can be used for any needs. Mechanism and working of the model are simple and robust.

Acknowledgements

The facilities for this study endeavor were provided by "Ansys 2023 and Solid edge 2023" which the authors gratefully thank. Additionally, a special thank you is given to our guide Nithin V K and Dr Vinod V the faculty of "NSS College of Engineering, Palakkad" for their ongoing assistance.

References

[1] Mohamad Ramadana, Mahmoud Khaleda, Hicham El Hage; Using speed bump for power generation –Experimental study; Energy Procedia 75; PP 867-872; 2015.

[2] Ahlam Lakshmi, Al Akwayn university; Speed bump generating electrical power; PP 1-38; 2019.

[3] K.Ravivarma, B.Divya, C.P.Prajith, A.Sivamurugan, K.Vengatesan; Power Generation Using Hydraulic Mechanism at Speed bumper; International Journal of Scientific Engineering Research 4; PP 258-266; 2013.

[4] Mohammadreza Gholikhania , Reza Nasouria, Seyed Amid Tahamia, Sarah Legetteb, Samer Dessoukya, Arturo Montoyaa; Harvesting kinetic energy from roadway pavement through an electromagnetic speed bump; Applied Energy 250 ; PP 503-511; 2019.

[5] B. Babu, V. Selvam; Design and Development of Power Generation from Speed Pump; International Journal of Multidisciplinary Educational Research 10; PP 50-56; 2021.

Fluid Flow and Heat Transfer Characteristics of Silver Granule Coated Minichannel with Graphene Oxide Nanofluid as Coolant

Athul P[1] and Dr. Jesseela S[2]

[1,2] Govt. Engg. College Kozhikode

[1]athulpallikkal@gmail.com, [2]jessyhamza@gmail.com

Abstract -

Micro/minichannel based circuits is one of the most effective solutions for the thermal management of electronics components due to its greater heat transfer coefficient and high heat transfer area. Coating in these channels further increase heat transfer rate by creating early turbulence. Fluid flow and heat transfer characteristics of flow through minichannel coated with silver granule under single phase flow conditions using Graphene oxide nanofluid of different volume concentrations is experimentally investigated. An enhancement of 58% in heat transfer coefficient is obtained for flow with nanofluid as compared to water. The heat transfer coefficient increases with increase in concentration of nanofluid.

Keywords -

Minichannel, Single phase flow, nanofluid

1 INTRODUCTION

High heat flux removal from electronic devices have been a challenging topic since after its origin. In some electronic components the heat produced has reached as high as 1000 W/cm2 which is approximately equal to ballistic entry [1]. According to Moore's law, the packing density of electronic components is doubling each year, with such a trend, a heat flux level of more than 2500 W/cm2 or higher can be seen in the near future. Due to miniaturization of electronic components, it is required to design heat transfer equipments which remove high heat flux from a small area.

Some of the recent technologies which were developed for high heat flux (HHF) removal includes minichannels, jet impingement, spray, enhanced surfaces and piezoelectric devices [2]. Minichannel heat exchangers are gaining its popularity in the field of HHF removal due to its compact size, dense packing, high heat removal capability and large surface area per unit volume. The above characteristics of minichannel make it an excellent candidate for high heat flux removal from electronic devices.

This work describes about the heat transfer and fluid flow analysis on a minichannel coated with silver granules. Silver granules due to its high thermal conductivity, large surface area and increased nucleation sites, when coated over the minichannel surface increases the heat transferred in both single phase and two-phase region.

The popularity of small flow passage in convective heat transfer applications is increasing mainly due to its capability to attain higher heat transfer enhancement, and also due to the emergence of micro scale devices that dissipate large amounts of heat [3]. Minichannel cooling can accomplish the task of high heat removal, but with an additional pressure drop. Electronic chip cooling using channel heat exchanger was first put forward by Tuckerman and Pease [4]. They circulated water on a microchannel fabricated on silicon chips and was able to remove heat flux of 790 W/cm2 without phase change on penalty in pressure drop of 1.94 bar. Since then several experimental and theoretical investigations (Philips et al. [5]; Mudawar et al. [6]; Harms et al. [7]; Lee et al. [8]; Morini et al. [9]) were carried out by several researchers in both single phase and two phase channel heat exchangers. Khanikar et al. [10] conducted experiments on a rectangular microchannel coated with vertically aligned carbon nanotube with titanium as the intermediate layer and its flow boiling characteristics is compared with bare microchannel. Morshal et al. [11] noticed an increase in pressure drop of 20% for copper nano wire coated surface. An increase in pressure drop was observed with increase in heat flux. With increase in mass flux pressure drop first increases and then decreases. The drop in pressure with increase in mass flux is due to segmented flow of water and vapour. Khanikar et al. [10] observed that the pressure drop was higher for CNT coated surface due to the additional wall shear stress imposed by CNT coating. Similar pressure drop characteristics was also observed by other nano coated surfaces.

Due to the presence of suspended nanoparticles with high thermal conductivity, nanofluids outperform traditional fluids in terms of thermal performance. Nanoparticles offer unique features that nanofluids potentially take use of, such as a large surface area to volume ratio, dimension-dependent physical properties, and reduced kinetic energy. At the same time, a greater surface area improves and stabilizes nanoparticle dispersion in base fluids.

Microfluids are more unstable than nanofluids. Flockhart et al. [12] were the first to propose the usage of metallic particles to improve the thermal properties of fluids. The influence of nanofluids in a tiny heat exchanger was examined by Mapa et al. [13]. Their studies used water and nanofluid with concentrations of 0.01 percent and 0.02 percent volume to assess heat transfer performance in the heat exchanger. They came to the conclusion that nanofluids improve heat transfer performance and lower the thickness of the thermal barrier layer. Garud et al. [14] examined the convective heat transfer performance of CNT–water nanofluid in a micro-channel with a hydraulic diameter of 355 m and Reynolds numbers ranging from 2 to 17 for particle concentrations of 1.1 to 4.4 percent. At the maximum concentration, the CNT–water nanofluid had a higher heat transfer coefficient.Present work focuses on the experimental analysis of the fluid flow and heat transfer characteristics of flow through silver granules coated minichannel with graphene oxide nanofluid as the working fluid.

2 EXPERIMENTAL SETUP

A mini channel coated with silver granule test facility has been fabricated and single phase experiments were conducted to observe the fluid flow and heat transfer characteristics in mini channel. The experiments were initially carried out using base fluid (water) and then with nanofluid. The experimental setup is shown in Figure 1.

The experimental facility consists of a mini channel test section with hydraulic diameter 761µm, a peristaltic pump (14 to 450 ml/min) for pumping fluid, a data acquisition system for measuring temperature, an autotransformer (0-260 V) for controlling heat input and two pressure transmitters (EQ-PT1000-2) for measuring pressure.

The main component of the experimental facility was the channel test section, which is shown in Fig.2.The test section includes a copper block, on the top of which there is a rectangular channel of length 30 mm, width 8 mm and depth 0.4 mm. Four cartridge heaters (each 500 W) were inserted at the horizontal holes drilled on the copper block. The copper block was thermally insulated by PEEK housing.

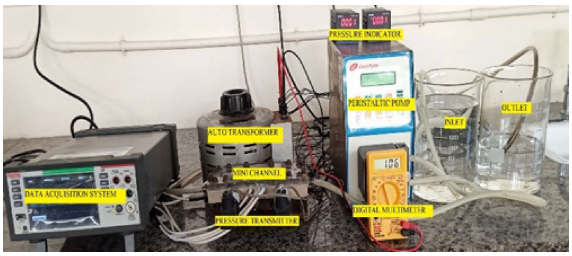

Figure 1. Experimental Facility

The channel bottom surface temperature was measured by four K type thermocouples (3 mm diameter probe). The thermocouples are located at a distance 6mm, 12mm, 18mm and 24mm from the inlet of the minichannel and 3 mm below the channel bottom surface. There were two thermocouples (K-type 1mm dia) one at inlet and other at outlet of mini channel to measure inlet and outlet temperature of working fluid. The thermocouples were attached to a Keithley data acquisition system (DAQ6510), which was used to record instantaneous temperatures.

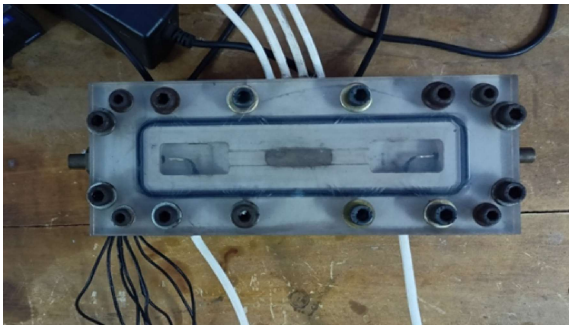

Figure 2. Minichannel Test Section

The experiment was conducted at first using de-ionized water and then using nanofluid as the working fluid. The working fluid at the desired flow rate was pumped using a peristaltic pump. The heat input to the section was given by cartridge heaters at the bottom of the channel, which is connected to the autotransformer. There were two pressure transmitters at the inlet and exit plenum to measure the pressure. A thick layer of glass wool insulation was provided at the bottom of the copper testing block to prevent heat loss to the surroundings.

2.1 Uncertainty Analysis

Uncertainty can be defined as an estimate of the interval or range that contains an error in the experimental measurement or result. The total error in a measurement is the difference between the measured value and the true value. For measured variable,

$$S_x = \sqrt{\frac{1}{N-1}\Sigma_i^N (x_i - \overline{x})^2} \tag{1}$$

For experimental result defined by an equation,

$$r = r(X_1, X_2, ...) \tag{2}$$

and

$$U_r = \sqrt{\left(\frac{\delta r}{\delta X_1}\right)^2 (U_{X_1})^2 + \left(\frac{\delta r}{\delta X_2}\right)^2 (U_{X_2})^2 + ...} \tag{3}$$

The uncertainties associated with each measurement is tabulated in table 1.

Table 1. UNCERTAINTY VALUES

Parameter	Uncertainty
Temperature	$\pm 1.4°C$
Pressure	$\pm 0.5°C$
Heat flux	$\pm 15.5°C$
Heat transfer coefficient	$\pm 17.8°C$

2.2 Nanofluid Preparation

Nanofluids were prepared by two step method. In the two steps method nanoparticles are first made as dry powders by various methods. Then powders will be dispersed into a base fluid in the second step with the help of magnetic stirrer and ultrasonic shaker. Stability of nanofluids is essential. The stability of nanoparticles in fluids can be ensured with giving sufficient time for mixing in magnetic stirrer. But the one step method consists of simultaneously making and dispersing the particles in the fluid.

Here nanofluids were prepared by two-step method. Graphene oxide nanoparticles were purchased from Shilpa Enterprises Bangalore. De-ionized water is taken as the base fluid for preparation of nanofluids. Initially the amount of nanoparticles required for preparation of given volume concentration of nanofluids are calculated using law of mixture formula and then nanoparticles are mixed with base fluid with the help of magnetic stirrer and then it was undergone for an ultrasonic vibration of 3 hours. Graphene oxide nanofluids of two different volume concentrations, 0.001%, and 0.01% were prepared to carryout this work.

2.3 Data Deduction

The pressure drop across the channel was measured using two pressure transmitters connected at the exit and inlet manifolds. The pressure drop thus measured is a combination of entrance and exit loss and the pressure drop across the channel. Hence, the net pressure drop along the channel was calculated as,

$$\Delta P = \Delta P_{experimental} - (K_c + K_e)\frac{1}{2}\rho u^2 \tag{4}$$

Where Kc and Ke are the entrance and exit loss coefficients respectively. The values of Kc and Ke are obtained from Shah and Sekulic [15].

Fanning friction factor,

$$f = \frac{\Delta P D_2}{2L^2} \tag{5}$$

Hydraulic diameter,

$$D_h = \frac{4HW}{2(H+W)} \tag{6}$$

Reynolds number,

$$R_e = \frac{\rho u D_2}{\mu} \tag{7}$$

Heat removed by fluid,

$$Q = \dot{m} C_p (T_o - T_i n) \tag{8}$$

Net heat input to the channel per unit area,

$$q = \frac{mcp(T_o - T_i n)}{As} \tag{9}$$

The local heat transfer coefficient is given by,

$$h = \frac{q}{Ts - Tm} \tag{10}$$

Nusselt number ,

$$f = \frac{hD_a}{kf} \tag{11}$$

For the single phase experiments the thermo physical properties of fluid were evaluated at the arithmetic mean of the inlet and exit temperatures. The operating conditions are given in Table 2.

Table 2. OPERATING CONDITIONS

Coolant	Inlet Temperature($°C$)	Flow rate (ml/min)	Heat Input(W)
Water	29	25-200	60
GO nanofluid	29	25-200	60

3 RESULTS AND DISCUSSIONS

Experiments have been conducted for different volume concentrations of nanofluid and the parameters such as pressure drop, friction factor, outlet fluid temperature, heat transfer coefficient, and Nusselt number were determined. The effect of volume concentration and the mass flow rate on these parameters have been studied.

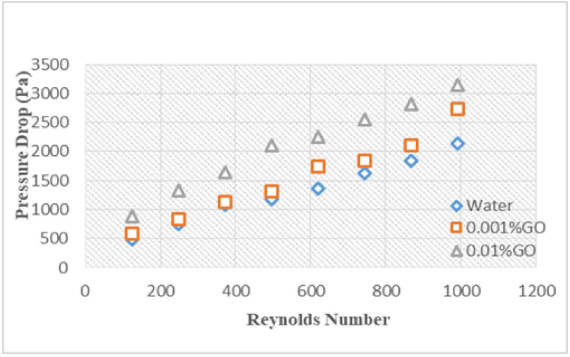

Figure 3. Variation of pressure drop with Reynolds number for different volume concentration

As shown in Fig.3, the pressure drop increases with Reynolds number and nanofluid particle volume concentration. Comparing water and nanofluid, the pressure drop

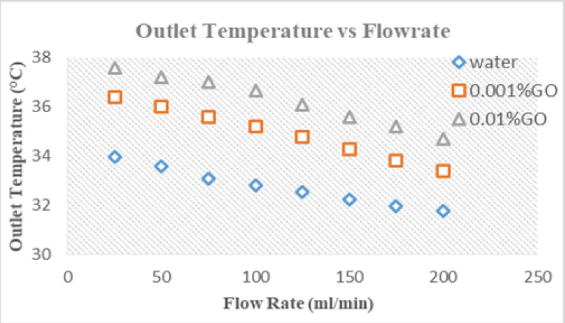

Figure 4. Variation of outlet temperature of fluid with flow rate for different volume concentrations of nanofluid

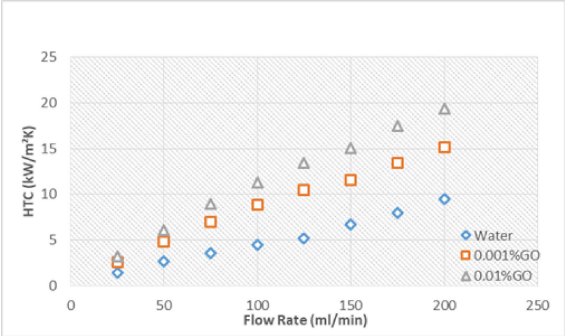

Figure 6. Heat transfer coefficient variation with flow rate for different concentration.

increased by about 34% while using nanofluid with 0.01% volume concentration.

Variation of outlet temperature of fluid with mass flow rate for different volume concentrations are shown in Fig.4. The outlet fluid temperature increases with increasing particle volume concentration and decreases with increasing mass flow rate. The maximum outlet temperature of fluid was discovered for 0.01 vol. %. This might be due to increased thermal conductivity of nanofluid.

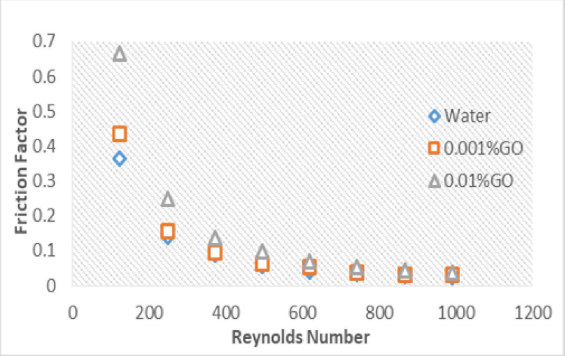

Figure 5. Variation of friction factor of fluid with Reynolds number for different volume concentrations of nanofluid.

Fig,5 shows the variation of friction factor with Reynolds number and it decreases with increase in Reynolds number as expected. At low Reynolds numbers the fiction factor is found to be increasing with increasing particle volume concentration and at higher flow rates the difference in values of friction factor for various concentrations is small and the value of friction factor approaches to zero.

For water and nanofluids, Fig.6 depicts the change of single-phase heat transfer coefficient with flow rate. The trend is same for both fluids, with nanofluid having a significant rise in heat transfer coefficient. The heat transfer coefficient tends to increase as the concentration of nanoparticles rises. The reason for this enhancement of heat transfer coefficient might be due to rise in thermal conductivity of nanofluid. The highest value of heat transfer coefficient is seen to be at higher flow rates. Compared to water the heat transfer coefficient of nanofluid is enhanced by about 58% at 0.01% volume concentration for 200ml/min. Fig.7 shows the variation of Nusselt number with Reynolds number and it shows the same trend as heat transfer coefficient as they are directly related.. This is due to increase in heat transfer coefficient. An enhancement of 56.2% in Nusselt number is observed for 0.01% volume percentage concentration as compared to water for a flow rate of 175 ml/min.

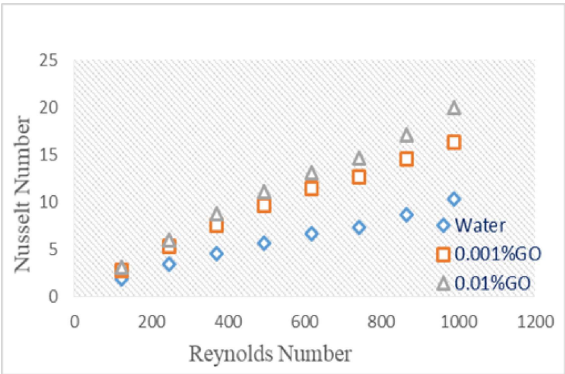

Figure 7. Nusselt number variation with Reynolds number for different concentrations.

The heat transfer coefficient for silver granule coated channel is compared with bare channel of same setup Sajith et al. (16). From fig. 8 we can see that the heat transfer coefficient for silver granule coated minichannel is 28.23% higher as compared to bare channel for a Reynolds number

of 495. The enhancement in heat transfer coeffient is due to the early turbulence created as a result of silver coating.

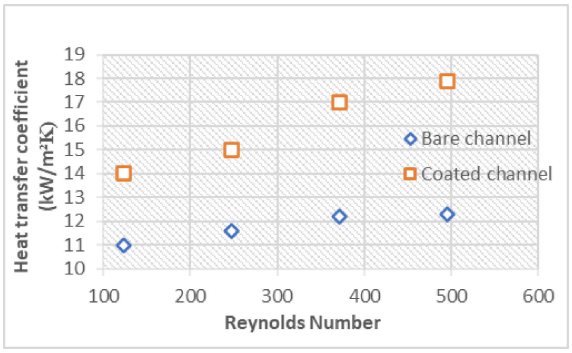

Figure 8. Comparison of heat transfer coefficient for bare and coated channel

4 CONCLUSIONS

Single phase flow experiments were performed using water and graphene oxide nanofluids as coolants. The results showed that use of nanofluids increases the heat transfer coefficient at the cost of increase in pressure drop. The percentage increase in pressure drop is negligible as compared with the enhancement in heat transfer. The main conclusions are

- With increase in concentration of nanofluids the heat transfer coefficient and pressure drop increases.
- An enhancement of 58% in heat transfer coefficient is obtained for 0.01% graphene oxide nanofluid as compared to water.
- For all ranges of Reynolds number heat transfer coefficient of mini channel with nanofluids was higher than that of water.
- Study recommends the graphene oxide nanofluid as an effective coolant in mini channel heat sink.

References

[1] I. Mudawar, “Assessment of high-heat-flux thermal management schemes,” Components and Packaging Technologies, vol. 24, no. 2, pp. 122 - 141, Jun 2001.J. Clerk Maxwell, A Treatise on Electricity and Magnetism, 3rd ed., vol. 2. Oxford: Clarendon, 1892, pp.68–73.

[2] M. A. Ebadian and C. X. Lin, “A Review of High-Heat-Flux Heat Removal Technologies,” J. Heat Transfer, vol. 133, no. 11, p. 11, Sep 02, 2011.

[3] S. G. Kandlikar, S. Garimella, D. Li, S. Colin and M. R. King, Heat transfer and fluid flow in minichannels and microchannels, Oxford: Elsevier, 2006.

[4] D. Tuckerman and R. Pease, “High-Performance Heat Sinking for VLSI,” Electron Device Letters, vol. 2, no. 5, pp. 126 - 129, 1981.

[5] R. Phillips, L. Missaggia, J. Walpole and Z. Liau, “Microchannel heat sinks for two-dimensional high-power-density diode laser arrays,” Quantum Electronics, vol. 25, no. 9, pp. 1988 - 1992, 1989.

[6] I. Mudawar and W. Qu, “Experimental and numerical study of pressure drop and heat transfer in a single-phase micro-channel heat sink,” International Journal of Heat and Mass Transfer, vol. 45, no. 12, p. 2549–2565, 2002.

[7] T. M. Harms, M. J. Kazmierczak and F. M. Gerner, “Developing convective heat transfer in deep rectangular microchannels,” International Journal of Heat and Fluid Flow, vol. 20, no. 2, p. 149–157, 1999.

[8] P. S. Lee, S. V. Garimella and D. Liu, “Investigation of heat transfer in rectangular microchannels,” International Journal of Heat and Mass Transfer, vol. 48, no. 9, p. 1688–1704, 2005.

[9] G. Morini, M. Spiga and P. Tartarini, “The rarefaction effect on the friction factor of gas flow in microchannels,” Superlattices and Microstructures, vol. 35, no. 3-6, p. 587–599, 2004.

[10] V. Khanikar, I. Mudawar and T. Fisher, “Effects of carbon nanotube coating on flow boiling,” International Journal of Heat and mass transfer, vol. 52, no. 15- 16, p. 3805–3817, 2009.

[11] A. Morshed, F. Yang, M. Y. Ali, A. A. Khan and C. Li, “Enhanced flow boiling in a microchannel with integration of nanowires,” Applied Thermal Engineering, vol. 32, pp. 68-75, 2012.

[12] S M Flockhart & R S Dhariwal, “Experimental and Numerical Investigation into the Flow Characteristics of Channels Etched in Silicon,” Journal of Fluids Engineering, vol. 120, pp. 291- 295, 1998.

[13] Daniel J. Faulkner, David R. Rector, Justin J. Davidson, Reza Shekarriz “Enhanced Heat Transfer Through the Use of Nanofluids in Forced Convection,” International Mechanical Engineering Congress and Exposition, November 13–19, Anaheim, California, USA, 2004.

[14] Garud, Kunal Sandip, and Moo-Yeon Lee. “Numerical Investigations on Heat Transfer Characteristics of Single Particle and Hybrid Nanofluids in Uniformly Heated Tube.” Symmetry (Basel), vol. 13, no. 5, MDPI AG, 2021, p. 876–, doi:10.3390/sym13050876.

[15] R.K. Shah and D.P. Sekuli (2003), ”Fundamentals of Heat Exchanger Design”, John Wiley & Sons Inc.

[16] Sajith Krishnan R, Jesseela S, “Fluid Flow and Heat Transfer Analysis on Single Phase Flow Through Microchannels with Single Side Heating” The Third National Conference on Emerging Trends in Engineering (NET 2015)

Design and Fabrication of an All-Terrain Vehicle Integrated with Sensors for the Identification of Materials in Landslide Affected Region

Kavya Suresh[1], Meenakshi Prakash[1], Musthafa Jalal[1], Sreehari K V S[1] and Dr. Rajesh Menon B[2]

[1] Department of Mechanical Engineering, NSS College of Engineering, Palakkad, Kerala, India
[2] Professor, Department of Mechanical Engineering, NSS College of Engineering, Palakkad, Kerala, India

Abstract -

This research paper presents an innovative approach to improve the detection of buried materials and trapped humans during landslides in India, aiming to save lives and minimize losses. By leveraging the proven rocker bogie mechanism used in interplanetary rovers, our searching protocol offers enhanced mobility across various terrains. Through a modular design, the system incorporates a Doppler radar module for trapped human detection, a fire extinguishing arm for rescue missions, and a future addition of a metal detector module. The principal results demonstrate the effectiveness of this approach in early detection and disaster response, contributing to improved efficiency and accuracy in landslide rescue operations.

Keywords -

Rocker bogie; Human; Landslide; Detection; Doppler radar

1 Introduction

The occurrence of earthquakes and landslides globally presents a significant threat to human lives and infrastructure. The devastating impact of landslides, including high mortality rates, infrastructural damages, and loss of resources, necessitates the development of more effective and efficient methods for rescue operations. Traditionally, rescue efforts rely on conventional techniques such as using sniffing dogs or optical devices, which are time-consuming and often inaccurate. Furthermore, the risks associated with deploying human personnel in hazardous environments limit their effectiveness. To overcome these challenges, our research focuses on designing and fabricating a modular all-terrain vehicle that integrates advanced sensing technologies to detect and locate trapped individuals. The integration of Doppler radar and PIR sensors enables the detection of human presence behind walls and under debris. The use of a rocker bogie mechanism, commonly employed in Mars rovers, ensures the vehicle's ability to traverse diverse terrains, thereby expanding its applicability in disaster-stricken areas. The significance of this research lies in its contribution to the field of disaster management and rescue operations. By developing an unmanned all-terrain vehicle capable of efficiently detecting trapped individuals, we aim to minimize the risk to both the victims and the rescue teams. The use of advanced sensing technologies, coupled with the versatility of modular design, allows for customization and adaptation to various scenarios, making the vehicle an invaluable tool in disaster response. Our research brings a practical and innovative approach to the field, addressing the limitations of current methods and technologies. By combining Doppler radar and PIR sensors, we provide a reliable and efficient means of detecting trapped individuals, reducing the critical time window for successful rescues. Additionally, the integration of metal detectors and fire extinguishing robotic arms further enhances the safety of both the trapped individuals and the rescue teams, ensuring a comprehensive rescue operation. In conclusion, this research paper presents a pioneering approach to disaster rescue and assistance through the development of a modular all-terrain vehicle. By integrating advanced sensing technologies and leveraging the versatility of the design, our research contributes to the field by providing an effective and efficient solution for life detection and safety enhancement. The practical applications of this research extend to disaster-stricken areas, where the all-terrain vehicle can be utilized for various tasks, such as logistics, reconnaissance, mapping, and medical assistance.

2 The object of the study (Model, Process, Device, Sample preparation etc.)

Worldwide, around 4,000 deaths per year in average are caused by landslides. As per the present methods of rescue, there are high chance of risking life of trapped ones and rescue teams. All of them are exposed to dangerous situations where the rescuers themselves can be a victim. Trained dogs are been currently used, but still, it is hard to totally depend on them. Dogs cannot work independently but need to be accompanied by their trainers. Therefore, it is necessary to develop an independent alternative like

robots. Contributions from each are highly valuable in these situation even if its impact isn't much and we would like to be a part of it. We are designing and manufacturing by considering faster identification of human bodies as well as safety and easiness of rescue team. We put forward an alternative method by automating the whole searching protocol. This motivates us to concentrate our final academic project in this field. We hope that our project will bring a tremendous development in the rescue process.

3 Methods

Initially the main objective was integration of GPR which detects the human bodies under the soil during landslide. Over the modular case in the chassis, GPR is attached and through remote control system the all-terrain I moves through the soil by and identify living bodies under trapped. The GPR is designed accordance to the dimensions of chassis and thus integration is made possible. Currently according to the ease of availability and cost effective, module used is the Doppler sensor and PIR sensor. These sensors receive signals that reflect from bodies trapped under soil. This is a main part for human rescue missions. The Doppler radar work by principle of transmission of microwave signal to target and its reflecting signal as a response. The variations in frequencies are measured so that using velocity signals results are obtained. For a PIR sensor external power is supplied since it is passive. It uses infrared light radiations from objects. These radiations cannot be detected using human eye and so electronic device are used.

3.1 Structure

The rocker bogie mechanism is a type of suspension system used in robotic vehicles, particularly in Mars rovers. It provides stability and mobility in challenging terrains by allowing the vehicle to traverse uneven surfaces and obstacles. The mechanism consists of a set of rocker arms and bogie arms. The rocker arms connect the vehicle's body to the rocker wheels, which are positioned in the center of the vehicle. The bogie arms connect the rocker wheels to the bogie wheels, which are located on the sides of the vehicle. The key feature of the rocker bogie mechanism is its ability to maintain constant contact between the wheels and the ground, even on uneven surfaces. When one wheel encounters an obstacle, the rocker arms pivot, allowing the other wheels to maintain contact with the ground. This enables the vehicle to smoothly navigate over obstacles and maintain stability. The rocker bogie mechanism also provides weight distribution and suspension flexibility. The weight of the vehicle is evenly distributed across multiple wheels, reducing the risk of overloading any single wheel. Additionally, the suspension system allows each wheel to move independently, ensuring that the vehicle maintains contact with the ground and can adapt to variations in terrain. Designing sensor boards for each sensors seems to be an ineffective and a bit costly in nature. So an idea of using a single board for all sensors can be proposed, which is said to be the modular approach. Modularizing the system, the sensor board can be reused for different sensors. This helps to make the process simple and inexpensive. Modular sensors are the design of the product in which different attributes can be interchange. It need not be limited with sensors but also packages etc. most of the suppliers are now embracing this approach. This methodology benefits both suppliers and customers. Its offers a versatile approach towards integration. With a modular design method, a product can be breakdown into parts and allow could assemble them. Thus each parts can be designed separately and could assemble accordance to the requirements. A modular approach for sensors involves designing and implementing sensors as individual modules that can be easily integrated into different systems or projects. Consider factors such as sensing range, accuracy, interface compatibility, power requirements, and cost. Choose sensors that come in modular form factors, such as breakout boards or sensor modules, which simplify integration. Determine the communication interface between the sensor module and the microcontroller or main control board. Common interfaces include I2C, SPI, UART, or analogue. Make sure the sensor module has an interface that is compatible with the microcontroller or can be easily adapted using additional modules or converters. If you cannot find a pre-made sensor module, you may need to design your own. This involves creating a PCB (Printed Circuit Board) that hosts the sensor, supporting components (e.g., resistors, capacitors), and the necessary interface circuitry. You can use PCB design software like Eagle, KiCad, or Altium to create the module. Once you have the sensor module ready, test it to ensure it functions correctly. Verify its accuracy and calibrate if necessary. Develop appropriate code or use existing libraries to interface with the sensor and retrieve data. Document the sensor module's specifications, pinout, and any special considerations for integration and usage. This documentation will be valuable for future projects or when sharing the module with others. Now that you have a functional sensor module, you can easily integrate it into different projects or systems. Connect the module to the microcontroller or control board using the designated communication interfaceBy following this modular approach, you can develop a library of sensor modules that are easily interchangeable and reusable. This makes it simpler to prototype new projects or adapt existing ones by selecting and integrating the appropriate sensor module(s) for the specific requirements.

Material Properties	Metrics
Ultimate strength	400 MPa
Yield strength	250MPa
Density	750kg/m3
Poisson's Ratio	0.3
Young's Modules	200GPa
Hardness	120
Thermal Conductivity	50W/mk

3.2 Construction

Selection of material is a main stage in designing a component. Main needs are increased reliability, strength, reduce cost and optimize weight of the product. The literature reviews and studies about different materials helped us to identify the proper raw material ie; MILD STEEL. It is been selected due to its outstanding mechanical properties and also its availability in India. It is one of the most widely used steel. Mild steel is a ferrous metal made up of iron and carbon. Amount of carbon presents 0.05 to 0.25 percent by weight and hence called as low-carbon steel. Applications are wider as from piping, fencing to automotive manufacturing and aerospace since known for its strength, durability, good weldability and ductility. Here we are using mild steel pipes of ½ cm in diameter. It has a low range of hardness and yield strength so that easy to shape. This doesn't mean it can be teared or stretches when shaped. Mild steel can be cleaned easily using chemical treatments and protecting shields can be provided to resist corrosion. This enhance and show long-lasting performance. Mild steel can be used as a best material for project as it can be graded accordingly considering its properties, composition and so on.

Welding technique is used for the whole fabrication process. It is the process if joining materials of same or different kind using heat with pressure or heat only. It is a permanent bonding process so that separation to former stage is impossible. Here the welding is done by the electrical torch with help of heat. Different types of joining are there like Butt joint, T joint, Lap joint etc. Melting point is in a range of 1450 -1520 degree Celsius. The parts need to be welded are kept closer and arranged as per the required shape. Then using heat torch the joining ends are heated and fused manually. Protective shields, gloves are necessary to ensure the safety of worker. After the fusion materials are allowed to cool for the fusion. Finally the welded product is obtained. The whole chassis in this project is joined by welding process. Rocker bogie is a suspension based mechanism used to overcome the difficulties through rough terrain by distributing vehicle load evenly. It is a passive spring-less and symmetric mechanism. The material used for the chassis, rocker and bogie is mild steel due to its strength and durability. Initially each parts are designed and its assemble is done using the CAD software Autodesk fusion 360.the whole body of a rocker bogie suspension system consist of supporting frame/ chassis, screws and bolts, joints, mounts and fixtures, and arms(rocker and bogie). The chassis is of size 465mm*300mm*70mm and mild steel pipe of ½ m in diameter. The pies are made up to required shape by cutting and joined by welding process. The structure of chassis is as shown in fig. The Arms consist of 2 parts: Rocker and Bogie and chassis has 2 arms as each on either side. The longer arm is the rocker that of a length of 550 mm and angle between is 160 degree. The middle point of rocker is attached with the chassis using screw and bolt. The shorter arm is the bogie and its mid-point is connected with one end of rocker using screw. 2 bearings are present in each side which is model of 6021 bearing. It is located as one between chassis and rocker and the other between rocker and bogie. Both end of the bogie and the remaining free end of rocker is attached with wheels. After the fabrication the chassis is completely polished and painted for better appearance. The locomotion system of the rover is controlled by microcontrollers and comprises motors, relays, wheels, and bearings. Due to the unavailability of the originally intended motor, a 30 rpm Geared center shaft 12V motor with an operating voltage of 6V to 18V is used instead. Each wheel is attached to an independent motor, with a total of 6 motors being used. The selected wheels are plastic and rubber robotic wheels, specifically REES52 10*4 robot wheels with a 6 mm shaft. The motor specifications include a rated voltage of 12V, providing a speed of 30 rpm and -2 kg cm torque. The gears used in the mechanism are made of metal, and the dimensions of the motor are 12*5*5 cm, weighing 150g. Each wheel is driven by its respective motor, and the chassis is designed to carry a total weight of 1.2 kg for the motors. Both propulsion and trajectory control functions are implemented through the forces applied by the wheels on the ground, which are caused by the deformation of both the bodies in contact (wheel and ground). As a consequence, the wheels of a vehicle are always operating with some sideslip and longitudinal slip and are never in pure rolling. In slip steering there is no steering mechanism, but the driving wheels can produce differential traction on the two sides of the vehicle. This can be achieved by using independent motors in the wheels or six motors actuating the wheels of the two sides independently, or by using a differential gear. The brakes can also be used in differential mode to achieve some slip steering. Very small trajectory curvature radius can be obtained by rotating backwards the wheels on one side, and turning on the spot is possible by using equal and opposite rotation speed. No kinematic steering is possible. The rover features a rocker bogie mechanism, allowing it to climb over obstacles. There are

no springs or stub axles in the wheels, ensuring tilt stability and preventing tilting up to an angle of 50 degrees. The differential mechanism is used to ensure that all wheels remain in contact with the ground and to distribute torque from the engine to the wheels. This prevents slipping and sliding during turning and provides better performance on various terrains. The rover does not have a steering mechanism but uses a slip system for wheel control. The traction produced on either side of the vehicle is differential, and each wheel is independently integrated with a motor. A differential mode brake is used for slip steering. The differential system allows the transmission of torque from the engine to the wheels, ensuring that each wheel can move at a different speed. This prevents power concentration on the least resistive part and reduces power loss and wheel spin. It also balances the load and redistributes torque to lower the slipping of wheels. The differential mechanism is particularly suitable for an all-terrain vehicle like the rover, as it ensures optimal performance on various grounds, including muddy and inclined terrains encountered during landslides. In summary, the rover utilizes microcontrollers to control locomotion, with motors, relays, wheels, and bearings forming the locomotive system. The rocker bogie mechanism, coupled with the differential system, allows the rover to navigate challenging terrains while maintaining stability and preventing wheel slipping. The selected motor and wheel specifications were chosen based on factors such as availability, cost, and suitability for the project's requirements. Relays are used in the project to control the movements of the rover's body. They act as electrically operated switches, allowing control of high current loads with a small amount of current. The DOAT d-3f-s-5vdc relay is utilized, with features including a trigger voltage of 5V DC, trigger current of 70mA, and maximum load currents of 10A for both AC and DC.After designing the rocker bogie mechanism with a differential system, a modular setup is implemented to integrate various modules. The modules are attached to the top portion of the chassis in a rectangular structure, with dimensions of 360mm in length and 300mm in total width. There is a fitting portion with a thickness of 12cm on each side, providing a hollow space of 300*50. The modules used in the project, based on availability and cost limitations, include a Doppler sensor and a robotic arm for fire extinguishing. Other possible modules include GPR, PIR sensors, and metal detectors. The electronic system of the rover comprises a microcontroller, control module, and human detection system. The ESP WROOM32 is used as the microcontroller, which is a Wi-Fi-BT-BLE MCU module integrating various peripherals such as capacitive touch sensors and Ethernet. Bluetooth is employed to control the rover's operation via a smartphone or by connecting to it for broadcasting. The control interface used is Blynk, a user-friendly system for building and controlling different projects. It utilizes a mobile app and a cloud-based server for performing the required functions. Human detection is achieved using Doppler sensors. Relays are used for controlling the rover's body movements, with the DOAT d-3f-s-5vdc relay being chosen for the project. A modular setup is implemented for integrating various modules, with a rectangular structure attached to the chassis. The electronic system consists of the ESP WROOM32 microcontroller, control module using Blynk interface, and human detection achieved through Doppler sensors.

3.3 Construction

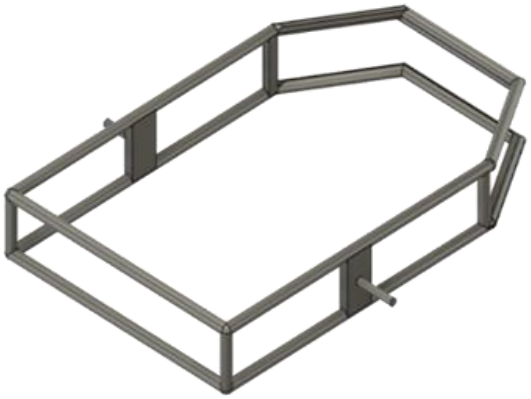

Figure 1.

Figure 2.

The bogie beams are parallel beams or bars that connect the rocker arms to the wheels. They provide support and stability while allowing vertical movement of the wheels. The rocker arms are the main linkage elements in the mechanism. They connect the suspension system to the chassis and allow the wheels to move

Figure 3.

3.4 Component

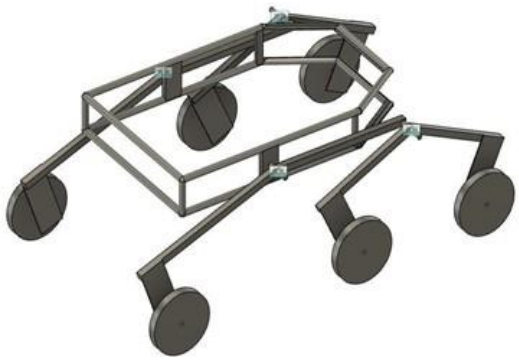

Figure 4.

Motor: The motor 12V 30 rpm Johnson geared DC motor- Grade A quality-Encoded Compatible is a sturdy construction. . Basically a motor converts electrical energy to mechanical and here the mechanical energy is for the movement of the system. This motor is a simple DC motor coupled with gearbox for delivering more power/torque. The gearbox material is of metal with gear ratio 540:1. Real time feedback of speed and rotating position of motor is given by Hall Effect Encoders in it. In the initial stages of our project, we had initially planned to use a Johnson motor type A with specific torque specifications. This motor had a stall torque of 1000 N-cm and a rated torque of 254 N-cm. Our circuit system was designed to accommodate a 12-volt motor driver unit. However, due to the unavailability of the Johnson motor type A and considering the nature of our project as a prototype, we had to explore alternative options. After careful consideration, we opted for a 30 RPM center shaft 12-volt motor. This motor had a rated torque of 2 kg-cm. We installed this motor on all six arms of our system. Despite the differences in torque specifications, we found that this motor was suitable for our needs. It successfully enabled our system to climb obstacles with a height of approximately 7 cm. It is important to note that the weight of the rocker bogie and additional robotic arms was taken into account when assessing the climbing capability of the system. Overall, this alternative motor selection, although different from our initial choice, proved to be effective in meeting our requirements within the scope of the prototype. Microcontroller: ESP WROOM 32 is a powerful, generic Wi-Fi-BT-BLE MCU module that targets a wide variety of applications, ranging from low-power sensor networks to the most demanding tasks, such as voice encoding, music streaming, and MP3 decoding.At the core of this module is the ESP32S chip, which is designed to be scalable and adaptive. There are 2 CPU cores that can be individually controlled or powered, and the clock frequency is adjustable from 80 MHz to 240 MHz. The user may also power off the CPU and make use of the low-power coprocessor to constantly monitor the peripherals for changes or crossing of thresholds. ESP32S integrates a rich set of peripherals, ranging from capacitive touch sensors, Hall sensors, low-noise sense amplifiers, SD card interface, Ethernet, high-speed SDIO/SPI, UART, and I^2C. Using Bluetooth, users can connect to their phone or broadcast low energy beacons for its detection. The use of Wi-Fi enables a large physical range, as well as a direct connection to the internet via a Wi-Fi router. Perfect for wearable electronic or battery-powered applications, the ESP32 chip uses less than 5μA.In addition, this module can support data rates of up to 150 Mbps and 22 dB output power at the PA in order to allow for the widest physical range. You can program the ESP32 in a variety of languages and programming environments, including C/C++, Micro python, Lau, and more. For programming environments, you can use Espressif's IoT Development Framework (IDF) or VSCode with PlatformIO. Control Interface: Blynk is an Internet of Things (IoT) platform that provides a user-friendly way to build and control IoT projects. It consists of a mobile app and a cloud-based server that work together to enable communication between IoT devices and a user's smartphone or tablet. With Blynk, users can create custom mobile apps for controlling and monitoring their IoT devices without needing to write complex code from scratch. The platform supports a wide range of popular hardware platforms and microcontrollers, such as Arduino, Raspberry Pi, ESP8266, and more. Users can connect their devices to the Blynk server using various communication protocols, including Wi-Fi, Ethernet, Bluetooth, and GSM. The Blynk mobile app allows users to design their own interfaces with drag-and-drop widgets, such as buttons, sliders, graphs, and displays. These widgets can be linked to IoT devices, enabling remote control and real-

time data visualization. Blynk also provides an extensive library of pre-built widgets and functions to simplify the development process. The Blynk cloud server acts as a bridge between the mobile app and the connected devices. It manages communication and data exchange, securely transmitting commands and receiving sensor data. The server also supports features like data logging, push notifications, and email alerts. Blynk offers a flexible and intuitive platform for hobbyists, makers, and professionals to quickly prototype and develop IoT projects. It simplifies the process of creating mobile apps for controlling and monitoring connected devices, allowing users to focus on the functionality and user experience of their projects. Human Detection Module : Doppler sensor and PIR sensors are used for the human detection in this project. Our system employs a novel passive Doppler sensor that collects signals reflected from people beneath rubble. Radar will detect and alter infrared radiation of micron wavelengths emitted by a human body. When a human target is found, the system is required to issue an alert that might assist in quickly locating and identifying the victim. The ”Human detection module,” which will be utilised to conduct the search activity, is the main component of the circuit design. It is a Doppler Radar Sensor, the RCWL-0516. Through the use of Doppler microwave technology, motion may be detected through walls and other obstructions. It will be activated by moving items in addition to people. To identify moving objects, the RCWL-0516 sensor employs microwave Doppler radar technology. The Doppler radar operates by sending a microwave signal to a target and then examining the shift in frequency of the signal that is received back. Target velocity relative to the radar may also be determined using variations in the received signal frequency The RCWL-0516 chip used in this sensor module allows repeat trigger and has a 360-degree detection range with no blind spots. It has a 7 metre sensitivity range and can detect motion through surfaces and other areas PIR is another sensing device used for human detection. An electronic sensor that measures the infrared (IR) light emitted by objects in its field of vision is known as a passive infrared sensor (PIR sensor). Most frequently, they are utilised in motion detection devices as PIR. Any item with a temperature greater than absolute zero radiates heat energy. Because it emits at infrared wavelengths, this radiation is often undetectable to the human eye, but it may be detected by electronic equipment made for that purpose. In this context, the word ”passive” refers to the notion that PIR devices don’t produce or emit any energy in order to detect objects. They are fully dependent on other things’ energy output to function. Instead of finding or measuring ”heat,” PIR sensors look for infrared radiation that emits or reflects from an object. To detect the movement of humans, animals, or other objects, a PIR-based mobility detector is utilised. They are often utilised in lighting control systems and burglar alarms. Arduino Uno: The Arduino Uno is a microcontroller board based on the ATmega328. It has 14 digital Input/output pins (of which 6 can be used as PWM outputs), 6 analog inputs, a 16 MHz crystal oscillator, a USB connection, a power jack, an ICSP header, and a reset button. It contains everything needed to Support the microcontroller; simply connect it to a computer with a USB cable or power it with an AC-to-DC adapter or battery to get started. The Uno differs from all preceding boards in that it does not use the FTDI USB-to-serial driver chip. The Uno and version 1.0will be the reference versions of Arduino, moving forward. The module designed utilizes a combination of Doppler radar and PIR sensor for human detection. We use Arduino Uno as the microcontroller to collect datas from both the radar and sensor and also control it for the smooth functioning. Datas collected and processed is sent to esp8266 which acts as the communication element of the module. A blynk IoT interface connected to the esp8266 using Wi-Fi communication protocol gives the user a bazzer alarm indicating human detection. It sounds like you have a setup where an Arduino Uno is used as a microcontroller to collect data from a radar and sensor, and control them for smooth functioning. The collected and processed data is then sent to an ESP8266 module, which acts as the communication element of the module. The ESP8266 is connected to a Blynk IoT interface using Wi-Fi communication, and it provides a buzzer alarm to indicate human detection. This setup seems to be designed for a human detection system that combines radar, sensors, microcontroller, and IoT communication. The Arduino Uno is a popular microcontroller board that can be programmed to interface with various sensors and devices. The ESP8266 module is commonly used for Wi-Fi communication and can connect to the Blynk IoT platform. By integrating the radar and sensor with the Arduino Uno, you can collect data from these devices and process it within the microcontroller. Once the data is processed, it can be sent to the ESP8266 module using a suitable communication protocol, such as serial communication. The ESP8266, with its built-in Wi-Fi capabilities, can establish a connection to your local Wi-Fi network. By configuring it to connect to the Blynk IoT platform, you can send the processed data to the Blynk server, which provides an interface for visualizing and controlling the data remotely. In your case, you have set up an alarm system where a buzzer is activated upon human detection. It’s worth noting that the specific implementation details and code would depend on the radar, sensor, and buzzer you are using, as well as the programming language and libraries you choose. However, the general idea outlined above should provide a good starting point for building your human detection

system using Arduino Uno, ESP8266, and Blynk

4 Results and Discussion

The locomotion of the Rocker Bogie is stable up to an elevation of 7cm and after that till 10cm, it takes time to elevate. After a height of 10cm the rocker bogie does not fully cross the elevation, instead only one side is able to cross the elevation. The human detection module is able to detect quickly till 30cm of depth, after that the detection takes time. There is no further detection after 50cm depth. The communication module is able to receive response properly at a circumference of 25 cm and after which the response takes time and eventually the response is not received at 35 cm

5 Conclusion

In this project, our primary objective was to detect humans or any other living being trapped during landslides. Landslides pose significant risks to human life and infrastructure, and the timely detection of individuals in these hazardous situations is crucial for effective rescue and evacuation operations for the quick and efficient detection module and the communication module are inculcated in locomotive module. The combined implementation of Doppler radar, PIR (Passive Infrared) sensor, and the rocker bogie mechanism provides an effective and comprehensive solution for the detection of humans in various scenarios. This report has explored the principles and capabilities of each component and their integration to achieve accurate and reliable human detection. Doppler radar utilizes the Doppler Effect to detect the movement of objects, including humans, by measuring the frequency shift in the radar signal. It is highly effective in detecting human presence and movement, even in challenging conditions such as low light or adverse weather. The PIR sensor, on the other hand, detects infrared radiation emitted by human bodies. It relies on the temperature difference between humans and their surroundings to trigger detection. PIR sensors are particularly useful for short-range detection and can be employed in applications such as automatic lighting systems, motion-activated cameras, and energy-saving devices. The rocker bogie mechanism provides mobility and stability to the system. It consists of a suspension system that allows the device to traverse uneven terrain, making it suitable for outdoor applications. The mechanism ensures that the radar and PIR sensor are appropriately positioned and oriented to maximize their detection capabilities, even in rough or inclined surfaces. The versatility and adaptability of the rocker bogie mechanism enable the system to be deployed in various environments and enhance the overall performance of the human detection system. Furthermore, the modularity of the rocker bogie mechanism opens up possibilities for future expansion and integration of additional sensors. As technology advances and new sensing capabilities emerge, it becomes feasible to incorporate complementary sensors onto the existing framework. However, it is important to note that no detection system is perfect, and each component has its limitations. Doppler radar may have difficulties in distinguishing between different moving objects, and PIR sensors may be susceptible to false positives caused by non-human sources of infrared radiation. The performance of the human detection system can be further improved through ongoing research and development, including advanced signal processing techniques, machine learning algorithms, and sensor fusion methodologies.

6 Future scope

Our all-terrain vehicle is designed to offer exceptional adaptability and versatility with its modular system. This innovative feature enables users to effortlessly swap and integrate different modules, allowing the vehicle to be effectively utilized in various scenarios. Whether it's for utility work, scientific expeditions, or disaster management, our all-terrain vehicle can be tailored to meet specific requirements. By incorporating different modules, you can enhance its capabilities and transform it into a specialized tool for a wide range of tasks. Experience the flexibility and versatility of our all-terrain vehicle as it seamlessly adapts to different situations, offering a reliable solution for diverse applications.

7 Acknowledgements

Any attempt at any level cannot be satisfactorily completed without the support and guidance of learned people. We owe to great many people whose constant support and motivation that has encouraged us to come up with this Project. We are immensely indebted to our very understanding Project guide, Dr. Rajesh Menon, Asst. Professor for his constructive suggestions, guidance, and advice. We are greatly obliged to Dr. Rajeev N, Head of the Department, Department of Mechanical Engineering, for the encouragement and support that he has provided. Our Project in charge Aneesh , Assistant Professor, Department of Mechanical Engineering for his valuable guidance, support and whole-hearted cooperation. We are thankful to our friends for their whole hearted co-operation during the preparation of our project. Last but not the least, we are grateful to our parents for their abundant blessing without which this Project would not be successful.

References

[1] D. S. Chinchkar1, S. S. Gajghate2, R. N. Panchal3, R. M. Shetenawar4, P. S. Mulik (2017)Design of Rocker Bogie Mechanism, International Advanced Research Journal in Science, Engineering and Technology 1,4

[2] K. Ranjithkumar, K. Sathyadharani, M. Preethi, et al.(2021) Identification of buried human bodies under landslides using GPR integrated with WIFI, AIP Conference Proceedings, 2387, 140004-1–140004-6

[3] Mr. S.P Vijayaragavan, Hardeep Pal Sharma,Guna sekar.C.H, S.Adithya Kumar(2013) Live Human Detecting Robot for Earthquake Rescue Operation, International Journal of Business Intelligents,1,2

[4] Shibu Prasath S V, Karthikeyan S, and Karthick C (2015) A Review on Artificial Intelligence System for Detection and Monitoring of Victims Trapped In Collapsed Building, RJPBCS, 6, 6

[5] Alvin Joseph Vishal Parmar Bagyaveereswaran V (2019) Design of Human Detection Robot for Natural calamity Rescue Operation, IEEE, 978-1-5386-8190-9/19.

[6] David W. Paglieroni,Christian T. Pechard, and N. Reginald Beer(2015) Change Detection in Constellations of Buried Objects,Extracted From Ground-Penetrating Radar Data, Ieee Transactions On Geoscience And Remote Sensing,53

[7] David W. Paglieroni,Christian T. Pechard, and N. Reginald Beer(2015) Change Detection in Constellations of Buried Objects,Extracted From Ground-Penetrating Radar Data, Ieee Transactions On Geoscience And Remote Sensing,53

[8] Rajavenkatesan.T1, Chinnadhurai.R2, Gowthamguhan.K.S3, Sangeetha.J4, Vijayasudha.A5 (2015) Detection of Human Beings Under BuildingRubble, International Journal of Electrical and Electronics Engineers, 1, 07

[9] Jinu Sebastian1, Lidiya KA2, Martha George3, Asst.Prof. Sija Gopinathan,(2017) Alive Human Detection System for Rescue Operations in Hazardous Areas, IJAREEIE,4,6

[10] Widodo Iqbal F. Aditama, Khalid Syaifulla, Muthi'a J. Mahya M. Hidayat (2016) Detecting Buried Human Bodies Using Ground-Penetrating Radar, Earth Science Research,2,5

Driver Drowsiness Detection and RiderMonitoring for Two Wheelers

Abhijith S R[1], Gokul V C[1], Aswin C[1], Devsooraj M C[1] and Abhay Rajan[2]

[1] B.Tech Students, NSS College of Engineering, Palakkad, Kerala, India
[2]Asst. Professor, Department of Mechanical Engineering, NSS College of Engineering, Palakkad, Kerala, India

Abstract -

In today's scenario, we can see a significant increase in the number of road accidents occurring around us. Many people suffer permanent injuries or lose their lives. A major share of these is accounted to by driver drowsiness not only in case of four wheelers but also in 2 wheelers. This project aims to prevent 2-wheeler accidents caused by drowsiness and, if such an accident occurs, to ensure that the person receives proper medical attention. Infrared signals are used, which are processed by a microcontroller, and the rider is alerted based on the output received. In the worst-case scenario, if the rider is involved in an accident, an accident emergency system is used to notify the appropriate people and provide them with the location of the accident. Later on using EEG (electroencephalograph) systems accuracy can be improved. The EEG signals are those which can be extracted from brain, during drowsy state these have a separate range of frequency than in normal state. So, using machine learning or other processing techniques we can detect them and warn the users. Another improvement is implementation of the same in Electric Vehicle where speed of vehicle can be reduced to reduce effect of accidents in case it occurs.

Keywords -

Drowsiness; infrared signals; micro controller; accident emergency system; EEG

1 Introduction

Drowsiness is an important factor in death in traffic accidents ,injury, with considerable efforts being made to mitigate its consequences. A case study conducted in Sweden found that approximately 8-15experiencing acute drowsiness [3] . The consequences of drowsy driving can be just as dangerous as the damage caused by alcohol intoxication. The term ”sleepy” simply means prone to falling asleep. Sleep researchers refer to ”sleepiness” as the transition period between wakefulness and first stage sleep. We will discuss a driver drowsiness monitoring system that uses infrared (IR) and rider monitoring system along with GPS module, IMU sensor, and SIM module. The proposed system aims to monitor the driver's alertness levels and send alerts to the driver when they show signs of drowsiness. The system integrates various sensors and modules to detect and analyse the driver's behaviour and send alerts accordingly. The IR sensor detects the driver's eye movements and determines if they are closing their eyes for a period. The system also includes a GPS module, which provides the location information of the vehicle. The IMU sensor is used to detect the vehicle's motion and determine the driver's fatigue levels based on their steering behaviour. The SIM module is used to send realtime alerts to the driver in case of any drowsiness detection, as well as send notifications to the emergency contacts in case of any accident. Recent research on driver drowsiness detection has been classified into three key methods, namely vehicle based methods, behavioural based methods, and physiological signal based methods. Physiological or Bio-signal-based measures are more reliable and accurate and have been found to outperform vehicle and behavioural measures because they provide fewer false positives and are less affected by environmental and road conditions. There are three main ones in this regard signals used to detect sleepiness, specifically Electroencephalography(EEG), Electrooculography (EOG) and Electrocardiography

2 Objective

a. Enhancing Road Safety: The primary objective is to improve road safety by detecting and preventing driver drowsiness. The system aims to identify signs of drowsiness in real-time and alert the driver, reducing the risk of accidents caused by drowsy driving.

b. Preventing Accidents: By monitoring driver behaviour and detecting signs of drowsiness, the system aims to prevent accidents caused by impaired attention and reduced reaction times. Timely alerts and interventions can help the driver stay alert and maintain safe driving practices.

c. Monitoring Rider Behavior: The rider monitoring system focuses on continuously monitoring the rider's actions, such as head movements and body posture, to detect any abnormal behaviour or risky manoeuvres. This objective aims to encourage safe riding habits and reduce the occurrence of accidents.

d. Providing Accurate Location Tracking: The integration of GPS technology allows for accurate tracking of the rider's location. This objective enables immediate assistance during emergencies or accidents by providing precise location information to authorized personnel or emergency services.

e. Enhancing Emergency Response: The system aims to improve emergency response times by automatically

transmitting distress signals, messages, or calls to predefined contacts when an accident or unusual event is detected. This objective ensures quick and appropriate response in critical situations.

f. Improving Rider Awareness: The system's alerts and notifications aim to increase rider awareness about their own behaviour, such as drowsiness or risky manoeuvres. By providing real-time feedback, the system encourages riders to adopt safer practices and maintain vigilance during their rides.

g. Developing Scalable and Cost-Effective Solutions: Another objective is to develop drowsiness detection and rider monitoring systems that are scalable and cost-effective, making them accessible to a wider range of riders. This objective aims to promote the widespread adoption of these technologies to enhance overall road safety.

3 Methods

The drowsiness detection system using ESP32, IR sensor, buzzer, DC-DC converter, and DC power source aims to detect driver drowsiness and provide timely alerts to prevent potential accidents on the road. This system utilizes a combination of hardware components and intelligent algorithms to monitor the driver's behaviour and detect signs of drowsiness. The system operates in real-time, continuously monitoring the driver's eye movements and analysing the data to determine drowsiness levels. When the system detects signs of drowsiness, it triggers the buzzer to alert the driver. Simultaneously, the system can also transmit alerts to a connected mobile device or a central monitoring station for further actions.

3.1 Components

The components used in the system are described below:

3.1.1 IR MODULE

The IR (Infrared) module used in the drowsiness detection system plays a crucial role in monitoring the driver's eye movements and detecting signs of drowsiness. The IR module typically consists of an IR transmitter and an IR receiver. The IR transmitter emits infrared light towards the driver's eyes, and the IR receiver detects the reflected light. By analysing the reflected light, the system can determine the driver's eye movements, including blinking patterns and the duration of eye closures. This information is vital in assessing the driver's level of drowsiness. The IR module operates based on the principle of reflection. When the emitted infrared light hits the driver's eyes, it reflects back to the IR receiver. The intensity and pattern of the reflected light vary depending on the position and movement of the eyes. The output of the IR module is typically in the form of electrical signals that represent the detected eye movements. These signals are then processed by the microcontroller (such as ESP32) or dedicated signal processing circuits to determine the drowsiness level of the driver. Algorithms can be implemented to analyze the duration and frequency of eye closures, enabling the system to detect signs of drowsiness accurately. Overall, the IR module serves as a vital component in the drowsiness detection system, providing real-time monitoring of the driver's eye movements. By leveraging the reflected infrared light, the module enables the system to detect and analyse blinking patterns, facilitating the timely identification of drowsiness and the initiation of appropriate alerts or interventions.

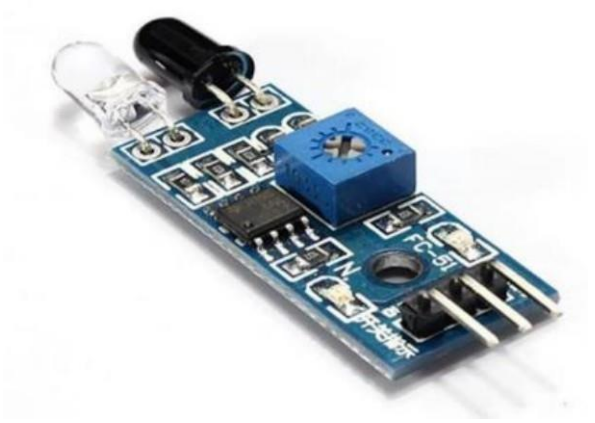

Figure 1. IR sensor

3.1.2 ESP 32 BOARD

The ESP32, a versatile microcontroller, has found valuable applications in drowsiness detection and rider monitoring systems. Its powerful processing capabilities and built-in wireless connectivity make it an ideal choice for such applications. In drowsiness detection, the ESP32 can be integrated with various sensors like infrared cameras or eye-tracking devices to monitor a rider's level of alertness. By continuously analyzing the driver's eye movements, blink patterns, and head position, the ESP32 can detect signs of drowsiness or distraction. It can then trigger alerts, such as sound alarms or haptic feedback, to help prevent accidents caused by driver fatigue. Furthermore, the ESP32's wireless capabilities enable real-time data transmission to a central monitoring system. This allows for remote monitoring of multiple riders simultaneously, making it suitable for fleet management or transportation companies. The data collected can be analyzed to identify patterns and trends, helping to improve safety protocols and implement preventive measures. The ESP32's com-

pact size and low power consumption make it an excellent choice for integration into wearable devices or vehicle systems. Its ability to run on battery power ensures uninterrupted operation, and its programmability allows for customization and the implementation of sophisticated algorithms for accurate drowsiness detection.

Figure 2. ESP 32 board

3.1.3 BUZZER

The buzzer plays a vital role in driver drowsiness detection systems, serving as an important component in alerting the driver when signs of drowsiness are detected. When the system detects that the driver is becoming drowsy or losing focus, it triggers the buzzer to emit a loud and attention-grabbing sound. This audible alert serves as a wake-up call for the driver, prompting them to regain their attention and take necessary actions to ensure their safety. The buzzer's loud and distinctive sound ensures that it can be easily heard even in noisy environments, allowing for effective warnings to be issued. Its integration into the drowsiness detection system helps prevent potential accidents caused by driver fatigue by providing an immediate and noticeable alert to the driver, urging them to take appropriate measures and avoid potential dangers on the road.

3.1.4 DC-DC CONVERTOR (BUCK)

The DC-DC converter plays a crucial role in a driver drowsiness detection system by providing efficient power management and voltage regulation. It converts the input voltage, typically from the vehicle's battery to a stable output voltage suitable for powering the various components of the system. The converter ensures that the sensors, microcontrollers, communication modules, and other electronic components receive a consistent and reliable power supply, regardless offluctuations in the vehicle's battery voltage. This stable power supply is essential for the accurate operation of the drowsiness detection system, as it

Figure 3. Buzzer

maintains the integrity of the sensor readings and enables precise data analysis. Additionally, the DCDC converter helps optimize power consumption, prolonging the system's battery life and minimizing energy waste. Its utilization in a driver drowsiness detection system contributes to the overall reliability and efficiency of the system, enhancing its performance in monitoring driver alertness and ensuring road safety.

Figure 4. Buck

3.1.5 IMU SENSOR -MPU 6050

The MPU6050 is a commonly used sensor in rider monitoring systems due to its ability to accurately detect and measure motion and orientation. It combines a three-axis gyroscope and a three-axis accelerometer into a single chip, making it ideal for monitoring the movements of a rider. In a rider monitoring system, the MPU6050 can be mounted on a helmet or integrated into a wearable device

to capture real-time data about the rider's head movements, posture, and overall body motion. By analyzing this data, the system can assess the rider's stability, detect any sudden or abnormal movements, and identify potential risks or incidents. The MPU6050's precise motion tracking capabilities, low power consumption, and compact size make it an excellent choice for rider monitoring systems, providing valuable insights to enhance safety and performance during various activities such as cycling, motorcycling, or horseback riding.

Figure 5. IMU sensor

3.1.6 GPS MODULE - NEO-6M

The Neo-6M GPS module plays a significant role in rider monitoring systems by providing accurate positioning and tracking capabilities. When integrated into a rider monitoring system, the Neo-6M module uses signals from multiple global navigation satellite systems (GNSS) to determine the rider's precise location in real-time. This information can be used to track the rider's movements, monitor their speed, and map out their route. Additionally, the Neo-6M module can assist in geo-fencing, allowing the system to define virtual boundaries and send alerts when the rider deviates from a designated area. This enables enhanced safety and security by enabling real-time tracking and monitoring of riders during various activities, such as cycling, motorcycling, or equestrian sports. The Neo-6M's reliability, accuracy, and compatibility with popular GNSS systems make it a valuable component in rider monitoring systems, ensuring effective tracking and improving overall safety measures for riders.

Figure 6. GPS module

3.2 SIM MODULE – SIM800L

The SIM800L module plays a vital role in rider monitoring systems by providing reliable and efficient communication capabilities. Integrated into a rider monitoring system, the SIM800L module enables real-time communication between the rider and the monitoring center or emergency services. It utilizes GSM networks to establish a connection, allowing the system to transmit important data, such as the rider's location, vital signs, or distress signals, in case of an emergency or an unforeseen event. The module's compact size and low power consumption make it suitable for integration into wearable devices or portable monitoring units. With the SIM800L module, rider monitoring systems can ensure seamless and effective communication, enabling timely assistance, and enhancing the safety and well-being of riders during their activities, be it cycling, motorcycling, or any other outdoor pursuits.

3.2.1 BATTERY (Li-Po)

The Li-Po (Lithium Polymer) battery serves a crucial role in both rider monitoring systems and drowsiness detection systems by providing reliable and portable power. These systems often consist of various sensors, microcontrollers, communication modules, and alert mechanisms that require continuous power to function effectively. The high energy density and lightweight nature of Li-Po batteries make them an ideal choice for powering wearable devices or compact monitoring units used in these systems. Li-Po batteries offer extended battery life, allowing for prolonged monitoring sessions without the need for frequent recharging. Additionally, Li-Po batteries can handle high discharge rates, ensuring stable voltage output even during peak power demands. The use of Li-Po batteries in rider

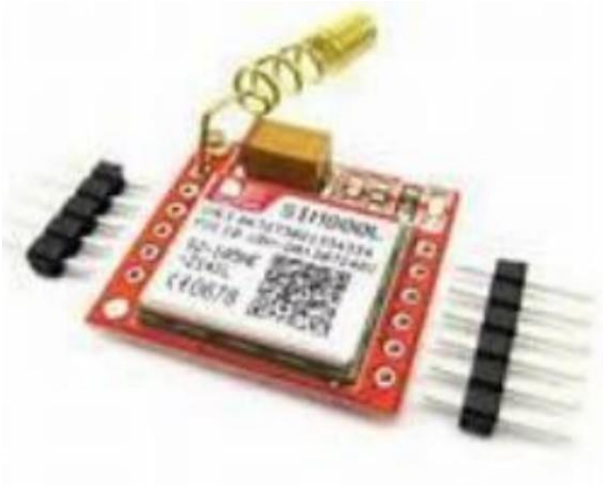

Figure 7. SIM module

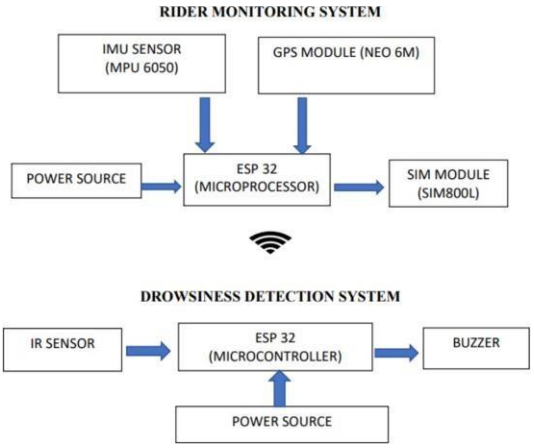

Figure 9. Block diagram of driver drowsiness detection and rider monitoring system

monitoring systems and drowsiness detection systems ensures uninterrupted operation and reliable power supply, enabling accurate monitoring of rider activities and timely detection of drowsiness or distraction to enhance overall safety on the road.

Figure 8. Battery

3.3 Block diagram

The drowsiness detection and rider monitoring system utilize a combination of components, including an IR sensor, ESP32 microcontroller, DC-DC converter, MPU6050 sensor, Neo-6M-0-001 GPS module, SIM800L communication module, buzzer, and a battery. The IR sensor monitors the user's eye movements, blink patterns, and head position. It detects signs of drowsiness or driver inattention based on these parameters. The ESP32 processes the data from the IR sensor and implements algorithms for drowsiness detection. It analyzes the input signals and triggers appropriate actions based on the detected drowsiness levels. The DC-DC converter regulates the power supply, converting the available input voltage from the battery to the required output voltage levels for the components. It ensures stable and efficient power delivery to the entire system. The MPU6050 sensor combines a gyroscope and an accelerometer to measure the rider's head movements, posture, and overall body motion. It provides real-time data to assess the rider's stability and detect any sudden or abnormal movements. The Neo6m GPS module determines the rider's precise location by receiving signals from multiple global navigation satellite systems (GNSS). It tracks the rider's movements, monitors their speed, and maps out their route. The SIM800L module enables wireless communication, allowing the system to transmit data, such as the rider's location, vital signs, or distress signals, to a central monitoring station or emergency services. The buzzer provides an audible alert to the rider when signs of drowsiness or distraction are detected. It emits a distinctive sound to immediately grab the rider's attention, encouraging them to regain focus and take necessary precautions. The battery supplies power to the entire system. It ensures uninterrupted operation and portable functionality, allowing the system to function even when not connected to a direct power source.

3.4 Software Components

AURDINO IDE

The Arduino IDE (Integrated Development Environment) is a software tool for writing, compiling, and uploading code to Arduino boards. It has an easy-to-use interface

and a simplified programming language based on C and C++. The IDE provides a code editor with features such as syntax highlighting, code completion, and debugging tools to make writing and debugging code easier. Furthermore, the IDE includes a library set that may be readily inserted into code to connect with various sensors, actuators, and other electronic components. It also includes a serial monitor, which enables real-time connection between the Arduino board and the computer. The Arduino IDE is open source and free to download from the Arduino website. It is compatible with a variety of operating systems, including Windows, Mac, and Linux. The IDE is intended to be user-friendly for beginners, making it simple for anyone to begin programming and working with Arduino boards.

3.4.1 Result obtained from IR Sensor

Figure 10. Result of IR sensor

3.4.2 Result obtained from GPS module

Figure 11. Result of IMU sensor

Figure 12. Result of GPS module

3.5 EEG Based drowsiness detection

An EEG (Electroencephalogram) based drowsiness detection system represents a significant advancement over an IR (Infrared) based system due to its ability to provide more accurate and comprehensive data on the user's brain activity. While an IR sensor primarily focuses on external cues like eye movements and blink patterns, an EEG system directly measures the electrical signals generated by the brain. By using specialized electrodes placed on the user's scalp, an EEG-based system can capture brainwave patterns associated with different states of consciousness, including drowsiness. This allows for a more precise and reliable detection of drowsiness, as it directly monitors the brain's activity. Additionally, an EEG-based system can provide insights into various brainwave frequencies, such as alpha, beta, theta, and delta waves, which can indicate different levels of alertness and cognitive states. This richer data can enable more accurate identification of drowsiness patterns and allow for more personalized and adaptive alerts or interventions. However, it's important to note that an EEG-based system typically requires more complex hardware, including the electrodes and amplifiers, as well as sophisticated signal processing algorithms to interpret the brainwave data. It may also be more intrusive and require more user preparation and setup compared to an IR-based system. Nevertheless, the utilization of EEG technology in drowsiness detection represents a promising advancement, offering a deeper understanding of the user's cognitive state and enabling the development of more advanced and precise alert systems to effectively mitigate the risks associated with driver drowsiness.

4 Results and Discussion

The development of a drowsiness detection system prototype integrated into spectacles, utilizing an IR sensor, ESP32, and a buzzer, holds significant potential for enhancing road safety. The prototype would leverage the IR sensor to monitor the user's eye movements, specifically detecting factors like eyelid closure duration, blink rate, and eye position. These data points would then be processed by the ESP32 microcontroller, which would employ advanced algorithms to analyze the user's alertness level. Upon detecting signs of drowsiness or driver inattention, the system would trigger the buzzer to provide an audible alert to the wearer. The buzzer's distinctive sound would be designed to immediately grab the wearer's attention, prompting them to regain focus and take necessary measures to ensure their safety.The integration of this prototype into spectacles provides several benefits. Spectacles are a commonly worn accessory, making the system inconspicuous and non-intrusive to the user. The compact size of the components, such as the IR sensor, ESP32, and buzzer, allows for seamless integration into the spectacles' frame, ensuring comfort and ease of use.

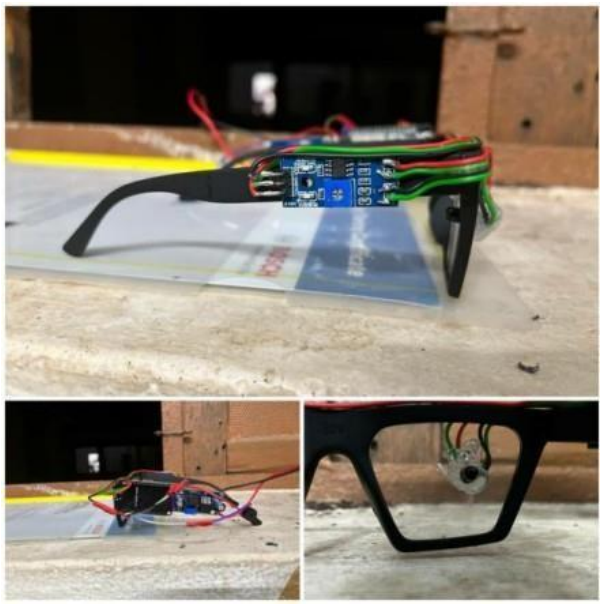

Figure 13. Prototype developed

5 Conclusion

The driver drowsiness detection and rider monitoring system, incorporating IR sensors, IMU sensor, GPS module, SIM module, and other components, presents a significant breakthrough in ensuring safety and enhancing the riding experience for two-wheeler users. This system effectively detects driver drowsiness, monitors rider behavior, and provides accurate location tracking. However, to further enhance the system's capabilities, the addition of an EEG-based drowsiness detection system would be a significant improvement. EEG technology measures brainwave activity, providing a direct insight into the rider's cognitive state and level of alertness. By monitoring brain activity, the system can detect drowsiness more accurately, enabling proactive intervention and preventing accidents caused by rider fatigue. The driver drowsiness detection and rider monitoring system, along with the proposed integration of an EEG-based drowsiness detection system, represents a major advancement in two-wheeler safety technology. By combining multiple sensor technologies, accurate location tracking, and proactive communication capabilities, this system aims to enhance rider safety and reduce the risks associated with drowsy riding. With the addition of EEG-based drowsiness detection, the system's ability to identify and address drowsiness will be further improved, creating a safer riding environment for two-wheeler users.

Acknowledgements

Any attempt at any level cannot be satisfactorily completed without the support and guidance of learned people.

We owe to great many people whose constant support and motivation that has encouraged us to come up with this Project. We are greatly obliged to Dr. Rajeev N, Head of the Department, Department of Mechanical Engineering, for the encouragement and support that he has provided. We are immensely indebted to our very understanding Project guide, Abhay Rajan, Assistant Professor ad hoc, Department of mechanical Engineering, for his constructive suggestions, guidance, and advice. Our Project in charge Madhu Mohan, Professor, Department of Mechanical Engineering for his valuable guidance, support, and whole-hearted cooperation. We are thankful to our friends for their whole-hearted cooperation during the preparation of our project. Finally, we wish our gratitude to our parents for their abundant blessing without which this project would not be successful.

References

[1] Jibo He, PhD William Choi , Yan Yang, Junshi Lu , Xiaohui Wu, Kaiping Peng (2017), Detection Of Driver Drowsiness Using Wearable Devices: A Feasibility Study Of The Proximity Sensor, Applied Ergonomics,Volume 65.

[2] Anil Kumar Biswal,1 Debabrata Singh, Debabrata Samanta, and Ming-Hour Yang (2021) IoT-Based Smart Alert System for Drowsy Driver Detection.

[3] Md Mahmudul Hasan, Christopher N. Watling, Grégoire S. Larue (2022), Physiological signal-based drowsiness detection using machine learning: Singular and hybrid signal approaches, Journal of Safety Research, Volume 80.

[4] Mohammed H.U. Bhuiyan, Mohamad Fard, Stephen R. Robinson (2022),Effects of whole-body vibration on driver drowsiness: A review, Journal of Safety Research, Volume 81.

[5] Abo Alzahab, N., Di Iorio, A., Apollonio, L., Alshalak, M., Gravina, A., Antognoli, L., Baldi, M., Scalise, L., Alchalabi, B. (2021). Auditory evoked potential EEG-Biometric dataset (version 1.0.0).

[6] Victor Javier Kartsch, Simone Benatti, Pasquale Davide Schiavone, Davide Rossi, Luca Benini,(2018)A sensor fusion approach for drowsiness detection in wearable ultra-low-power systems, Information Fusion, Volume 43.

[7] Christopher N. Watling, Md Mahmudul Hasan, Grégoire S. Larue, (2021) Sensitivity and specificity of the driver sleepiness detection methods using physiological signals: A systematic review, Accident Analysis Prevention, Volume 150.

[8] Gupta, Sheifali & Garima, Er. (2014). Road Accident Prevention System Using Driver's Drowsiness Detection by Combining Eye Closure and Yawning. International Journal of Research (IJR).

[9] Daniel Mollicone, Kevin Kan, Chris Mott, Rachel Bartels, Steve Bruneau, Matthew van Wollen, Amy R. Sparrow, Hans P.A. Van Dongen, (2019) Predicting performance and safety based on driver fatigue, Accident Analysis Prevention, Volume 126.

[10] M. Miranda, A. Villanueva, M. J. Buo, R. Merabite, S. P. Perez and J. M. Rodriguez, (2018) Portable Prevention and Monitoring of Driver's Drowsiness Focuses to Eyelid Movement Using Internet of Things.

Multi Lug Nut Remover with Differential Diameters

Kiran R Chandran[1], Aswin Kumar K N[1], Maneesh Mohan M [1], Sreeram K K [1] Varun M [1] and Abhay Rajan [2]

[1] Department of Mechanical Engineering, NSS College of Engineering, APJ Abdul Kalam Technological University, India
[2] Asst. Professor, Department of Mechanical Engineering, NSS College of Engineering, Palakkad, Kerala, India

Abstract -
Nowadays we can see the increment in number of cars on the road, so the failure of tires in vehicles are also gradually increasing. The most common way of removing a tire is through the use of a lug wrench which requires an excessive amount of human effort and time. So to reduce the loss of time, a multi nut wheel remover has already been made. The aim of this project is to further develop the multi nut wheel remover such that we can accommodate more wheel hub diameters. This development allows for better flexibility and considerably reduces the time for wheel nut removal. The wheel hub diameters chosen are the standard diameters generally used by car manufacturers and the pitch circle diameters are 108mm, 110mm, 114.3mm. The component used to switch between the three pitch circle diameters is the scroll plate. It can be used successfully as a standard tool regardless of the vehicle model. The remover is ergonomic and easy to use.

Keywords -
lug wrench; pitch circle diameters; scroll plate; multi wheel nut;

1 Introduction

Transportation plays an important role in the economic growth and globalization. In the modern world, the use of automobiles has increased rapidly. Especially during the pandemic period, people have changed their mode of transportation from the public transport system to their own vehicles. Tires play a crucial role in the performance of a vehicle. During an uncertain event such as tire puncture or flat tires, we need to remove the tires from vehicle and replace it with good ones. Wheel nut removal is a common challenge faced by mechanics and vehicle owners. Traditional lug wrenches or impact tools often struggle to remove tightened or corroded wheel nuts, causing frustration and wasting valuable time. This project focuses on developing a specialized tool capable of effectively and efficiently removing wheel nuts from various vehicles. In each vehicle there is tool provided by the manufacturer for removing the tires. Removal of tire is a tedious task when performed manually with the tool provided by manufacturer. It needs a lot of effort and consumes a lot of time to change tires by an individual, especially for women and senior citizens. The consumption of more time is because of each wheel nut is loosen or tighten one by one. Another issue posed by using a lug wrench is that all the lug nuts are uniformly tightened which can lead to slip between the threads of the lug nut and screw causing damage to the threads of the screw. Researches have been conducted to build a model that can remove all nuts simultaneously, but a common problem that arises with these models is that, it can only be used for a particular type of vehicles. Because the design comprises of a single standard pitch circle diameter (PCD). This led to separately design the multi-lug wheel nut remover tool for each vehicle. Because the pitch circle diameter is not same for all vehicles. To solve the above problems, an innovative solution has been developed: The Adjustable Multi-Lug Wheel Nut Remover. This project aims to find a design which can solve the issues of the currently existing model. Through research an idea has been developed that provides the model to switch between various PCD of vehicles with four lug nuts. By using this tool, we can remove or tighten all the four nuts of a wheel simultaneously. This tool significantly reduces the time for removal and tightening of wheel nuts. The effort required for the removal and tightening of nut is reduced up to an extent. From studies, most of the automobiles of body type hatchbacks and compact sedans mainly having four nuts in a wheel and their standard pitch circle diameters (PCD) are 100mm, 108mm, 114.3mm. So, the adjustable multi lug nut remover is designed based on these pitch circle diameter. The switching of pitch circle diameter depending on the vehicle is achieved through the use of a scroll plate. A centre shaft is provide which carries gears of varying diameters. At a time, a set of four planetary gears are connected to one of the three gears mounted on centre shaft. The shaft on which the planetary gears are mounted are inserted into the scroll plate. The scroll plate is provided with gear teeths on its outer surface and slots present on its surface. The scroll plate is controlled using another pinion gear. This arrangement helps to switch between the pitch circle diameters when required. The sun and planetary gear arrangement help to reduce the effort needed to remove or tighten the wheel nut by an individual. The tool incorporates adjustable features that allow it to adapt to different wheel nut sizes, providing compatibility with a wide range of vehicles. The design also focuses on maximizing grip, torque transmission, and leverage to ensure efficient and effective removal of wheel nuts. The Adjustable Multi-wheel Nut remover offers numerous ad-

vantages over traditional tools, such as versatility, ease to use, time and cost savings, enhanced safety. The adjustable multi-wheel Nut remover for vehicles represents a significant advancement in the field of wheel maintenance. By addressing the challenges associated with corroded & worn out wheel nuts, this tool offers increased efficiency. The subsequent sections deals with the design, development, and evaluation of this solution, thereby providing valuable insights for common vehicle users, automotive professionals and enthusiasts alike.

2 Objectives

The objectives for the Multi Lug Nut Remover with Differential Diameters can vary depending on the specific requirements and goals of the project. However, here are some common objectives that such a system might aim to achieve:

• To effectively remove / tighten the lug nuts: It provides a reduction in effort during the removal of all lug nuts of a wheel. It also ensures the uniform tightening of lug nuts reducing wear and tear of the lug nut threads.

• Time efficiency in the removal of lug nuts: Compared to the removal of lug nuts manually with a wrench, a planetary mechanism could potentially reduce the time, due to its mechanical advantage. It allows for faster rotation and higher torque, enabling quick removal of lug nuts.

• Versatility (flexibility between standard PCD): The shifting between the standard Pitch Circle Diameter (PCD) of a differential multi-lug remover is to enable compatibility with a wider range of vehicles. By incorporating an adjustable or interchangeable PCD feature, the multi-lug remover can accommodate various PCD sizes commonly found on different car models. And thus improving the versatility and compatibility of the product.

• Simple design which can be manually operated: The simple design of the multi lug nut remover utilizing a hand driven mechanism with a planetary gear system providing users with an efficient and versatile tool for lug nut removal. This design concept combines practicality and ease of use.

• User friendly model: This model offers numerous advantages in terms of efficiency, convenience, and safety. Its innovative design and ergonomic features make it a valuable tool for professionals and daily users. By simplifying the lug nut removal process, this tool enhances productivity and contributes to a more user-friendly experience for maintenance tasks involving wheels.

• Safety of the user: This model incorporates the safety features that prevent slippage or damage to the wheel nuts or wheel. It also ensures that the user id far from potential injuries during removal process.

• Durability and reliability: A multi wheel nut remover is a tool that is used under high load and torque. So as to withstand all the external forces acting on it, its built using high quality materials that endures the torque and forces involved in wheel nut tightening or removal. It also provides for a minimum wear and tear of components during usage.

3 Methods

The setup used here is mainly composed of the scroll plate, the sun gears, the planetary gears, tool end key. The setup involves 4 planetary gears meshed with a specific sun gear, which together constitute the 100,108 and 114 PCD. The movement of the sun gear causes movement in the 4 planetary. This type of power transmission method is called the planetary mechanism. For the setup's torque requirement, the diameters of the planetary gears have been increased. When the PCD has to be changed, the scroll plate comes into play. Using the scroll plate's slits, the planetary and sun gears can be disengaged and move to the appropriate PCD. During switching movement of the shaft is done through a pulling or pushing movement which is assisted by a spring. To induce movement in the scroll plate a key which can be moved upwards and downwards is inserted.

3.1 Planetary

The planetary gear mechanism is the main working principle of the wheel nut remover. A planetary gear system is utilized to provide efficient torque multiplication and facilitate the removal of wheel nuts simultaneously. The purpose of the planetary gear system for a multi-wheel nut remover would be to provide the necessary torque and rotational force to loosen or tighten the nuts efficiently. The basic design concept for a planetary gear system used here is: Sun Gear: The central gear is driven directly by the user's input, such as a handle or power source. The sun gear is fixed at the centre and transmits power to the planet gears. Here there are three sun gears with varied diameter in order to engage three different pitch circle diameter. These sun gears are mounted on to a main shaft that helps in switching these gears for different pitch circle diameter arrangement. Planetary Gears: There are four gears that are arranged around the sun gear known as the planetary gears. These are gears that receive torque from users input through the sun gears. They are bigger than sun gears so as to transmit more torque effectively. These gears are connected to a shaft that contains a socket tool that aligns with the size of the wheel nut. Operation: When the user applies torque the main shaft transfers the user's torque from the hand lever or power source towards the sun gear

mounted on it.The sun gear receives the input force or torque and then transfers it to the four planetary gears. The planetary gears are held on a shaft that is kept inside the guide ways of the scroll plate and these shafts helps to transfer the torque received from the planetary gear to the socket tool resulting in torque multiplication. The gear ratios and the number of planet gears determine the overall torque multiplication achieved. When the mechanism is at play all the components in it remains at a stationary position and rotates within that position. Each planetary gear shafts should contain a socket attached to it in order to engage with the wheel nut. When applying input torque to the sun gear manually, the planetary gear system multiplies the input torque and transmits it to the socket attachments on the planet gears. As the planet gears rotate, the wheel nuts are simultaneously loosened or tightened.

3.2 Locking and shifting

The multi wheel nut remover contains a locking mechanism that prevents the planetary shaft from slipping inside the scroll plate guide ways.and socket from slipping or disengaging during use. To achieve the locking mechanism a metal plate is welded to the cylindrical casing. This metal plate consists of three holes that are aligned according to the position at which the planetary gears tightly engages the required pitch circle diameter sun gears (100 PCD, 108 PCD, 114.3 PCD). The metal plate is provided at the base of the key hole so that the key can be locked on that metal plate at the required PCD. This locking provides the tight meshing of the scroll plate and the pinion gear without any slip. The arc shape of the scroll plate guide way also provide a stability to the planetary shaft from slipping inside the guide ways. The multi lug nut remover is adjustable to three different standard diameters. As the design is manually controlled, the shifting between different diameters is also done manually. The shifting facilitates for varying of the pitch circle diameter and it is achieved by using the pinion gear. The pinion gear is attached to a shaft with a key hole at its end. A key is used to rotate the pinion gear from the key hole end and thereby roaring the scroll plate. The rotation of scroll plate facilitates the inward and outward movement of planetary shaft and successively disengaging and engaging the planetary gears from the sun gear. Disengaging the planetary gears from the sun gear makes provides the main shaft to freely move. Then to shift the setup from one PCD to another, the sun gear of the required PCD is set at the planetary gear axis by moving the main shaft and the planetary gear is engaged by pushing the key. This makes the planetary gears to once again mesh with the sun gear and the tool is ready to use. The upward movement of the key disengages the planetary gears from the sun gear and the downward movement engages the planetary gears.

4 Design calculations

To remove a lug nut in a vehicle we must provide adequate torque. Each lug nuts are loosened and tightened to a specific torque specification. To remove and tighten lug nuts we need a torque wrench or an impact wrench. On experimentation, the torque wrench was inserted to a lug nut of a car and hanged by mass on the other side. Therefore, the amount of torque required to loosen one lug nut of a car is 83 N-m.

4.0.1 For sun gear and pinion gears:

For pinion gear:
Pith circle diameter for pinion, $d1 = 68mm$
Thickness = $20mm$
Let, Module,$m_1 = 2$
No of teeth, $Z_1 = d_1/m_1 = 68/2 = 34$
Tangential force,$F_t = 2M_t/d = 2 * 83/0.068 = 2441.2N$

For 100 PCD:
Pitch circle diameter for gear, $D1 = 36mm$
Pressure angle= 20^o
Gear ratio, i = PCD of gear/ PCD of pinion = $68/36 = 1.88$
No of teeth: $D_1/Z_2 = m1ßZ2 = D1/m1 = 36/2 = 18$
From power equation, $T_S = (4 * T_p)/1.9 = 174.8N - m$
Tangential force,$F_{t1} = 2M_t/D_1 = 2 * 174.8/0.036 = 9711.11N$

Permissible Bending stress:
For driven gear and driver gear permissible bending stress are same.
$bp = Sut = 550N/mm^2$
$bp * Yp < bg * Yg$, Therefore driven gear is more prone to bending than the driver gears.

Beam strength:
$Y_p = \pi * y = \pi * 0.118 = 0.37$
$F_b = m * b * bp * Yp = 2 * 20 * 550 * 0.37 = 8140N$
When driven gear and driver gear are constructed using same material then at that time driving gear is found to be stronger than driven gear in bending, so we have to find out effective force (F_{eff}) for calculating factor of safety (FOS).

Effective load for precise estimation:
$F_{eff} = (K_a * K_m * F_t)/K_v$
Where, Load Distribution Factor, Km = 1.2 for face width upto 50 mm.
K_a = 1.25 for moderate shock & precise gearing.
$V = 22m/s$ for fine hobbing process.
F_t = Tangential Component of Force.
Dynamic Factor,$K_v = 5.6/(5.6 + (V)^{1/2}) = 5.6/(5.6 + (22)^{1/2}) = 0.5441$

Table 1. Abbreviations used for calculations

SYMBOLS	PARAMETERS
PCD	Pitch circle diameter
FOS	Factor of safety
T	Input torque
d_1, d_2	PCD of pinion gear and scroll plate pinion
D_1, D_2, D_3, D_4	PCD of 3 sun gears and scroll plate
$Z_1, Z_2, Z_3, Z_4, Z_5, Z_6$	Number of teeth of pinion gear, 3 sun gears, scroll plate pinion gear and scroll plate gear
α	Pressure angle
$F_t, F_{t1}, F_{t2}, F_{t3}$	Tangential force of pinion and 3 sun gears
$M_t, M_{t1}, M_{t2}, M_{t3}$	Turning moment of pinion and 3 sun gears
m_1, m_2	Module of pinion-sun gears, scroll plate-scroll plate pinion
σ_d	Allowable static strength
y	Lewis form factor
S_{ut}	Ultimate tensile strength
S_{yt}	Yield strength
E	Young's modulus
BHN	Brinell hardness number
σ_{bg}, σ_{bp}	Permissible bending stress of sun gears and pinion gear
Y_g, Y_p	Form factor of sun gears and pinion gears
F_b	Beam strength
F_{eff}	Effective load for precise estimation
P	Power
N	Speed of center shaft
l_c, l_p	Length of the center shaft and pinion shaft
d_c, d_p	Diameter of the center shaft and pinion shaft
BM_1, BM_2, BM_3, BM_p	Bending moment of center shaft when each gear is engaged and pinion shaft
Z_c, Z_p	Section modulus of center shaft and pinion shaft
J_c, J_p	Polar moment of inertia of the center shaft and pinion shaft
r_c, r_p	Radius of center shaft and pinion shaft
$\tau_c max, \tau_p max$	Maximum shear stress of center shaft and pinion shaft
l_s	Free length of spring
l_1, l_2, l_3	Length of spring when each sun gear is engaged
d	Wire diameter of spring
D_O, D_i	Outside and inside diameter of spring
N	Number of coils
i	Number of active coils
k	Spring constant
G	Shear modulus of corresponding material
F_1, F_2, F_3	Force acting on spring when different gears are engaged
τ_1, τ_2, τ_3	Shear modulus of spring when different gears are engaged
y_1, y_2, y_3	Deflection of spring when different gears are engaged
x	Displacement of spring
t_S, t_P	Number of teeth of sun and pinion gears
N_S, N_P	Speed of sun and pinion gears
P_S, P_P	Power of sun and pinion gears

Table 4. Mechanical Properties of EN 8 material

Ultimate tensile strength (Sut) = 550 N/mm^2
Yield strength (Syt) = 280 N/mm^2
Young's modulus (E) = 200000 N/mm^2
Poisson's Ratio = 0.3
BHN = 255 HB

Table 5. Dimensions of shafts

PARAMETERS	MAIN SHAFT	PINION SHAFT
Length (mm)	340	330
Diameter (mm)	25	12
Material	EN19	

$F_{eff} = (K_a * K_m * F_t)/K_v = (1.25 * 1.2 * 2441.2)/0.5441 = 6730N$
$ie, FOS = F_b/F_{eff} = 8140/6730 = 1.22$
As the available FOS is greater than 1, so the design of gears is safe.

Power:
Assuming humans can turn the driving gear at the rate of 30 rpm,
Power,$P = 2/60 = 2 * \pi * 30 * 255/60 = 801.1W$

4.1 For scroll plate:

For scroll plate pinion:
Pitch circle diameter, d2 = 66 mm
Thickness = 10 mm
No of teeth, Z5 = 42
Gear ratio, i = PCD of gear/ PCD of pinion = 150/66 = 2.3
Module, m2 = d2 / Z5 = 66/42 = 1.55

For scroll plate with gear:
Pitch circle diameter, D4 = 150 mm
Thickness = 10 mm Gear ratio,
i = PCD of gear/ PCD of pinion = 150/66 = 2.3
No of teeth: D4 / Z6 = m2 $\rightarrow$ Z6 = D4 / m2 = 150/1.55 = 100

4.2 For center shaft and pinion shafts:

Bending moment: When 100 PCD is engaged,
$BM_1 = F_{t1} * 0.245/4 = 9711.11 * 0.245/4 = 594.81Nm$

Equivalent bending moment: When 100 PCD is engaged
$= (T2 + BM12)1/2 = (2552 + 594.812)1/2 = 647.16Nm$
Section Modulus: $Z_c = \pi dc3/32 = \pi * 0.0253/32 = 1.53 * 10 - 6m3$
Polar moment of inertia:$J_c = 4/64 = \pi * 0.0254/64 = 1.91 * 10 - 8m4$
Max shear stress: $_{cmax} = T_c * r_c/J_c = 255 * 0.011/1.14 * 10^{-}8 = 246.05MPa$
Max shear stress for Mild steel = 320 MPa
Factor of safety, FOS = Max shear stress for Mild steel / Max shear stress = 320/246.05 = 1.3
Since FOS is greater than 1, the design is safe.

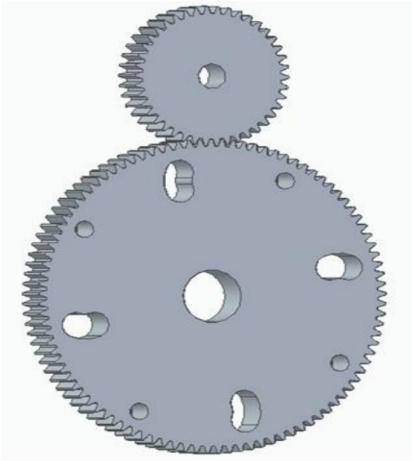

Figure 1. Front view of Experimental Setup

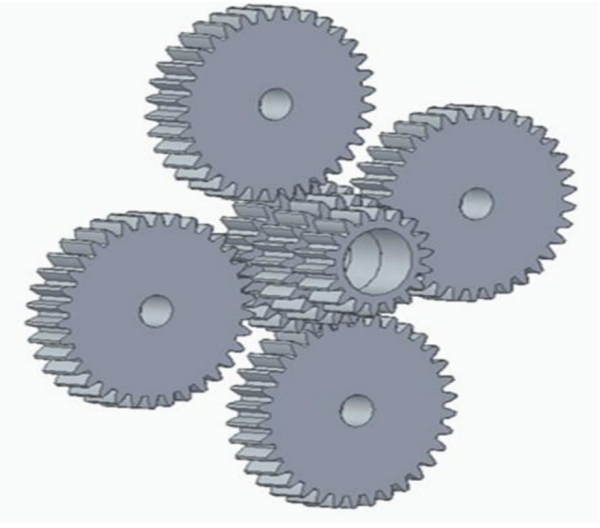

Figure 2. Side view of Experimental Setup

4.3 Design and Analysis

In this work, SOLIDEDGE software has been used to implement design ideas of different parts of the model and

Table 6. Properties of shafts under different gear engagements

PARAMETERS	100 PCD ENGAGED	CENTER SHAFT 108 PCD ENGAGED	114.3 PCD ENGAGED	PINION SHAFT PINION SHAFT
Bending moment (Nm)	594.81	620.68	603.33	657.08
Equivalent bending moment (Nm)	647.16	671.02	655	662.3
Section modulus (m^3)		1.53*10⁻6		1.69*10⁻4
Polar moment of inertia (m^4		1.91°10⁻8		1.01*10⁻9
Max shear stress (MPa)		246.05		493.1
Factor of safety		1.3		1.72

animate the assembly of the Multi lug nut with differential diameters. For analysis, ANSYS WORKBENCH is used to analyze the stress and deformation values of different gear arrangements. The torque of 83 Nm at the ends of the planetary shafts is obtained by applying 174.8 Nm, 214.2 Nm, 255 Nm of torques when 100, 108, 114.3 PCD gears are engaged respectively. The analysis for stress, deformation, moment reactions are performed and the results obtained are comparable with the calculated values. The factor of safety obtained for gear is1.22, main shaft is 1.3 and for planetary shaft is 1.72. The FOS values shows that the designed model is safe and can be operated. The detailed drawing and Analysis results is shown in section 5.2 and 5.3 respectively. The maximum stress and deformation values is shown in table 7.

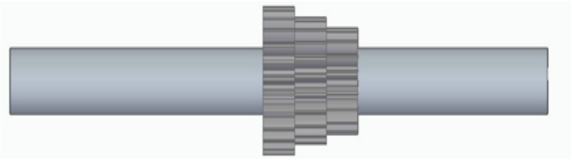

Figure 3. Arrangement of sun gears in main shaft

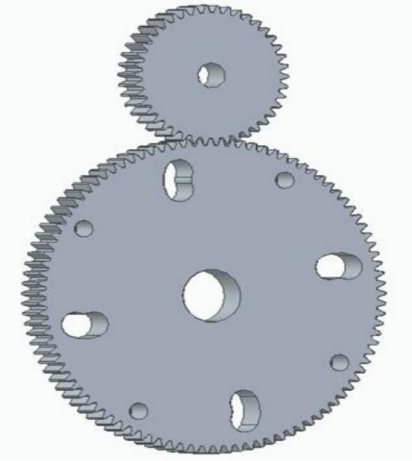

Figure 4. Scroll Plate meshed with pinion gear for Radial Expansion

4.4 List of materials

Sun gear
- Planetary gears
- Pinion gear
- Scroll plate
- Bearing
- Socket tool
- Shaft (For sun gear)
- Shaft (For pinion gear)
- Spring
- Hand lever
- Stand

4.5 CAD drawings & Analysis

5 Results and Discussion

After evaluating the feasibility conditions, including economic feasibility, operational feasibility, and technical feasibility, an multi lug nut remover with differential diameters was designed. This design was then implemented in real-world problems, and the outcome was successful, meeting the desired objectives.

- After proper calculation, designing and analysis a model prototype for the Multi wheel nut remover with differential diameters is developed and fabricated. This prototype was then implemented in real-world problems, and the outcome was successful, meeting the desired objectives.
- For the use of Multi wheel nut remover on actual wheel

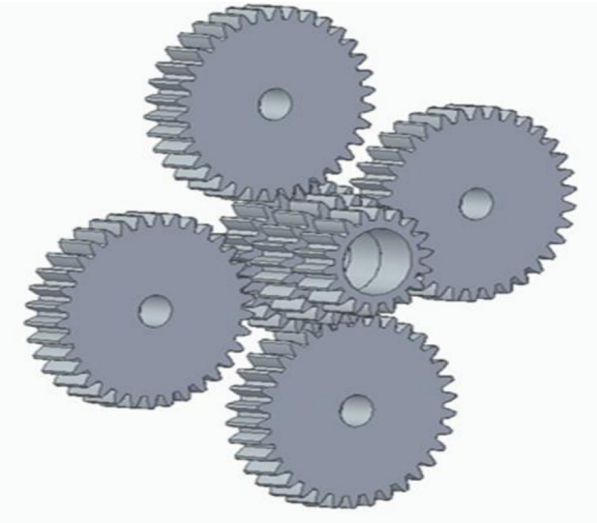

Figure 5. Assembly of sun gear meshed with planetary gears

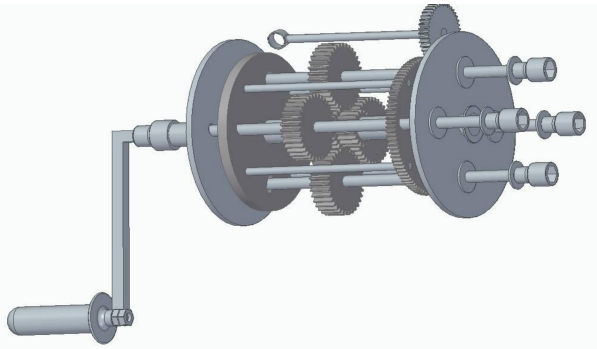

Figure 6. Final assembly of the model

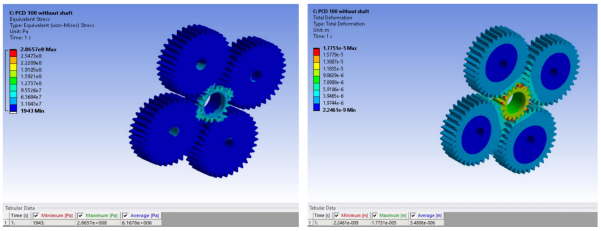

Figure 7. 100 PCD engagement, (i)stress analysis; (ii)deformation analysis

nuts, it was found that each of the wheel nuts require a torque of 83 N-m for its removal and tightening.

• The model is provided with an adjustable PCD design, it has proven that it can accommodate different PCDs of wheel especially the incorporated three PCD of 100 mm, 108 mm and 114.3 mm.

• While engaging the 100, 108 and 114 PCD, it is found

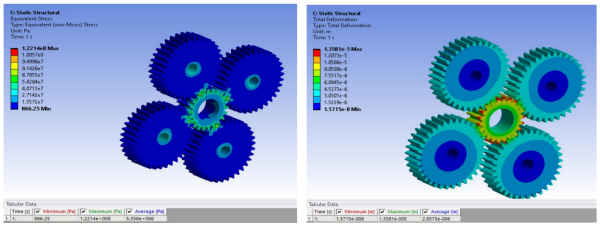

Figure 8. 108 PCD engagement, (i)stress analysis; (ii)deformation analysis

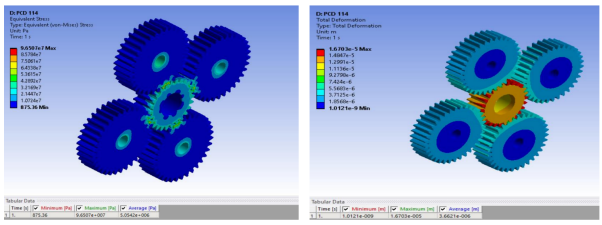

Figure 9. 114.3 PCD engagement, (i)stress analysis; (ii)deformation analysis

Table 7. Stress and deformation values for different gear engagements

PARAMETERS	MAXIMUM STRESS (N/m^2)	MAXIMUM DEFORMATION (m)
100 PCD Engaged	2.86×10^{8}	1.77×10^{-5}
108 PCD Engaged	1.22×10^{8}	1.35×10^{-5}
114.3 PCD Engaged	9.65×10^{7}	1.67×10^{-5}

that a torque of 174.8 N-m, 214.2 N-m, 255 N-m should be inputted for successful loosening or tightening of the lug nut.

• The factor of safety (FOS) for the sun gear is obtained as 1.22, which greater than 1. This meets the minimum requirement for safety and the material choice of medium carbon grade steel (EN 8 steel).

• By assuming that an average person can produce a speed of 30 rpm using hand, then the maximum power required to run the model using hand is estimated to be 801.1 W.

• The bending moment experienced by the center shaft during the engagement of three different PCD are:

o For 100 PCD: 594.81 N-m

o For 108 PCD: 620.68 N-m

o For 114.3 PCD: 603.33 N-m

• While the bending moment experienced by the pinion

shaft is calculated to be 657.08 N-m
• The factor of safety (FOS) in both results for main shaft is 1.3 and for planetary shaft is 1.72 , which is greater than 1.
• For the feasibility of the using multi wheel nut remover in real life an analytical study was conducted on ANSYS software.
Analysis was mainly conducted for the stress distribution, deformation distribution and meshing of the gears and shafts.

Figure 10. Fabricated model

Table 8. Comparison of the tool with conventional tools

Tool	Time (s)	Torque (Nm)
L-shaped wrench	75-85	140
Impact wrench	15-20	125
Multi lug nut with differential with differential diameters	20-30	255

5.1 Advantages and Limitations

The main advantages which come with the usage of this model are:
• The main selling point of the model is that it has the ability to unscrew 4 lug nut simultaneously through the use of human effort.
• The model allow has the added benefit of being simple in build which allows for easy construction and modifications.
• The concept of using a single tool to remove lug nuts of different wheel hub diameters proves it's versatility.
• The structural rigidity of the model is not compromised as the stress is mostly present on the Central shaft which has sufficient cross section and length.

Every tool has certain limitations as well. Some of the limitations are as follows:
• The time taken to align and fix the tool end onto lug nut takes longer compared to other methods.
• It is heavier causing a portability issue.
• The model is not optimized for use in different terrains.
• Depending on condition of lug nut removal rate and tightening rate may not be uniform for all nuts.
• Can result in over-tightening or under-tightening of the lug nuts.

6 Conclusion

The tool is designed for wheels which adopts 100mm,108mm,114.3mm PCD for the wheel nuts which is commonly seen in most of the cars. This tool is manually operated and requires the same amount of torque as an L-shaped spanner, providing a practical and efficient solution for tightening or loosening lug nuts on wheels. By incorporating these different PCD measurements, the tool can be used with a variety of wheels that have corresponding PCD sizes. This makes it versatile and compatible with a wide range of cars. The stress is mostly concentrated on the Central shaft and it is solved through the use of shaft supports and scroll plate supporter. The scroll plate with gear teeth, which is a key component of the mechanism, plays a vital role in the adjustable nature of the product. The wire wound across the pinion shaft allows the shafts to remain in place while holding it tightly to reduce instability. It is important to note that torque generated by the tool is found to be the same as a simple wrench. However, it is possible to encounter cases of over-torquing, where some lug nuts undergo more rotation compared to others. This can lead to a non-uniform removal and tightening process. Based on the calculation results, the ability of the mechanism to generate a torque that surpasses the requirement and the factor of safety for the gears in the mechanism has been determined to be 1.6, which is higher than the required value 1. The factor of safety for centre shaft has been determined to be 1.3, which is greater than required value. Overall, the higher factor of safety for the gears and the unique adjustable nature provided by the scroll plate with gear teeth contribute to the reliability, durabil-

ity, and versatility of the product. The analysis is done using ANSYS work bench. The analysis obtained gives us conclusive results which prove that the stress in 100 PCD is maximum and the minimum stress is in the 114 PCD. The stress distribution is skewed maximum in the 108 PCD, which shows that the stress is distributed over a larger surface area. This allows helps us to infer that the calculated torque is viable.

7 Future scope

One of the problems of the model is over-torquing the lug nuts which can lead to loss of thread of the tool and shape of lug nut. To solve this problem the principle of the torque wrench is used where the rated torque for each lug nut can be achieved by placing an adjustable spring in the pinion shaft which slips when the required torque is reached, which reduce over-tightening and under-tightening.

• The weight of the model weighs too heavy so we will try to reduce the weight of the overall model by using modern materials for different components which weighs less than that of the previous model.

• This project model is purely mechanical and the operations in this model is done manually. As a part of future extension, the model can be supplied with an electric motor which drives the center shaft and thus exempts the torque given manually. It can also be powered pneumatically.

• The torque required may exceed the torque generated, a mechanism which is based on the epicyclic gear train can be used. High torque can be achieved by making the ring gear stationary.

Acknowledgements

Any attempt at any level cannot be satisfactorily completed without the support and guidance of learned people. We owe to great many people whose constant support and motivation that has encouraged us to come up with this Project. We are immensely indebted to our very understanding Project guide, Abhay Rajan, Asst. Professor (ADHOC) for his constructive suggestions, guidance, and advice. We are greatly obliged to Dr. Rajeev N, Head of the Department, Department of Mechanical Engineering, for the encouragement and support that he has provided. Our Project in charge Madhu Mohan, Assistant Professor, Department of Mechanical Engineering for his valuable guidance, support and whole-hearted cooperation. We are thankful to our friends for their whole hearted co-operation during the preparation of our project. Last but not the least, we are grateful to our parents for their abundant blessing without which this Project would not be successful.

References

[1] Das T, Samantaray S, Thacker B, Danish MD, Kumar RR, Kumar P. Design and analysis of multi nut remover/tightener for car wheel. Materials Today: Proceedings. 2022 Jan 1;67:1170-4.

[2] Abdullah MA, Sulaiman N, Mat Idera IH, Mohd Razi MZ, Ngadiman MN. Design and Fabrication of Vehicle All-Wheel-Nuts Remover. International Journal of Computer Science and Electronics Engineering (IJCSEE). 2013:381-4.

[3] Sivabalan R, Vignesh M, Vairamuthu S, Hameed MS. Design and fabrication of adjustable unified wheel opener. International Journal of Innovative Research in Science, Engineering and Technology. 2014;3(2):516-8.

[4] Srivastava K, Sinha AA, Sahani R. Effect of heat treatment on hardness and toughness of EN8 steel. Materials Today: Proceedings. 2021 Jan 1;42:1297-303.

[5] Gurumurthy G, Sharma SS, Gowrishankar GS, Devar A. Study of Mechanical Properties of Dual Phase EN19 Steel (AISI4140). Indian Journal of Science and Technology. 2016 Oct 1;9(37):97422.

[6] Kumar SN, Reddy KB, Kumar KM, Rao DV. Design Fabrication of Multi Nut Removing and Tightening Tool for a Car Wheel. International Journal of Innovative Technology and Research. 2018 Jan;6(1):7848-51.

[7] Ananthu P, Dileep P I, Johnson Chacko, Sammon S, Mathew Mathew. Design and Development of Multi-Nut Tightener. International of creative research thoughts (IJCRT). 2020; Volume 8. ISSN: 2320-2882.

[8] A. R. Abd Aziz "Improvement and Optimization of Tire Nut Removal with 114 PCD". University Malaysia Pahang, Thesis Degree, 2008. Pawar SS, Pardeshi V, Khade V, Sayed S, Katara C. Design and Analysis of Flywheel for different Geometries and Materials. International Journal of Engineering, Science and Mathematics. 2018;7(3):293-301.

[9] Bhanage A, Bedse S, Devare K, Batte V, Dixit K. Design and Development of All Wheel Nut Remover for Automotive. International Journal of Applied Engineering Research. 2015;10(7):17631-41.

[10] Mahadevan, K., and K. Balaveera Reddy, Design Data Handbook, Mechanical Engineers in SI and Metric Units, CBS Publishers Distributors, New Delhi, 2018

Fire Extinguisher Automatic Robot

Gopan R[1], Kailas Chand P[1], Mohammed Riyas M P[1], Rohan[1]and Ajay Krishnan V[2]

[1] B.Tech Students, NSS College of Engineering, Palakkad, Kerala, India
[2]Asst. Professor, Department of Mechanical Engineering, NSS College of Engineering, Palakkad, Kerala, India

Abstract -

An uncontrolled fire is a dangerous act with many negative effects. Detecting a fire at an early stage and extinguishing it can aid in prevention of various accidents. Our main resource up till now has been people. As a result, the person's life is frequently put in danger. Fire safety becomes a crucial factor in saving human lives. In this project, a fire extinguishing robot is proposed and constructed, which recognizes the position of the fire and extinguishes it by activating sprinklers and triggering the pump. First, the user sends a robot to an impacted area to obtain a live view of the field using a thermal camera and data transfer via Bluetooth module. If any indicators of fire appear in the image, the user should move the robot in that direction for confirmation. Fire and temperature sensors detect and measure the readings, and following confirmation, the robot sprays water over the impacted field.

Keywords -

Drowsiness; : Fire extinguisher;

1 Introduction

Casualties and property damage from fire continue to exist in fire disasters and new measures are continuously introduced. Toxic gases and flames continue to threaten disaster victims and rescue workers alike. While a range of fire-fighting robots have been developed and put in action worldwide, they have not yet contributed greatly to the fight. Most robots assist only in small ways, helping fight fires from a distance or monitoring outside fire scenes. An indoor fire-fighting robot is capable of performing rescue operations without risking personnel, including fire extinguishing and helping people at risk. The application of robotics field is broadly used in the field of research, laboratory-based work, industrial work to automate process and reduce the human errors. With the right control systems and automation software, robots can perform complex tasks and operate 24/7 with greater efficiency than their human counterparts. In fact, studies have shown manufacturers can reduce overtime and increase efficiency by 1525with greater accuracy. They are able to achieve a variety of tasks rather than specializing in one task, unlike a traditional assembly worker. On the other hand, software automation such as implemented RPA can improve employee workflows and allow them to focus on high-value tasks. It can streamline various business tasks through help desk support with chatbots, efficient meeting scheduling, or offering analytics on employee performance. This paper describes the design of mechanical structure of a robotic arm with a fire extinguisher built in is called a fire extinguisher robot. The robot's fire quencher was attached, and the mechanization extinguished the fire in the affected area. This paper describes the design and operation of a fire-suppression and detection robot. The fire detection and extinguishment concept is carried out by this robot. It makes use of fire sensors to identify areas that have been burned. The reenacted fires at the factory, school, house, and forest were all extinguished by a robot. For the first identification of the fire, flame sensors are utilized. If the flame is identified, the robot then resonances those alerts with the use of a ringer that is installed on the prototype, the robot quench the fire. This initiative promotes interest in robotics and developments in the industry while working toward a workable and attainable approach to save lives and reduce the likelihood of property harm. Where humans fail to detect fire, this robot fire detector will step in. When 2 putting out fires and rescuing people, fire fighters often find themselves in hazardous situations; this is maybe an inevitable element of their job. In contrast, a robot can function on its own and can even be remotely controlled. In essence, firefighting robots have reduced the need for fire fighters to intervene in dangerous situations

2 Objective

i. Reduce human risk Every year a lot of people die in accidents caused by fire. One of the main objectives of this project is to reduce the risk of human life. With the help of this device, we can ensure the safety of the fire fighters since they do not have to make direct contact with fire.

ii. Avoid disaster The impact of any accident caused by fire is really high. The death rate as a result of this accident is also very high. This condition mainly occurs due to the high temperature in the neighboring area of the accident and also since there is chance for the occurrence of another explosion. All of these can be prevented by using this automatic fire extinguishing robot.

iii. Reduce the response time Number of victims in any accident can be reduced if the respond time is low. Risk for human life is very low while using this robot. Firefighters can easily use this device from a safe distance and clear the fire and also locate if people are trapped in the site.

iv. To find a good escape route In most cases of fire accidents people are likely to be trapped in the building. There is a chance that these places are filled with toxic gases and other smoke. This makes it very difficult for the people to carry out the rescue mission. Also, it makes the trapped people unable to find a way outside. All these problems can be addressed by using this fire extinguishing automatic robot.

3 Methodology

In every project the basic thing to do is to find a problem and address it. After that we brainstormed to obtain more than one solution for the problem. From these solutions we selected the most feasible one. The next step was literature review. We referred through various journal papers to obtain more knowledge about robotics, different classes of fire and statistical analysis system etc. After this we made a rough design of our design just to determine its dimensions and shape. Next step was to calculate the force to be applied at the nozzle, to select the temperature range of the fire in which this device should be used, to select which foam to be used based on the temperature range of the fire and how much amount of this foam should be carried in the device. After this we had to select which suspension should be used in the base, for which we selected the rocker bogy suspension. This was because it will help the fire extinguishing robot to easily move though the obstacles. In next step we designed every single part of the arm with the help of the calculations done before. This is what we have done in phase one. In phase two we will make every part of this device and assemble them. The next step is testing of the device.

3.1 MECHANICAL STRUCTURE

The mechanical design of a robotic arm is based on a robotic manipulator with similar function like a human arm. In order to establish a generalized operating system and the technological systems for the analysis, design, integration and implementation of a humanoid robotic arm. The command flow when operating is illustrated below. It shows the path of command and the order of process taken when given a command to the robotic arm. For operating DC motor, we need DC power supply that's way we attached an AC to DC converter for getting DC power. This DC power supplies each motor. Using a single command centre, we can control different part of the arm by giving commands to the corresponding Arduino. Even though separate commands are given for each separate process, all the process are interlinked. The base for the robotic fire extinguisher is a rocker bogie. This is done so that the vehicle could even travel on uneven surfaces with obstacles in front of it. The rocker bogie mechanism is a unique design used in some types of robotic vehicles, particularly in space exploration rovers like NASA's Mars rover such as spirit and curiosity. It's a suspension system that allows the rover to traverse rough and uneven terrains while maintaining stability and preventing from tipping over.

Figure 1. Robotic Arm

Figure 2. Rocker Bogie

3.2 POWER SUPPLY

The ac voltage, typically 220V rms, is connected to a transformer, which steps that ac voltage down to the level of the desired dc output. A diode rectifier then provides a full wave rectified voltage that is initially filtered by a simple capacitor filter to produce a dc voltage. This resulting dc voltage usually has some ripple or ac voltage variation. A regulator circuit removes the ripples and also remains the same dc value even if the input dc voltage varies, or the load connected to the output dc voltage changes. This voltage regulation is usually obtained using one of the popular voltage regulator IC units.

Working Principle

1) Transformer The potential transformer will step down the power supply voltage (0-230V) to (0- 6V) level. Then the secondary of the potential transformer will be connected to the precision rectifier, which is constructed with the help of op–amp. The advantages of using precision rectifier are it will give peak voltage output as DC, rest of the circuits will give only RMS output.

2) Bridge Rectifier When four diodes are connected as shown in figure, the circuit is called as bridge rectifier.

The input to the circuit is applied to the diagonally opposite corners of the network, and the output is taken from the remaining two corners. 3) IC Voltage Regulators Voltage regulators comprise a class of widely used ICs. Regulator IC units contain the circuitry for reference source, comparator amplifier, control device, and overload protection all in a single IC. IC units provide regulation of either a fixed positive voltage, a fixed negative voltage, or an adjustably set voltage. The regulators can be selected for operation with load currents from hundreds of milli amperes to tens of amperes, corresponding to power ratings from milli watts to tens of watts.

3.3 FABRICATION

3.3.1 Robotic Arm

Fabricating a robotic arm with a nozzle for spraying water or fire extinguishing substances involves several key steps. Initially, the specifications and requirements of the arm are defined, and a detailed 3D model is created using CADsoftware. Mild steel is selected as the material for the arm due to its strength and durability. The individual components, including arm segments, joints, and the nozzle system, are then fabricated using machining techniques suitable for mild steel. Through precise measurements and tolerances, the components are assembled, ensuring smooth movement and alignment. Actuators such as electric motors are integrated into the arm, along with sensors like proximity and temperature sensors, to enable control and feedback. Wiring connections are established, and a control system is programmed to govern arm movement, nozzle activation, and sensor response. The fabricated arm is thoroughly tested, calibrated, and fine-tuned to ensure optimal functionality and performance.

3.3.2 Rocker Bogie

Designing and fabrication of the project are done as several stages. The whole system can be divided to 2 parts as the all-terrain vehicle using rocker bogie mechanism and a modular structure for sensors like GPR, Doppler, PIR, metal detectors etc. Initial step was the design and analysis of rocker bogie. Material for manufacturing chassis need to be strong enough so that it could carry the sensors or fire extinguishing robotic arm and also resistive towards corrosion. By considering the strength required, usage, lifespan AL6061 is selected as the material to build the chassis. Bogie seems to be heavy since all the components are integrated over it and effect the proper balance and movement to the body. Thus the wheels are kept wider which increase the area of contact by wheels over the ground surface. The weight is been distributed to a larger surface area by using 6 wheels. Six 12 V 30 rpm Johnson Geared motor is used for enough traction and torque to move through the rough terrain. Differential mechanism is used for avoiding tipping and overturning.

3.4 MANEUVERING

3.4.1 Robotic Arm Movement

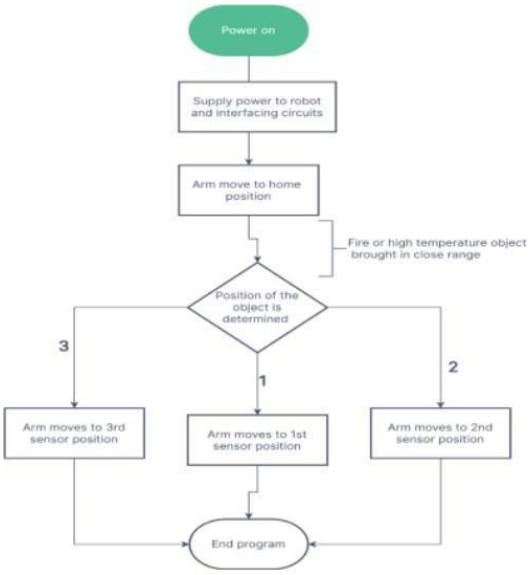

Figure 3. Flow chart of robotic arm movement

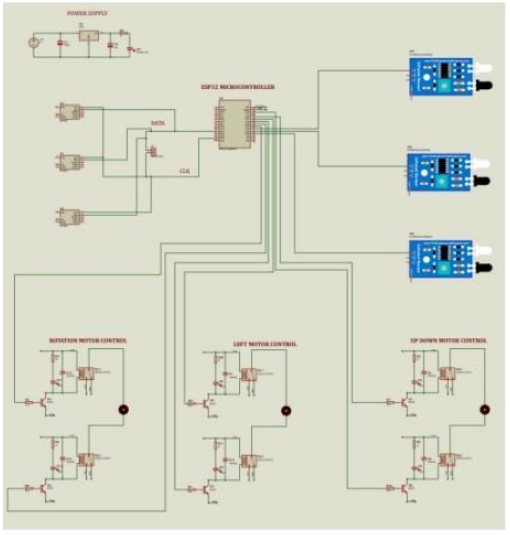

Figure 4. control system circuit diagram

3.4.2 Rocker Bogie Steering System

A central axis steering system is a type of steering system used in vehicles, particularly motorcycles and tricycles, where the front and rear wheels are connected by a central pivot or axis. This design allows for a unique steering mechanism that provides improved stability, maneuverability, and handling characteristics.In a central axis steering system, the front and rear wheels are linked together through a central pivot, typically located near the midpoint of the vehicle. The handlebars or steering mechanism are connected to the front wheel, while the rear wheel follows the steering inputs through the central 25 axis.Consists of advantages such as Stability since The central axis provides a stable platform, as both front and rear wheels move together, reducing the tendency for the vehicle to tilt or lean excessively during turns or maneuvers , then Enhanced Maneuverability because The central axis allows for a tighter turning radius, making it easier to navigate in tight spaces or make sharp turns. Also Improved Handling because The design provides a more direct and responsive steering feel, allowing for precise control and better handling characteristics, especially at higher speeds and reduces Steering Effort as the central axis steering system often requires less physical effort to steer the vehicle compared to other steering systems, making it more comfortable for the rider. While central axis steering systems offer certain advantages, they also have some limitations and considerations. The design may require additional components and complexity, which can increase the weight and cost of the vehicle. Additionally, the handling characteristics may differ from traditional steering systems, requiring some adaptation and familiarity for riders. Overall, the central axis steering system is a unique approach to vehicle steering that offers improved stability, manoeuvrability, and handling. Its application is primarily seen in motorcycles and tricycles, where these benefits can be particularly advantageous.

3.4.3 DC Motor Forward - Reverse Control

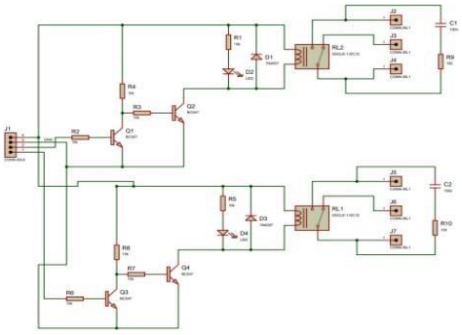

Figure 5. Motor movement circuit diagram

3.4.4 Control Interface

Blynk is an Internet of Things (IoT) platform that provides a user-friendly way to build and control IoT projects. It consists of a mobile app and a cloud-based server that work together to enable communication between IoT devices and a user's smartphone or tablet. With Blynk, users can create custom mobile apps for controlling and monitoring their IoT 27 Fig 4.18 Control interface devices without needing to write complex code from scratch. The platform supports a wide range of popular hardware platforms and microcontrollers, such as Arduino, Raspberry Pi, ESP8266, and more. Users can connect their devices to the Blynk server using various communication protocols, including WiFi, Ethernet, Bluetooth, and GSM. The Blynk mobile app allows users to design their own interfaces with drag-anddrop widgets, such as buttons, sliders, graphs, and displays. These widgets can be linked to IoT devices, enabling remote control and real-time data visualization. Blynk also provides an extensive library of prebuilt widgets and functions to simplify the development process. The Blynk cloud server acts as a bridge between the mobile app and the connected devices. It manages communication and data exchange, securely transmitting commands and receiving sensor data. The server also supports features like data logging, push notifications, and email alerts. Lynk offers a flexible and intuitive platform for hobbyists, makers, and professionals to quickly prototype and develop IoT projects. It simplifies the process of creating mobile apps for controlling and monitoring connected devices, allowing users to focus on the functionality and user experience of their projects

4 Results and Discussion

Figure 6. Sensor Performance

Types of sensors	Detection Range & Status
Temperature Sensors	Rated specification: 1 cm, 3 -5 V Through Experiments: In front of the lighter about 1 cm, sensor will respond in 2 seconds.
I R Sensor	Rated specification: 3.3V-5V voltage, effective distance range is 2cm to 80cm Through Experiments: it detects object in 5 cm to execute the program.

The incorporation of three temperature sensors and three IR sensors into the firefighting robot proved to be instrumental in enhancing its temperature detection ca-

pabilities. The sensors worked seamlessly in tandem, interconnected through a multiplexer board, facilitating efficient data collection and analysis.

4.1 Robot Motion and Positioning

The firefighting robot works efficient and precise motion control through its three degrees of freedom. The gear motors responsible for controlling the movement of the nozzle, shoulder extension, and base of the arm operated flawlessly, enabling the robot to navigate and position itself effectively within its environment. The base of the robot provided smooth 360-degree rotation at a speed of 30 rpm, allowing the robot to swiftly change its orientation to face the fire source. The synchronized upand-down motion of the nozzle at a speed of 30 rpm facilitated effective water spraying and fire suppression. Additionally, the shoulder extension, with its 30-degree vertical motion at a rate of 10 rpm, further enhanced the robot's agility and flexibility in adjusting the nozzle's height to effectively target the flames.

4.2 Autonomous Fire Response

The autonomous fire response mechanism implemented in the robot proved to be highly effective in minimizing response time and maximizing firefighting effectiveness. When power was switched on, the robot automatically returned to the home position (position 1) within 7 seconds, ready for immediate deployment. Upon fire detection by sensor 2, the robot autonomously moved to position 2, initiating firefighting measures without any human intervention. The robot swiftly sprayed water within 2 seconds, efficiently suppressing the flames and preventing further fire spread. Similar response mechanisms were implemented for the other two sensors, ensuring comprehensive coverage and quick deployment of the robot in emergency situations.

5 Conclusion

When a fire breaks out in a building used for business, education, or healthcare, a firefighting robot can be used to save lives quickly, easily, and automatically. Fire-fighting Robots are space-efficient because they have many motors and sensors, are lightweight and compact, and have rechargeable batteries. The prototype helps us detect the flame, temperature, and gas more effectively in the impacted region. Before a fire develops out of control and poses a threat to human life, the extinguisher robot successfully puts it out. By employing a robotic arm to clear the road, the firefighting robot is also successful in removing obstacles from the way to another area. Consequently, the robot has a significant future in our civilization. The main problems in fire safety measurements where taken into consideration and a suitable solution was obtained

Acknowledgement

Any attempt at any level cannot be satisfactorily completed without the support and guidance of learned people. We owe to great many people whose constant support and motivation that has encouraged us to come up with this Project. We are greatly obliged to Dr. Rajeev N, Head of the Department, Department of Mechanical Engineering, for the encouragement and support that he has provided. We are immensely indebted to our very understanding Project guide, Ajay Krishnan V, Assistant Professor (Ad-hoc), Department of mechanical Engineering, for his constructive suggestions, guidance and advice. We are thankful to our friends for their whole hearted cooperation during the preparation of our Project. Last but not the least we wish our gratitude to our parents for their abundant blessing without which this project would not be successful.

References

[1] Memon AW, Du J, Abro AH, Shah SI, Bhutto MA. Design and implementation of fire extinguisher robot with robotic arm. InMATEC Web of Conferences 2018 (Vol. 160, p. 06008). EDP Sciences .

[2] uoglu HS, Bogrekci I, Demircioglu P. Development of mobile robot with sensor fusion fire detection unit. IFAC PapersOnLine. 2018 Jan 1;51(30):430- 5.

[3] Khoon TN, Sebastian P, Saman AB. Autonomous firefighting mobile platform. Procedia Engineering. 2012 Jan 1;41:1145-53

[4]] ur Rehman A, Necsulescu DS, Sasiadek J. Robotic based fire detection in smart manufacturing facilities. IFACPapersOnLine. 2015 Jan 1;48(3):1640- 5.

[5] AlHaza T, Alsadoon A, Alhusinan Z, Jarwali M, Alsaif K. New concept for indoor fire fighting robot. Procedia-Social and Behavioral Sciences. 2015 Jul 3;195:2343-52

Fabrication and Characterization of AZ91d Mg Matrix Composite with Hybrid Reinforcement using Friction Stir Processing

Muhammed Safwan C T [1], Nithin P [1], Sanil Sabu [1], Aravind S [1] and Chamind E C [2]

[1] Mechanical Engineering, Jawaharlal College of Engineering and Technology, Kerala
[2] Faculty of Mechanical Engineering, Jawaharlal College of Engineering and Technology, Kerala

Abstract -

Potential of widespread industrial applications of magnesium has been realized in recent years. A variety of magnesium alloy matrix composites are now being studied for mechanical properties. Magnesium (Mg) alloys have been extensively used in various fields, such as aerospace, automobile, electronics, and biomedical industries, due to their high specific strength and stiffness excellent vibration absorption, electromagnetic shielding effect, good machinability, and recyclability Since magnesium is the lightest structural metal, it can replace aluminium in existing applications for further weight savings. The ability to improve mechanical properties with the use of smaller volume fraction of reinforcements while keeping density low makes magnesium composites an attractive choice for lightweight engineering. The Biomedical & Automotive domains mainly use the Magnesium composites because of its mechanical properties. Many works were carried out to improve the strength and yield properties of the composite by adding different reinforcements, but the ductility factor is decreasing in most cases. This work focuses to prepare a composite of AZ91D Mg with unique composition of hybrid reinforcements TiB2 (Titanium diboride) and Y2O3 (Yttrium Oxide). The work aims to improve the ductility of the composite without compromising the yield properties. Mechanical and Metallurgical testing of the composite are carried out for the characterization of the composite material. There are various ways for the preparation of Mg composites and different works were carried out with different processes. This work is carried out in friction stir processing (FSP) process. Friction Stir Processing (FSP) is a severe plastic deformation technique, based on the principle of Friction Stir Welding Processing quality is depending on process parameters like tool rotation, Travel speed, axial force etc. The variation of these process parameter of friction stir processing directly affects the mechanical and microstructural properties of the composite. Reinforcements can be mixed with the matrix material in different forms but the studies show that mixing of reinforcement in form with the matrix material enhances the results. The intermetallic changes and the stress-strain variations of the composite is prepared.

Keywords -

Mg Composites, Ductility, Titanium diboride, Yttrium Oxide, Friction Stir processing (FSP).

1 Introduction

Magnesium which has an excellent combination of mechanical properties, corrosion resistance, and castability is the commonly used material now a days.

Magnesium alloys and composites are widely used in several components such as automobile components, sporting goods, mobile and telephones, housings etc. Owing to the high specific strength of magnesium alloys, there is a great interest in broadening their use in transportation industries in order to achieve weight reductions and fuel savings. Mg density (1.74 g/cm3) is lower compared with the other wellknown light metal, aluminium (2.4 g/cm3). Their utility in wrought form is low and there are expectations to increase in the upcoming years. Although magnesium alloys and composites has good impact toughness and fatigue strength, it is sensitive to stress concentration and has high chemical reactivity making the conventional fusion welding process difficult. Some of the available studies already conducted on various types of magnesium alloy and their composites, the addition of reinforcements of different types, sizes and volume fraction and their influence on the mechanical and metallurgical behaviour Mg/Mg alloy matrix is reviewed in this chapter. The addition of reinforcements gives better results for the composite prepared and it also develops a better intermolecular distribution of the reinforcements which helps to achieve good metallurgical characteristics. There are different processes to prepare a metal matrix composite and a number of different reinforcements are added to get improved properties.

1.1 Friction Stir Processing

Friction Stir Processing (FSP) is an ecofriendly process which works on the identical principle as Friction Stir Welding (FSW). A rotating and moving non consumable tool with shoulder and pin of several geometries is utilized

for performing FSP. The tool is utilized to produce frictional heat and mix the material by inserting the rotating tool into the work piece. Tool plunging and traversing results in dynamic recrystallization of material caused by severe plastic deformation and consequently forms fine equiaxed grains in the processed region. The influence of material movement and plastic deformation during FSP results in the formation of various zones and the region where material mixing takes place is represented by the nugget zone or stir zone (SZ) adjoined by thermomechanically affected zone (TMAZ) and heat affected zone (HAZ). Among the three zones developed in FSP, the transition between the SZ and TMAZ is most important because this reformed area defines the properties of the processed material in the FSP. Sufficient axial force is required to insert the rotating tool into the workpiece surface to perform FSP.

2 METHADOLOGY

2.1 REINFORCEMENTS USED

2.1.1 TITANIUM DIBORIDE (TIB2, 99.5%PURITY)

Titanium diboride (TiB2) is an extremely hard ceramic which has excellent heat Conductivity, oxidation stability and wear resistance. TiB2 is also a reasonable electrical conductor ,so it can be used as a cathode material in aluminum melting and can be shaped by electrical discharge machining.

2.1.2 YTTRIUM OXIDE (Y2O3, 99.9%PURITY))

Yttrium oxide,also known as yttria, is Y2O3 .It is an air-stable,white solid substance.The thermal conductivity of yttrium oxide is 27 W/(m.K). Yttrium oxide, or yttria, has a range of uses including the tough structural ceramic yttria-stabilized zirconia (YSZ) that has many uses including protective coatings on the turbine blades of jet engines, allowing them to run at higher temperatures where they are more efficient. Yttrium oxide is an excellent mineralizing agent for spinel formation. It has a high melting point (2450oC), chemical stability, low coefficient of thermal expansion, high transparency for both visible (70%) and infrared (60%) light, low cut off energy of photons.

2.2 PROCEDURE AND EXPERIMENTAL SETUP

2.2.1 PREPARATION OF AZ91D MAGNESIUM ALLOY PLATE AZ91D

Mg powder of density 1.74 and melting point 648°C is going to be use Preparation of AZ91D Magnesium alloy plate of dimension 100mm x 50mm x 6mm is done in milling machine and the cutting process is done by Wire EDM . Length: 100 mm Width: 50mm Thickness: 6mm.

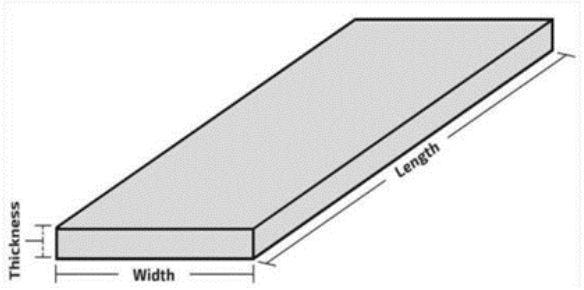

Figure 1. Dimension of alloy plate

2.2.2 CUTTING OF THE V-GROOVE ON THE PLATE

Groove Cutting is the technique to offer control joints in the concrete to guide cracks along the predetermined line, and it will also help to accommodate the movement of the concrete and avoid concrete cracks. The tool used here is made of H13 (steel chromium molybdenum hot work steel).Dimensions of the groove done here are width 1.5mm and depth 2.5mm. The machine used for groove cutting is the same machine used for Friction Stir Welding (FSW).

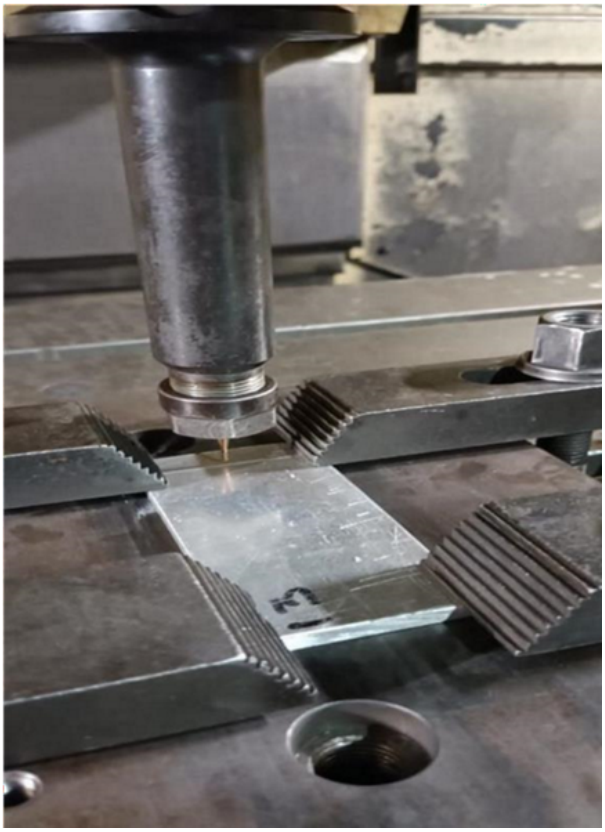

Figure 2. V-groove cutting

2.2.3 BLENDING OF REIFORCEDPARTICLE WITH A COMPOSITION OF TiB2 (25%) AND Y2O3 (5%)

Titanium diboride (TiB2,99.5%purity) molecular weight 69.50 ,melting point 3225°C,4.38 density and -325 mesh and Yttrium oxide (Y 2O3, 99.9% purity) of molecular weight 225.81,melting point 2410 ° C and density 5.01 are blended together to make reinforcements to add in the Mg alloy plate. The AZ91D Mg (99% purity) will be mixed and blended with 25 % weight of TiB 2 and 5% weight of Y2O3 at 200 rpm in both clockwise and anticlockwise direction.

BLENDING PROCESS

The actual process of blending the powder is ball milling. Due to the unavailability of a ball milling machine, we adopted an alternative method. The alternative method adopted for ball milling involves using a lathe. In this method, TiB2 (25%), Y2O3 (5%), and marble balls are added to a tube, which is fixed on the chuck of the lathe. The tube is then rotated at about 600 RPM clockwise and anticlockwise for 30 minutes in the lathe.

Figure 3. Ball milling using lathe machine

2.2.4 FRICTION STIR PROCESSING (FSP)

FILLING THE GROOVE WITH BLENDED REINFORCED PARTICLE The blended reinforcement particles with a composition of TiB2 (25%) Y2O3 (5%) are filled inside the v-groove. CLOSING Closing is done with a stroke of tool to preserve the spilling of reinforced particle. The tool rotates through the surface and begins to weld the surface to prevent the spilling RP's. The machine used for the closing is FSWM 20CNC – VMX 42,which is same machine used for FSP. PROCESSING In this process the deformation happens by forcibly inserting a non-consumable tool into the workpiece, and revolving the tool in a stirring motion as it is pushed laterally through the workpiece. When ideally implemented, this process mixes the material without changing the phase (by melting or otherwise) and creates a microstructure with fine, equiaxed grains. This also enhances the tensile strength and fatigue strength of the metal.

Table 1. Tool process parameters

Tool rotation speed	1240rpm
Travel speed	30mm/min
Stroke length	100mm

Figure 4. Closing tool image

3 RESULT AND DISCUSSION

3.1 TENSILE TEST

For tensile test the specimen size is 24 mm length, 4mm breadth and 4mm thickness. The specimen cut to the required standard by wire EDM as shown in figure.

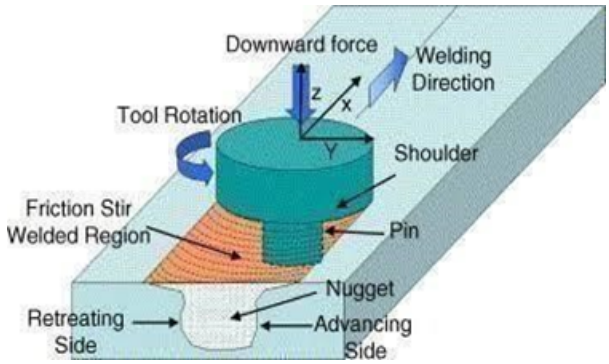

Figure 5. FSP process diagram

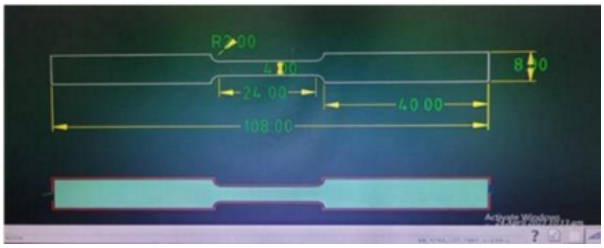

Figure 6. Specimen for tensile test

Equation and calculation:-
Percentage of elongation = ((final gauge length – initial gage length)/ initial gauge length) * 100
= ((26.13 – 24)/24)*100 = 8.87%
The parent material,Mg alloy AZ91D have % elongation of 5.3%. The increase in the percentage of elongation with parent metal is 3.57%. Based on the proportionality between the percentage of elongation and ductility, we can conclude that the ductility has increased.

3.2 HARDNESS TEST

Brinell hardness is a common method used to measure the hardness of a material. It determines the resistance of a material to indentation by a spherical indenter under a specified load. The Brinell hardness value is obtained by measuring the diameter of the indentation left on the material's surface. From the comparison of results between the parent metal (AZ91D Mg alloy) and the composite, it was found that the parent metal has a hardness ranging from 60 to 63 HRB. The hardness test conducted on the fabricated composite yielded a value of 62 HRB.

Initial Length	24mm
Extension	2.13mm
Elongation	8.87%
Final Length	26.13mm

Table 2. Hardness test result

TEST	SAMPLE	OBSERVED VALUES IN HRB
Brinell hardness	Mg alloy composite	62,64.5,65

3.3 SEM ANALYSIS

The samples were tested FESEM to visualize very small topographic details on the surface or entire or fractioned sample. Micrographic image of the composite shown using scanning electron microscope.

SEM ANALYSIS OF PARENT MATERIAL:- Based on the comparison between the parent metal

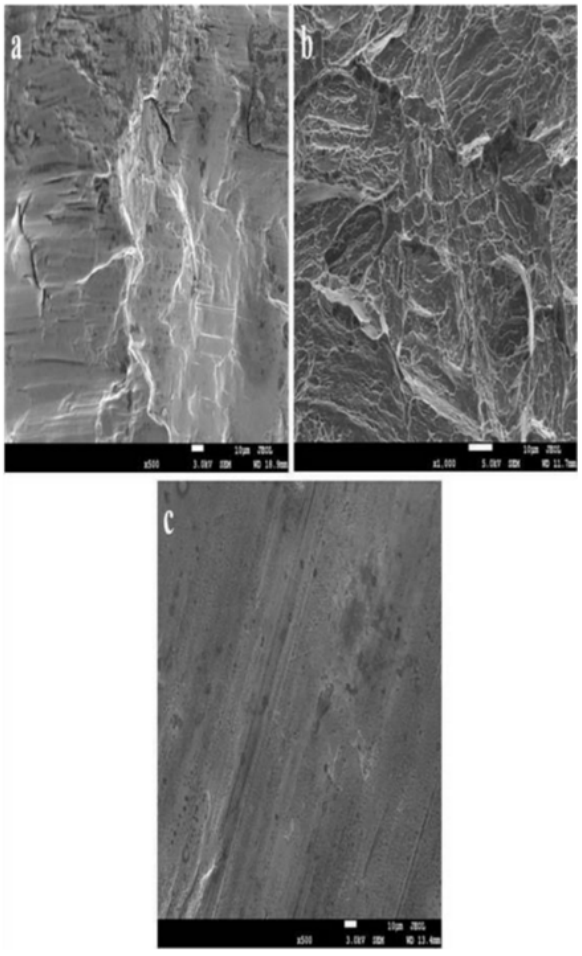

Figure 7. SEM analysis of Mg alloy AZ91D

and the composite, the SEM analysis revealed that the microscopic images indicated a uniform grain distribution.

SEM ANALYSIS OF COMPOSITE MATERIAL:-

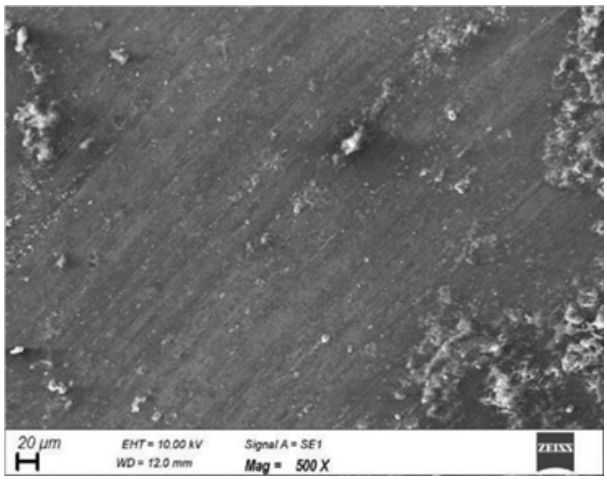

Figure 8. SEM analysis of the composite

4 Conclusion

• Literature studies suggest that the ductility and strength of the material increases with the addition of nano hybrid reinforcements Y2O3 and TiB2. • The AZ91D alloy processed at 1240rpm showed higher ultimate tensile strength from the parent metal. • The increase in the percentage of elongation with parent metal is 3.57%. Based on the proportionality between the percentage of elongation and ductility, we can conclude that the ductility has increased. • The expected result from the friction stir processing composite with enhanced properties compared with the base metal. • The particles addition would have given the composite better tensile (TiB2) and ductile strength (Y2O3).

References

[1] Abhishek Chauhan & Sanjeev Kumar (2018), Effect of friction stir welding parameters on impact strength of the AZ31 magnesium alloy joints, International Journal of Mechanical and Production ISSN (P): 2249-6890; ISSN (E): 2249-8001 Vol. 8, Issue 2, Apr 2018, 615-622.

[2] S. Mironov et.al. (2015), Microstructure evolution during Friction stir welding of AZ31 Mg alloy,ActaMaterialia301-312

[3] Won-Bae Lee, Chang-Yong Lee, Myoung-Kyun Kim, Jung-II-Yoon, Young-Mo Yoen, Seung-Boo Jung (2006), Microstructure and wear property of Friction stir welded AZ91 Mg/SiC particle reinforced composite, Composites Science and Technology 66(2006) 1513-1520.

[4] Amin Abdolahzadeh & Hamid Omidvar & Mohammad Ali Safarkhanian Mohsen Bahrami (2014), Studying microstructure and mechanical properties of SiCincorporated AZ31 joints fabricated through FSW: the effects of rotational and traveling speeds, Int J Adv Manuf Technol (2014) 75:1189–1196.

[5] A. Abdollahzadeh, A Shokuhfar, H Omidvar, JM Cabrera, A Solonin, A Ostovari and M Abbasi (2017), Structural evaluation and mechanical properties of AZ31/SiC nanocomposite produced by friction stir welding process at various welding speeds, Materials: Design and Applications 0(0) 1–11.

[6] Lee, W. B., Kim, J. W., Yeon, Y. M., & Jung, S. B. (2003, a). The joint characteristics of friction stir welded AZ91D magnesium alloy. Materials Transactions, 44(5), 917923.

[7] Lee, W. B., Yeon, Y. M., & Jung, S. B. (2003, b). Joint properties of friction stir welded AZ31B–H24 magnesium alloy. Materials Science and Technology, 19(6), 785-790.

[8] Pareek, M., Polar, A., Rumiche, F.,& Indacochea, J. E. (2007). Metallurgical evaluation of AZ31B-H24 magnesium alloy friction stir welds. Journal of materials engineering and performance, 16(5), 655-662. DOI: 10.1007/s11665007-9084-5.

[9] Commin, L., Dumont, M., Masse, J. E.,& Barrallier, L. (2009). Friction stir welding of AZ31 magnesium alloy rolled sheets: Influence of processing parameters. Acta materialia, 57(2), 326334.

[10] Chowdhury, S. M., Chen, D. L., Bhole, S. D., & Cao, X. (2010). Tensile properties of a friction stir welded magnesium alloy: Effect of pin tool thread orientation and weld pitch. Materials Science and Engineering: A, 527(21), 6064-6075.

Design and fabrication of folding stairs for train

Jaganathan K S[1], Jayanth T K[1], Abhay U[1], Arjun O V [1]and Dr. Rajeev N[2]

[1] B.Tech Students, NSS College of Engineering, Palakkad, Kerala, India
[2] Professor, Department of Mechanical Engineering, NSS College of Engineering, Palakkad, Kerala, India

Abstract -

A folding stair is a mechanical extension used to fill the gap between the train and the platform. The platform gap also known technically as the platform train interface or PTI is the space between a railway station platform and any train represents a major hazard and risk for all passengers boarding and exiting trains. Many accidents have been reported due to passengers falling in the gap between train and the platform. In that scenario we are trying to fill the gap between the train and platform so as to reduce these accidents. We are planning to fix a metal sheet on the platform side of the train and with the help of a sensor while train approaches the platform this metal sheet automatically comes and align at the level of platform. The main objective is to offer an automated way to reduce the gap between train and platform using sensors. As there has not been any such works previously done, we believe this project will be the best possible solution for the problem that the train passengers are facing in Indian Railways.

Keywords -

Platform train interface

1 Introduction

A platform gap also known technically as the platform train interface or PTI in some countries is the space between a train car or other mass transit vehicle and the edge of the station platform. So as of now lots of lives have been lost between the tracks. In that scenario we are trying to fill the gap between the train and platform so as to reduce these accidents. We are planning to fix a metal sheet on the platform side of the train and by the help of a sensor while train approaches the platform this metal sheet automatically comes and align at the level of platform. So, while the train is stationary at the platform there will be no gap between train and platform edge. In the world of transportation, trains continue to play a crucial role in providing efficient and reliable mass transit solutions. To enhance passenger safety and accessibility, it is essential to design innovative solutions that cater to the diverse needs of commuters

2 The object of the study (Model, Process, Device, Sample preparation etc.)

2.1 Project Planning

a. Perform a throughout assessment of train stairs details , considering its dimensions, weights, and suitable structural integrity. b. Research and select suitable motor for the prototype c. Determine the appropriate material for the structure, and platform

2.2 Sensor arrangement

a. suitable sensor determined by research b. ultrasonic sensor used this project using the time calculation

3 Methods

This is the simple way by which the working methodology of the project is explained easily. In this method the safety guard is attached in the bottom of the locomotives and the sensor is also attached in the train itself. Initially the train reaches the platform, and the working of this project starts. While train reaching the platform the senor attached in the locomotive is started to work. Sensor measures the distance between the train and to the platform by sending the light signal. Immediately the sensor sends the signal to the Arduino. The Arduino is the one which receives the signal and the program which is done in the Arduino is helpful to operate the motor driver. The motor drive is used to operate the motor which make the motion of the safety guard which is attached in the bottom of the locomotive compartment.

3.1 Structure

Structure of folding stairs for train is created by metal sheet. We provided a extension to the structure to fill the gap between train and platform. This extension automatically operated by Arduino using sensor and motor drives. Maximum extension of the structure is 15cmWe used 0.5-inch GI pipe for extension purpose. Two clamp which is provided opposite sides structure for fixing motors.

3.2 components

3.3 Ultrasonic sensor

Figure 1. Ultrasonic sensor

The sensor head emits an ultrasonic wave and receives the wave reflected back from the target. Ultrasonic Sensors measure the distance to the target by measuring the time between the emission and reception. Ultrasonic sensors shown in the fig work on the principle of reflected sound waves and are used to measure distance. One sensor can detect others operating nearby. Distance is then estimated by the time interval between sensor and object. Basic Sonar Illustration – A transducer generates a sound pulse and then listens to the echo It emits an ultrasound at 40 000 Hz which travels through the air and if there is an object or obstacle on its path It will bounce back to the module. Considering the travel time and the speed of the sound you can calculate the distance.

3.4 Arduino

Figure 2. Arduino

Arduino is an open-source electronics platform built on simple-to-use hardware and software, as seen in Fig. A motor can be started, an LED can be turned on, and something may be published online by using an Arduino board to receive inputs like light on a sensor, a finger on a button, or a tweet. Sending a set of instructions to the board's microcontroller will instruct your board what to do. You achieve this by using the Arduino Software (IDE), which is based on Processing, and the Wiring-based Arduino Programming Language. Over the years, countless of projects, ranging from simple household items to intricate scientific instruments, have used Arduino as their brain. This open-source platform has attracted a global community of makers, including students, hobbyists, artists, programmers, and professionals. Their efforts have added up to an astounding quantity of accessible knowledge that may be very helpful to both beginners and specialists.

3.5 Motor driver

Figure 3. Motor driver

The L293D is quadruple high-current half-H drivers. It is designed to provide bidirectional drive currents of up to 600-mA at voltages from 4.5 V to 36 V. Both devices are designed to drive inductive loads such as relays, solenoids, dc and bipolar stepping motors, as well as other high-current/high-voltage loads in positive-supply applications. All inputs are TTL compatible. Each output is a complete totem-pole drive circuit, with a Darlington transistor sink and a pseudo- Darlington source.

3.6 DC Motor

A DC motor is any of a class of rotary electrical machines that converts direct current electrical energy into mechanical energy. The most common types rely on the forces produced by magnetic fields. Nearly all types of DC motors have some internal mechanism, either electromechanical or electronic, to periodically change the direction of current flow in part of the motor. DC motors were the first form of motor widely used, as they could be powered from existing direct-current lighting power distribution systems. A DC motor's speed can be controlled over a wide range, using either a variable supply voltage or by changing the strength of current in its field windings. Small DC motors are used in tools, toys, and appliances. The universal motor can operate on direct current but is a lightweight brushed motor used for portable power tools and appliances. Larger DC motors are currently used in propulsion of electric vehicles, elevator and hoists, and in

drives for steel rolling mills. The advent of power electronics has made replacement of DC motors with AC motors possible in many applications.

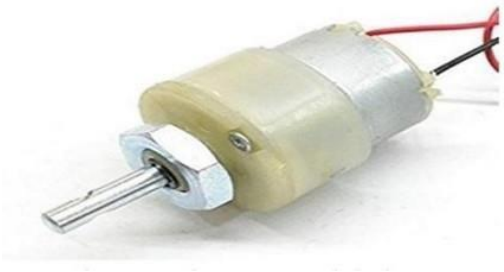

Figure 4. Motor driver

4 Equations

L = 1/2 * T* C

Were,

L is the distance

T is the time between the emission and reception

C is the sonic speed (The value is multiplied by ½ because T is the time for go-and-return distance)

5 Results and Discussion

The folding stairs of train model are carried out successfully completed. The project team analyzed various train models and platform configurations to identify the design requirements for the folding stairs. Multiple design concepts were generated, considering factors such as structural integrity, compatibility, and passenger comfort. Through evaluation criteria and feedback, a suitable design concept was selected for further development.

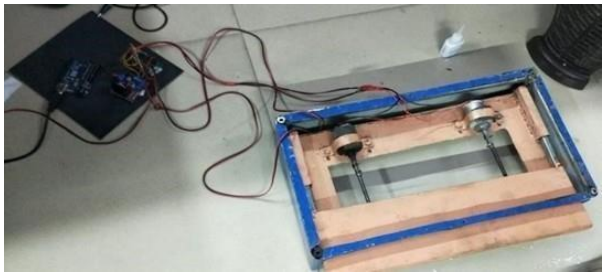

Figure 5. Experimental setup

6 Conclusion

Overall, the project successfully achieved its objectives of designing and fabricating folding stairs for trains. The folding stair system showcased enhanced safety, accessibility, and user experience, contributing to the continuous improvement of mass transit systems. The outcomes of this project serve as a stepping stone for further advancements in train boarding and alighting mechanisms, ultimately making public transportation more inclusive, efficient, and user-friendly. An extensive review of the literature provided was done and the team have acquired clarity on how to proceed with the project. Since the system works on railway track using sensor, method that will helps to reduce accident due to gap. The successful design and fabrication of a folding stair system for trains will significantly enhance the boarding and alighting experiences of passengers. By addressing platform- train gaps and accommodating various train configurations, this innovative solution aims to minimize risks associated with passenger transfers and improve overall safety. Furthermore, the project aims to set a new benchmark for accessibility standards and contribute to the continuous improvement of mass transit systems, fostering a more inclusive and efficient public transportation environment.

Acknowledgements

Any attempt at any level cannot be satisfactorily completed without the support and guidance of learned people. We owe to great many people whose constant support and motivation that has encouraged us to come up with this Project. We are greatly obliged to Dr. Rajeev N, Head of the Department, Department of Mechanical Engineering, for the encouragement and support that he has provided. We are immensely indebted to our very understanding Project guide, Dr.Rajeev N, Professor and Head of Department, Department of mechanical Engineering, for his constructive suggestions, guidance, and advice. Our Project in charge Dr. Aneesh Kumar P, Assistant Professor and Madhu Mohan, Professor, Department of Mechanical Engineering for his valuable guidance, support, and whole-hearted cooperation

References

[1]] Elamvazhudib Bala, P. Arun Vetrivel, A. Mohamed Asarudheen. Design of Safety Grill to avoid Railway Platform Accidents in 2019 .

[2] Indian Railways Statistical Publications 2015-16: Statistical Summary. Ministry of Railway. Retrieved 26 February 2017

[3] Vincent Moug1, Etal, 'An Analysis of Station Infrastructure Design to Improve Accessibility Between the Platform and Suburban Train Carriages', 2 - 4 October 2013, Brisbane, PP 1-19

Dynamic Response Testing on Control Valve with EVSP Packing

Gokul K[1], Karthik K[2], Nidhun P M[3], Salmanul Faris K[4] and Vishnu Narayan[5]

[1,2,3,4,] Department of Mechanical Engineering, Affiliated to APJ Abdul Kalam Technological University, Kerala

[5] Asst. Professor, Department of Mechanical Engineering, Affiliated to APJ Abdul Kalam Technological University, Kerala

[1]goku.valloor@gmail.com, [2]karthikdas462@gmail.com [3]nidhunalfa@gmail.com [4]salmanulfariska1@gmail.com
[5]vishnunarayan@jawaharlalcolleges.com

Abstract -

This venture work is an endeavour to lessen the hour of control valve presenting different pressing materials. In loops, the response time of the valves is crucial and must be taken care of. In process industry the progression of liquid in a huge line is to be controlled from a control room. The administrator gives input sign to the control unit which Will open or close the valve according to the sign. An excessive number of fluid flows is caused by the lag in response time. This brings about unreasonable material use. The response time is influenced by a variety of factors, including packing box friction, valve plug and stem unbalance, spring and diaphragm hysteresis, and so on. In this way, to conquer these issues, the organization utilizes additional extras like supporters furthermore, fast exhaust valves and so on. the system focuses on packing box friction. We suggested the Expandable Valve Stem Packing (EVSP) alternative to get around the friction and speed up the response time. In a 3" valve, the above-mentioned method is implemented. The proposed approach is then put through its paces using a Dynamic Response Testing Apparatus, and the outcomes are compared to those of the current approach. It reduces response time to desired value and eliminates the use of additional accessories, both of which contribute to an increase in profit.

Keywords -

Dynamic response Testing, packing box friction, EVSP (Expandable valve stem Packing).

1 Introduction

In order to produce a product that can be sold, process plants have hundreds or even thousands of control loops that are connected in a network. The purpose of each of these control loops is to maintain important process variables like pressure, flow, level, temperature, etc. within a predetermined operating range to guarantee the final product's quality. In addition to receiving and internalizing disturbances that have a negative impact on the process variable, interactions with other loops in the network also produce disturbances that have an impact on the process variable. The reaction season of valves is significant in process ventures where all these progression of liquid in enormous pipelines should be controlled from a control room. The valve ought to open or close in accordance with the operator's input signal to the control unit. However, excessive fluid flow and material consumption can occur if the response time is delayed. The undertaking intends to address the elements that add to the reaction season of control valves, explicitly zeroing in on pressing box grating. The project suggests an alternative method called EVSP (Expandable Valve Stem Packing) to get around this friction and speed up the response time. This method is used in a 3" valve, and a Dynamic Response Testing Apparatus is used to test how well it works. The outcomes acquired from testing the proposed technique are then contrasted and the current strategy.

2 Literature Survey

[1] Marvin R.Havens: Extremely hot systems for packing high-pressure valves, patent number 4234317; Mar17, 1981: Where the temperature is below 30 degrees Celsius, asbestos-based materials are frequently used. At higher temperatures, however, asbestos loses its water and hydration, and the binder frequently decomposes, causing packing to leak. Graf oil is a brand name for the expanded graphite material, which is one of the best packing materials for high temperatures. It is equipped for activity at temperature up to 650°C. However, some expended graphite packings were found to have a high failure rate. The most significant issue was that expanded graphite could extrude out of the stuffing box because it becomes somewhat fluid under pressure

[2] Michael S. Fink; Broadened stem globe valve, US pat no 6302374; Oct 16, 2001 Teflon has desired as the friction coefficient, yet the Teflon contracts at more noteworthy degree than the encompassing material exposed climate. The position may experience frosting and leakage as a result of this relative shrinkage. Additionally, the Teflon packaging can only function properly between 100 and 260 °C. This issue was survived by utilizing graphite base pressing material. due to the fact that graphite is a material that can function at temperatures up to 650 °C. So, the system iis based on Teflon.

[3] Danny L. Schnitzler; Packing ring containing flexible graphite; US pat no 4190257, Feb. 26) 1980: Highly effective packing ring made of compressed flexible graphite undergoes a lot of flow when put under pressure,

allowing it to form a better interference fit in the stuffing box. These packing rings do not need to be precisely sized to the dimensions of a particular stuffing box because they are able to flow and change their dimensions under pressure.

[4] White et al; Staffing box packing system and methods, US pat no 4328974 May 11,1982: A lowemission packing article, apparatus, and method, especially for valve stems in the petrochemical and power industries, with one or more low-density preform rings. material that can be molded and compressed, such as, ideally, flexible graphite. The material of the low density preform ring is re-formed (i.e., deformed and caused to move) against the stem and/or the stuffing box by tightening the gland. This results in the formation of an LD. as well as an O.D. seal Each low density preform ring is preferably in contact with a high-density adapter ring (preferably also made of graphite), and the pair of rings form either an ID or an OD sealing assembly.

[5] Donald R. Fields: High Temperature, High pressure valve packing system; US pat no 4256317. Mar 17, 1981: The valve stem was held in place by a small amount of expanded graphite. The production stem had a finish of 10-14 microns and a projection resembling a tooth (a light grinding mark can be seen) to pick up expanded graphite. Silver and chrome plating on the stem was inadmissible from process contemplations. Chrome isn't a good choice for expanded graphite material's surface. The stems were tested and found to work by simply polishing them to a mirror finish with diamond rouge. Polishing the valve stem was found to reduce expanded graphite material transfer and make the valves work better.

3 Methodology

A parameter that incorporates both the dead time and the time constant is typically used to measure response time. It is essential that the valve reach a particular position quickly for optimal control of numerous processes. One important aspect of providing optimal process control is the speed with which one responds to minor signal changes (less than one percent). The majority of signal changes received from the controller in automatic regulatory control pertain to minute shifts in position. Process variability will be reduced if a control valve assembly can react quickly to these minor changes. Valve response time is measured using the parameters T63.5 and T86. Dynamic means the valve is moving. Dynamic reaction can be estimated without process stacking in seat top tests with animated or dynamic stacking in a stream research center or under a mal process working condition utilizing DRT arrangement. Dynamic Response Testing (DRT) is planned to gauge the time reaction of a valve regarding input signal. The

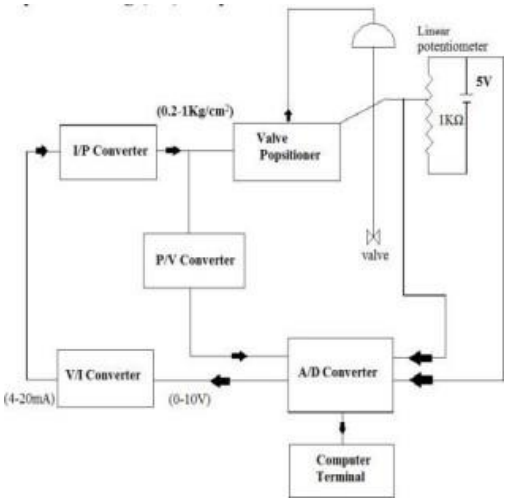

Figure 1. DRT Set up

Dynamic Response Testing gives imperative data to a possible client and gives him a thought regarding how the valve will perform. The Dynamic Response Testing is carried out in a room with air conditioning that is free of any and all external disturbances. A linear potentiometer, an A/D convertor, a V/I convertor, an I/P convertor, and a P/V convertor are typically the components of a Dynamic Response Testing apparatus. These components are all connected to a computer that receives data and analyzes the results. The outcome is as a chart with info and result signals It likewise shows dead time and rise season of the interaction. The Unique Reaction Testing is doing in INSTRUMENTATION Restricted according to the standard ISA-TR 75.25.02- 2000. The valve should pass the preliminary test before the Dynamic Response Test The test setup for evaluating the control valve's dynamic response at Instrumentation Limited Palakkad is shown in the figure above (fig. 1). The test arrangement and the methodology according to the norm ISA - TR 75.25.02-2000. The analog-to-digital converter feeds the signal to the V/I converter, which converts the voltage (0-10V) into a current signal (4-20mA). The analog-to-digital converter feeds the signal to the V/I converter, which converts the voltage (0-10V) into a current signal (4-20mA). The IP converter then transforms the current signal into an air pressure signal (0.2-1 kg/cm2) This sign is taken care of to valve through positioner. Valve reaction (development) is switched over completely to electrical sign by a straight potentiometer and taken care of to the PC for investigation. To gauge the dead season of valve of a valve, the valve is exposed to a stage reaction test. For instance, in this instance, the valve is given a signal that actuates it by +/-5% from the middle position, which

is between 45 percent and 55 percent of the valve stroke (depending on the customer's requirements).The selected valve's stroke length is as follows:
Stroke = 37.5mm
Mid position = 50% of stroke = 18.75mm
+5% from mid position = 55% of stroke
= 20.625mm
-5% from mid position = 45% of stroke
= 16.875mm
45% to 55% position = 16.875 to 20.625mm
Signal span = 4-20Ma
For 50% response = 4+(4-20)/2
= 12mA
Therefore, 10% of signal = 1.6mA
And 5% of signal = 0.8mA
For 45% -55% response = (12-0.8) to (12+0.8)
=11.2mA to 12.8mA
For this corresponding signal and position the dead time and time constant is obtained from DRT test

3.1 Expandable valve stem packing (evsp)

EVSP pressing is made of high - immaculateness jewel finished graphite tape in cup and cone shape design. The low-density performing ring, the high-density OD and ID adapter ring, and the braided end ring are the three types of rings in this packing. The preforming ring has the thickness of 0.7gr/cc, also, the connector ring has the thickness of around 1.8 gr/cc. This packing's controlled radial flow results in effective sealing and reduced friction due to the design's cup-and-cone shape and variation in density. Preferably, the high- and lowdensity rings' facing surfaces are oriented at an acute angle to the packing's longitudinal axis. The confronting surface of the connector ring is ideally around 300 and the confronting surface of the perform ring is ideally around 450 to such longitudinal pivot, in this manner giving a best contrast in points of around 150. One way to control the deformation or re-formation of the lower density flexible graphite preform ring to ensure the formation of the I.D. or O.D. seal is through the difference in angles. When compared to the standard flat ring that is currently in use, this packing experiences 15 to 25of approximately 70 Mpa and a temperature range of 200 °C to 650 °C. To prevent leaks, 5 to 7 ring sets are typically used. Less than five rings can cause leaks, while more than seven rings can cause drag. Seven rings should be used whenever possible.

Application condition

Working temperature = -200℃ to 650℃
Maximum working pressure = 70Mpa
Ph range = 0-14(except strong oxidizers)
friction = 25% lesser than flat ring packing
Suitability for nuclear service = Yes

Figure 2. EVSP

Lubrication =Not needed
With oxidizing agent =Form coke at the temperature of about 350
The packing box dimension of 3" valve is:
Depth = 80mm
Bore diameter = 23mm
Stem diameter = 10mm
Based on stuffing dimension the thickness of the ring is calculated using the formula:
Cross section = (Box bore ID- stem Diameter)/2
= (23-10)/2
=6.5mm
So, each ring of the packing should be of thickness 6.5mm.
For seven ring the total depth required is =6.5 x7=45.5mm.
Bushing height = (stuffing box depth - required packing height - thickness of retaining ring).
So, Bushing height = 80 -38-(2X3) = 36mm.

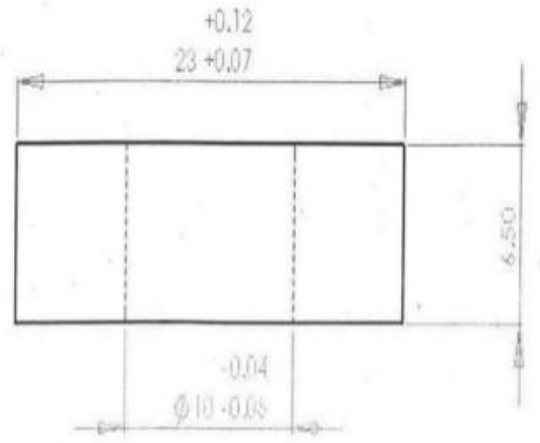

Figure 3. Dimension of Braided Ring

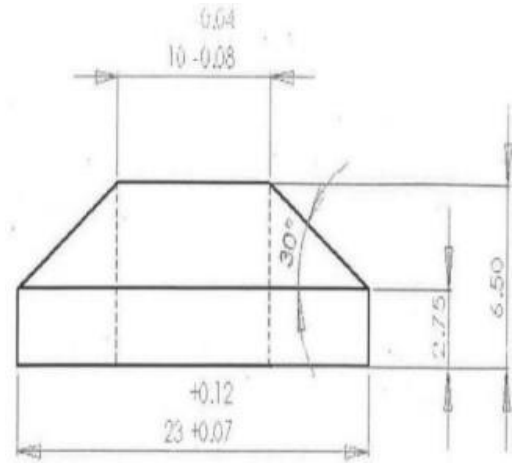

Figure 4. Dimension of OD Adapter Ring

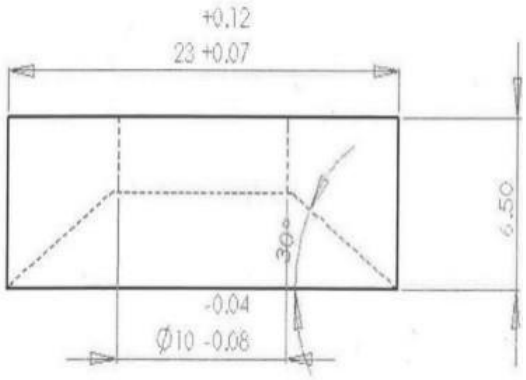

Figure 5. Dimension of Performing Ring

4 Results and Discussion

The 3" size valve is used. Specifications are:
Valve size: 3"
Actuator type: VA1 Direct
Packing: Graf oil
Process temperature: 400^{o}C

RESULTS:
Avg Dead time of Graf oil (TD1) = 0.26
Avg T63.5 of Graf oil (T63.5 1) = 0.63
Avg T86 of Graf oil (T86 1) = 1.08
Avg Dead time of EVSP (TD2) = 0.20
Avg T63.5 of EVSP (T63.5 2) = 0.44
Avg T86 of EVSP (T86 2) = 0.68
Dead time difference = TD1 – TD2
= 0.26 - 0.20
= 0.06
Percentage decrease in dead time = 6%
T63.5 difference = T63.5 1- T63.5 2
= 0.63 – 0.44
= 0.19
Percentage decrease in dead time = 19%
T86 difference = T86 1- T86 2
= 1.08 – 0.68
= 0.40
Percentage decrease in dead time = 40%
Avg T63.5 of Graf oil (rise time) = 0.7095
Avg T86 of Graf oil (rise time) = 0.9303
Avg T63.5 of EVSP (rise time) = 0.6364
Avg T86 of EVSP (rise time) = 0.7873
Avg T63.5 of Graf oil (fall time) = 1.02
Avg T86 of Graf oil (fall time) = 1.206
Avg T63.5 of EVSP (fall time) = 0.793
Avg T86 of EVSP (fall time) = 0.9697
T63.5(rise time) difference = 0.7095-0.6364 = 0.0731
Percentage decrease in rise time (T63.5) = 7.31%
T86 (rise time) difference = 0.143
Percentage decrease in rise time(T86) = 14.3%
T63.5(fall time) difference = 0.227
Percentage decrease in fall time (T63.5) = 22.7%
T86 (fall time) difference = 0.2363
Percentage decrease in fall time(T86) = 23.63%

5 Conclusion

The project on using Expandable Valve Stem Packing (EVSP) for dynamic response testing (DRT) of control valves has shed light on the capabilities and advantages of this cutting-edge packing method. The goal of the undertaking was to assess the unique reaction of control valves furnished with EVSP and evaluate their appropriateness for different functional circumstances. Control valves that make use of EVSP have superior dynamic response characteristics to those of conventional packing systems, as demonstrated by extensive testing and analysis. The EVSP packing material exhibits improved wear and degradation resistance, reduced frictional losses, and superiorsealing capabilities. Control valve longevity, efficiency, and performance all benefit from these properties. The EVSP-equipped control valves consistently provided precise control, minimal hysteresis, and a rapid response to changes in flow rates, pressures, and temperature differentials during the dynamic response testing. This exhibits their capacity to keep up with exact command over liquid stream, guaranteeing ideal interaction execution and wellbeing. In addition, despite being subjected to harsh operating conditions, the EVSP packing exhibited remarkable durability and dependability. It showed very little leakage and kept its sealing properties over long periods, reducing the need for frequent maintenance and improving the integrity of the system as a whole.

References

[1] Burnishing; Walter E. Burton; sep 1957; page 205-216

[2] Surface effects in adhesion, friction, wear and lubrication; Donald H. Buckley; page578-585Process specification for dry film lubrication application; Julie A. Henkener

[3] Control of cutting temperature and cutting fluid application; version 2 ME, KharagpurMoS2 in Lubrication application; Yakov Epshteyn and Thomas J Risdon.

[4] Marine engineering log; Volume 85 Simmons. Boardman Pub. Co;1980.

[5] Gauging the Force Effects of Valve Stem Packing on Valve Stem Actuation; James Drago, Wayne Evans, December 5, 2017.

[6] B. Nesbitt, Handbook of Valves and Actuators: Valves Manual International, 1 st edn. (Elsevier, Oxford, 2007).

[7] K. Sotoodeh, Piping and valve materials for offshore use, part 2. Stainl. Steel World Mag. 28(July/August), 35–40 (2016)

Study On Novel Multisegment Replaceable Profiled Steel Shear Links Under Cyclic Loading

Manikandan P V[1] **and Dr. Keerthy M Simon** [2]

[1] M Tech Student, Department of Civil Engineering, NSS College of Engineering, Palakkad Kerala, India
[2] Asst.Professor, Department of Civil Engineering, NSS College of Engineering, Palakkad Kerala, India

Abstract -
Replaceable steel shear links are structural elements that are often placed between the main structural elements in a multi-story building, such as columns and beams, and are meant to disperse energy under lateral loads, such as those experienced during an earthquake. These shear links are designed to break or deform under severe lateral stresses, which helps to distribute energy and prevent structure damage, and can be easily replaced after an earthquake. Multi-segment shear links is a modified form of replaceable shear links that can limit structural damage by dissipating more energy under lateral loads than a common replaceable shear link. These shear links are made up of a sequence of I sections with web stiffeners, with each segment designed to bend or break under severe loads. These I section can be replaced with stiffened profiles (profiled steel shear links) which occupies more space, providing increased strength and buckling resistance. The purpose of this paper is to analyse the structural behaviour of replaceable profiled steel shear links using ANSYS finite element software. This paper also includes a numerical study on the effect of cyclic loading on these shear links by varying link length and profile parameters like wave type, thickness and width. Hysteretic curve was acquired through cyclic load testing for stiffened I sections. These curves are plotted between applied load and the resulting deformation of the element, and can provide insight into how the structure will respond to repeated loading and unloading cycles.

Keywords -
Multi-segment shear links, Stiffened profiles, Hysteretic curves

1 Introduction

Under the premise of ensuring life safety, the philosophy of earthquake resilience mandates in order that the structure should swiftly regain its function after earthquakes and should minimize the impact on daily activities and productivity. According to this theory, earthquake resilient structures concentrate damage on replaceable elements or components by utilizing the four mechanisms of rocking, self-centering, replaceability, and energy dissipation to render the primary structures damage-free or easily repairable. Steel shear links that can be replaced In seismic-resistant building constructions, replaceable steel shear links are widely employed to safeguard the primary structural parts from damage during an earthquake. These links are designed to break or deform in the event of high lateral stresses, which helps to diffuse energy and reduce structure damage. Shear links are typically constructed of steel and are situated between the main structural members. They are designed to be easily removable, allowing for rapid and easy replacement following an earthquake. These replacement shear connections have a restricted energy dissipation capacity, a set deformation capacity, and the inability to alter performance. To alleviate these problems, a modified type of shear links is created; such shear links are known as multi-segment replaceable shear links.

1.1 Multi-segment replaceable steel shear links

Multi-segment shear connections are a form of energy-dissipating device that is often utilised in the design of seismic-resistant buildings. To improve the behaviour of the typical replaceable shear link in the connected columns frame, a multi-segment replaceable shear link is proposed. The multisegment replaceable shear link is made up of a central shear link that acts as a fuse and two linked beams, with the central shear link connected to linked beams at both ends and the linked beams attached to the columns through demountable connections. When this structural system is subjected to severe ground motion, all damages of the central shear links dissipating seismic energy as they undergo large inelastic deformation are concentrated in the central shear link, and the damaged link can then be easily replaced after the earthquake, while the linked beams remain undamaged to transfer the forces generated by the fully yielded and strain hardened link. Overall, multi-segment shear links are a significant component of seismic-resistant structure design, and their application can help to safeguard buildings and inhabitants from earthquake damage.

2 Analysis of multi-segment replaceable steel shear links

The material properties and dimension for validation is taken from work by Men J, et.al (2022) [8]. The experimental study on Multi-segment replaceable steel shear links is carried out, boundary condition assigned is bottom frame hinged and cyclic load acting on the top of the frame [8]. Total deformation and shear force is obtained using analysis using ANSYS workbench. Mesh of

size 50mm shape of mesh is hexahedron with 20 nodes is modelled and is shown in Fig 1.

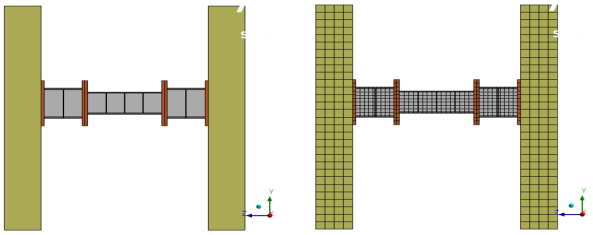

Figure 1. Geometry of the model and Finite element model

Table 1. depicts the dimensions of shear link, the shear link consists of primary link and secondary link both are I sections.

Table 1. Material Properties

Properties	Value
Young's modulus of Flange	199000Mpa
Yield strength of flange	391Mpa
Ultimate tensile strength of flange	538.3Mpa
Young's modulus of Flange	211000Mpa
Yield strength of web	291.7Mpa
Ultimate tensile strength of web	441.7Mpa
Poisson's ratio	0.3

2.1 Cyclic loading

Cyclic loading is applied at the top of the column in the frame. For the application of load Men J, et.al (2022) use a loading protocol called AISC/FEMA Protocol [5]. The protocol says, for seismic loading criteria the drift of the structure varies from 0.375structure is stable. So these shear links are designed such a way that it should withstand till 6drift or corresponding loading. Table 2. depicts the cyclic loading protocol used for analysis of the shear link model.

2.2 Results

Fig. 2 (a) and (b) depicts the total deformation and plastic strain distribution of the shear link models. From the plastic distribution image, the damage is only in the primary link web and there is no damage in secondary shear links

2.3 Validation

Fig 3 and Table 3 are the validation results from literature and Finite Element Analysis. The shear force

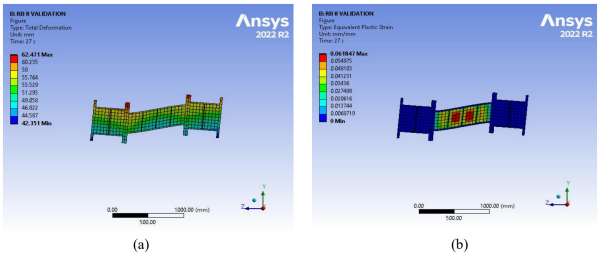

(a) (b)

Figure 2. (a) Total deformation and (b) Plastic strain distribution

occurred on shear links as per literature is 790kN [10] and shear force obtained from the finite element analysis (FEA) is 770.5kN.

The percentage error was found to be 2.5%. The percentage error was found to be 0.84%, hence the model is validated. Both the specimens are failed by web buckling and web tearing with the application of cyclic loading.

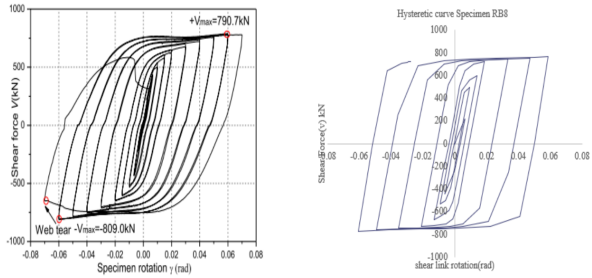

Figure 3. Hysteretic curves from experiment and FEA

3 Analysis of multisegment steel shear links with varying primary link length

Analysis of multi-segment steel shear links was conducted using Ansys Workbench. AISC protocol cyclic loading is applied to the multi-segment steel shear links with varying primary link length. The maximum value of primary link length that can be used is calculated from the equation.

$$e \leq \frac{2x1.2M_p}{1.5v_p} = 1.6\frac{M_p}{v_p} \quad (1)$$

Where,
V_p is the plastic shear strength of I section
M_p is the plastic moment strength of I section
The values for v_p and M_p can be calculated from the equation;

$$v_p = \frac{F_{yw}}{\sqrt{3}} * t_w(d - 2t_f) \quad (2)$$

Table 2. AISC protocol cyclic loading scheme

Storey height(m)	Drift (rad)	Drift(degrees)	Drift(%)	Displacement (mm)
3	0.00375	0.21	0.375	11.26
3	0.005	0.29	0.5	15.01
3	0.0075	0.43	0.75	22.5
3	0.01	0.57	1	30.02
3	0.015	0.86	1.5	45.03
3	0.02	1.15	2	60.04
3	0.03	1.72	3	90.07
3	0.04	2.29	4	120.13
3	0.05	2.86	5	150.2
3	0.06	3.43	6	180.31

Table 3. Validation of the model

	Shear Force(kN)	Link rotation(rad)
Experimental Results	790	0.06
FEA	770.5	0.0605
Percentage error	2.47	0.834

Table 4. Section details

Link	Section (mm)	Link Length (e) (mm)	Model Designation
Primary Shear link	I-300×150×10×18	500	RB8 500
		600	RB8 600
		700	RB8 700
		800	RB8 800
		900	RB8 900
		1000	RB8 1000
Secondary shear link	I-400×200×10×18	400	

$$M_p = F_{yf} * t_f(b - t_w).(d - t_f) + \frac{F_{yw} t_w d^2}{4} \quad (3)$$

t_w and t_f is the web and flange thickness of the I section
b and d is the flange width and overall beam depth of the I section
The maximum primary link length obtained as per AISC code (AISC 341 -Seismic Provisions for Structural Steel Buildings) is 1020mm.

3.1 Material Property

The material properties and dimensions of multi-segment steel shear links were taken from Men J, et.al (2022) [10]. The primary link length varying from 500mm to 1000mm was modelled. The material properties of the components are given in Table 4.

Modelling and analysis of project was carried out using ANSYS Workbench R21. There are 6 cases of each vary in primary link length in multi-segment steel shear link were modelled. The elements were modelled using Solid 186 with a mesh size of 50mm. Solid 186 is a higher order element which exhibit the quadratic displacement behaviour. The column of the specimen was hinged at the bottom with lateral cyclic load applied at the top of the column. Similar models were generated for all cases also.

4 Analysis of multisegment steel shear links with varying primary link length and web width

Analysis of multi-segment profiled steel shear links was conducted using Ansys Workbench. AISC protocol cyclic loading is applied to the multi-segment steel shear links by varying primary link length and web width (profiled sections).

4.1 Modelling

Modelling and analysis of study was carried out using ANSYS Workbench Fig 4.3(a) and (b) shows the design dimensions and model of corrugated steel web. The corrugations were provided in a trapezoidal manner [8]. This pattern reduces the chance of web buckling and web tearing due to repeated cyclic loading and it allows the use of

thin plates and can reduce the use of stiffeners. Thus, by reducing the cost of fabrication and improves fatigue life. The width of parallel and inclined folds was 56mm and 10mm. The width of web profile or corrugation ranges from 15mm to 75mm respectively. Initially the thickness of the profiled section is fixed at 10mm as that of the validated model (RB8 Specimen). Series of corrugations were modelled according to this. Fig 4.3(b) indicates the model of the steel shear link, web width of 45mm and web thickness 10mm. The six cases of each with constant primary link length are modelled by correspondingly varying the web width ranging 15mm, 30mm, 45mm, 60mm and 75mm respectively as shown in Table 4.4[4].

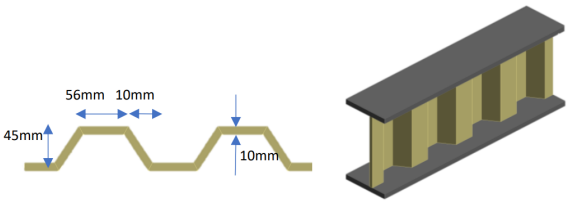

Figure 4. (a) Profile pattern, (b) Model of profiled primary steel shear link

Fig. 5. (a) to (f) shows the secondary link deformation of shear link models with fixed primary link length and varying web width using ANSYS workbench software.

5 Analysis of multi-segment steel shear links with varying primary link web thickness

Analysis of multi-segment profiled steel shear links was conducted using Ansys Workbench software. AISC protocol cyclic loading is applied to the multi-segment steel shear links models, where the primary link length is fixed at 500mm and web width fixed at 30mm. The behavior of shear link model by varying the primary link profiled web thickness is analyzed. The material data is same as that of previous model depicted in the above Table 1.

The elements were modelled using Solid 186 with a mesh size of 50mm. Solid 186 is a higher order element which exhibit the quadratic displacement behaviour. The column of the specimen was hinged at the bottom with lateral cyclic load applied at the top of the column. Similar models were generated for all cases also. Fig. 6. (a) to (f) shows the secondary link deformation of shear link models while varying primary link length and web width using ANSYS workbench software.

6 Results

6.1 Varying primary link length

The shear link model with higher value of shear force and primary link rotation as well as lesser value of secondary link deformation will be the optimal section, as the primary link of the shear link go higher limit of link rotation and lesser damage on the secondary link. Additionally, with the increase of link length ratio, the performance of the long links in terms of the strength, inelastic deformation, and energy dissipation capacity is considerably lower than that of the short links [3]. From the Table 7 the shear linkmodel with 500mm primary link length have higher value of shear force about 862.77kN, minimum secondary link deformation of 3.16 and higher link rotation of 0.12428rad.

For an increase in primary link length shear capacity and link rotation of the shear links reduces [3]. From the FEA of multi-segment steel shear links, upon increasing the link length, the shear capacity and primary link rotation is found to reduce with an increase in secondary link deformation.

6.2 Varying primary link length and web width

As the primary link of the shear link goes higher limit of link rotation with less damage on the secondary link, the shear link model with higher value of shear force, primary link rotation, and secondary link deformation will be an optimal section. Furthermore, as the primary link web width the performance long links in terms of shear strength, link rotation decreases significantly. As per the literature study for increase in link length the shear capacity as well as the link rotation reduces, it is because of, under the cyclic loading which is acting laterally on the shear links, while the link length increases the chance of occurring deflection or buckling is more than the chance of rotation of primary link [3]. The Table 8 indicates the same, with increase in primary link length the rotation capacity as well as the shar capacity reduces.

From the Table 8 the shear link model with 500mm primary link length have higher value of shear force about 738.39kN, secondary link deformation of 2.7mm and higher link rotation of 0.1267rad. Compared to the other models the shear link with 30mm web width had the larger value of link rotation, which means the primary link can rotate without causing any damage to the main structural elements. Compared to the section (15mm width), which had lesser primary link rotation as well as the shear capacity than 30mm model, which implies the model with an higher value of link rotation is the optimum section that can be used under seismic effects on multi-storey building.

Table 5. Cases of varying Primary link and web width

Primary Link Length	Width of Web in primary link					Model Designation
500mm	15mm	30mm	45mm	60mm	75mm	C(15-75)- CSL 500

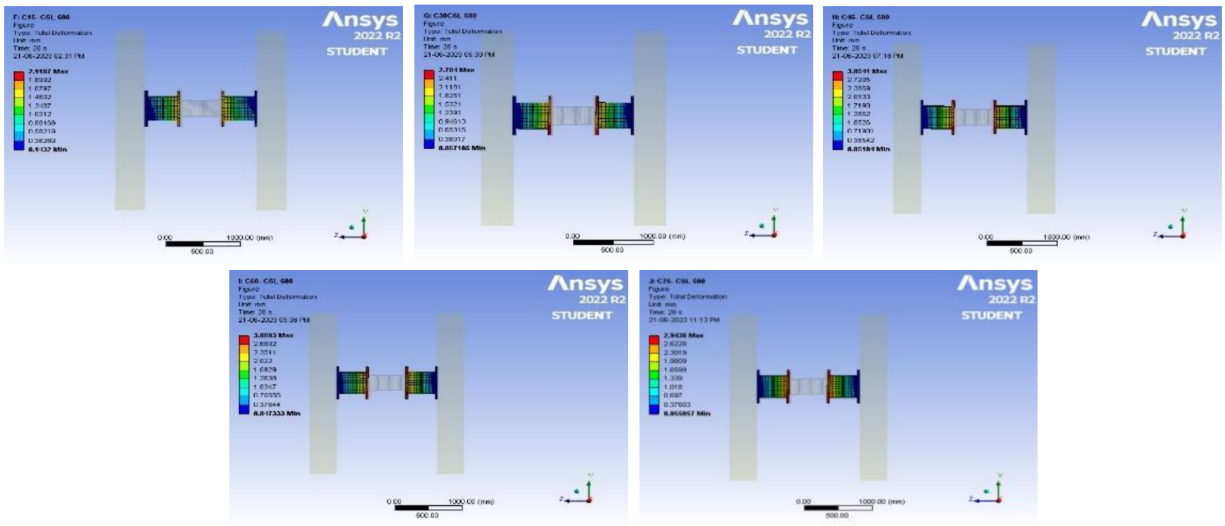

Figure 5. Deformation of secondary link for vary in web width

Table 6. Cases of varying Primary link web thickness

Model Designation	Primary Link Length	Width of Web in primary link	Thickness of Web in primary link
C30-6-CSL500	500 mm	30mm	6mm
C30-7-CSL 500	500 mm	30mm	7mm
C30-8-CSL500	500 mm	30mm	8mm
C30-9-CSL 500	500 mm	30mm	9mm
C30-10-CSL500	500 mm	30mm	10mm
C30-10-CSL500	500 mm	30mm	11mm
C30-10-CSL500	500 mm	30mm	12mm

Table 7. Analysis results for cases of varying Primary link length

Model Designation	Deformation in Secondary link (mm)	Secondary Link rotation(rad)	Primary (rad) Link rotation	Shear Force (kN)
RB8 500	3.16	0.0206	0.12428	862.77
RB8 600	3.1471	0.01727	0.10361	820
RB8 700	2.8148	0.01418	0.08074	789.28
RB8 800	3.1539	0.01262	0.0765	770.55
RB8 900	3.2587	0.01109	0.06788	764.6
RB8 1000	3.6441	0.01005	0.06124	754.03

6.3 Varying primary link length web thickness

Table 9 depicts the analysis results for cases of varying primary link length web thickness by fixing the length at 500mm, width at 30mm and thickness of web at 10mm.

Upon increasing web thickness, the primary link rotation is found to be reducing as well as the shear force increases with an increase in secondary link deformation. From the Table 9 the shear link model with 500mm primary link length have higher value of shear force about 659.52kN, secondary link deformation of 2.3655mm and

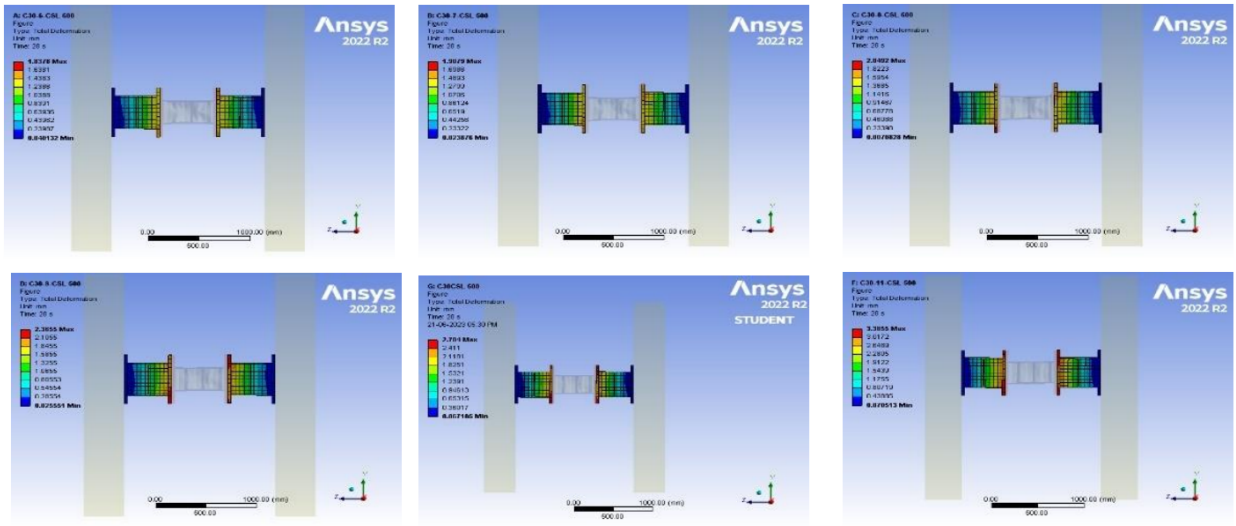

Figure 6. Deformation of secondary link for vary in primary link web thickness

Table 8. Analysis results for cases of varying primary link length and web width

Model Designation	Primary Link Length	Width of Web in primary link	Secondary link deformation	Primary Link rotation (rad)	Shear Force (kN)
C15- CSL 500	500 mm	15mm	2.1	0.125	725.6
C30-CSL-500	500 mm	30mm	2.7	0.1267	738.39
C45-CSL-500	500 mm	45mm	3.05	0.1261	800.35
C60-CSL-500	500 mm	60mm	3	0.1256	819.83
C75-CSL-500	500 mm	75mm	2.94	0.1255	814.44

Table 9. Analysis results for cases of varying primary link length web thickness

Model Designation	Primary Link Length	Width of Web in primary link	Thickness of Web in primary link	Deformation of Secondary link (mm)	Link rotation (rad)	Shear Force (kN)
C30-6-CSL500	500 mm	30mm	6mm	1.8378	0.1306	478.09
C30-7-CSL 500	500 mm	30mm	7mm	1.9079	0.1292	533.81
C30-8-CSL500	500 mm	30mm	8mm	2.0492	0.1279	595.19
C30-9-CSL 500	500 mm	30mm	9mm	2.3655	0.1275	659.52
C30-10-CSL500	500 mm	30mm	10mm	2.704	0.1267	738.39
C30-11-CSL500	500 mm	30mm	11mm	3.3855	0.1263	837.46
C30-12-CSL500	500 mm	30mm	12mm	4.1173	0.1216	932.6

link rotation of 0.1275rad.

6.4 Interpretation of results

Table 10 depicts the comparison of shear force and link rotation obtained from the study of Men J et al., (2022) for replaceable shear link model and optimum section obtained from the current study of profiled steel shear links.

Compared to the model (validation model), which has lesser primary link rotation as well as the shear capacity than the obtained optimum model, which implies the

Table 10. Comparison of Shear force and Link rotation

	Shear Force (kN)	Link rotation (rad)
Literature study	770.5	0.0605
Optimum Section obtained	660	0.1275
Percentage change	-14.2	110.74

model with a higher value of link rotation is the optimum section that has only lesser secondary link deformation

7 Conclusions

The behavior of multi-segment shear links under cyclic loading can be studied effectively using finite element analysis by comparing the primary link rotation and shear force. Upon increasing the link length, the primary link rotation as well as the shear force is found to reduce with an increase in secondary link deformation. Primary link of length 500mm show higher shear force of 862.77kN and higher link rotation of 0.12428rad with a secondary link deformation of 3.16mm. By replacing the primary link web with profiled section (corrugated web) and fixing the primary link length as 500mm and varying web width of primary link, the shear force and link rotation found to reduce with an increase in primary link length. Hence, primary link of length 500mm with 30mm web width have shear force of 738.39kN and link rotation of 0.1267rad with a minimum deformation of secondary link of 2.704mm is obtained as the optimal section. For the profiled steel shear link, where the primary link parameters are fixed, upon increasing web thickness, the primary link rotation reduces as well as the shear force increases with an increase in secondary link deformation. Under cyclic loading primary link of length 500mm with 30mm web width and 9mm web thickness have shear force about 660kN, secondary link deformation of 2.3655mm and higher link rotation of 0.1275rad, which is taken as optimum section. While comparing the profiled steel shear links, with that of a common replaceable steel shear link, the primary link rotation was found to be higher, whereas the shear force and secondary link deformation found to be reducing. In literature study the shear force and secondary link deformation is more because the majority of the cyclic load is resisted by secondary link, causing more damage in secondary link. In optimum model the damage withstands only in primary link, by having only lesser secondary link deformation. Hence, the optimum model for the multi-segment shear link is the section with 500mm link length,30mm width,10 mm thickness and secondary link thickness of 10mm.

References

[1] Eatherton, M. R., Ma, X., Krawinkler, H., Deierlein, G. G., Hajjar, J. F.: Quasistatic cyclic behavior of controlled rocking steel frames. Journal of Structural Engineering, 140 (2014).

[2] Imani, R., Bruneau, M. I. C. H. E. L.: Effect of link-beam stiffener and brace flange alignment on inelastic cyclic behavior of eccentrically braced frames. AISC Eng. Journal, 52(2), 109-124 (2015).

[3] Daneshmand, A., and Hashemi, B. H.: Performance of intermediate and long links in eccentrically braced frames. Journal of Constructional Steel Research, 70, 167-176 (2012).

[4] Ji, X., Wang, Y., Ma, Q., Okazaki, T.: Cyclic behavior of very short steel shear links. Journal of Structural Engineering, 142 (2016).

[5] Ji, X., Wang, Y., Ma, Q., Okazaki, T.: Cyclic behavior of replaceable steel coupling beams. Journal of Structural Engineering, 143 (2017).

[6] Krawinkler, H., Gupta, A., Medina, R. and Luco, N.: Loading Histories for Seismic Performance Testing of SMRF Components and Assemblies. Report No. SAC/BD-00/10, SAC Joint Venture (2000).

[7] Li, W., Li, Q. N., Jiang, W. S and Jiang, L.: Seismic performance of composite reinforced concrete and steel moment frame structures–state-of-the-art. Composites Part B: Engineering, 42(2), 190-206 (2011).

[8] Mansouri, A and Sharif, M. M.: Development of a corrugated web shear link for steel moment-resisting frames. Journal of Constructional Steel Research, 193, 107-281 (2022).

[9] Men, J., Guo, Z. F., and Shi, Q. X.: Experimental research on seismic behavior of novel composite RCS joints. Steel and Composite Structures, 19 (2019).

[10] Men, J., Xiong, L., Wang, J., and Zhang, Q.: Experimental and numerical study on the behavior of novel multi-segment replaceable steel shear links. Journal of Constructional Steel Research, 194 (2022).

[11] Vetr, M. G., Ghamari, A., Bouwkamp, J.: Investigating the nonlinear behavior of Eccentrically Braced Frame with vertical shear links (V-EBF). Journal of Building Engineering, 10, Pages 47-59 (2017).

[12] Wang, F., Su, M., Hong, M., Guo, Y., Li, S.: Cyclic behaviour of Y-shaped eccentrically braced frames fabricated with high-strength steel composite. Journal of Constructional Steel Research, 120, 176-187 (2016).

[13] Yao, Z., Wang, W., Fang, C., Zhang, Z.: An experimental study on eccentrically braced beam-through steel frames with replaceable shear links. Engineering Structures, 206 (2020).

[14] Xu, J., Wang, S. L., Mohamed, H. S., Han, J., Han, Z., Tu, J., Li, Z.: Seismic performance of shear energy dissipation beams in D-shaped eccentrically braced steel frames. Journal of Constructional Steel Research, 180 (2021).

Effect of Dynamic Coupling of Liquid Propellant Sloshing on the Response at Satellite of a Typical Liquid Propellant Rocket

Ganga S[1], Rojan Mathew [2] and Deepthy S Nair [3]

[1] M tech Student, N.S.S College of Engineering, Akathethara, Palakkad, 678008, Kerala, India
[2] Scientist SD/Engg, STR, Vikram Sarabhai Space Center, Thiruvananthapuram, 695022, Kerala, India
[3] Asst. Professor, N.S S College of Engineering, Akathethara, Palakkad, 678008, Kerala, India

Abstract -

A liquid propellant rocket has an engine that employs liquid as propellants. Liquid hydrogen is primarily utilised as a fuel, and liquid oxygen is used as an oxidizer. Slosh can occur with liquid propellants. Slosh works as a tailored damper, lowering the vehicle's dynamic response. Propeller slosh is a potential source of disturbance that is critical to the stability of the spacecraft. A mechanical model of a spring-mass-damper system is often used to represent sloshing dynamics. The MSC NASTRAN / PATRAN software is used to simulate a conventional liquid propellant rocket with and without propellant. Dynamic characterization of liquid propellant rockets with and without propellant is carried out. Transient analysis of launch vehicles with and without propellant is performed, and satellite responses are evaluated. The structural dynamic characterization and reaction of a liquid propellant rocket at satellite locations are investigated in this study. The primary goal of the project is to investigate the influence of coupling between propellant sloshing and vehicle modes.

Keywords -

Coupling; Dynamic characterisation; Liquid propellant rocket; Propellant sloshing; Transient analysis

1 Introduction

A rocket is powered by high-speed exhaust. A rocket is powered by fuel so that it can fly in the vacuum of space. The force that propels any aircraft through the air is called thrust. The aircraft's propulsion system produces thrust.[1] Every thrust is produced through the application of Newton's third law of motion in some way, different propulsion systems produce thrust in various ways. In any propulsion system, the system accelerates the working fluid, and the working fluid's reaction to this acceleration exerts a force on the system. Fuel and an oxygen source, known as an oxidizer, are combined and ignited in a combustion chamber to create a rocket engine. Hot exhaust from the combustion is sent through a nozzle to speed up the flow and create thrust. The hot exhaust created upon combustion serves as the rocket's accelerated gas or operating fluid. Liquid rockets and solid rockets are the two major types of rocket engines.[3] In a liquid rocket, the fuel and the oxidizer, the two propellants, are stored separately as liquids and poured into the nozzle's combustion chamber, where burning takes place. The propellants are combined and crammed into a solid cylinder for a solid rocket. A liquid rocket's propulsion can be stopped by stopping the propellant flow, whereas a solid rocket's engine must be destroyed to be stopped. Due to the pumps and storage tanks, liquid rockets typically weigh more and require more intricate design. Just before launch, the rocket is loaded with propellants. Liquid-propellant systems store the propellant in tanks outside the combustion chamber. The majority of these engines use liquid fuel and liquid oxidizer, which are transferred from their respective tanks through pumps. Propellers are then pumped into the engine in a way that ensures atomization and quick mixing after the pumps raise the pressure above the engine's operating pressure. [3] A liquid rocket propulsion system typically consists of an engine, fuel tanks, and a vehicle frame to hold everything in place while connecting to the payload and launch pad (or vehicle). Considering that they function at low pressure, the fuel and oxidizer tanks are often made of very lightweight materials.[1] The spaceship's liquid fuel vibrates, resulting in powerful coupled vibrations that have a complex effect on the main body's dynamic behaviour. This is a significant challenge for high-attitude precision astronomical imaging satellites. Prior to deployment, it is necessary to specify the dynamic interaction behaviour of a flexible space structure with onboard liquid to improve the stability and dependability of space structures. The liquid having free surface so that there will be a slosh dynamics problem, where there is a coupling of liquid i.e. liquid can interact with the container and drastically change the dynamics of the system. Engineers in the fields of nuclear, civil, and aerospace still have a lot of concerns about the issue of liquid sloshing in moving or stationary containers.[5] The slosh of propellant in the tanks and rockets of spacecraft are two significant examples. Spacecraft attitude destabilization may occur as a result of liquid sloshing in the tanks holding the propellants because it causes rapid energy loss during resonant modes. The liquid's free surface begins to slosh or oscil-

lation when a container is put in motion.[14] The dynamic or modal coupling phenomena is of tremendous relevance in the design of space structures. The standard method in the space business is to avoid dynamic coupling between the launcher and the satellites it transports, or between a satellite and its equipment. The main goal is to avoid the negative effects that occur when the frequency range of the dynamic loads generated during the launch phase and other events such as landing, testing, or ground operations coincide with the main natural frequencies of the structures, causing structural resonance and the generation of undesirable structural damages. The launcher authority establishes minimal limit values for both the lateral and longitudinal natural frequencies of the satellite to avoid structural resonance at low frequency vibrations induced by the launch vehicle.[15] Here we are concerned with the effect of dynamic coupling of liquid propellant sloshing on the response at satellite location of a typical liquid propellant rocket. MSC PATRAN and MSC NASTRAN is used for modelling and analysis of the propellent sloshing and typical rocket with liquid propellant. The main objective of the project is to study the effect of coupling between the propellant sloshing and the vehicle modes.

2 Literature Review

1. M Chin et.al In this paper, the influence of liquid sloshing on the pitching dynamics of flexible space structures with liquid on board is studied. In the analysis, the main body of spacecraft is considered as rigid tank and on board liquid as ideal liquid. It was found that during the operation of satellite, decrease in fuel would introduce strong coupling of two motions, that is liquid sloshing and system vibration.[5]

2. A. Prashanthan et.al studied the response of launch vehicle with liquid propellant slosh as a dynamic vibration absorber underground wind response. The response of the liquid vehicle depends on the slosh characteristics of the propellant tanks of the vehicle and also on the vehicle flexibility and type of disturbance. In case of PSLV it is found that the slosh frequencies are very close to first cantilever bending frequency. The response studies showed that slosh has acted as a tuned damper and helped in reducing the dynamic response of the vehicle.[14]

3. Zhong Wen et.al studied the coupling effects of a launch vehicle's lateral mode, longitudinal mode, and torsional mode cannot be taken into account in standard dynamic analysis utilizing the lateral beam model and longitudinal spring-mass model separately. To address the issue, propellant analogy methods based on the beam model are proposed, and a coupled mass-matrix of liquid propellant is built using additional mass in this work. Then, an integrated model of the launch vehicle for free vibration analysis is constructed, allowing study on the interactions between the launch vehicle's longitudinal and lateral modes, as well as its longitudinal and torsional modes, to be carried out in this work.[17]

4. Shageer. H et.al presented an overview of the pendulum analogy model of a spaceship with fuel slosh dynamics and investigate adaptive control for such a model in this research. Nonlinear dynamics of the selected models are also studied.[20]

5. Xu. J et.al studied on long booster clustered launch vehicle, taking core and boosters into account. Then, due to the high proportion of liquid propellant in the total mass of the launch vehicle, a dynamic equation incorporating elastic deformation and liquid sloshing is created on the basis of the multi-beam model. Simulation is used to investigate the dynamic properties of the launch vehicle as well as the interplay between liquid sloshing and aeroelasticity. The results shows that the multi-beam model can more accurately represent the dynamic features of the long booster clustered launch vehicle, and that the connection form between the core and the boosters also has an impact on liquid sloshing and elastic deformation.[24]

3 Objectives

Main objectives of the project are:
1. To develop the finite element model of a typical rocket with liquid propellant.
2. To develop the finite element model of propellent sloshing.
3. To obtain the structural dynamic characterization of the liquid propellant rocket with and without propellant.
4. To obtain the response at satellite location of a liquid propellant rocket.
5. To study the effect of coupling between the propellant sloshing and the vehicle modes.

4 Methodology

• Literature Review: Various periodicals and research articles pertaining to the subject are collected, and a literature survey is undertaken.
• Software familiarization: PATRAN software is utilized for modelling launch vehicle and propellant slosh. NASTRAN software is also used for dynamic analysis of the launch vehicle.
• Validation: A comparison of the mode shapes and frequencies of cylindrical beams and shells of varying

diameters, heights, and mesh sizes was performed while keeping the aspect ratio constant. PATRAN software was used to model the launch vehicle with and without propellant.
• Dynamic Characterization of a Propellant Rocket: A modal analysis of a typical Propellant Rocket with propellant was performed.
• Estimation of Responses at Satellite Location: Responses at the launch vehicle's satellite location were estimated using transient analysis.
• Interpretation of Results: The effect of interaction between the propellant sloshing and the vehicle modes was investigated.

5 Finite Element Modelling

5.1 Typical Launch Vehicle Modelling

Launch vehicles are used to transport spacecraft into orbit. The launch vehicle has numerous stages, each with its own propulsion system. A PLA, propulsion for end tank, fuel tank, inter tank, oxidizer tank, shroud, and fin are typical components of a liquid propellant rocket. MSC PATRAN is used to create the structure's finite element model. The structure is represented by shell elements. Shell elements are iso parametric quadrilaterals with 4 to 8 nodes or triangular elements with 3 to 6 nodes. All pieces have a mesh size of 0.05m. Steel was employed, which has a Young's modulus of 2x1011 N/m2 and a density of 7280 kg/m3.

•Modelling details of parts

1. PLA

A PLA with a length of 1 metre, a thickness of 0.1 metre, a diameter of 0.5 metre at one end, and a diameter of 1 metre at the other end is modelled.

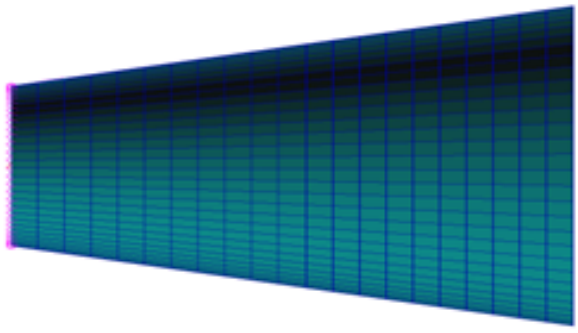

Figure 1. FE model of PLA

2. Propulsion for end structure

The propulsion for an end structure of 1 metre length, 0.05 metre thickness, and 2 metre diameter is modelled.

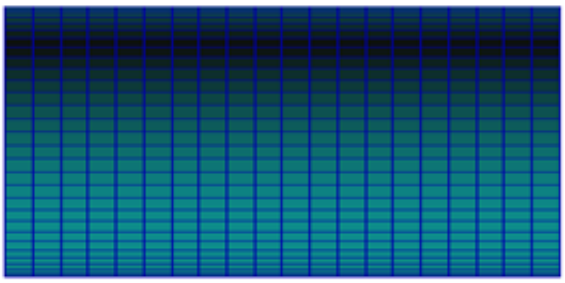

Figure 2. FE model of Propulsion for end tank

3. Fuel tank and Oxidizer tank

Fuel tank and oxidizer tank of thickness 0.05 meter, 10 meter length excluding dome and l meter diameter were modelled. At each 1meter distance a RB3 coupling is provided.

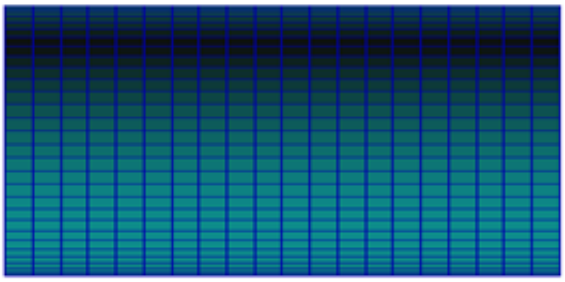

Figure 3. FE model of Fuel tank and Oxidizer tank

4. Inter tank

The inter tank has a thickness of 0.05 metre, a length of 2 metres, and a diameter of l metre. A RB3 connector is provided at 1 metre distance. 5. Shroud

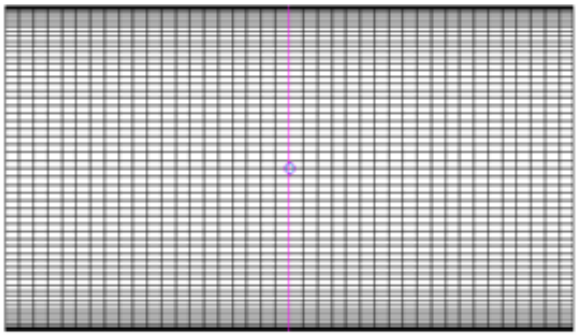

Figure 4. FE model of Fuel tank and Oxidizer tank

A shroud with a thickness of 0.1 metre, a length of 5 metres, and a diameter of l metre is modelled. A RB3

connection is provided at each 1 metre distance, and a 2 metre long fin is modelled in four directions.

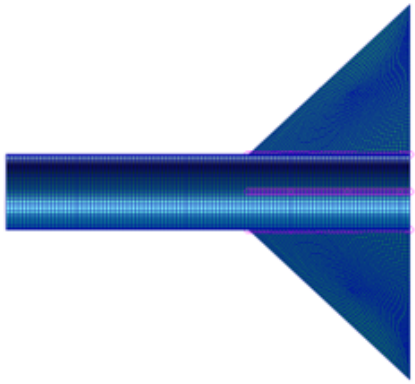

Figure 5. FE model of Shroud

6. Fin

The fins at the bottom of a rocket give stability. A 2 metre long fin is modelled in four directions around the bottom half of the shroud.

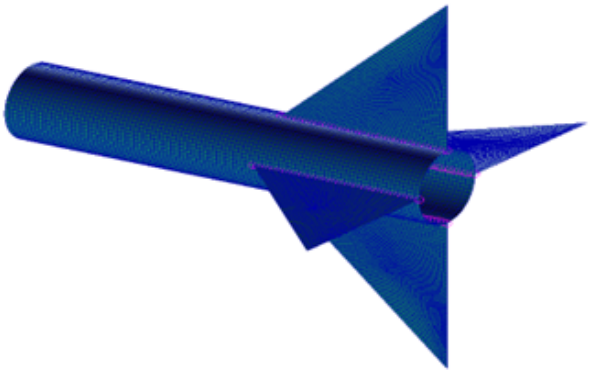

Figure 6. FE model of Shroud with Fin

7. Propellant Modelling

The propellant is represented as an analogous spring mass model in the lateral direction at the relevant point. This propellant model is attached to the two center nodes where RB3 connection is provided, at the bottom of the fuel tank and oxidizer tank.

8. Satellite modelling

RB2 coupling is given at the top of the launch vehicle, i.e. at the top of the PLA. A satellite mass of 1000 kg is attached to a spring. And this spring mass system is linked to the center node, which has an RB2 connection at the top of PLA.

9. Engine Modelling

A 300kg engine is coupled to the center node, where an RB3 coupling is provided at a distance of 2 meters from the top of the shroud section.

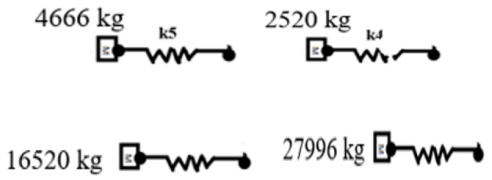

Figure 7. Propellant model

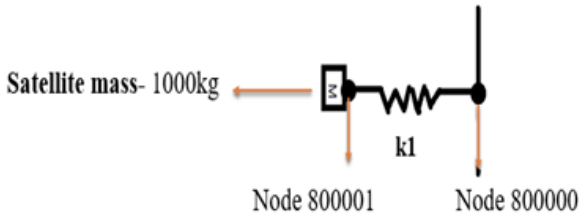

Figure 8. Satellite model

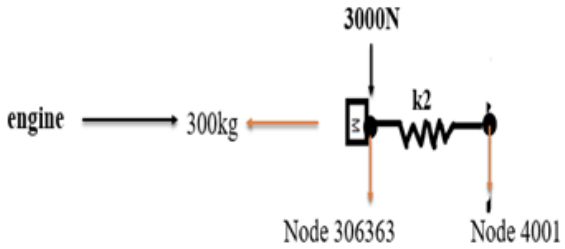

Figure 9. Engine model

• Finite element model of typical launch vehicle

A typical launch vehicle of 27.5 metres in length and 1 metre in diameter is modelled with and without propellant. The RB2 coupling connects the payload to the interstage, the interstage to the fuel tank, the fuel tank to the inter tank, the inter tank to the oxidizer tank, and the oxidizer tank to the shroud. RB3 connector is given every 1 metre along the length of the fuel tank, inter tank, oxidizer tank, and shroud. A RB2 connection is supplied at the top of the launch vehicle, i.e. at the top of the payload, and a 1000 kg satellite in the form of a spring mass system is attached to the centre node where an RB2 coupling is provided at the top of the payload. A 300kg engine simulated as a mass spring system is coupled to the centre node, where an RB3 connection is given at a distance of 2 metres from the top of the shroud section. An engine in the form of a spring mass system is attached to node 400l. A force of 3000 N is applied in the y direction, that is, vertically downwards, to the node 306363, to which a mass of 300kg is linked. A spring mass system is given at node 800000 (i.e. center node at PLA portion). A satellite mass of 1000kg is linked

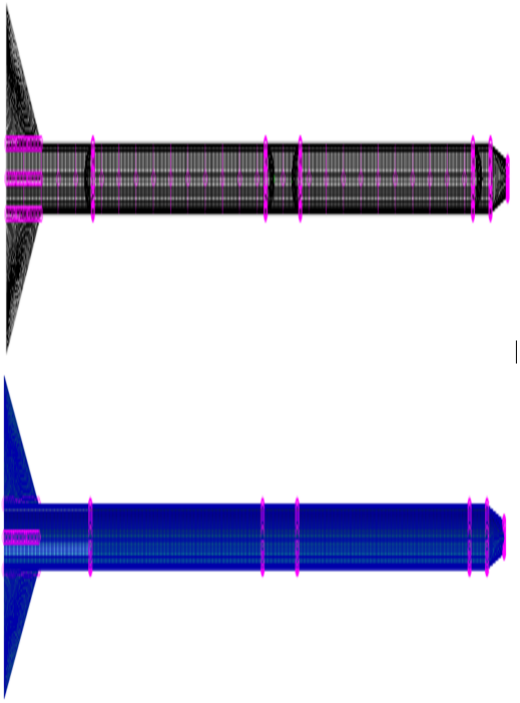

Figure 10. FE model of a typical liquid propellant rocket

to this spring mechanism. k1 is the spring stiffness where the satellite is mounted. k2 is the spring stiffness where the engine is mounted. At the bottom of the fuel tank and oxidizer tank, propellant models are coupled to the two centre nodes with RB3 coupling. In a liquid propellant rocket with propellant, k4 represents the stiffness of the lower mass of propellant in the fuel tank, and k5 represents the stiffness of the lower mass of propellant in the oxidizer tank. Liquid propellant rocket with propellant model is shown in Figure 11

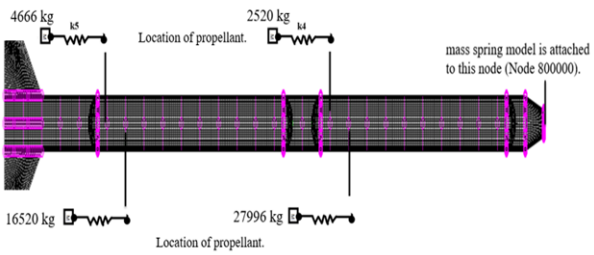

Figure 11. FE model of Launch Vehicle with propellant

Table 1. Dynamic characterization of liquid propellant rocket without propellant

Mode no.	Radians (Rad/sec)	Cycles (Hz)	Modes
1	0.00068	0.000108	Rigid body modes
2	0.000315	5.02E-05	Rigid body modes
3	0.000154	2.45E-05	Rigid body modes
4	0.000282	4.5E-05	Rigid body modes
5	0.000378	6.02E-05	Rigid body modes
6	0.000498	7.93E-05	Rigid body modes
7	36.03361	5.754927	1st bending mode
8	36.03368	5.754938	1st bending mode
9	107.1608	17.05517	torsion mode
10	107.1688	17.05644	torsion mode
11	119.6931	19.04975	torsion mode
12	127.9899	20.37022	2nd bending mode
13	128.014	20.37405	2nd bending mode
14	131.1138	20.8674	shell mode
15	217.6807	34.64496	3rd bending mode
16	217.6837	34.64543	3rd bending mode
17	283.1047	45.05751	torsion mode
18	360.4692	57.37045	4th bending mode
19	360.472	57.37091	4th bending mode
20	423.831	67.4548	1st axial mode

6 Dynamic Analysis

6.1 Dynamic Characteristics of liquid propellant rocket with and without launch vehicle

The first bending mode for a liquid propellant rocket without propellant was discovered to be 5.75 Hz and 5.35 Hz for a liquid propellant rocket with propellant. The second bending mode for a liquid propellant rocket without propellant was discovered to be 20.37 Hz and 20.03 Hz for a liquid propellant rocket with propellant. The first axial mode for a liquid propellant rocket without propellant is found to be 67.45 Hz and 46.42 Hz for a liquid propellant rocket with propellant. Table 3 shows the dynamic characteristics of slosh model, it can seen that the slosh modes are near to the first and second bending modes of liquid propellant rocket with and without propellant. Effect of propellant sloshing on satellite location of launch vehicle is done by finding responses corresponding to the first bending modes.

6.2 Transient Analysis

An engine is connected to node 400l. A force of 3000 N is applied in the y direction, that is, vertically downwards, to the node 306363, to which a mass of 300kg is linked. A spring mass system is given at node 800000 (i.e. node at PLA portion). A satellite mass of 1000kg is linked to

Table 2. Dynamic characterization of liquid propellant rocket with propellant

Mode no.	Radians (Rad/sec)	Cycles (Hz)	Modes
1	0.000575	9.15E-05	Rigid body mode
2	0.000229	3.65E-05	Rigid body mode
3	0.00014	2.24E-05	Rigid body mode
4	0.000313	4.99E-05	Rigid body mode
5	0.000434	6.91E-05	Rigid body mode
6	0.000456	7.26E-05	Rigid body mode
7	33.64024	5.35401	1st bending mode
8	33.64032	5.354024	1st bending mode
9	86.7081	13.80002	fin mode
10	86.70996	13.80032	Fin mode
11	119.6931	19.04975	fin mode
12	125.8662	20.03223	2nd bending mode
13	125.8965	20.03704	2nd bending mode
14	131.1137	20.8674	fin mode
15	168.271	26.78116	3rd bending mode
16	168.2719	26.7813	3rd bending mode
17	283.1047	45.05751	torsion mode
18	291.666	46.42009	1st axial mode
19	300.5196	47.82918	4th bending mode
20	300.5214	47.82947	4th bending mode

Table 3. Dynamic characterization of slosh model

Mode No.	Radians (Rad/sec)	Cycles (Hz)
1	6.642973E-04	1.057262E-04
2	2.776092E-04	4.418287E-05
3	2.040673E-04	3.247832E-05
4	9.487526E-05	1.509987E-05
5	2.695650E-04	4.290260E-05
6	3.375440E-04	5.372180E-05
7	3.051583E+01	4.856745E+00
8	3.199138E+01	5.091587E+00
9	3.311882E+01	5.271024E+00
10	3.364028E+01	5.354016E+00
11	3.635964E+01	5.786817E+00
12	8.670903E+01	1.380017E+01
13	9.143440E+01	1.455224E+01
14	1.196931E+02	1.904975E+01
15	1.242586E+02	1.977637E+01
16	1.258814E+02	2.003465E+01
17	1.286079E+02	2.046858E+01
18	1.311137E+02	2.086740E+01
19	1.682714E+02	2.678123E+01
20	1.843193E+02	2.933533E+01

this spring mechanism. When thrust is given to the motor (at node 306363), the reaction at nodes 800001 (where the satellite mass is attached) and 306363 (where the motor is attached) is recorded. The first bending mode of the launch vehicle with and without propellant was discovered to be at 5.35 Hz and 5.75 Hz, respectively. The spring is first strengthened. The stiffness is then changed. k1 is the stiffness of the spring to which the satellite is mounted, k2 is the stiffness of the spring to which the engine is attached, and k3 is the excitation force applied between 0.01 and 35 seconds. In a liquid propellant rocket with propellant, k4 represents the stiffness of the lower mass of propellant in the fuel tank, and k5 represents the stiffness of the lower mass of propellant in the oxidizer tank. Transient analysis is done by varying the stiffness of two propellants.

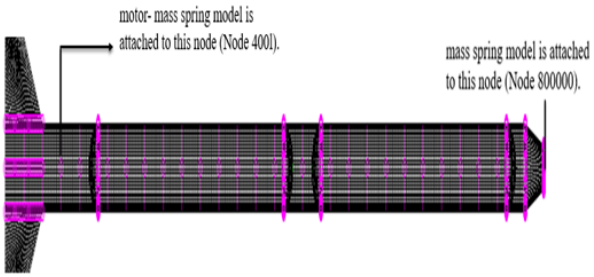

Figure 12. Node where response has to be estimated

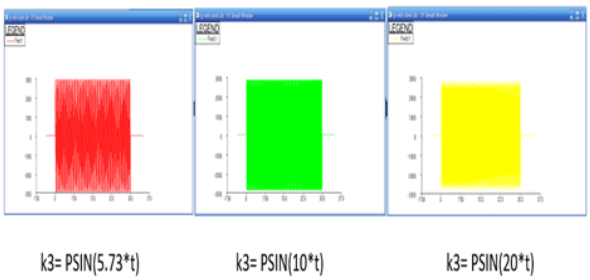

Figure 13. Excitation force applied at engine gimbal point

7 Results and Discussions

7.1 7.1.1 Responses at satellite of a liquid propellant rocket with propellant sloshing

• Case 1: k4 varying, k5 rigid, k1=5.13Hz, k2=20 Hz and k4 rigid, k5 varying, k1=5.13Hz, k2=20 Hz
• Excitation force applied at engine gimbal point- k3= PSin(5.75, 20, 10*t)

• Response:

Graph showing acceleration response at satellite and force applied nodes obtained from analysis of launch vehicle with propellant sloshing -:

1. k4 varying, k5 rigid, k1=5.13Hz, k2=20 Hz

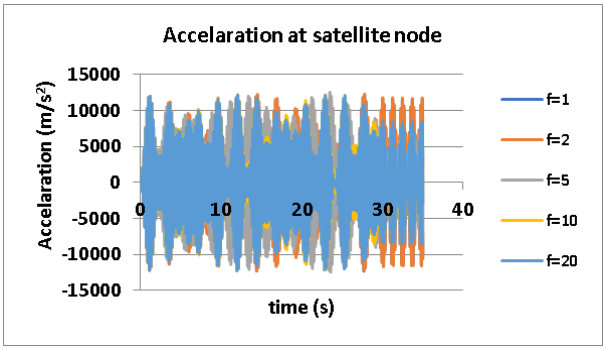

Figure 14. k3=5 Hz

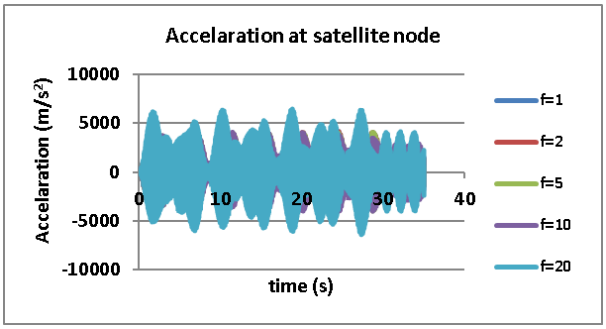

Figure 15. k3=20Hz

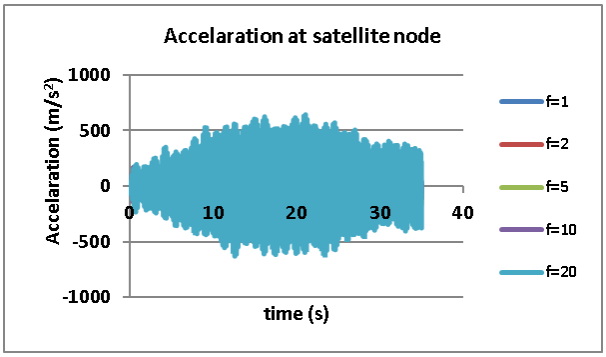

Figure 16. k1=30 Hz

*k1 is the stiffness of spring where satellite is attached
*k2 is the stiffness of spring where engine is attached
*k3 is the stiffness of excitation force applied

Table 4. Table showing peak value of acceleration response at node where satellite is connected

K3(Hz)	K5	K4 (Hz)	Peak acceleration value(m/s^2)
5	Rigid	1	12233.2
	Rigid	2	12265.18
	Rigid	5	12546.38
	Rigid	10	12148
	Rigid	20	12180.23
K3(Hz)	**K5**	**K4 (Hz)**	**Peak acceleration value(m/s^2)**
20	Rigid	1	4142.067
	Rigid	2	4139.862
	Rigid	5	4029.208
	Rigid	10	4084.011
	Rigid	20	6404.352
K3(Hz)	**K5**	**K4 (Hz)**	**Peak acceleration value(m/s^2)**
30	Rigid	1	178.5426
	Rigid	2	177.780
	Rigid	5	172.1924
	Rigid	10	200.6943
	Rigid	20	642.5085

Table 5. Peak value of acceleration response (k3) at node where satellite is connected

K3(Hz)	K5	K4 (Hz)	Peak value(m/s^2)
5	Rigid	5	12546.38
20	Rigid	20	6404.352
30	Rigid	20	642.5085

*k4 is the stiffness of lower mass of propellant in fuel tank
*k5 is the stiffness of lower mass of propellant in the oxidizer tank

Discussions

• k4 is varying and k5 is rigid, k1=5.13Hz, k2=20 Hz

When sloshing occurs i.e. in case 4 , when k4 is varying and k5 is rigid, k1=5.13Hz, k2=20 Hz, when excitation force applied k3=5.35Hz, stiffness of lower mass of propellant in fuel tank k4=5Hz shows greater response, when k3=20Hz, stiffness of lower mass of propellant in fuel tank k4= 20Hz shows greater response, when k3= 30Hz, stiffness of lower mass of propellant in fuel tank k4=20Hz shows greater response at node where satellite is attached is shown in Figure 15. It is seen that when excitation force k3= 5Hz applied , stiffness of lower mass of propellant in fuel tank k4=5Hz is having greater responses at node where satellite is connected and when excitation force k3= 20 Hz applied. It is seen from Figure 15 that vibration has reduced thus response has reduced. Thus indicating that slosh acts as a good vibration absorber and a good damper.

· **k4 rigid, k5 varying, k1=5.13Hz, k2=20 Hz**

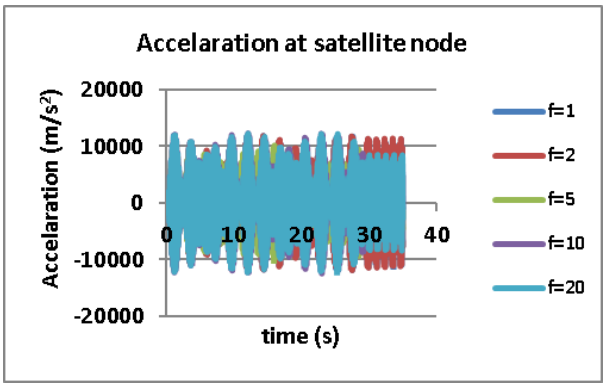

Figure 17. k3=5 Hz

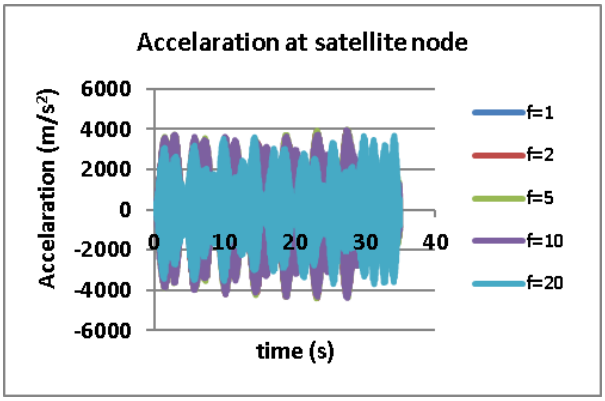

Figure 18. k3=20Hz

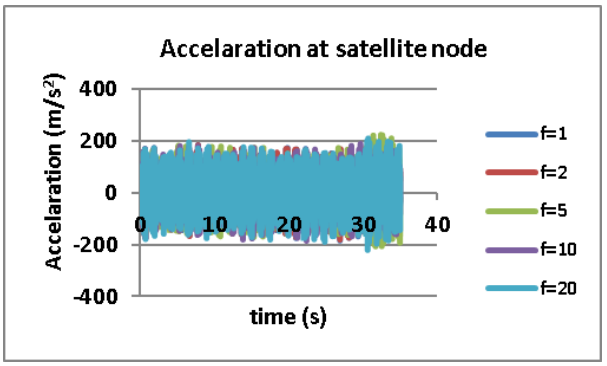

Figure 19. k1=30 Hz

*k1 is the stiffness of spring where satellite is attached *k2 is the stiffness of spring where engine is attached *k3 is the stiffness of excitation force applied *k4 is the stiffness of lower mass of propellant in fuel tank *k5 is the stiffness of lower mass of propellant in the oxidizer tank

Discussions:

· **k4 rigid, k5 varying, k1=5.13Hz, k2=20 Hz**

When k4 is rigid and k5 is varying, k1=5.13Hz, k2=20 Hz, when excitation force k3=5.35Hz, stiffness of lower mass of propellant in the oxidizer tank k5=10Hz shows

Table 6. Table showing peak value of acceleration response at node where satellite is connected

K3(Hz)	K4	K5 (Hz)	Peak Accelaration Value(m/s^2)
5	Rigid	1	11856.39
	Rigid	2	11804.81
	Rigid	5	10125.75
	Rigid	10	12293.36
	Rigid	20	12255.99
K3(Hz)	**K4**	**K5 (Hz)**	**Peak Accelaration Value(m/s^2)**
20	Rigid	1	3852.8
	Rigid	2	3850.056
	Rigid	5	3925.645
	Rigid	10	3913.888
	Rigid	20	3648.585
K3(Hz)	**K4**	**K5 (Hz)**	**Peak Accelaration Value(m/s^2)**
30	Rigid	1	183.0313
	Rigid	2	181.7233
	Rigid	5	222.6939
	Rigid	10	188.174
	Rigid	20	208.445

Table 7. Peak value of acceleration response (k3) at node where satellite is connected

K3(Hz)	K4	K5 (Hz)	Peak value(m/s^2)
5	Rigid	10	12293.36
20	Rigid	5	3925.645
30	Rigid	5	222.6939

greater response, when k3=20Hz, stiffness of lower mass of propellant in the oxidizer tank k5=5Hz shows greater response, when k3= 30Hz, stiffness of lower mass of propellant in the oxidizer tank k5=5Hz shows greater response at node where satellite is attached is shown in Figure 16. It is seen that when excitation force k3= 5Hz applied, stiffness of lower mass of propellant in oxidizer tank k5=10Hz is having greater responses at node where satellite is connected and when excitation force k3= 20 Hz applied. It is seen from Figure 16 that vibration has reduced thus response has reduced. Thus indicating that slosh acts as a good vibration absorber and a good damper.

From this result, it is clear that based on the location of propellant, slosh frequencies, sloshing will cause changes in responses at specified locations i.e. at nodes where satellite is attached. And it is seen that as sloshing occurs vibration has reduced.

8 Conclusion

Launch vehicle are used to carry spacecraft to space. Launch vehicle contains multiple stage, each of which contains a propulsion system. A typical launch vehicle with and without propellant was modelled and dynamic analysis was carried out. Dynamic analysis includes structural characterisation and transient analysis of launch vehicle with propellant. From the modal analysis done, first bending mode was found to be at 5.75Hz for launch vehicle without propellant and 5.35Hz for launch vehicle with propellant. With respect to these frequencies transient analysis i.e. effect of propellent and propellant sloshing on the structure were carried out. This case is done by applying propellant sloshing. It is seen that when excitation force k3=5Hz applied , stiffness of lower mass of propellant in fuel tank, k4=5Hz and stiffness of lower mass of propellant in oxidizer tank, k5=10Hz is having greater responses at node where satellite is connected. Therefore, is clear that based on the location of propellant, slosh frequencies, sloshing will cause changes in responses at satellite location. From the analysis results, it can be concluded that based on structural frequencies, location of force applied, location of propellant model connected, changes in responses at certain locations of launch vehicle and the effect of coupling between the propellant sloshing and the vehicle modes is studied.

References

[1] Launchers, https://www.isro.gov.in/Launchers.html

[2] Nasa(.gov), https://software.nasa.gov/software/LAR-16804-GS

[3] Nasa(.gov), https://www.grc.nasa.gov/www/k-12/airplane/lrockth.html

[4] Adler. J.M, Lee. M.S and Saugen. J.D, “Adaptive control of propellant slosh for launch vehicles,” In Sensors and sensor integration, vol. 1480, pp. 11-22, 1991.

[5] Chiba. M. and Magata. H, “Coupled pitching dynamics of flexible space structures with on-board liquid sloshing,” Acta Astronautica., vol. 181, pp. 151-166, 2021.

[6] Cho. S, McClamroch. M and Reyhanoglu. M, “Feedback control of a space vehicle with unactuated fuel slosh dynamics,” In AIAA guidance, navigation, and control conference and exhibit, 2000.

[7] Constantin. L, De Courcy. J, Titurus. B, Rendall. T.C. and Cooper. J.E, “ Nonlinear damping effects in vertically vibrating systems with violently sloshing liquid,” Journal of Sound and Vibration, vol. 544, p. 117405, 2023.

[8] Craig Jr. R.R and Kurdila. A.J, “ Fundamentals of structural dynamics. John Wiley & Sons” , 2006.

[9] Cui. D.L, Yan S.Z, Guo. X.S. and Gao. R.X, “Parametric resonance of liquid sloshing in partially filled spacecraft tanks during the powered-flight phase of rocket,” Aerospace Science and Technology, vol. 35, pp. 93-105, 2014.

[10] Gasbarri. P, Sabatini. M and Pisculli. A, “ Dynamic modelling and stability parametric analysis of a flexible spacecraft with fuel slosh,” Acta Astronautica, vol. 127, pp. 141-159, 2016.

[11] Ibrahim. R.A, Pilipchuk. V.N and Ikeda. T, “ Recent advances in liquid sloshing dynamics,” pp. 113-119, 2001.

[12] Khoshnood. A.M, Aminzadeh. A, Hasani. M and Nikpey. P, “Dynamic Modeling and Controller Design for a Space Vehicle with Fuel Sloshing,” Journal of Solid and Fluid Mechanics, vol. 11, pp. 25-40, 2021.

[13] Kim. D.H and Choi. J.W, “ Attitude controller design for a launch vehicle with fuel-slosh,” In SICE 2000. Proceedings of the 39th SICE Annual Conference, International Session Papers (IEEE Cat. No. 00TH8545), pp. 235-240, 2000.

[14] K.S. Rao, Prashanthan, “Ground wind response of launch vehicles with liquid propellant – Slosh as a dynamic vibration absorber”, Proceedings of 48th AGM, 1997.

[15] Manguan. M.C, Garcia-Perez. A, Sanz-Andres. A and Alonso. G, "Dynamic coupling on the design of space structures," Aerospace Science and Technology., vol. 84, pp. 1035-1048, 2019.

[16] Noorian. M.A, Haddadpour. H. and Ebrahimian. M, " Stability analysis of elastic launch vehicles with fuel sloshing in planar flight using a BEM-FEM model," Aerospace Science and Technology, vol. 53, pp. 74-84, 2016.

[17] Pan. Z, Xing. Y, Zhu. L, Dong. K and Sun. M, " Liquid propellant analogy technique in dynamic modeling of launch vehicle," Science China Technological Sciences, vol. 53, pp. 2102-2110, 2010.

[18] Reyhanoglu. M, " Maneuvering control problems for a spacecraft with unactuated fuel slosh dynamics," In Proceedings of 2003 IEEE Conference on Control Applications, vol. 1, pp. 695-699. 2003.

[19] Reyhanoglu. M, " Modeling and control of space vehicles with fuel slosh dynamics," 2011.

[20] Shageer. H and Tao. G, " August. Modeling and adaptive control of spacecraft with fuel slosh: overview and case studies," In AIAA guidance, navigation and control conference and exhibit, 2007.

[21] Sierikova. E, Strelnikova E, Kriutchenko. D and Karaiev. A, " Coupled boundary and finite element method for stability analysis of launch vehicle," Doctoral dissertation, IKSAD Publications-2023.

[22] Sudermann. E.J, Gangadharan. N.S, Marsell. B,"CFD fuel motorling of fluid structure interaction in spacecraft propellant tanks with diaphragms,"ntrs.nasa.gov/api/citations.

[23] Sutton. G.P, " History of liquid propellant rocket engines," AIAA, 2006.

[24] Xu. J, Yang. Y, Fu. B and Zhang. D, " Modeling and analysis of long booster clustered launch-vehicle," Scientific Reports, vol. 10(1), p.1611, 2020.

[25] Zhang. D, Qi. H, Xu. J, Yang. Y and Fu. B, " Modeling and analysis of aeroelasticity and sloshing for liquid rocket," IEEE Access, vol. 7, pp. 4453-4465,2018.

[26] Zhang. H and Wang. Z, " Attitude control and sloshing suppression for liquid-filled spacecraft in the presence of sinusoidal disturbance," Journal of Sound and Vibration, vol. 383, pp. 64-75, 2016.

Experimental Investigation On Sugarcane Bagasse Ash Based Geopolymer Bricks

Aiswarya Anil[1], Anchala Monichan B[1], Sony T Saji[1], Divya S Nair[2] and Dr. Meena T[3]

[1] College of Engineering Kidangoor,Kottayam,686583,India
[2] Assistant Professor College of Engineering Kidangoor,Kottayam,686583,India
[3] Associate Professor, VIT, Velloor,632014, India

Abstract -

Carbon dioxide (CO2) emissions from the manufacture of cement and the fire of clay bricks both have a significant impact on global warming. On the other hand, brick manufacturing is unavoidable due to the high demand for bricks in the housing industry. The Geopolymer brick is the latest innovation in the brick industry. As Portland cement consumption rises, CO2 emissions into the atmosphere also increases there by increases the rate of global warming. One tonne of cement production results in the release of 900 kg of CO2 into the atmosphere. In 1979 it was discovered that the Fly ash and other by-product materials having cementitious property(commonly called as source material) when react with an alkaline liquid(activator solution) to produce binders. The source material selected should be rich in silica and alumina content. Material commonly used as source material are fly ash, silica fume, red mud, sugarcane bagasse ash etc. Activator solution used are combination of sodium silicate and sodium hydroxide or potassium silicate and potassium hydroxide. Most commonly used one is sodium hydroxide and sodium silicates, because they are reasonably priced and abundantly available. When aluminosilicate materials are activated by alkalis, inorganic polycondensation results in the creation of geopolymers. Chemical reactions are necessary to transform materials containing aluminate and silicate, such as fly ash or slag from the manufacturing of iron and metal, into geopolymer brick. It can function as a workable substitute for ordinary Portland cement (OPC). Due to their low energy requirement and substantial waste incorporation, geopolymer bricks appear to be advantageous. Research has been concentrated on using agricultural and industrial waste products in the sector for economic, environmental, and technological reasons. The purpose of this research is to create affordable, environmentally friendly bricks in order to preserve environmental harmony and prevent the ash disposal issue. In this paper sugarcane bagasse ash based geopolymer bricks are studied. In addition, this research investigates the possible advantages of adding locally available agro-industrial waste such sugarcane bagasse ash to geopolymer brick and the impact of NaOH molarities and curing techniques on the compressive strength of geopolymer brick.

Keywords -
Geopolymer; Sugarcane bagasse ash

1 Introduction

Sugarcane bagasse ash (SBA) has recently become the subject of research. Scientists have begun investigating the sugarcane bagasse ash's (SBA) potential for sustainable use. Bagasse ash (BA) has a wide range of applications, including the synthesis of phillipsite zeolite, sodium water glass (SWG), geopolymer, raw materials for ceramics, mesoporous silica as a catalyst, etc. SiO2 is the primary component of bagasse ash (BA), which has attracted numerous academics interested in its possible use in the cement sector. The amorphous silica in bagasse ash combines with calcium hydroxide, which further improve the binding characteristics. Sugarcane bagasse ash (SBA) is a type of agricultural waste that, after being calcined, is well known for being a pozzolanic substance. However, this research makes use of its potential to be exploited as a geopolymerisation precursor. The fly ash-based geopolymer is incredibly eco-friendly. There may be a decrease in greenhouse gas emissions as a result of the manufacture of geopolymers. Most of the components of geopolymer (Al) are natural materials, such as silica (Si) and alumina. In addition to being high in silica, sugarcane bagasse ash also has a sizable amount of alumina. Between 60°C and 90° C, the polymerization process moves swiftly. Additionally, silica and alumina are necessary for the polymerization bond. Alkali activator solvents like NaOH and Sodium Silicate, with a NaOH concentration of roughly 8–14 M, were utilised after the reaction of these essential components. The primary ingredient in this geopolymer research is sugarcane bagasse ash waste. Geopolymer is a brand-new, green building material that can take the place of cement. The compressive and tensile strengths of geopolymer are higher, it takes less time to reach full strength (cure time), it shrinks less, and it does not produce CO2. Additionally, it is more fire and corrosion resistant. Fly ash, sodium hydroxide, sodium silicate, sugarcane bagasse ash

, and fine aggregates are the components of geopolymer brick. Practically every state in India has thermal power plants, which increases the accessibility of fly ash. Sodium hydroxide and sodium silicates, the components of alkaline solution, are readily available and reasonably priced in local markets. Bagasse ash can be collected nearby jaggery mills. In this regard, geopolymer technology holds out a lot of promise for usage in the construction industry as a binder alternative to Portland cement.

2 The object of the study

• To create low-cost, environmentally friendly, high-strength bricks.
• To study the effect of NaOH molarity on compressive strength of geopolymer bricks.
• To develop a method for the manufacture of geopolymer bricks.
• To study the properties of sugarcane bagasse ash based geopolymer bricks.
• To find the optimum percentage of fly ash to sugarcane bagasse ash ratio (70:30, 80:20, or 90:10).
• To evaluate the impact of ambient and oven curing on compressive strength of geopolymer bricks.

3 Methods

3.1 Materials

The materials used in the construction of geopolymer bricks are: Flyash, Sugarcane bagasse ash and fine aggregate. fly ash is a waste product obtained from thermal powerplant. The sugarcane bagasse ash was collected from the jaggery factory in Kidangoor, Kottayam district. Sodium hydroxide and sodium silicates are used for the alkali activator solution as they are reasonably priced. The fine aggregate used in the experiment is M-Sand which was obtained locally.

3.2 Determination of optimum mix

Since there is no IS code for the mix design of geopolymer brick, the trial and error method was applied. Fly ash and sugarcane bagasse ash were blended in the following ratios: 70:30, 80:20, and 90:10, respectively, to determine the mix proportion. The mixtures were then transferred into brick moulds of standard dimension and allowed to cure for 28 days at room temperature. This paper discuss the evaluation compressive strength of geopolymer brick for different molarities of sodium hydroxide (NaOH) in molar concentrations of 8M, 10M, 12M. Only 8M NaOH is considered for determining optimum proportion of fly-ash and sugar cane bag ash. The molecular weight of sodium oxide is 40 grams (added atomic masses: Na=23, O=16, and H=1). In other words, 8M Sodium Hydroxide Solution requires 320 gms. With a steady NaOH molarity of 8 M, several experimental mixes containing fly ash and sugarcane bagasse ash and fly ash were created, and the brick specimens were prepared. Measurements of the specimens' compressive strength were made, and tests lasting seven days and 28 days were run on each trial mix. The project was carried forward with the final mixture that had the highest likelihood of success.

3.3 Preparation of alkaline activator solution

In the geopolymerisation reaction, the alkaline activator solution (AAS) plays a significant role. Si and Al in the raw material or cement are activated by AAS. 8M, 10M, and 12M solutions were used in this study. 12x40=480 g of NaOH in fragment form were combined with water to create a solution with a 12 M molarity, where 40 is the molecular weight of NaOH. Because of the exothermic reaction, heat is generated when water and NaOH are combined. To avoid any fate, it should be handled carefully with help of hand gloves. To make AAS sodium silicate was mixed with the solution of sodium hydroxide. Solution was agitated for 4 to 5 min for accurate mixing of Na2SiO3 and NaOH.

Table 1. Weight of sodium hydroxide with respect to required molarity

Required Molarity	Wt. of NaOH (g)
8M	320
10M	400
12M	480
14M	560

3.4 Preparation of test samples of different NaOH molarities

Once the ideal mix fraction is determined, the effects of different NaOH molarities on the brick are revealed. The test samples were created using sugarcane bagasse ash with different NaOH molarities. For molarities 8M, 10M, and 12M, samples were cast.

3.5 Mixing casting and curing

Rectangular moulds having a cross section of 20 cm x 10 cm x 10 cm is prepared. Fly ash is replaced with the Sugarcane bagasse ash in optimum ratio. The molarity of the alkali activator solution is fixed based on the result obtained. The dry ingredients are mixed for a duration of three minutes and then the solution is incorporated; mixing is continued until a uniform blend is achieved. The mix is then immediately poured into the moulds, and the

necessary degree of compaction and surface polishing is done. The specimens were demoulded after one day. For 28 days, some of the demoulded specimens underwent ambient curing at room temperature. At an ideal temperature of 80°C, some specimens were oven cured. The brick samples were allowed to air-dry in the lab until the day of the test after completing the necessary curing duration of 24 hours inside the oven.

3.6 Testing of trial samples

To establish the mix percentage, the ratio of fly ash to sugarcane bagasse ash was changed in the following orders:70:30, 80:20, and 90:10. The fly ash to sugarcane bagasse ash which gives the highest compressive strength would be taken as the optimum ratio.

3.7 Testing of compressive strength of samples

While one set is dried in an oven, the remaining sets of 8M, 10M, and 12M are subjected to ambient curing. The oven was preheated to 80°C to cure the brick mixture in the moulds. The samples that had been demolded were kept at room temperature until testing. Measurements of compressive strength were made on a compression testing equipment, and the compressive strength was calculated from the applied load at failure point.

Figure 1. Compression Testing Machine

3.8 Testing of water absorption of bricks

To find out how much moisture brick will absorb in harsh conditions, such as rain, a water absorption test is performed on the material. The absorption test can be used to determine a brick's durability characteristics, including its quality, degree of burning, and how it reacts to the elements.

Figure 2. Testing of water absorption of bricks

3.9 Testing of efflorescence of bricks

Efflorescence is the term used to describe the development of white powder material on the surface of bricks. When the alkaline salt in the brick dries, it deposits powder on the surface after absorbing moisture from the air. To check for the presence of alkaline materials, bricks are subjected to an efflorescence test.

Figure 3. Testing of efflorescence

4 Results and Discussion

4.1 Determination of Optimum Ratio

The brick specimen with 80:20 ratio was found to have the highest compressive strength, hence 80:20 was determined to be the ideal ratio of fly ash to sugarcane bagasse ash.

Table 2. Determination of Optimum Ratio

Sample Ratios (8M)	Compressive Strength 7 Day (N/mm^2)	Compressive Strength 28 Day (N/mm^2)
90:10	11.30	12.23
80:20	14.12	15.25
70:30	13.21	14.42

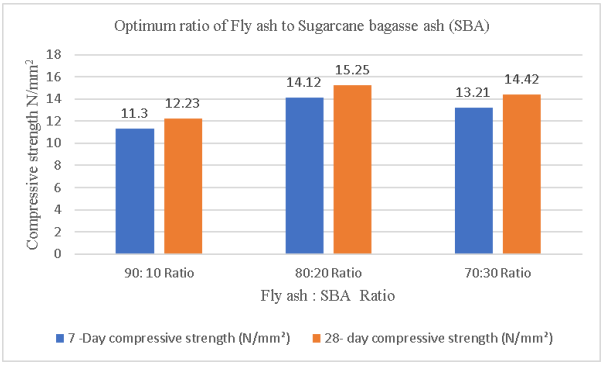

Figure 4. Optimum ratio of fly ash to sugarcane bagasse ash

4.2 Ambiently cured samples

The test is done on geopolymer bricks in compressive testing machine to determine its compressive strength after the age of 7 days and 28 days for ambiently cured. The compressive strength results obtained are given in. The compressive strength of ambient cured sample with sugarcane bagasse ash is found to increase in 28-day test in comparison with the 7-day test. The increase in NaOH molarity will increase the compressive strength of the ambiently cured sample as the 12 M sample is found to have higher compressive strength compared to 8M and 10 M.

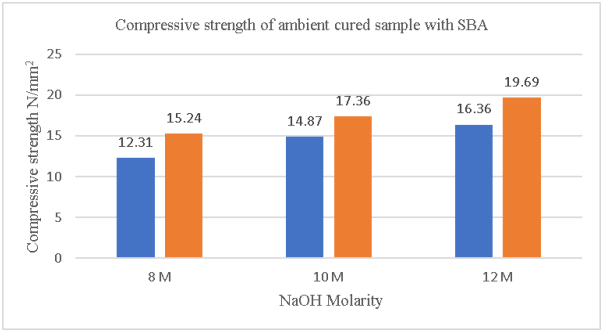

Figure 5. Compressive strength of ambient cured sample with SBA

Table 3. Compressive strength of ambiently cured samples with sugarcane bagasse ash.

Samples	Compressive Strength 7 Day (N/mm^2)	Compressive Strength 28 Day (N/mm^2)
8M	12.65	15.63
	11.87	14.54
	12.42	15.24
Avg.	12.31	15.24
10M	15.23	17.45
	14.85	17.65
	14.54	16.98
Avg.	14.87	17.36
12M	15.94	19.26
	16.35	19.66
	16.78	20.16
Avg.	16.36	19.69

4.3 Oven drying

The compressive strength of oven dried sample with sugarcane bagasse ash is found to increase in comparison with the ambient cured samples. The increase in NaOH molarity will increase the compressive strength of the oven cured sample as the 12 M sample is found to have higher compressive strength compared to 8M and 10 M.

Table 4. Compressive strength of oven dry samples with sugarcane bagasse ash

Samples	Compressive Strength (N/mm^2)
8M	17.24
	17.20
	17.20
	17.14
Avg.	17.19
10M	19.46
	19.06
	19.2
Avg.	19.24
12M	20.36
	20.06
	21.06
Avg.	20.49

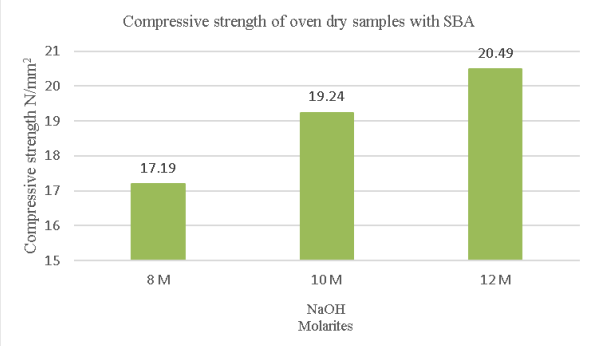

Figure 6. Compressive strength of oven dry samples with SBA

4.4 Water absorption of bricks

As per IS code the minimum percentage of water absorption of bricks is 15%. The SBA based geopolymer absorbed 5% of water

Table 5. Mesh Properties

Sl.No	Types of Bricks	Water Absorption (%)
1	SBA based geopolymer brick	5

4.5 Efflorescence of bricks

The efflorescence is caused due to the presence of alkalis in bricks. When the bricks get exposed to moisture; water is absorbed by them. Due to evaporation this water absorbed dries out from the exposed faces. As a result of this, the soluble Salts contained within them crystallize out on to the surface. This process continues for several years depending on the amount of salts present in the bricks and their solubility. All the samples tested showed very slight effloresce which is acceptable.

5 Conclusion

Fly ash, sugarcane bagasse ash, and alkali activated solution are polymerized to produce geopolymer brick.
• The ideal ratio of fly ash to sugarcane bagasse ash was determined to be 80:20.
• The compressive strength of NaOH was calculated at several molarities, including 8M, 10M, and 12M. The results reveal that the compressive strength increases with increasing molarity, with 12 M having the highest measured compressive strength.
• Bricks dried in an oven have a higher compressive strength than bricks dried at room temperature.
• Fly ash, sugarcane bagasse ash, and alkali activated solution can be polymerized to create low-cost, environmentally friendly, high-strength bricks.
• Since the main raw materials have no emissions, energy-efficient bricks were created.
• Since only locally accessible waste materials were utilised to make the bricks, this solid waste management strategy is sustainable.

Acknowledgements

We take this opportunity to express our deep sense of gratitude and sincere thanks to all who helped us to complete this project work successfully. We express our sincere gratitude to our Principal Dr. Indu P Nair for providing all the facilities needed for the completion of this project. We are greatly thankful and deeply indebted to our Guide and Head of Civil Engineering Department, Ms. Divya S Nair, for her excellent guidance, positive criticism, valuable comments, and support. We are greatly thankful to Dr.T Meena Associate Professor, VIT, Velloor for her support and guidance. We thank our parents, friends and dear ones who directly or indirectly contributed to the successful completion of our project work. We thank God Almighty for showering his blessing throughout.

References

[1] Hamza Karakas, Serhan İlkentapar, Uğur Durak; Ezgi Örklemez, Sümeyye Özuzun, Okan Karahan, Cengiz Duran Atiş; Properties of fly ash-based lightweight-geopolymer mortars containing perlite aggregates: Mechanical, microstructure, and thermal conductivity coefficient; Construction and Building Materials :Volume 362, 2 January 2023, 129717

[2] Ankur LaxmanYadava, V.SairamaK.Srinivasana, L.Muruganandamb; Synthesis and characterization of geopolymer from metakaolin and sugarcane bagasse ash;Construction and Building Materials;Volume 258, 20 October 2020, 119231.

[3] Saloma, Hanafiah1, and Kartika Ilma Pratiwi1; Effect NaOH Concentration on Bagasse Ash Based Geopolymerization: MATEC Web of Conferences,2016.

[4] Arslan Akbar, Muhammad Shafique, Fahid Aslam, Rayed Alyousef, Hisham Alabduljabbar; Sugarcane bagasse ash-based engineered geopolymer mortar incorporating propylene fibers; Journal of Building Engineering Thermo-chemico-mechanical activation of bagasse ash to develop geopolymer based cold-pressed block,2020.

[5] IdreesZafa, KhuramRashid, MadihaAhmad, MounirLtifi ; Thermo-chemico-mechanical activation of bagasse ash to develop geopolymer based cold-pressed block Construction And Building Materials:Volume 33, January 2021, 10149.

Validation of Modular Gridded Base Platform for the Static Structural Testing of Aerospace Structures Using M S Adaptor

Fathima N[1] and Deepthy S Nair[2]

[1] PG student, Civil Engineering Department, NSS College of Engineering, Palakkad – 8, Kerala
[2] Asst. Professor, NSS College of Engineering, Palakkad, 678008, Kerala, India

Abstract -

A static structural testing is a method for verifying that, the realised structure has enough strength to withstand the loads, for which it is designed. In any space mission, safety holds utmost priority. Structural qualification tests are necessary in order to verify structural adequacy and to qualify the design. The primary objective of a structural qualification test is to assess the exact real performance of a structure and to validate its design. This project focuses on the analysis of modular gridded base platform. Previously anchoring plates which are embedded in concrete strong floor is provided for mounting the test adaptor or loading elements. A modular grid test platform is a replacement for this concept. The finite element analysis for the modular base gridded platform is already carried out. And the validation of this modular gridded base platform is done in this paper. The design of the components was done manually and through finite element analysis using ABAQUS software.

Keywords -

Structural testing; Structural qualification test; Modular gridded base platform; Anchoring plates;

1 Introduction

Aerospace structures which are differ from other structures due to their high demands for performance and lightweight. Modern aerospace structures typically require the use of composite materials, advanced multifunctional materials and thin-walled constructions. To obtain the level of performance required from flight structures, thorough knowledge of material limitations, structural stability, structure health and strength considerations are needed [15]. A static structural test is to be conducted in order to build up confidence in the design capability to withstand the expected flight loads. Qualification tests are conducted on flight quality hardware to demonstrate that all structural design requirements have been achieved. And margin evaluation test are conducted in order to check the margin of safety of structures. The entire load is applied on the base structure, where the test article is anchored. The reactions to the base structures are transfer through the loading portals. So, the base structure should be very strong enough to withstand high localized loads. Moreover, it should not alter the natural response of the test article during the load application. Hence, design of base structure or ground anchoring configuration holds utmost importance in the configuration of a proper test set-up. At present anchoring plates are used over the reinforced floors for providing anchoring to the test article and test rigs. In order to overcome the drawbacks of the present system a new base platform having modular gridded construction is introduced. The qualification tests have been already done and in this paper a validation of this base platform is performed.

2 The object of the study

The main objective of this study is to validate this modular gridded base platform using an MS adaptor. And to find it's margin of safety.

3 Methods

3.1 Modular Gridded Base platform

A modular gridded base platform is a platform which consists of standard interchangeable modules for making test bed for different test rig assemblies. The main purpose of having a base platform is to support and anchor the test rigs. This modular gridded base platform consists of a L plate, cross plate, long beams, short beams, and base plates. All together to give this base platform.

3.2 M S Adaptor

For the validation of this project, a MS adaptor is used. The test set-up of this assembly consists of test adaptors, that is MS adaptor and the base beams. Mild steel (MS) adaptor is used at top with loading locations. The loading locations are arranged equi-spaced over the top flange of this MS adaptor. And this will provide proper load diffusion. The MS Adaptor is a cylindrical shell of 2742mm diameter and 16mm thick, which is made of mild steel (MS). Gussets are provided for the bending stiffness of the rings. The fore end ring(top flange) of the test adaptor is of diameter 2942mm and 30 mm thick, and they are provided with 10mm thick gussets on the external side

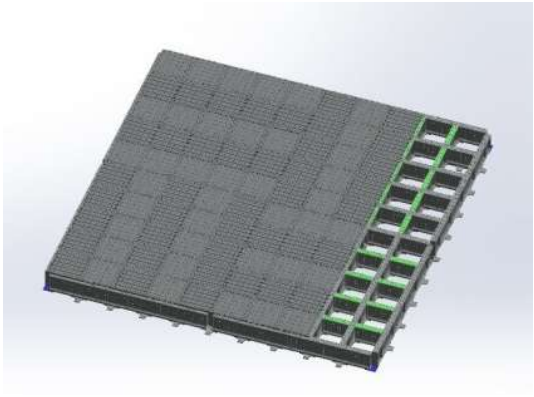

Figure 1. Assembly of base platform

Description	Material	Dimension (mm)
Top flange	IS2062	OD 2942 x ID 2712 x 30 thick
Shell	IS2062	OD 2742 x ID 2710 x 16 thick
Bottom flange	IS2062	OD 3340 x ID 2090 x 30 thick
Stiffener (top)	IS2062	120x90x10
Stiffener (bottom)	IS2062	500x300x20

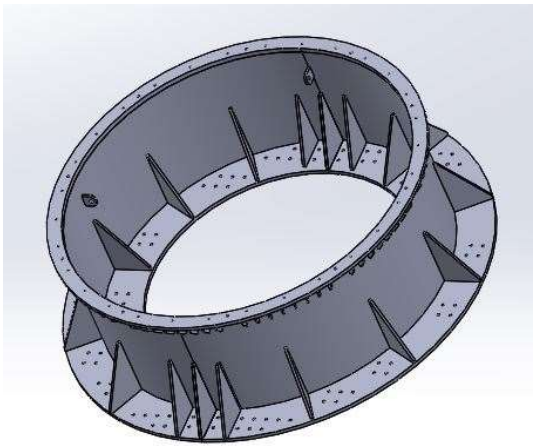

Figure 2. M S Adaptor

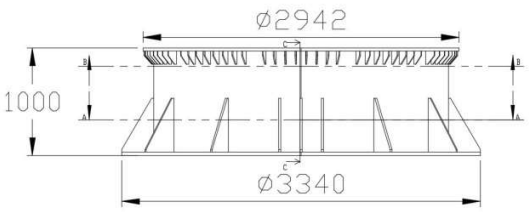

Figure 3. Dimensional details of MS Adaptor

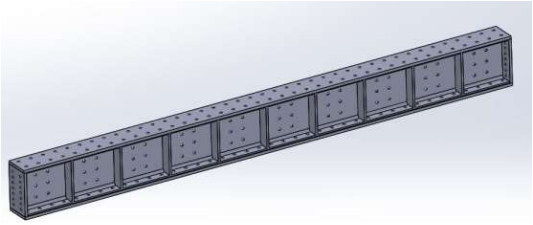

Figure 4. Dimensional details of MS Adaptor

of the flange. The aft end (bottom flange) is of diameter 3340mm and has a thickness of 30mm. The bottom flange is stiffened with gussets of 20mm thickness in interior as well as in exterior side of the flange. Fig 2 shows the 3D model of MS Adaptor.

3.3 Loading Beams

This MS adaptor rest on 8 bottom beams of 4m length and is made up of ISNPB 450 built up section. This bottom beam is anchored to the gridded platform by using bolts. The bottom beams are also provided with intermediate stiffeners of 374x85mm and having a thickness of 16 mm. Also, the stiffeners are equally spaced at 400mmc/c throughout its length. 3D view of the loading beam is shown in fig 4 and the detailed view is shown in fig 5.

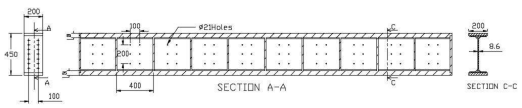

Figure 5. Dimensional details of MS Adaptor

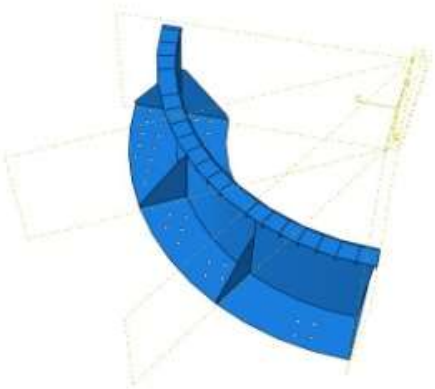

Figure 6. FE model of Adaptor

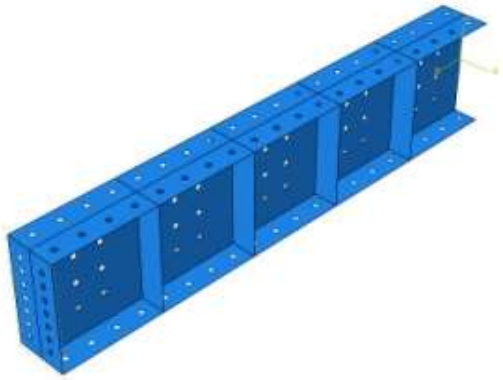

Figure 7. FE model of base beam

3.4 Finite Element Analysis

The finite element analysis (FEA) involves subdividing a continuum into a finite number of regions called elements connected at finite number of points called nodes to which loads are applied. For that, at first idealize the actual physical continuum problem into a mathematical model. A mathematical model is an integral structure consisting of boundary condition, geometry, loads applied and material properties. Linear static analysis is performed here. The finite element analysis is done using the software ABAQUS. The FE model of test rig structure includes the test adaptor and the bottom beams. The MS adaptor as well as the bottom beams are created using mid surface model and are dicretized using shell elements. Also for the ease of calculation only small portion is modeled. Fig 6 shows the FE model of MS adaptor The bottom beam is provided beneath the MS adaptor and the tie constraints are given in-order to restrict the movement. There are total of 8 numbers of beam is used. FE model of beam is shown below as fig 7

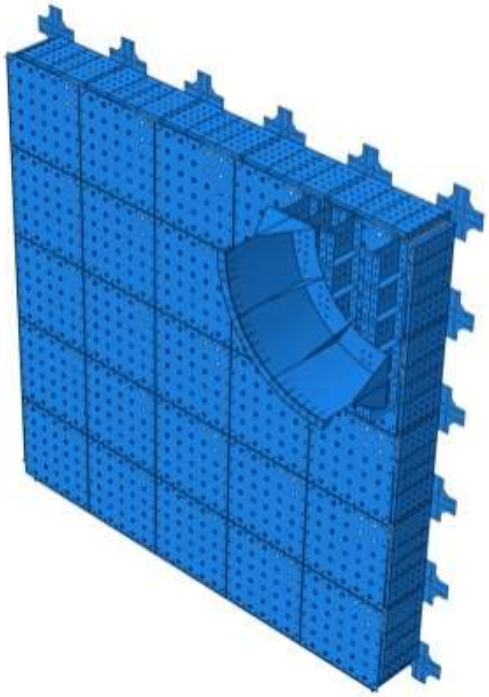

Figure 8. FE model of entire assembly

3.5 Mesh, Boundary condition and Loads applied

A mesh convergence study was done. And it is found that after the mesh size of 15 there is no fluctuations in the von- Mises value and displacement. So a mesh size of 15 was taken into account. Also, a fixed boundary condition is given to the bottom of the platform and a symmetric boundary condition is given to the sides since only a quadrant portion is taken for the analysis. The tension load of 2800kN and compression load of 3000kN is applied and the analyses were done. Loads were applied per nodes on the top flange of this MS adaptor, these are shown in figure given below.

Figure 9. Meshed model of MS adaptor

Figure 10. meshed model of entire assembly

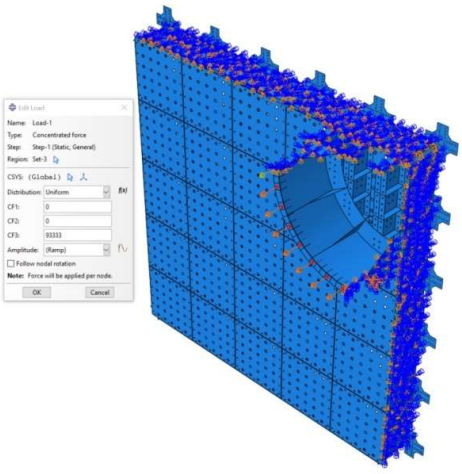

Figure 11. Tension loads on assembly

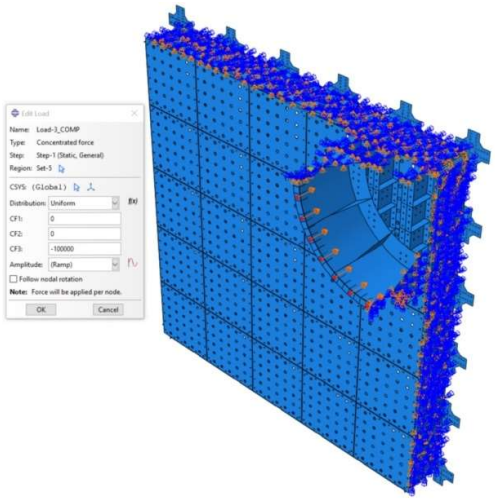

Figure 12. Compression loads on assembly

4 Results and Discussion

Through finite element analysis, the von-Mises stress of the entire assembly in tension and in compression is found out. The stress components S11 (Local 11 direct stress), S22(Local 22 direct stress) and S12 (Local 12 shear stress) of each components are noted. And it is noted that the von- mises stress for tension and compression is around 160 N/mm2. These values are less than 240 N/mm2, that is less than yield stress. So the design is found to be safe.

Components	Stress (N/mm^2)	Yield Stress (N/mm^2)	MOS
L plate	44.75	240	4.363
Cross plate	87.28	240	1.749
Base plate	101.6	240	1.36
Long beam	197.4	240	0.215
Short beam	48.86	240	3.911
Assembly –Tension	154.6	240	0.552
Assembly- Compression	120	240	1

5 Conclusion

Validation of modular gridded base platform using MS adaptor was carried out in this paper. Margin of safety the entire assembly in both condition were analyzed. It is found that the margin of safety in both case are greater than zero. So it is safe. From the above conclusion the modular gridded base platform can be used a superior for the present condition. And through finite element analysis using ABAQUS, it was found that the proposed configuration is safe by design.

6 Acknowledgement

This work was done at VSSC-ISRO, Thiruvananthapuram, Kerala. Special thanks to the director of VSSC for permitting to carry out this work. Also special thanks to the external guide, VSSC and internal guide for the help and support they have given for the project work.

References

[1] Asyraf, M.R.M., Ishak, M.R., Sapuan, S.M., Yidris, N., Ilyas, R.A., Rafidah, M. and Razman, M.R., 2020, "Evaluation of design and simulation of creep test rig for full-scale crossarm structure", Advances in Civil Engineering, pp.1-10.

[2] Dongming, L., Wei, T., Caijun, X. and Pengfei, Z., 2014, "Static test rig development and application for an airliner's hyperstatic aero-engine pylon structure", Journal of Measurements in Engineering, 2(3), pp.145-153.

[3] Favato, L.F. and Magalhães, P.A.A., "Linear Static and Dynamic Analysis of Rocket Engine Testing Bench Structure using the Finite Element Method", International Journal of Engineering Research and Applications, pp.70-77.

[4] Huang, C.C., 2000. "Overview of modular product development" Proceedings-National Science Council Republic of China Part a Physical Science and Engineering, 24(3), pp.149-165.

[5] IS 816-1969, Code of practice for use of metal Arc welding for General Construction in Mild Steel.

[6] ISRO Design Manual, Volume 1, Design Data, Fasteners Circlips, Vikram Sarabhai Space Centre, Thiruvananthapuram, November 2005

[7] Jain, U., Shukla, H., Kapoor, S., Pandey, A. and Nirwal, H., 2020. "Design and analysis of 2-axis rocket motor stand for thrust vectoring", In AIAA propulsion and energy 2020 forum (p. 3920).

[8] Ramly, R., Kuntjoro, W., Wisnoe, W. and Nasir, R.E.M., 2010, "Design and analysis for development of a wing box static test rig" International Conference on Science and Social Research (CSSR 2010) (pp. 113-117). IEEE.

[9] Reddy, T.S. and Reddy, K.V.K., 2010. "Design and analysis of vibration test bed fixtures for space launch vehicles". Indian Journal of Science and Technology, 3(5), pp.592-595.

[10] Report- An Overview on Standard Interchangeable Modular Sections (SIMs) for Test Rig Design Configuration, A Report VSSC/STG/INSTEF/TM-MISC/08/20

[11] Report-Design And Analysis Of Test Rig For Thermo-structural qualification Of Integral Tps , A Report of VSSC/SDE/TM-ITPS/1140/2017

[12] Report -"Design report of test rig elements for the structural qualification test of 4m composite ogive payload fairing (OPLF) for GSLV for phase-I test , A Report of the ISRO-VSSC-DR-0073-0-20

[13] Soares, D.M., Telöken, F., Severo, T.C. and Poletto, M., 2018. "Development of a vertical static test bench for amateur rocket engines". International Journal of Advanced Scientific and Technical Research, 5(8), pp.45-49.

[14] ABAQUS User Manual

[15] https://aero.engin.umich.edu/research/research-areas/structures-materials/

Sustainability studies and life cycle assessment of construction materials – An overview

Parvathy A Nair [1], Dr. G Madhu[2] and Dr. Roy M Thomas[3]

[1] Research Scholar, Division of Civil Engineering,School of Engineering, Cochin University of science and Technology,Cochin Kerala.

[2] Professor, Division of Civil Engineering,School of Engineering, Cochin University of science and Technology,Cochin Kerala.

[3] Professor, Division of Chemical Engineering,School of Engineering, Cochin University of science and Technology,Cochin Kerala

Abstract -

Now a days due to uncontrolled human activities enormous amount of greenhouse gases are released into the atmosphere and its persistent accumulation consequently generates potential threats to the earth as well as mankind. Global warming, drastic climatic changes, rapid increase in the atmospheric temperature, shortage of water etc to enlist a few. Sustainable development focuses on fulfilling the present needs without causing much harm to the environment and thus catering the needs of future generations also. Efficient use of natural resources by careful planning and design principles which ultimately reduces the energy intake is one of the principal goals towards sustainable development. Life Cycle Assessment is one among the powerful tools which is used to analyze the environmental impacts caused by the processes involved in the entire life of a particular product. This article includes a discussion on use of sustainable materials in construction industry, significance of recycle and reuse of materials which eventually reduces the embodied energy in comparison with virgin materials. The paper also incorporates a study on application of Life cycle analysis to construction materials

Keywords -

sustainable development; life cycle assessment; embodied energy; life cycle analysis

1 Introduction

The accelerated level of industrialization, urbanization together with infrastructure development led to escalated energy demands as well as accumulation of wastes. Considering the material level of a construction domain, most of the raw materials are extracted from the earth in the impure form and their extraction as well as purification involves extensive processes which demand high level of energy ,along with generation of waste .components which are left behind adds up to a large portion of waste .Loss of natural habitat of wide varieties of flora and fauna, highly disturbed ecosystem etc are the outcomes of unrestricted and over usage of natural resources. To make sure the conservation of natural resources as well as to create a more stabilized ecosystem, sustainable development is crucial. Furthermore, it reduces the impact of alarming climatic changes due to overexploitation of naturally occurring assets. Since the construction industry involves diverse, complicated and laborious processes, it contributes a major part to the formation of greenhouse gases and atmospheric pollution. Incorporation of LCA technique in different stages of building industry like, material selection, process design, usage phase, maintenance and final disposal helps to clearly identify the sustainable mechanisms compared to the conventional one. In each of the stages direct (during phase of construction and demolition) as well as indirect (in the form of embodied energy of raw materials used) energy consumption occurs [1]. Life Cycle Assessment is the technique which is used to analyze the environmental impacts which are an outcome of the processes involved in the life cycle of a particular product. LCA involves the collection and evaluation of quantitative data on the inputs and outputs of material, energy and waste flows associated with a product over its entire life cycle so that the environmental impacts can be determined. Recent research papers discusses LCA as a systematic analysis to quantify industrial methods and materials by analyzing the energy flow and usage of elements, environmental emissions and evaluate alternatives for environmental improvement[2].As LCA method can be applied on a wider field encompassing much complicated building sector ,it is recognized worldwide as a tool to improve processes and designs environmentally [3], [4]. Architects, designers, engineers as well as decision makers are benefitted by the accomplishment of LCA by providing data about the environmental impacts associated with a construction. Moreover life cycle analysis includes a comprehensive approach focusing on environmental benefits rather than capital expenditure incurred in a project [5]. Principal stages of LCA in construction industry includes –raw material extraction, processing, construction, usage phase , end of life and final disposal. Use of LCA will improve and demonstrate the "green-ness" of the project and help significantly in increasing long-term paybacks by better decision making . Life cycle analysis for new building materials, locally available building materials and their

alternatives, supplementary cementitious materials, building blocks, structural concrete, industrial by-products etc helps to identify the best choice for green building construction.

2 Sustainable Construction materials

Although several efforts were made towards environmental protection earlier ,a prominent sustainability paradigm in construction industry started in early 1990s .One of the essential requirement in this respect is the material and resource efficiency .

2.1 Factors influencing selection of sustainable construction materials

A building which is planned ,designed ,constructed ,operated ,maintained and finally reused or disposed in an ecological and resource efficient manner is termed as sustainable building .According to international standards ,a building should meet different parameters like reduction in green house gas (GHG) emission ,resource efficiency, waste management ,energy utilization in order to be sustainable .Among all these parameters the material efficiency is the crucial factor which determines the overall performance and energy expenditure of a structure .Appropriate selection of building materials from sustainable point of view can be accomplished by considering their entire period of life and those having minimal impact on the environment. Since the life -cycle of renewable or recycled materials can be closed, it is widely accepted as a better way for sustainable development. It is important to understand that the materials which satisfy the criteria must be sustainable throughout their life and consume low energy during usage and maintenance phase .They must not emit harmful pollutants which has negative impact on human health and comfort .Some of the major aspects regarding selection of building materials are their cost ,aesthetic beauty, availability, strength and durability [6]. Conventional materials including concrete, glass, aluminium ,steel etc have high energy content in them .Therefore selection of these materials have huge impact on the overall energy usage as well as waste generation [7] . Another important strategy to achieve sustainability would be to improve the functionality and environmental performance of traditional materials through the use of more sustainable technologies, for example, utilizing nanotechnology. Producers of sustainable building materials will also have to make them more affordable and harmless for human health and the environment [8] . Analysis on the sustainability of building materials in Nigeria suggested the top three barriers encountered in practice while selecting building materials in the country and they are “perception of extra cost being incurred”, “lack of sustainable material information” and “lack of comprehensive tools and data to compare material alternatives [9]. However when considering the natural reserves which cannot be replenished and are insufficient in nature , an acceptable goal for achieving sustainable future is by the reduction in use of raw materials .The amount of waste generated also plays significant role during the construction ,service life and also upto the final disposal of a building.

2.2 Comparative studies on alternate building materials used in the construction industry

Recent studies regarding the structure and properties, applications and sustainability of bamboo as a renewable construction material showsbthat bamboo has superior properties in view of sustainability. Properties like rapid renewability , lower embodied energy compared to concrete ,steel and plastic, ability to recycle (since their products can be incinerated or digested in sewage) make it a superior material in thesustainability point of view [10]. Researches on the applicability of bamboo as a construction material shows that bamboo bars are suitable rebars for non-load-bearing and lightweight-reinforced concrete flexural members. Because of its rapid renewability, material strength, and availability of variety of species across the globe, bamboo is widely accepted as a sustainable solution in construction. Moreover, It has least hazardous waste generation and can be easily recycled. The sustenance of bamboo for construction application offers benefits, such as prefabrication, simple assembly, simple replacement of structural parts, and moreover, the bamboo elements could easily be dismantled and reused for another application [13].Studies conducted on cement stabilized rammed earth (CSRE) as a sustainable construction material concluded that it can be used as a building material with sufficient strength and durability but low in embodied energy. CSRE can be used in the construction of boundary walls, load bearing walls of buildings, retaining walls and road pavement construction [11].Sustainability studies on using recycled plastic fiber in concrete reveals that Only 9% of the global production of plastic fibre is recycled. LCA results show that 100% recycled polypropylene (PP) fibers produced by mechanical recycling of industrial plastic waste have substantially lower resource consumption and emissions compared to both virgin PP fibers and steel reinforcing mesh (SRM) [12].

3 Concept of life cycle assessment

3.1 General

Basic strategy that is included in the life cycle evaluation is to measure the environmental impact of a product over its entire life cycle stages, i.e from cradle to grave. The method evaluates in detail the resources inputs, including energy, water and materials, and environmental

loadings including CO2 emissions, solid wastes and liquid wastes of a product. Within the last decade, research on LCA has increased covering from construction process to manufacturing of building materials. The methods to assess buildings are diverse as buildings have different functions, materials, sizes and locations [1]. Based on the study on intake and emissions in sequential stages of building construction and maintenance conducted ,it is realised that despite differences in focuses of evaluation and complexities of methodologies, all of them pointed to the same conclusion that the use-phase of a building contributes the largest life cycle environmental impacts with their structural materials dominating the share [14].

3.2 Key elements of LCA

The key elements associated with the method are :- functional unit ,system boundary and impact categories . functional unit is the basic unit which is considered for the study based on which evaluations and quantification of energy and emissions (both input and output) are measured. The 'functional unit' appropriately describes the product or process being studied. It reflects the function the system delivers at the product unit level [14]The functional unit is a description of the product or system being assessed, defined with great specificity so that the resulting LCA can be compared to the LCA of a similar product or system on a one-to-one basis [15]. The functional unit should as far as possible relate to the functions of the product rather than to the physical product. The primary purpose of a functional unit is to provide a reference to which the inputs and outputs are related [16].It forms the basis of calculation for the indicators and impact categories later .In addition to that the ease of comparison of the outcome of the study to other known quantities should also be taken into consideration while fixing the functional unit [17], [18]. System boundary is set of criteria that determines which unit processes, inputs, outputs, and impacts are considered in an LCA. A unit process is a discrete step in the life cycle of a product, such as extraction, manufacturing, transportation, use, or disposal. A system boundary is the set of criteria that determines which unit processes, inputs, outputs, and impacts are considered in an LCA. A unit process is a discrete step in the life cycle of a product, such as extraction, manufacturing, transportation, use, or disposal. There can be several basis for selecting a system boundary for a buildings LCA. Cradle to grave is the most popular system boundary adopted in buildings LCA [1].figure 1 illustrates the possible system boundaries when considering the construction of a building . Another key element in the life cycle analysis method is the environmental impact categories An impact category groups different emissions into one effect on the environment. During the course of the LCA, a large amount of emission data is collected:

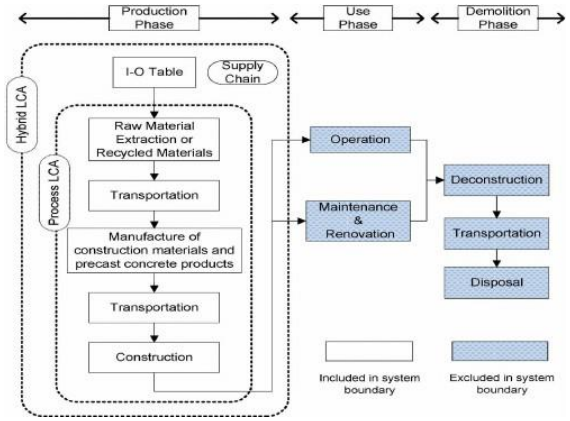

Figure 1. system boundary for LCA in building construction process .[19]

Impact category	Abbreviation	Scale	LCI data i.e., classification	Characterization factor
Global warming	GW	Global	Carbon Dioxide (CO_2) Nitrogen Dioxide (NO_2) Methane (CH_4) Chlorofluorocarbons (CFC_S) 'Hydro chlorofluorocarbons' ($HCFC_S$) Methyl Bromide (CH_3B_r)	Global warming potential
Acidification	A	Regional Local	Sulphur Oxides (SO_X) Nitrogen Oxides (NO_X) Hydrochloric Acid (HCL) Hydrofluoric Acid (HF) Ammonia (NH_4)	Acidification potential
Eutrophication	E	Local	Phosphate (PO_4) Nitrogen Oxide (NO) Nitrogen Dioxide (NO_2) Nitrates, and Ammonia (NH_4)	Eutrophication potential
Ozone depletion	OD	Global	Chlorofluorocarbons (CFC_S) Hydro chlorofluorocarbons ($HCFC_S$) Halons, and Methyl Bromide (CH_3B_r)	Ozone depletion potential

Figure 2. Major impact categories in construction process

emissions from energy production, the waste produced, the raw material production, etc. These emissions come in different shapes and formats since the emissions from harvesting raw materials are very different from the emissions from producing electricity. Different emissions that cause the same impact- are converted into one unit that translates into one impact category. Some of the major impact categories that are incorporated in LCA are global warming ,climate change ,ozone depletion ,acidification,eutrophication etc.

4 Framework of LCA

The description of the LCA methodology is based on the International standards of series ISO 14040 and consists of four distinct analytical steps; defining the goal and scope, creating the inventory, assessing the impact and finally interpreting the results[20] Goal and scope definition - The goal and scope definition step includes identification

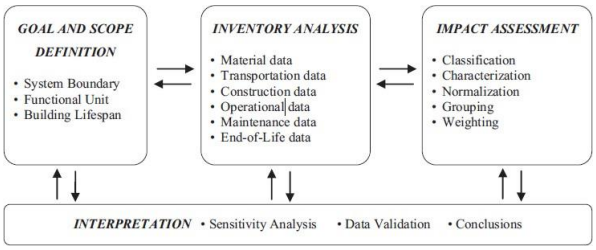

Figure 3. Frame work of LCA in construction industry [1]

of the purpose and boundary of the study, establishing the functional unit of analysis, and defining the key processes, material, and energy flows for analysis [21]. In this phase, the product(s) or service(s) to be assessed are defined, a functional unit is chosen, and the required level of detail is defined. The type of analysis, impact categories to be evaluated, and set of data that needs to be collected are identified. System boundary and functional unit definition are important elements of this component [15] .The accuracy and reliability of the LCA work depends on defining clearly the goal and scope of the work .This encompasses setting of system boundaries ,specifying the functional unit and also fixing the building lifespan

Next major step is inventory analysis which is the most strenuous stage in the frame work of life cycle analysis .It involves collection and aggregation of datas ,material and energy comsumption in each unit processes ,quantity of waste generated and also the emission of GHG etc . In other words, an inventory of all the inputs and outputs to and from the production system is prepared in this step. In the inventory analysis stage, software tools and databases are critical. It is not possible to analyze each individual material and process from scratch each time an LCA is performed. Instead, software tools tied to extensive product and process databases are used to complete the inventory analysis. The simplest software tools are spreadsheets, in which material quantities can be entered [15].The third step in this process is impact assessment . In this step translation of the emissions from a given product or process into impacts on various human and terrestrial eco-systems are done . Data from the inventory analysis is attributed to an appropriate impact category defined in scoping [15] . Impact assessments differ among the LCA tools used, and there is no one dominant impact framework. Different researcher uses different impact categories but most commonly used are global warming potential, acidification, ozone depletion and eutrophication [1]. The final step in LCA is the interpretation of results where values from the impact assessment will be analysed for robustness and sensitivity to inputs and conclusions are drawn with reference to the goals and objectives of the LCA . Data validation also will be conducted by comparing to other published research works [1]. LCA results are reported in the most informative way possible and the need and opportunities to reduce the impact of the products or services on the environment are systematically evaluated. The results are often presented in the form of tables or graphs, which is especially helpful when comparing two competing design options or products. The outcome of this step is directly useful in making environmentally friendly decisions. Like any other design feedback tool, LCA can be an iterative process; the interpretation of the LCA can lead to changes in the proposed design and feeds to the previous step [15]

5 Life cycle impact of construction materials

In majority of the cases construction materials are selected at early stage that suits the need of owner and undergo the studies of sustainability or they are incorporated in the design stage parallelly as the work progresses. Generally the life cycle assessment of materials is done on a cradle to gate basis, because it is innately connected to the pre-use phase of building [22] . According to a research study by [23] selection of materials should be carried out at early stage as they could be subjected to life cycle analysis to study the environmental performance of the same [23] .The major stages in the life cycle of a building material consist of raw materials extraction ,manufacturing ,installation , usagephase ,maintenance and final disposal . To begin with the primary stage of extraction from nature ,the process demands high energy ,generates dirt as well as smoke together with loud noise creating direct harm to the environment .In addition to that it causes serious impact on health of the workers related to it .Heavy machines used for extraction process have very high primary energy consumption and is considered as initial embodied energy of the materials [23]. Onsite construction as well as installation involves laborious hours of marking, cutting ,fixing ,aligning, finishing etc and all these operations generates some amount of waste with input of high energy .Greater part of these materials can be reused or recycled if planned and executed efficiently in the design stage itself. Since the building industry is vast by size as and its complicated operations ,each stage during the period need to be kept minimal .Another significant factor is the transportation of materials ,whether it is the raw materials ,finished products ready for installation ,any waste and byproducts generated in between the processes etc need to be carried to and from site ,factory and finally upto the land fill at the time of disposal [24].Utilizing materials which are locally sourced can significantly reduce the embodied energy of materials which eventually have direct impact associated with each stage [23]. Examining the next stage of a building product's life cycle which is considered as the most

energy consuming phase is the operation phase. It comprises of maintenance , repair and renovation until end of building life .Initially the materials which are used have direct correlation with the maintenance stage . Designers need to make sure that products used for construction have minimal emission of harmful gases and other volatile organic compounds as it is detrimental to the occupants [7].The final stage is analyzed under two conditions .First condition where further maintenance is not fruitful or becomes uneconomical . Second condition is the end of life of building itself even though some of the materials used are still in operable stage. Complete replacement of materials eventually leads to disposal in land fill. Materials that can be recycled or reused should be categorized separately ,so that the amount of waste being disposed off to landfill is reduced considerably .[7]

6 Conclusion

The concept of ecologically sustainable development is a broad area of research .It needs more clarity in terms of selection criteria for materials ,process design ,waste disposal etc . However right selection of materials have significant impact on all subsequent stages of building. Utilization of locally available ,recyclable materials is highly recommended .Adaptation to life cycle assessment procedure in selecting the materials could bring clarity to the environmental repercussions made by them. The ultimate goal of LCA is to provide users with comprehensive results and enable the evaluation of specific improvement alternatives, based on economic, social and environmental criteria. LCA case studies on commonly used building materials have been carried out in developed countries but there are insufficient studies in developing countries using local data. Therefore, more LCA studies of building materials are to be developed and used in order that environmental and energy considerations can be implemented worldwide. Inclusion of LCA as a criteria for ranking using energy rating systems is also viable solution.

References

[1] A. F. Abd Rashid and S. Yusoff, “A review of life cycle assessment method for building industry,” Renew. Sustain. Energy Rev., vol. 45, pp. 244–248, 2015, doi: 10.1016/j.rser.2015.01.043.

[2] R. Fay, G. Treloar, and U. Iyer-Raniga, “Life-cycle energy analysis of buildings: A case study,” Build. Res. Inf., vol. 28, no. 1, pp. 31–41, 2000, doi: 10.1080/096132100369073.

[3] J. Fava, S. Baer, and J. Cooper, “Increasing demands for life cycle assessments in North America,” J. Ind. Ecol., vol. 13, no. 4, pp. 491–494, 2009, doi: 10.1111/j.1530-9290.2009.00150.x.

[4] O. Ortiz, F. Castells, and G. Sonnemann, “Sustainability in the construction industry: A review of recent developments based on LCA,” Constr. Build. Mater., vol. 23, no. 1, pp. 28–39, 2009, doi: 10.1016/j.conbuildmat.2007.11.012.

[5] G. Han and J. Srebric, “Life-Cycle Assessment Tools for Building Analysis,” Pennsylvania Hous. Res. Cent., no. Lcc, p. 7, 2011, [Online]. Available: http://www.engr.psu.edu/phrc/Publications/RB0511-Life-cycle assessment tools for bldg analysis .pdf

[6] U. G. Y. Abeysundara, S. Babel, and S. Gheewala, “A matrix in life cycle perspective for selecting sustainable materials for buildings in Sri Lanka,” Build. Environ., vol. 44, no. 5, pp. 997–1004, May 2009, doi: 10.1016/J.BUILDENV.2008.07.005.

[7] G. K. C. Ding, “Life cycle assessment (LCA) of sustainable building materials: An overview,” Eco-Efficient Constr. Build. Mater. Life Cycle Assess. (LCA), Eco-Labelling Case Stud., pp. 38–62, 2013, doi: 10.1533/9780857097729.1.38.

[8] P. Joseph and S. Tretsiakova-McNally, “Sustainable non-metallic building materials,” Sustainability, vol. 2, no. 2, pp. 400–427, 2010, doi: 10.3390/su2020400.

[9] P. O. Akadiri, “Understanding barriers affecting the selection of sustainable materials in building projects,” J. Build. Eng., vol. 4, pp. 86–93, 2015, doi: 10.1016/j.jobe.2015.08.006.

[10] M. Asif, T. Muneer, and R. Kelley, “Life cycle assessment: A case study of a dwelling home in Scotland,” Build. Environ., vol. 42, no. 3, pp. 1391–1394, 2007, doi: 10.1016/j.buildenv.2005.11.023.

[11] C. Jayasinghe and N. Kamaladasa, “Compressive strength characteristics of cement stabilized rammed earth walls,” Constr. Build. Mater., vol. 21, no. 11, pp. 1971–1976, 2007, doi: 10.1016/j.conbuildmat.2006.05.049.

[12] R. Tuladhar and S. Yin, Sustainability of using recycled plastic fiber in concrete. Elsevier Ltd, 2018. doi: 10.1016/B978-0-08-102676-2.00021-9.

[13] M. Yadav and A. Mathur, “Bamboo as a sustainable material in the construction industry: An overview,” Mater. Today Proc., vol. 43, pp. 2872–2876, 2021, doi: 10.1016/j.matpr.2021.01.125.

[14] R. K. Rosenbaum, Selection of Impact Categories, Category Indicators and Characterization Models in Goal and Scope Definition. Chapter 2 “Goal and Scope Definition in Life Cycle Assessment” (Curran M. ed). 2017. doi: 10.1007/978-94-024-0855-3.

[15] C. Bayer, M. Gamble, R. Gentry, and S. Joshi, “Guide to Building Life Cycle Assessment in Practice,” Am. Inst. Archit., pp. 1–193, 2010.

[16] M. N. Nwodo and C. J. Anumba, “A review of life cycle assessment of buildings using a systematic approach,” Build. Environ., vol. 162, no. July, p. 106290, 2019, doi: 10.1016/j.buildenv.2019.106290.

[17] B. Weidema, H. Wenzel, C. Petersen, and K. Hansen, “The product, functional unit and reference flows in LCA,” Environ. News, vol. 70, p. 46, 2004, [Online]. Available: http://gfc.force.dk/resources/777.pdf

[18] R. Hughes, Life cycle assessment; origins, principles...,

[19] A. Abdelmonteleb and M. Ali, “Process by using Life Cycle Assessment Tool,” no. December, 2014, doi: 10.13140/2.1.1857.6965.

[20] M. Finkbeiner, “The International Standards as the Constitution of Life Cycle Assessment: The ISO 14040 Series and its Offspring,” pp. 85–106, 2014, doi: 10.1007/978-94-017-8697-3_3.

[21] A. Singh, G. Berghorn, S. Joshi, and M. Syal, “Review of Life-Cycle Assessment Applications in Building Construction,” J. Archit. Eng., vol. 17, no. 1, pp. 15–23, 2011, doi: 10.1061/(asce)ae.1943-5568.0000026.

[22] E. Franzoni, “Materials selection for green buildings: Which tools for engineers and architects?,” Procedia Eng., vol. 21, pp. 883–890, 2011, doi: 10.1016/j.proeng.2011.11.2090.

[23] T. Esin, “A study regarding the environmental impact analysis of the building materials production process (in Turkey),” Build. Environ., vol. 42, no. 11, pp. 3860–3871, 2007, doi: 10.1016/j.buildenv.2006.11.011.

[24] Berge, Bjorn. The ecology of building materials. Routledge, 2009.

[25] Halliday, S. ”Sustainable Construction Butterworth Heinemann.” (2008).

An Isolated Soft Switched High Power Factor Rectifier With Multiple Output

Elsa J Nalappat[1] and Dr. Saju Narendran[2]

[1] PG Scholar, Dept of Electrical & Electronics Engineering, NSS College of Engineering, Palakkad
[2] Professor, Dept of Electrical and Electronics Engineering, NSS College of Engineering, Palakkad

Abstract -

A high power factor rectifier is an electronic circuit that is used to convert alternating current (AC) power into direct current (DC) power while maintaining a high power factor. A high power factor rectifier that uses a boost input and an asymmetrical half-bridge flyback converter is described in this project. This type of rectifier allows for single input and multiple output bridgeless AC-DC conversion, and also reduces the voltage stress on the switches while achieving zero voltage turn-off. Additionally, a closed loop is provided using a PI controller.The resonant nature of the asymmetrical half-bridge flyback converter is utilized in the design procedure of the proposed model. This detailed design procedure can be executed using MATLAB/SIMULINK. Finally, the performance of this converter is compared to that of other converters

Keywords -

MATLAB, SIMULINK

1 Introduction

Active PFC circuits typically use a boost converter configuration to regulate the dc output voltage and shape the input current waveform. This involves sensing the ac line voltage and current and adjusting the switching frequency and duty cycle of the boost converter to ensure that the input current waveform follows the input voltage waveform, resulting in a high power factor. Other techniques such as interleaved PFC and bridgeless PFC can also be used to further improve the power factor and reduce the size and cost of the PFC circuit. High power factor rectifiers are commonly used in applications such as ac-dc power supplies for computers, tvs, and other electronic equipment, as well as in industrial and commercial applications where high efficiency and low harmonic distortion are required. Soft switching is an important factor in high power factor rectifiers. Soft switching is a technique used in power electronics to reduce switching losses in power converters. In hard switching, the power switch is turned on and off at high voltage and current levels, which can cause high power dissipation and stress on the switching components. In soft switching, the switching losses are minimized by manipulating the circuit in such a way that the power switch is turned on and off at low voltage and current levels, thereby reducing the switching losses. This is achieved through the use of resonant circuits that store and release energy, allowing the power switch to turn on and off with minimal voltage and current stress. Soft switching techniques include zero voltage switching (ZVS) and zero current switching (ZCS), which can be implemented using a variety of circuit topologies, such as the resonant converter, the quasi-resonant converter, and the LLC converter, among others. Soft switching can improve efficiency, reduce EMI, and increase the power density of power converters.

In this project high power factor rectifier is designed based on AHBFC (Asymmetrical half-bridge flyback converter). An AHBFC is a type of dc-dc converter used in power electronics that uses a flyback transformer to convert a dc input voltage to a regulated dc output voltage. The converter consists of a half-bridge circuit, where two transistors are used to switch the current through the primary winding of the flyback transformer. The flyback transformer then stores the energy during the on-time of the transistor and releases it during the off-time of the transistor, allowing for voltage regulation. In an AHBFC, the duty cycle of the two transistors is not equal. This allows for greater flexibility in the design, as it can be used to optimize the converter for a specific load or operating condition. By adjusting the duty cycle of the two transistors, the converter can be designed to achieve high efficiency, low voltage ripple, or a combination of both. An isolated soft-switched high-power factor rectifier based on an asymmetrical half-bridge flyback converter is a type of power electronics topology that combines the benefits of an asymmetrical half-bridge flyback converter with soft switching techniques to improve power efficiency and power factor correction. The converter uses an isolation transformer to provide electrical isolation between the input and output sides of the circuit, and a soft-switching technique to reduce switching losses and improve efficiency. The converter operates by using a half-bridge circuit to control the current through the primary winding of the isolation transformer. The half-bridge circuit consists of two switching devices (usually mosfets or ig-

bts) that are driven by a controller circuit. The controller circuit controls the duty cycle of the switching devices, which determines the voltage and current delivered to the primary winding of the transformer. The asymmetrical duty cycle of the two switching devices is used to achieve ZVS for one of the devices and ZCS for the other device. This reduces the switching losses and improves the efficiency of the converter. The converter also includes a power factor correction (PFC) stage, which uses a boost converter to shape the input current waveform and improve power factor. Overall, the isolated soft-switched high-power factor rectifier based on an asymmetrical half-bridge flyback converter is a powerful and efficient power electronics topology that is commonly used in applications such as renewable energy systems, electric vehicles, and industrial motor drives.

2 Objective

This project presents a novel approach for designing a high-power-factor rectifier using a combination of a DCM-operated Boost input stage and an AHBFC. The converter design procedure takes advantage of the resonant nature of the AHBFC to ensure zero-voltage switching (ZVS) for both switches over the entire input voltage and load range. Additionally, the project proposes a simple feed-forward control scheme that adjusts the switching frequency based on the line root-mean-square (rms) voltage, reducing the need for duty-cycle variation. Overall, this project offers a comprehensive and practical solution for achieving high-power-factor rectification in a variety of applications.

3 Converter Operation

This project presents a novel approach for designing a high-power-factor rectifier using a combination of a DCM-operated Boost input stage and an AHBFC. The converter design procedure takes advantage of the resonant nature of the AHBFC to ensure zero-voltage switching (ZVS) for both switches over the entire input voltage and load range. Additionally, the project proposes a simple feed-forward control scheme that adjusts the switching frequency based on the line root-mean-square (rms) voltage, reducing the need for duty-cycle variation. Overall, this project offers a comprehensive and practical solution for achieving high-power-factor rectification in a variety of applications.

3.1 DCM Boost Analysis

Assuming a constant dc link voltage $v_b(t) \approx V_b$ and a generic switching period within the line half-cycle, the inductor current exhibits a triangular waveform. Three sub-intervals can be identified in relation to the boost cell only. It is worth noting that the subinterval $(1—d_b\text{-}d'_b)T_S$ is a result of the input bridge diodes turning off since the

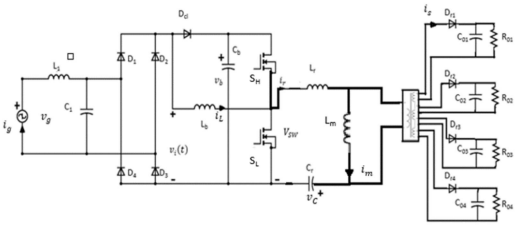

Figure 1. Schematic of high power factor rectifier

boost cell operates using synchronous rectification. This fact carries practical implications that must be considered, including the necessity of utilizing fast input diodes. By defining $m_B = \frac{V_b}{V_{gpk}}$ as the boost voltage gain, it becomes apparent that the following condition must be fulfilled at all times to achieve proper discontinuous conduction mode (DCM) operation of the boost cell:

$$m_b = \frac{V_b}{\sqrt{2}V_g} > \frac{1}{1-d_b} \tag{1}$$

Taking into account the inductor flux balance equation, which states that $|v_g|\, d_b = (V_b - |v_g|)\, d'_b$ the average inductor current within a switching period can be expressed as follows:

$$\bar{I}_L(\theta) = \frac{1}{T_s}\int_0^{T_s} i_L(t)\mathrm{dt} = \frac{d_b^2}{2L_b f_s}\frac{m_B V_{gpk}|\sin(\theta)|}{m_B - |\sin(\theta)|} \tag{2}$$

The average inductor current will be proportional to the input voltage, resulting in a unity power factor only if $m_B \to \infty$. However in all other The average input power is given by:instances, low-frequency distortion arises and the power factor falls below one The average input power is given by:

$$\begin{aligned} P_g &= \frac{1}{\pi}\int_0^{\pi} v_g(\theta)\bar{I}_L(\theta)d\theta = \frac{d_b^2 V_{gpk}^2}{2\pi f_s L_b}\int_0^{\pi}\frac{m_B \sin^2(\theta)}{m_B - |\sin(\theta)|}d\theta \\ &= \frac{d_b^2 V_g^2}{f_s L_b} f(m_B) \end{aligned} \tag{3}$$

with

$$\mathrm{f}(m_B) = \frac{m_B^3}{\sqrt{(m_B^2-1)}}\left[1 + \frac{2}{\pi}\arctan\left(\frac{1}{\sqrt{(m_B^2-1)}}\right)\right] - \frac{2}{\pi}m_B - m_B^2 \tag{4}$$

Upon examining equation (3), it becomes apparent that, as the output power decreases, the duty cycle must be reduced and/or the switching frequency must be increased to preserve the input/output power balance. Another possible

solution would be to increase the boost inductance L_b using a variable inductor arrangement, although this would entail a more complicated inductor construction. When the boost cell is combined with a dc-dc stage, regardless of the topology used, it shares the same control variables, namely duty cycle and switching frequency. However, these control variables are now utilized to regulate the output voltage of the dc-dc stage, leaving the DC link voltage V_b unregulated, which is a function of the converter operating point. Assuming $m_{DC} = V_o/V_b = \mathrm{g}\,(d_c, P_o, f_s)$ as the voltage gain of the dc-dc stage, which can be generally regarded as a function of duty cycle, load, and switching frequency, the combined Boost+dc-dc stage must adhere to the following system of equations:

$$\frac{d_b^2 V_g^2}{f_s L_b} f\left(\frac{V_o}{\sqrt{2} V_g m_{DC}}\right) - \frac{P_o}{\eta} = 0; m_{DC} = g\,(1 - d_b, P_o, f_s) \tag{5}$$

In equation (5), which utilizes the relationship $d_c = 1 - d_b$ and where η represents the estimated overall conversion efficiency, the boost duty cycle d_b, along with the dc link voltage V_b, can be determined for a specific combination of parameters, namely P_o, V_g and f_s.

In contrast to the LLC converter, the voltage gain of the AHBFC increases as the duty cycle d_c is increased. During light-load conditions, the boost duty cycle d_b must decrease to compensate for the reduced power transfer. This results in an increase in the AHBFC duty cycle $d_c = 1 - d_b$, causing a reduction in the dc link voltage ($V_b = V_o/m_{DC}$). This is why the AHBFC cell is connected in parallel to the bottom switch in figure 3.1, rather than the upper switch. Connecting it to the upper switch would result in an unacceptable increase in the dc link voltage during light-load conditions.

3.2 AHBFC Analysis

All figures should be numbered with Arabic numerals (1,2,3. . . .). Every figure should have a caption. All photographs, schemas, graphs and diagrams are to be referred to as figures. Line drawings should be good quality scans or true electronic output. Low-quality scans are not acceptable. Figures must be embedded into the text and not supplied separately. In MS word input the figures must be properly coded. Lettering and symbols should be clearly defined either in the caption or in a legend provided as part of the figure. Figures should be placed at the top or bottom of a page wherever possible, as close as possible to the first reference to them in the paper. The relationships obtained from the volt-second balance of inductors and the charge balance of capacitors under steady-state conditions are expressed as follows:

$$\left\{\begin{array}{c} \bar{v}_c = \bar{v}_{sw} = d_c V_b \quad \text{inductor flux} - \text{balance} \\ \bar{I}_r = 0 \quad \text{resonant capacitor charge balance} \\ \bar{I}_m = n_{21}\bar{I}_s = n_{21} I_o \quad \text{capacitors charge balance} \end{array}\right\} \tag{6}$$

The third equation is a distinctive characteristic of the suggested configuration, resulting from the half-wave rectification process that causes the switched current values to be contingent on the load, thereby influencing the zero voltage switching (ZVS) condition of the switches. The parameters of two distinct resonant tanks are determined by the state of the rectifier diode $\mathrm{D_r}$

$$\left\{\begin{array}{ll} Z_r = \sqrt{\frac{L_r}{C_r}}, \omega_r = \frac{1}{\sqrt{L_r C_r}} & D_r \text{ is } ON \\ Z_{ro} = \sqrt{\frac{L_r + L_m}{C_r}}, \omega_{ro} = \frac{1}{\sqrt{(L_r + L_m) C_r}} & D_r \text{ is } OFF \end{array}\right\} \tag{7}$$

The ratio of inductances, $\lambda = L_r/L_m$, will be utilized in the upcoming explanation. If the voltage fluctuation across capacitor C_r is insignificant, current waveforms that are piecewise linear can be achieved, and the converter is expected to function in continuous conduction mode (CCM). In such a scenario, the AHBFC operates in a manner similar to that of an isolated Buck converter and displays a voltage gain that is proportional to the duty cycle. Specifically, disregarding the brief subinterval $d_f T_s$ illustrated in Fig. 3.2(b), the volt-second balance of the magnetizing inductance can be neglected.

$$\frac{(1 - d_c) V_b}{1 + \lambda} d_c \approx \frac{V_o}{n_{21}} (1 - d_c) \longrightarrow m_{DC}^{\text{ideal}} = \frac{V_o}{V_b} = \frac{n_{21}}{1 + \lambda} d_c \tag{8}$$

A more precise equation, valid for CCM operation is:

$$\boldsymbol{m}_{DC}^{(CCM)} = \frac{V_O}{V_b} = m_{DC}^{ideal} \left(\frac{1}{\frac{d_c(1-d_C)}{k_1} + m_{DC}^{ideal} \frac{k_2}{n_{21}}}\right) \tag{9}$$

with coefficients k_1 and k_2 given by

$$\begin{aligned} k_1 &= \frac{f_s}{\omega_{ro}} \frac{\sin(\beta)(1-\cos(\alpha))}{1-\cos(\alpha)\cos(\beta)} \\ k_2 &= 1 + \frac{n_{21}^2 z_r}{R_o} \left[1 + R_N (1 - d_c)\right] \frac{\sin(\alpha)}{1-\cos(\alpha)} \\ &+ \frac{n_{21}^2 z_{ro}}{R_o} \left[1 - R_N (1 - d_c)\right] \frac{(1+\cos(\alpha))(1-\cos(\beta))}{\sin(\beta)(1-\cos(\alpha))} \end{aligned} \tag{10}$$

In these expressions, $R_N = \frac{R_o}{2 n_{21}^2 L_m f_s}$ is the normalized load resistance, $\alpha = \omega_r (1 - d_c) T_s$, and $\beta = \omega_{ro} d_c T_s$. In the derivation of equation (10), only two approximations have been made: neglecting the subinterval $d_f T_s$ in Fig 3.2(b), and assuming that the waveform of the magnetizing current is precisely triangular.

4 Simulation and Results

The system design, was simulated in Matlab-Simulink due to Matlab's extensive capabilities, Simulink integration, specialized toolboxes and customization options. The simulation parameters are mentioned in table 1.

Parameter	Value
Input Voltage,	230V
Input Inductance,	1mH
Input Capacitance,	50
Boost Inductance,	0.1mH
Boost Capacitance,	50
Resonant Inductance,	0.01mH
Resonant Capacitance,	2
Magnetizing Inductance,	55
Output Resistance,	160Ω
Output Capacitance,	200
Transformer Turns ratio,	1:5

Table 1. Simulation Parameters

4.1 Simulation Diagram and Simulation Results

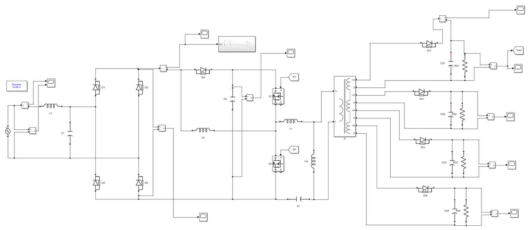

Figure 2. Main Simulation Diagram

The simulation diagram includes input from a AC supply. First stage is rectification of the input voltage using diode rectifier. Next is the Boost Converter followed by AHBFC converter. Closed loop is achieved using PI controller.

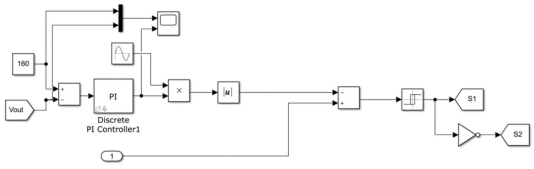

Figure 3. Control Block Diagram

The output voltage is compared with a reference voltage of 160V in the control block diagram shown in figure 3. The switching pulse is produced by the PI controller.

The input voltage can be obtained by connecting a voltage source across the input supply and the input current can be obtained by connecting a current source in series with the input supply. The input voltage and current waveforms are shown in figure 4.

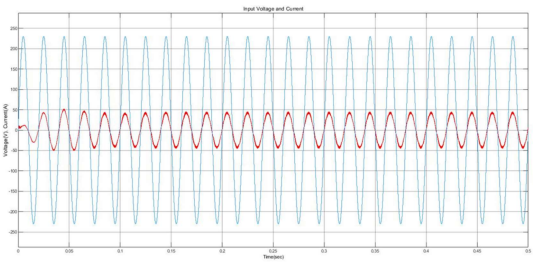

Figure 4. Input voltage and current waveforms

Output voltage is taken across the load resistor. An output voltage of around 155 V to 165 V is obtained in figure 5. The output current waveform is shown in figure 6.

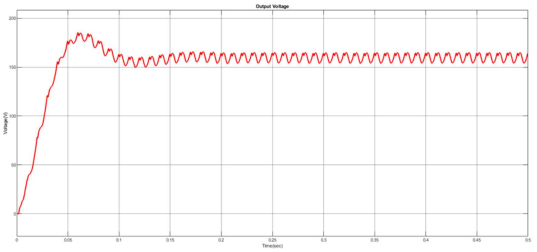

Figure 5. Output voltage waveform

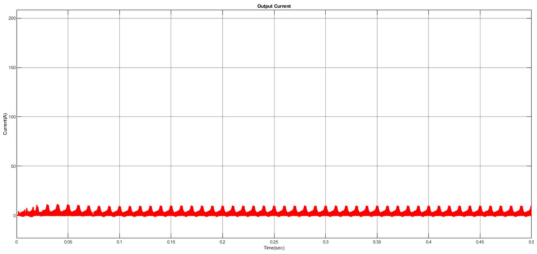

Figure 6. Output current waveform

5 Hardware Implementation

5.1 Hardware Parameters

The components utilized to actualize the hardware segment of the high power factor rectifier project are MOSFET, Inductor, Capacitor, Diode, Transformer, ,Resistors, Microcontroller, TLP 350

Parameters	Values
Input Voltage	24V
Inductors	1mH,0.1mH,0.01mH
Capacitors	470µF 25V,10µF 63V,4.7µF 63V(3),100µF 160V,220µF 250V(2)
Load Resistors	1kΩ(2)
Mosfets	IRF840,IRF440
Diodes	BY399(7),IN4007(5)
Resistors	4.7 kΩ(7),560 Ω(2),2.7 kΩ(1),100 kΩ(1)
Microcontrollers	DSPIC30F2010(1)
IC	TLP350(2) , LM358(1)
Transformer	EI 33 Ferrite Core
LCD Display	16*2(1)
Output Voltage	135V,220V

Table 2. Hardware Parameters

5.2 Prototype Implementation

The whole circuit is integrated into a single board. The input 24V for the converter is provided from a transformer. The input to the driver circuit and microcontroller circuit is provided by the rectification of input AC voltage. The input voltage from transformer is rectified and applied to TLP350 circuit and Microcontroller circuit. LM358 IC is used for ZCS detection. The main converter is designed in two separate boards. An input of 24 V AC is applied to the EMI filter. This voltage is rectified and applied to the boost cell. The output of the boost cell is connected to the AHBFC stage. By making use of a transformer multiple output can be obtained.

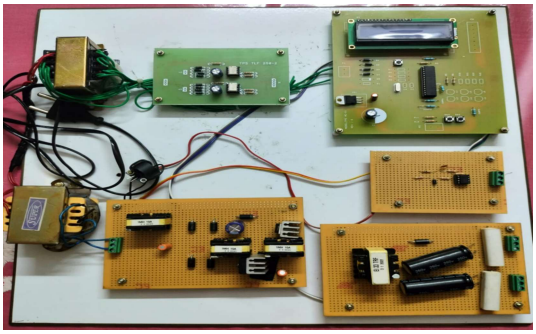

Figure 7. Prototype

6 Results

The circuit can be switched on by connecting the wire. Output voltage 1 can be obtained by connecting the DSO probes across load resistor 1. The output voltage 2 can be obtained by connecting the DSO probes across load resistor 2. Output voltage of around 135 V and 226 V is obtained in figures 8 and 9 respectively.

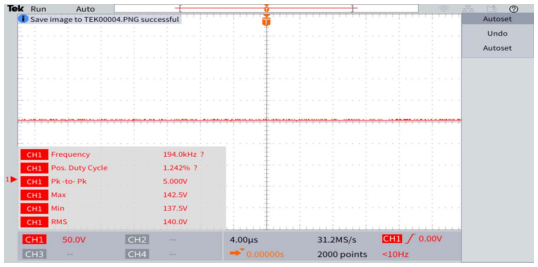

Figure 8. Output Voltage 1

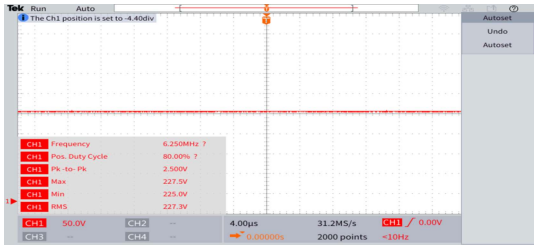

Figure 9. Output Voltage 2

7 Conclusion

This project work presents a thorough examination of a high-power-factor rectifier that merges a DCM operated Boost input cell with an AHBFC. Its key contributions include: 1) a meticulous design procedure that utilizes the resonant nature of the AHBFC stage to compute all converter parameters, while guaranteeing zero-voltage-switching turn-ON for the switches within the designated input voltage and load ranges; 2) a digital control strategy that combines feedforward-feedback techniques to leverage both duty-cycle and switching frequency control parameters; and 3) the exploration of a specific kind of input current crossover distortion triggered by the DCM operation of the boost input cell. The validity of the theoretical analysis is confirmed through experimental results. The advantages of a high power factor rectifier based on an asymmetrical half-bridge flyback converter include improved power factor, compact size, simplified design, reduced switching losses, high voltage conversion ratio, output voltage regulation, and cost-effectiveness. These benefits make it a suitable choice for various applications, including power supplies, LED lighting, renewable energy systems, and more.

Acknowledgements

Ack I wish to record my indebtedness and thankfulness to all those who helped me to do this project titled "Isolated soft switched high power factor rectifier with multiple outputs ". First and foremost, I thank God Almighty for His providence and for being the guiding light throughout the Project. I express my gratitude to our honorable Principal, Dr. Suresh P R and Head of the Department Dr. Saju Narendran for making the project a successful one. I would like to thank my guide Dr. Saju Narendran without their help I would have been far from completion of this project. I also thank my staff in charge and all other faculty members in our department for the help they had extended. This acknowledgement will stand incomplete if my parents and friends are not thanked, whose constant encouragement and moral support have helped me to a great extent and was the fuel of my determination.

References

[1] MD. D. Lu, H. H. Iu, and V. Pjevalica, "Single-stage AC/DC boost-forward converter with high power factor and regulated bus and output voltages," IEEE Trans. Ind. Electron., vol. 56, no. 6, pp. 2128–2132, Jun. 2009.

[2] S. Lee and H. Do, "Boost-integrated two-switch forward AC–DC LED driver with high power factor and ripple-free output inductor current," IEEE Trans. Ind. Electron., vol. 64, no. 7, pp. 5789–5796, Jul. 2017.

[3] H. Ma, Y. Ji, and Y. Xu, "Design and analysis of single-stage power factor correction converter with a feedback winding," IEEE Trans. Power Electron., vol. 25, no. 6, pp. 1460–1470, Jun. 2010.

[4] A. Abasian, H. Farzaneh-fard, and S. Madani, "Single stage soft switching ac/dc converter without any extra switch," IET Power Electron., vol. 7, no. 3, pp. 745–752, 2014.

[5] A. Abasian, H. Farzaneh-fard, and S. Madani, "Single stage soft switching ac/dc converter without any extra switch," IET Power Electron., vol. 7, no. 3, pp. 745–752, 2014.

[6] S. Lee and H. Do, "A single-switch AC-DC LED driver based on a boost-flyback PFC converter with lossless snubber," IEEE Trans. Power Electron., vol. 32, no. 2, pp. 1375–1384, Feb. 2017.

[7] C. Lai, R. Lee, T. Wang, and K. Shyu, "Design and implementation of a single-stage llc resonant converter with high power factor," in Proc. IEEE Int. Symp. Ind. Electron., 2007, pp. 455–460.

[8] C. M. Lai and K. K. Shyu, "A single-stage AC/DC converter based on zero voltage switching LLC resonant topology," IET Electric Power Appl., vol. 1, no. 5, pp. 743–752, Sep. 2007

SOLAR-POWERED BICYCLE TEASHOP

Aneesh M[1], Deepika R [2], Diya Das[3], Saranya P[4] and Lekshmipriya J[5]

[1,2,3,4,5] Instrumentation and Control Engineering NSS College of Engineering Palakkad, India

[1]aneeshmuralinssce@gmail.com, [2]deepikarajendran212@gmail.com [3]diyadas200144@gmail.com
[4]saranyacheriyodath5@gmail.com [5]lekshmipriyaj@nssce.ac.in

Abstract -

The solar-powered bicycle teashop utilizes solar energy to power its battery and motor, and excess solar energy can be used for cooking. By promoting solar cycling and cooking, it is possible to reduce carbon dioxide emissions and fuel costs. Additionally, solar cooking can help to reduce the risk of respiratory diseases caused by smoke from traditional wood- burning stoves. The average speed of the cycle ranges between 12to 15 km/hr, making it an affordable and practical alternative. India's abundant sunny climate makes it an ideal location for solar bicycle teashops as a sustainable alternative to traditional fuel-based vehicles and cooking stoves.

Keywords -

Solar-powered bicycle, sustainable, MPPT, Solar cooking, Solar panels, Eco-friendly, Clean energy

1 Introduction

The need for clean energy sources is one of the greatest engineering concerns to be tackled. Our world is highly depen- dent on coal and natural gases for the production of electricity. Even if these power sources are abundant, they assist in global warming. Also, the methods used for extracting such fuels have a detrimental effect on our environment. Fossil fuel vehicles also emit carbon and create pollution. The traditional stoves which use wood as fuel emit smoke that can lead to many chronic respiratory diseases and stoves which use CNG as fuel are too costly. So, all these types of energy sources should be replaced. As solar energy is easily available and efficient it can be seen as a feasible option to replace energy obtained from fossil fuels. Also advances in materials used for solar energy conservation have laid the foundations for using solar energy as a renewable resource that can meet the energy demands that society has become adapted to. The project focuses on the construction of a solar-powered Bicycle. The cycle runs with the help of solar energy obtained using solar panels as well as the stored pedaling energy. The outgoing solar energy is also used for cooking and operating the teashop. This idea lies in its combination of several concepts, such as sustainability, mobility, and entrepreneurship. By using a solar-powered bicycle, this teashop concept also promotes environmental sustainability by reducing carbon emissions and reducing dependence on non-renewable energy sources.Additionally, it offers a unique and mobile experience that allows the tea shop to move around to different locations and cater to different audiences.

2 Objective

There are three objectives for this initiative that include making a hardware model of a bicycle that has onsite charging ability and can be powered by both solar and manual pedaling energy with the intention to reduce environmental pollution. The next one is to manage power consumption using solar renewable energy, store the power gained in a rechargeable battery, and maximize the utilization of the sun by tracking the sunlight during the day. The last objective is to use the ongoing solar energy for cooking and operating the teashop

3 Purpose

3.1 To reduce carbon emissions created by fossil-fueled vehicles.

The purpose of using a solar bicycle to reduce carbon emissions created by fossil-fueled vehicles is to promote sustainable and environmentally-friendly transportation. Solar bicycles use clean, renewable energy from the sun to power the electric motor that drives the bicycle, which means they do not emit any carbon dioxide or other harmful pollutants that contribute to climate change and air pollution.

3.2 To reduce the detrimental effect on the environment due to the extraction of Fossil fuels.

Solar bicycles offer a solution to reduce the negative impact on the environment caused by the extraction and combustion of finite resources such as coal, oil, and gas. The extraction process and usage of these resources lead to environmental degradation through air and water pollution, habitat destruction, and greenhouse gas emissions that contribute to climate change. In contrast, solar bicycles rely on renewable energy from the sun to operate their

motors, thereby providing a cleanand sustainable form of transportation.

3.3 To reduce the use of traditional stoves

Solar cooking is employed as an alternative to conventional wood stoves in developing countries to decrease the reliance on biomass fuels like wood, charcoal, and animal dung for cooking and heating. The usage of such fuels in traditional stoves leads to the emission of dangerous smoke and pol- lutants like carbon monoxide, volatile organic compounds, and particulate matter, which contribute to various respiratory illnesses such as asthma, pneumonia, and chronic obstructive pulmonary disease (COPD). By using solar energy to prepare food, solar cooking eradicates the necessity for biomass fuels, thereby reducing the health risks associated with their usage.

4 Literature review

The paper [1] proposes a design for a bicycle that uses two batteries, with the ability to run on one battery while charging the other. Another paper [2] explores the idea of using longer tires to improve the bike's ability to absorb impacts from the road. Additionally, a power lock that requires a key and a battery charge indicator are suggested in paper [3]. As discussed in paper [4], the Solar Powered bicycle can travel at an average speed of 15 km/hr in the absence of pedalling and at a speed of at most 25 km/hr with pedalling. According to the research paper [5], the MPPT based Solar Charge Controller works better and optimizes the battery charging. The average output power values of MPPT and PWM are 38.89 watts and 29.92 watts respectively. The journal paper [6] states that there are two stages for the system; the "boost stage" is used to boost voltage from the Solar panel and the "inverter stage" which converts DC to AC. A low-power and high-efficiency based stand - Solar Electric Cookstove can be designed, consisting of an efficient Cookstove, a solar panel, battery, charge controller, inverter, and essential electrical controls. It meets the requirements of heating, over-temperature control and insulation. These are the main aspects that have been discussed in paper [7]. Journal paper [8] tells that the specifications of the battery used are 12V, 24AH, and only two panels of 20V, 50W are used to obtain the desirable output. The system has the ability to operate smoothly for over 12 hours and can continue to run for an additional 4 hours using stored energy. This means it can function continuously for more than 16 hours. A research paper [9] reports that the maximum temperature reached by the cooker when it is not loaded is 250°C. The paper also mentions various types of panel cookers such as polyhedral, semi-cylindrical, bi-rectangular, and parabolic. Another research paper [10] describes the impact of vehicle direction, panel tilt, partial shading on solar generation, etc., and concludes that a low- cost SEV has real advantages for the power grid, driver, and environment. The primary idea presented in paper [11] is to enhance the safety of bikers by utilizing a GPS tracker device that can be fixed on the top tube of the bicycle. The device includes an Arduino-based microcontroller, a standalone GPS smart antenna chip, and a transceiver. According to the article [12], the glow plug consists of two types of coils: the heating coil and the regulator coil. The heating coil heats up to a specific temperature of around 900°C, and the regulator coil assists in maintaining the high temperature. The research paper [13] employs the perturb and observe technique to achieve maximum power point tracking in photo- voltaic panels. This method is grounded on the mathematical equation that represents the condition for maximum power, which states that dp/dv=0. When the PV panel operates to the left of the maximum power point, power increases, and when it operates to the right of the MPP, power decreases with decreasing voltage. The perturbation should be adjusted depending on the value of dp/dv. If dp/dv is greater than zero, then the perturbation should remain the same, and if dp/dv is less than zero, the perturbation should be reversed. The process should be repeated until dp/dv equals zero. The journal paper [14] states that the angle at which solar panels are mounted on rooftops or on the ground depends on the latitude of the location. For instance, the ideal angle for Kolkata, India, is around 22 degrees from the horizontal. However, this elevation angle may not be optimal for solar panels mounted on moving vehicles, as it could reduce energy yield during certain times of the day. To address this issue, it is recommended to mount the top panel without any elevation angle or with a small angle of 10 to 15 degrees. The back panel, on the other hand, should be mounted at an angle of 10- 15 degrees to allow air to pass through and reduce drag. The research paper [15] states that the use of bicycles is recognized as a healthy, efficient, and eco-friendly mode of transportation that can be faster than driving in some areas. The paper outlines the creation of an electric motor drive for a motorized bicycle using readily available commercial components. The paper proposes an electric propulsion system utilizing a BLDC motor equipped with sensory speed control to achieve a smooth operation. The system's efficiency could be enhanced by utilizing renewable energy sources such as solar power, which would contribute to a safer driving environment and a better world overall.

5 Methodology

5.1 Design of the solar-powered bicycle

Solar panels convert the sun's energy into electrical energy by using multiple photovoltaic cells to generate DC electricity. To ensure maximum sunlight exposure, the

panels are mounted on the bicycle frame. The solar charge controller regulates the solar panel's current and voltage, efficiently and safely charging the battery. The battery, which is typically a deep cycle battery designed for repeated discharge and recharge, stores the DC electricity generated by the solar panel and providesa constant supply of power to the system, even when sunlight is not available. The motor, which is powered by the battery, supplies the necessary power to the bicycle wheel to propel it in the desired direction. The motor's type and power rating depend on the weight of the rider and the terrain on which the bicycle will be used. The bicycle wheel is connected to the motor and rotates to move the bicycle forward.

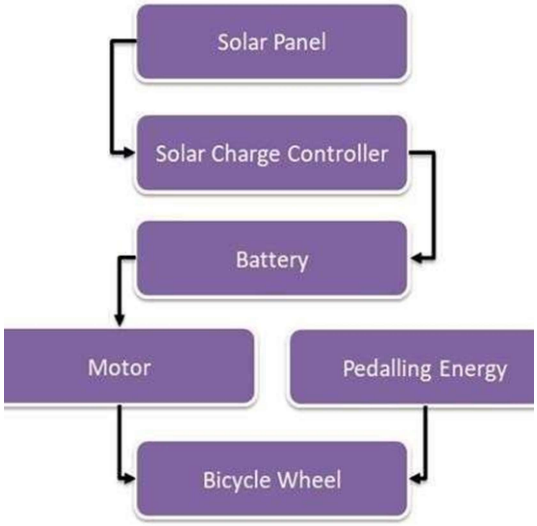

Figure 1. Methodology for Design of Solar Powered Bicycle

The bicycle can also be operated by pedaling, using the stored pedaling energy. It is essential to choose a battery with a suitable capacity for the motor's power requirements and the distance to be covered by the bicycle. The solar charge controller prevents overcharging of the battery and extends its life.

5.2 Usage of solar energy for cooking

The solar panel is the main component of a solar power system that captures sunlight and converts it into electrical energy. It is made up of multiple photovoltaic cells that generate DC electricity when exposed to sunlight. The charge controller is an electronic device that regulates the amount of current and voltage that is sent to the battery from the solar panel. It ensures that the battery is not overcharged or undercharged, which can damage the battery and reduce its lifespan. The battery stores the DC electricity generated by the solar panel and provides a steady supply of power to the system even when the sun is not shining. It is typically a deep- cycle battery, designed to be discharged and recharged repeatedly. The battery provides power to the inverter which converts the DC electricity to AC for use to power the heating element. A heating element is an appliance that converts electrical energy into heat energy. In this system, a heating element is used as an example of an appliance or device that requires AC power to operate.

6 Implementation scope

The implementation scope of a solar-powered bicycle teashop will depend on various factors such as the intended

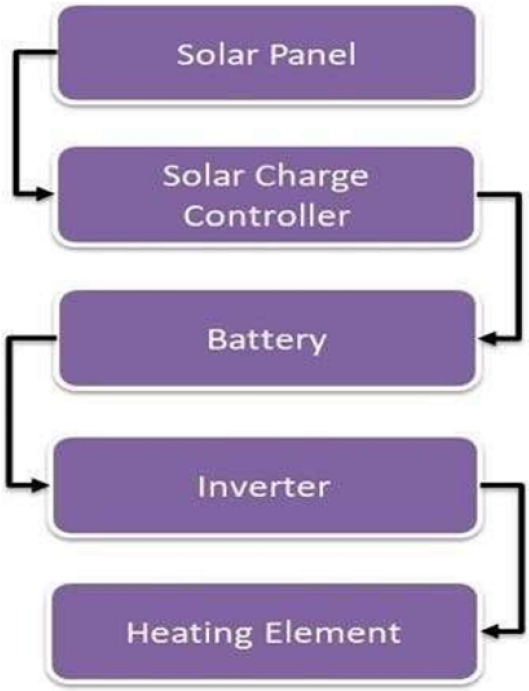

Figure 2. Methodology for Usage of Solar Energy for Cooking

location, target audience, budget, and resources available. However, here are some general considerations that may help determine the implementation scope: Business plan: Developing a detailed business plan is essential to determine the feasibility of the project and outlinethe scope of implementation. The plan should include market research, a financial analysis, marketing strategies, and operational details. Legal requirements: It is important to research and comply with all legal requirements and regulations for starting a teashop, such as permits and licenses, food safety regulations, and zoning restrictions.

Solar power system: The implementation scope will include the design and installation of the solar power system, which should be based on the estimated energy needs of the teashop, the available sunlight in the location, and the budget. Bicycle modification: A bicycle will need to be modified to accommodate the teashop equipment and solar panels, which will require expertise in bicycle mechanics and design. Equipment and supplies: The implementation scope will includeselecting and sourcing equipment and supplies such as a tea brewing system, cups, saucers, napkins, and other necessary items. Staffing: The implementation scope will include hiring and training staff to operate the teashop, handle customer service, and prepare and serve tea and other beverages. Marketing and promotion: The implementation scope will include developing a marketing and promotion strategy to attract customers, such as social media advertising, flyers, and partnerships with local businesses and events.

Figure 3. SOLAR-POWERED BICYCLE TEA SHOP

7 Result

Made a hardware model of a bicycle that has onsite charging ability and can be powered by both solar and manual pedaling energy with the intention to reduce environmental pollution manage power consumption using solar renewable energy, store the power gained in a rechargeable battery, and maximize the utilization of the sun by tracking the sunlight during the day. The solar energy was also utilized for cooking and for operating the teashop

8 Conclusion

A solar-powered bicycle teashop has been presented as an innovative solution to promote sustainable energy and eco- friendly business practices. The paper has discussed the design and implementation of the bicycle and teashop using solar powered system. The solar-powered bicycle teashop is a novel approach that combines mobility, sustainability, and entrepreneurship. It is an excellent example of how small businesses can leverage renewable energy to reduce their carbon footprint and operate in an environmentally conscious manner. The teashop can be used as a model for other businesses looking to incorporate renewable energy and sustainable practices into their operations. In addition to its environmental benefits, the solar-powered bicycle teashop also has economic and social benefits. It provides a platform for entrepreneurship, creates job opportunities, and brings people together over a cup of tea. The teashop also serves as an educational tool for promoting sustainable energy and raising awareness about environmental issues. Overall, the solar-powered bicycle teashop is a promising solution for sustainable business practices and renewable en- ergy promotion. Its design and implementation can serve as a model for future similar endeavors, and it is a valuable addition to the field of sustainable energy and entrepreneurship.

References

[1] Ajmayen Fayek, Shah Md. Salimullah,Md. Shadman Hasan Shakib,Ariful Islam Anik,Moynul Hossen Khan," Wind and Solar Powered Bicycle: Lessening the Dependency over Grid Electricity", 30 January 2020 IEEE

[2] Christen Roger, Hamid El Omari, "Solar-E-Cycles, Empowering People Project 2014-2019", 27 April 2020 IEEE xplore.

[3] P Rampulla Reddy; K.S Shivani Gowda; S Charitha; R. Mahalakshmi, "Review and Redesign of Pedal Energy - Solar Power Augmented Hybrid Bicycle" 06 October 2020 IEEE.

[4] T. Suresh, T.D Subha, C.Surendra Kumar, T.D Subash"A study of novel technique - solar powered bicycle" Volume 43, Part 6, Pages 3595- 3602, ScienceDirect 2021.

[5] Lorenzo Stilo, Diana Segura-Velandia, Heinz Lugo, Paul P.Conway, Andrew A.West, "Electric bicycles, next-generation low carbon transport systems: A survey", Transportation Research Interdisciplinary Perspec- tives, Volume 10, June 2021,100347.

[6] Jagmohan Singh, Pritpal Singh, "Solar Electric Cookstove - A First Gen- eration, High-Efficiency Solar Electric Cooking Device Prototype",2019 IEEE.

[7] Sundaram. R Meenakshi; S Lokesh; S Sundaramahalingam," Solar Powered Induction Cooking System", 2019 IEEE.

[8] Mohamad Aramesh, Mehdi Ghalebani, Hosein Zamani, Giulio Lorenz- ing, Omid Mahian Somchai Wongwises," A review of recent advances in solar cooking technology", Renewable Energy Volume 140, Pages 419- 435, ScienecDirect September 2019.

[9] Aurora, Fathkur Rohman, Elka FaizalMuhamad," The Design And Performance Investigation Of Solar E-Bike Using Flexible Solar panel By Different Battery Charging Controller", Vol. 10, Issue 3, Jun 2020, 14431–14442.

[10] Chia-Chen Lin, Ying-Chuan Lai, Chih-Chiang Wang, Liren Tsai, Jing-Wein Wang, "Development and Implementation of Solar-Assisted Elec- tric Bicycle with GPS Tracking Service over Cloud", 2019 IEEE.

[11] Bayram Akdemir, Bayram Volkan reisoglu, "A Novel Glow Plug Design to Improve Heating Capability via Induction Heating",Vol. 6 Issue2,pp 85-94, IEEE 2019.

[12] Arghya Saha,Fahmida Sulthana, Md.Asrarul Haque, Dr. S.M Nasif Shams, "Design of MPPT mounted Solar Based Double Coil DC Electric Cooker With Smart Temperature Control Device",2019,ICAEE.

[13] Indrashis Halder,Dipanakar Dcbnath,Tanmoy Roy Choudhury, "Design of a Battery Charger Fed from Two Solar Panels Arranged at Different Inclination for E-rickshaw and DC Microgrid Applications", ICPEE- 2021.

[14] C.Sivapragash,c.Shankar,M.Nageena,B.Reetha Devi,K.Kiruthiga, "An innovative solar powered electric bicycle, ICON-STEM 2015.

Design of a Smart Car

Abitha Aravindan[1], Adersh Babu[2], Arun C Abraham[3], Shijil M S[4] and Dr. Anish M N[5]

[1,2,3,4,5] Dept. of Instrumentation and Control Engineering, NSS College Of Engineering Palakkad

[1]abithaaravindan22@gmail.com, [2]adershbabuo16@gmail.com [3]aruncabraham2020@gmail.com [4]shijilms2001@gmail.com [5]anishmn@nssce,ac.in

Abstract -

Vehicles are the key factor for transportation. The safety of the people inside the vehicle should be the primary concern of vehicle manufacturer. In this current era, different technologies are implemented in automobiles, that ensures safety and comfortable to the users. By designing a smart car, the main intentions are to provide safety to the passengers and to reduce accidents. Accidents happens by the careless driving, improper behaviour of vehicle modules. In this project there are different modules, alcohol detection and fine reporting, automatic light dimming system, driver drowsiness detection, speed control. Most of the technologies already exist. Constituting different technologies helps to make the system more efficient. In this project, the data collected by using corresponding sensors and manipulated the signals according to the measurements. Controlling unit is based on micro controller. Various controller units such as Arduino Uno, Raspberry Pi are available. The controlling unit can handle the process in control within few seconds and can make it economical. Index Terms—smart car, alcohol detection, drowsiness detection, light dimming, adaptive cruise control.

Keywords -

smart car, alcohol detection, drowsiness detection, light dimming, adaptive cruise control.

1 Introduction

The primary intention of a car is to make transportation. But nowadays it is giving more importance to comfortable and safe travelling experience. According to the study report, there are lot of reasons for accidents. Drunken driving, malfunction of vehicle parts, improper organization of roads and so on. The importance of designing a smart car is very high in this scenario. Selecting common reason for accidents and building new system for preventing that constraint causing accidents. Accident rate due to drunken driving is always a headache. In order to overcome the issue, an alcohol detection system and giving corresponing alerts. Drowsiness detection module is also added to itso that accidents due to carelessness can be reduced. An- other problem in urban area is the accidents due to speed. This project includes solution to this problem which is byadjusting the speed by detecting the obstacles around it. It can reduce the accident rate. When there is a situation, a vehicle which approaches with full intensity light or dur-ing night travel there may be situations like no need of headlights under street lights. Under such circumstances if it is possible to decrease the intensity of head light it will be helpful for the reduction of accidents due to splash of light and also for energy saving. Hence updates are made with-in these objectives. This work tends to make this system with more economical and cost-efficient ways.

2 Objectives and Purposes

2.1 Objectives

1. To detect the presence of alcohol and to impose corresponding penalty.
2. To design and implement automatic speed control and breaking.
3. To design and implement automatic light dimming system.
4. To detect drowsiness of drivers.
5. Cruise control.

2.2 Purposes

1. To reduce to drunken driving tendency and impose people to follow the rules.
2. To reduce the accidents.
3. To create comfortable driving experiences and reduce consumption of energy.
4. To provide safe driving experience.
5. Accident prevention.

3 Methodology

The detailed methodology of the project is described below. It includes four units. Alcohol detection unit, light dimming unit, drowsiness detection and automated braking system.

3.1 Alcohol detection and penalty imposing

Alcohol detection is done by using MQ-3 sensor. The signal corresponding to the measurement is transferred to control unit. When presence of alcohol is detected, the signal is transferred to the ignition locking unit and the data trans- mission unit. The ignition locking unit consists of the motor driving IC which on receiving high signal (which indicates the absence of alcohol) will enable the IC. When the presence of alcohol is detected, the signal is transmitted to the server which includes the basic details of the vehicles which helps in calculating the penalty. When the alcohol presence is detected, ESP8266 Wi-Fi module sends data to the specific channel that hold by 'thinkSpeak' IoT server. Figure 1 shows the block diagram represen- tation of Alcohol detection and penalty imposing system.

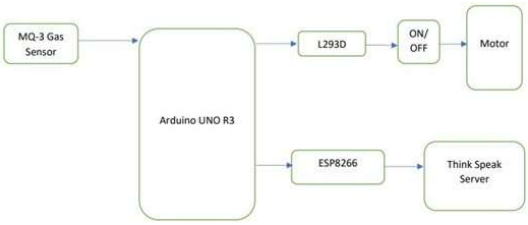

Figure 1. Alcohol Detection and Penalty Imposing System

3.2 Driver drowsiness detection

Drowsiness detection can be done by measuring heart pulse rate, forces on the hand palm, and analysing char- acteristics of eye. Here drowsiness is detecting by using eye blinking sensor (IR based). The infrared waves that are transmitted to our eyes by the IR transmitter. The infrared photons that are reflected from the eye are collected by the IR receiver. The output of an IR receiver is higher when the eye is closed because light rays are not reflected off the eye, but it is lower when it is open. This is done in order to determine if the eye is closed or open. The alarm and igni- tion locking system are controlled by the microcontroller using this output. Consequently, drowsiness detection is accomplished via an eye blink sensor, and the microcon- troller then issues an auditory alarm, which causes the carto stop. The basic diagram for the drowsiness detection system is shown in Figure 2.

3.3 Automatic light dimming system

In this design, LDR is used for measuring light inten- sity. LDR stands for Light Dependent Resistance / Photo Resis- tance, it measures intensity of light. When light is

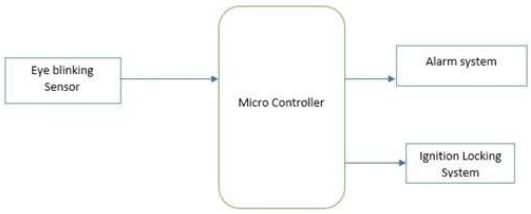

Figure 2. Driver drowsiness detection unit

absent the resistance value of the LDR is very high. The reduction of the light is happens when the LDR sensor is exposed to the light. Characteristics of LDR with light intensity is shown below. In this unit, arduino UNO is used for controlling purposes. There is two way of getting

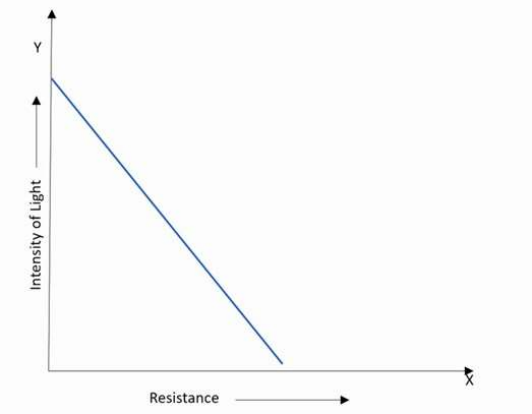

Figure 3. Characteristics of LDR

signals. One is digital and another one is analog. Here using analog siganl, because the intensity level of light is the primary concern. In arduino UNO, there is six analog pins are present. Using one of those pins and using a 1 K ohm resistor to read the analog value according to the intensity of the light. The block diagram representation of automatic light dimming unit is shown in figure 4. Auto- matic light dimming units control the intensity of the head lamp of the vehicle. The dimming process achieved by switching off the bright light.

Relay is used as a switch to control the bright light. Presetting a set point of light intensity in arduino code. If the light intensity become high, then the resistance value of LDR become minimum and also the analog value become maximum. And vice versa. The relay switch become normally open, when the analog value become higher than the set point. And the relay switch become normally open, when the analog value become lower than set point.

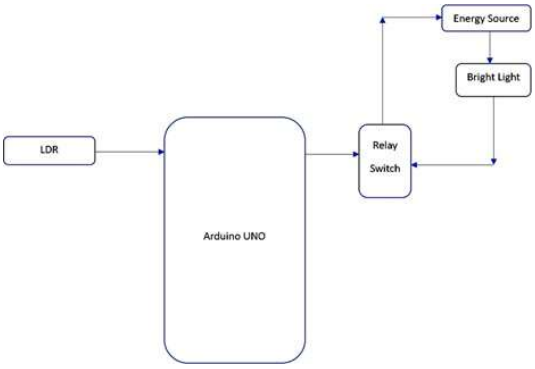

Figure 4. Block diagram for automatic light dimming unit

3.4 Automatic Speed Control and Speed Limit Unit

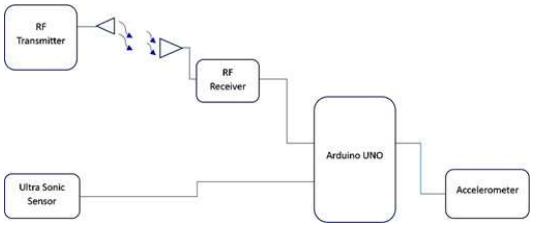

Figure 5. Block diagram of automatic speed control and speed limit unit

3.5 Adaptive Cruise Control: Accident Alerting Unit

In this unit, the primary sensing unit is Piezo-electric sensor. It produces a proportional signal when crash occurs. Arduino UNO is connected with the sensor to process the required signal. When the sensor generates signal, the unit will dispatch the current location to the pre-planned hospitals. The communication is designed through GPS module. It sends message to the desired location. The value form the sensor will taken as analog, because analog value will give the exact measure of crash intensity. The controlling and transmission unit should be protected. Because all the action is dependent on these unit.

4 Images

This project consist of different working units such as alcohol detection and penalty imposing unit, driver drowsiness detection, speed limit and speed control, and automatic light dimming unit. For each unit, there is separate circuit diagram and those hardware implemented in a unite.

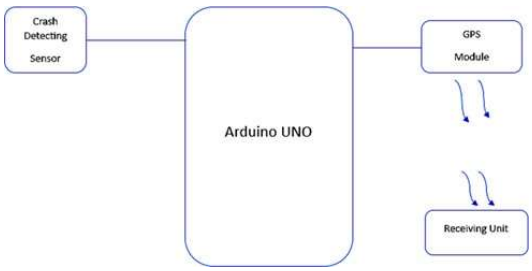

Figure 6. Block diagram of Adaptive Cruise Control: Accident Alerting Unit

4.1 Circuit Diagram

.

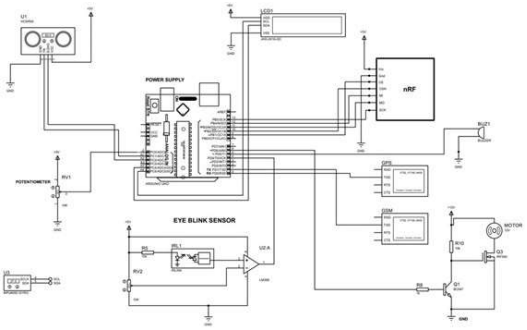

Figure 7. Vehicle Unit

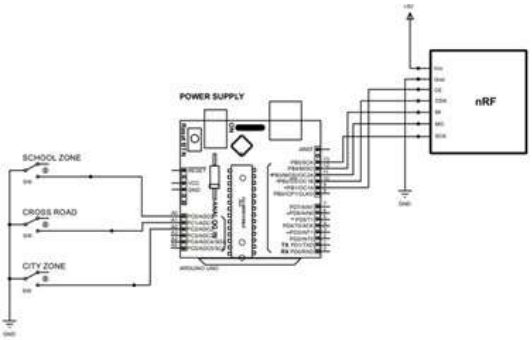

Figure 8. Transmitter Unit

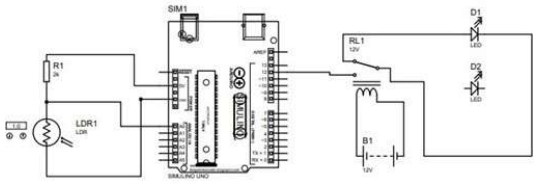

Figure 9. Automatic Light dimming unit

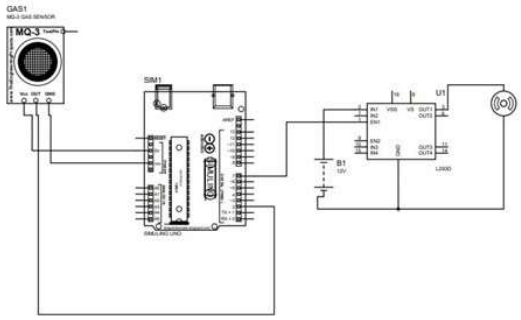

Figure 10. Alcohol detection and penalty imposing unit

4.2 Real- time Image

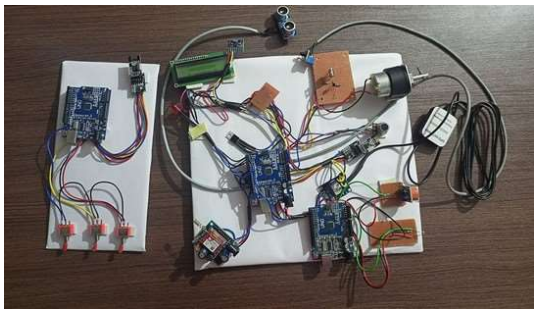

. Figure 11. Real-time Image of Project

5 Conclusion

The increasing population and innovation of new technology demands new trends in the vehicle industries. Thi technology would have a promising future when more electro-mechanical safety enchantments are produced for the vehicle industry. With this project eliminating the major causes to accidents is of prime importance. Alcohol detection and penalty imposing system, drowsiness detection, automatic speed control, auto- matic light dimming and cruise control are incorporated which will help to reduce the causes of accidents.

References

[1] Al-Youif, S., Ali, M. A., Mohammed, M. N. (2018, April). Alcohol detection for car locking sys- tem. In 2018 IEEE Symposium on Computer Ap- plications Industrial Electronics (ISCAIE), (pp. 230-233). IEEE.

[2] Das, R., Chattopadhyay, O., Biswas, P., Das, M., Chatterjee, S., Paul, A. (2020). Intelligent alcohol detection system for car drivers. Proceedings of In- dustry Interactive Innovations in Science, Engineer- ing Technology (I3SET2K19), (pp. 1-9).

[3] Gasparesc, G. (2018). Driver alcohol detection system based on virtual instrumentation. IFAC-PapersOnLine, 51(6), (pp. 502-507).Research 4; PP258-266; 2013.

[4] Hassan, S. A., Iqbal, S. (2019, November). Automatic car braking system using fuzzy logic controller with environmental factors. In 2019 22nd Interna- tional Multitopic Conference (INMIC), (pp. 1-8). IEEE.

[5] He, X., Wang, H., Cao, J., Lei, D. (2020, June). De- sign of High-power LED Automatic Dimming Sys- tem for Light Source of On-line Detection System. In 2020 IEEE 5th Information Technology and Mecha- tronics Engineering Conference (ITOEC), (pp. 1487- 1491). IEEE.

[6] Kommey, B., Tamakloe, E., Nunoo-Mensah, H., Opoku, D. (2022). Smart vehicle ignition interlock: A car ignition interlock device for alcohol impaired. Proceedings on Engineering, 4(1), (pp. 51-62).

[7] Pal, S., Bhaskaran, S. (2020, July). Arduino based Conventional Head- light with Multi Trait. In 2020 International Conference on Electronics and Sustain- able Communication Systems (ICESC), (pp. 1039- 1044). IEEE.

[8] Rezwan, M. S., Islam, M. A., Islam, M. M., Hasan, M. R. (2018, April). Vehicle Breaking Support Sys- tem. In 2018 3rd International Conference for Con- vergence in Technology (I2CT), (pp. 1-4). IEEE.

Advanced Helmet for Two Wheelers

Praveena A R[1], Swathi Krishnanunni[1], Vrinda V[1], Kiran R Nair[1] and Lekshmipriya J [2]

[1] Student,Department of ICE NSS College of Engineering Palakkad, India
[2] Asst.Professor, Department of ICE NSS College of Engineering Palakkad, India

Abstract -

The purpose of this technology is to give motorcycle riders a smart helmet with better safety features. The helmet has a number of advanced features built in, such as impact detection and an alert system.Motorcycles, often known as two-wheelers or motorbikes, are used more frequently than other kinds of vehicles because they are more affordable. However, this is the most dangerous vehicle. Speeding and drunk driving are two factors that might lead to accidents. Safety and security are the main concerns of everyone while they are in an automobile. Due to the remarkable rise of transportation networks, Road safety and bike security, which now also include two-wheeled vehicles and the growing urbanisation, are unavoidable issues for us. Accidents occur more frequently now, resulting in greater damage and fatalities. In many cases, we are unable to determine where the accident occurred. A type of safety attire worn to shield the head from harm is a helmet. The helmet primarily helps the skull protect the brain. A smart helmet can locate the scene of an accident, which can help save lives and make two- wheeler driving safer than it was in the past. Here, we suggest using an intelligent helmet system to prevent accidents. When an accident occurs, the system notifies the emergency contacts via a database. Only when both drivers are wearing helmets and there is no sign of drinking do vehicles start. Force-sensing resistors are used to detect two wheelers with three or more occupants. Speed reduction and accident reduction are both aided by speed optimization.

Keywords -

Helmet, Accident detection, Overload, Alcohol detection

1 Introduction

Everywhere in the world, we hear the word ”technology,” especially in the fields of education, product manufacturing, transportation, communication, and health. Industries relating to transport have long been essential to the economy.Even if there are various ways to travel the world, motorcycles are the wildest kind of transportation for young people ev- erywhere. Motorcycle rider views towards motorcycles are distinctive, and various aspects of the motorcycle are related to safety.However, due to the lack of a protective body, the smallest act of negligence can result in severe harm or even death.In addition to carelessness, driving too fast, driving recklessly, drinking too much alcohol, and breaking traffic

laws can all result in fatalities. But the lack of a helmet on the victim was the primary cause of brain injury, which results in instant death. Every individual riding a two-wheeler is required to wear protective headgear that complies with BIS (Bureau of Indian Norms) norms, under Section 129 of the Motor Vehicles Act of 1988. According to the Motor Vehicle Act of 1939, drunken driving while intoxicated is a crime for which the bike rider will face penalties.Determine if the helmet is on or off as the first step. If a helmet is on, the ignition will turn on; otherwise, it will not.The Flex Sensor is used for this. The second step is alcohol detection. If the amount is higher than the permitted limit, a breath analyzer that employs an alcohol sensor to detect the presence of alcohol in the rider's breath prohibits the ignition from starting.This is accomplished using the MQ-3 sensor. Ignition doesn't start unless these two conditions are met. The third significant issue is accidents and delayed medical attention. When a motorcyclist suffers an accident, one of the leading causes of death is that he might not receive medical care right away. Every second, someone dies because medical assistance was delayed or there was no one on duty at the scene of the accident. Numerous nations throughout the world are dealing with the issue of a sharp increase in the number of individuals hurt or killed while using two-wheeled vehicles, such as motorbikes and bicycles. Injuries to the head are a major cause of fatalities and serious injuries. Helmets are helpful in lowering both the frequency and severity of head injuries. Thus, promoting helmet wear is a crucial step in raising road safety in a nation. According to studies, wearing a helmet lowers your risk of death and severe brain injuries since the helmet absorbs the majority of the impact energy during a fall or collision rather than your head and brain. But choosing the correct helmet is just as crucial as wearing one. A helmet that doesn't fit correctly or doesn't provide enough padding might make you feel more secure than you should while still not offering the necessary amount of protection. In comparison to alternative methods, the accident victim will have a higher survival rate. We lower the number of fatalities from accidents

and also help users locate their vehicles by using technology that automatically detects accidents and theft.

2 METHODOLGY

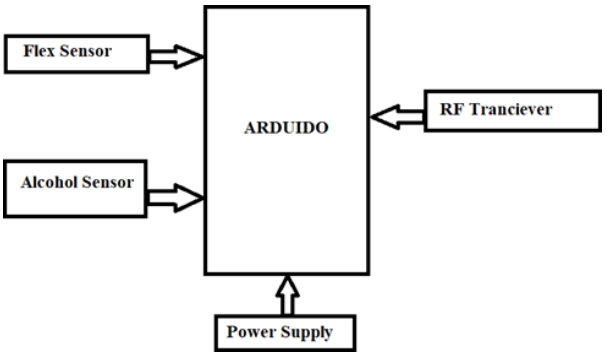

Figure 1. Helmet unit

The system consists of two units,helmet unit and motorbike unit.The helmet unit consist of alcohol sensor ,flex sensor and RF transceiver.The motorbike unit consist of force sensing re- sistors(FSR),accelerometer and gyroscope sensor,Global Posi- tioning System (GPS) and Global System for Mobile commu- nication (GSM).It also consist of RF transceiver and LCD.The receiver is placed in motorbike unit, and the transmitter is placed in the helmet unit.So that the helmet unit components will able to communicate wirelessly with motorbike unit . The helmet unit's sensors will measure the values and then compare them to the threshold value.If the measured value falls exceeds the threshold value, the motorbike will not be able to start. The microcontroller in the motorbike unit will decide whether to start the bike after reading all the information on the helmet. In order to ignite the bike, some requirements must be satisfied. The rider and the co-passenger should wear helmet and the rider should not consume alcohol.The system will detect the overload in the vehicle using force sensing resistors.The accelerometer and gyroscope sensors monitor the angle of the motorbike during a fall, triggering an indication of an accident if the angle falls within the specified range. If so, a quick warning will be sent through GSM to the emergency contact number, also the location of the accident. They may transport the casualty immediately to the medical clinic, where they can oversee clinical consideration, thus they can likewise report the event to the police headquarters.

2.1 Ignition of the vehicle only if both persons are wearing a helmet

The opposition of the metal cushion changes as the flex sensors, which are strips with metallic cushions, are twisted.Depending on how far the strip has been twisted, the analog pin's values range from 0 to 1023. One of these strips is attached to the inside of the helmet. At the point when a Helmet is worn, the client's head twists the strip, permitting the head protector to decide whether it has been utilized. To ensure that it is able to precisely identify helmet wear, our threshold value is set at 100. A type of sensor known as a flex sensor measures the amount of deflection or bending that has taken place.Materials like plastic and carbon can be utilized to assemble this sensor. This sensor, according to the bending strip theory, detects changes in resistance whenever the strip is bent. Measurement of this can be done with any controller. This sensor functions similarly to a variable resistance because its resistance changes as it rotates. Since the obstruction will vary when the surface is level, the obstruction change might be subject to the surface's linearity.The mounted flex sensors When the helmet is worn, within will flex to some degrees such that It has been embedded inside of the helmet in such a way that the head will press against it. As a result, the sensor is able to accurately detect when the helmet is removed and worn. The flex sensor generates analog data ranging from 0 to 1023 in response to the degree to which the strip has been bent.100 is our wear detection threshold. This is crucial to prevent erroneous allegations to the police that the rider was intoxicated and operating without a helmet. However, there is no considerable risk because the rider is not wearing a helmet.

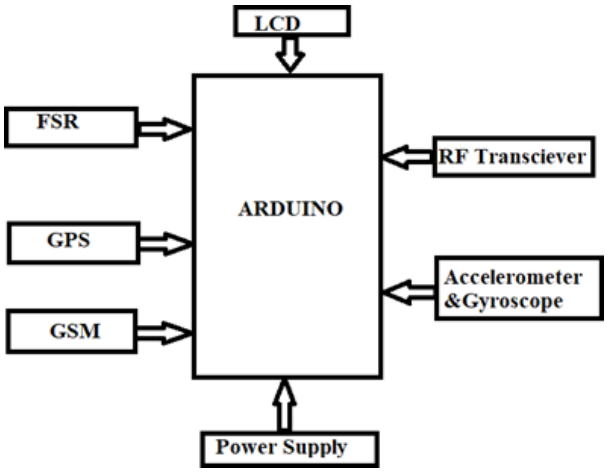

Figure 2. Helmet unit

2.2 Alcohol detection using MQ3 sensor

An alcohol sensor will test the rider's breath for alcohol in order to cut down on accidents caused by drunk driving, which is a major cause of accidents.The MQ-3 sensor is a fuel sensor module designed to detect alcohol vapor in the air. It is widely used in breathalyzer applications and car systems to detect alcohol levels in a driver's breath. The MQ-3 sensor is based on a tin dioxide semiconductor sensor element that changes its resistance in the presence of alcohol vapor. The main sensor is in a small module that also has a heating element, an analog-to-digital converter and a load resistor. When the MQ-3sensor is energized, the heating element heats the tin dioxide sensor element, making it sensitive to alcohol vapors.

An analog-to-digital converter then converts the resistance value of the sensor into a digital signal that can be read by a microcontroller or other digital circuit.The output of the MQ-3 sensor is usually a voltage that varies with the alcohol vapor concentration in the air. .A threshold value of 0.04mg/l is given to the Helmet units microcontroller. This sensor identifies any expansions in riders' breath alcohol content and communicates the outcomes to the microcontroller in the helmet unit. The microcontroller consistently looks at the sensor's outcomes to the limit esteem. If the alcohol content rises above the threshold, the buzzers on both units go off. The relay then cuts off the ignition system, stopping the motorcycle.

2.3 Detection of accidents and alert emergency contacts by message

The goal of the subtopic is to devolop a system to detect when an accident occurs and send the location of the accident location to the set emergency contact through text message. it can help to inform the accident to inform ambulance,locate nearest hospital and seek emergency help fastly.Accelerometer,gyrometer,GPS and GSM modules are used for this.Because of the lengthy procedures for reporting an accident to the police and the accompanying investigation, witnesses and bystanders commonly decide not to help when an accident is serious. This inspires us to devise a system that will enable us to save the victim without depending on anybody else. Additionally, the injured person, if awake frequently struggles to supply the emergency medical per- sonnel with information about his or her precise position, local landmarks, etc.either as a result of the shock or the fact that they are unfamiliar with the area. In light of this, it is essential that the accident scene be automatically com- municated to the emergency facility.Accident occurrence is detected by the MPU6050 sensor using a 3-axis gyroscope and 3-axis accelerometer. Using the automatic dialer, the victim's family is contacted. When the car has fallen, the system has already been taught using the 3+3 axis data. Therefore, it identifies accidents when the value falls within the range (250 – 1200°/s). When the GPS module is activated, it locates the accident scene with pinpoint accuracy and texts the emergency services the location information.. The precise position of the accident site is determined by the GPS module and communi- cated to the emergency services. By effectively reporting the accident to the hospitals, this approach has helped to shorten the reaction time to the incident.

2.4 Detection of more than two people

Systems for detecting weight, pressure, and force accelera- tion over the seat typically employ mechanical sensors.Force sensing resistors (FSR), which are the least expensive and easiest to measure or sense the weight or pressure exerted to that body. Mechanical sensors, however, have trouble telling apart between people and things put or placed over the seat. Usually, this may be resolved by merging the data from many types of sensors or by comparing the collection of data to known patterns. A substance known as a force-sensitive

resistor (FSR) adjusts its resistance in response to pressure or force.Force-sensitive resistor is a sensor that can recognize weight, squeezing and pressure from the body. While FSRs can sense weight, they are unable to determine the precise number of pounds that are on them.Three or more FSR's are placed in the seats of the vehicle adjusting the space and gap in the seat.So when a person sits on the two-wheeler seat, a force or pressure is applied to the FSR, which is mounted on the seat. It has been calibrated with a threshold value equal to the maximum weight of two people equivalent to newtons so that it can detect overweight when two or more persons sit rides it. The sensor sends the appropriate data to the micro controller, the ignition switch, and a relay to disconnect the ignition when it detects a value greater than the threshold value. Consequently, it can detect whether there are two or more people riding the bike which ensures top safety to the bike.

2.5 Implementation of accident detection through machine learning

Accident detection is excuted by machine learning in python platform using micromlgen algorithm.Usually fall detection is used as a method to detect accidents but it has several disadvantages such us fault recognition,sometimes when the motorbike may fall while parking or other times it may produce fault message showing it as an accident so to mitigate these machine learning is used.The values for falling are tested and found out in different angle for x,y,z axis respectively and these set of values are trained to the system through machine learning by python platform.When the vehicle undergoes a fall,these datas are

excuted and the dataset is analysed whether the vehicle is fallen or not.The datas recieved when tested is as follows -58,0 -63,0 -63,0 -70,0 -82,0 -76,0 -68,0 -75,0 -82,0 -75,0 -63,0 -65,0 -79,0 -81,0 -67,0 -60,0 -71,0 -77,0 -84,0 -69,0

3 RESULT

The bike will only start if both the rider and the passenger wear a helmet. The MQ3 sensor is designed to detect the alcohol content in rider's breath and prevent the vehicle from starting if alcohol is detected.To determine load, a force sensing resistors is employed.If the sensor detects more than two people, the vehicle will not start. The accelerometer and gyroscope will continuously monitor the angle of the motorbike during a fall. If the measured angle falls within the specified range, an alert message will be generated.The location of the accident will be automatically transmitted via GSM to the emergency contact number.This will enable im- mediate transportation of the injured individuals to the hospital for prompt treatment, while also notifying the relevant police station about the incident.With the specific integration of all these components into helmet and bike enhance safety features in vehicles, including motorcycles.The system represents a hypothetical concept that showcases the potential for integrat- ing various sensors, controls, and communication systems to improve rider safety and response incase of accidents.

4 Conclusion

This technique was primarily created to prevent motorbike accidents. The primary objective of the advanced smart helmet system is to mitigate accidents that are primarily caused by al- cohol consumption or the absence of helmets. This technology progressively verifies driving under the influence and helmet use. We can lower the number of head injuries that occur by putting this strategy into place. And it is the simplest and most affordable to use. It has strong social dimensions and authority. Using a cutting-edge helmet to prevent accidents is preferable to unpleasant ones. In the event of an unfortunate fall. The suggested method aims to reduce fatal accident rates while simultaneously preventing motorbike collisions. Accidents are reported to close family members and the near by hospital, along with the accident's location. By promoting the habit of helmet use among motorcycle riders, this strategy enhances safety and security during motorbike excursions, particularly when equipped with the smart helmet.

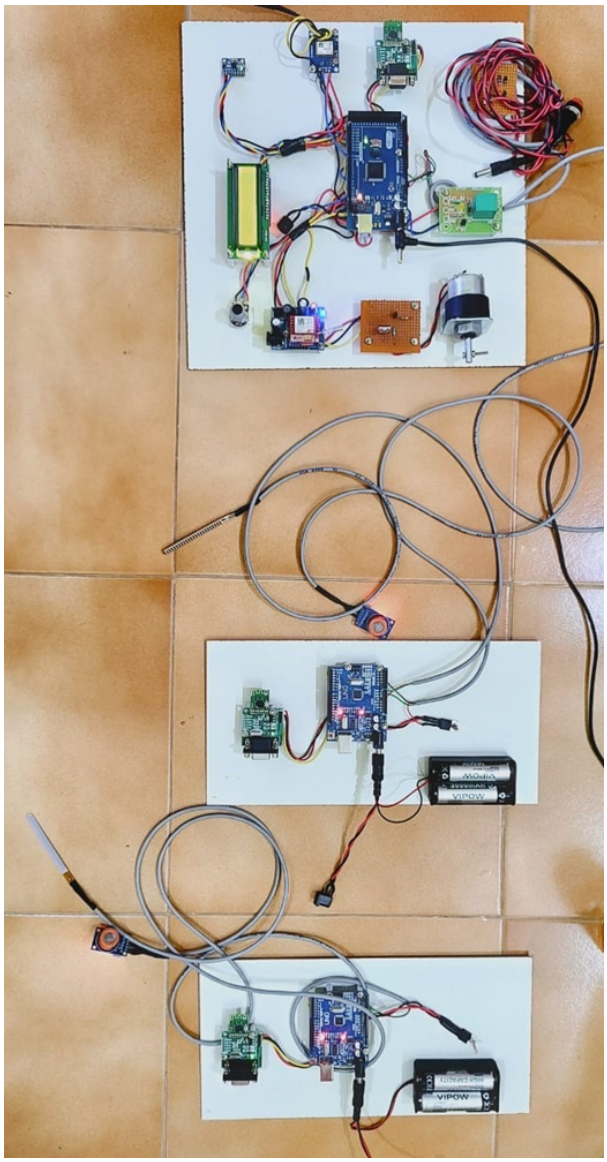

Figure 3. circuit model

References

[1] Pathak, P. (2020). IoT based Smart Helmet with Motor- bike Unit for Enhanced Safety. 2020 2nd International Con- ference on Advances in Computing, Communication Control and Networking (ICACCCN), 528-534.

[2] M. A. Rahman, S. M. Ahsanuzzaman, I. Rahman, T. Ahmed and A. Ahsan, "IoT Based Smart Helmet and Accident Identification System," 2020 IEEE Region 10 Symposium (TENSYMP), Dhaka, Bangladesh, 2020, pp. 14-17.

[3] A. Jesudoss, R. Vybhavi and B. Anusha, "Design of Smart Helmet for Accident Avoidance," 2019 Interna- tional Conference on Communication and Signal Processing (ICCSP), Chennai, India, 2019, pp. 0774-0778.

[4] P. Karmokar et al., ”A Novel IoT based Accident Detection and Rescue System,” 2020 Third International Con- ference on Smart Systems and Inventive Technology (ICSSIT), Tirunelveli, India, 2020, pp. 322-327.

[5] Dr. K.Thilagam “smart helmet wear detection for mo- torbike riders” International Journal of Applied Engineering Research ISSN 0973-4562 Number 6, 2019 volume 14.

[6] Amrutha Madhusan, Lavanya Viswanathan, Vaishnavi Ravindran, Dr.ShantaRangaswamy,” A survey on Road Acci- dent Detection and Reporting” Volume 7, Issue 4, April-2016.

[7] C. Prabha, R.Sunitha , R.Anitha,“Automatic Vehicle Accident Detection and Messaging System Using GSM and GPS Modem”, Vol. 3, Issue 7, July 2014 DOI: 10.15662/ija- reeie.2014.0307062.

[8] Aboli Ravindra Wakure, Apurva Rajendra Patkar, Man- isha VitthalDagale, Priyanka Pradeepkumar Solanki,”Vehicle Accident Detection and Reporting System Using GPS and GSM” Volume 10, Issue (April 2014), PP.25-28 [IJERD]

[9] Hemangi S. Ahire, Madhuri B. Kamble, Prajakta K. Khade, Rohini A.Ghare, Prof. B.V. Jadhav, “Vehicle Accident Detection and Alerting System”, Volume 6 Issue I, January 2018.

[10] Akansha Rajputa, Amit Saxenaa, Achint Agarwalb, Aman Bhatiab and Aman Mishrab, “Smart Helmet with Rider Safety System, Volume 4,Issue 3, 2017[IJAERE]

[11] V.Krishna Chaitanya, K. Praveen Kumar, “Smart helmet using arduino”, Hyderabad, 2013.

[12] SudharsanaVijayan, Vineed T Govind, Merin Mathews, SimnaSurendran, Muhammed Sabah,” Alcohol detection using smart helmet system”, IJETCSE, Volume 8 Issue 1 – APRIL 2014.

[13] Bhandari Prachi, Dalvi Kasturi,” Intelligent Accident- Detection and Ambulance- Rescue System” VOLUME 3, ISSUE 6, JUNE 2014.

[14] Hemendra Kumar, Mohit Kumar, “Smart Helmet for Two-Wheeler Drivers”,Volume. 02 Issue.05, May-2016.

[15] M. K. A. Mohd Rasli, N. K. Madzhi and J. Johari, ”Smart helmet with sensors for accident prevention,” 2013 (ICEESE), Kuala Lumpur,2013, pp.21-26. doi: 10.1109/ICEESE.2013.6895036.

Implementation of Lean Manufacturing in a Small and Medium Enterprise using Value Stream Mapping

Shravan E R [1], Sourav Dharmanand[1], Krishnaunni V[1] Vyshnav S[1] and Dr. Kiron K R [2]

[1] Department of Mechanical Engineering, NSS College of Engineering, Palakkad, Kerala- 678008
[2] Professor, Department of Mechanical Engineering, NSS College of Engineering, Palakkad, Kerala- 678008

Abstract -

Lean manufacturing was initially designed to reduce waste and maximize resource usage. Later, lean was developed in response to the competitive and ever-changing business environment. Businesses nowadays must contend with problems and complexity as a result of the fast-changing business environment. Any organisation, whether manufacturing or service-focused, may ultimately rely on its capacity to consistently and methodically react to these changes in order to increase the value of the output in order to survive. Lean manufacturing system implementation is therefore becoming a key capability for any type of firm to sustain, since value-adding processes are required to reach this excellence. Only a small percentage of studies concentrate on more than one lean element, yet for the organization to successfully implement lean, it had to concentrate on all the features, including Value Stream Mapping (VSM), inventory control, Kanban, etc. The study is about implementing lean manufacturing in an SME by using VSM as the lean tool. The Current VSM for the organization is done using the data collected from the organization. Time is used as the main parameter for preparing a Future VSM for the organization. Comparing of both VSM will bring light on the benefits of future state mapping over the current state mapping. The benefits include increased efficiency, waste reduction etc.

Keywords -

Lean manufacturing; Value Stream Mapping; Steel Rebars; Takt Time;

1 Introduction

Adopting manufacturing practices that increase competitiveness is necessary due to the intense rivalry in worldwide marketplaces. Lean practices implementation is one such strategy to enhance the manufacturing process. The Toyota Production System, now known as ”lean manufacturing,” was used to reorganize manufacturing processes in order to cut down on production waste and raise the caliber of the final product. In an organization, ”wastage” involves excess inventory, flaws, insufficient processing, holding up work, overproducing, superfluous motions, and avoidable transportation. The implementation of quality functions, Total Productive Maintenance, Total Quality Management, 5S, Kanban, Kaizen, and Value Stream Mapping are some of the several lean tools employed in this situation. Each industry’s shop floor contains a number of stations that collaborate to complete certain activities on time and in accordance with the schedule established to satisfy production goals. The inability to satisfy demand is hampered by equipment failure, inventory shortages, and a lack of tools. the extra stock in the workplace. To meet client demand, improvements and a rise in production rate have been contemplated for the worldwide boom’s fabrication line. To fulfil the actual demand, it has been planned to boost the fabrication line’s efficiency. Before applying methods, the value stream mapping captures the current state of the production line using a current state map. Some of the issues found throughout the fabrication line include the underutilized press station due to the lack of fixture provision, the higher setup at welding station of center section due to improper clamping of center section, excess inventory at foot boss a center boss tacking station catches rust and requires regrinds, and so on. Lean implementation removes superfluous inventory and shortens setup and cycle times overall at various stations. Previously, the manufacturing sector operated on a traditional model that involved producing a large number of goods at a low cost. Lean manufacturing is currently receiving both a lot of attention and a wide range of applications from industries across the globe. It is known as ”Lean” because it enables businesses to produce more with less effort, inventory, money, and other resources. The major goal is to demonstrate how the concepts of lean manufacturing assist us in learning how to better manage inventory, cut waste, and shorten production lead times. A number of industrial businesses have noticed an abrupt shift after using the lean approach, and they are currently undergoing both physical and cultural transition to adopt lean thinking. The book ”The Machine That Changed the World” defines the lean. Industrial engineering and lean manufacturing share a number of tasks and concepts. In plain English, lean manufacturing enables us to maintain a constant flow of goods and services by minimizing non-value-added processes, eliminating waste, and shortening the overall production lead time through managed inventories. Lean is maximizing the use of people, equipment, and resources by removing processes that don’t add value. The foundation of the lean home is built on the lean system, which emphasizes stability and uniformity. The lean house’s walls are built with jidoka, which combines automation with human intelligence and just-in-time instruction to produce goods just when they are needed. The house’s roof is designed with a key component that emphasizes the importance of the

consumer and offering them the highest-quality goods at the most affordable prices. The system's core message relates to the harmony of the workplace, which will support sustaining the company's ongoing progress as well as its ongoing search for a more fruitful future.

2 Methodology

It starts with a survey of relevant literature on the subject. Following that, the product family was selected. The product's current status map was developed. Site visits, motion studies, observation, interviews, and document analysis were utilized to collect data for the present state map. The current map was then used to identify issues and potential remedies. A complete examination of the whole plant involving the plant manager, supervisors, and operators is required prior to applying the VSM approach. Interviewing these people will help us identify the critical shop floor areas where we can increase efficiency.

· Flow of processes Study.
· Waste identification.
· A look at whether the process might be reorganized in a more efficient manner.
· An improved flow pattern is being considered, which may involve a modified flow structure or transit routing.
· Consider if everything being done at each stage is indeed necessary, and what would happen if non-essential tasks were eliminated.

2.1 Developing Current State Value Stream Map

Developing product families: Since every order is different due to the bespoke nature of the order from the customer, a concept of reconfigurable manufacturing systems can be used where the products can be classified into product families based on their weight, shape, size, changeover time, material type, etc. Identifying common operations: In this step, all the components from the SME are laid out. Using commonality analysis over any other method would provide more precise data about routing of a product family as there could be shared sub processes or assemblies in a product family and also provides the most common operations that are being performed on that product family. The advantage of using this approach is that it provides the estimated lead time for each operation which could be later analyzed for continuous improvement purposes. Creating the Current Value Stream Map: The current value stream is created using the data gathered. The VSM points out all the bottleneck processes, inventories, cycle times, lead time, efficiency and information flow. Mapping the value stream constantly starts with customer expectations. To create current value stream map those following step are accompanied. Step I - Takt time calculation. Step II - Understand Customer expectations: Customer demand may be monthly or daily as per the customer's requirement. Step III- Process Flow Mapping: This step involves various strategies which can be in series to complete product development and calculation of cycle time, changeover time and technique performance. Step IV- Material Flow mapping: The flow of material from raw material to finished goods is given through supplier to customer. Step V- Map Information Flow: The data drift is likewise incorporated to offer demand facts that is a vital parameter for figuring out the process inside the manufacturing device. Various data concerning cycle time (c/t), changeover time (c/o), total lead time and many others. Step VI- Total Product Cycle Time Calculation: After both material and data streams have been mapped, a course of events is shown at the base of the map demonstrating the preparing time for every activity and the exchange delays between tasks. The course of events is utilized to recognize the value-added steps, as well as squanders, in the present framework

2.2 Future State Value Stream Map

The purpose of creating a VSM is to expose hidden inefficiencies in a value stream. A future state map outlining the system's improvement paths can be shown once all hidden inefficiencies have been found. The future state VSM might be created using the approach listed below. Calculating takt time: Since the concept of pure takt time is not to be considered in SME as it has a highly diverse product range and could be low volume as well hence an average takt time is more appropriate. Thus, average takt time is calculated. Creating a continuous flow between the processes: Multiple factors could affect the continuous flow of a product on the shop floor such as unbalanced cycle times of each process, shared resources and the skills of the operator. During this step, continuous flow is achieved wherever possible. Creating a pull-based system: Creating a pull rather than a push system is highly recommended. Defining pacemaker process: The pacemaker process is responsible for controlling the pace of the upstream by pulling the parts through. It also controls the process downstream by regulating the release of work or products to maintain First in First out (FIFO) processing flow to the customer. Levelling the production mix and volume: There are various benefits of levelling the production mix. Batching products during a production process might increase the lead time and could also increase the inventory between the processes. Levelling the production would eliminate the three main factors i.e., waste, overburden and unevenness which are responsible for the loss of productivity. In a SME this could often be achieved by good forecast. If the bottleneck process and pacemaker operation are two different processes then

the capacity constraints must be taken into consideration while planning to level the volume upstream. Release of pre-defined work at a certain point in time i.e., pitch could be used to release work to the pacemaker process in order to control the pace of the work. Also, labor could be added to level the takt time with cycle time. In high demand and low variety, supermarket scenarios could be also used to level the production volume.

2.3 Value stream mapping in a TMT steel bars industry

As the backbone of India's infrastructure, TMT steel bars are vital for construction projects, fuelling economic development and job creation. With their superior strength and durability, TMT bars support the nation's growing urbanization, housing initiatives, and industrial expansion. Thus, we chose an ISO 9001-2015 certified leading TMT steel bar manufacturer, who has a manufacturing unit at Kanjikode, Palakkad -the industrial heart of Kerala for our study. The organization falls under Small and Medium Enterprises (SME) category as per government norms. They have adopted the latest technologies available globally to manufacture high quality TMT steel bars. The processes involved in the industry are such that in the quality control department, the raw materials (billets and ingots) supplied by the supplier are first tested for composition and quality. If the raw materials fulfil the requirements, they are accepted and processed. They are returned to the supplier if the quality test fails. The ingots are then placed in the furnace, which warms them to the desired temperature of 1000-1250 degrees Celsius in three stages. The red-hot ingots from the furnace are next rough rolled to significantly decrease their diameter in seven stages. Intermediate and continuous rolling are only done in one step. Intermediate rolling steel bars with diameters of 16mm, 20mm, and 25mm are used. Continuous rolling produces 8mm, 10mm, and 12mm diameter bars. The steel bars are cooled using a German process known as THERMEX, in which water is sprayed with pressure over the bars to provide consistent cooling. The bars are then sheared at 48mm and sent to a cooling bed to cool naturally. Then the bars further sheared down to 12m. They are extracted and bent using conveyer belts to produce the finished product. The product taken into account for this study is 8mm TMT steel bars, as it is manufactured in more quantity by the organization. Thus, current value stream map is drawn for this particular product. The various data collected for the same are cycle time, changeover time, inventory between each process, number of workers per process/machinery, available time and uptime. The whole process from unloading the billets to loading the finished TMT bars to the trucks were observed, studied and data were collected. The readings were also cross checked in the reverse order i. e. from loading of finished bars to unloading the billets. The cycle time, changeover time and the number of workers for each process/machinery is given in Table3.1. Ten readings were taken and the average is shown in the table. Then the current VSM is drawn using the collected data and lead time is calculated based on inventory, takt time and available time per day.

Table 1. Data for current value stream map

Process	Cycle Time (*t*)	Change Over Time (*t*)	Number of Workers
Unloading	2700	300	Nil
Segregation	9.27	292.93	6
Furnace	22689.81	8.428	3
Rough Rolling	37.338	8.773	6
Intermediate Rolling	23.735	3.638	2
Continuous Rolling	24.01	1.31	3
Thermex Cooling	20.5	0.3	Nil
Flying Shear	19.696	4.65	Nil
Cooling Bed	338.965	6.35	1
End Shear	6.35	300	1
Bending	27.75	8.3	12
Loading	1800	Nil	Nil

The Overall Equipment Efficiency (OEE) chart of the plant for the month of January was taken as a reference for calculating the available time and production per day. As per the OEE chart, the plant functioned for 11 days. The total available time excluding the breakdowns was 249588 seconds (sec) and the total 8mm bars manufactured was around 570.69 tonne of which 510 tonne was finally accepted following the stringent quality tests and measures. 624 tonnes of ingots were charged into the furnace for 8mm production.

The takt time is calculated as per equation.

$$TaktTime = AvailableTime / CustomerDemand \quad (1)$$

The customer demand is taken as 510 tonne per month assuming all the 8mm bars manufactured were as per order. Thus, the takt time is calculated as below.

Takt Time =249588 sec per month/ 510 tonne Per month= $489.38 sec/tonne$

The lead time is based on inventory, takt time and available time per day.

$$LeadTime = (Inventory * Takttime) / Availabletimeperday \quad (2)$$

$$Averageavailabletimeperday = \frac{totalavailabletimeinsec}{numberofdaysfunctioned} \quad (3)$$

=24588/ 11 = 22681.81 sec

The production per day was calculated based on the total weight accepted as per equation

= 510 tonne / 11 days = 46.36 tonne per day

The total consumption i.e., ingots and billets consumed was calculated as per equation

$$Consumptionper\ day = \frac{Totalweightconsumed}{Numberof\ days\ functioned} \quad (4)$$

= 624 tonne / 11 days = 56.72 tonne per day

From the current value stream map, the total lead time was 7.36 days and the total processing time is 27697.404 sec. The value-added ratio is the ratio of total processing time to the total lead time.

$$ValueAddedRatio = \frac{Totalprocessingtime}{TotalleadTime} \quad (5)$$

= 27697.404 sec / 7.36 days =0.16585

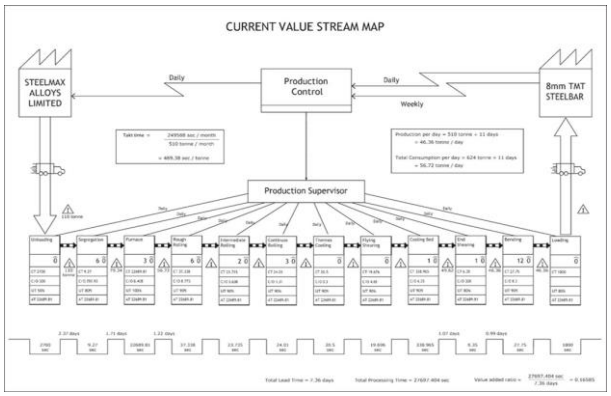

Figure 1. Current value stream map

= 16.585The main objective is to reduce the total lead time and thereby increasing the value-added ratio. The potential areas for improvement and bottlenecks were identified with the help of appropriate personnel from the organization by lean thinking. From the current value stream map, it is clear that the total processing time is very small compared to the total lead time. Heating in the furnace consumes a lot of time and capital in terms of fuel. Ingots and billets are being mixed and heated. This reduces the furnace capacity and increases the lead time. Using either ingots or billets specifically can reduce the lead time and fuel consumption. V Dhandapani et al. (2014) used value stream mapping in a steel plant and demonstrated that using only billets or ingots can reduce the lead time by 33.33%. Another non value adding activity identified was during the manual activities. Unloading and segregation was done by the same workers which increased the lead time. Similarly, bending and loading was done by the same workers. Simultaneous operations can reduce lead time in these activities as demonstrated by Pandian R. Sudhakara et al. (2020). An average reduction in lead time about 24.613% can be achieved by splitting and distributing workers for these processes. With these reduction in lead times, the future value stream map is prepared and shown in figure 3.3. The changes in lead time are calculated and new lead time is obtained

. For unloading the current lead time was 2.37 days.

Future lead time for unloading = 2.37 – (24.613% of 2.37) = 1.78 days

For segregation, the current lead time was 1.71 days

Future lead time for segregation = 1.71- (24.613 % of 1.71) = 1.70 days

For end shear, the current lead time was 0.99 day.

Future lead time for end shear = 0.99- (24.613 % of 0.99) = 0.74 days

In case of furnace, 33.33% reduction in lead time can be

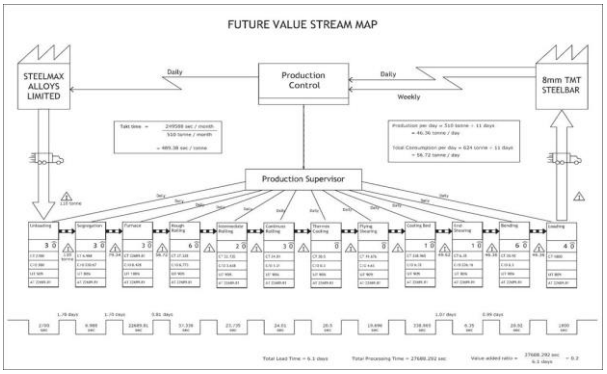

Figure 2. Future value stream map

achieved. Current lead time was about 1.22 day.

Future lead time for furnace = 1.22 – (33.33% of 1.22) = 0.81 days

From the future value stream map, it is clear that the lead time has reduced to 6.1 days from 7.36 days in the current value stream map. By applying the improvements, there has also been a reduction in the cycle time of select processes.

The actual cycle time for segregation was 9.27 sec.

The improved cycle time for segregation = 9.27 – (24.613 % of 9.27) = 6.988 sec

The actual cycle time for bending was 24.75 sec.

The improved cycle time for bending = 27.75 – (24.613% of 27.75) = 20.92 sec

The changeover time for end shear has reduced. The actual changeover time was 300 sec. The improved change over time for end shear = 300 – (24.613 % of 300) = 226.16 sec

Thus, the total processing time has reduced to 27688.292 sec from 27697.404 sec. Therefore, the value-added ratio increases.

The improved value added ratio = 27688.292 sec/ 6.1 days = 0.2

Table 2. Comparison of current and future processing time

Process	Current Processing Time (sec)	Graduating students
Unloading	2700	2700
Segregation	9.27	6.988
Furnace	22689.81	22689.81
Rough Rolling	37.338	37.338
Intermediate Rolling	23.735	23.735
Continuous Rolling	24.01	24.01
Thermex Cooling	20.5	20.5
Flying Shear	19.696	19.696
Cooling Bed	338.965	338.965
End Shear	6.35	6.35
Bending	27.75	20.92
Loading	1800	1800
Total	27697.404	27688.292

Table 3. Comparison of current and future VSM

	Current VSM	Future VSM
Total Process Time	27697.404 sec	27688.292 sec
Total Lead Time	7.36 days	6.1 days
Value Added Time	0.16585	0.2

3 Results and Discussion

In this study, twelve processes are considered for study purposes to make an attempt in minimizing total lead time using value stream mapping by eliminating non-value-added activities. It is shown in table 2., the comparison of existing lead time and the lead time calculated after eliminating the non-value-added activities. There is a considerable reduction in lead time. Total lead time is reduced by 17.12% and the value-added ratio is increased to 20%.

Table.2 shows the reduction in total processing time, total lead time and value-added ratio.

Loading the furnace with either billets or ingots reduces the lead time by 33.33 (Dhandapani et al.). splitting and distributing the workers for bending, segregation, unloading and loading can have a reduction in lead time of about 24.613% (Pandian R. Sudhakara et al.).

4 Conclusion

In this study, it was attempted to reduce the lead time of the manufacturing process by eliminating all possible Non Value-Added activities using the value stream mapping process as one of the management decision making processes for achieving customer satisfaction through the implementation of modern techniques and also by using methods such as cellular manufacturing (simultaneous operation) and the use of only one type of raw material for production. This research has proved that there is potential for the deployment of lean thinking in India to provide process improvement and cost savings. Based on its yearly income and the South Indian economy, the selected industry is classified as a small and medium enterprises (SME). According to the interpretation of the data, the percentage of reduction in overall lead time in this study may be reached to an average of 17.119The ideas mentioned above have been submitted to the case study company for consideration for implementation. It should be highlighted that none of the improvements need large investments in new apparatus or technology. The company's overall profit may rise as a result of the significant lead time decrease, which in turn enables processing more client orders. As a result, consumer satisfaction has increased, and future growth is now likely. The research work might be advanced by considering the following considerations.

Rough rolling automation has the potential to significantly reduce non-value-added time. Automation lowers both mistakes and manpower costs. A safer atmosphere with a lower risk of accidents. Similar businesses have previously converted to completely automated facilities. To remain competitive in the market, the organization must be willing to innovate. Implementation is costly in the near term but helpful in the long run. Rough rolling stands must be replaced or altered in order to deploy rough rolling automation. The factory layout must also be changed in order to adopt rough rolling automation.

Steel bar splitting and counting before bending: This is accomplished using machine vision approaches such as the triangulation method. Alternatively, photoelectric sensors can be used to count objects. Manual counting takes a lot more time. Because it avoids human subjectivity and the challenges associated with geometric variances between rebars, the combination of cameras and the innovative 3D technique offers substantial benefits over previous counting systems. The accuracy ratio of segmentation for steel bars with diameters ranging from 8mm to 20mm is greater than 99.90%, which meets the industry requirement.

Blast furnace installation: This can cut inventory by 40%. Additionally, this avoids paying for shipping, replenishing raw materials, etc. In the same factory, scrap materials including scales, random rolls, and scrap may be re-melted into ingots. With a single scheduling point, the blast furnace and rolling mill activities would be coordinated. Hot charging is the method of directly charging billets from the continuous billet casting machine to the rolling mill with little warming. Energy savings, lower inventory

levels, and quicker cycle times are advantages of the technology.

Acknowledgements

The facilities for this study endeavour were provided by ”SteelMax Rolling Mills Pvt Ltd,” which the authors gratefully thank. Additionally, a special thank you is given to the faculty of ”NSS College of Engineering, Palakkad” for their ongoing assistance.

References

[1] Suman Kundgol, Praveenkumar Petkar, V.N. Gaitonde “Implementation of value stream mapping (VSM) upgrading process and productivity in aerospace manufacturing industry” Materials Today: Proceedings, 2020.

[2] B. Rajesh Menon, P.R. Shalij, K.R. Kiron, J. Sreejith, P. Sajeesh “Cost value stream mapping as a lean assessment tool in a small-scale industry” International. Journal of Productivity and Quality Management, Vol. 30, No. 1, 2020.

[3] Rajesh Menon B, P.R. Shalij, P. Sajeesh, G. Tom Pramod V.R “Cost value stream mapping as a lean assessment tool in a surgical glove manufacturing company” South African Journal of Industrial Engineering May 2021 Vol 32(1), pp 157-170.

[4] P.M. Masuti, U.A.Dabade “Lean manufacturing implementation using value stream mapping at excavator manufacturing company” Materials Today: Proceedings,2019.

[5] Mahadeo M Narkea, Dr.C. T Jayadevab “Value stream mapping: effective lean tool for SMEs” Materials Today: Proceedings 24 (2020) 1263–1272,2018.

[6] Devanshu Mudgal, Emanuele Pagone, Konstantinos Salonitos “Approach to value stream mapping for make-to-order manufacturing” 53rd CIRP Conference on Manufacturing Systems 2020.

[7] Pradip Gunaki, S. Devaraj, Shanawaz Patil “Process optimization by value stream mapping” Materials Today: Proceedings,2020.

[8] Vijay Dhandapani, Andrew Potter, Mohamed Naim “Applying lean thinking: a case study of an Indian steel plant” International Journal of Logistics Research and Applications: A Leading Journal of Supply Chain Management, 2014.

[9] Pandian R. SUDHAKARA, Robert SALEK, Dhanashri VENKAT and Katarzyna CHRUZIK “Management of non-value-added activities to minimize lead time using value stream mapping in the steel industry” Acta Montanistica Slovaca, Volume 25 (3), 444-454,2020.

Analysis Of Defects For Reducing The Rejection Losses In A Forging Industry

Aiswarya K Prakasan[1] and Sunil D T[2]

[1] PG Student, Dept of Production Engineering, Govt Engineering College, Thrissur, Kerala, India
[2] Assistant Professor, Dept of Production Engineering, Govt Engineering College, Thrissur, Kerala, India

Abstract -

This study is conducted in a leading forging industry. The objective of this project is to investigate the various forging defects that occur in the forging industry that causes high rejection rates and the remedial measures to reduce these defects. The forging defects that are repeatedly occurring are discussed along with their causes and remedies. With the help of Pareto-diagram, the most significant defects based on cost are identified. Then the fish-bone diagram is used to explore possible causes of defects through literature review and brainstorming sessions with the managers. These causes are aggregated and grouped further and analysed. Based on the analysis, practical and feasible solutions are recommended to reduce the forging defects, and thereby save the financial loss incurred to the firm.

Keywords -

: Forging Defects; Rejection Losses; Pareto Chart; Fish-bone diagram

1 Introduction

Productivity is the major factor determining the success of any organization. In today's competitive business world, companies strives to increase their productivity and profitability. The demand for more efficient manufacturing processes has been increasing. The forging process is presented as a possible solution, because it allows the production of simple to relatively complex configurations with a good surface finish and with the desired mechanical properties. Forging is considered as the cornerstone of the manufacturing industry and it is almost always used where, reliability and human safety are critical considerations. The objective of this project is to investigate the various forging defects that occur in the forging industry that causes high rejection rates in the components and the remedial measures that can reduce these defects in the hot forging. This study is carried out in a leading forging industry located at Kerala. The rejections in the industry is incurring a huge financial loss to the firm and is obviously effecting their goodwill and productivity. The investigation was done with the help of the quality assurance department within the industry. The forging defects that are repeatedly occurring are discussed along with their causes and remedies. With the help of Pareto diagram, the most significant defects based on cost are identified. Then the cause and effect diagram is used to explore possible causes of defects through literature review and a brainstorming session with the managers, to determine the causes which have the greatest effect. These causes are aggregated and grouped further and analyzed. Based on the analysis, practical and feasible solutions are recommended to reduce the forging defects, and thereby save the financial loss incurred to the firm by rejection of the forged components.

2 The objective of the study

The defects that occur in the industry which leads to the rejection of the forged components has to be reduced in order to reduce the rejection losses. The purpose of this project is to reduce these defects which will in turn reduce the rejection losses and thereby increase their productivity. The objectives of the study involves studying the die forging process in the industry and the rejection of forged components. This is followed by the identification of the causes leading to the forging defects and the analysis of root causes for reducing the forging defects. Finally, some practical recommendations are suggested for reducing the rejection losses.

3 Methods

The project begins with the selection of the industry. By conducting discussions with technical department head and the managers, the factors that hinders the productivity of the industry is identified. The rejection of the forged components causes huge financial loss to the firm and hence the project aims to reduce the rejection losses and thereby improve the productivity. Thorough literature review is done on forging defects, their root causes and their remedial actions. This is followed by the study of forging processes and data collections. The root causes of each defects are identified through literature reviews and brainstorming sessions with the managers and the employees. Different quality tools such as the pareto chart and the

fish bone diagrams are used for prioritizing the defects and finding the root causes. The identified root causes are then aggregated and reduced based on their commonalities. These root causes are further reduced based on their controlling parameters for effective analysis. Finally some practical recommendations are provided which when implemented in the industry, the defects can be reduced and thereby the rejection losses.

3.1 General Framework

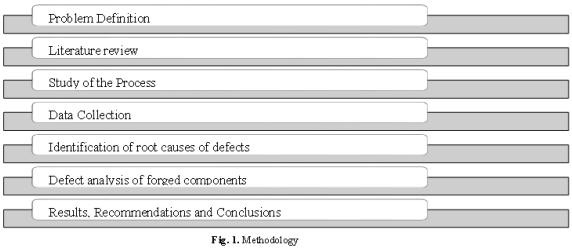

Figure 1. General Framework

3.2 Data Collection

The industry was visited and the processes has been studied to identify the factors effecting the productivity. The customer returns data of the forging industry during a specific period is collected. During this period, there was customer returns during seven months. Further from the data's collected, it is observed that the defects such as underfilling, residual stress, undersize, cracks and mismatch where causing the rejection of the forged components and this incurred a huge financial loss to the firm. On collecting the details of customer returns of the industry during a particular period, it was found that, there were rejections in gear forgings, top deck centre, top deck end ,crank shaft forgings, flange, etc. and this incurred considerable loss to the firm. Among this, the highest rejection was for top deck end. Twenty six percentage of top deck end, out of the data collected during the period of study was returned during a specific month and this caused a loss of Rs.5,08542 to the firm. Similarly, thirteen percentage of axle wheel was returned during a particular month and this incurred a loss of Rs.4,47,000 to the firm. It was followed by gear forgings, top deck center etc. The identified defects in the observed data's are underfilling, cracks, residual stress, mismatch undersize. These defects are therefore hindering the productivity and causing a huge financial loss to the firm. Proper mitigation of these defects will eliminate the forging defects and hence the rejection rates. The details of defects identified for a period of time at the forging industry are as shown below,
U/F – Underfilling or Unfilling
M/M – Mismatch
O/S – Oversize
C/R – Cracks
T/M – Tool Mark
F/P – Flash Projection
P/M – Punch Mark
R/S – Residual Stress
U/S – Undersize
Bulged surface
Ovality
However, during the period of study, the following defects are identified at the forging industry,
Underfilling
Residual Stress
Undersize
Cracks
Mismatch

3.3 Analysis

In this analysis, the Pareto tool is used to find the significance of the defects and to identify which defect to focus on based on the 80-20 rule. The chart is plotted from the table below.

Table 1. Data table

Sl .No	Defect	Cost	Cumulative Cost	Cumulative %
1	Underfilling	1125320	1125320	50.57
2	Residual stress	508542	1633862	73.43
3	Undersize	499628	2133490	95.88
4	Cracking	50470	2183960	98.15
5	Mismatch	41160	2225120	100.00

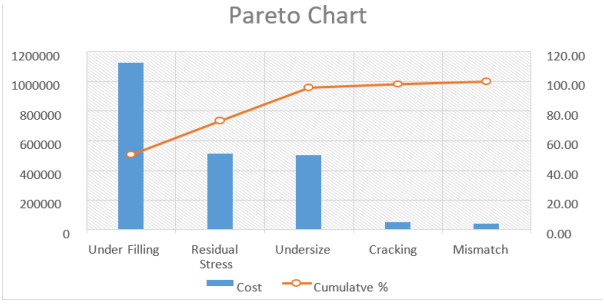

Figure 2. Pareto Chart

From the pareto chart, it is clear that underfilling and residual stress are the most significant defects that are responsible for 80

3.3.1 Underfilling Defect

It refers to a situation where the metal in the forging does not completely fills the die cavity, resulting in a portion of

the final product being missing or incomplete. Underfilling can have a significant impact on the quality and performance of the final product. It can weaken the structure and cause cracks or other defects that may compromise the integrity of the final component. This can lead to failures during use or testing, which can result in safety hazards, increased costs, and decreased customer satisfaction. The various root causes of the underfilling defect was determined through the theoretical and practical perspectives by considering its effectiveness during the implementation. These are listed below.

Table 2. Causes of Underfilling defect

SL. NO	CAUSES
1	Less raw material
2	Seam crack of billet
3	Obliquely cut billet
4	Die geometry variations
5	Insufficient number of skilled workers
6	Lack of training & motivation
7	Insufficient heating
8	Wrong position of perform
9	Lack of maintenance
10	Shape complexity
11	Vibrations
12	Crude Technology
13	Improper scale removal
14	Non-optimum no. of blows
15	Early withdrawal of billet

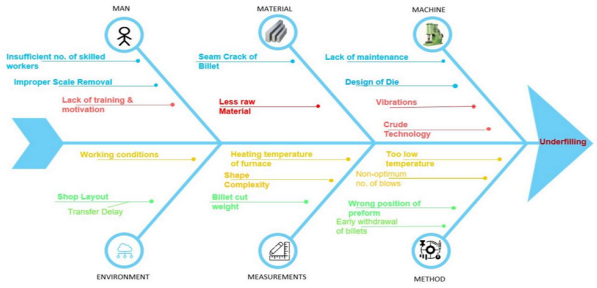

Figure 3. Ishikawa diagram for underfilling

3.3.2 Residual Stress

Residual stress is a common defect that can occur in the forging process. It is caused by the thermal and mechanical forces that are applied on to the material during the forging process, which can cause the material to warp or deform. This can result in uneven distribution of stress within the material, leading to residual stress defects. Residual stress defects can lead to a number of issues, including weakening of the material, distortion, cracking, or making it more susceptible to cracking or failure under load. The various root causes of the residual stress defect was determined through the theoretical and practical perspectives by considering its effectiveness during the implementation. These are listed below.

Table 3. Causes of Residual Stress defect

SL. NO	CAUSES
1	Shape complexity
2	Micro structure
3	Insufficient number of skilled workers
4	Lack of training and motivation
5	Non optimum no. of blows
6	Improper cooling
7	Inhomogeneous deformation
8	Lack of maintenance
9	External forces
10	Too low temperature
11	Greater Thermal Loads
12	Lubricating oil
13	Working conditions
14	Shop Layout

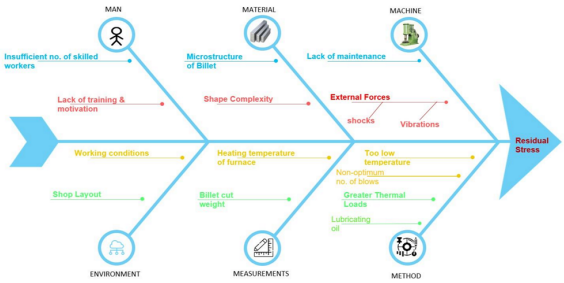

Figure 4. Ishikawa diagram for Residual Stress Defect

3.3.3 Undersize Defect

Undersize defect in forging refers to a situation where the forged part is smaller in size than the required specifications. Undersize defects can have negative impacts on the performance and functionality of the final product. In some cases, undersize can lead to a weakened structure, which may cause the component to fail prematurely or even during use. Undersize can also lead to the need for additional machining or processing, which can increase the overall cost of production and decrease the overall efficiency of the manufacturing process. The various root causes of the undersize defect was determined through the theoretical and practical perspectives by considering its effectiveness during the implementation. These are listed below (Table 4.).

Table 4. Causes of Undersize Defect

SL. NO	CAUSES
1	Low cut weight
2	Quality of Billet
3	Die geometry variations
4	Impurities on die
5	Sharp edges
6	Insufficient number of skilled workers
7	Lack of training & motivation
8	Inhomogeneous deformation
9	Insufficient heating
10	Wrong position of perform
11	Lack of maintenance
12	Obliquely cut billet
13	Working conditions
14	Shop Layout

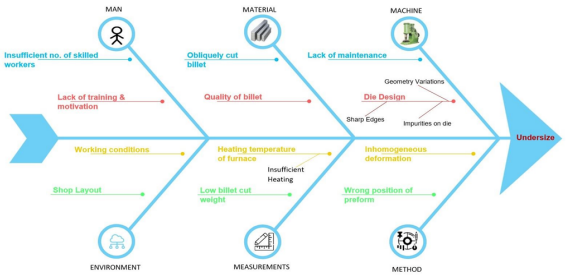

Figure 5. Ishikawa diagram for Undersize Defect

Table 5. Causes of cracks

SL. NO	CAUSES
1	Micro structure of billet
2	Cavities in billet
3	Insufficient numbers of skilled workers
4	Lack of training & motivation
5	Lubricating oil
6	Too low temperatures
7	Greater thermal loads
8	Surplus blows
9	Lack of maintenance
10	Vibrations
11	Lazy Cleaning
12	Working conditions
13	Shop Layout

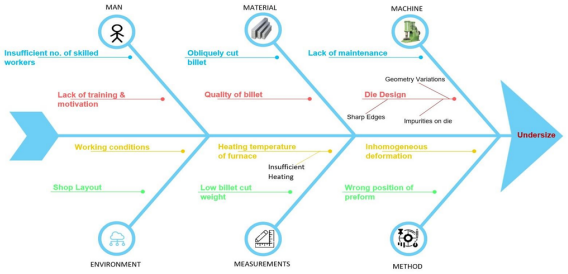

Figure 6. Ishikawa diagram for Cracks

3.3.4 Cracks

Cracks in forging refer to the formation of fissures or fractures that occur during the forging process. Cracks are one of the major concerns in forging, as they can have significant impacts on the performance and safety of the final product. In some cases, cracks can propagate and lead to catastrophic failure of the component, which can cause safety hazards and significant costs for repairs or replacements. Cracks can also decrease the strength and durability of the component, reducing its lifespan and efficiency. They can weaken the finished product and compromise its structural integrity, leading to potential failure or safety hazards. The various root causes of cracks was determined through the theoretical and practical perspectives by considering its effectiveness during the implementation. These are listed below (table.5).

3.3.5 Mismatch

Mismatch or die shift forging defect is caused when the upper and lower dies are not aligned with each other. In this type of defect, the final forged component has a noticeable or significant difference between its two or more surfaces, such as an uneven thickness, an irregular shape, or a misaligned feature. This will result in improper dimensions and geometry of the product. It can also have negative impacts on the performance and functionality of the final product. In some cases, mismatch can lead to weakened areas or reduced functionality, which may cause the component to fail prematurely or even during use. Mismatch can also lead to the need for additional machining or processing, which can increase the overall cost of production and decrease the efficiency of the manufacturing process. The various root causes of the mismatch defect was determined through the theoretical and practical perspectives by considering its effectiveness during the implementation. These are listed below.

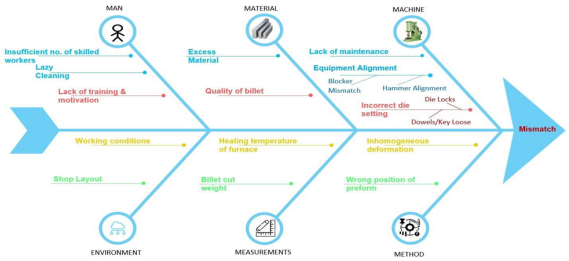

Figure 7. Ishikawa diagram for Mismatch

Table 6. Causes of cracks

SL. NO	CAUSES
1	Excess material
2	Lazy cleaning
3	Lack of training & motivation
4	Equipment Alignment
5	Incorrect Die setting
6	Die locks
7	Blocker mismatch
8	Insufficient no. of skilled workers
9	Inhomogeneous deformation
10	Wrong position of preform
11	Lack of maintenance
12	Working Conditions
13	Shop Layout

3.4 Agregating the Root Causes

Aggregating the root causes is an important step in analysing and addressing the defects in forging. When a defect occurs, there may be multiple root causes that contribute to the problem, and it is important to identify and address all of these causes in order to prevent the defect from recurring. By aggregating the root causes, a better understanding of the underlying issues that are leading to the occurrence of the defects can be attained, and take targeted and effective corrective actions to address them. Here, the defects have been prioritized using the pareto chart and the root causes for each defects have been explored using the ishikawa or fish bone diagram. Further, the causes with similar nature or characteristics are grouped so that the number of root causes for each defects have been reduced for effective analysis. The aggregated root causes of defects are tabulated as shown on table 7.

3.5 Causal Diagram

A causal diagram, also known as a causal loop diagram or a system dynamics diagram, is a graphical representation of a system or process that shows the cause-and-effect relationships between different variables or factors that influence the system. Causal diagrams are commonly used in engineering, management, healthcare and other fields to model complex systems and analyze the impact of different factors on the overall performance of the system. The diagram consists of a series of interconnected nodes, which represents the different variables or factors in the system, and arrows or lines that shows the causal (cause and effect) relationships between them. By analyzing the causal diagram, one can understand the complex interactions between different factors that affect the system. Overall, causal diagrams are a powerful tool for understanding complex systems and helps to make decisions by identifying the key factors and relationships that contribute to a particular outcome. By constructing a causal diagram, the commonality of the factors could be derived. In this project, for practical convenience, the root causes are first aggregated and then further reduced, based on their commonalities with the help of a causal diagram. Interpreting a causal diagram involves understanding the relationships between different factors and how they contribute to a particular outcome or result. The following figure shows the causal diagram constructed based on the root causes identified for the forging defects.

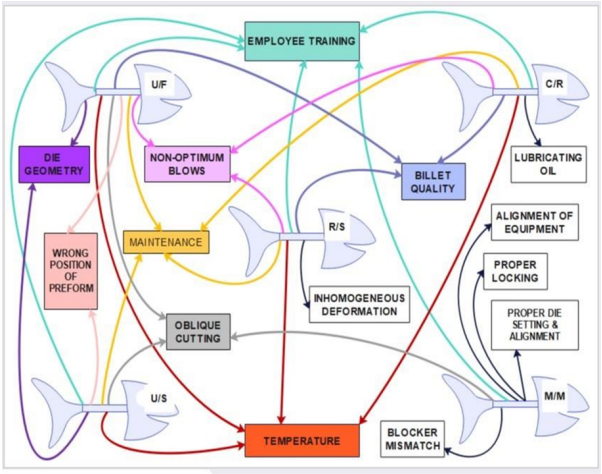

Figure 8. Causal diagram

3.6 Analysis and Remedial Measures

The main causes that triggers all the identified defects and their possible remedial actions are discussed below.

3.6.1 Forging Hammer Parameter

Forging hammer parameters refers to the specific characteristics and specifications of a forging hammer that determines its performance and capabilities. This includes the number of blows, hammer weight, stroke length, striking force, etc.

Number of Blows : In the concerned forging industry, the number of blows required for each work is determined by the worker. However, the non optimum number of blows often causes defects such as underfilling, cracks, and residual stress. For the axle wheel, which incurs the most rejection losses due to underfilling, the number of blows is about 25. From the observation and the discussions conducted with the managers, increasing the number of blows to 28, can reduce the underfilling defect.

Table 7. Aggregated Root Causes

Sl. No	CAUSES				
	U/F	**R/S**	**U/S**	**C/R**	**M/M**
1	Oblique cutting	Inhomogeneous deformation	Oblique cutting	Lubricating oil	Oblique cutting
2	Die geometry	Non-optimum number of blows	Die geometry	Non-optimum number of blows	Proper Die setting & alignment
3	Temperature	Temperature	Temperature	Temperature	Alignment of equipment
4	Employee Training	Employee Training	Employee Training	Employee Training	Employee Training
5	Non-optimum no. of blows	Maintenance	Maintenance	Maintenance	Blocker mismatch
6	Wrong position of preform	Billet Quality	Wrong position of preform	Billet Quality	Proper locking
7	Billet Quality				

3.6.2 Temperature

Non optimum temperature effects the smooth deformability of the billet and effects all the discussed defects. Some remedies for maintaining optimum temperature are stated below.

Monitor the billet temperature : Using non-contact temperature sensors, such as infrared thermometers or thermal imaging cameras, can help to monitor the temperature of the billet during forging and ensure that it remains within the desired temperature range.

Use a temperature-controlled forging press : Modern forging presses have sophisticated temperature control systems that can monitor and adjust the temperature of the billet during the forging process. This helps to maintain the desired temperature range and prevent overheating or under heating of the material.

Use a heat-resistant forging die : The forging die can absorb heat from the billet during the forging process. Using a heat-resistant forging die can help to minimize heat loss and maintain the billet temperature. Heat resistant forging dies are made from special materials that have high resistance to heat and wear, such as tool steels, high-speed steels, and tungsten carbide.

The proper calibration of the furnaces must be done.

Proper soaking time for the billets must be given for attaining the required temperature to the inner part of the work-piece.

Reducing the delays of moving the work-piece to the furnace .

Adequate spraying of furnace oil.

3.6.3 Maintenance

The following are the possible solutions for reducing the defects caused by improper or irregular maintenance activities.

Proper and regular maintenance, identifying opportunities for improvement and making changes to improve maintenance processes can eliminate the defects aroused by misalignment of Equipment and Die, Die wear and Oblique Cutting.

This can be done through regular audits, calibration, predictive and preventive maintenance, feedback from maintenance personnel, monitoring of maintenance metrics etc.

Preventive Maintenance : This includes tasks such as cleaning, lubricating, inspecting, and adjusting equipment as needed, alignment checks, cleaning and lubrication of dies, and wear checks.

The scale removal during the forging process must be properly done by using high pressure air cleaners which thereby reduces the clogging of scales on the path of metal flow.

The mechanized method of lubrication by spraying lubricants over the workpiece and die for better and uniform lubrication will help in reducing the friction between workpiece and die allowing the metal to flow more easily.

Predictive maintenance : This includes using sensors to measure equipment performance and detect potential issues before they become problems.

Corrective maintenance : This includes emergency repairs, component replacement, or major repairs to the equipment.

Calibration : Proper and regular calibration of equipments

and furnaces ensures accurate and reliable measurements and control during the forging process.
Inventory management : This ensures that spare parts and consumables are available when needed, reducing downtime and increasing efficiency.
Record keeping: Maintaining detailed records of the maintenance activities and equipment performances can help to identify the trends, identify potential issues, and make informed decisions about the equipment repair or replacement and also helps for future references.
Employing trained and qualified maintenance personnel.

3.6.4 Billet Quality

The following are some of the remedies for ensuring the billet quality and thereby reducing the defects.
Full matrix capture (FMC) ultrasonic testing – This technique uses multiple ultrasonic probes unlike the traditional ultrasonic testing method, to obtain the detailed images of the internal structure of the billet.
Perform a chemical analysis of the billet to ensure that it meets the required composition specifications.
Automated ultrasonic testing systems can reduce the risk of operator induced errors and also increase the speed and accuracy of the test.
Ensuring uniform cross sectional area – purchasing good quality billets.
Increasing the cut weight of the billet can reduce the undersize defect.

3.6.5 Employee Training

Employee training is critical in the forging industry as it helps to ensure that workers have the necessary skills and knowledge to carry out their job effectively and safely. The following are some remedies to ensure effective employee training.
Set clear goals and expectations. This helps the workers to have a clear idea about what they should do, how to do when to do.
Recognize and reward the performances of workers. This will increase their enthusiasm and nourish the sense of integrity.
Simulation training : Trainings are provided in controlled environments. It helps them to be well prepared to the situations before really being in the situation.
Communicate effectively : Effective communication is a critical factor to get the best results by effectively exchanging the ideas and perspectives.
Frequent trainings on new equipment, and other job-related skills.
Cross-training : This involves training employees to perform tasks outside of their usual job responsibilities such as training on safety procedures, troubleshooting techniques, and equipment-specific maintenance procedures. This can help to increase employee versatility and improve productivity.

4 Results and Discussion

The study for the reduction of the rejection losses of forged components in the forging industry is successfully done. The processes were studied and rejection data's were collected. The root causes for each defects were identified and they are aggregated based on their commonalities. Finally five causes that trigger the identified defects were listed and analysed. The following are the major corrective measures for reducing the defects and the rejection losses.
Using a non-contact temperature sensors, such as the infrared thermometers or thermal imaging cameras, to monitor the temperature of the billet during the forging process helps to ensure that the temperature of the billet remains within the desired range.
Introducing advanced forging presses with temperature control systems that can monitor and adjust the temperature of the billet during the forging process.
The mechanized method of lubrication and cleaning by spraying lubricants and air over the work piece and die.
Automated ultrasonic testing systems can reduce the risk of operator error and increase the speed and accuracy of the quality tests.
Simulation training : It helps them to be prepared to the situations before really being in the situation.
Cross-training : This involves training employees to perform tasks outside of their usual job responsibilities.

5 Conclusion

The industry was visited and the processes were studied. Forging defects that occur in the industry that causes high rejection losses in the components are identified. The various defects identified are unfilling, residual stress, undersize, crack, and mismatch. From the Pareto chart it was found out that 80 percnt of the total rejection were due to unfilling and residual stress defect. The cause and effect diagram was drawn to explore the root causes of the defects. Defects and their root causes were analyzed and grouped by their nature. The identified factors have been further aggregated and reduced for effective analysis. The feasible factors that can be improved are selected and analyzed further. Finally, some practical solutions and recommendations are provided so as to reduce the rejection losses. These are,

Infrared thermometers can be incorporated to monitor the temperature of the billet.
Introducing advanced forging presses with temperature control systems that can monitor and adjust the temperature of the billet during the forging process.
Mechanized method of spraying lubricant and cleaning.

More systematic maintenance plans were suggested.
Advanced billet inspection methods were suggested (Automated ultrasonic testing systems).
Cross training of employees. It is concluded that the proper implementation of the proposed corrective plans will reduce the occurrence of the defects and thereby the present rejection losses in the firm.

6 Acknowledgements

The authors would like to thank following persons for their continuous support and guidance throughout the work.Quality Dept. of the concerned forging industry. Dr. Boby K George, Head of the Department, Department of Production Engineering, Govt. College of Engineering college, Thrissur.

References

[1] Christy Mathew, Justin Koshy, Dr.Deviprasad Varma,(2022)- Study of Forging Defects in Integral Axle Arms, International Journal of Engineering and Innovative Technology (IJEIT) Volume 2, Issue 7 .

[2] Amitkumar B. Solanki, Sunilkumar S. Sonigra, Vivek Vajpayee,(2021)Implementation of quality tools and effective strategies to boost production market standards for forged crankshafts: A case study of forging industry, Materials Today: Proceedings, 2021.04.537 .

[3] Dr. R.K Kaushik, Poonam Thakur,(2017)- To Investigate Forging Processes and its Defect, International Journal of Engineering Research Technology (IJERT) Volume 5, Issue 03 .

[4] Marek Hawryluk, Joanna Jakubik,(2016)- Analysis of Forging Defects For Selected Industrial Die Forging Processes, Engineering Failure Analysis 9.

[5] Rohan K. Soyaliya V. Parmar Jayendra B. Kanani, (2015)- A Review on Unfilling Defect Found in Forging Process, International Journal for Scientific Research Development— Vol. 3, Issue 10, 2015

[6] Mr.Bhavesh V Patel, et al (2014)-Review of Analysis on Forging Defects for Quality Improvement in Forging Industries, Journal of Emerging Technologies and Innovative Research (JETIR) Volume 1 Issue 7

[7] Mahendra G. Rathi, Nilesh A. Jakhade,(2014)- An Overview of Forging Processes with Their Defects, International Journal of Scientific and Research Publications, Volume 4, Issue 6, June 2014

[8] Meetinder Singh Sekhon, et al.,(2014)- A six sigma approach to detect forging defects in a small scale industry: A case study, International Journal of Engineering and Technical Research (IJETR) ISSN: 2321-0869, Volume-2, Issue-8

[9] Pankaj Chandna, Arunesh Chandra,(2009)- Quality Tools to Reduce Crankshaft Forging Defects: An Industrial Case Study, Journal of Industrial and Systems Engineering Vol. 3, No. 1, pp 27-37

[10] Bhoop Singh,(2017)- Study of Various Factors Related to Quality in Forging Industry, ICADEMS-volume 5,issue-3

[11] Forging Magazine,(2000)- Focus your attention on Forging Process and equipment,A penton publication; 17-23

[12]]Official Website of the forging industry.

Characterization and Estimation of Area Biased Shukla Distribution with Applications of Medical Sciences

Roshni C[1], Venkatesan D[2] and Prasanth C B[3]

[1]Research Scholar, Department of Statistics, Annamalai University, Tamilnadu, India
[2]Professor, Department of Statistics, Annamalai University, Tamilnadu, India
[3]Assistant Professor, Department of Statistics, Sree Keralavarma College, Thrissur, India

[1]roshnic.balan2@gmail.com [2]sit_san@hotmail.com [3]cbpwarrier@gmail.com

Abstract -

In this paper, a new study of Shukla distribution called as area biased Shukla distribution has been proposed. Some of its statistical properties which include moments, harmonic mean, survival function, hazard rate function, reverse hazard rate function, moment generating function, order statistics, entropy, Bonferroni and Lorenz curves have been discussed. For estimating its parameters the method of maximum likelihood estimation has been used. Finally, a real life data set has been fitted to discuss the goodness of fit of new distribution.

Keywords -

Shukla distribution, Weighted distribution, Survival analysis, Order statistics, Maximum likelihood estimation.

1 INTRODUCTION

The concept of weighted distributions is applied in various research areas related to reliability, biomedicine, ecology and branching process. The study of weighted distribution was proposed firstly by Fisher (1934) to model the ascertainment bias. Later, Rao (1965) developed this concept in an integrated manner when the standard distributions were not appropriate to record the observations with equal probabilities. The weighted distributions are utilised to modulate the probabilities of events as observed and transcribed. The concept of weighted distributions provides a collective access for the problem of model specification and data interpretation problems. The study of weighted distributions is useful in distributions theory, because it provides a new understanding of the existing standard distributions. The weighted distributions are used as a tool in selection of appropriate models for observed data especially when samples are drawn without a proper frame. The weighted distributions take into account the method of ascertainment by adjusting the probabilities of actual occurrences of events to arrive at a specification of the probabilities of those events as observed and recorded. The weighted distribution reduces to length biased distribution especially when the weight function considers only the length of units of interest. The concept of length biased sampling was introduced by Cox (1969) and Zelen (1974). More generally, when the sampling mechanism selects units with probability proportional to measure of the unit size, resulting distribution is called size biased. Size biased distributions are special case of more general form known as weighted distributions. Many researchers have developed some important weighted probability models along with their applications in handling data sets from various practical fields. Warren (1975) was the first to apply the weighted distributions in connection with sampling wood cells. Patil and Rao (1978) introduced the concept of size biased sampling and weighted distributions by identifying some of the situations where the underlying models retain their form. Subramanian and Rather (2018) studied the weighted exponentiated Mukherjee-Islam distribution. Mudasir and Ahmad (2017) presented the weighted Erlang distribution with characterizations and information measures. Hassan et al. (2018) constructed the three parameters weighted quasi Akash distribution with properties and Applications. Saghir et al. (2017) discussed on the weighted distributions with a brief review, perspective and characterizations. Bashir and Rasul (2016) discussed the poisson area biased Lindley distribution with its applications in biological data to prove that it gives a better fit than poisson distribution. Perveen et al. (2016) constructed the area biased weighted weibull distribution. Dar et al. (2020) studied the weighted gamma-Pareto distribution and its applications. Mudasir et al. (2018) studied the weighted new Weibull Pareto distribution with some characteristics and applications. Sharma et al. (2018) discussed on the length and area biased Maxwell distribution. Recently, Ade et al. (2021) presented the characterization and estimation of area biased quasi Akash distribution.

Shukla distribution is a two parametric lifetime distribution proposed by Shukla and Shanker (2019) which is a particular case of exponential, Shanker, Pranav, Ishita, Rani and Ram Awadh distributions. Its various statistical properties which include moments, hazard rate function, mean residual life function and stochastic ordering have been discussed. For estimating its parameters the method

of maximum likelihood estimation has been discussed. Application of the proposed Shukla distribution has been discussed with real life data sets has been fitted and it is found that the proposed Shukla distribution provides better fit over well known lifetime distributions.

2 Area Biased Shukla (ABS) Distribution

The probability density function of Shukla distribution is given by:

$$f(x;\theta,\alpha) = \frac{\theta^{\alpha+1}}{\theta^{\alpha+1}+\Gamma(\alpha+1}\,(\theta+x^{\alpha})\,e^{-\theta x} \qquad (1)$$

x>0,θ>0,$\alpha \geq 0$

and the cumulative distribution function of Shukla distribution is given by:

$$F(x;\theta,\alpha) = 1 - \frac{\theta^{\alpha}\,(\theta+x^{\alpha})\,e^{-\theta x} + \alpha\Gamma(\alpha,\theta x)}{\theta^{\alpha+1}+\Gamma(\alpha+1)} \qquad (2)$$

x 0,θ ,$\alpha \geq 0$

Let X be a non-negative random variable with probability density function f(x).Let w(x) be its non-negative weight function, then the probability density function of weighted random variable $X_w$is given by

$$f_w(x) = \frac{w(x)f(x)}{E(w(x))}, x > 0.$$

Where w(x) be the non-negative weight function and E(w(x))=$\int$ w(x)f(x)dx<∞

For different weighted models, we have different choices of the weight function w(x),when w(x)=x^c, the resulting distribution is termed as weighted distribution. In this paper, we have to find the area biased version of Shukla distribution, so we will take c = 2 in weights x^c,in order to get the area biased Shukla distribution and its probability density function (pdf) is given by:

$$f_a(x) = \frac{x^2 f(x)}{E(x^2)} \qquad (3)$$

Where, E(x^2)=$\int_0^{\infty} x^2$f(x)dx

$$E(x^2) = \frac{2\theta^{\alpha+1}+(\alpha+2)!}{\theta^2(\theta^{\alpha+1}+\alpha!)} \qquad (4)$$

By using the equations (1) and (4) in equation (3), we will obtain the probability density function of area biased Shukla distribution as:

$$f_a(x) = \frac{x^2\theta^{\alpha+3}}{2\theta^{\alpha+1}+(\alpha+2)!}(\theta+x^{\alpha})e^{-\theta x} \qquad (5)$$

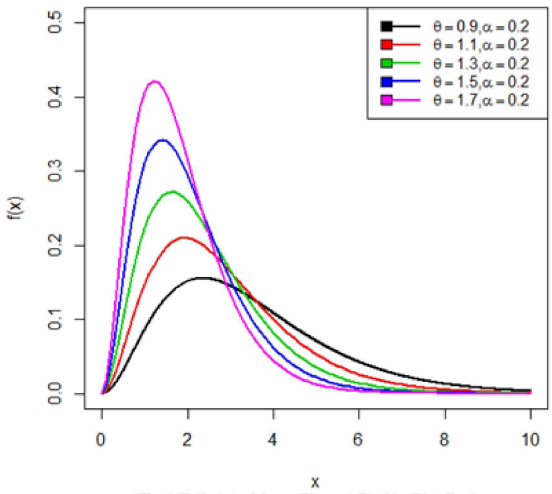

Fig.1:Pdf plot of Area Biased Shukla Distribution

and the cumulative distribution function of area biased Shukla distribution can be obtained as:

$$F_a(x) = \int_0^x f_a(x)dx$$

$$F_a(x) = \int_0^x \frac{x^2\theta^{\alpha+3}}{2\theta^{\alpha+1}+(\alpha+2)!}(\theta+x^{\alpha})e^{-\theta x}dx$$

$$F_a(x) = \frac{1}{2\theta^{\alpha+1}+(\alpha+2)!}\int_0^x x^2\theta^{\alpha+3}(\theta+x^{\alpha})e^{-\theta x}dx \qquad (6)$$

After the simplification of equation (6), we will obtain the cumulative distribution function of area biased Shukla distribution as:

$$F_a(x) = \frac{1}{2\theta^{\alpha+1}+(\alpha+2)!}(\theta^{\alpha+1}\gamma(3,\theta x)+\gamma(\alpha+3,\theta x)) \qquad (7)$$

3 Survival Analysis

In this section, we will discuss the survival function, hazard rate and Reverse hazard rate functions of the proposed area biased Shukla distribution.

3.1 Survival function

The survival function is also known as reliability function or complement of the cumulative distribution function. The survival function of proposed model can be

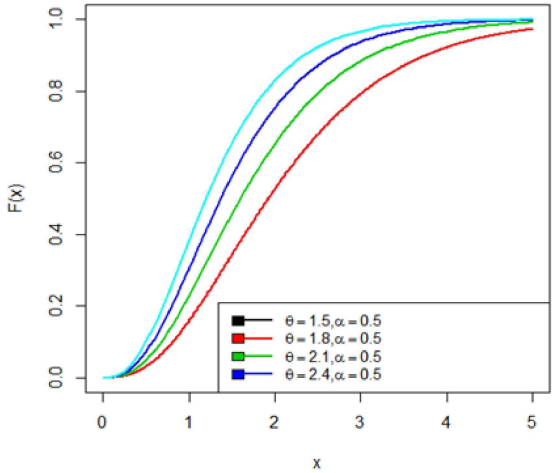

Fig.2:Cdf plot of Area Biased Shukla Distribution

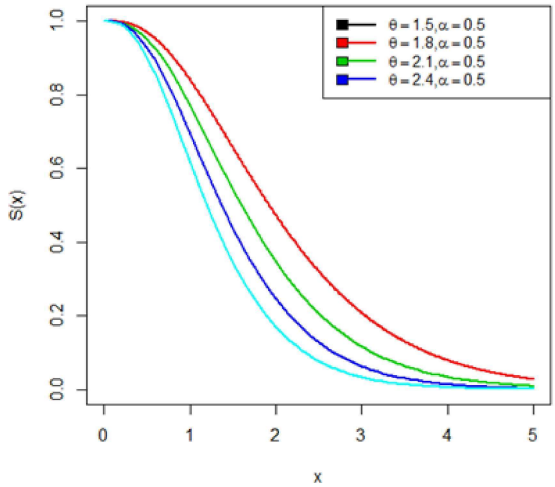

Fig.3:Survival plot of Area Biased Shukla Distribution

computed as

$$S(x) = 1 - F_a(x)$$

$$S(x) = 1 - \frac{1}{2\theta^{\alpha+1}+(\alpha+2)!}\left(\theta^{\alpha+1}\gamma(3,\theta x) + \gamma(\alpha+3,\theta x)\right)$$

3.2 Hazard function

The hazard function is also known as instantaneous failure rate or force of mortality and is given by:

$$h(x) = \frac{f_a(x)}{1-F_a(x)}$$

$$h(x) = \frac{x^2\theta^{\alpha+3}}{(2\theta^{\alpha+1}+(\alpha+2)!)-(\theta^{\alpha+1}\gamma(3,\theta x)+\gamma(\alpha+3,\theta x))}(\theta + x^{\alpha})\, e^{-\theta.}$$

3.3 Reverse hazard function

The reverse hazard function is given by:

$$h_r(x) = \frac{f_a(x)}{F_a(x)}$$

$$h_r(x) = \frac{x^2\theta^{\alpha+3}}{\theta^{\alpha+1}\gamma(3,\theta x)+\gamma(\alpha+3,\theta x)}(\theta + x^{\alpha})\, e^{-\theta x}$$

4 Statistical Properties

In this section, we will discuss the various statistical properties of area biased Shukla distribution which includes moments, harmonic mean, MGF and characteristic function:

4.1 Moments

Let X be the random variable following area biased Shukla distribution with parameters θ and α then the rth order moment $E(X^r)$ of area biased Shukla distribution can be obtained as:

$$E(X^r) = \mu_r' = \int_0^{\infty} x^r f_a(x)dx$$

$$E(X^r) = \mu_r{}' = \int_0^{\infty} x^r \frac{x^2\theta^{\alpha+3}}{2\theta^{\alpha+1}+(\alpha+2)!}(\theta + x^{\alpha})\, e^{-\theta x}dx$$

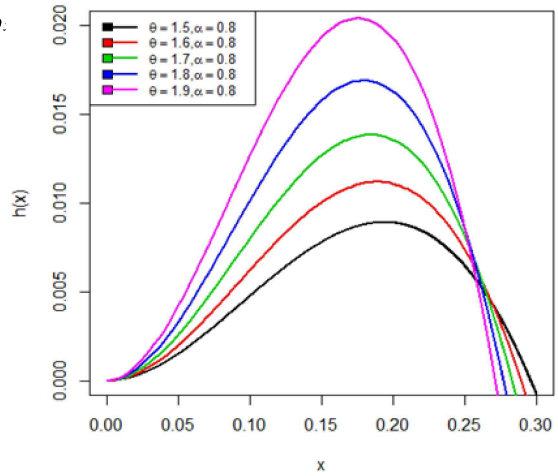

Fig.4:Hazard function of Area Biased Shukla Distribution

$$E\left(X^r\right) = \frac{\theta^{\alpha+3}}{2\theta^{\alpha+1}+(\alpha+2)!}\int_0^{\infty} x^{r+2}\left(\theta + x^{\alpha}\right)e^{-\theta x}dx$$

$$E\left(X^r\right) = \frac{\theta^{\alpha+3}}{2\theta^{\alpha+1}+(\alpha+2)!}\left(\theta\int_0^{\infty} x^{(r+3)-1}e^{-\theta x}dx + \int_0^{\infty} x^{(\alpha+r+3)-1}e^{-\theta x}dx\right) \quad (8)$$

After the simplification of equation (8), we obtain:

$$E\left(X^r\right) = \mu_r' = \frac{\theta^{\alpha+1}(r+2)! + (\alpha+r+2)!}{\theta^r\left(2\theta^{\alpha+1}+(\alpha+2)!\right)} \quad (9)$$

By putting r = 1, 2, 3 and 4 in equation (9), we will obtain the first four moments of area biased Shukla distribution.

$$E(X) = \mu_1' = \frac{6\theta^{\alpha+1}+(\alpha+3)!}{\theta\left(2\theta^{\alpha+1}+(\alpha+2)!\right)}$$

$$E\left(X^2\right) = \mu_2' = \frac{24\theta^{\alpha+1}+(\alpha+4)!}{\theta^2\left(2\theta^{\alpha+1}+(\alpha+2)!\right)}$$

$$E\left(X^3\right) = \mu_3' = \frac{120\theta^{\alpha+1}+(\alpha+5)!}{\theta^3\left(2\theta^{\alpha+1}+(\alpha+2)!\right)}$$

$$E\left(X^4\right) = \mu_4{}' = \frac{720\theta^{\alpha+1}+(\alpha+6)!}{\theta^4\left(2\theta^{\alpha+1}+(\alpha+2)!\right)}$$

$$\text{Variance}\ (\mu_2) = \frac{24\theta^{\alpha+1}+(\alpha+4)!}{\theta^2(2\theta^{\alpha+1}+(\alpha+2)!)} - \left(\frac{6\theta^{\alpha+1}+(\alpha+3)!}{\theta(2\theta^{\alpha+1}+(\alpha+2)!)}\right)^2$$

$$S.D(\sigma) = \sqrt{\left(\frac{24\theta^{\alpha+1}+(\alpha+4)!}{\theta^2(2\theta^{\alpha+1}+(\alpha+2)!)} - \left(\frac{6\theta^{\alpha+1}+(\alpha+3)!}{\theta(2\theta^{\alpha+1}+(\alpha+2)!)}\right)^2\right)}$$

4.2 Harmonic Mean

The harmonic mean for the proposed area biased Shukla distribution can be obtained as:

$$H\cdot M = E\left(\frac{1}{x}\right) = \int_0^{\infty}\frac{1}{x}f_a(x)dx$$

$$H\cdot M = \int_0^{\infty}\frac{x\theta^{\alpha+3}}{2\theta^{\alpha+1}+(\alpha+2)!}\left(\theta+x^{\alpha}\right)e^{-\theta x}dx$$

$$H\cdot M = \frac{\theta^{\alpha+3}}{2\theta^{\alpha+1}+(\alpha+2)!}\left(\theta\int_0^{\infty} xe^{-\theta x}dx + \int_0^{\infty} x^{\alpha+1}e^{-\theta x}dx\right)$$

$$H\cdot M = \frac{\theta^{\alpha+3}}{2\theta^{\alpha+1}+(\alpha+2)!}$$

$$\times\left(\theta\int_0^{\infty} x^{3-2}e^{-\theta x}dx + \int_0^{\infty} x^{(\alpha+3)-2}e^{-\theta x}dx\right)$$

After simplification of above equation, we obtain:

$$H.M = \frac{\theta^{\alpha+3}}{2\theta^{\alpha+1}+(\alpha+2)!}(\theta\gamma(3,\theta x) + \gamma(\alpha+3,\theta x))$$

4.3 Moment Generating Function and Characteristic Function

Let X be the random variable following area biased Shukla distribution with parameters and , then the MGF of X can be obtained as:

$$M_X(t) = E\left(e^{tx}\right) = \int_0^{\infty} e^{tx}f_a(x)dx$$

Using Taylor's series, we obtain,

$$= \int_0^{\infty}\left(1 + tx + \frac{(tx)^2}{2!} + \ldots\right)f_a(x)dx$$

$$= \int_0^{\infty}\sum_{j=0}^{\infty}\frac{t^j}{j!}x^j f_a(x)dx$$

$$= \sum_{j=0}^{\infty}\frac{t^j}{j!}\mu_j{}'$$

$$= \sum_{j=0}^{\infty}\frac{t^j}{j!}\left(\frac{\theta^{\alpha+1}(j+2)!+(\alpha+j+2)!}{\theta^j(2\theta^{\alpha+1}+(\alpha+2)!)}\right)$$

$$M_X(t) = \frac{1}{(2\theta^{\alpha+1}+(\alpha+2)!)}\sum_{j=0}^{\infty}\frac{t^j}{j!\theta^j}\left(\theta^{\alpha+1}(j+2)! + (\alpha+j+2)!\right)$$

Similarly, the characteristic function of area biased Shukla distribution can be obtained as:

$$\phi_x(t) = M_X(it)$$

$$M_X(it) = \frac{1}{(2\theta^{\alpha+1}+(\alpha+2)!)}\sum_{j=0}^{\infty}\frac{it^j}{j!\theta^j}\left(\theta^{\alpha+1}(j+2)! + (\alpha+j+2)!\right)$$

5 Order Statistics

Order statistics is a useful concept in statistical sciences and have wide range of applications in the field of reliability and life testing. Let $X_{(1}, X_{(2)}, \ldots, X_{(n)}$ denotes the order statistics of a random sample $X_1, X_2, \ldots, X_n$ from a continuous distribution with probability density function $\tilde{f_x}(x)$ and cumulative distribution function $F_X(x)$, then the probability density function of r^{th} order statistics $X_{(r)}$ is given by

$$f_{x(r)}(x) = \frac{n!}{(r-1)!(n-r)!}f_X(x)\left(F_X(x)\right)^{r-1}\left(1-F_X(x)\right)^{n-r}$$

By using the equations (5) and (7) in equation (10), we will obtain the probability density function of r^{th} order statistics of area biased Shukla distribution as:

$$f_{x(r)}(x) = \frac{n!}{(r-1)!(n-r)!}\left(\frac{x^2\theta^{\alpha+3}}{2\theta^{\alpha+1}+(\alpha+2)!}\left(\theta+x^{\alpha}\right)e^{-\theta x}\right)$$

$$\times\left(\frac{1}{2\theta^{\alpha+1}+(\alpha+2)!}\left(\theta^{\alpha+1}\gamma(3,\theta x) + \gamma(\alpha+3,\theta x)\right)\right)^{r-1}$$

$$C\times\left(1 - \frac{1}{2\theta^{\alpha+1}+(\alpha+2)!}\left(\theta^{\alpha+1}\gamma(3,\theta x) + \gamma(\alpha+3,\theta x)\right)\right)^{n-r}$$

Therefore, the probability density function of higher order statistic $X_{(n)}$ of area biased Shukla distribution can be obtained as

$$f_{x(n)}(x) = \frac{nx^2\theta^{\alpha+\bar{j}3}}{2\theta^{\alpha+1}+(\alpha+2)!}\left(\theta+x^{\alpha}\right)e^{-\theta x}$$

$$\times\left(\frac{1}{2\theta^{\alpha+1}+(\alpha+2)!}\left(\theta^{\alpha+1}\gamma(3,\theta x) + \gamma(\alpha+3,\theta x)\right)\right)^{n-1}$$

and the probability density function of first order statistic $\overline{\bar{X}}^{=}_{(l)}$ of area biased Shukla distribution can be obtained as

$$f_{x(1)}(x) = \frac{nx^2\theta^{\alpha\bar{F}+3}}{2\theta^{\alpha+1}+(\alpha+2)!}\left(\theta+x^{\alpha}\right)e^{-\theta x}$$

$$\times\left(1 - \frac{1}{2\theta^{\alpha+1}+(\alpha+2)!}\left(\theta^{\alpha+1}\gamma(3,\theta x) + \gamma(\alpha+3,\theta x)\right)\right)^{n-1}$$

6 Likelihood Ratio Test

Let the random sample $X_1, X_2, \ldots., X_n$ of size n drawn from the area biased Shukla distribution. To test we set up the hypothesis:

$$H_o : f(x) = f(x;\theta,\alpha) \quad \text{against} \quad H_1 : f(x) = f_a(x;\theta,\alpha)$$

In order to analyse, whether the random sample of size n comes from Shukla distribution or area biased Shukla distribution, the following test statistic is used.

$$\Delta = \frac{L_1}{L_o} = \prod_{i=1}^{n} \frac{f_a(x;\theta,\alpha)}{f(x;\theta,\alpha)}$$

$$\Delta = \frac{L_1}{L_o} = \prod_{i=1}^{n} \left(\frac{x_i^2 \theta^2 \left(\theta^{\alpha+1} + \alpha!\right)}{2\theta^{\alpha+1} + (\alpha+2)!} \right)$$

$$\Delta = \frac{L_1}{L_o} = \left(\frac{\theta^2 \left(\theta^{\alpha+1} + \alpha!\right)}{2\theta^{\alpha+1} + (\alpha+2)!} \right)^n \prod_{i=1}^{n} {x_i}^2$$

We should reject the null hypothesis, if

$$\Delta = \left(\frac{\theta^2 \left(\theta^{\alpha+1} + \alpha!\right)}{2\theta^{\alpha+1} + (\alpha+2)!} \right)^n \prod_{i=1}^{n} x_i^2 > k$$

Equivalently, we also reject the null hypothesis, where

$$\Delta^* = \prod_{i=1}^{n} x_i^2 > k \left(\frac{2\theta^{\alpha+1} + (\alpha+2)!}{\theta^2 \left(\theta^{\alpha+1} + \alpha!\right)} \right)^n$$

$$\Delta^* = \prod_{i=1}^{n} {x_i}^2 > k^*, \text{ Where } k^* = k \left(\frac{2\theta^{\alpha+1} + (\alpha+2)!}{\theta^2 \left(\theta^{\alpha+1} + \alpha!\right)} \right)^n$$

For large sample of size n, $2\log\Delta$ is distributed as chi-square distribution with one degree of freedom and also the chi-square distribution is used for getting the p value. Thus, we reject the null hypothesis, when the probability value is given by $p\left(\Delta^* > \lambda^*\right)$, Where $\lambda^* = \prod_{i=1}^{n} {x_i}^2$ is less than a particular level of significance and $\prod_{i=1}^{n} {x_i}^2$ is the observed value of the statistic Δ^*.

7 Bonferroni and Lorenz Curves

The Bonferroni and Lorenz curves are used in economics to study the distribution of inequality in income or poverty. The bonferroni and Lorenz curves are given by

$$B(p) = \frac{1}{p\mu_1'} \int_0^q x f(x) dx$$

and

$$L(p) = pB(p) = \frac{1}{\mu_1'} \int_0^q x f(x) dx$$

Where

$$\mu_1' = \frac{6\theta^{\alpha+1} + (\alpha+3)!}{\theta\left(2\theta^{\alpha+1} + (\alpha+2)!\right)}$$

and

$$q = F^{-1}(p)$$

$$B(p) = \frac{\theta\left(2\theta^{\alpha+1}+(\alpha+2)!\right)}{p\left(6\theta^{\alpha+1}+(\alpha+3)!\right)} \int_0^q \frac{x^3\theta^{\alpha+3}}{2\theta^{\alpha+1}+(\alpha+2)!} \left(\theta + x^{\alpha}\right) e^{-\theta x} dx$$

$$B(p) = \frac{\theta^{\alpha+4}}{p\left(6\theta^{\alpha+1}+(\alpha+3)!\right)} \int_0^q x^3 \left(\theta + x^{\alpha}\right) e^{-\theta x} dx$$

$$B(p) = \frac{\theta^{\alpha+4}}{p\left(6\theta^{\alpha+1}+(\alpha+3)!\right)} \left(\theta \int_0^q x^{4-1} e^{-\theta x} dx + \int_0^q x^{\alpha+4-1} e^{-\theta x} dx\right)$$

After simplification, we obtain

$$B(p) = \frac{\theta^{\alpha+4}}{p\left(6\theta^{\alpha+1}+(\alpha+3)!\right)} \left(\theta\gamma(4,\theta q) + \gamma(\alpha+4,\theta q)\right)$$

$$L(p) = \frac{\theta^{\alpha+4}}{\left(6\theta^{\alpha+1}+(\alpha+3)!\right)} \left(\theta\gamma(4,\theta q) + \gamma(\alpha+4,\theta q)\right)$$

8 Entropy

The concept of entropy is important in different areas of knowledge such as probability, statistics, physics, communication theory and economics. Entropies quantify the diversity, uncertainty, or randomness of a system. Entropy of a random variable X is a measure of variation of the uncertainty. umm

8.1 Renyi Entropy

The Renyi entropy is important in information theory as it generalizes the Shannon, Hartley, collision and min entropies. The Renyi entropy is also important in quantum information, where it can be used as a measure of entanglement. For a given probability distribution, Renyi entropy is given by

$$e(\gamma) = \frac{1}{1-\gamma} \log\left(\int f^{\gamma}(x) dx\right)$$

Where $\gamma > 0$ and $\gamma \neq 1$

$$e(\gamma) = \frac{1}{1-\gamma} \log \int_0^{\infty} \left(\frac{x^2\theta^{\alpha+3}}{2\theta^{\alpha+1} + (\alpha+2)!} \left(\theta + x^{\alpha}\right) e^{-\theta x} \right)^{\gamma} dx$$

$$e(\gamma) = \frac{1}{1-\gamma} \log\left(\left(\frac{\theta^{\alpha+3}}{2\theta^{\alpha+1} + (\alpha+2)!} \right)^{\gamma} \int_0^{\infty} x^{2\gamma} e^{-\theta\gamma x} \left(\theta + x^{\alpha}\right)^{\gamma} dx \right)$$

Using Binomial expansion in equation (11), we obtain

$$e(\gamma) = \frac{1}{1-\gamma} \log\left(\left(\frac{\theta^{\alpha+3}}{2\theta^{\alpha+1}+(\alpha+2)!} \right)^{\gamma} \sum_{j=0}^{\infty} \binom{\gamma}{j} \theta^{\gamma-j} x^{\alpha j} \int_0^{\infty} x^{2\gamma} e^{-\theta\gamma x} dx \right)$$

$$e(\gamma) = \frac{1}{1-\gamma} \log\left(\left(\frac{\theta^{\alpha+3}}{2\theta^{\alpha+1}+(\alpha+2)!} \right)^{\gamma} \times \sum_{j=0}^{\infty} \binom{\gamma}{j} \theta^{\gamma-j} \int_0^{\infty} x^{(2\gamma+\alpha j+1)-1} e^{-\theta\gamma x} dx \right)$$

$$e(\gamma) = \frac{1}{1-\gamma} \log\left(\left(\frac{\theta^{\alpha+3}}{2\theta^{\alpha+1}+(\alpha+2)!} \right)^{\gamma} \sum_{j=0}^{\infty} \binom{\gamma}{j} \theta^{\gamma-j} \frac{\Gamma(2\gamma+\alpha j+1)}{(\theta\gamma)^{2\gamma+\alpha j+1}} \right)$$

8.2 Tsallis Entropy

The generalization of B-G statistics was proposed firstly by introducing the mathematical expression of Tsallis entropy (Isallis, 1988) for a continuous random variable is defined as follows

$$S_{\lambda} = \frac{1}{\lambda - 1} \left(1 - \int_0^{\infty} f^{\lambda}(x) dx\right)$$

$$S_{\lambda} = \frac{1}{\lambda - 1} \left(1 - \int_0^{\infty} \left(\frac{x^2\theta^{\alpha+3}}{2\theta^{\alpha+1} + (\alpha+2)!} \left(\theta + x^{\alpha}\right) e^{-\theta x} \right)^{\lambda} dx \right)$$

$$S_\lambda = \frac{1}{\lambda-1}\left(1 - \left(\frac{\theta^{\alpha+3}}{2\theta^{\alpha+1}+(\alpha+2)!}\right)^\lambda \times \int_0^\infty x^{2\lambda} e^{-\lambda\theta x}\,(\theta + x^\alpha)^\lambda\, dx\right)$$

Using Binomial expansion in equation (12), we get

$$S_\lambda = \frac{1}{\lambda-1}\left(1 - \left(\frac{\theta^{\alpha+3}}{2\theta^{\alpha+1}+(\alpha+2)!}\right)^\lambda \times \sum_{j=0}^\infty \binom{\lambda}{j} \theta^{\lambda-j} x^{\alpha j} \int_0^\infty x^{2\lambda} e^{-\lambda\theta x} dx\right)$$

$$S_\lambda = \frac{1}{\lambda-1}\left(1 - \left(\frac{\theta^{\alpha+3}}{2\theta^{\alpha+1}+(\alpha+2)!}\right)^\lambda \times \sum_{j=0}^\infty \binom{\lambda}{j} \theta^{\lambda-j} \int_0^\infty x^{(2\lambda+\alpha j+1)-1} e^{-\lambda\theta x} dx\right)$$

$$S_\lambda = \frac{1}{\lambda-1}\left(1 - \left(\frac{\theta^{\alpha+3}}{2\theta^{\alpha+1}+(\alpha+2)!}\right)^\lambda \times \sum_{j=0}^\infty \binom{\lambda}{j} \theta^{\lambda-j} \frac{\Gamma(2\lambda+\alpha j+1)}{(\lambda\theta)^{2\lambda+\alpha j+1}}\right)$$

9 Maximum Likelihood Estimation and Fisher's Information Matrix

In this section, we will discuss the method of maximum likelihood estimation to estimate the parameters of area biased Shukla distribution. Let $X_1, X_2, \Longrightarrow X_n$ be a random sample of size n from the area biased Shukla distribution, then the likelihood function can be written as

$$L(x) = \prod_{i=1}^n f_a(x)$$

$$L(x) = \prod_{i=1}^n \left(\frac{x_i^2\theta^{\alpha+3}}{2\theta^{\alpha+1}+(\alpha+2)!}\left(\theta + x_i^\alpha\right) e^{-\theta x_i}\right)$$

$$L(x) = \frac{\theta^{n(\alpha+3)}}{\left(2\theta^{\alpha+1}+(\alpha+2)!\right)^n} \prod_{i=1}^n \left(x_i^2\left(\theta + x_i^\alpha\right) e^{-\theta x_i}\right)$$

The log likelihood function is given by

$$\log L = n(\alpha+3)\log\theta - n\log\left(2\theta^{\alpha+1}+(\alpha+2)!\right) + 2\sum_{i=1}^n \log x_i + \sum_{i=1}^n \log\left(\theta + x_i^\alpha\right) - \theta\sum_{i=1}^n x_i \quad (13)$$

Now differentiating the log likelihood equation (13) with respect to parameters θ and α. we must satisfy the normal equations as

$$\frac{\partial \log L}{\partial\theta} = \frac{n(\alpha+3)}{\theta} - n\left(\frac{2\theta^\alpha(\alpha+1)}{\left(2\theta^{\alpha+1}+(\alpha+2)!\right)}\right) + \sum_{i=1}^n \left(\frac{1}{\left(\theta + x_i^\alpha\right)}\right) - \sum_{i=1}^n x_i = 0$$

$$\frac{\partial \log L}{\partial\alpha} = n\log\theta - n\left(\frac{1}{2\theta^{\alpha+1}+(\alpha+2)!}\right) = 0$$

The above likelihood equations are too complicated to solve it algebraically. Therefore we use R and wolfram mathematics for estimating the parameters of the proposed distribution.

In order to obtain the confidence interval, we use the asymptotic normality tests. We have that if $\hat\beta = (\hat\theta, \hat\alpha)$ denotes the maximum likelihood estimate of $\beta = (\theta, \alpha)$. We can state the result as

$$\sqrt{n}(\hat\beta - \beta) \to N_2\left(0, I^{-1}(\beta)\right)$$

Where $I(\beta)$ is Fisher's Information matrix. i.e.

$$I(\beta) = -\frac{1}{n}\begin{pmatrix} E\left(\frac{\partial^2 \log L}{\partial\theta^2}\right) & E\left(\frac{\partial^2 \log L}{\partial\theta\partial\alpha}\right) \\ E\left(\frac{\partial^2 \log L}{\partial\alpha\partial\theta}\right) & E\left(\frac{\partial^2 \log L}{\partial\alpha^2}\right) \end{pmatrix}$$

$$E\left(\frac{\partial^2 \log L}{\partial\theta^2}\right) = -\frac{n(\alpha+3)}{\theta^2} - n\left(\frac{\left(2\theta^{\alpha+1}+(\alpha+2)!\right)2\alpha\theta^{\alpha-1}(\alpha+1) - (2\theta^\alpha(\alpha+1))\,2(\alpha+1)\theta^\alpha}{\left(2\theta^{\vec{\alpha+1}}+(\alpha+2)!\right)^2}\right) - \sum_{i=1}^n \left(\frac{1}{\left(\theta + x_i^\alpha\right)^2}\right)$$

$$E\left(\frac{\partial^2 \log L}{\partial\alpha^2}\right) = n\left(\frac{1}{\left(2\theta^{\alpha+1}+(\alpha+2)!\right)^2}\right)$$

$$E\left(\frac{\partial^2 \log L}{\partial\theta\partial\alpha}\right) = \frac{n}{\theta} - n\left(\frac{\left(2\theta^{\alpha+1}+(\alpha+2)!\right)2\theta^\alpha - (\alpha+1)2\theta^\alpha}{\left(2\theta^{\alpha+1}+(\alpha+2)!\right)^2}\right)$$

Since β being unknown, we estimate $I^{-1}(\beta)$ by $I^{-1}(\hat\beta)$ and this can be used to obtain asymptotic confidence intervals for θ and α.

10 Application

In this section, we have used a real life data set in area biased Shukla distribution to discuss its goodness of fit and the fit by area biased Shukla distribution has been compared over Shukla, Shanker and Lindley distributions. The following real life data set is given below as The following real data set represents 40 patients suffering from blood cancer (leukemia) reported from one of ministry of health hospitals in Saudi Arabia (see Abouammah et al.). The ordered lifetimes (in years) is given below as:

In order to estimate the unknown parameters along with the model comparison criterion values, the R software is employed. In order to compare the area biased Shukla distribution with Shukla, Shanker and Lindley distributions, we use the criterions like AIC (Akaike Information Criterion), BIC (Bayesian Information Criterion), AICC (Akaike Information Criterion Corrected) and -2logL. The better distribution is which corresponds to the lesser values of AIC, BIC, AICC and -2logL. For the calculation of criterions like AIC, BIC, AICC and -2logL following formulas are used.

$$AIC = 2k - 2\log L, BIC = k\log n - 2\log L$$

$$\text{and} \quad AICC = AIC + \frac{2k(k+1)}{n-k-1}$$

Where k is the number of parameters in the statistical model, n is the sample size and $-2\log L$ is the maximized value of log-likelihood function under the considered model.

Table 1. Data regarding blood cancer (leukemia) patients reported by Abouammah et al. (2000)

0.315	0.496	0.616	1.145	1.208	1.263	1.414	2.025	2.036
2.162	2.211	2.37	2.532	2.693	2.805	2.91	2.912	3.192
3.263	3.348	3.348	3.427	3.499	3.534	3.767	3.751	3.858
3.986	4.049	4.244	4.323	4.381	4.392	4.397	4.647	4.753
4.929	4.973	5.074	5.381					

Table 2. Performance of fitted distributions

Distributions	**MLE**	**S.E**	**-2logL**	**AIC**	**BIC**	**AICC**
Area Biased Shukla	$\hat{\alpha}$ =4.7239868	$\hat{\alpha}$ =1.3367639	139.9006	143.9006	147.2783	144.2249
	$\hat{\theta}$ =2.3484695	$\hat{\theta}$ =0.4599152				
Shukla	$\hat{\alpha}$ =6.441769	$\hat{\alpha}$ =1.504546	140.6503	144.6503	148.028	144.9746
	$\hat{\theta}$ =2.098150	$\hat{\theta}$ =0.469815				
Shanker	$\hat{\theta}$ =0.54874483	$\hat{\theta}$ =0.05724169	157.8358	159.8358	161.5247	159.9410
Lindley	$\hat{\theta}$ =0.52692132	$\hat{\theta}$ =0.06074766	160.5012	162.5012	164.19	162.6064

From table 2 given above, it has been observed that the area biased Shukla distribution have the lesser AIC, BIC, AICC and -2logL values as compared to the Shukla, Shanker and Lindley distributions. Hence, it can be concluded that the area biased Shukla distribution leads to a better fit over Shukla, Shanker and Lindley distributions.

11 Conclusions

In this study, a new continuous two parameter distribution called as area biased Shukla distribution has been proposed. The introduced distribution is generated by using the area biased technique to the standard baseline distribution. Its several statistical properties along with some survival measures have been discussed. the estimation of parameters have also been studied by employing the method of maximum likelihood estimation. Finally, the new distribution has been demonstrated with real life data set to discuss its goodness of fit test and it is found from the results that the area biased Shukla distribution fits quite satisfactory over Shukla, Shanker and Lindley distributions.

References

[1] Abouammoh, A. M., Ahmed, R. and Khalique, A. (2000). On new renewal better than used classes of life distribution. Statistics and Probability Letters, 48, 189-194.

[2] Ade, R. B., Teltumbade, D. P. and Tasare, P. W. (2021). Characterization and estimation of area biased quasi Akash distribution. International Journal of Mathematics Trends and Technology, 67(1), 53-59.

[3] Bashir, S. and Rasul, M. (2016). Poisson area-biased Lindley distribution and its applications on biological data. Biometrics & Biostatistics International Journal, 3(1), 27-35.

[4] Cox, D. R. (1969). Some sampling problems in technology, In New Development in Survey Sampling, Johnson, N. L. and Smith, H., Jr .(eds.) New York Wiley- Interscience, 506-527.

[5] Dar, A. A., Ahmad, A. and Reshi, J. A. (2020). Weighted Gamma-Pareto distribution and its Application. Pak.J.Statist., 36(4), 287-304.

[6] Fisher, R. A. (1934). The effects of methods of ascertainment upon the estimation of frequencies. Ann. Eugenics, 6, 13-25.

[7] Hassan, A., Dar, S. A. and Para, B. A. (2018). On three Parameter Weighted Quasi Akash Distribution: Properties and Applications, IOSR Journal of Engineering (IOSR-JEN), 08(11), 01-10.

[8] Mudasir, S. and Ahmad, S. P. (2017). Characterization and Information measures of weighted Erlang distribution. Journal of Statistics Applications & Probability Letters An international journal, 4(3), 109-122.

[9] Mudasir, S., Bhat, B. A., Bhat, A. A. and Ahmad, S. P. (2018). The weighted new Weibull Pareto distribution: Some Characteristics and Applications. International Journal of Scientific Research in Mathematical and Statistical Sciences, 5(5), 153-163.

[10] Patil, G. P. and Rao, C. R. (1978). Weighted Distributions and Size-Biased Sampling with Applications to Wildlife Populations and Human Families. Biometrics, 34(2), 179. doi:10.2307/2530008.

[11] Perveen, Z., Munir, M., Ahmed, Z. and Ahmad, M. (2016). On area biased weighted weibull distribution. Sci. Int.(Lahore), 28(4), 3669-3679.

[12] Rao, C. R. (1965). On discrete distributions arising out of method of ascertainment, in classical and Contagious Discrete, G.P. Patiled; Pergamum Press and Statistical publishing Society,Calcutta. 320-332.

[13] R core team. R version 3.5.3 (2019): A language and environment for statistical Computing. R foundation for statistical computing, Vienna, Austria. URL http://www.R-project.org/.

[14] Saghir, A., Hamedani, G. G., Tazeem, S. and Khadim, A. (2017). Weighted distributions: A Brief Review, Perspective and Characterizations. International Journal of Statistics and Probability, 6(3), 109-131.

[15] Sharma, V. K., Dey, S., Singh, S. K. and Manzoor, U. (2018). On length and area-biased Maxwell distributions. Communications in Statistics-Simulation and Computation, 47(5), 1506-1528.

[16] Shukla, K. K. and Shanker, R. (2019). Shukla distribution and its Application. R. T & A, 3(54), Volume 14.

[17] Subramanian C. and Rather, A. A. (2018).Weighted exponentiated mukherjee-islam distribution, International Journal of Management, Technology and Engineering, 8(11), 1328-1339.

[18] Warren, W. (1975). Statistical distributions in forestry and forest products research. In: Patil, G.P., Kotz, S. and Ord, J.K. (eds) Statistical Distributions in Scientific Work, Vol. 2. D. Reidel, Dordrecht, The Netherlands, pp. 369-384.

[19] Zelen, M. (1974). Problems in cell kinetic and the early detection of disease, in Reliability and Biometry, F. Proschan & R.J. Sering, eds, SIAM, Philadelphia, 701-706.

Sujit Distribution and Its Applications

Rekha Radhakrishnan[1], Venkatesan D[2] and Prasanth C B[3]

[1] Research Scholar, Department of Statistics, Annamalai University
[2] Professor, Department of Statistics, Annamalai University
[3] Assistant Professor, Department of Statistics, Sree Keralavarma College ,Thrissur

Abstract -

A new one parameter lifetime distribution named "Sujit distribution" has been proposed for modeling lifetime data. This model is a mixture of Exponential and Gamma distribution. Some important properties of the proposed distribution including its shape, moments, Skewness , Kurtosis, hazard rate function, mean residual functions has been discussed. The estimation of the parameters has discussed using maximum likelyhood estimation. A simulation study was carried out to assess the performance of the proposed model.

Keywords -

Lifetime distribution, Moments, Hazard rate function, Mean residual life function, Estimation of parameter, Simulation.

1 Introduction

The modeling and statistical analysis of lifetime data are necessary in many applied sciences including medicine, engineering, insurance and finance . There are a lot of continuous distributions for modeling lifetime data such as Exponential, Lindley, Gamma, Lognormal, Weibull and their generalizations. The Exponential, Lindley and Weibull distributions are more popular than the Gamma and the Lognormal distributions because the survival functions of the Gamma and the Lognormal distributions cannot be expressed in closed forms and both require numerical integration. Though each of Exponential and Lindley distributions has one parameter, Lindley distribution has one advantage over Exponential distribution that the Exponential distribution has constant hazard rate whereas the Lindley distribution has monotonically decreasing hazard rate. The probability density function (p.d.f.) and the cumulative distribution function (c.d.f.) of Lindley distribution are given by (1958).

$$f(x,\theta) = \frac{\theta^2}{\theta+1}(1+x)e^{-\theta x}; x > 0, \theta > 0$$

$$F(x,\theta) = 1 - [1 + \frac{\theta x}{\theta+1}]e^{-\theta x}; x > 0, \theta > 0$$

The density is a two-component mixture of an Exponential distribution having scale parameter θ and a Gamma distribution having shape parameter 2 and scale parameter θ with their mixing proportions $\frac{\theta}{\theta+1}$ and $\frac{1}{\theta+1}$ respectively. The Lindley (1958) are popular for modeling lifetime data from biomedical science and engineering. But, Shanker et al (2015) have conducted a comparative study on modeling of lifetime data from various fields of knowledge and observed that there are many lifetime data where these two distributions are not suitable due to their shapes, nature of hazard rate functions, and mean residual life, amongst others. Shanker (2015 a, 2015 b, 2016 b, 2016 c,2016 d, 2017) has introduced few one parameter lifetime distributions namely Akash, Shanker, Aradhana, Sujatha, Devya, and Suja and produced that these distributions give better fit than the classical Exponential and Lindley distributions. Each of these life time distributions has advantages and disadvantages over one another due to its shape, hazard rate function and mean residual life function. There are many situations where these distributions are notifiable for modeling lifetime data from theoretical or applied point of view. Therefore, an attempt has been made in this paper to obtain a new distribution which is flexible than these one parameter lifetime distributions including Akash, Shanker, Aradhana, Sujatha, Devya, Suja and Exponential for modeling lifetime data in reliability and in terms of its hazard rate shapes.

2 The objective of the study

In this paper we have proposed a new continuous distribution, which is better than Akash, Shanker, Lindley and Exponential distributions for modelling lifetime data. The new one parameter lifetime distribution is based on a two component mixture of an Exponential distribution having scale parameter θ and a Gamma distribution with shape parameter 4 and scale parameterθ with their mixing proportion $\frac{\theta^2}{\theta^2+6}$ and $\frac{6}{\theta^2+6}$. We would call this distribution as Sujit Distribution.The Probabilty density function of the new one parameter lifetime distribution can be introduced

as

$$f(x) = \frac{\theta^3}{\theta^2+6}(1+x^3\theta)e^{-\theta x}; x > 0, \theta > 0 \qquad (2.1)$$

This distribution can be easily expressed as the mixture of Exponential (θ) and Gamma (4, θ) with their mixing proportion $\frac{\theta^2}{\theta^2+6}$ and $\frac{6}{\theta^2+6}$ respectively.

We have $f(x,\theta) = pg_1(x) + (1-p)g_2(x)$

where p = $\frac{\theta^2}{\theta^2+6}$ and $g_1(x) = \theta e^{-x\theta}$ and

1-p = $\frac{6}{\theta^2+6}$ and

$$g_2(x) = \frac{\theta^4.x^3.e^{-x\theta}}{6}$$

The corresponding cumulative distribution function is given as

$$F(x) = 1 - [1 + \frac{\theta x * (\theta^2x^2 + 3\theta x + 6)}{\theta^2+6}]e^{-\theta x}, x > 0, \theta > 0 \qquad (2.2)$$

The graph of pdf and cdf for varying values of θ are shown in the figure 1 and 2.

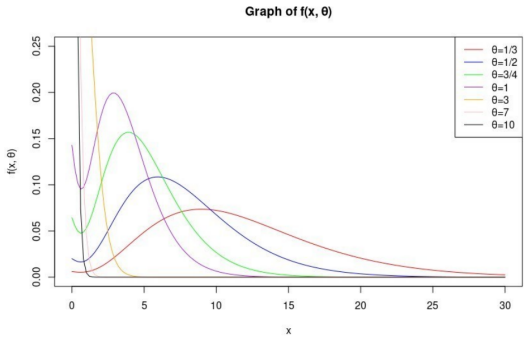

Figure 1. Graph of the pdf of the distribution with different values of the parameter

3 Moments and its related measures

The rth moment of the new distribution is given by

$$\mu = E[X^r] = \frac{r!}{\theta^r}[\frac{\theta^2 + (r+3)(r+2)(r+1)}{\theta^2+6}], r = 1, 2, 3, \ldots \qquad (3.1)$$

and then the first four moments about origin as.. . .

$$\mu_1 = \frac{\theta^2+24}{\theta(\theta^2+6)}, \mu_2 = \frac{2(\theta^2+60)}{\theta^2(\theta^2+6)}$$

$$\mu_3 = \frac{6(\theta^2+120)}{\theta^3(\theta^2+6)}, \mu_4 = \frac{24(\theta^2+210)}{\theta^4(\theta^2+6)}$$

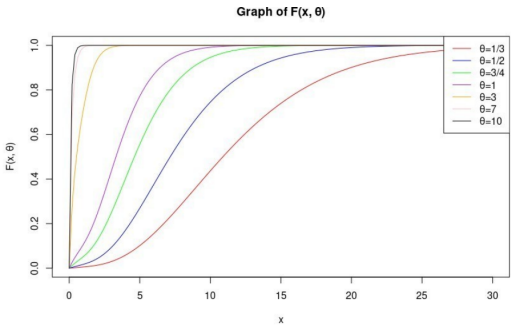

Figure 2. Graph of the cdf of the distribution with different values of the parameter

Thus the central moments(moments about orgin) are obtained as

$$\mu_2 = \frac{(\theta^4+84\theta^2+144)}{\theta^3(\theta^2+6)^2}\mu_3 = \frac{2(\theta^6+198\theta^4+324\theta^2+864)}{\theta^3(\theta^2+6)^3}$$

$$\mu_4 = \frac{9(\theta^8+312\theta^6+2304)\theta^4+10368\theta^2+10368}{\theta^4(\theta^2+6)^4}$$

The coefficient of variation (CV), Coefficient of Skewness ($\sqrt{\beta_1}$) and Coefficient of Kurtosis (β_2) and index of dispersion (γ) of the above distribution are thus obtained as

$$CV = \frac{SD}{mean} = \frac{\sqrt{(\theta^4+84\theta^2+144)}}{\theta^2+24} \qquad (3.2)$$

$$\sqrt{\beta_1} = \frac{2(\theta^6+198\theta^4+324\theta^2+864)}{(\theta^4+84\theta^22+144)^{3/2}} \qquad (3.3)$$

$$\beta_2 = \frac{9(\theta^8+312\theta^6+2304)\theta^4+10368\theta^2+10368}{\theta^4+84\theta^2+144)^2} \qquad (3.4)$$

$$\gamma = \frac{(\theta^4+84\theta^2+144)}{\theta(\theta^2+6)(\theta^2+24)} \qquad (3.5)$$

4 Hazard Rate Function and Mean Residual Life Function

Let f(x) and F(x) be the pdf and cumulative distribution functions of a continuous random variable, then the hazard function h(x) (also known as the failure rate function) is

$$h(x) = \lim_{\delta x \to} \frac{P(X < x + \delta x / X > x)}{\delta x}$$

$$= \frac{f(x)}{(1-F(x)}$$

the mean residual life function,

$$m(x) = \frac{1}{1 - F(x)_x} \int_x^\infty 1 - F(t)\, dt$$

The corresponding hazard rate function h(x) and mean residual function m(x) of the distribution thus obtained as

$$h(x) = \frac{\theta^3(1 + x^3\theta)}{\theta^2x^2(3 + \theta x) + 6(\theta x + 1) + \theta^2} \tag{4.1}$$

$$m(x) = \frac{\theta^2(6x^2 + 1) + 24 - x\theta(x^2\theta^2 + 6)}{\theta[(\theta^2 + 6) + \theta x(\theta^2x^2 + 3\theta x + 6)]} \tag{4.2}$$

It can be easily verified that h(0) = $\frac{\theta^3}{6+\theta^2}$ = f(0) and m(0) = $\frac{\theta^2+24}{\theta(\theta^2+6)}$ = μ. The graph of hazard function and mean residual life function of Sujit distribution is given in Figure 3 and 4.

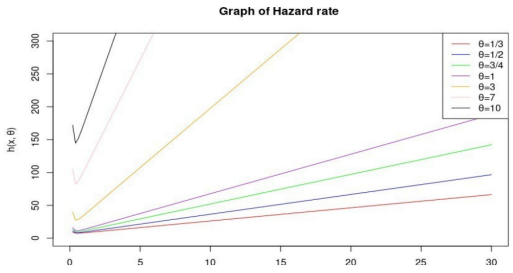

Figure 3. Graph of the hazard rate function for different values of the parameter

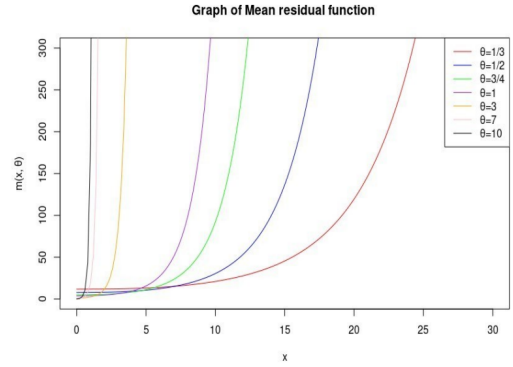

Figure 4. Graph of mean residual function with different values of the parameter

5 Estimation of Parameters

Maximum Likelihood Estimation

Let (x1,x2,....xn) be a random sample from a distribution with pdf

$$f(x) = \frac{\theta^3}{\theta^2 + 6}(1 + x^3\theta)e^{-x\theta}, x > 0, \theta > 0.$$

The likelihood function L of f(x) is

$$L = (\frac{\theta^3}{\theta^2 + 6})^n \prod_{i=1}^{n}(1 + \theta x_i^3)e^{-n\bar{X}\theta} \tag{5.1}$$

$$ln(L) = nln(\frac{\theta^3}{\theta^2 + 6})^n \sum_{i=1}^{n}(1 + \theta x_i^3) - n\theta\bar{X} \tag{5.2}$$

$$\frac{dlnL}{d\theta} = 0$$

$$\frac{3n}{\theta} - \frac{2n\theta}{\theta^2 + 6} - n\bar{X} + \sum_{i=1}^{n}\frac{x_i}{(1 + x_i\theta)} = 0 \tag{5.3}$$

Where $\bar{x}$ is the sample mean MLE of the θ is the solution of the equation $\frac{dlnL}{d\theta} = 0$

Simulation Study

From the simulation study we obtained the sample values for different values of the parameter θ. As the parameter value increases from zero the range of the sample values decreases. For θ ¿ 1 the range of the sample values are less than one.The graph of the pdf (2.1) for simulated values and mean residual function for the simulated values are given in the Figure 5 and 6.

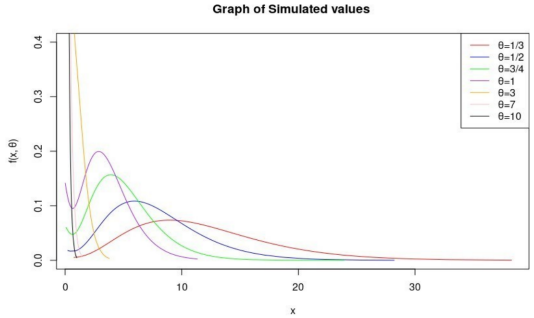

Figure 5. Graph of pdf with simulated values for different values of the parameter

The MLE for the parameter θ is calculated with the simulted data. Six different sets of data are concerned

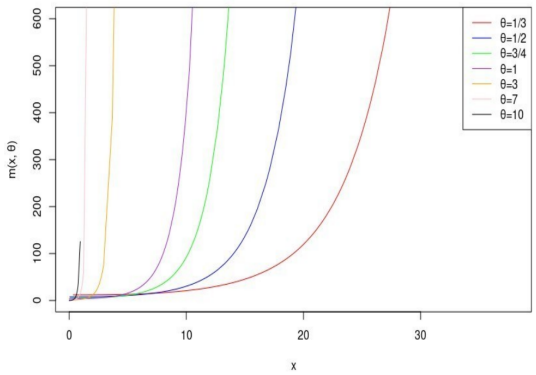

Figure 6. Graph of mean residual function with simulated values for different values of the parameter

and MLE for θ is estimated .The mean and SD are also calculated for the same.The results are given in the Table 1.

Table 1. Shows the mean, SD and MLE for six different sets of data

	Mean	**SD**	**Theta**
Set1	4.686707 5632792	3.082244 6877587	0.750441 491149994
Set2	5.415859 57088973	2.833451 15594328	0.663324 861213589
Set3	47.009754 5527387	28.921018 8022171	0.078654 4808672582
Set4	46.182077 9503323	29.942176 4767621	0.079858 4823762708
Set5	474.265060 976613	295.547724 759827	0.007801 54604362678
Set6	493.147635 455243	287.132659 89987	0.007552 96357017229

From the above table we can see that for the data ranges from 0-10 the estimated value of the parameter is 0.75, for the data ranges from 10-100 the estimated value of the parameter is .07 and for the data ranges from 100- 1000 the estimated value of the parameter is .007.

6 Conclusion

A one parameter lifetime distribution named Sujit distribution has been proposed. The statistical properties of the distribution Shape, Moments, Skewness, Kurtosis, Hhazard rate function,mean residual life function have been discussed.Maximum likelyhood estimation has been discussed for estimating the parameter.Finally the simulation study of the distribution has also carried out.The more characteristics of the above distribution is under progress.

Acknowledgements

The author expresses the gratefulness to the reviewers for their constructive comments

References

[1] Lindley,D .V.(1958);Fiducial distributions and Bayes theorem,Journal of the Royal Statistical Society, Series B,20,102-107

[2] Shanker, R. (2015 a): Akash distribution and its2. Applications, International Journal of Probability and Statistics, 4(3), 65 – 75.

[3] Shanker, R. (2015 b): Shanker distribution and its Applications, International Journal of Statistics and Applications, 5(6), 338 – 348.

[4] Shanker, R. (2016 b): Aradhana distribution and its Applications, International Journal of Statistics and Applications, 6(1), 23 – 34.

[5] Shanker, R. (2016 c): Sujatha distribution and its Applications, Statistics in Transition-new series, 17(3), 1 – 20.

[6] Shanker, R. (2017) : Suja Distribution and Its Application,International Journal of Probability and Statistics 6(2): 11-19

[7] Shanker, R. (2016 d): Devya distribution and its Applications, International Journal of Statistics and Applications, 6(4), 189 – 202.

Impact of COVID-19 on Learners Learning Behavior with Specially for the Adolescent Group

Shiny C Raj[1], Prasanth C B[2], Vijayakumar M [3]

[1]Research Scholar, Department of Statistics, Annamalai University,
[2]Assistant Professor, Sree Kerala Varma College, Thrissur, Kerala,
[3]Associate Professor, Department of Statistics, Annamalai University,

[1]shinycraj@gmail.com [2]cbpwarrier@gmail.com [3]mvkumar1975@gmail.com

Abstract -

The main issues that students had in studying during the post-COVID era and in concentrating and paying attention to their course during the online classes that their universities offered are described below. It is noticed that due to network issues, some difficulties in understanding lectures delivered in online mode. Students face socio-psychological issues like career concerns, lack of motivation, anxiety, and depression due to school closures. The study reveals the impact of internet usage on boys and girls. Schools, colleges, and institutions all across the world are now required to conduct lessons and other activities remotely due to the COVID-19 epidemic. For both students and instructors, switching from traditional face-to-face instruction to virtual instruction presents a number of difficulties. Principals, teachers, and behavioural experts reported a significant increase in behavioural issues among schoolchildren, such as aggression, attention deficit disorder, insomnia, and emotional disturbances, especially among those who lost loved ones in COVID as schools across the nation reopened after two years of online instruction. So it is emphasising the necessity to introduce the socio-emotional learning programmes and counselling sessions at schools. The basic data used in this study was gathered using a questionnaire.

Keywords -

Post covid, Pandemic, Aggression, Attention Span Deficit, Covid 19, Socio psychological issues

1 Introduction

Nearly 1.6 billion pupils in more than 200 countries have been impacted by the largest disruption to the educational system since the country-wide lockdown. Numerous studies have been conducted in relation to the influence of COVID-19 on numerous areas. The limited access to technical resources, transactional distance, mental health, social isolation, and peer-to-peer learning has all had an impact on enrollment in COVID-19. Stress variables that have a significant impact on most students' mental health include financial hardship and loneliness. Academic performance is also likely to be impacted by social isolation brought on by the lack of a peer group, the sense of community created by spending time alone with family members, and the entrepreneurial spirit cultivated by students who use internet platforms to develop and sell their products. Closing schools, colleges, and universities is one of the actions the Indian government has taken to provide access to ongoing education during the pandemic. More than 120 million children and adolescents are worldwide have been impacted by the COVID-19 epidemic. Over 32 crore students in India have been impacted by the restrictions and the nationwide lockdown. This has opened up a wide range of possibilities for a new era of digital learning, including rapid adoption of digital technologies, increased use of learning management systems, increased usage of soft copies of learning materials, and enhanced collaborative work. The government's digital strategy for India is becoming increasingly important. Important classes have been cancelled, tests have been rescheduled, and the admissions process has all been delayed as a result of the epidemic. Additionally, most recruitment has been delayed, and student placements have been impacted. The epidemic has had an effect on unprepared teachers and students for online learning as well as on career possibilities worldwide. Many Indians have lost their overseas jobs as a result of the COVID-19 pandemic and have returned home. Due to school closings, children now have more parental responsibility for their education, have access to the internet, and are given access to global education. Due to these problems, many Indian students who were enrolled in numerous colleges abroad have had to leave those nations, which has had a substantial influence on the higher education system. Payment of school and college fees has been delayed as a result of COVID-19, which has had a huge impact on India's education industry. In order to address the situation, the Government of India has investigated the potential of open and distance learning (ODL) by putting various digital technologies into practise. It is time for vocational institutions to improve their internal knowledge and IT infrastructure in order to better prepare them to handle issues like the COVID-19 pandemic. India

needs to come up with innovative strategies to guarantee that all kids will continue to access education despite the pandemic. Investigating the effect of COVID-19 on India is a major concern in all categories of the power pyramid. The COVID-19 pandemic has had a negative effect on education, with 80% of public schools reporting ”stunted behavioral and socio-emotional development” in their students, a 56% increase in classroom disruptions, a 49% increase in rowdiness outside of the classroom, a 42% increase in chronic teacher and student absenteeism, and a 61% increase in the number of public schools reporting it is ”much more difficult” to find in addition to out-of-class learning frameworks that address some of the uncertainties.

2 Review of Literature

Both teachers and students have to take into account a number of issues as a result of the quick transition from traditional face-to-face sessions to virtual ones. To develop a meaningful and collaborative learning and social atmosphere, students and instructors must work together and actively engage in one another's lessons. In this situation, it is critical to comprehend how students behave throughout synchronous and asynchronous learning activities. The success of online education is also significantly impacted by students' opinions of the teacher-student relationship and their preferences for learning modes. The COVID-19 pandemic's negative effects on scientific education have further shown the necessity for creative frameworks and methods to mitigate their effects and offer equal and effective learning opportunities.

Lorenz S. Neuwirth. et al. (2020) studied the need for faculty and students to address a number of issues and reach an agreement in order to create a meaningful and collaborative learning and social environment as a result of the rapid shift from traditional face-to-face classes to virtual classrooms. With adult learners, the necessity for collaboration between students and instructors is even more important because both sides must have the flexibility to actively engage through the employed online platform. Consider the definition that follows to begin reliably concentrating on these issues: (1) the conduct of the students during live lectures, such as turning on their computer cameras, using the raised hand tools, chat boxes, and unmuting their microphones; (2) in asynchronous formats, the conduct of the students during discussion boards immediately following or prior to lectures, such as by completely responding to questions.

Taneja and I Dutt (2021) find out that the COVID-19 pandemic has led to a shift in teaching methods in India, with 75.32% of students favouring offline learning and 48.1% favouring virtual teaching. The survey indicated that while 79.75% of students prefer regular engagement, 98.73% of students think the teacher is competent when in an offline setting. While 55.06% of students prefer the online mode, 69.62% are at ease using the offline mode. The study offers suggestions for enhancing teaching-learning strategies in times of crisis.

Watonga Michael Ope´ra (2021) explained that a framework for analysing the detrimental consequences of the COVID-19 issue on science education is provided by Michael Ope´ra (2021). It is divided into four sections: a simulation model, a model for a home experiment, a model for a theoretical virtual lecture, and a model for interactive feedback. The suggested technique can be incorporated into the decision analysis framework to clearly address negative consequences and give students options on how they participate, what they study, or how they demonstrate science understanding. It also provides chances for equity, value, and efficiency once it is put into practise, all of which could be advantageous for students.

Anil Kumar Yadav (2021) described the main difficulties pupils encounter during learning, including their inability to focus, the absence of a conducive learning environment at home, and their lack of drive. Additionally, students have experienced problems such as worry about their future careers, anxiety, despair, and a lack of social and moral support. Students' post-lockdown activity shows that they prefer both in-person and online learning methods from their schools. As a result, online teaching and learning techniques are now included in the standard learning process and are treated similarly to traditional classroom instruction.

Marta Migocka. et al. (2021) detailed how, in addition, distance learning offers a remedy for common infrastructural issues. However, a teacher using a distance learning approach might not give their pupils enough chances to develop new abilities and successfully transfer existing knowledge. E-learning offers various benefits, including flexible time management, increased student participation in education due to different access points, lower costs, etc. The benefits and drawbacks of remote teaching should be understood by those in higher education. However, practically all reports show that teachers' commitment and capacity for knowledge transfer have a significant impact on students' performance and happiness.

Graduate students exhibited more concern about the pandemic's impact than undergraduate students did, according to Mona Alhasani et al. (2022). With the help of the viral interface, technology interventions might be created to help students feel more in control over their learning over time, which would relieve tension and anxiety. The students' performance in accomplishing their goals may have been hindered by a lack of motivation and focus on their part. Failure to meet desired or prescribed goals may have a negative impact on students' perception

of their ability to handle time.

From these studies, we understand that it's critical to address the challenges and worries students encounter when education moves to online platforms. Students' learning experiences might be hampered by problems like a poor learning environment, a lack of concentration and motivation, and insufficient social support. However, with students expressing a preference for both in-person and online learning methods, the incorporation of online teaching and learning methodologies into the traditional learning process has become crucial. Opportunities for flexible time management, greater student involvement, and cheaper expenses are provided through distance learning. However, teachers' dedication and ability to promote information transfer continue to be significant determinants affecting students' achievement and happiness. The gendered effects of the pandemic on students' levels of stress and anxiety also highlight how crucial technology solutions are for improving students' perceptions of control over time and easing their psychological loads. Teachers may create a more inclusive and productive learning environment for students by addressing these issues and utilising the benefits of online education.

3 Method of Analysis

The course was abruptly switched from classroom mode to online mode due to COVID-19 epidemic and ensuing lockdown. A total of 380 responses were received to an online questionnaire distributed to students in the adolescent period in order to examine the change in students' behavior.

3.1 Research Objectives

- To research how students now feel about the use of technology in education.
- To investigate how COVID-19 affects students' learning habits.
- To investigate the sociopsychological effects of COVID-19 on graduate and higher education students in Kerala.
- To analyze the learning behavior of the students in two modes, that is traditional class room method and virtual learning method.
- To compare the efficiency of students in studying the course in pre and post covid period.
- An analytical study of pre and post covid result of higher secondary and matric students Develop a regression model for the existing result.

3.2 Hypothesis testing

- To test the independence of gender wise sleeping time and concentration after post covid period using chi – square method
- Correlation between internet usage and concentration power

3.3 Statistical Analysis

- Using frequency, mean, and standard deviation, we computed descriptive statistics.
- Calculate the average score for each scale and run an independent sample chi square test to look for any gender-based differences in the students' stress, anxiety, internet use, sleep patterns, and behavior. Analyze the effectiveness of the learning process as well.

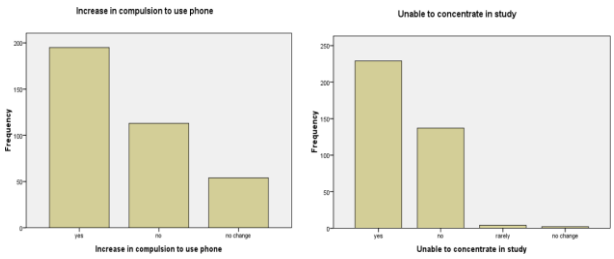

Figure 1. Figure indicates that the smart phone makes great influence in day to life and that will negatively cause the concentration or memory power of students.

Consider the Null hypothesis H0: phone usage and concentration power are independent, Against Alternate hypothesis H1: phone usage and concentration power are not independent

Table 4: chi-square Tests.

6 cells (50.0%) have expected count less than 5. The minimum expected count is .30

Result of chi square test of independence presented in table 2 indicate that phone usage and concentration power is associated. The value of chi square is 7.133, p=0.309 greater than α=.05

Table 5. Correlations

*. Correlation is significant at the 0.05 level (2-tailed).

The association among the above two factors are negatively correlated. That is increase in usage off digital media cause the decrease in the concentration power of the students.

4 Analytical Study of Students Result in Pre and Post Covid Period

Table 6: Descriptive Statistics

Descriptive analysis shows that great variations shown in pass percentage of class12.

Table 1. Descriptive Statistics

		age of respondent	covid +ve	Digital usage increase after covid	Gender of the Respondent	Mode of learning method prefer	Unable to concentrate in study	time spend for doing home work	How much time you sleep every day
N	Valid	379	376	357	378	376	372	367	372
	Missing	16	19	38	17	19	23	28	23
Mean		4.33	1.27	2.35	1.51	2.07	1.41	2.03	1.41
Median		4.00	1.00	2.00	2.00	2.00	1.00	2.00	1.00
Mode		4	1	2	2	2	1	2	1
Std. Deviation		.784	.442	1.172	.501	.462	.544	.880	.544
Variance		.614	.196	1.373	.251	.213	.296	.775	.296
Range		5	1	4	1	2	3	3	3
Percentlies	25	4.00	1.00	1.00	1.00	2.00	1.00	1.00	1.00
	50	4.00	1.00	2.00	2.00	2.00	1.00	2.00	1.00
	75	5.00	2.00	3.00	2.00	2.00	2.00	2.00	2.00

Table 2. Frequency TableMode of learning method preferred

		Frequency	Percent	Valid Percent	Cumulative Percent
Valid	Online digital media	27	6.8	7.2	7.2
	traditional class room	294	74.4	78.2	85.4
	self study	55	13.9	14.6	100.0
	Total	376	95.2	100.0	
Missing	System	19	4.8		
Total		395	100.0		

Table 3. Cross Tabulation - Increase in compulsion to use * Unable to concentrate in study

Count		Unable to concentrate in study				Total
		Yes	No	Rarely	No Change	
Increase in Compulsion to use phone	yes	110	81	2	2	195
	no	73	36	2	0	111
	no change	38	16	0	0	54
Total		221	133	4	2	360

Table 4. chi-square Tests

	Value	df	Asymp. Sig. (2-sided)
Pearson Chi-Square	7.133[a]	6	.309
Likelihood Ratio	8.439	6	.208
Linear-by-Linear Association	5.258	1	.022
N of Valid Cases	360		

Var (10) ¡Var (12). So, efficiency of higher secondary students is comparatively less efficient than Matric students.

The graph shows the pass percent of 10 th and 12 th class students from 2015 to 2023 in Kerala state board examination. At 2020 or 21 the pass percent of10 th was 98.82 and 99.47. These students are now appearing 12 board examinations with result 87.94 and 82.95 percentages. During these two years, the most of the teaching learning process done through the on-line methods. These indicates that the virtual method of learning is adversely influenced by their learning process.

Table 7: Correlations

**Correlation is significant at the 0.01 level (2-tailed).

Table 5. Correlations

		Unable to concentrate in study	Increase in compulsion to use phone
Unable to concentrate in study	Pearson Correlation	1	-.121*
	Sig. (2-tailed)		.022
	N	372	360
Increase in compulsion to use phone	Pearson Correlation	-.121*	1
	Sig. (2-tailed)	.022	
	N	360	362

Table 6. Descriptive Statistics

	N	Minimum	Maximum	Mean	Std. Deviation
percentage12	9	80.94	95.98	88.3167	5.63146
percentage10	7	95.98	99.47	97.9114	1.23892
Valid N (list wise)	7				

Table 7. Correlations

		Percentage 12	Percentage10
Percentage12	Pearson Correlation	1	.661**
	Sig. (2-Tailed)		.004
	N	17	17
Percentage10	Pearson Correlation	.661**	1
	Sig. (2-Tailed)	.004	
	N	17	17

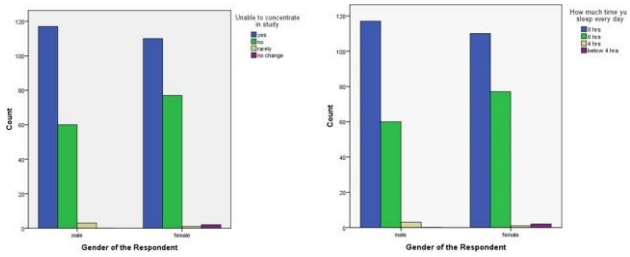

Figure 2. The above multiple bar diagrams indicates that there is no variation in gender wise sleeping time and concentration

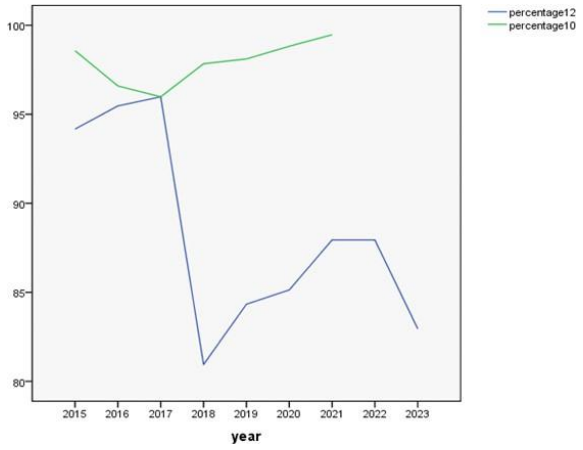

Figure 3. Time series graph

Correlation coefficient between the pass percentage is 0.661; positively correlated

Coefficient of determination R^2 is nearest to 0.45.

Table :8 Coefficients

From the Table 8, 'a' = 0.494 (Y-intercept) and the value of 'b' =35.306 (the slope)

The regression equation is Y = 0.494 X +35.306 which can be used to calculate the percentage of class 12 (dependent variable).

Besides from the survey we can understand that children were found to be facing several health problems such as generalized weakness, headache, sleeplessness and some other issues. Mainly, the diseases due to the intense use of Smartphone.

5 Conclusions and Suggestions

This study examines how students learn when they are exposed to traditional classroom instruction and virtual internet instruction. According to the responses, 74.4%

Table 8. Coefficients

Model		Unstandardized Coefficients		Standardized Coefficients	t	Sig.
		B	Std. Error	Beta		
1	(Constant)	35.306	13.660		2.585	.021
	Percentage10	.494	.145	.661	3.413	.004

A. Dependent variable: percentage 12

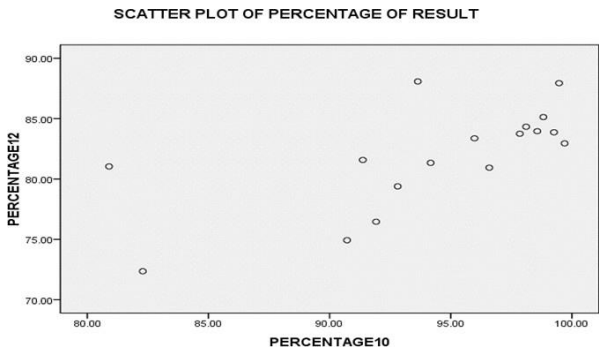

Figure 4. Scatter plot of pass percent percentage between matric & higher secondary classes

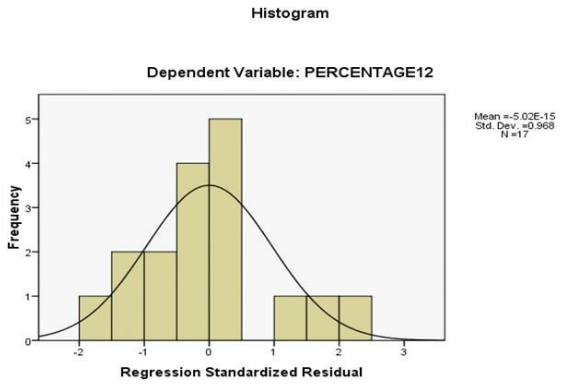

Figure 5. Histogram

of the students support offline instruction. Students also believe that classroom instruction allows for better teacher-student connection. Due to the e-learning method, most students are simultaneously greatly addicted to social media like WhatsApp, Facebook, etc. This seriously affected their concentration. After the epidemic, kids' perceptions of their instructors, schools, friends, and other people have significantly changed. Their ability to focus has decreased, and their writing abilities have undoubtedly suffered. Their sleep patterns have also changed drastically, which has made them irritable. Additionally, due to an increase in internet use, gaming, and excessive cellphone use, behavioral disorders among students have become more prevalent. Following that, because they are unable to sit still for even 30-35 minutes in class, the pupils are frequently taking breaks. We expose an overview of learning disabilities in students due to the COVID pandemic and the excess usage of the internet and mobile phones.

References

[1] Lorenz S Neuwirth et.al. "Reimagining higher education during and post covid-19 challenges and opportunities." Journal of Adult and Continuing Education 27(3), (2020) doi:10.1177/1477971420947738

[2] Taneja Ashur and Dutt Ishwar. "COVID-19 and its implications on students' learning behavior". Library Philosophy and Practice (e-journal), (2021). https://digitalcommons.unl.edu/libphilprac/5103

[3] Wasonga Michael Opera "Negative Impacts of the Current COVID-19 Crisis on cience Education in Kenya: How Certain Can We Be about the Efficacy of the Science Learning Framework Online?", (2021). doi**:** https://doi.org/10.1128/jmbe.v22i1.2559

[4] Marta Migocka et.al. " The Attitude of the Academic Community towards Distance Learning: A Lesson from a National Lockdown", (2021). doi: http://doi.org/10.34190/ejel.19.4.2405

[5] 1. Mona Alhasani et.al. " Mental health and time management behavior among students during covid -19 pandemic", (2022). Article ID 7376748 — https://doi.org/10.1155/2022/7376748.

[6] Anil Kumar Yadav & Uddipla Nayana Medhi. "Impact of covid -19 on student learning behavior with reference to a district in Assam". Inspira-Journal of Commerce, Science (JCECS) 62. ISSN: 2395-7069, Impact Factor: 6.289, 08(02), pp. 62-66, April-June, (2022).

Entrepreneurship Opportunities in the Mechanical Engineering Sector: Challenges and Success Factors in the Indian Context

Dilip Bhattarai

LEAD College of Management, Dhoni, Palakkad

Abstract -

Mechanical engineering is a broad field encompassing design, analysis, testing, manufacturing and maintenance of mechanical systems. The mechanical engineering sector in India presents immense potential for entrepreneurship and business creation due to factors like rapid infrastructure growth, manufacturing expansion, automation trends, and rising exports. However, those venturing into entrepreneurship in this sector face considerable challenges as well. This paper aims to analyze the key opportunities for entrepreneurship in mechanical engineering in India across industries like automotive, manufacturing, robotics, aerospace, energy and more. It also assesses the significant challenges faced by these entrepreneurs including technical complexity, high costs, manpower issues, market fluctuations etc. that require mitigation to ensure success. Based on secondary research and examples of successful Indian entrepreneurs in this sector, the factors that can lead to successful establishment and operation of mechanical engineering startups and enterprises in India are identified. These encompass aspects like strong technical skills, innovation and creativity, understanding industry needs, access to latest technologies, funding and investments, partnerships and networks, perseverance and calculated risk-taking. Recommendations are provided for potential and existing mechanical engineering entrepreneurs on how to leverage opportunities while tackling challenges through specific actions in areas like product development, human resources, financials, and company growth strategy. The study contributes insights on translating the potential of mechanical engineering entrepreneurship into profitable and sustainable ventures that can positively impact India's economic growth.

Keywords -

Mechanical engineering, entrepreneurship, startups, India

1 INTRODUCTION

India's engineering R&D and manufacturing sectors have continued to expand post pandemic, driven by policy support, rising investments and new opportunities across aerospace, automotive, machinery and renewable energy domains.

According to NASSCOM, the market share of the Indian engineering, research, and development (ER&D) market to the global market is projected to grow at a compound annual growth rate (CAGR) of 12-13% to reach US$ 63 billion by 2025. The Indian ER&D market share to the global market is expected to grow from US$ 31 billion in 2019. This growth is being powered by global enterprises across telecom, automotive, semiconductor, aerospace, medical devices, consumer electronics, industrial and energy, who are focusing on the Indian ER&D's capabilities for innovation to boost efficient service delivery. Investments in R&D by both public and private sector are rising driven by reforms outlined in the Draft Science, Technology and Innovation Policy 2020 which aims to increase India's R&D spend from 0.7% to 2% of GDP over this decade.

Specifically, the mechanical engineering space is gaining increasing prominence, with Tracxn data showing over 4,200 mechanical engineering startups in India as of 2022, compared to 3,500 in 2020. Funding in the sector touched $6.1 billion during 2021-22, a 95% annual growth as per Venture Intelligence. Some major deals include ION Energy ($25 million), Pravaig Dynamics ($10 million) and NuSpace ($8 million) (Mint, 2022).

India also witnessed a major fillip in space tech startups like Skyroot, Agnikul, Dhruva etc. propelled by ISRO initiatives to boost private sector participation. This puts the spotlight on precision manufacturing capabilities. Established institutions like ISRO, DRDO and CSIR have built strong technical expertise over decades that can now be leveraged by entrepreneurs.

However, challenges continue to exist for startups in terms of technical complexity, hiring, infrastructure, market access and funding requirements. By focusing on frugal innovation, partnerships, emerging technologies and calculated risk-taking, India's mechanical engineers can enable hardware startups to develop globally competitive innovations across automotive, robotics, renewables and other key sectors.

2 Opportunities for Mechanical Engineering Startups in India

2.1 Automotive and Auto Components

- The Automotive Mission Plan 2016-26 by Government of India aims to grow the sector's contribution to GDP from 2.3% to 12% and increase localization to 80% by 2026 (Ministry of Heavy Industries and Public Enterprises, 2016).
- McKinsey estimates reveal that electric and shared mobility trends will help the auto sector reach $300 billion by 2026 (Gupta et al, 2021).
- Opportunities for startups exist in EV components, automotive IoT solutions, testing and simulation tools, custom fabrication etc. India already has over 1,000 auto component startups as per Tracxn.

2.2 Industrial Equipment Manufacturing

- Driven by expanding food processing, textile, plastic, packaging and construction machinery demand, India's industrial machinery market is projected to reach $28-35 billion by 2024-25 (TechSci Research, 2019).
- Custom fabrication, servomechanisms, precision engineering and niche machine manufacturing provide prospects. Tracxn data shows there are over 300 industrial equipment startups in India.

2.3 Robotics and Automation

- According to Mordor Intelligence, India's robotics market has been growing at a CAGR of 20% since 2013 on account of rising adoption across industries. It is forecast to reach $4 billion by 2024.
- Developing robotic automation for warehouses, factories, commercial buildings etc. provides an emerging opportunity. Inc42 estimates show India already has over 800 active robotics startups.

2.4 Engineering Design Services

- Driven by cost advantages and availability of ME talent, India's engineering design, R&D and services exports grew 14% YoY to reach $6.1 billion in FY22 (Economic Times, 2022).
- Low-cost offerings in 2D drafting, 3D modeling, simulation, prototyping, product data management etc. give an edge.

2.5 Technical Support Services

- India's industrial maintenance market is anticipated to expand at over 10% CAGR to reach $34 billion by 2027 due to lack of in-house servicing expertise in most companies as per Stratview Research.
- Installation, preventive maintenance, commissioning and technical support services surrounding industrial equipment, systems and machinery offer prospects.

2.6 Medtech Devices

- India's medical device market is expected to grow from $10 billion to $21 billion by 2025 as per Invest India estimates.
- Leveraging mechanical engineering capabilities to design and manufacture clinical instruments, implants, prosthetics etc. provides opportunities.

2.7 Aerospace and Defense

- The Indian aerospace and defense sector is projected to reach $70 billion by 2030 according to a EY-FICCI report. Indigenous manufacturing is being promoted under 'Make in India'.
- Prospects exist in precision engineering, components manufacturing and MRO services for the defense, space and civil aviation sectors.

2.8 Renewable Energy

- To meet its goal of achieving 175 GW installed renewable energy capacity by 2022, India needs to ramp up localization in solar, wind, hydro and bioenergy technologies (CEEW, 2021).
- Innovative product development in these domains by leveraging mechanical engineering expertise provides potential.

3 Challenges Faced by Mechanical Engineering Startups

- Technical Complexity and High Risks: Most mechanical engineering products, tools and systems require complex simulations, design analysis, prototypes and rigorous testing. Failure risks are inherently high.
- Capital Expenditure Requirements : Major investments needed in product R&D, prototyping, certifications, product trials and setting up manufacturing. This constrains early-stage startups.
- Scarce Skilled Labor : Limited availability of high-quality talent with niche mechanical engineering skills like measurement science, machining, metallurgy etc. Attracting and retaining talent is challenging.
- Lack of Domestic Capabilities: Nascency in some futuristic mechanical domains like nanotech, alter-

native materials, additive manufacturing etc. Low access to hubs for such emerging technologies.
- Long Product Development Cycles: Lengthy conceptualization, design analysis using CAD/CAE tools, prototype construction, compliance testing and certification requirements.
- Market Competition : Multinational corporations and large domestic firms dominate established mechanical engineering domains. Difficult for startups to compete.
- Infrastructure and Logistics Issues : Deficiencies in basic infrastructure regarding roads, utilities, testing facilities etc. Supply chain constraints especially in manufacturing.

4 Key Success Factors for Mechanical Engineering Startups

- **Technical Expertise :** In-depth knowledge of mechanical engineering principles and hands-on design, prototyping and troubleshooting skills.
- **Understanding User Needs :** Aligning product development with precise needs and pain points of target user segments for optimal product-market fit.
- **Frugal Innovation :** Innovating engineering solutions creatively despite constraints of limited resources and infrastructure.
- **Leveraging Advanced Technologies :** Adopting digital tools like CAD/CAE, simulation software, 3D printing, industrial IoT etc. to accelerate development.
- **Building IP Portfolio :** Creating patentable intellectual property in designs, technologies and processes through robust R&D.
- Forging Strategic Partnerships Collaborations with research institutions, larger companies and even competitors to gain technical and business resources.
- **Focus on Quality and Reliability :** Rigorous quality control and reliability engineering allowing products to thrive in demanding industrial conditions.
- **Calculated Risk Appetite :** Willingness to experiment, learn quickly and iterate - but with calculated risks tied to addressable market potential.

5 The path forward: Key Recommendations

- **Spot unmet needs:** Identify niche problems areas to develop proprietary solutions. Avoid duplicating existing products.
- **Leverage frugal innovation:** Reengineer expensive technologies for affordability constraints of Indian markets.
- **Prioritize quality:** Implement robust QA and reliability testing. This builds confidence in innovations from India.
- **Adopt digital tools:** Mainstream usage of CAD, CAE, 3D printing, IoT etc. Democratization initiatives like SWAYAM can assist.
- **Encourage partnerships:** Policy and ecosystem support for university-industry partnerships. Platforms for startup collaboration.
- **Improve infra:** Ensure access to advanced prototyping labs, testing facilities and fab spaces through institutions like TBIs.
- **Promote clusters:** Develop region-specific mechanical engineering clusters harnessing local talent, universities and industries.
- **Support incubators:** Expand high-quality incubation programs tuned to long gestation hardware startups. Provide mentoring.

6 Conclusion

The mechanical engineering sector in India holds vast potential for startups to create globally competitive products and companies. Though challenges exist, they can be overcome through innovation focus, partnerships, quality and calculated risk-taking. Policy reforms to improve access to infrastructure, digital technologies, investors and talent can significantly boost innovation outcomes. With targeted support, India's talented mechanical engineers can build innovative products and solutions for not just domestic but also global markets in the coming decade.

References

[1] Gupta, S., Sharma, A., Sinha, A.K. et al. (2021). Shaping the future of mobility in India: Reimagining mobility with electric and autonomous vehicles. McKinsey & Company.

[2] Ministry of Heavy Industries and Public Enterprises (2016). Automotive Mission Plan 2016-26. Government of India.

[3] National Association of Software and Service Companies (Nasscom) (2018). $63 billion ER&D opportunity for India by 2022. Nasscom Perspective.

[4] Council on Energy Environment and Water (CEEW) (2021). Localising India's renewable energy technology manufacturing. CEEW Policy Brief.

[5] TechSci Research (2019). India Industrial Machinery Market By Type, Competition Forecast and Opportunities. TechSci Research Report.

[6] Economic Times (2022). Engineering R&D services exports record 14% growth in FY22: EY report. The Economic Times.

Statistical Analysis and Characterisation of Diabetes Mellitus Data

Ramya M S[1], Prasanth C B[2], Subramanian C [3], Mary George[4]

[1]Research Scholar, Department of Statistics, Annamalai University
[2]Assistant Professor, Department of Statistics, Sree Kerala warma College,Kerala
[3]Associate Professor, Department of Statistics, Annamalai University
[4]Research Scholar, Department of Statistics, Annamalai University

[1]msramyaotp@gmail.com [2]cbpwarrier@gmail.com [3]manistat@yahoo.co.in [4]joicykunjumon@gmail.com

Abstract -

Diabetes is a standout amongst the most well-known non-transmittable diseases in the world. It is assessed to be the seventh leading cause for death. It is predicted that the diabetes rate in adults worldwide will become 642 million in 2040. Diabetes and obesity are associated with non-modifiable and modifiable risk factors. Non-alcoholic fatty liver disease (NAFLD) and type 2 diabetes (T2DM) are common conditions that regularly co-exist and can act synergistically to drive adverse outcomes. The presence of both NASH and T2DM increases the likelihood of the development of complications of diabetes as well as augmenting the risk of more severe NASH, including cirrhosis, hepatocellular carcinoma and death. Also, cardiovascular disease is the most prevalent and detrimental complication of diabetes mellitus. Type 2 diabetes (T2D) is the result of interaction between environmental factors and a strong hereditary component. In this paper, summarised and critically evaluated the available data, with the aim of helping to inform the reader as to the most pertinent issues when managing patients with co-existent NASH, CVD, HEREDITY and T2DM and fit appropriate statistical distribution to the collected real data.

Keywords -

Type 2 DM, NASH, CVD, Heredity, NAFLD, and Pascal Distribution.

1 Introduction

INTRODUCTION

Type 2 diabetes (T2DM) is a complex metabolic disorder that has become a major public health problem worldwide in the past three decades. About one in 11 adults worldwide now have diabetes mellitus, of which 90% have T2DM. T2DM can cause injury not only to the pancreas and insulin system but also the liver, cardiac, kidneys, gut, muscle, fat cells and even the brain. Diabetes can affect many different organ systems in the body and, over time, can lead to serious complications, such as non-alcoholic fatty liver disease. The correlation between NASH and type 2 diabetes mellitus (T2DM) is complicated and bidirectional. NASH increases the risk of incident diabetes and is common in T2DM patients.

Insulin resistance and type 2 diabetes mellitus are generally accompanied by low HDL cholesterol and high plasma triglycerides, which are major cardiovascular risk factors. This review describes abnormalities in HDL metabolism and reverse cholesterol transport, i.e. the transport of cholesterol from peripheral cells back to the liver for metabolism and biliary excretion, in insulin resistance and type 2 diabetes mellitus. Cardiovascular disease remains the leading cause of death in women. Both obesity and diabetes mellitus are important independent risk factors for the development of cardiovascular disease. Obesity is the leading risk factor for type 2 diabetes. Central obesity as well as obesity in general is associated with physiological changes that may cause the development of diseases like high blood pressure, heart disease, high blood cholesterol and type 2 diabetes.

Cholesterol is a waxy substance that's made by the body and found in some animal-based foods. Blood cholesterol levels describe a group of fats also known as lipoproteins (lipids) which include HDL-C, "good" cholesterol and LDL-C or "bad"cholesterol. Cholesterol is important to overall health, but when LDL-C levels are too high, it can contribute to narrowed or blocked arteries. Unfortunately, people with diabetes are more prone to having high cholesterol, which contributes to cardiovascular disease (CVD).In individuals who have diabetes, there are higher incidences of liver function test abnormalities than individuals who do not have diabetes. The most common liver function tests (LFTs) include the Serum Glutamic Pyruvate Transaminase (SGPT) activity, to measure the concentration of intracellular hepatic enzyme that has leaked into the blood and serves as a marker of hepatocytic injury. In this study we analyse the risk factors which affects type 2 diabetes mellitus and developing a predictive model with the aim to identify important risk factors for the development of NAFLD in patients with T2DM and try to

fit appropriate statistical distributions to the collected real data.

2 Review of Related Literature

AlaAmourah et al.,(2022) conducted study on Exploiting the Pascal Distribution Series and Gegenbauer Polynomials to Construct and Study a New Subclass of Analytic Bi-Univalent Functionsto construct a new subclass of analytic bi-univalent functions defined on symmetric domain by means of the Pascal distribution series and Gegenbauer polynomials.

Annabel Acs et al., (2018) studied Prevalence of cardiovascular disease in type 2 diabetes: a systematic literature review of scientific evidence from across the world in 2007–2017 and concluded that globally, overall CVD affects approximately 32.2% of all persons with T2DM. CVD was a major cause of mortality among people with T2DM, accounting for approximately half of all deaths over the study period. Coronary artery disease and stroke were the major contributors.

Abraham TM et al., (2015) conducted a study on Trends in diabetes incidence: the Framingham Heart Study and established the result as the risk of new-onset diabetes continued to be higher in the 2000s compared with the 1970s. In the past decade, diabetes incidence remained steady despite the on-going trend of rising adiposity.

Sarwar N et al ., (2010) explained in the study Diabetes mellitus, fasting blood glucose concentration, and risk of vascular disease: a collaborative meta-analysis of 102 prospective studies as Diabetes confers about a twofold excess risk for a wide range of vascular diseases, independently from other conventional risk factors. In people without diabetes, fasting blood glucose concentration is modestly and non-linearly associated with risk of vascular disease.

Fox CS, et al., (2008) proposed a study on Lifetime risk of cardiovascular disease among individuals with and without diabetes stratified by obesity status in the Framingham heart study and explained as the lifetime risk of CVD among individuals with diabetes is high, and this relationship is further accentuated with increasing adiposity.

Van Hateren KJ et al., (2009) conducted a study on The lipid profile and mortality risk in elderly type 2 diabetic patients and stated as the lipid profile was not predictive in the overall group of elderly patients, higher lipids were related to increased cardiovascular mortality in patients with diabetes of long duration.

Muhammad AmmaarAslam et al., (2 019) proposed a study on prevalence of cardiovascular disease in type 2 diabetes- systematic literature review and concluded that CVD is one of the major cause of death in T2DM with coronary artery disease having the high prevalence.

MarsoSPet al., (2016) studied Liraglutide and cardiovas- cular outcomes in type 2 diabetes and concluded that the rate of the first occurrence of death from cardiovascular causes, nonfatal myocardial infarction, or nonfatal stroke among patients with type 2 diabetes mellitus was lower with liraglutide than with placebo.

Mills EPet al.,(2018) examined in the study Treating nonalcoholic fatty liver disease in patients with type 2 diabetes mellitus and reviewed that all reviewed treatment options are safe for management of NAFLD in patients with T2DM but long-term histological improvements are minimal. TZDs are efficacious for resolution of NASH and improvements in fibrosis but long-term use is required to maintain the results.

Alessandro Mantovaniet.al., (2018) [16] studied "Non-Alcoholic Fatty Liver Disease and Risk of Incident Type 2 Diabetes: A Meta-analysis" and found that NAFLD is significantly associated with a twofold increased risk of incident diabetes. However, the observational design of the eligible studies does not allow for proving causality.

Bhatt KN et.al., (2017) [17] conducted study 0n "Prevalence of Nonalcoholic Fatty Liver Disease in Type 2 Diabetes Mellitus and its Relation with Insulin Resistance in South Gujarat Region." The study revealed a high incidence of NAFLD in Type 2 diabetes patients stressing the need for early screening.

Carrie R. Wong, et. Al., (2018) [18] conducted study on "The Association between Non-alcoholic Fatty Liver Disease and Cardiovascular Disease Outcomes" and concluded that the causal relationship of CVD and NAFLD remains under investigation, but the strong bidirectional association between CVD and NAFLD warrants clinical intervention in patients with NAFLD to modify metabolic risk factors, including T2DM, dyslipidemia, hypertension, and obesity.

Claudio Tana et.al., (2019) [19] conducted study on "Cardiovascular Risk in Non-Alcoholic Fatty Liver Disease: Mechanisms and Therapeutic Implications" to conclude that all cardio-metabolic risk factors should be carefully and routinely screened among patients with NAFLD, and that disease management should be focused on both specific lifestyle modifications and aggressive risk factors modification, which would not only reduce the risk of liver disease progression, but may also provide benefits by reducing the risk of developing cardiac complications.

Dharmalingam M, Yamasandhi P G (2018) [20] conducted a study on "Alcoholic Fatty Liver Disease and Type 2 Diabetes Mellitus" and concluded that T2DM and NAFLD have a common association. The increasing prevalence makes it a public health problem.

Targher G et. al., (2007) [21] conducted study on "Non-alcoholic Fatty Liver Disease is Independently Associated with an Increased Incidence of Cardiovascular Events in Type 2 Diabetic Patients." The findings suggest

that NAFLD is associated with an increased incidence of CVD in type 2 diabetic patients, independent of traditional CVD risk factors and metabolic syndrome components.

Dyson JK, et.al., (2014) [22] studied "Non-alcoholic Fatty Liver Disease: A Practical Approach to Treatment" concluded that lifestyle interventions aimed at weight loss and increased activity are essential for all patients with NAFLD and if sustained are effective in the treatment of NAFLD.

Hagstromet.al., (2019) [23] studied "Cardiovascular Risk Factors in Non-alcoholic Fatty Liver Disease." The study concluded that patients with NAFLD are at an increased risk for CVD compared to matched controls, but histological parameters do not seem to independently predict this risk.

Carrie et.al.,(2018) conducted a study on "The Association between Non-alcoholic Fatty Liver Disease and Cardiovascular Disease Outcomes and found that the causal relationship of CVD and NAFLD remains under investigation, but the strong bidirectional association between CVD and NAFLD warrants clinical intervention in patients with NAFLD to modify metabolic risk factors, including T2DM, dyslipidemia, hypertension, and obesity.

Jonathan M. Hazlehurst, et.al., (2016) studied "Non-alcoholic Fatty Liver Disease and Diabetes and concluded Turkish Journal of Physiotherapy and Rehabilitation; that diabetes and NAFLD are reciprocal risk factors and when they occur together, an increasing body of data demonstrates that diabetes is more difficult to manage and that NAFLD is more likely to progress.

Mathews et.al.,(2018) conducted a study on "Non-alcoholic Steatohepatitis, Obesity, and Cardiac Dysfunction." It summarises obesity as a major factor in the development of Nonalcoholic Fatty Liver Disease (NAFLD) and its progression to steatohepatitis. Patients with NAFLD have a significant increase in cardiovascular disease risk. For biopsy-proven NASH, Vitamin E and Pioglitazone are the recommended medical treatments in addition to lifestyle modification.

NasrinAmiriet.al., (2017) conducted the study, "Type 2 Diabetes Mellitus and Non-Alcoholic Fatty Liver Disease: A Systematic Review and Meta-analysis." The findings indicated that the overall prevalence of NAFLD among type 2 diabetes mellitus patients is significantly higher. It can be concluded that type 2 diabetes mellitus patients should be managed to prevent NAFLD.

Prasanth et.al., (2017) conducted a study on "Prevalence of NAFLD in Patients with Type 2 Diabetes Mellitus" and concluded that prevalence of NAFLD and NASH in our cohort of type 2 DM patients is high and increases with multiple components of metabolic syndrome. NASH and advanced fibrosis can occur in diabetic patients without any symptoms, signs or routine laboratory test abnormalities.

Rashmee and Gagan (2017) studied "Non-alcoholic Fatty Liver Disease and Cardiovascular Risk and concluded that Non-alcoholic Fatty Liver Disease (NAFLD) is often associated with insulin resistance and is strongly associated with type 2 diabetes mellitus and obesity. NAFLD is now recognized as a risk factor for poor cardiovascular outcomes including mortality and morbidity from major vascular events. As a whole, NAFLD patients may benefit from more careful surveillance and early treatment interventions

Shunquan Wu et.al., (2016) conducted a study "Association of Non-alcoholic Fatty Liver Disease with Major Adverse Cardiovascular Events: A Systematic Review and Meta-analysis." The main results of meta-analysis were NAFLD was not associated with overall mortality and CVD mortality. NAFLD was associated with an increased prevalence and/or incidence of other adverse cardiovascular events, including CVD, CAD, hypertension, and atherosclerosis; (3) NASH was not associated with overall mortality and CVD mortality but was associated with an increased incidence of CVD.

Targher, et.al., (2005) conducted study on "Nonalcoholic Fatty Liver Disease and Risk of Future Cardiovascular Events Among Type 2 Diabetic Patients" and suggested that the metabolic syndrome predicts incidents of cardiovascular disease (CVD), so it is possible to hypothesize that NAFLD patients might portend a greater CVD risk and that NAFLD itself might confer a CVD risk above that associated with individual metabolic syndrome risk factors.

Wenjie Dai et.al.,(2017) studied "Prevalence of Nonalcoholic Fatty Liver Disease in Patients with Type2 Diabetes Mellitus" and concluded that the high pooled prevalence of NAFLD in T2DM patients found in this study significantly underscores the need for early assessment of NAFLD and the importance of strengthening the management of NAFLD in T2DMpatients.

3 Methodology and Data Analysis

The proposed study aims to summarize the evidence of the association with NASH and CVD with risk factors such as age, height, weight, waist circumference, blood sugar, cholesterol level, sgot, sgpt, TG, heredity, bmi, systolic pressure, diastolic pressure in childbearing diabetic women. 603 subjects were randomly selected from various hospitals in the two districts, Palakkad and Malappuram - at Kerala to make a real data analysis.

Baseline information for this study was obtained via a questionnaire on general information, physical examination (height, weight, and blood pressure), laboratory tests (triglycerides, total cholesterol, blood glucose, aspartate aminotransferase (AST) or serum glutamic-oxaloacetic

Table 1. Residual Statistics

Minimum		Maximum	Mean	Std. Deviation	N
Predicted Value	155.66	272.96	211.64	20.250	543
Residual	-76.149	95.823	.124	35.167	543
Std. Predicted Value	-2.885	3.090	-.034	1.032	543
Std. Residual	-2.144	2.698	.003	.990	543

Table 2. Summary Statistics

Clinical Characteristics	Min/Max	Mean	Median	Mode	Skewness	Kurtosis
Age	20/48	30.8±5	31	28	0.163827	-0.40751
Height	140/176	157±7.3	155	152	0.456	-0.789
Weight	48/99	68.97±8.8	68	65	0.525	0.206
Blood sugar(pp)	122/312	209.9±39.6	203	210	0.505	-0.05
BMI	22.5/35.5	27.7±2.3	27.4	27.4	0.397	0.647
WC	27/44	37.13±3.1	37	35	-0.584	1.184
SGOT	11.4/48.6	18.95±5.09	18.4	18.6	1.34	3.35
SGPT	17/59	36.15±8.64	36.8	28.6	0.1007	-0.238
Cholesterol	115/321	217.29±42.5	214	265	0.1634	-0.466
TG	92/356	218.19±66.9	227.9	269	-0.1598	-0.7345
SP	110/160	130±15	130	120	0.393	-0.666
DP	70/100	84±8	85	90	-0.414	-0.814

transaminase (SGOT) and alanine aminotransferase (ALT) or Serum glutamic pyruvic transaminase (SGPT)), Body mass index (BMI) and waist circumference (WC). Prevalence of T2DM patients is high and increases with multiple components of metabolic syndrome (Metabolic syndrome is a cluster of conditions that occurs together, increasing risk of heart disease, stroke and type2 diabetes. These conditions include increased blood pressure, high blood sugar, excess body fat around the waist, and abnormal cholesterol or triglyceride levels).

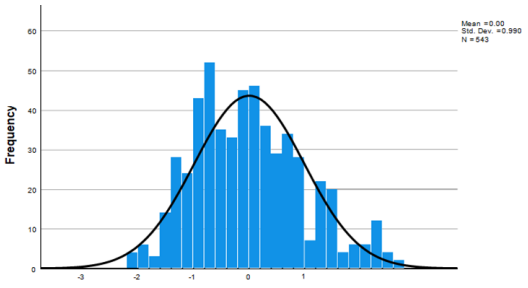

Figure 1. Histogram - Dependent variable BLOOD SUGAR (PP)

4 Residual Statistics

The residual is the vertical distance (or deviation) from the observation to the predicted regression line. Predicted values are points that fall on the predicted line for a given point on the x-axis.

a. Dependent Variable: BLOODSUGAR (PP)

The summary statistics of these variables are given in table.

5 Association Of Blood Sugar, BMI And Waist Circumference

Body mass index has a strong relationship to diabetes and insulin resistance. Overweight and obesity are defined by an excess accumulation of adipose tissue to an extent that impairs both physical and psychosocial health and well-being. The influence of obesity on type 2 diabetes risk is determined not only by the degree of obesity but also by where fat accumulates. Increased upper body fat including visceral adiposity, as reflected in increased abdominal girth or waist-to-hip ratio, is associated with the metabolic syndrome, type 2 diabetes, and cardiovascular disease. Excess body weight has a well-established link with decreased insulin sensitivity which in turn is a correlate of cardiovascular risk factors and a defining characteristic of type 2 diabetes.

An excessive BMI and visceral obesity are the most common and well-documented risk factors for NAFLD, also contributing to metabolic syndrome and other com-

Table 3. Adult Body Mass Index (BMI)

BMI	**Considered**
Below 18.5	Underweight
18.5 to 24.9	Healthy weight
25.0 to 29.9	Overweight
30 or higher	Obesity
40 or higher	Class 3 Obesity

plications. In diabetes, individuals with excessive fat storage have been noted to have higher insulin levels and are said to have insulin resistance, which is described as the cause of T2DM. The entire spectrum of obesity, ranging from overweight to obese and severely obese, is associated with NAFLD.

Table 4. Correlations between PP, WC, BMI

	BLOOD SUGAR (PP)	WAIST CIRCUM-FERENCE	BMI
BLOOD SUGAR(PP)	1		
WAIST	0.100653	1	
BMI	0.551416	0.297895	1

The correlations among the variables were positive; blood sugar and BMI have medium correlation. ANOVA indicates the model is also good for the data since p ¡ 0.05.

Table 5. Regression coefficients

	Coefficients
Intercept	3.941855
BMI	7.859242
WAIST CIRC	-0.73303

The graph of each data set shows that there is linear relationship.

Linear Regression Model: 1

Blood sugar (PP) = 7.968517 bmi-0.7330wc+ constant

6 Association Of Blood Sugar, Systolic and Diastolic Pressure

Hypertension and type 2diabetes are common comorbidities. Hypertension is twice as frequent in patients with diabetes compared with those who do not have diabetes. Moreover, patients with hypertension often exhibit insulin resistance and are at greater risk of diabetes developing than are normotensive individuals. The major cause of morbidity and mortality in diabetes is cardiovascular disease, which is exacerbated by hypertension. Accordingly, diabetes and hypertension are closely interlinked because of similar risk factors, such as endothelial dysfunction, vascular inflammation, arterial remodelling, atherosclerosis, dyslipidemia, and obesity. There is also substantial overlap in the cardiovascular complications of diabetes and hypertension related primarily to microvascular and macrovascular disease. Diabetes is associated with both macrovascular (involving large arteries such as con- duit vessels) and microvascular (involving small arteries and capillaries) disease.Hypertension is an important risk factor for diabetes-associated vascular complications, be- cause hypertension itself is characterized by vascular dys- function and injury.

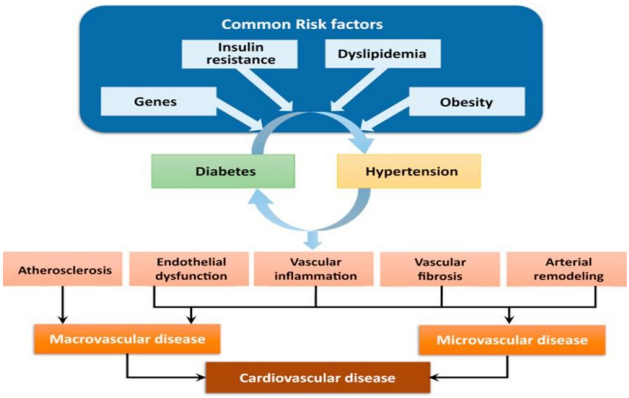

Figure 2. Common Risk factors of CVD

Figure 2: Vascular processes whereby diabetes and hypertension predispose to cardiovascular disease. Common risk factors promote diabetes and hypertension, which are associated with atherosclerosis, vascular inflammation, endothelial dysfunction, and structural remodelling, which lead to macrovascular and microvascular disease. Vascular damage and endothelial dysfunction is amplified when diabetes and hypertension coexist.

In this study also the correlation between blood sugar, systolic and diastolic pressure is positive and the linear regression model is

Blood sugar (pp) = 0.099405 SP+1.037123 DP+ constant

7 Association Between Blood Sugar, Nash and CVD

Non-alcoholic fatty liver disease (NAFLD) and type 2 diabetes mellitus are common conditions that regularly co-exist and can act synergistically to drive adverse outcomes. There are many ways to image NAFLD and NASH, including abdominal ultrasound, CT scan, and magnetic resonance imaging (MRI) or MR spectroscopy. More recently, elastography performed with ultrasound or MR has gained traction in diagnosing different stages of NAFLD

and NASH.

Cardiovascular disease is the most prevalent and detrimental complication of diabetes mellitus. The incidence of cardiovascular mortality in diabetic subjects without a clinical history of previous cardiac events is as high as the incidence in nondiabetic subjects with a history of myocardial infarction. This inordinate increase in the risk of coronary events in diabetic patients is attributed to multiple factors, including glycation and oxidation of proteins and increased prevalence of classic risk factors of coronary disease, such as hypertension, obesity, and dyslipidemia. Chronic hyperglycemia leads to many long- term complications in the eyes, kidneys, nerves, heart, and blood vessels. Individuals with pre-diabetes, undiagnosed type 2 diabetes, and long-lasting type 2 diabetes are at high risk of all complications of macrovascular disease, coronary heart disease (CHD), stroke, and peripheral vas- cular disease. More than 70% of patients with type 2 diabetes die of cardiovascular causes. Therefore, the epi- demic of type 2 diabetes will be followed by an epidemic of diabetes-related cardiovascular disease (CVD).

Out of 603 children bearing diabetic women 373 (62%) had fatty liver or more risk for NASH. Majority of person's level of SGPT and SGOT are in normal range. Only countable number of persons was in the above risk level.

While considering the cholesterol and triglyceride level of fatty liver diabetic patients nearly 50% persons higher cholesterol level. Graph of cholesterol level of fatty liver Diabetic patients is given below.

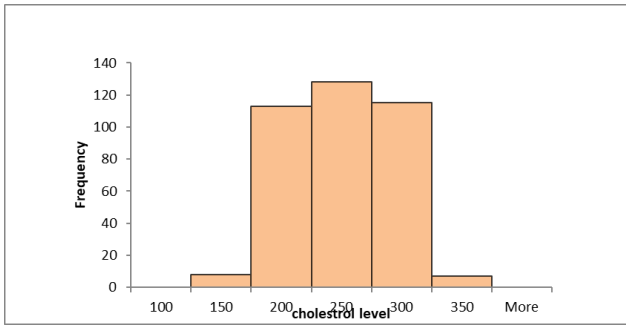

Figure 3. Histogram of cholesterol level

8 Association Between Heredity and Blood Sugar

Type 2 diabetes (T2D) is the result of interaction between environmental factors and a strong hereditary component. Hereditary factors clearly play a role in the development of diabetes; the actual genetic variants involved in this inherited risk were completely unknown prior to the advent of modern genetic technologies. The study reveals that the risk of developing type 2 DM increases with the number of affected family members through parents or through influence of genetic factors. There is 62% of child bearing diabetic women have influenced by heredi- tary factors while the remaining were not influenced.

Table 6. Modelling Anova

	Model	Sum of Squares	df	Mean Square	F	Sig.
1.	Regression	97837.689	1	97837.689	67.275	.000[b]
	Residual	775141.649	533	1454.300		
	Total	872979.338	534			
2.	Regression	147951.725	2	73975.862	54.281	.000[c]
	Residual	725027.613	532	1362.834		
	Total	872979.338	534			
3.	Regression	185942.793	3	61980.931	47.904	.000[d]
	Residual	687036.545	531	1293.854		
	Total	872979.338	534			
4.	Regression	198884.178	4	49721.044	39.093	.000[e]
	Residual	674095.161	530	1271.878		
	Total	872979.338	534			
5.	Regression	205780.634	5	41156.127	32.631	.000[f]
	Residual	667198.705	529	1261.245		
	Total	872979.338	534			

a: Dependent Variable: BLOODSUGAR(PP)

b: Predictors: (Constant), BMI

c: Predictors: (Constant), BMI, DIASTOLIC PRESSURE

d: Predictors: (Constant), BMI, DIASTOLIC PRESSURE, TG

e: Predictors: (Constant), BMI, DIASTOLIC PRESSURE, TG, CHOLESTROL

f: Predictors:(Constant), BMI, DIASTOLICPRESSURE, TG, CHOLESTROL, AGE

The model is perfectly significant for the predictor variables BMI, Diastolic pressure, TG, Cholestrol, and Age corresponding to the dependent variable Bloodsugar(PP).

9 Fitting Best Probability Distributions to the Data

In statistics and probability, distributions of random variables play a basic role and are used extensively to describe and model a lot of real-life phenomena; they de- scribe the distribution of the probabilities over the random variable values. Some distributions are used in practice and have been given special names to clarify the importance of these distributions and the random experiments behind them. Appropriate distributions were derived using statistical tools; the collected data were fitted to four distributions named as Pascal Distribution, Poisson Distributions for two different means, discrete uniform Distribution. Using goodness of fit, Pascal Distribution is the best fitted distribution for the collected data. Comparison of fitted distributions were given below:

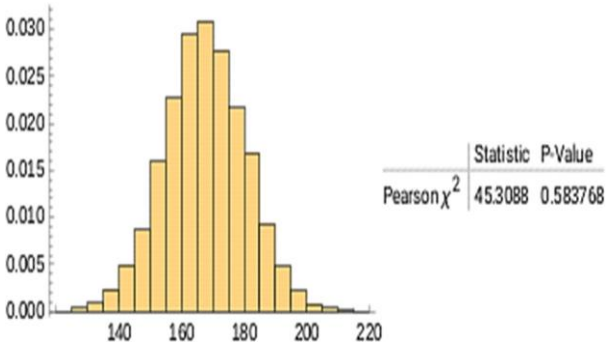

Figure 4. Fitted Poisson distribution (207.788)

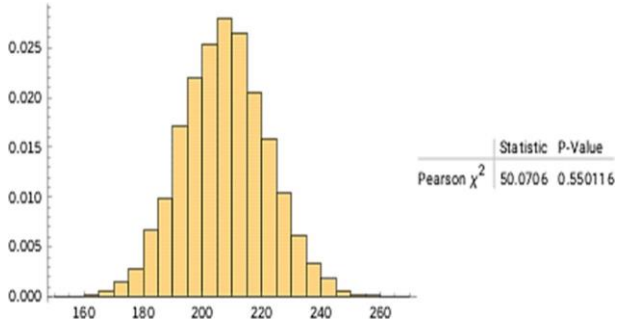

Figure 5. Poisson distribution (167.095)

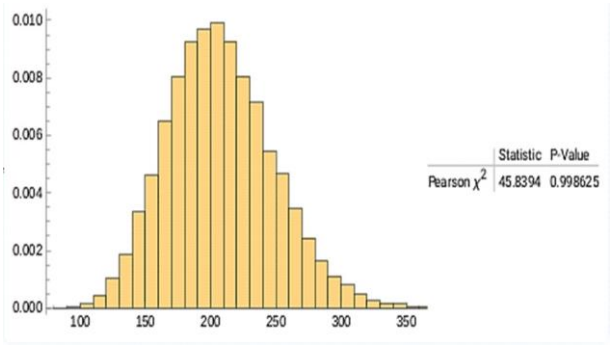

Figure 6. Pascal Distribution

1 CDF of Pascal Distribution for the Col- lected Data

The best fitted distribution follows the Pascal Distribu- tion.So CDF is also drawn for the best fitted distribution for the collected data.

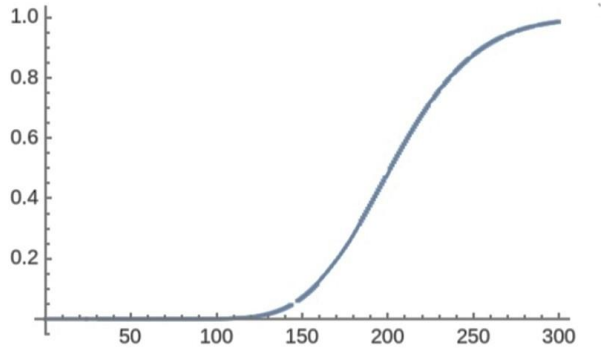

Figure 7. Pascal Distribution – CDF

2 Conclusion

The study supports the finding that diabetes develop- ment and obesity were positively and significantly associ- ated. When it comes to type 2 diabetes mellitus patients who are childbearing, BMI and WC are more strongly linked to diabetes than other risk factors. The degree of connection with diabetes risk was drastically raised when BMI and WC were used. This shows that when determin- ing the risk for diabetes, waist circumference should also be examined in addition to BMI. Therefore, preventing central obesity and being overweight at the same time has significant public health consequences for the prevention of diabetes.

Also, it might be advisable to maintain blood pressure between 130-139/80-85 mm Hg, supported by other ther- apeutic and lifestyle interventions to improve cardiovas- cular outcomes in patients with diabetes. Patients with T2DM and NASH should be considered at high risk of CVD and could benefit from more intensive CV preven- tion. Additional long-term follow-up is needed to demon- strate that the treatment of NASH effectively reduces the risk of CVD. Type 2diabetes has a stronger link to family history and genetics play a very strong role in the develop- ment of type 2 diabetes. Here 62% of childbearing diabetic women have been influenced by hereditary factors.

In fitting a distribution to a collected set of biological data, say, it is also important for the mathematical model underlying the theoretical distribution to have a reasonable biological meaning. The fitted Pascal Distribution offers interesting possibilities in this direction. This study is an exposure to medical science to predict different aspects of blood sugar in relation to its components.

References

[1] Abraham, Tobin M., et al. “Trends in Diabetes Incidence: The Framingham Heart Study.” Diabetes Care, vol. 38, no. 3, 31 Dec. 2014, pp. 482–487, https://doi.org/10.2337/dc14-1432.

[2] Amourah, AA, et al. Exploiting the Pascal Distribution Series and Gegenbauer Polynomials to Construct and Study a New Subclass of Analytic Bi-Univalent Functions. Vol. 14, no. 1, 13 Jan. 2022, pp. 147–147, https://doi.org/10.3390/sym14010147.Accessed 31 May 2023.

[3] Barchetta, Ilaria, et al. “Strong Association between Non-Alcoholic Fatty Liver Disease (NAFLD) and Low 25(OH) Vitamin D Levels in an Adult Population with Normal Serum Liver Enzymes.” BMC Medicine, vol. 9, no. 1, 12 July 2011, https://doi.org/10.1186/1741-7015-9-85.

[4] Dai, Wenjie, et al. “Prevalence of Nonalcoholic Fatty Liver Disease in Patients with Type 2 Diabetes Mellitus.” Medicine, vol. 96, no. 39, Sept. 2017, p. e8179, www.ncbi.nlm.nih.gov/pmc/articles/PMC5626318/, https://doi.org/10.1097/md.0000000000008179. Accessed 13 May 2019.

[5] Dyson, J K, et al. “Non-Alcoholic Fatty Liver Disease: A Practical Approach to Treatment.” Frontline Gastroenterology, vol. 5, no. 4, 22 Jan. 2014, pp. 277–286, https://doi.org/10.1136/flgastro-2013-100404.

[6] Einarson, Thomas R., et al. “Prevalence of Cardiovascular Disease in Type 2 Diabetes: A Systematic Literature Review of Scientific Evidence from across the World in 2007–2017.” Cardiovascular Diabetology, vol. 17, no. 1, 8 June 2018, cardiab.biomedcentral.com/articles/10.1186/s12933-018-0728-6, https://doi.org/10.1186/s12933-018-0728-6. Accessed 12 Sept. 2019.

[7] 2008, pp. 1582–1584, https://doi.org/10.2337/dc08-0025. Accessed 14 May 2020.

[8] Francque, Sven M., et al. “Non-Alcoholic Fatty Liver Disease and Cardiovascular Risk: Pathophysiological Mechanisms and Implications.” Journal of Hepatology, vol. 65, no. 2, Aug. 2016, pp. 425–443, https://doi.org/10.1016/j.jhep.2016.04.005. Accessed 13 Dec. 2021.

[9] Gerstein, Hertzel C, et al. “Dulaglutide and Cardiovascular Outcomes in Type 2 Diabetes (REWIND): A Double-Blind, Randomised Placebo-Controlled Trial.” The Lancet, vol. 394, no. 10193, July 2019, pp. 121–130, https://doi.org/10.1016/s0140-6736(19)31149-3. Accessed 12 Mar. 2020.

[10] GiBeom Kim, et al. Association between Non-Alcoholic Fatty Liver Disease and Cancer Incidence Rate. Vol. 68, no. 1, 1 Jan. 2018, pp. 140–146, https://doi.org/10.1016/j.jhep.2017.09.012.Accessed 31 May 2023.

[11] Hagstro¨m, Hannes, et al. “Cardiovascular Risk Factors in Non-Alcoholic Fatty Liver Disease.” Liver International, vol. 39, no. 1, 17 Oct. 2018, pp. 197–204, https://doi.org/10.1111/liv.13973. Accessed 18 Dec. 2021.

[12] Hazlehurst, Jonathan M., et al. “Non-Alcoholic Fatty Liver Disease and Diabetes.” Metabolism, vol. 65, no. 8, Aug. 2016, pp. 1096–1108, https://doi.org/10.1016/j.metabol.2016.01.001. Accessed 13 Oct. 2020.

[13] Mills, Elizabeth P., et al. “Treating Nonalcoholic Fatty Liver Disease in Patients with Type 2 Diabetes Mellitus: A Review of Efficacy and Safety.” Therapeutic Advances in Endocrinology and Metabolism, vol. 9, no. 1, 7 Dec. 2017, pp. 15–28, https://doi.org/10.1177/2042018817741852. Accessed 6 Oct. 2021.

[14] Tana, Claudio, et al. “Cardiovascular Risk in Non-Alcoholic Fatty Liver Disease: Mechanisms and Therapeutic Implications.” International Journal of Environmental Research and Public Health, vol. 16, no. 17, 1 Sept. 2019,

www.ncbi.nlm.nih.gov/pmc/articles/PMC6747357 /: :text=New%20evidence%20suggests%20that %20non, https://doi.org/10.3390/ijerph16173104 .Accessed 21 Sept. 2021.

[15] Targher, G., et al. "Non-Alcoholic Fatty Liver Disease Is Independently Associated with an Increased Prevalence of Chronic Kidney Disease and Proliferative/Laser-Treated Retinopathy in Type 2 Diabetic Patients." Diabetologia, vol. 51, no. 3, 6 Dec. 2007, pp. 444–450, https://doi.org/10.1007/s00125-007-0897-4. Accessed 8 Feb. 2021.

[16] Targher, Giovanni, et al. "Non-Alcoholic Fatty Liver Disease and Risk of Incident Cardiovascular Disease: A Meta-Analysis." Journal of Hepatology, vol. 65, no. 3, Sept. 2016, pp. 589–600, www.sciencedirect.com/science/article/pii/ S0168827816301994, https://doi.org/10.1016/j.jhep.2016.05.013.Ac- cessed 13 Sept. 2019.

[17] vanHateren, Kornelis J. J., et al. "The Lipid Profile and Mortality Risk in Elderly Type 2 Diabetic Patients: A Ten-Year Follow-up Study (ZODIAC-13)." *PLoS ONE*, vol. 4, no. 12, 24 Dec. 2009, p. e8464, https://doi.org/10.1371/journal.pone.0008464. Accessed 25 Feb. 2021.

[18] Wu, Shunquan, et al. "Association of Non-Alcoholic Fatty Liver Disease with Major Adverse Cardiovascular Events: A Systematic Review and Meta-Analysis." *Scientific Reports*, vol. 6, no. 1, 16 Sept. 2016, https://doi.org/10.1038/srep33386. Accessed 1 Jan. 2021.

Customer Receptivity of a Telecom Service supply Chain

Dr. Pramod V R[1] and Dr. Banwet D K[2]

[1]Professor, Department of Mechanical Engineering, NSS College of Engineering, Palakkad-8, Kerala, 678008
[2]Former Professor, Department of Management Studies INDIAN INSTITUTE OF TECHNOLOGY, Delhi, 110016

[1]pramodram68@yahoo.com, [2]dkbanwet@dms.iitd.ac.in

Abstract -

Purpose – The major theme of this paper is to highlight the customers' attitudes towards the various aspects of a telecom service supply chain in the Indian context. Service sectors are gaining more and more popularity among the industrialists in this ever-vibrant global competitive scenario. They call for more attention to external customers, who are the major stakeholders of a service providing organization. customers aspirations and expectations have to be given considerable attention. In such a milieu, the receptivity of service supply chain among external customers becomes extremely important. Design/methodology/approach –The firm in the present study is an Indian MNC in the telecom service sector. It is having core business activities, wide spread across the globe. They are 1. Consultancy 2. Project Execution and 3. Training and quality control. External customers are national and international clients/organizations from which the firm receives the orders against tenders/ bids. The views and expectations of the firm's external customers were studied by analyzing their feedbacks. Findings – A closed ended questionnaire was specially designed to collect feedback of customers were analyzed during the termination of each project. 50 responses have been analyzed. The results indicated that customers' receptivity is high in all aspects. The results were quantified by two indices namely (i). Average Performance Index (With out prioritization) and (ii) Weighted Performance Index (AHP based prioritization). Both showed appreciable values Originality/value – Research on service supply chain especially telecom consultancy and project related services has not been well explored. In the current research, responses from customers have been quantified accordingly.

Perceptions of Internal Customers on a Telecom Service Supply Chain

Dr. Pramod V R[1] and Dr. Banwet D K[2]

[1]Professor, Department of Mechanical Engineering, NSS College of Engineering, Palakkad-8, Kerala, 678008
[2]Former Professor, Department of Management Studies Indian Institute Of Technology, Delhi, 110016

[1]pramovdram@gmail.com,, [1]pramodvram@redifmail.com,, [2]dkbanwet@hotmail.com [2]dbanwet@gmail.com

Abstract -

Service sectors are gaining more and more popularity among the industrialists in this ever-vibrant global competitive scenario. Internal customers are the one among the major stakeholders of an organization. In this milieu, an attempt to analyze their receptivity on various departments and authorities of a service sector supply chain is of extreme relevant. Collecting the responses of employees through a questionnaire survey and subsequent statistical analysis of the elicitations gave valuable insights on employee receptivity. The study revealed that employees are having high receptivity on various authorities and departments. The receptivity was quantified by an index named receptivity index. The results were appreciable having high receptivity indices which clearly indicate that the organization is taking care of the expectations of internal customers. Understanding the perceptions of internal customers on various organizational aspects helps to have better policy decisions. The study has been conducted in an Indian MNC, having their business wide spread among the globe.

Expert System for Cost-Integrated V SM Implementation in MSMES- A Case Study

Dr. Rajesh Menon Balakrishnan[1] Dr Shalij Poovathumkadavil Ramakrishnan[2]
Dr. Mahima Ganeshan[3] and Geemon Tom[4]

[1]Professor, Department of Mechanical Engineering, NSS college of Engineering, Palakkad, Kerala-678008, India, Phone: +91 9496466899
[2]Dean-Research, Kerala APJ Abdul Kalam Technological University, Thiruvananthapuram, Kerala-695016, India.
[3]Assistant Professor, Ahalia School of Engineering and Technology, Palakkad- 678557.
[4]Manager-Operations & Administration, Sanrea Healthcare Products Private Limited, Palakkad, Kerala-678621, India.

[1]brmenonnssce@gmail.com, [2]shalij123@gmail.com [3]ganeshanmahima@gmail.com [4]tomgeemon@gmail.com

Abstract -
The implementation of Lean tools in different sectors is considered a potential source for increasing the productivity of small and medium-sized enterprises. In this context, the Cost Integrated Value Stream Map (CVSM) is a versatile tool that can visualize the production process completely, allowing for further analysis of production-related parameters at a micro-level for each production process. The internet-enabled data collection software, MSME Value Tracker, is designed for the collection and analysis of production parameters to determine the company's leanness in operation. This tool helps assess the cost-wise status of production and suggests remedial lean measures for better future productivity. The design of the new lean tool is carried out by combining the conventional VSM with the incorporation of cost aspects of production. The test implementation of this new tool was carried out in two different industries. As part of the implementation procedure, an easy-to-operate expert system was developed.

1 Introduction

The implementation of Lean tools in small and medium-scale enterprises in India has been an initiative by the Ministry of MSMEs to improve productivity. These measures enhance competitiveness and subsequently improve the quality of products of these companies, ensuring that all existing manufacturing firms survive global competition and contribute to the Indian economy. MSMEs typically have an optimal number of operators in their organization due to the higher overhead component of employee wages when considering the cost of production. Many of the companies in Kerala registered as small or medium enterprises are facing severe competition from other parts of the world. The cost of raw materials, labour, utilities, administration, etc. are the primary components that decide the cost of a product. MSMEs usually have the scope for optimization only in the area of production-related expenses. The cost of raw materials remains the same among competing companies. In this situation, the cost of a product can be further reduced by eliminating the waste associated with the production process. Shifting traditional manufacturing into the Lean manufacturing paradigm is one solution to this problem. To eliminate manufacturing waste, MSMEs should assess their processes to identify various costs incurred in the processes. The need for an assessment tool to quantify lean competitiveness is relevant in the Lean manufacturing paradigm. As part of the research work, the principles of CVSM were used to develop an assessment tool to visualize the changes due to the implementation of Lean tools.

1.1 CVSM as a Lean Assessment Tool

The Cost Integrated Value Stream Map (CVSM) is a versatile tool that can comprehensively visualize the production process and analyze production-related parameters at a micro level for each production process. CVSM provides a clear representation of the entire spectrum of production transactions, which even lower-level operators on the production floor can understand. These transactions encompass information, material, and activity flow during production in terms of both money and time. The analysis and final reports generated from CVSM can be easily understood by employees, empowering them to drive change and improve competitiveness by reducing costs and ensuring better product quality. However, enterprises seeking to implement Lean tools may find it difficult to spare employees for this exercise due to the busy schedule typically present in industrial environments.

1.2 Unavailability of a standard format for the data collection for lean analysis

Standard format for implementing different lean tools in MSMEs in India is not well established as in other countries like Japan. This is supposed to be the most important hurdle in the lean implementation initiative for small and medium enterprises.

1.3 Sparing employees for meeting, data collection and brainstorming

In MSMEs, all employees, supervisors and managers are normally preoccupied with their routine job responsibilities in every company. This is because, the cost of maintaining an employee is considerable compared to the other overheads of production. With this optimum number of employees, companies are not normally able to spare the time for some other additional work such as lean auditing and related meetings.

1.4 Manual Data Collection

Data collection needs to be done with the help of supervisors of each process station and it should be accurate for further analysis. This is the next most challenging factor in the implementation of Lean, because the data can vary in a wide range of value. Picking the exact value from such a wide range can only be done with the help of an experienced operator. They can arrive at the most likely value of the production parameter in their process station.

1.5 Large number variants for products

Every enterprise makes a variety of product in their production line suiting different customer requirements. Analyzing each of this product individually is another difficulty in the manual lean analysis.

1.6 Regular review regarding the results of analysis

The results obtained through lean analysis is to be conveyed back to the team so that in the next brain storming session each one of the committee members will have some simple suggestion that can considerably change or eliminate the wastes associated with those production areas during the production of a specific product.

1.7 Data sharing and collection

The data which is collected from each organization specific to a single product is to be first recorded, processed and then interpreted for taking remedial measures such as suggesting the most appropriate lean technique for waste elimination. Manual data collection, processing and interpretation method have got their own disadvantages. All the above-mentioned challenges of data collection and analysis point towards the use of Information Technology solutions to overcome the entire issues regarding this situation.

2 Literature Review

Marko et al. (2018) implemented the Lean tool by ensuring the sustainability of the production process while improving efficiency by at least 8–10% on a monthly basis [1]. The Value Stream Map was applied to visually see the entire production process, as well as to identify the root causes of losses. It was identified that application of the Lean and PDCA approach based on the developed action plan the performance of efficiency was significantly increased by 10.67% compared to the state before process improvement. Indrajit Bhattacharyaa & Anandhi Ramachandran (2021) did multi-case study approach based on the primary implementation of Lean manufacturing techniques in the MSMEs under the Lean manufacturing competitive Scheme (LMCS) Scheme of the Ministry of Micro, Small, Medium and Medium Enterprises (MSME), Govt. of India since 2014 [2]. A sample size of 6 clusters each representing a specific sector has been selected for the study and the sectors covered were brass, pump and machinery, packaging, auto, textile and garments. The validation study carried out by the national monitoring committee on randomly selected 23 MSME units has also been explored for understanding the quality of benefits achieved by the MSMEs post implementation of Lean. There has been a reduction in cost, reduction in waste, improvement in quality and increase in lead time. The study established that up-scaling of Lean manufacturing technique practice is required en-masse across the entire MSME sector quickly so that they can realize the benefits of Lean and invest in sustainable Industry 4.0 techniques leading to Advanced Digital Production (ADP) techniques. The data driven smart manufacturing would enable the MSMEs to maintain competitiveness in the global markets through innovation and internationalization, resource optimization and flexible manufacturing. Expert systems utilizing the capabilities of Information Technology (IT) is the order of the day. The complex industrial production processes can be accurately simulated with predictable deviation from the actual real-life situation [3]. The changes in these production parameters from time to time can also be accommodated using the capability of IT tools. There are a lot of attempts done in this sector to simulate and automate the data collection, processing and analysis in the lean manufacturing domain in the context of improving the productivity of manufacturing processes. IT tools are also integrated into many well-known lean tools such as 5S, VSM, KANBAN, TPM, Poka Yoke etc. [4-13]. Misha Matharu & Neena Sinha (2019) used SAP LAP framework to address critical questions regarding lean adoption by Indian manufacturing MSMEs in the context of the government scheme 'LMCS'. The study adds the importance of soft issues while implementing lean and helps the stakeholders by suggesting suitable actions that can be taken to further improve the competitive priorities of MSMEs [14]. This case study detailed existing weakness despite lean interventions and progress made so far. Yadav V. et al. (2019) measured the degree of lean adoption in SMEs

and to test its influence on operational performance [15]. The SMEs primarily uses eight practices, namely, customer involvement, employee involvement, pull system, 5S, TPM, statistical process control, SMED and production levelling resulting in a positive impact on the operational performance. The results suggest that even with the limited number of implemented practices, lean may help to enhance the operational performance in SMEs and also valuable for practitioners because it suggests that even a partial implementation of lean may be beneficial for SMEs. The practitioners in SMEs are also encouraged to perform customer involvement, employee involvement, pull system, 5S, TPM, statistical process control, SMED and production levelling for the successful implementation of lean in their organization. Dave et al., (2016) presented an insight into the field of lean construction management systems such as VisiLean and KanBIM [16]. These tools are improved by utilizing IoT techniques in order to report real-time task status from the field, while enhancing interoperability between all major information systems and organizations throughout the construction project. These standardized IoT interfaces are considered potential as well as maintaining the information flow consistency in lean construction management systems. Ante et al., (2018) recommended a hierarchical structure for the key Performance Indicators (KPI) which are useful for manufacturing engineers in measuring the performance of the studied Bosch Production System and allow identifying the relationships among the different KPIs, consistently with operational improvement and floor shop control [17]. Das K. (2018) introduced a model-based approach for integrating contributions and outcomes of Lean tools and practices in Supply Chain planning process for improving sustainability performances of the overall business [18]. The work helped Supply Chain managers in choosing Lean and green practices in addition to benign technology based on their unique business situations for accomplishing their triple-bottom-line targets. A significant conclusion made by Kruse et al., (2019) showed that outcomes of an integrated-lean management system, such as value-added and reduced waste and risk, were supported by the specific management, structural and financial strategies adopted by the sampled companies [19]. The aforementioned areas back up the overall focus of management systems for continuous improvement. A standard procedure devised by Passath and Mertens (2019) to adapt dynamically with the rapidly changing industrial production scenario to manage the maintenance [20]. This can significantly reduce the human effort and create a standard independent of the data quality and reduce the human factors influencing such maintenance decisions and to create a more objective and comparable evaluation. Antosz et al., (2019) presented the possibility of using intelligent decision support systems in the Maintenance management paradigm [21]. The use of AI for the assessment of the Lean Maintenance methods. Antony pearce et al. (2018) identified critical success factors for lean implementation and it followed two first-time implementations of lean in small to medium-sized enterprises (SMEs) [21]. The paper provided new visions into the role of knowledge as a causal factor in the successful implementation of lean and especially in organisations with inadequate resources. Vinodh et al. (2016) presented a method for value stream mapping (VSM) integrated with life-cycle assessment (LCA) for ensuring sustainable manufacture [23]. The projected framework is capable of visualizing and evaluating manufacturing process performance from sustainability view point. They compared the key performance measures from environment, economy, and societal perspective and percentage improvement was computed. The scientific value showed that it has contributed a new framework for VSM integrated with LCA to ensure sustainable performance. A structured literature review was conducted on lean implementation in SMEs with a perspective of identifying the main challenges faced and comprehensive analysis along three stages: planning, conducting, and reporting. The main aim was to establish the current position of global understanding of Lean implementation in SMEs, including examining the main categories of Lean implementation in the context of SMEs [24-26]. The review stipulated well-advertised benefits (increase market share, increase customer satisfaction, increase sustainability of the company) along with improvising the internal performance of the company (such as increasing flexibility, introduction of realistic and meaningful key performance indicators, desire). Sunil kumar et al. (2019) elaborated the opportunities to reduce cost and improve productivity and quality in the existing production system through the application of Lean-Kaizen concept using value stream mapping (VSM) tool of an Indian Small-Scale Enterprise (SSE) [27]. The void between current state map and future state map and to synchronize cycle time of each station with talk time, Kaizen event (KE) was suggested. The findings can inspire the SSEs to adopt the Lean-Kaizen concept for optimizing continuous improvement opportunities in their production industry. This study also used SAP LAP framework to report critical questions concerning lean adoption by Indian manufacturing MSMEs related to the government scheme 'LMCS'. Andreadis, L et al. 2017 investigated issues related to lean philosophy and in correlation with some of its main tools [28]. Five hypotheses and three complementary research questions were articulated and verified using a combination of descriptive statistics and Pearson correlation, 2-Sample proportion, One-way ANOVA, 1-Sample t-tests and Tukey-Pairwise comparison tests. A survey questionnaire was conducted with 168 manufac-

turing organisations worldwide and results were based on different prospects of using VSM efficiently. Few other methods were suggested by different researchers employing lean management in manufacturing world [29-31]. An extensive review on the lean managament system and its ambiguity in practical sense is also detailed in various papers [32-35]. Rajesh Menon et al. (2021) developed cost-integrated value-stream mapping (CVSM) as a lean assessment tool for identifying wastage in the production process [36]. Comparing to conventional VSM, the cost of production is also accounted for in the proposed CVSM, along with the time domain of conventional value-stream mapping. The method is used to evaluate the value addition in monetary terms, and thus the actual production cost of the processes is acknowledged precisely. The wastage is also quantified in the cost domain and thus the processes in which lean tools need to be implemented can be recognised. Review summarises the progression of VSM from the conventional pencil and paper method to smart implementation over the years. The challenging variations in the production process and production quantity, smart techniques have to be incorporated into the traditional VSM method. This will assist the Lean implementation procedure for enhancing the accuracy of analysis and reduces the efforts of the Lean team. Finally, a new feature of integrating the cost aspect of production along with the incorporation of information Technology is introduced.

3 Cost Time Integration Principle

Industry 4.0 is supposed to be the fourth industrial revolution that represents the new concept of organization and control of various activities of the industrial value chain. Smart systems integrated into every manufacturing system making use of IoT as the tool for this change. In this perspective, we make use of an expert decision support system for the data collection and analysis of lean implementation in a small-scale industrial unit. Indirect cost for the product includes utility cost and the fixed cost which has to be collected from the company. Cost of utility consists of the cost of water consumed, electricity charges and fuel. The fixed cost associated with every production process is related to the cost involved in the salary of administrative and security personals, bank charges, audit expenses, travelling expenses, unloading of goods arrived and loading of goods in despatch section, lab expenses, employee welfare, annual employee insurance charges, various taxes, festival allowance and rent of building or equipment. Total cost of production can be found by adding the direct cost, indirect cost and the non-value-added cost. In this stage, the cost of waiting (Cw) for the different processes are added along with the timeline of VSM. Cw is determined by accounting the total investment cost due to the waiting of raw material, Work in Process inventory and finished goods waiting to be sold to the market.

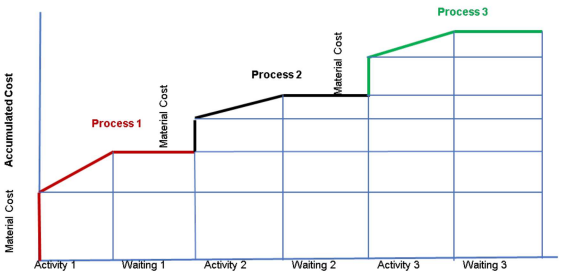

Figure 1. Total Cost Investment as the Area under CTP Curve

As shown in Figure 1, Cw is the product of the area under the CTP line and %IRR. Cw is calculated using equation 1.1.

$$C_w = \Sigma_i[Cmat_{i,k} * Tc_i) + 1/2(Ca_{i,k} * Tc_i) + (Ca_{i,k} + Cmat_{i,k}) * Tw_{i,k}] * IRR\% \quad (1.1)$$

Where
Cw - Total cost investment due to waiting
Cmat - Material cost
Tc - Cycle time
Ca - Activity cost
Tw - Waiting Time
i, j & k - different activities, materials, and machines respectively
Total cost of production (Cp) is calculated using the equation 1.2.

$$Cp = \Sigma_i(Ca + Cmat + Cw + Cu + Cf + Crej) \quad (1.2)$$

Where
Cp - Cost of Production
Ca - Activity cost
Cmat - Material cost Cw - Total cost investment due to waiting
Cr - Cost of Manufacturing Resources (Cost depreciation and Maintenance)
Cu - Utility cost per product
Cf - Fixed cost per product
Crej - Cost of rejection of defective product at each machine
Activity cost refers to the sum of operator cost (Co) and the cost of the various resources (Cr) that are consumed. Operator cost can be calculated from the annual emoluments given to the operator. Cost of resources (Cr) is the sum of depreciation cost (Cd) of the machine and machine maintenance cost (Cm). Machine depreciation cost rate ($\dot{C}$ dk) can be found out by dividing the cost of the equipment with the product of the equipment's service life and

the time the equipment was used in a year as shown in equation 1.3

$$\dot{C}dk = Ce_k/(Ly * Tl_k) \tag{1.5}$$

Tl – Time units it is used in a year
Ce - Cost of Equipment
Ly – Expected life of equipment in years

The machine maintenance cost rate (Cm_k) is found out by dividing the maintenance cost per year with the time units it was used in a year. This calculation is shown in equation 3.4.

$$\dot{C}m_k = Cm/Tu_k \tag{3.4}$$

The resource cost rate ($\dot{C}$ r) can be found by adding the machine depreciation cost rate ($\dot{C}$ d) and machine maintenance cost rate ($\dot{C}$ m) as shown in equation 3.5.

$$\dot{C}r_k = \dot{C}d_k + \dot{C}m_k$$

(3.5)

$\dot{C}$ r - Resource cost rate (Resource cost/hour)
$\dot{C}$ d - Depreciation cost rate
$\dot{C}$ m - Machine maintenance cost rate

Effective cost rate of the operator ($\dot{C}$o) is calculated by dividing the annual remuneration with the effective time of work in the company. Resoure cost rate can be added with the operator cost rate for obtaining the activity cost rate ($\dot{C}$a). Activity cost rate and the corresponding activity cost in the production can be found from equations 3.6 and 3.7 respectively.

$$\dot{C}a_k = \dot{C}o_k + \dot{C}r_k$$

(3.6)

$\dot{C}$ a - Activity Cost Rate $\dot{C}$ o - Labour Cost per hour (Operator & Supervisor) $\dot{C}$r - Resource Cost Rate

$$Cai = \dot{C}a_i Tc_i$$

(3.7)

Ca - Activity Cost
$\dot{C}$ a - Activity Cost Rate
Tc - Cycle Time
Waiting cost of the work in process (WIP) inventory, which is the major non-value-added cost in manufacturing a product, is further termed as 'Cost of Waiting'. From the conventional CTP, horizontal lines indicate the waiting cost for WIP and the area below the horizontal lines in CTP will imply the term Cw.

4 Development of Current State CVSM

Combining the time data from VSM and cost investment data from CTP, a current state map of the CVSM is to be developed. In the present state CVSM, a cost line is also drawn along with the timeline that depicts the cost and the time of all non-value-added activities. Information related to production parameters, including lot size for an activity, cycle time, available time, uptime, number of operators and supervisors, the distance between work stations, percentage rejections activity and waiting period for the various production processes are recorded by the implementation team in the CVSM. The cycle time, uptime, change over time, work in process inventory and the number of operators is entered with the corresponding symbols in the prepared CVSM. During this process Takt time for the product is also to be calculated. For calculating the takt time data on the daily demand of the selected product and net available working time in a day for manufacturing the product are required. A comparison of the cycle time and the takt time can be made in a bar chart. Non-value-added time during the production can be identified from this bar chart.

5 Development of Expert System for CVSM Implementation

Implementation of Lean tools in small and medium scale enterprises in India had been an initiative by the Ministry of MSMEs for improving its productivity. These measures improve the competitiveness and subsequently enhance the quality of products of these companies. This ensures all the existing manufacturing firms to survive the global competition and contribute towards Indian economy. MSMEs normally have optimum number of operators in their organization due to the higher overhead component of employee wages when considering the cost of production. Many of the companies in Kerala registered as small or medium enterprises are facing severe competition from even other parts of the world. The cost of raw materials, labour, utilities, administration, etc. are the primary components deciding the cost of a product. MSMEs usually have the scope for optimization only in the area of production related expenses. Cost of raw materials remain same among competing companies. In this situation, cost of a product can be further reduced by eliminating the wastes associated with the production process. Shifting the traditional manufacturing into Lean manufacturing paradigm is one of the solutions to this problem. In order to eliminate the manufacturing wastages, MSMEs should be able to assess their process for identifying various costs incurred in the processes. The need of an assessment tool for quantifying the lean competitiveness is relevant in the Lean manufacturing paradigm. As a part

of the research work, the principles of CVSM were used to develop an assessment tool to visualize the changes due to the implementation of the Lean tools.

6 CVSM as a Lean Assessment Tool

Cost Integrated Value Stream Map (CVSM) is a versatile tool which can completely visualize the production process for further analysis of production related parameters in a micro level as far as each production process is concerned. CVSM establishes the entire spectrum of production transactions in a clear manner which is even understood by the lower-level operators in the production floor. Transactions in production includes the information, material and the activity flow during the production in terms of money and time. This analysis and the final reports can be easily understood by the employees and it empowers them to be a change agent in the improvement of competitiveness and thereby reducing cost and ensuring better quality of products. Enterprises aspiring to implement Lean tools in their organization can hardly spare employees for this exercise due to the busy schedule normally prevailing in the industrial environment. The following difficulties are found in every organization which acts as a barrier for the implementation of the Lean tools:

6.1 Unavailability of a standard format for the data collection for lean analysis

Standard format for implementing different lean tools in MSMEs in India is not well established as in other countries like Japan. This is supposed to be the most important hurdle in the lean implementation initiative for small and medium enterprises.

6.2 Sparing employees for meeting, data collection and brainstorming

In MSMEs, all employees, supervisors and managers are normally preoccupied with their routine job responsibilities in every company. This is because, the cost of maintaining an employee is considerable compared to the other overheads of production. With this optimum number of employees, companies are not normally able to spare the time for some other additional work such as lean auditing and related meetings.

6.3 Manual Data Collection

Data collection needs to be done with the help of supervisors of each process station and it should be accurate for further analysis. This is the next most challenging factor in the implementation of Lean, because the data can vary in a wide range of value. Picking the exact value from such a wide range can only be done with the help of an experienced operator. They can arrive at the most likely value of the production parameter in their process station.

6.4 Large number variants for products

Every enterprise makes a variety of product in their production line suiting different customer requirements. Analyzing each of this product individually is another difficulty in the manual lean analysis.

6.5 Regular review regarding the results of analysis

The results obtained through lean analysis is to be conveyed back to the team so that in the next brain storming session each one of the committee members will have some simple suggestion that can considerably change or eliminate the wastes associated with those production areas during the production of a specific product.

6.6 Data sharing and collection

The data which is collected from each organization specific to a single product is to be first recorded, processed and then interpreted for taking remedial measures such as suggesting the most appropriate lean technique for waste elimination. Manual data collection, processing and interpretation method have got their own disadvantages. All the above-mentioned challenges of data collection and analysis point towards the use of Information Technology solutions to overcome the entire issues regarding this situation.

7 MSME Value Tracker

A software named "MSME Value Tracker" is designed for data collection, analysis and interpretation of results of the lean implementation in MSMEs. This internet enabled software equips the entire team to share the data collected in their own comfort and convenience. This software can be installed and operated by the entire team members through their mobile phone or computer. This package ensures convenience of uploading the concerned values of parameters related to a specific team member which can be consolidated in a common platform for further analysis. Every team member is free to see the values in each process stage. Finally, everyone in the team will get an overall view of the costs of operations during the production. This helps in identifying the wastages in each department during production.

7.1 Design and Functions of MSME Value Tracker

The welcome page of the MSME Value Tracker is shown in Figure 6.1. Upon clicking the Go to Admin Dashboard, the Dashboard for adding a company will be displayed. As shown in Figure 6.2, the name of the company can

be added by the administrator. Login details of the team leader is also created by the administrator of the company. Login details are assigned to the team members by the team leader. Actual data of a company M/s SANREA Healthcare Products Pvt Limited are entered into the MSME Value Tracker, in order to explain the working of the system.

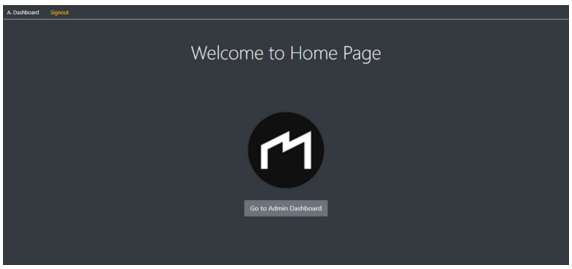

Figure 2. Home page of Value Tracker

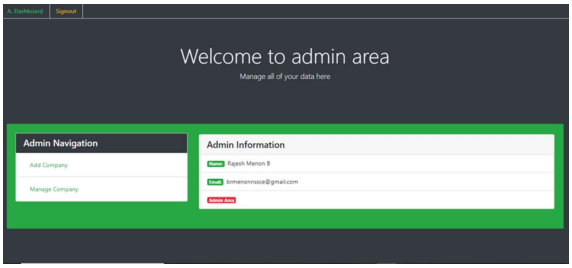

Figure 3. Dashboard for adding Company

7.2 Company Profile

The following general details about the company are initially uploaded at the time of adding the company.
Company Name
Company Description (A general description of products and the category)
Company Address
Company Contact (Team Leader for this Lean Implementation)
Products (All products and its variants)
Annual Turn Over (INR)
Investment Cost (INR)
Customers (Regular clients/customers for the last two years)
Monthly Demand (number of product pieces)
Monthly Production Capacity (Numbers)
Number of Employees
Departments (Production, Marketing, Quality, Maintenance, etc.)
Utilities (Water, Electricity, Fuel, Oil, etc.)
Temporary Employees (Not included in the company Roll)
Area of Land (cents/acres)
Area of Factory Building (Sq ft/Sq m)

The company details entered for M/s Sanrea Healthcare Products Pvt. Ltd. is shown in Table.1

7.3 Add Product

After adding the company and company details, the products details are added in the screen shown in Figure 6.3. The products of M/s SANREA Healthcare Products Pvt Ltd, as added are shown in Table 2. After adding all the products, the screens for entering Information flow, Material flow and Activity flow will be displayed by clicking the 'eye' symbol near the product name.

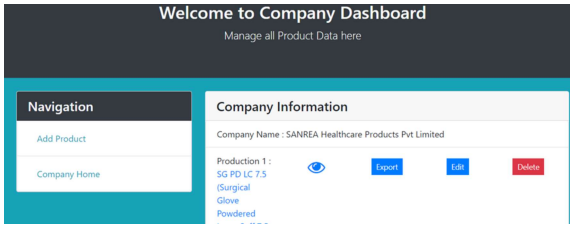

Figure 4. Add product screen

7.4 Material Flow

Tracing the material flow of the production process is another important aspect of visualising the production with the help of VSM. These details are entered in the 'Materials Flow Details' screen shown in Figure 4. On clicking the 'Add' button, a screen for entering the details will be displayed. This screen is shown in Figure 5. There are provisions for adding material and denoting the type of material handling for all the processes. A sample of the materials flow data entered is shown in Table 3.

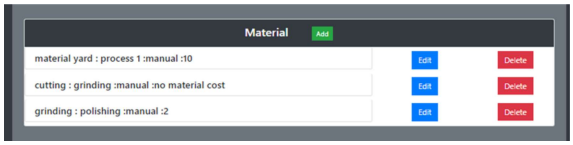

Figure 5. Material Flow Details Window

7.5 Activity Flow

Process parameters are uploaded by the concerned department team member into the main pool of data. These data are entered through the 'Activity Flow Window' shown in Figure 6. A sample of the activity flow entered is shown in Table. 4. Activity details of all the

Table 1. Company Details entry to the MSME Value Tracker

Details	**Data to be entered**
Company Name	SANREA Healthcare Products Pvt Limited
Description	SANREA HEALTHCARE PRODUCTS PRIVATE LIMITED is a Medical Glove manufacturing company established in 2012 located in KINFRA Integrated Industrial & Textile Park, Palakkad, Kerala, India. The factory is equipped with state-of-the-art multi glove production facility capable of manufacturing disposable gloves using natural and synthetic latex. The promoters of SANREA with their past experience in the glove manufacturing field have come up with this facility (having a capacity of 2 Million Pairs per month), for development of disposable gloves with innovative production technologies keeping at par with the international standards. SANREA guarantees a safe and reliable glove manufactured under stringent production hygiene and quality check parameters.
Address	KINFRA Integrated Industrial & Textile Park, Pearl Road, Kanjikode, Palakkad, Kerala, INDIA
Contact Details	XXXXXX3076
Products	SURGICAL/PHARMA GLOVES
Annual Turnover	49.8 Cr
Investment Cost	9.12 Cr
Customers	Sun Pharma Industries, Lupin, Sreeji Distributors
Monthly Demand	21,00,000 Pairs
Monthly Production Capacity	16,00,000 Pairs
Number of Employees	140
Departments	Production, Quality, Marketing & Finance
Utilities	Water, Firewood, Furnace Oil
Temporary Employees	5
Area of Land	185 cents
Area of Factory Building	80000 SQ FT

Table 2. Products added into the MSME Value Tracker

Product	**Product Code**	**Lot Size (Nos)**
Powdered Long Cuff Palm size 7.5 inch	SG PD LC 7.5	120,000
Powdered Long Cuff Palm size 8 inch	SG PD LC 8.0	119,000
Powder Free Long Cuff Palm size 7.5 inch	SG PF LC 7.5	120,000
Powder Free Long Cuff Palm size 8 inch	SG PF LC 8.0	119,000
Powdered Short Cuff Palm size 7 inch	SG PD SC 7.0	122,000
Powdered Short Cuff Palm size 7.5 inch	SG PD SC 7.5	120,000
Powdered Short Cuff Palm size 8 inch	SG PD SC 8.0	119,000
Powder Free Short Cuff Palm size 7 inch	SG PF SC 7.0	122,000
Powder Free Short Cuff Palm size 7.5 inch	SG PF SC 7.5	120,000
Powder Free Short Cuff Palm size 8 inch	SG PF SC 8.0	119,000

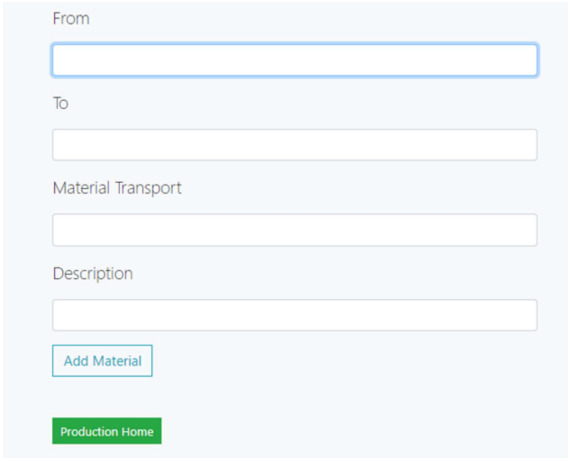

Figure 6. Materials Flow Entry Window

sections as shown in Table 6.4 are entered into the MSME Value Tracker.

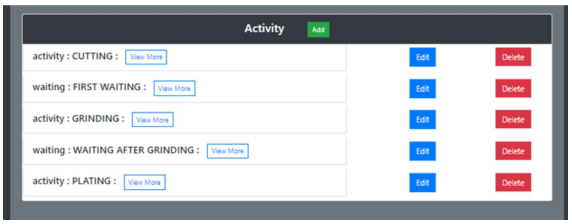

Figure 7. Activity Details Window

The following parameters are uploaded in a production line.

Name and code of the Process
Activity cycle Time
Value Added Time (VA)
Non-Value-added time (NVA)
Lot Size (if any)
Material cost
Operator cost rate and Number of operators
Supervisor cost rate and number of supervisors
% Rejection
Distance between processing stations
% Internal Rate of Return
Machines, Investment on machinery, Annual Maintenance cost and age of the machine

7.6 Activity Parameters

By clicking the add button of the screens 'Activity' and 'Waiting', the listed parameters are entered as shown in Figure 6.7 and 6.8 respectively. These data are to be entered for all the activities.

Table 3. Sample data of Material Flow

From	Type of Flow	To
Store	Manual	Compounding
Compounding	Through Pipes	Dipping & Curing
Dipping & Curing	Manual	Tumble Dryer
Dipping & Curing	Manual	Tumble Dryer
Tumble Dryer	Manual	Inspection Section
Inspection section	Manual (Trolly)	Glove Washing
Glove washing	Manual	Glove Drying
Glove Drying	Manual	Despatch
Despatch section	Truck	Kochi Unit
Warehouse	Manual	Packing Unit
Packing Unit	Trolly	Sterilization unit

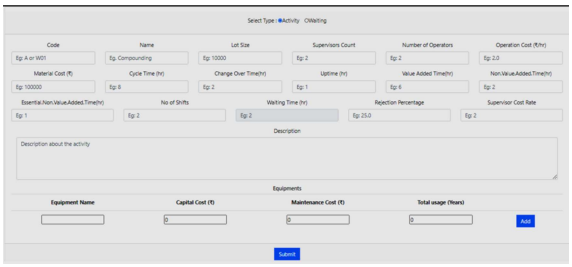

Figure 8. Activity parameters Window

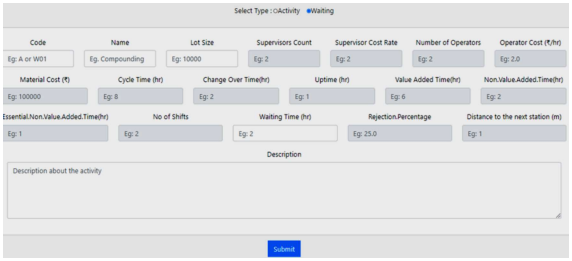

Figure 9. Waiting parameters Window

7.7 Information Flow

Details of Information flow are mainly used for the preparation of Value Stream Map for picturizing the complete transactions involved in the production. These data are entered in the 'Information Flow' screen shown in Figure 9. The flow of information between the customers and company, within the company and the communication between the company and its suppliers are entered in this screen. By clicking the 'Add' switch the screen shown in

Table 4. Activity Details of each Processing Station

Activity Code	Activity Name	Distance to the Next Station(M)	Description
A	Compounding	5	Mixing of chemicals with latex
B	Dipping & Curing	5	Dipping The ceramic former into latex compound and then curing with heat
C	Tumble Drying	6	Drying the gloves after curing
D	Inspection	6	Inspecting the acceptable quality level
E	Glove Washing	5	Chlorinated to remove the powder present in the gloves
F	Glove Drying	5	Drying the gloves after washing
G	Despatch	150000	Sending the finished gloves for packing and sterilization to kochin plant
H	Packing	5	Packing the gloves in a pouch (both left and right hand), packing pouches into inner carton and finally placing the inner cartons to master carton
I	Sterilization	5	Sterilization is done to a lot of 88000

Figure 10 will be displayed, Information entry screen.

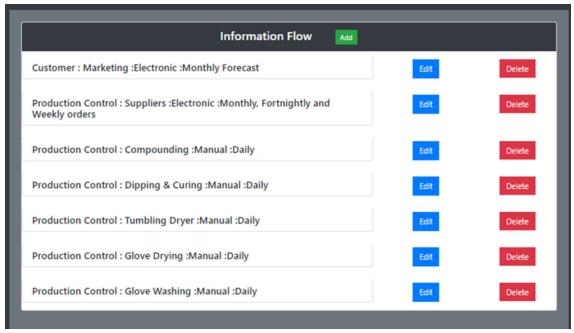

Figure 10. Information Flow Add / Edit Window

After completing the data entry, by clicking the 'Export' button, in screen shown in Figure 11, the details of costs and other information will be exported in the Excel format. The information obtained are shown in Tables 5 to 7. Table 5 gives the details of cycle time, costs and cost rates arrived at using Equations 1 to 6.

7.8 CTI Calculation

The time and costs of waits in the processes as exported from the MSME Value tracker are given in the table 6.

Finally, all the direct, indirect and investment cost is accounted for calculating the actual production cost.

8 Validation of Value Tracker

Actual set of product data for a company was entered into MSME Value Tracker. Costs of 10 variants of products as obtained from MSME value tracker are shown in

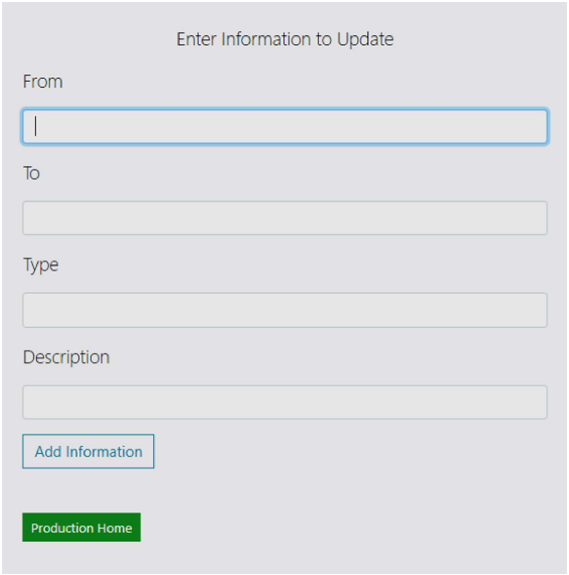

Figure 11. Information Flow Entry Window

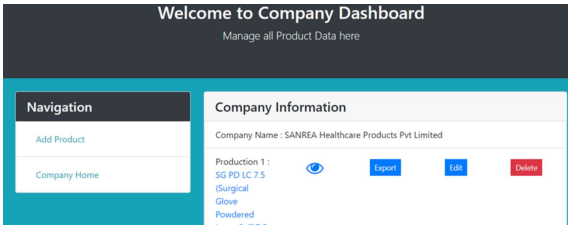

Figure 12. Export the results of analysis Window

Table 6.8. The system was able to perform the following

Table 5. Process Parameters in Time and Cost Domain

Activity Code	A		B		C
Process	Compounding		Dipping & Curing		Tumble Drying
In between stage/ waiting		Maturation1		Waiting1	
Lot Size	120000	120000	120000	118050	6000
Supervisors	1	-	3	-	-
Operators	2	-	10	-	3
Cycle Time	60	-	24	-	24
Waiting time before	-	60	-	2	-
Operator cost rate	37.5	-	37.5	-	43.75
Supervisor cost rate	76.92	-	76.92	-	76.92
Depreciation Cost Rate	21.69	-	42.94	-	4.95
Maintenance Cost	0.18	-	0.61	-	0.04
Resource Cost	21.87	-	43.55	-	4.98
Activity Cost Rate	136.29	-	157.97	-	125.65
Material Cost	286000	-	-	-	-
Activity Cost	8177.53	-	3791.19	-	3015.71
Total Cost	294178	-	3791.2	-	3015.7
% Rejection	-	-	0.5	-	-
Cost with rejection	294177.5	-	3810.15	-	3015.71
CTI*IRR%	550.25	-	120.89	-	906.57

H	G		F		E		D	
Packing	Despatch	Waiting 4	Glove Drying	Waiting 3	Glove Washing	Maturation 2	Inspection	Waiting 2
120000	480000	120000	8000	112000	8000	12000	120000	114000
1	-	-	-	-	1	-	1	-
10	3	-	4	-	3	-	30	-
72	288	-	75	-	15	-	8	-
-	-	72	-	3	-	168	-	168
76.12	43.75	-	37.5	-	62.5	-	76.13	-
76.92	76.92	-	76.92	-	76.92	-	76.92	-
0.15	-	-	3.81	-	4.57	-	0.55	-
0.01	-	-	0.04	-	0.04	-	0.04	-
0.16	-	-	3.84	-	4.60	-	0.59	-
153.20	120.67	-	118.26	-	144.02	-	153.64	-
14500	-	-	-	-	-	-	-	-
11030.39	34752.96	-	8869.74	-	2160.36	-	1229.09	-
25530	34753	-	8869.7	-	2160.4	-	1229.1	-
-	-	-	-	-	-	-	4.5	-
25530.39	34752.96	-	8869.74	-	2160.36	-	1284.4	-
838.21	1494.92	-	717.72	-	85.76	-	835.01	-

	Waiting 5	12000	-	-	-	72	-	-	-	-	-	-	-	-	-	-	-	-
I Sterilization		88000	1	3	24	-	62.5	76.92	105.02	0.09	105.11	244.53	-	5868.82	5868.8	-	5868.82	141.85

Table 6. Time line Costs

	Process	Wait	Process	Wait	Process	Wait	Process	Wait	Process	Wait	Process	Wait	Process	Wait	Process	Wait	Process	Wait
Process	A		B		C		D		E		F		G		H		I	
Time (VA) in min	60		24		24		8		15		75		96		72		24	
Time (NVA) in min		0		0		0		0		0		0		0		0		0
Cost (VA) in Rs.	294,177.5		3,810.15		30,15.71		12,84.4		2,160.36		8,869.74		34,752.96		25,530.39		5,868.82	
Cost (NVA) in Rs.		550.25		120.89		906.56		835.00		85.763		717.71		1,494.92		838.20		141.84

Table 7. Unit Production cost

Cost Time Investment (Rs.)	Utility Cost (Rs.)	Fixed Cost (Rs.)	Total Unit Cost (Rs.)
5,691.17	0.52	0.75	4.47968

Table 8. Cost comparison between CVSM and from Accounting data

Product	Product Code	Lot Size	Cost (CVSM Analysis)	Cost as per Accounts	% deviation
Powdered Long Cuff Palm size 7.5 inch	SG PD LC 7.5	120000	4.48	4.22	1.062
Powdered Long Cuff Palm size 8 inch	SG PD LC 8.0	119000	4.52	4.26	1.061
Powder Free Long Cuff Palm size 7.5 inch	SG PF LC 7.5	120000	4.78	4.51	1.060
Powder Free Long Cuff Palm size 8 inch	SG PF LC 8.0	119000	4.82	4.57	1.055
Powdered Short Cuff Palm size 7 inch	SG PD SC 7.0	122000	4.41	4.15	1.063
Powdered Short Cuff Palm size 7.5 inch	SG PD SC 7.5	120000	4.42	4.17	1.060
Powdered Short Cuff Palm size 8 inch	SG PD SC 8.0	119000	4.45	4.19	1.062
Powder Free Short Cuff Palm size 7 inch	SG PF SC 7.0	122000	4.74	4.39	1.080
Powder Free Short Cuff Palm size 7.5 inch	SG PF SC 7.5	120000	4.72	4.46	1.058
Powder Free Short Cuff Palm size 8 inch	SG PF SC 8.0	119000	4.76	4.49	1.060

functions.

Collection of all production related data from the production floor

Time related data such as cycle time, waiting time, etc. can be recorded

Cost related data can be recorded (Material, activity, etc.)

Analysis can be carried out and a timeline and cost line can be drawn for each process

A distance line is drawn to assess the efficiency of the production layout

By conducting the lean costing of the entire range of products coming under the production, the production cost determined based on CVSM analysis was pretty close to the value predicted by the accounting department, considering the cost of material, employees, infrastructure, utility and indirect overheads related to the production of each product.

9 Conclusion

MSMEs in India are forced to undergo some kind of productivity improvement exercises as envisioned by the Government of India under the schemes of the MSME ministry. These measures will improve our GDP, exports, employment opportunities and quality of products. Hence, it is high time the studies had concentrated on the contemporary research on MSMEs so that they can be managed effectively. All the general methods of implementing lean in MSMEs, are by utilising the many well-known lean tools evolved from Toyota Production System. There are lot of published research works associated with Lean Implementation in various industrial sectors and Value Stream Map has a vital role in initially visualising and assessing the productivity and suggesting the lean tool to be adapted in improving the current state of an enterprise. Many modifications are attempted by many authors in this regard.

The methodology can be considered as the standard procedure for implementing cost integrated Value Stream Mapping in a company which is classified under the MSME sector. The Lean analysis is done by drawing the value stream of the current production process. The shortcomings of VSM analysis are identified by incorporating the cost information in connection with the production process. The data collected for VSM is to be augmented with the cost data associated with the production in visualizing the process in terms of Cost of production. From the Cost integrated VSM, we are able to visualize the production streamline not only in terms of time but also in cost terms. So, the wastages in production can be visualized easily at each processing stage in the production streamline. Then the remedial measures for eliminating these wastages can be done using various available lean tools that exist as per the Toyota Production System.

The results of this analysis show the timeline and cost line below the Cost Value Stream Map similar to the timeline in VSM. From the cost-line, any operator with minimum awareness about the production process can understand the entire value addition happening along with the production streamline. Normally the cost involved in a production process can only be effectively read and understood by a person from financial background so as to interpret the efficiency of the production process and to suggest and decide upon any lean improvement initiatives. CVSM gives a simple and very effective analysis tool in any MSME for the pre-lean implementation analysis to assess the present condition of functioning and propose an effective lean tool which is suitable for implementation considering the future state to be reached. CVSM gave a direct opportunity to identify wastes in the production line in terms of cost. This enables everyone, irrespective of the hierarchical position in the company, to quantify the wastages in production in cost terms. Identification of 'muda' and selection of the suitable lean tool to eliminate it is made easy by implementation of CVSM.

Industries can use MSME value tracker to collect all production data and calculate the cost of production of each product manufactured in the facility. This costing can be used to identify nonvalue-adding activities. Measures can be taken for improving the processes. This tool can be used as an assessment tool for measuring leanness in a company producing different variants of products and to accurately identify the wastages during production. This becomes an efficient tool to predict the production wastage and to suggest a suitable remedial lean tool for resolving the issue. The accuracy of this tool is validated by comparing the cost determined by the tool with the cost calculated using the conventional accounting methods. The accuracy of cost calculation is found to be varying in a consistent deviation range.

This newly developed CVSM model was test implemented in a manufacturing industry and a process industry and the evaluation was carried out. The results of this implementation study revealed that CVSM can be adopted by any MSMEs for assessing the productivity and for using lean analysis for wastage reduction. CVSM tool enables everyone to understand the areas of improvement for wastage removal better and to have an upper edge compared to the interpretation of traditional accounting systems for productivity analysis.

Acknowledgement

The author would like to express gratitude to the management of Nair Service Society for granting permission to successfully complete the research. The author also gratefully acknowledges the permission given by the management of Sanrea Healthcare Products Pvt Limited,

Palakkad, for undertaking the Lean implementation study. Furthermore, the author would like to extend thanks to the professors of GEC Thrissur for their guidance, which was invaluable in completing the research work on time

References

[1] Marko Milosevic, Marko Djapan, Roberto D'Amato, Nicolae Ungureanu, Alessandro Ruggiero, Sustainability of the Production Process by Applying Lean Manufacturing Through the PDCA Cycle – A Case Study in the Machinery Industry, International Conference on Manufacturing engineering and materials , (2018) 199-211.

[2] Indrajit Bhattacharyaa, Anandhi Ramachandran, Lean Manufacturing Techniques – Implementation In Indian Msmes and Benefits Realized Thereof, Indian Journal of Engineering & Materials Sciences 28 (2021) pp. 89-101.

[3] M. Mohan Prasad, J. M. Dhiyaneswari, J. Ridzwanul Jamaan, S. Mythreyan, S. M. Sutharsan, A Framework for Lean Manufacturing Implementation in Indian Textile Industry, Journal home page for Materials Today: Proceedings, 33 (7) (2020) 2986-2995.

[4] M. M. Shahriar, M. S. Parvez, M. A. Islam, S. Talapatra, Implementation of 5S in A Plastic Bag Manufacturing Industry: A Case Study, Cleaner Engineering and Technology, 8(2022).

[5] Seyed Mojib Zahraeea, Ali Tolooieb, Salman Jameh Abrishamic, Nirajan Shiwakotia, Peter Stasinopoulosa, Lean Manufacturing Analysis of A Heater Industry Based on Value Stream Mapping and Computer Simulation, Procedia Manufacturing, 30th International Conference on Flexible Automation and Intelligent Manufacturing (FAIM2021) 15-18 June 2021, 51 (2020) 1379–1386.

[6] Biman Das, Uday Venkatadri, Pankajkumar Pandey, Applying Lean Manufacturing System to Improving Productivity of Airconditioning Coil Manufacturing, The International Journal of Advanced Manufacturing Technology, 71 (2014) 307–323.

[7] P. Masuti, U. Dabade, Lean Manufacturing Implementation Using Value Stream Mapping At Excavator Manufacturing Company, Materials Today: Proceedings, 19 (2019) 606-10.

[8] Kashmir Singh Ghatorha, Rohit Sharma, Gurraj Singh, Parveen Sharma, Implementing Lean Through Value Stream Mapping for Productivity Improvement: A Case Study of Link Frame Mechanical Press Manufacturing Industry, International Journal of Six Sigma and Competitive Advantage, 13 (2021) 182-194.

[9] Ahmad Naufal, Ahmed Jaffar, Noriah Yusoff, Nurul Hayati, Development of Kanban System at Local Manufacturing Company in Malaysia–Case Study, Procedia Engineering, 41 (2012) 1721-1726.

[10] Krishnan Krishna Iyer, F. Frank Chen, A Cloud-based Kanban Decision Support System for Resource Scheduling Management, Procedia Manufacturing, 11 (2017) 1489-1494.

[11] Rajan Kumar, Premanand S. Chauhan, Ravi Kumar Dwivedi, Anoop Pratap Singh, Jagdish Prasad, Design And Development Of Ball Dispenser Machine Through Lean Manufacturing Tool Poka-Yoke Technique in Automobile Industries, Materials Today Proceedings, 62(12) (2022) 6530-33.

[12] Omar Bataineh, Tarek Al-Hawari, Hussam Alshraideh, Dorid Dalalah, A Sequential TPM-Based Scheme for Improving Production Effectiveness Presented With A Case Study, 25 (1) (2019) 144-161.

[13] J. D. Morales Méndez, R. S. Rodriguez, Total Productive Maintenance (TPM) as A Tool For Improving Productivity: A Case Study of Application in The Bottleneck of An Auto-Parts Machining Line, The International Journal of Advanced Manufacturing Technology, 92 (2017) 1013–1026.

[14] Misha Matharu, Neena Sinha, Lean Implementation in Indian Manufacturing MSMEs: A SAP-LAP Analysis, Management and Production Engineering Review, 10 (1) (2019).

[15] V. Yadav, R. Jain, M. L. Mittal, A. Panwar, A. Lyons, The Impact of Lean Practices on The Operational Performance Of SMEs in India, Industrial Management Data Systems, 119 (2) (2019) 317-330.

[16] B. Dave, S. Kubler, K. Främling, L. Koskela, Opportunities for Enhanced Lean Construction Management Using Internet of Things Standards, Automation in Construction, 61 (2016) 86–97.

[17] G. Ante, F. Facchini, G. Mossa, S. Digiesi, Developing A Key Performance Indicators Tree For Lean And Smart Production Systems, IFAC-PapersOnLine, 51 (11) (2018) 13–18.

[18] K. Das, Integrating Lean Systems in The Design of A Sustainable Supply Chain Model, International Journal Of Production Economics, 198(1) (2018) 177–190.

[19] T. Kruse, A. Veltri, and A. Branscum, Integrating Safety, Health and Environmental Management Systems: A Conceptual Framework for Achieving Lean Enterprise Outcomes, Journal of Safety Research, 71(11) (2019) 259–271.

[20] T. Passath and K. Mertens, Decision Making in Lean Smart Maintenance: Criticality Analysis as a Support Tool, IFAC-PapersOnLine, 52 (10) (2019) 364–369.

[21] K. Antosz, L. Pasko, and A. Gola, The Use of Intelligent Systems to Support the Decision-Making Process in Lean Maintenance Management, IFAC-PapersOnLine, 52 (10) (2019) 148–153.

[22] Antony Pearce, Dirk Pons, Thomas Neitzert, Implementing lean—Outcomes from SME case studies, Operations Research Perspectives, 5 (2018) 94-104.

[23] Vinodh R., Ben Ruben, P. Asokan, Life Cycle Assessment Integrated Value Stream Mapping Framework To Ensure Sustainable Manufacturing: A Case Study, Clean Techn Environ Policy, 2015

[24] Alkhoraif, Abdullah, Lean Implementation in Small And Medium Enterprises: Literature Review. Operations Research Perspectives, (2018)

[25] Mohammed Al Manei, Konstantinos Salonitis, Yuchun Xu, Lean Implementation Frameworks: The Challenges for SMEs, Procedia CIRP, 63 (2017) 750-755.

[26] S. P. Leo Kumar, Knowledge-Based Expert System in Manufacturing Planning: State-of-The-Art Review, International Journal of Production Research, 57 (1) (2018) 4766–4790.

[27] Sunil Kumar, Ashwani Kumar Dhingra, Bhim Singh, Kaizen Selection for Continuous Improvement through VSM-Fuzzy-TOPSIS in Small-Scale Enterprises: An Indian Case Study. Advances in Fuzzy Systems, (2018) 1–10.

[28] L. Andreadis, J.A. Garza-Reyes, V. Kumar, Towards A Conceptual Framework for Value Stream Mapping (VSM) Implementation: An Investigation Of Managerial Factors, International Journal of Production Research, Taylor and Francis (2017).

[29] D. Romero, P. Gaiardelli, D. Powell, T. Wuest, and M. Thürer, Rethinking Jidoka Systems Under Automation & Learning Perspectives in The Digital Lean Manufacturing World, IFAC-PapersOnLine, 52 (13) (2019) 899–903.

[30] P. Perico, E. Arica, D. J. Powell, and P. Gaiardelli, MES as An Enabler of Lean Manufacturing, IFAC-PapersOnLine, 52 (13) (2019) 48–53.

[31] S. Jing, P. Luo, Z. Niu, J. Yan, and Z. P. Ho, The Application of Term Mining Techniques and Fuzzy Proximity For Driving Force Study in Lean Management, Computers and Industrial Engineering, 148 (2020).

[32] S. S. Kamble, A. Gunasekaran, A. Ghadge, and R. Raut, A Performance Measurement System for Industry 4.0 Enabled Smart Manufacturing System in SMMEs- A Review And Empirical Investigation, International Journal of Production Economics, 229 (7) (2020).

[33] D. T. Weldeslasie and M. Ahmed, The Application of Expert Systems in Manufacturing Sector, International Journal of Innovative Technology and Exploring Engineering, 9 (1) (2019) 4744–4749.

[34] R. Secchi and A. Camuffo, Lean Implementation Failures: The Role of Organizational Ambidexterity, International Journal of Production Economics, 210 (1) (2019) 145–154.

[35] P. Wang, P. Wu, H. L. Chi, and X. Li, Adopting Lean Thinking in Virtual Reality-Based Personalized Operation Training Using Value Stream Mapping, Automation in Construction, 119 (3) (2020).

[36] B. Rajesh Menon, P.R. Shalij, P. Sajeesh, G. Tom, Pramod V.R., Cost Value-Stream Mapping As A Lean Assessment Tool in A Surgical Glove Manufacturing Company, South African Journal of Industrial Engineering, 32 (1) (2021).

Navigating Service Quality: A Comprehensive Review of SERVQUAL Applications Across Diverse Industries

Harisankar T[1] and Dr. Pramod V R [2]

[1] Department of Mechanical Engineering, NSS College of Engineering, Palakkad, Kerala, India
[2] Professor, Department of Mechanical Engineering, NSS College of Engineering, Palakkad, Kerala, India

Abstract -

This literature survey explores the application and findings of the SERVQUAL model, a well-established framework for evaluating service quality across diverse industries. The study synthesizes insights from various works that employ SERVQUAL, highlighting its effectiveness in assessing service quality in contexts such as wireless communication, public transportation, education, banking, healthcare, and the hospitality industry. The survey examines dimensions such as reliability, responsiveness, empathy, assurance, and tangibility, offering a comprehensive overview of how these factors influence customer perceptions and satisfaction. The research findings underscore the model's versatility in multicultural environments and its ability to uncover critical areas for improvement in service delivery. From telecommunications in the UAE to public bus transport in Ghana, higher education programs in the United States, retail banking in Malaysia, rural services in India, and healthcare in the National Capital Region of India, the study showcases the wide-ranging applicability and impact of SERVQUAL.

Keywords -

SERVQUAL, Reliability, Responsiveness, Empathy, Assurance, Tangibility

1 Introduction

In the dynamic landscape of service industries, ensuring and enhancing service quality is paramount for organizations aiming to thrive in competitive markets. One proven and widely accepted model in this pursuit is SERVQUAL, introduced by Parasuraman et al. in 1985. This model delineates five key dimensions—Reliability, Responsiveness, Empathy, Assurance, and Tangibility—to evaluate the quality of services provided. Over the years, SERVQUAL has found applications in diverse sectors, providing a standardized framework for assessing and improving service quality.

This literature survey delves into recent works that employ the SERVQUAL model to evaluate service quality in various domains. The dimensions of reliability, responsiveness, empathy, assurance, and tangibility are examined in studies spanning wireless communication services in the UAE, public bus transport in Ghana, higher education programs in the United States, retail banking in Malaysia, rural services in India, healthcare in the National Capital Region of India, and the hospitality industry in Malaysia. Each study contributes unique insights into the application of SERVQUAL, shedding light on the specific challenges and opportunities within different service contexts.

The survey aims to provide a comprehensive overview of recent literature on SERVQUAL, synthesizing findings from different industries and geographies. By analyzing the successes and challenges faced in implementing SERVQUAL, this survey seeks to offer valuable insights for organizations striving to improve service quality in an ever-evolving global landscape.

2 Literature Survey

SERVQUAL is one among the well proven and widely accepted model in the current scenario to evaluate service quality. Current scenario witnesses the application of SERVQUAL in various fields of service. In order to have an assessment on the recent works in SERVQUAL, certain literatures are surveyed and results are shown here with. SERVQUAL (Parasuraman et al.1985) has five dimensions named as (i) Reliability, (ii) Responsiveness, (iii) Empathy, (iv) Assurance and (v) Tangibility.

Jadayil et al. (2020), explored SERVQUAL to evaluate the quality of wireless communication services in UAE. They use the five dimensions to measure the quality of the telecommunication services offered by the Etisalat company by instrumenting a questionnaire among four age groups from men and women. The main aim was the comparison between the expectations, perceptions and gaps of the five dimensions for men and women. The results showed that the tangibility has the highest concern from both men and women and needs a great improvement and the responsiveness is fair and need only less improvement. Men thinks that the provided service is reliable and assured whereas women have an opposite opinion. Women are very happy with the empathy of the provided service, but the men completely are not. The findings of this research revealed that the SERVQUAL can still be applicable to measure service quality in a multi-cultural environment, in other countries providing similar telecommunication services. Sam et al. (2017), describes using SERVQUAL methodology to analyse the core public bus transport users' service quality expectations and perceptions, and its influence on overall satisfaction with public

bus transport services in Kumasi, Ghana. A sampling scheme of clusterised random sampling approaches were employed for the study. After the survey a total of 103 questionnaires were found to be valid and useful for data analysis. Most of the customers are workers who use transportation for travelling to work places. The gap in service quality is being calculated by comparing the perception score with that of expectation score. The positive score indicates that customer's expectations have been met or exceeded and the negative score indicates the opposite of positive score. The results concludes that the service quality expectations of the participants far exceeded their perceptions resulting in vast differences (negative gap values) between the two causing the "The Quality Paradox Effect". According to the study, the transport operators are not providing accurate services as expected, the buses are not time-scheduled-based. A gap score of -3.68 were obtained indicating a gap of 50% between the current level of satisfaction and the expected level. The services were deemed unreliable and less empathic contrary to the expectation. Furthermore, the study revealed that central to the public bus transport service quality was the service reliability and responsiveness. The journal concluded that appropriate steps and measures should be taken to increase the service quality of the bus service provided in Kumasi. Gregory (2019), discusses service quality as a gap between a student's expectations and his/her perception of their experience. This study describes how measuring perceptions of service quality can provide higher education programs information that aids in the efficient allocation of limited resources. The study uses a survey approach by collecting data from 57 students in October of 2017. The survey included a single open-ended comment box to allow for qualitative feedback on the domains or survey. Demographic questions were not included in the survey, but the program reports that 63.8 percent of students identified as female and 36.2 percent male. The results of this work identified opportunities for program improvement in each of the five SERVQUAL areas, but the gaps were not equivalent. The largest gap exists in the dimensions of reliability (the ability to perform the promised service dependably and accurately) and tangibles, with the smallest in the dimensions of empathy and responsiveness. Assurance (represents the interpersonal interactions) had the third largest gap for this program. The SERVQUAL model provides a quantitative framework to remove any ego investment from prior initiatives and identify areas ripe for growth. The current study illustrates how SERVQUAL can provide concrete information about a program to inform decisions and assess change efforts with a smaller commitment of resources than larger self-study models. Hamzah et al. (2017) examined the dimensions of service quality (SERVQUAL) from the perspective of the customers and its relationships with perceived overall SERVQUAL in retail banking and also investigate the relationships between perceived overall SERVQUAL and customer trust, customer satisfaction, and bank reputation. The research identified the three traditional dimensions of SERVQUAL (i.e., tangibles, empathy, reliability) and security, and internet banking as extra dimensions that influence the overall perceived SERVQUAL, and how these overall perceptions will eventually influence customer trust, customer satisfaction, and bank reputation is valid and reliable in retail banking industry. A survey questionnaire was constructed, and data were collected from 375 regular customers of local banks. The convenience sampling method was employed to collect data from existing customers of local banks operating in the Klang Valley area of Malaysia. Structural equation modelling was applied to analyse the data. The results of the study indicate four key dimensions of SERVQUAL – tangibles, empathy, reliability and security, and internet banking – all of which are significantly and positively related to customer's perceived overall SERVQUAL. The results concluded that local banks should improve SERVQUAL, if they want to build and enhance customer trust, satisfaction and reputation. It also concludes that customer experience on the overall SERVQUAL affects the customer trust towards a bank, customer satisfaction, and bank reputation. Hirmukhe (2013) explored to measure the quality of services provided in a rural Tehsil office of Maharashtra using the SERVQUAL instrument. A questionnaire with 24 questions was devised on a Likert scale 1 to 7 and was used to analyse the 'gap' in the five dimensions of service quality. Genuine customers were selected at random; help was provided to those who were illiterate. The questionnaire was filled by 26 customers, out of which 24 were valid. The result generated from the study revealed that reliability had the greatest gap score (-1.438) followed by responsiveness (-1.074) and tangibles (-1.072). From the results generated the service experiences are generating unsatisfactory perceptions among the customers and the organisation should seriously consider about quality issues and measures to tackle them. Lai and Hutchinson (2007) conducted an empirical assessment and application of SERVQUAL in mainland China's mobile communication Industry. The purpose of the study was to check the reliability and validity of SERVQUAL instrument and apply them in the China's mobile communication setting to understand the service quality. Slight modification from Parasuraman's SERVQUAL instrument was done to tailor it to China's mobile communication setting. For checking the reliability and validity Cronbach coefficients was used, Exploratory and Confirmatory factor analysis were also done. After the analysis a 3-Tier structure was created which included Empathy, Assurance, Responsiveness in

Tier 1, Reliability, Convenience in Tier 2, Tangible in Tier 3. An additional Dimension of "Convenience" was added along with Parasuraman's five dimensions of SERVQUAL for customers to adequately judge the service quality of China's mobile communication companies. The dimension of "convenience" measures how easy it is to access the business office, how easy it is to change service options (like call-waiting, call-forwarding), and how convenient it is to pay bills or reach customer service representatives. By analysing competitive gap scores between service quality perceptions of the focal company and its primary competitor, they were able to evaluate its strengths and weaknesses on service quality. Mehrotra and Bhartiya (2019) studied about the service quality at multi-speciality hospitals located in National Capital Region (NCR) of India. Prominent cities of NCR include Delhi, Faridabad, Ghaziabad, Gurugram, and Noida. The objective of the study was to understand the key factors that patient find critical in providing quality health services using SERVQUAL. The two types of quality possessed by a hospital are: technical (the extent to which, diagnoses and procedures are accurate) and functional quality (the form in which the services are provided). SERVQUAL Model determines gap between perception and expectation of the consumers, A five-dimensional tool RATER (Reliability, Assurance, Tangibility, Empathy and Responsiveness), was proposed using exploratory factor analysis from a questionnaire of 97 items. The first part collected demographic details of the patient, whereas the second part included questions related to different quality service dimensions in a hospital. The variables that load high on factor 1 relate to 'EMPATHY' which means the "Ability of Healthcare Provider to understand the feelings and need of the patient". Factor 2 has been labelled 'RELIABILITY', concerned with 'Reliability of Healthcare Services' extended by the hospitals. Factor 3 are related to 'RESPONSIVENESS' that indicate behaviour skills of the hospital staff'. Factor 4, labelled as 'ASSURANCE' loads the variables that can 'enhance trust and confidence' of patient in obtaining services from the hospital. Factor 5 labelled as 'TANGIBILITY' relate to 'Physical and Visible Aspects' affecting the decisions made by patients while selecting the hospitals. 'TANGIBILITY' gets a low weightage in total share of the variance. The study was further extended to observe a change in decision based on the categorization of patients, namely, gender, in-door/outdoor, age, and frequency of visit. The analysis found a significant variation in patient's opinion depending on their age and the number of times they require visiting any hospital. Shafiq et al. (2018), uses SERVQUAL to measure Generation Y's (Gen Y) perceived service quality and its effects on their satisfaction toward the Malaysian hotel industry. Generation Y (Gen Y) also known as "Travellers of the Future" are a generation of people born between 1980 and 2000. The five dimensions which include Tangibility, reliability, Responsiveness, Assurance and Empathy influenced Gen Y 's satisfaction toward Malaysian Hotel industry. This research was conducted in Malaysia and constituted distribution of questionnaire within selected regions of its Klang Valley. A questionnaire of 400 were distributed among the Gen Y hotel guests and their review was analysed with reliability test, Correlation test and Multiple linear regression. It was found that all SERVQUAL dimensions strongly correlate to customer satisfaction, while four of these dimensions (tangibility, reliability, assurance and empathy) have significant influence on customer satisfaction It can be concluded that this study provided sufficient evidence to use SERVQUAL to understand Gen Y's satisfaction toward Malaysian hotel industry. The result implies that the higher level of service quality can lead to greater satisfaction which ultimately leads to higher success in Malaysian hotel industry as it will increase the chances to generate and maximize sales revenue. Singh and Singhi (2018), analyses the impact of SERVQUAL on overall satisfaction and brand loyalty in the healthcare industry. The study has been initiated by conducting a survey of various hospitals of Delhi NCR. SERVQUAL helps in identifying the difference between the customer's preferences and what they experience and specifying the gaps in the areas which need improvement. The gap in service quality is being calculated by comparing the perception score with that of expectation score. The positive score indicates that customer's expectations have been met or exceeded and the negative score indicates the opposite of positive score. The objective of the research is to find out the effect of five dimensions of SERVQUAL model of service quality, i.e., reliability, empathy, responsiveness, tangibility and assurance. A sample of 328 patients has been taken. A set of 24 questions has been framed evaluating each dimension of SERVQUAL, overall satisfaction and brand loyalty on the Likert scale ranging from 1 to 7. Data is analysed using the SPSS software and AMOS software. The results shows that SERVQUAL has a positive effect on overall satisfaction and overall satisfaction has a positive effect on brand loyalty thus both the hypotheses have been achieved successfully. Chuenyindee et al. (2022), used the SERVQUAL dimensions to measure the service quality of Public Utility Vehicles (PUV) in the Philippines during the Covid-19 pandemic. The Study was targeted at all residents in the Philippines who have experienced riding PUV in the pandemic times. The questionnaire was distributed online through google forms. A total of 564 participants answered the online questionnaire which consist of 58 questions exploring all the SERVQUAL dimensions. Structural equation modelling (SEM) was applied to derive the casual relationships between SERVQUAL

dimensions, Covid-19 safety protocol, and customer satisfaction. The dimensions that were used in the study were tangibility, responsiveness, reliability, assurance, empathy, COVID-19 protocols, perceived service quality, and perceived customer satisfaction. The three significant dimensions are COVID-19 protocols, tangibility, and assurance. Among the three significant dimensions, COVID-19 protocols showed to be the most significant. The positive reaction of commuters from the COVID-19 protocols indicates the PUV operator's compliance with the government. the remaining three dimensions: reliability, responsiveness, and empathy, proved insignificant towards PUV service quality and customer satisfaction.

3 Conclusion

Understanding of the specific dimensionalities of SERVQUAL is critical to all service industries, including banks, hotels, hospitals etc, as they need to deliver high quality of services in order to fulfil customers' demands and to survive in a competitive business environment. SERVQUAL refers to the customer's overall evaluation of service firms' attributes by comparing their expectations and actual performance. The five dimensions of SERVQUAL that rely on customers to form their judgement on perceived SERVQUAL are: assurance – employees' knowledge and courtesy and their ability to convey trust and confidence; empathy – caring and individual attention given to customers; reliability – ability to perform the promised service dependably and accurately; responsiveness – willingness to help customers and provide prompt service; and tangibles – appearance of physical facilities, equipment, personnel, and written materials. By conducting this study many advantages and limitations of SERVQUAL model were understood. The study not only provides insights on SERVQUAL, but also provide future proceedings for checking the Quality of the Service.

References

[1] Abu Jadayil, W., Shakoor, M., Bashir, A., Selmi, H. and Qureshi, M.R.N.N. (2020), "Using SERVIQUAL to investigate the quality of provided wireless communication services in UAE", International Journal of Quality and Service Sciences, Vol. 12 No. 1, pp. 109-132.

[2] Chuenyindee T., Ong A.K.S., Ramos J.P., Prasetyo Y.T., Nadlifatin R., Kurata Y.B., Sittiwatethanasiri T., (2022), "Public utility vehicle service quality and customer satisfaction in the Philippines during the COVID-19 pandemic", Utilities Policy, Vol. 75, 101336, ISSN 0957-1787.

[3] Gregory, J.L. (2019), "Applying SERVQUAL: Using service quality perceptions to Improve student satisfaction and program image", Journal of Applied Research in Higher Education, Vol. 11 No. 4, pp. 788-799.

[4] Hamzah, Z.L., Lee, S.P. and Moghavvemi, S. (2017), "Elucidating perceived overall service quality in retail banking", International Journal of Bank Marketing, Vol. 35 No. 5, pp. 781-804.

[5] Hirmukhe, J. (2013). "Measuring the customer's perception of service quality using SERVQUAL in public services", International Journal of Services Technology and Management, Vol. 19 No. 4/5/6, pp.267–277.

[6] Lai, F., Hutchinson, J., Li, D. and Bai, C. (2007), "An empirical assessment and application of SERVQUAL in mainland China's mobile communications industry", International Journal of Quality Reliability Management, Vol. 24 ,No. 3, pp. 244-262.

[7] Mehrotra, D., Bhartiya, S., (2020) "Results of mapping patients expectation using SERVQUAL", Journal of Healthcare Quality Research, Vol. 35 No. 6, pp. 381- 390.

[8] Parasuraman, A., Zeithaml, V.A. and Berry, L.L. (1985) "SERVQUAL, a multiple item scale for measuring perceptions of service quality", Journal of Retailing, Vol. 64, No. 1, pp.12–40.

[9] Sam E.F., Hamidu O., Daniels S. (2018), "SERVQUAL analysis of public bus transport services in Kumasi metropolis, Ghana: Core user perspectives", Case Studies on Transport Policy, Vol. 6 No. 1, pp. 25-31.

[10] Shafiq, A., Mostafiz, M.I. and Taniguchi, M. (2019), "Using SERVQUAL to determine Generation Y's satisfaction towards hoteling industry in Malaysia", Journal of Tourism Futures, Vol. 5 No. 1, pp. 62-74.

[11] Singh, B. and Singhi, R. (2018) "SERVQUAL impact on overall satisfaction and brand loyalty: an empirical study in Delhi-NCR hospitals", International Journal of Healthcare Technology and Management, Vol. 17, No. 1, pp.49–60.

Quality Cost Analysis: A Literature Review

Viswas K[1] **and Dr. Pramod V R** [2]

[1] Department of Mechanical Engineering, NSS College of Engineering, Palakkad, Kerala, India
[2] Professor, Department of Mechanical Engineering, NSS College of Engineering, Palakkad, Kerala, India

Abstract -

Quality cost is a multifaceted aspect crucial for organizational success, encompassing expenses incurred due to deficiencies in products, processes, or services. This abstract explores the intricate relationship between quality and cost, aiming to unveil the strategic implications for businesses.The pursuit of higher quality often leads to increased costs in production, inspection, and rectification. However, this investment can mitigate expenses related to rework, returns, and customer dissatisfaction, ultimately enhancing brand reputation and customer loyalty.his paper examines various models and methodologies employed by organizations to strike an optimal balance between quality and cost. It delves into the nuances of prevention, appraisal, internal failure, and external failure costs, dissecting their impacts on overall operational efficiency and bottom-line performance.Furthermore, the abstract scrutinizes the influence of quality management systems, technological advancements, and evolving consumer demands on the dynamics of quality cost. It highlights the shift from reactive approaches to proactive quality management strategies that integrate cost-effective measures without compromising quality standards.The findings of this study emphasize the necessity for businesses to adopt a comprehensive approach, integrating quality initiatives within their strategic frameworks. By embracing a culture of quality and leveraging innovative tools and methodologies, organizations can effectively manage quality costs, optimizing resources while delivering superior products and services to consumers.In conclusion, this abstract proposes a holistic perspective on quality cost, advocating for a balanced strategy that considers both short-term expenditure and long-term benefits. It underscores the pivotal role of quality in driving competitive advantage and sustainable growth in today's dynamic business landscape.

Keywords -

Quality Costing Cost of Quality , Quality Management , Operational Efficiency

1 Introduction

In the realm of business operations, the interplay between quality and cost stands as a pivotal determinant of organizational success. The concept of quality cost encapsulates the intricate relationship between the expenses incurred in ensuring superior product or service quality and the ramifications of shortcomings in meeting those standards. Understanding and strategically managing this relationship is fundamental for businesses seeking sustainable growth and competitive advantage in today's dynamic markets.Quality, in its essence, is not merely an abstract attribute but a tangible asset that directly impacts the bottom line. Achieving and maintaining high-quality standards involves a series of investments across various phases of production, including initial development, meticulous inspections, and continuous improvement measures. These investments, often construed as costs, form the foundation of a company's commitment to delivering excellence. Conversely, overlooking quality can lead to a cascade of expenses. Deficiencies in products or services not only incur direct costs related to rectification, rework, or warranty claims but also inflict indirect expenses through damaged reputation, decreased customer satisfaction, and potential loss of market share. Such expenditures, classified under the umbrella of quality costs, possess the potential to significantly erode profitability and undermine an organization's long-term viability.The landscape of quality cost analysis encompasses four primary categories: prevention, appraisal, internal failure, and external failure costs. Each category represents a facet of the quality management process, from preemptive measures to detect and prevent defects (prevention costs) to the expenses incurred due to defects identified before delivery (appraisal costs) and those found after delivery (internal and external failure costs).

2 Literature Review

Biadacz (2020) examined the research problem that represents an attempt to approximate the importance of quality costing in managing a modern enterprise using the selected enterprises from small and medium-sized enterprises (SMEs) in Poland. It conducted in SMEs in the form of questionnaire interview and analyse quality cost management (QCM). Quality is a difficult concept to define, and it results from its ambiguity implementation of quality costing should be considered by both manufacturing and service companies wishing to increase efficiency

and effectiveness of their operations, quality costing can be used to complement traditional cost accounting system; companies planning to implement cost accounting should be aware that QCM systems do not have to be too comprehensive (especially in the initial phase of their use). The creation of QCM, however, allows management to optimize quality control planning in terms of quality, reveals areas with high cost, and allows for more accurate observation and more efficient analysis of non-compliances occurring and removal of sources of costs.

Brennanh et al. (1990) quality is now more widely acknowledged as a component of competitive strategy. There are two main dimensions to the idea of "fitness for use," which is included in many definitions of quality: quality of design and quality of conformance. The latter aspect involving "conformance to requirements and specifications" is the one that this article focuses on. The most effective way to get and keep upper management's attention on quality is to frame quality objectives in terms of "costs.". Costs related to quality are incurred as a result of production line issues. There are various causes for these issues. Several support functions, including Customer Quality Assurance, Line Quality Assurance, Product Engineering, Process Engineering, Purchasing or Production Control, and Customer Services, are used to help them find a solution. Quality expenses must be kept under control. These expenses must be determined and estimated in order to do this. Analysing quality costs can show areas where money can be saved while quality is improved

Chatzipetrou and Moschidis (2017) is about the study of Quality costing and evolution of variables that have been used for this. It points out and analytically present specific demographic characteristics. The Total Quality Cost Indices (QCIs) are the typical ratios of total quality costs as a percentage of sales revenue, value added, direct material/labour costs etc. Longitudinal speciation of quality costs between 1985 and 2016 identification of the most prominent cost categories and cost components, in relation to the date of publication of each study. Quality costs is mainly to 'attack' failure costs and to invest in the right prevention activities.

Cheah and Shah (2010) is used to evaluate on the implementation of a quality cost program in a continuous-process manufacturing company. It was sum of total expenses t on the implementation of a quality cost program in a continuous-process manufacturing company, another component is quality. The cost of quality refers to the total expenditure that an organization incurs for its overall quality. It comprises two basic components: (1) the cost of conformance; and (2) the cost of non-conformance. Further studies are therefore needed to find out how the case company makes use of the quality cost information to formulate a survival strategy at this time of economic downturn, and a growth strategy for its future expansion.

Chopra and Grag (2011) it mainly focused different quality cost categories that helps to take proper decisions in allocating resources for reducing quality costs. Quality is a critical success factor for achieving competitiveness, Quality costing is an increasingly important issue in the debate over quality. Good quality leads to increase in production and reduced quality costs and eventually to increased sales, market penetration and hence higher profits. Quality costs are measure of cost related with achievement or non-achievement of product or service quality, it represents the difference between the actual cost of a product or service. it mainly discusses about various quality costs that are Prevention costs, Appraisal costs, Internal failure cost, External failure cost. It is also observed that there is a strong positive correlation between prevention costs and appraisal costs as well as between internal failure costs and external failure costs quality cost will help them to allocate funds and justify investments to reduce the total quality costs and tell them how a cost element will respond if we increase or decrease another quality cost element.

Chopra and Singh (2015) examined about how companies unleashing a decisive approach to manage quality costs through behavioural investigation. In service sectors also, behavioural investigation of quality costs through the presented quantitative approach will surely bring paradigm shift and would cause rapid economic growth. This work will indeed help the entrepreneur to fine tune their financial policies and budgets for generating more economic quality control programmes in future. In service sectors also, behavioural investigation of quality costs through the presented quantitative approach will surely bring paradigm shift and would cause rapid economic growth

Lorente et al. (1998) examined that both the price of achieving the desired level of quality and the costs incurred as a result of failing to do so are referred to as quality costs. If quality is defined as the fulfilment of customer requirements, then the product's design and the way that design is implemented will determine the required level of quality. The investigator could be led astray if internal and external quality requirements weren't taken into consideration. Therefore, the next stage of model development would involve the creation of scales to assess the intensity of specific variables, including prevention effort, TQC intensity, internal and external quality requirements, and most importantly, time factor.

Omachonu et al. (2004) examines the components of quality cost (internal failure, external failure, appraisal cost, and prevention cost) in the context of two important manufacturing inputs, materials and machines. The goal of this study is to examine the elements that affect quality in a manufacturing setting. The research has three main conclusions. Four categories—prevention, appraisal, in-

ternal failure, and external failure—are used to classify the cost of quality. The total cost of prevention is the sum of all the resources used to stop errors from happening across all business functions. The quality cost data can be used to be proactive and to pinpoint the root of issues. It offers a method for identifying the top priorities for improvement

Walsh and Antony (2007) discussed the usability and potential of incorporating quality costs into an electronic adverse incident recording system within a healthcare sector. finds that quality costs are a valid and useful approach for measuring the impact of individual adverse incidents or trends in order to support managers and clinicians to develop appropriate action plans to reduce levels of patient harm and thereby improve patient safety greets of quality costs. The quality cost associated with individual adverse incidents combined in the rising health care quality cost needs to be further understood and prioritised. The key to future development of electronic adverse incidents recording and reporting systems is in relation to how organisations in healthcare will be able to demonstrate clear outcomes and improve patient safety by demonstrating an improvement in their delivery of quality care by using a combination of quality costing and electronic adverse incident recording and reporting processes.

Wang and Yin (2021) examined the variation management consists of process-oriented tolerance and maintenance planning, and the optimal variation management strategy for each KCC (Key control characteristics) is assigned based on its impact to the manufacturing system. A new variation management method is proposed for KCCs in MMPs (Multi machining process) with the consideration of quality-cost equilibrium. In response to the above limitations, it presents a new variation management framework for KCCs in MMPs considering quality-cost equilibrium simultaneous optimization with machining parameters is an interesting issue for variation management. Secondly, preventive maintenance can update the maintenance schedule based on the online measurement of process conditions, reflecting the dynamics of the maintenance. Therefore, the choice of maintenance methodology based on the consideration of measurement cost and feasibility is also a subject worthy of further study.

3 conclusion

The behavior of quality costs tends to vary across different industries due to their unique operational structures and market demands. These costs are typically classified into four categories: prevention costs, appraisal costs, internal failure costs, and external failure costs. Each category relates to both positive and negative factors impacting the overall quality costs within an organization.

Statistical generalizations often rely on a limited scope, such as considering cost data from just three consecutive years. However, practitioners advocate for a broader view, suggesting the utilization of five to ten years of data for more accurate and reliable predictions. This extended timeframe allows for a more comprehensive understanding of quality cost fluctuations and trends, enabling better-informed decisions.

Recognizing these limitations opens doors for innovative approaches, particularly in implementing methodologies like ”quality cost optimization” within large and intricate industries. By addressing these limitations, there is an opportunity to refine strategies and tailor them to the complex dynamics of such industries.

The significance of understanding quality costs lies prominently in their impact on the decision-making process. They serve as a critical tool in providing relevant reports on quality to top management. These reports enable informed decisions, facilitating improvements in processes, products, and services to meet or exceed established quality standards. Ultimately, a thorough comprehension of quality costs aids in steering organizations towards enhanced efficiency and excellence.

References

[1] Biadacz, R., (2020). “Quality cost management in the SMEs of Poland”. The TQM Journal. Vol. 33, No.7, pp. 1-38

[2] Brennanh .L, Cullinanec. O, Connor. D, PunchJ. Sheil, (1990),”Quality Costs Determination on a Production Line”, International Journal of Quality and Reliability Management, Vol. 7 Iss.3

[3] Chatzipetrou.E, Odysseas Moschidis, ”A multidimensional longitudinal meta-analysis of Quality Costing Research”, International Journal of Quality and Reliability Management, Vol. 67 Iss 1 pp. 171-191

[4] Cheah, S. J., Shah, A. (2011). “Tracking hidden quality costs in a manufacturing company: an action research”, International Journal of Quality and Reliability Management. Vol. 28 No. 4, 2011 pp. 405-425

[5] Chopra. A Dixit Garg, (2011),”Behavior patterns of quality cost categories”, The TQM Journal, Vol. 23 Iss 5 pp. 510 – 515

[6] Chopra. A Bikram Jit Singh, (2015),” Unleashing a decisive approach to manage quality costs through behavioural investigation ”, Business Process Management Journal, Vol. 21 Iss 6 pp. 1206 - 1223

[7] Lorene. A, Alejandrino Gallego Rodriguez, Louise Rawlins, (1998) ”The cumulative effect of preven-

tion", International Journal of Operations and Production Management, Vol. 18 Issue: 8, pp.727-739

[8] Omachonu. V, Sakesun Suthummanon Norman G. Einspruch, (2004),"The relationship between quality and quality cost for a manufacturing company", International Journal of Quality Reliability Management, Vol. 21, pp. 277 – 290

[9] Walsh, K., Antony, J. (2007). "Quality costs and electronic adverse incident recording and reporting system: Is there a missing link? " , International Journal of Health Care Quality Assurance. Vol. 20 No. 4, pp. 307-319

[10] Wang, K., Yin, Y., Du, S., Xi, L. (2021). "Variation management of key control characteristics in multistage machining processes considering quality-cost equilibrium", Journal of Manufacturing Systems, Vol. 59, pp. 441-452

[11] Biadacz, R., (2020). "Quality cost management in the SMEs of Poland". The TQM Journal. Vol. 33, No.7, pp. 1-38

[12] Brennanh .L, Cullinanec. O, Connor. D, PunchJ. Sheil, (1990),"Quality Costs Determination on a Production Line", International Journal of Quality and Reliability Management, Vol. 7 Iss.3

[13] Chatzipetrou.E, Odysseas Moschidis, "A multidimensional longitudinal meta-analysis of Quality Costing Research", International Journal of Quality and Reliability Management, Vol. 67 Iss 1 pp. 171-191

[14] Cheah, S. J., Shah, A. (2011). "Tracking hidden quality costs in a manufacturing company: an action research", International Journal of Quality and Reliability Management. Vol. 28 No. 4, 2011 pp. 405-425

[15] Chopra. A Dixit Garg, (2011),"Behavior patterns of quality cost categories", The TQM Journal, Vol. 23 Iss 5 pp. 510 – 515

[16] Chopra. A Bikram Jit Singh, (2015)," Unleashing a decisive approach to manage quality costs through behavioural investigation ", Business Process Management Journal, Vol. 21 Iss 6 pp. 1206 - 1223

[17] Lorene. A, Alejandrino Gallego Rodriguez, Louise Rawlins, (1998) "The cumulative effect of prevention", International Journal of Operations Production Management, Vol. 18 Issue: 8, pp.727-739

[18] Omachonu. V, Sakesun Suthummanon Norman G. Einspruch, (2004),"The relationship between quality and quality cost for a manufacturing company", International Journal of Quality and Reliability Management, Vol. 21, pp. 277 – 290

[19] Walsh, K., Antony, J. (2007). "Quality costs and electronic adverse incident recording and reporting system: Is there a missing link? " , International Journal of Health Care Quality Assurance. Vol. 20 No. 4, pp. 307-319

[20] Wang, K., Yin, Y., Du, S., Xi, L. (2021). "Variation management of key control characteristics in multistage machining processes considering quality-cost equilibrium", Journal of Manufacturing Systems, Vol. 59, pp. 441-452

5s Principles: A Review of the Literatures

Yedhu Gopan[1] **and Dr. Pramod V R** [2]

[1] Department of Mechanical Engineering, NSS College of Engineering, Palakkad, Kerala, India
[2] Professor, Department of Mechanical Engineering, NSS College of Engineering, Palakkad, Kerala, India

Abstract -

This paper aims to provide an extensive overview of the literature on 5S and identify any potential gaps from the perspectives of practitioners and scholars. The paper provides an overview of the application of 5S and emphasizes the successes that have been attained through the deployment of 5S initiatives for long-term organizational performance.

Keywords -

Quality, 5S, sort, set in order, shine, standardize, sustain

1 Introduction

The five pillars of a continuous improvement program are called 5S, or, in Japanese, Sort, Set in Order, Shine, Standardize, and Sustain. Seiri (i), Seiton (ii), Seiso (iv), Seiketsu (v), and Shitsuke (vi). A 5S program aims to reduce wastage of time and materials by arranging and labeling objects in close proximity to workers and operations. There is a place for everything and everything in its place according to the 5S principle, which also helps to reduce wastage of inventory, time, and space. The application of 5S leads to increased productivity and improved product quality, which in turn reduces expenses and boosts efficiency.

2 Initial challenges faced when initiating 5s

Avishkar et al. (2021) look into organizations that want to produce well while making constant improvements. A well-designed tool, 5S creates a methodical workplace with visible controls and organization. Each member of the organization's dedication, involvement, and contributions, as well as unwavering support from the higher authority of the organisation, are the two most crucial components of a successful 5S implementation. Lack of 5S awareness and poor communication between upper management and workers and employees contributed to poor management. The 5S initiative initially faced many challenges because the workers and employees were resistant to the 5S activity. Many of these challenges were overcome with the aid of inspiration for the organization's staff in the form of awards and recognition. When 5S was first implemented, there were a lot of challenges since workers and employees did not adapt to the 5S activities. Many of these challenges were solved with the use of incentives such as awards and recognition for the members of the organization. Research conducted on the manufacturing and packaging industries found that integrating 5S significantly increases worker efficiency. As a result, after applying 5S, process effectiveness has been noticeably increased by 25 Percent. Thus, it can be concluded that proper workplace upkeep, item organisation based on frequency of use, and sorting of things all increase productivity.

3 Problems occurred before implementation of 5s principles

Gupta et al. (2022) interprets the following issues that existed before the 5S Principle was implemented in the company (automotive industry); (i) misusing storage space for bins, completed goods, and raw materials. (ii) Time lost looking for raw materials because there isn't a permanent place to store them. (iii) Low productivity as a result of inefficient workplace management, which wastes time looking for tools and supplies. (iv) The presence of undesirable materials at work, which lowers employee morale while they are working. There are various benefits that follow the application of the 5S principles in the automotive industry. (i) The 5S concept is very straightforward and simple enough for everyone to understand, requiring only a high level of commitment and familiarity with conventional discipline. It is possible to use this technique at all levels. (ii) 5S will promote discipline, teamwork, and a greater sense of responsibility and compassion for the business. (iii) 5S will guarantee the delivery system toward a world-class standard and produce hygienic, productive work environments. (iv) The cornerstone for the effective adoption of 5S practices is the management's ongoing commitment and involvement, which is provided by all citizens. (v) Maintaining exceptional service delivery performance requires constant application of 5S. All things considered, the 5S system is a good place to start for any improvement initiatives hoping to reduce waste in the manufacturing process and, in the end, boost a business's production by raising the quality of goods and services while cutting costs.

4 5s concept to evaluate the performance of a Manufacturing company

Ratanakvisal et al. (2021) inspects the 5S concept to evaluate the performance of a Malaysian manufacturing company. Globalization has altered the requirements for the effective application of the 5S concept, including product designs, life cycles, production modifications, and technological advancements in manufacturing capacities. As a result, manufacturing industries have had to adapt by putting proactive measures in place to stay competitive. Nonetheless, an organization's performance is important because it can show how well or poorly a business is running. Empirical findings showed that 5S had a major impact on an organization's productivity. Every variable in the 5S concept has a significant relationship with productivity, according to the analysis. By properly applying the 5S concept and identifying errors and defects, the company's productivity can be increased by using the research as a guide.

5 Impact of 5s implementation on occupational safety in an automotive industry

Fernandez et al. (2019) analyzed how implementing 5S has affected workplace safety in the automotive industry. Lean is emerging as a preeminent body of work that epitomizes both the value of concentrating on value creation and ongoing improvement. Lean Manufacturing was put into practice, which improved quality while cutting costs and getting rid of non-value-added tasks. The ISO 45001: 2018 - Occupational Health and Safety Management Systems standard was released in March 2018 by the International Organization for Standardization (ISO). This new standard, which is meant to replace OHSAS 18001, is based on the same high-level framework as environmental (ISO 14001) and safety systems (ISO 9001). The document offers a set of ready-to-use, straightforward procedures and guidelines for enhancing workplace safety in international supply chains. This standard is applicable everywhere, including factories, partners, and production facilities. This is anticipated to lower the amount of illnesses and injuries related to the workplace. This paper examines how the application of lean tools, specifically 5S, could improve occupational safety conditions in a case study conducted in one of the biggest automakers' plants in Europe. The results demonstrated that the total risk could be reduced by up to 64 percent using the used risk assessment tool by applying 5S+1S, or 6S, on the designated location. Furthermore, the implementation of 2S (Seiton or Set in Order) was found to have the greatest influence on overall safety..

6 5s technique by implementation of lean manufacturing

Goswamy et al. (2019) examined in today's world, the 5S technique for continuous improvement of the manufacturing process through the application of lean manufacturing helps to meet and satisfy end users by enabling the production of products based on customer demand. This research paper's primary goal is to examine and analyze how applying 5S to an automotive ancillary unit can reduce waste and increase productivity. The low level of awareness regarding the 5S terminology in manufacturing units can be attributed to inadequate training and communication gaps between upper management and shop floor employees. The company EECL Limited is currently engaged in the production of automotive components and operates production facilities in India. It supplied parts to a significant Indian automaker, with a 50 million dollar turnover in 2017. The management of the company wishes to enhance the current system in order to increase productivity because it is not a smooth line. The industry as a whole is cleaner, safer, and has a better environment as a result of applying 5S, and product quality has increased.

7 Impact of 5s methodology

Sangode et al. (2018) examined the effects of the 5S methodology—which emphasizes sorting, organizing, shining, standardizing, and sustaining—in manufacturing companies. Using this methodology, the manufacturing system can become lean by removing waste that would otherwise arise from an untidy and unhealthy work environment. This essay aims to comprehend how several manufacturing companies in the Nagpur area of India have adopted the 5S methodology. For the study, a sample of ten manufacturing facilities was selected. The chi-square test was employed to substantiate the hypothesis that companies adopting 5S achieve operational efficiency. It was a conceptual model that put 62 engineers from a chosen organization's manufacturing department to the test. The results demonstrated that every hypothesis contributed significantly to the productivity prediction. The research study conducted on the ten manufacturing units demonstrated that the implementation of 5S has a notable effect on improving workplace efficiency. The manufacturing sector's automotive divisions had the highest efficiency level mean. Therefore, it can be said that keeping the workspace neat and orderly, properly sorting objects, and arranging all necessary items according to frequency of requirement all directly affect productivity.

8 Impact in an automotive company

Veres et al. (2017) investigated the effects of the 5S method in a car company that sets an example for developed nations to follow in the dynamically changing economic environment. The Toyota Production System, which includes the 5S method, is the most widely used management model in the automotive industry. Its goal is to maximize efficiency and productivity by promoting discipline and cleanliness in the workplace. The Austrian business Hirschman Automotive, which manufactures auto parts and has facilities in Morocco, Mexico, China, the Czech Republic, and Romania, is the subject of this case study. Its total revenue in 2016 was 300 million euros, with investments accounting for 12.5Randhawa et al. (2017) examined the manufacturing performance gains made by Indian manufacturing companies using strategic 5S methods. This paper's goal is to assess the qualitative and quantitative advantages that the strategic 5S implementation initiatives have brought to the Indian automotive parts industry. Based on the study's empirical findings, the manufacturing industry has seen significant improvements in quality, production, cost optimization, employee morale, and work culture when the 5S program is implemented effectively. The industry benefited from the comprehensive application of 5S principles in both tangible and intangible ways. The research shows that because of the many benefits that 5S provides, industries across the globe have been using it continuously, from Asia and Europe to the United States and the United Kingdom. Furthermore, case studies and literature have shown that all practitioners, industrial managers, personnel managers, and HR professionals view the 5S technique as a useful tool for bringing about overall organizational improvement, beginning with the foundation and establishment of various quality programs. Overall, the study unequivocally shows that the implementation of the 5S program has enabled manufacturing organizations to significantly improve plant performance in comparison to its prior state. Agrahari et al. (2015) examines 5S, a fundamental manufacturing system, in the context of the small-scale industry. The 5S methodology shows notable gains in cleanliness, productivity, and efficiency. The 5S methodology shows notable gains in cleanliness, productivity, and efficiency. In India's economy, the small-scale sector holds a prominent and unique position. It has become a very effective instrument in creating comparatively more jobs than agriculture. The demands of the world's markets are always shifting, and they call for affordable, high-quality products. Small-scale industries in India must be able to innovate, increase operational effectiveness, and boost productivity in order to survive and grow. A workspace that is well-maintained, spotless, efficient, and of superior quality is a key component of the 5S methodology. The study was carried out in the manufacturing company V.M. Auto Pvt. Ltd. During the study, it was executed that selection of process parameters/procedure in chosen production process, on each workplace. The objective of their research was to increase the storing place with 30 create and preserve standards and service procedures specific to the workshop, reduce unproductive time with 10Patel et al. (2014) conducted research on how to use the lean manufacturing 5S methodology to address the issues facing the Indian ceramics industry in order to improve process efficiency across the board and eliminate losses for the business. Through a case study, the paper aims to decrease process wastes, streamline workflow, uphold appropriate quality control, and enhance storage facilities, safety, security, and process cost savings in an organization. Components made of ceramics are manufactured in batches. Certain processes are completed on an individual basis, while others are completed on a lot basis. A flowchart explaining the ceramic insulator product manufacturing process is created using the operation data. There are two processes for producing. The use of the 5S principle and the visual management system (GAMBA) has improved space utilization, employee safety, reduced error scope, increased productivity, and improved inventory management. It has also increased machine efficiency, maintained and cleaned devices, improved machine efficiency, promptly informed about damages (or potential sources of damages), improved the work environment, and eliminated the company's causes of accidents.

9 CONCLUSION

Instead of being seen as a one-time project, the 5S strategy requires standardization and consistency in rules in order to guarantee long-term implementation plans that meet organizational objectives. Updating the organization's education and training programs is essential for a successful 5S implementation. This study can also serve as a guide for properly applying the 5S concept to identify errors and defects and increase productivity within the organization. It is advised that all businesses concentrate on appropriately separating the essential and superfluous products in the production line in order to increase productivity even further..

References

[1] Avishkar A. Ahire, Amit B. Chaudhari, Omkar S. Ahirrao, Vijay B. Sarode (2021). Increasing Productivity Through Implementation of 5S Methodology in A Manufacturing Industry: A Case Study International Journal of Scientific Research. Multidisciplinary Studies, Vol. 7, No. 7, pp 51-57.

[2] Agrahari, R.S., Dangle, P.A. Chandratre, K.V., (2015) Implementation Of 5s Methodology in The Small-Scale Industry: A Case Study", International Journal of Scientific Technology Research, Vol. 4, No.4, pp.180-187.

[3] Fernandes, J.P., Godina, R. Matias, J.C., (2018)." Evaluating the Impact of 5s Implementation on Occupational Safety in An Automotive Industrial Unit". In International Joint Conference on Industrial Engineering and Operations Management, Vol.281, No.11, pp-139-148.

[4] Goswami, D., Gupta, R.K. Choudhary, B, (2019)." An Experimental Examination of 5S 'technique For Continuous Improvement of The Manufacturing Process". International Journal for Innovative Technology

[5] Gupta, K., (2022)." A Review on Implementation Of 5s For Workplace Management——. Journal Of Applied Research on Industrial Engineering, Vol. 9, No 3, pp 323-330.

[6] Patel, V.C. Thakkar, H., (2014)," A Case Study: 5S Implementation in Ceramics Manufacturing Company". Bonfring International Journal of Industrial Engineering and Management Science, Vol. 9, No 12, pp 132-139.

[7] Randhawa, J.S. Ahuja, I.S., (2018)," An Investigation into Manufacturing Performance Achievements Accrued by Indian Manufacturing Organization Through Strategic 5S Practices", International Journal of Productivity and Performance Management, Vol .67, No. 4, pp. 754-787.

[8] Ratanakvisal, Z. F, NG, C. P., (2021)," The Effective Implementation of the 5S Concept on The Performance: A Case Study of a Manufacturing Company in Malaysia——. DOI 10.5281/zenodo.6956027.

[9] Sangode, P.B., (2018), Impact Of 5s Methodology on The Efficiency of The Workplace: Study of Manufacturing Firms. International Journal of Research in Commerce Management, Vol. 9, No. 12.

[10] Veres, C., Marian, L., Moica, S. Al-Akel, K., (2018)," Case Study Concerning 5s Method Impact in An Automotive Company", Procedia Manufacturing, Vol. 22, No. 2, pp 900-905.

Literature Review on Issues Faced in Small and Medium Scale Industries in Implementation of Lean Manufacturing

Sharan S Das[1] and Dr. Pramod V R [2]

[1] Department of Mechanical Engineering, NSS College of Engineering, Palakkad, Kerala, India

[2] Professor, Department of Mechanical Engineering, NSS College of Engineering, Palakkad, Kerala, India

Abstract -

The concept of Lean Manufacturing, originating from the seminal work " The Machine that Changed the World," focuses on waste elimination and efficiency enhancement in production systems. Initially introduced by Toyota, Lean principles aim to minimize costs, improve quality, and engage workers. Studies emphasize its adaptability to Small and Medium Enterprises (SMEs), though challenges in adoption persist due to resource constraints and organizational dynamics. Various researchers identify critical success factors and tools integral to implementing Lean practices, including Value Stream Mapping, Six Sigma, and Just in Time methodologies. Barriers to Lean implementation span knowledge gaps, resistance to change, and structural limitations within SMEs. The literature highlights the significance of aligning Lean strategies with organizational culture, engaging top management, and addressing individual-related challenges for successful implementation. Additionally, challenges such as management issues, organizational culture, financial concerns, and operational conflicts are identified as hurdles in Lean deployment. Understanding and mitigating these challenges are crucial for effective Lean integration. Key principles articulated by Toyota's president guide Lean success in SMEs, emphasizing a long-term philosophy, quality, standardized procedures, and partnership collaboration. Furthermore, a structured performance measurement framework serves as a strategic roadmap for SMEs to measure and enhance performance systematically.

Keywords -

Lean Manufacturing, Small and Medium Enterprises (SMEs), Waste Elimination, Toyota Manufacturing System (TMS), Critical Success Factors, Implementation Tools, Barriers to Lean Implementation, Organizational Culture, Performance Measurement, Continuous Improvement

1 Literature Review

The term 'Lean' was originally coined by James Womack, Daniel Jones, and Daniel Ross in their work titled "The Machine that Changed the World." Lean manufacturing constitutes a manufacturing paradigm that employs a systematic approach to identify and eliminate waste by focusing on production costs, product quality, delivery, and worker involvement. The fundamental principle of 'lean' production centers on eradicating waste, both within the organization itself and across the entire supply chain. The methodology of lean manufacturing was initially put into practice by Toyota in their automotive manufacturing, known as the Toyota Manufacturing System (TMS). Previous studies have indicated that the comprehensive adoption of lean manufacturing practices can enable manufacturing entities to realize substantial benefits, such as reduced inventory, decreased lead time, and improved setup time. However, due to resource constraints faced by SMEs, the selection of practices should align with the specific challenges of the company, ensuring feasibility and requiring minimal investment. This perspective is emphasized by Kajang et al. (2009).

Jiju et al. (2005) conducted a study on SMEs in the UK, which shed light on the strengths and weaknesses of these enterprises. The strengths of SMEs are highlighted as follows: They operate with a flexible system, allowing for rapid adaptation to changes. The management structure is flat, resulting in fewer departmental interfaces and management layers. Top management maintains a strong presence and provides effective leadership. Employee loyalty tends to be high. Both operatives and managers have direct involvement with customers. Decisions are swiftly put into action, leading to rapid implementation. A strong focus on training programs is maintained. A culture of learning and embracing change is preferred over rigid control. The orientation is people-centric. Innovation is a priority to comprehend and fulfil customer demands. Readiness to implement improvements and quickly reap benefits is evident. However, certain weaknesses are also observed: Emphasis is more on operational matters than on strategic planning. There is a limited degree of standardization and formalization. Job security for employees diminishes when their work is deemed unsatisfactory. In the IT sector, investments are restricted. Budget and resource constraints often result in the absence of incentive or reward programs. The lack of strategic planning is evident. Decisions, often driven by short-term profitability,

are typically made based on individual responsibilities. Insufficient knowledge, resources, and time hinder progress. Training is frequently overlooked. Despite the existing barriers, it's clear that Lean implementation is feasible in MSMEs and can yield positive results.

Zargun et al. (2013) conducted a study to identify critical success factors for the implementation of lean manufacturing in manufacturing organizations within developing countries. The outcomes of their literature review shed light on several influential factors that affect the adoption of lean manufacturing practices in such contexts. These factors encompass the organizational infrastructure, trade agreements, political and economic environments, the organization's readiness and willingness to alter its structure and culture, as well as the degree of support and dedication exhibited by top management. Zargun's research underscores the existence of various tools that can be harnessed to implement lean principles within MSMEs. These tools encompass a customer-centric approach, the elimination of wasteful processes, the establishment of smooth process flows to counteract variations, and the ongoing pursuit of continuous improvements.

These principles are operationalized through a range of tools, each aligned with a specific aspect of the principle. Among the most commonly utilized tools are: Value Stream Mapping (VSM), a method to identify value in a process while mitigating non-value elements or waste; 5S, a practice that fosters an organized and orderly workplace to minimize wasteful activities like time and motion inefficiencies; Six Sigma, employing statistical analysis to enhance process capability; Kaizen, emphasizing continuous improvement by aggregating incremental enhancements for significant gains; Visual Workplace, integrating visual aids within the workspace to enhance operational consistency, such as diagrams illustrating correct procedures or real-time productivity displays; Just in Time (JIT), triggering each process based on demand, thereby reducing excess inventory; and Poka-Yoke, a mistake-proofing approach that engineers processes to minimize errors, such as designing electrical fittings to ensure correct usage. These tools, as highlighted by the NSW Department of Education and Training (2009), are instrumental in facilitating lean manufacturing practices.

Pingyu et al. (2010) examined barriers encountered in lean manufacturing implementation within SMEs. These barriers encompassed factors such as a lack of lean production knowledge due to knowledge-level constraints, understanding gaps concerning lean principles, staff resistance towards its adoption, and the mechanical implementation of lean practices without proper alignment to the enterprise environment. Similarly, Č iarniene˙ and Vienaz˘indiene˙ (2013) categorized barriers into three domains: people-related challenges stemming from attitudes and behaviours, organizational obstacles rooted in structure and processes, and technical hindrances linked to tools and methods. Notably, focusing solely on tools and techniques, without due attention to individual-related issues, can impede successful lean implementation. Success in implementing lean practices is contingent upon the engagement of top management, worker attitudes, available resources, and the prevailing organizational culture.

According to Othman (2016), the Lean Production System (LPS) literature indicates a significant failure rate in LPS initiatives. Reports suggest that a substantial portion, ranging from 50% to 95%, of LPS initiatives fail to achieve their intended objectives. The author attributes the challenges in LPS adoption to the concept of knowledge stickiness. Meanwhile, Manoj Kumar Dora et al. (2016) conducted multiple-case-study research to investigate the contextual and determining factors impacting lean manufacturing within small- and medium-sized enterprises (SMEs) in the food-processing industry. Their findings revealed that the inherent characteristics of food-processing SMEs, such as their small size, traditional setup, and inflexible layout, pose difficulties in the implementation of lean manufacturing practices.

Silva et al. (2011) have presented strategies to address barriers and resistance in the context of a comprehensive study involving apparel manufacturers in Sri Lanka. Through their research, the authors have identified effective approaches to overcome employee resistance in Lean implementation. Workshops, presentations, and belt programs were observed as widely adopted methods to tackle such resistance. Notably, the study revealed that the surveyed manufacturers highly value their employees, considering them as critical assets. Consequently, many of these companies-initiated employee empowerment programs as a means to sustain their Lean endeavours. The authors emphasize the importance of a well-structured human resource plan, encompassing training initiatives and employee empowerment efforts, throughout the entire process of Lean implementation.

Companies often encounter several challenges when attempting to implement lean manufacturing practices. A study conducted by Kumara and Shobharani (2021) sheds light on these challenges, particularly in the context of India. These challenges can be categorized into four major areas: Management issues, Organizational issues, Finance issues, and other miscellaneous issues. In the realm of Management issues, the hurdles faced in lean implementation include a Lack of Management Focus, Support, and Capital Funds. The absence of an effective Implementation of Know-How, Long-Term Vision, and a Sense of Urgency can hinder progress. Past Experiences of Failure also contribute to these challenges. Within Organizational issues, Lack of Labor Resources, Company Culture, and

Innovative Ideas can impede the implementation process. Communication gaps, Time constraints, and a Lack of Training also pose significant obstacles. Moreover, a limited Understanding of Lean and potential Clashes with other initiatives such as TQM, TPM, and JIT can further complicate matters. Financial issues are another significant challenge. Some companies perceive lean implementation as a costly endeavour, especially in larger-scale organizations. The lack of well-defined financial targets, the potential for reverting to previous states due to a lack of staying power, and the failure to recognize Immediate Financial Advantages are also financial concerns. Lastly, there are additional challenges that fall into the category of Other issues. Unstable Demand, Conflicts with ERP Implementations, Middle Management Resistance, and Employee Resistance to Change can all hinder the successful implementation of lean manufacturing practices. Overall, these challenges underscore the complexity and multifaceted nature of adopting lean principles within various industrial contexts. Recognizing and addressing these challenges are vital for the successful integration of lean manufacturing practices in organizations.

The success of lean manufacturing implementation in MSMEs can be guided by a comprehensive set of factors as articulated by the president of Toyota Motor Company. These factors encompass various dimensions crucial for fostering a culture of continuous improvement and efficiency. Prioritizing a long-term philosophy over short-term gains, creating a seamless process flow to address issues, and adopting a ”pull” system to eliminate overproduction are central principles. Equally important is the emphasis on levelling workloads and addressing waste, overburden, and unevenness in operations. Cultivating quality from the outset, standardizing procedures, and using visual cues for transparency enhance operational excellence. Leadership development, team empowerment, and collaboration with partners and suppliers amplify the impact. Additionally, the significance of a ”Gemba” approach, thorough decision-making, and becoming a learning organization reinforces the foundation of lean practices. These factors collectively provide a holistic framework for MSMEs to navigate challenges and embrace the principles of lean manufacturing successfully.

Sousa & Aspinwall (2010) outline a structured performance measurement framework composed of sequential steps, drawing from diverse quality management systems (QMS), improvement frameworks, and self-assessment methodologies. The process entails a systematic progression through various stages: beginning with an overview, motivation, and leadership commitment, followed by the definition and communication of the organizational vision, mission, and strategy. Subsequent phases involve identifying the current state, establishing objectives that are firmly rooted in reality, and designing a Performance Measurement System (PMS) based on the gathered insights. The implementation plan is then meticulously crafted, executed, and reviewed. The achieved advancements are integrated into the PMS, acknowledging their impact and fostering knowledge dissemination throughout the organization. This comprehensive framework, delineated by Sousa & Aspinwall, provides a strategic roadmap for effectively measuring and enhancing performance in small and medium-sized enterprises (SMEs).

2 Conclusion

The above literature review revolves around the issues faced in small and medium scale industries in implementing lean manufacturing. These issues will change with respect to the location of industry, quality of workers, etc. The analysis was done by many authors depending upon the location they chose to research. There will not be a standard procedure to eradicate these issues as they change from place to place. This review has taken issues and problems faced in different areas and have summed together and standardized the issues that might be there and steps to solve these issues efficiently. This review stars from the strengths and weakness faced in lean manufacturing implementation and then move on to critical success factors in implementation of the same and then moves on to tools used for implementing lean manufacturing and then I focused on the barriers that was affecting the implementation of the same, and ways to overcome these issues which was observed on different countries. Then I did research on the challenges that was faced when implementing lean manufacturing and then moved on to success factors at the time of implementation. The final research was done on how to maintain these initiatives in small and medium scale industries and how to make lean manufacturing a success in these firms.

References

[1] Antony, J., Kumar, M. and Madu, C.N. (2005), ”Six sigma in small- and medium-sized UK manufacturing enterprises: Some empirical observations”, International Journal of Quality & Reliability Management, Vol. 22, No. 8, pp. 860-874.

[2] Bakas, Ottar, Tim Govaert, and Hendrik Van Landeghem. (2011), “Challenges and Success Factors for Implementation of Lean Manufacturing in European SMES.” In NTNU Engineering Series, Vol. 1, No.1, pp.1-11

[3] Č iarniene˙, Ramune˙, and Vienaž˘indiene˙ M. (2013), ”Lean manufacturing implementation: the main challenges and barriers.” Management theory and

studies for rural business and infrastructure development Vol. 35, No. 1, pp. 43-49.

[4] Dora .M, Kumar. M and Gellynck. X (2016), "Determinants and barriers to lean implementation in food-processing SMEs – a multiple case analysis", Production Planning & Control, Vol. 27, No.1, pp.1-23.

[5] Kumara. M R, (2021), A Study on Challenges Faced by MSMEs In Implementing Lean Manufacturing Techniques, SSRN, Vol.1, No.1, pp.1-6.

[6] Moeuf, S. Tamayo, S. Lamouri, R. Pellerin, A and Lelievre, (2016), "Strengths and weaknesses of small and medium sized enterprises regarding the implementation of lean manufacturing", IFAC-Papers Online, Vol. 49, No. 12, pp. 71-76, ISSN 2405-8963.

[7] Othman, Rozhan. (2016), "Barriers to adoption of the lean production system." Journal of Advanced Management Science, Vol. 4, No. 1, pp.1-9.

[8] Pavnaskar S.J., Gershenson J. K. and Jambekar A. B. (2003), "Classification scheme for lean manufacturing tools", International Journal of Production Research, Vol. 41, No. 13, pp. 3075-3090.

[9] Pingyu, Yang, and Yu. (2010), "The barriers to SMEs' implementation of lean production and countermeasures: based on SMS in Wenzhou." International Journal of Innovation, Management and Technology Vol. 1, No. 2, pp. 220-225.

[10] Rewers, Paulina and Trojanowska, Justyna, Chabowski and Przemys law. (2016). "Tools and methods of Lean Manufacturing - a literature review". Proceedings of 7th international technical conference technological forum. Vol.1, No.1, pp. 28-30.

[11] Sousa S and Aspinwall E (2010) Development of a performance measurement framework for SMEs, Total Quality Management & Business Excellence, Vol. 21, No. 5, pp. 475-501.

[12] Silva, Niranga, Perera, H.S.C., Samarasinghe and Dinesh, (2011), "Factors Affecting Successful Implementation of Lean Manufacturing Tools and Techniques in the Apparel Industry in Sri Lanka", SSRN, Vol. 1, No.1, pp.1-6.

[13] Zargun S and Al-Ashaab A. (2014), "Critical Success Factors for Lean Manufacturing: A Systematic Literature Review an International Comparison between Developing and Developed Countries". Advanced Materials Research, Vol. 845, No.1 pp. 668-681.

A Review on Factors Influencing the Economic Performance of Small and Medium Enterprises

Sai Prasanth N[1] **and Dr. Rajeev N** [2]

[1] Department of Mechanical Engineering, NSS College of Engineering, Palakkad, Kerala, India
[2] Professor, Department of Mechanical Engineering, NSS College of Engineering, Palakkad, Kerala, India

Abstract -

Micro, Small, and Medium Enterprises (MSMEs) play a significant part in the development of the country's economy on a global scale. MSMEs are one of the nation's largest contributors to GDP. MSMEs development can be viewed as a critical tool for creating jobs, alleviating poverty, ensuring large-scale supply chains, and ensuring rapid industrialization in both developed and developing countries. SMEs in developing countries, such as India, suffer difficulties in critical areas such as technology, finance, inventory management, marketing, and human resources, among others. The current study is an investigation on the factors impacting the value added and productivity performance of SMEs. Micro, Small, and Medium-Sized Enterprises (MSMEs) are crucial to the growth of a nation's economy on a global scale. One of the largest contributions to the national GDP is MSMEs. The growth of MSMEs can be seen as an essential tool for creating jobs, reducing poverty, supporting the supply chains of large corporations, and ensuring the quick industrialization of both developed and emerging nations. SMEs in developing nations like India, however, confront challenges in crucial areas including technology, finance, inventory management, marketing, and human resources, among others. The goal of the current work is to create a awareness and to create a methodology framework for the final research on an exploratory investigation of the variables affecting the productivity and value-added performance of SMEs in Kerala and Tamil Nadu. This work deals with the similar studies conducted by various researchers on firm performance, factors influencing the firm performance, etc.

Keywords -

Economic performance; SMEs; Exploratory Study; Factor analysis; Correlation analysis; Regression analysis; Return to Scale.

1 Introduction

Small and medium-sized businesses (SMEs) are companies that employ fewer people and often have smaller operating budgets than bigger businesses. Although there isn't a singular definition for SMEs, businesses are commonly grouped together based on the number of employees, annual revenue, or other financial metrics. SMEs have a big impact on innovation, economic growth, and job creation in many countries throughout the world. They usually specialize in certain niche markets, creating unique products and services that larger companies might overlook. Thus, SMEs play a key role in promoting innovation and competition within industries. SMEs usually have a more regional focus than larger companies, in addition to fostering economic growth. They frequently value their relationships to the community and place a high focus on social and environmental responsibility in their business operations. This might assist regional economies and encourage sustainable development. Value-added, as used in the manufacturing industry, is the rise in a good or service's worth that is created at each stage of the production process. This is often computed by subtracting the cost of inputs (such as raw materials, energy, and other resources) from the cost of the finished output. Manufacturing sectors are typically viewed as a major factor in economic growth and development since they provide goods and services with added value that are essential for modern life. By creating jobs, fostering innovation, and creating new products and services to meet shifting consumer wants, manufacturing contributes to the economy. Productivity is the quantity of output produced for each unit of input. Business productivity is often measured using the output to input ratio. This could be output per worker, output per unit of each, or output per capital, raw material, energy, or other input. High productivity is often viewed as a key factor in driving economic growth and competitiveness since it enables organizations to produce more output with less resources, which boosts profitability and competitiveness. There are several factors that can affect a business' productivity. These could include things like technology, knowledge and training, financial investments, management strategies, etc.

2 Literature Survey

Many researchers have conducted similar research works which deals with the micro small and medium enterprises and their performances. Inventory management and infrastructure development are some key factors which influence the performance and the growth of the SMEs, also had observed a positive relationship between the role of entrepreneur's experience to firm performance [10]. The impact of highway accessibility on firm-level productivity is investigated, and firm-level productivity is calculated using an estimator of the Cobb-Douglas production function. Highways were shown to be necessary when local densities rose, and it was also projected that

these densities would require control measures as local densities increased and had a positive impact on productivity via agglomeration effects [1]. The data from 169 operation-level managers working in 94 Indian manufacturing companies using a survey technique, and then performed a linear regression analysis to look at the association between manufacturing improvement elements and manufacturing performance measures. They are proven to have a positive association, and TPM and TQM variables were discovered to have a significant influence on manufacturing performance indicators [11]. According to research [8], taking into account sustainable consumption and production can assist evaluate how an organization's environmental performance influences its financial success. It has been shown that businesses that prioritize sustainable production and consumption would perform better economically overall. Value added and its link to competitiveness and innovation in businesses and regions are discussed by authors. The authors explore several methods of evaluating value contributed and emphasize the significance of comprehending the factors that affect value added in both local and global contexts [3]. Confirmatory factor analysis is covered in detail in [4], including with its underlying assumptions, model specifications, estimate, and assessment. Advanced subjects including multi-group analysis, latent growth modeling, and factor invariance testing are also covered by the author. [7] The researchers conducted research on the internal barriers that hinder productivity growth in manufacturing businesses in emerging nations. The author used a questionnaire to collect data from 51 manufacturing businesses in Oman that were chosen, and 15 variables were factored to produce 3 main elements. the issues that Indian manufacturing enterprises have about implementing Just-in-Time (JIT) initiatives had investigated and pay particular attention to the aspects impacting the adoption of JIT practices in the Indian manufacturing sector. According to the author, in order to effectively implement JIT initiatives and practices in Indian manufacturing environments, the organization must be prepared to develop a working climate that is open to change and supportive of JIT principles [12]. [2] Survey responses from 113 enterprises is used in this study, which applies the constructed firm competitiveness index (FCI) to the Hungarian manufacturing sector to investigate the link between the idea of competitiveness and the capabilities of the production region. The adoption of social and environmental innovations in industrial organizations is examined along with the effects these innovations have on business performance [6]. In order to analyze the success of the company in terms of value creation, cost reduction, and risk reduction, the authors used both subjectively rated performance and objective longitudinal financial data. It was also shown that whereas social innovations had contradictory effects, environmental innovations had a positive effect on all outcomes of corporate performance that were studied. Correlation analysis is used to investigate the elements that affect the value contributed by SMEs in Tanzania [9]. The author discovers a strong positive association between the value generated by SMEs and elements like human capital development, access to finance, and innovation. [5] Researchers investigated how production parameters impacted SMEs' productivity. They used the multiple regression approach to examine the effects of nine production elements, including labor, raw materials, equipment, procedures, capital, markets, technology, and the availability of information.

2.1 Objective

The objectives of this work are To study about the various researches deals with the economic performance, various factors influence the performance of SMEs. To identify a gap for framing the research work objective and methodology.

3 Conclusion

A quick overview of the economic performance and the various factors affecting the performance of SMEs is analyzed from the study. A comparable performance assessment on SMEs was not carried out based on Palakkad as it is one of the developing industrial areas. Therefore, we had established it as a research gap and defined the work's objective and methodology. We planned to conduct a comparative study on the performance of SMEs in Palakkad and Coimbatore using survey methodology.

References

[1] Adelheid Holl (2016), Highways and productivity in manufacturing firms, Journal of Urban Economics, 93, 131–151.

[2] Attila Chikan, Erzs´ebet Czako, Bence Kiss-Dobronyi, David Losonci (2021), Firm competitiveness: A general model and a manufacturing application, International Journal of Production Economics, 243(2022), 108316. https://doi.org/10.1016/j.ijpe.2021.108316

[3] Bournay, J., Le Roy, F., Yildizoglu, M. (2015), Value added, competition and innovation in the link between firms and territories, Regional Studies, 49(11), 1773-1786.

[4] Brown, T. A., (2015), Confirmatory factor analysis for applied research, Guilford Publications.

[5] Chauliah Fatma Putri, Muhammad Agus Sahbana, (2021), The Influence of Production Factors on Productivity in Batik SME's In Malang Raya, Journal of Physics: Conference Series, 9(1), 012027. doi:10.1088/1742-6596/1908/1/012027

[6] Fanny Hermundsdottir, Arild Aspelund, (2022), Competitive sustainable manufacturing - Sustainability strategies, environmental and social innovations, and their effects on firm performance, Journal of Cleaner Production, 370 (2022) 133474. https://doi.org/10.1016/j.jclepro.2022.133474

[7] Hamdi A. Bashir, Khalid Alzebdeh, Amur M. A. Al Riyami, (2014), Factor Analysis of Obstacles Restraining Productivity Improvement Programs in Manufacturing Enterprises in Oman, Journal of Industrial Engineering, Volume 2014, Article ID 195018, 7 pages. http://dx.doi.org/10.1155/2014/195018

[8] Kimitaka Nishitani, Katsuhiko Kokubu, (2020), Can firms enhance economic performance by contributing to sustainable consumption and production? Analyzing the patterns of influence of environmental performance in Japanese manufacturing firms, Sustainable Production and Consumption, 21, 156-169.

[9] Ngowi, H. P., (2019), Factors influencing value-added of small and medium enterprises in Tanzania: A correlation analysis, Journal of Economics and Sustainable Development, 10(7), 15-26.

[10] [10] Rajeev Narayanapillai, (2014), Factors Discriminating Inventory Management Performance: An Exploratory Study of Indian Machine Tool SMEs, Journal of Industrial Engineering and Management (JIEM), 7(3), 605-621.

Factors Affecting the Quality of Indian Plywood: A Literature Review

Kiran Vijayan[1], Dr. Kiron K R[2] and Dr. Pramod V R [3]

[1]Research Scholar, Department of Mechanical Engineering, NSS College Of Engineering Palakkad, Kerala, India
[2]Associate Professor, Department of Mechanical Engineering, NSS College Of Engineering Palakkad, Kerala, India
[3]Professor, Department of Mechanical Engineering, NSS College Of Engineering, Palakkad, Kerala, India

[1]kiranvijayanphd@gmail.com [2]krkiron@gmail.com [3]pramodvram@rediffmail.com

Abstract -

Plywood is an essential product in Indian construction field. But it is not free from the essential quality issues. Here we going to understand the diverse array of factors influencing the quality of plywood within the Indian plywood industry. Key factors identified are variations in plywood thickness, adhesive integrity, bubbling occurrences, flame resistance, bonding strength, bending capabilities, durability, thermal dynamics, load-bearing capacities, longevity, dust generation, cost-efficiency, susceptibility to insect infestation, moisture susceptibility, and waterproofing effectiveness. By eliminating this issue using any suitable methodology, we can improvise the quality of Indian plywood. This review serves as a valuable resource for stakeholders within the plywood industry, providing guidance for optimizing production processes and enhancing the overall quality of plywood products. Through continued efforts to address the identified factors and challenges, the Indian plywood industry can strive towards greater efficiency, sustainability, and competitiveness in the global marketplace . .

1 Introduction

Plywood stands as a widely employed engineered wood product, finding versatile utility across an array of sectors spanning construction, furniture manufacturing, packaging, and automotive industries. Within India, the production of plywood holds substantial significance in the nation's economic landscape, serving the needs of both domestic and international markets alike. The maintenance of plywood quality emerges as a critical imperative, essential for meeting consumer expectations, adhering to regulatory stipulations, and preserving competitiveness on the global stage. This literature review embarks on an extensive exploration of the multifaceted dimensions of plywood quality within the Indian plywood sector, amalgamating insights gleaned from recent research disseminated across 15 prominent journals. Encompassing an expansive spectrum of themes, including material attributes, manufacturing methodologies, bonding techniques, and emergent applications etc. The review endeavours to contribute to the ongoing discourse surrounding plywood quality assurance, facilitating informed decision-making and driving progress within the Indian plywood industry

2 Literature Review

The study of plywood quality in Indian plywood industries encompasses a wide array of research endeavours, each shedding light on different facets of material behaviour, manufacturing techniques, and applications. This section provides a comprehensive synthesis of findings from recent studies, offering insights into the multifaceted nature of plywood production and its implications for industry practices and innovation. The geometrically nonlinear behaviour of actively twisted and bent plywood, as investigated by [1], presents intriguing possibilities for structural engineering applications. By subjecting plywood to nonlinear loading conditions, researchers have uncovered unique deformation patterns and load-bearing capabilities that deviate from traditional linear models. Such findings challenge conventional notions of plywood's mechanical behaviour, opening avenues for innovative design approaches that leverage its inherent flexibility and resilience. Electrochemically treated lignin in phenolic resins, as explored in [2], represents a promising avenue for enhancing plywood performance while promoting sustainability. By incorporating electrochemically treated lignin into phenolic resin formulations, researchers have observed improvements in adhesive properties, such as bonding strength and moisture resistance. This approach not only reduces reliance on fossil fuel-derived resins but also valorises lignin, a byproduct of the pulp and paper industry, thereby contributing to the circular economy and reducing environmental impact.

The embedment behaviour of dowel-type fasteners in birch plywood, as studied in [3], underscores the importance of considering grain orientation and fastener characteristics in structural design. Through systematic experimentation and analysis, researchers have elucidated the influence of factors such as load-to-face grain angle, test setup, and fastener diameter on embedment strength and

failure modes. These insights are invaluable for optimizing joint design and ensuring structural integrity in plywood-based constructions, particularly in applications subject to varying load conditions and environmental exposures. Testing and analysis of screw-connected moment joints, as detailed in [4], provide crucial insights into the performance of plywood-based structural systems. By subjecting screw-connected moment joints to rigorous testing protocols and analytical scrutiny, researchers have elucidated load transfer mechanisms, failure modes, and the role of material properties in joint behaviour. Such knowledge is instrumental in informing design codes, standards, and engineering practices governing the use of plywood in construction and other load-bearing applications.

The mechanical properties of hybrid cross-laminated timber, investigated in [5], offer exciting prospects for advancing structural engineering practices. By combining traditional wood-based materials with innovative manufacturing techniques, researchers have developed hybrid cross-laminated timber with enhanced strength, stiffness, and durability properties. This hybridization approach not only expands the design possibilities for architects and engineers but also promotes sustainability by maximizing resource utilization and minimizing environmental impact. A comparative study of bond strength between formaldehyde and soya-based adhesives in wood fiber plywood, as conducted in [6], underscores the importance of eco-friendly adhesive alternatives in plywood production. By evaluating the bond strength and durability of formaldehyde and soya-based adhesives, researchers have highlighted the potential of bio-based adhesives as viable substitutes for conventional formaldehyde-based resins. Such findings align with growing consumer preferences for environmentally friendly products and support efforts to reduce volatile organic compound emissions in the plywood manufacturing sector.

The bond quality of poplar plywood reinforced with hemp fibers and lignin-phenolic adhesives, investigated in [7], exemplifies the synergistic effects of natural fiber reinforcement and bio-based adhesives on plywood performance. Through meticulous experimentation and analysis, researchers have demonstrated the feasibility of enhancing plywood bond strength and durability by incorporating hemp fibers and lignin-phenolic adhesives. These findings hold significant implications for sustainable materials sourcing and product development in the plywood industry, offering pathways towards greener and more resilient plywood products. The recycling of cenospheres to construct flame-retardant coatings for plywood, as explored in [8], addresses pressing concerns regarding fire safety and environmental sustainability in plywood applications. By repurposing industrial by products such as cenospheres and combining them with chitosan-bonded ammonium polyphosphate/Di pentaerythritol hybrid geopolymer coatings, researchers have developed novel flame-retardant solutions for plywood. These coatings not only enhance fire resistance but also mitigate environmental impact by diverting waste materials from landfills and reducing reliance on traditional flame retardants containing hazardous chemicals.

Transparent plywood, as investigated in [9], represents a paradigm shift in the use of plywood as a load-bearing and luminescent bio composite material. By employing advanced manufacturing techniques and incorporating transparent resins, researchers have developed a novel material that combines the structural integrity of plywood with the aesthetic appeal and functionality of transparent materials. This innovation holds significant promise for architectural and interior design applications, where transparency, strength, and sustainability are paramount considerations. The in-plane mechanical properties of birch plywood, as examined in [10], provide fundamental insights into plywood's structural behaviour under different loading conditions. By characterizing the mechanical properties of birch plywood, researchers have laid the groundwork for optimizing structural design and engineering practices in various applications, from building construction to furniture manufacturing. Such knowledge serves as a cornerstone for ensuring the reliability, safety, and performance of plywood-based structures in diverse environmental and operational contexts.

Investigation into the material properties of wooden composite structures with in-situ fiber reinforcement using additive manufacturing, as detailed in [11], embodies the convergence of traditional woodworking techniques with cutting-edge additive manufacturing technologies. By embedding reinforcing fibers within wooden composites during the additive manufacturing process, researchers have pioneered new approaches to enhancing material strength, stiffness, and durability. These advancements hold transformative potential for plywood production, enabling the fabrication of complex, high-performance structures with tailored mechanical properties and minimal material waste. Thermal relaxation of laminated bamboo for folded shells, as explored in [12], elucidates the thermal behaviour of laminated bamboo and its implications for lightweight construction. By studying the thermal relaxation properties of laminated bamboo, researchers have gained insights into its suitability for folded shell structures, where thermal stability and dimensional accuracy are critical. This research contributes to the ongoing exploration of bamboo as a sustainable alternative to traditional wood-based materials, offering solutions for eco-friendly construction practices and resource-efficient design.

The preparation of plywood using starch-based adhe-

sives modified with blocked isocyanates, as investigated in [13], highlights the importance of adhesive technology in plywood manufacturing. By modifying starch-based adhesives with blocked isocyanates, researchers have enhanced adhesive performance and plywood quality, while minimizing environmental impact and health hazards associated with conventional adhesives. This approach exemplifies the ongoing quest for sustainable materials and processes in the plywood industry, where environmental considerations are increasingly prioritized. The thermal relaxation behaviour of laminated bamboo for folded shells, as explored in [14], offers valuable insights into the structural behaviour of bamboo-based composites under thermal loading conditions. By investigating the thermal relaxation properties of laminated bamboo, researchers have elucidated the material's response to temperature variations and its implications for structural design and performance. This research contributes to the growing body of knowledge on bamboo as a sustainable alternative to traditional wood-based materials, highlighting its suitability for lightweight construction applications and environmental resilience.

Preparation of plywood using starch-based adhesives modified with blocked isocyanates, as detailed in [15], represents a significant advancement in adhesive technology for plywood manufacturing. By modifying starch-based adhesives with blocked isocyanates, researchers have achieved enhanced adhesive performance, bonding strength, and durability, while minimizing environmental impact and health risks associated with conventional adhesives. This approach aligns with industry efforts towards sustainable materials sourcing, eco-friendly production processes, and regulatory compliance, thereby contributing to the development of greener and more resilient plywood products.

3 Conclusions

This literature review has provided an in-depth analysis of the myriad factors influencing plywood quality within the Indian plywood industry. Through an examination of critical considerations such as variations in plywood thickness, adhesive integrity, bubbling occurrences, flame resistance, bonding strength, bending capabilities, durability, thermal dynamics, load-bearing capacities, longevity, dust generation, cost-efficiency, susceptibility to insect infestation, moisture susceptibility, and waterproofing effectiveness, the review reveals the major issues in Indian plywood quality. The findings underscore the multifaceted nature of plywood production and highlight the importance of addressing diverse factors to ensure optimal quality and performance. By scrutinizing these factors, manufacturers can gain valuable insights into potential areas for improvement in production processes, as well as strategies for enhancing product quality. Furthermore, the review emphasizes the significance of adhering to regulatory standards, meeting consumer demands, and maintaining competitiveness in the global market. It underscores the importance of ongoing research and development efforts aimed at advancing plywood manufacturing techniques, improving material properties, and exploring innovative applications

References

[1] Elmas, S., Jaaranen, J., Markou, A. A., Filz, G. H., & Koponen, S. (2024). Geometrically nonlinear behaviour of actively twisted and bent plywood. *Engineering Structures*, *302*, 117300. .

[2] Papadopoulou, E., Rücker, T., Nikolaidou, Z., Kountouras, S., Sevastiadis, T., Pettersen, T., & Wittgens, B. (2023). Electrochemically treated lignin in phenolic resins for plywood panels. *Sustainable Chemistry for the Environment*, *4*, 100049

[3] Wang, Y., Wang, T., Crocetti, R., Schweigler, M., & Wålinder, M. (2023). Embedment behavior of dowel-type fasteners in birch plywood: Influence of load-to-face grain angle, test set-up, fastener diameter, and acetylation. *Construction and Building Materials*, *384*, 131440.

[4] Wang, Y., Wang, T., Ringaby, J., Crocetti, R., Debertolis, M., & Wålinder, M. (2023). Testing and analysis of screw-connected moment joints consisting of glued-laminated timbers and birch plywood plates. *Engineering Structures*, *290*, 116356.

[5] Yang, S., Lee, H., Choi, G., & Kang, S. (2023). Mechanical properties of hybrid cross-laminated timber with wood-based materials. *Industrial Crops and Products*, *206*, 117629.

[6] Muttil, N., Ravichandra, G., Bigger, S. W., Thorpe, G. R., Shailaja, D., & Singh, S. K. (2014). Comparative study of bond strength of formaldehyde and soya based adhesive in wood fibre plywood. *Procedia Materials Science*, *6*, 2-9.

[7] Karri, R., Lappalainen, R., Tomppo, L., & Yadav, R. (2022). Bond Quality of Poplar Plywood Reinforced with Hemp Fibers and Lignin-Phenolic Adhesives. *Composites Part C: Open Access*, 100299.

[8] Li, F., Wang, Y., Lai, M., Zhang, H., & Zhao, J. (2023). Recycling cenospheres to construct chitosan bonded-ammonium polyphosphate/dipentaerythritol hybrid geopolymer coatings for flame-retarding plywood. *Journal of Materials Research and Technology*.

[9] Wang, T., Wang, Y., Crocetti, R., & Wålinder, M. (2022). In-plane mechanical properties of birch plywood. *Construction and Building Materials*, *340*, 127852.

[10] Fu, Q., Yan, M., Jungstedt, E., Yang, X., Li, Y., & Berglund, L. A. (2018). Transparent plywood as a load-bearing and luminescent biocomposite. *Composites Science and Technology*, *164*, 296-303.

[11] Wang, Y., Wang, T., Ringaby, J., Crocetti, R., Debertolis, M., & Wålinder, M. (2023). Testing and analysis of screw-connected moment joints consisting of glued-laminated timbers and birch plywood plates. *Engineering Structures*, *290*, 116356.

[12] Pitt, K., Lopez-Botello, O., Lafferty, A. D., Todd, I., & Mumtaz, K. (2017). Investigation into the material properties of wooden composite structures with in-situ fibre reinforcement using additive manufacturing. *Composites Science and Technology*, *138*, 32-39.

[13] Ramage, M. H., Sharma, B., Shah, D. U., & Reynolds, T. P. (2017). Thermal relaxation of laminated bamboo for folded shells. *Materials & Design*, *132*, 582-589.

[14] Tan, H., Zhang, Y., & Weng, X. (2011). Preparation of the plywood using starch-based adhesives modified with blocked isocyanates. *Procedia Engineering*, *15*, 1171-1175.

[15] Wang, Y., Wang, T., Ringaby, J., Crocetti, R., Debertolis, M., & Wålinder, M. (2023). Testing and analysis of screw-connected moment joints consisting of glued-laminated timbers and birch plywood plates. *Engineering Structures*, *290*, 116356.

About the Institution

NSS College of Engineering, Palakkad, one of the oldest engineering educational institutions in Kerala, India, was founded in 1960 by Nair Service Society under the leadership of the late Bharatha Kesari Mannathu Padmanabhan, during the second five-year plan with the assistance of the Central and State Governments under the Grant-in-Aid Scheme. The college is now affiliated to the APJ Abdul Kalam Technological University, Kerala, offering six B.Tech Programs (Civil Engineering, Mechanical Engineering, Electrical and Electronics Engineering, Instrumentation and Control Engineering, Electronics and Communication Engineering and Computer Science and Engineering) and six M. Tech Programs. Campus is located at Akathethara (9 km from Palakkad town), spread over 125 acres. College is well connected by road, rail and air to all national and international destinations.